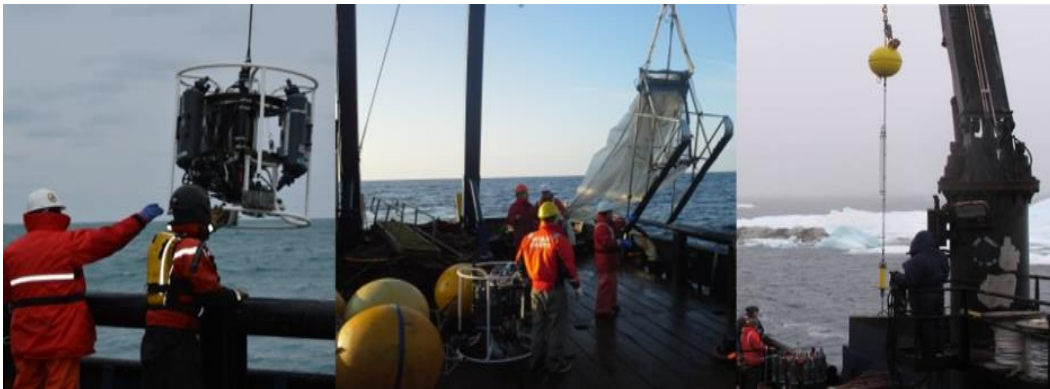


Chukchi Offshore Monitoring in Drilling Area (COMIDA): Factors Affecting the Distribution and Relative Abundance of Endangered Whales and Other Marine Mammals in the Chukchi Sea

Final Report of the Chukchi Sea Acoustics, Oceanography, and Zooplankton Study



**NOAA
FISHERIES**

National Marine Mammal Laboratory
Alaska Fisheries Science Center
National Marine Fisheries Service
National Oceanic and Atmospheric Administration
7600 Sand Point Way NE, Seattle, WA 98115-6349



Funding Agency:
Bureau of Ocean Energy Management
Alaska Outer Continental Shelf Region
U.S. Department of the Interior
3801 Centerpoint Drive, Suite 500
Anchorage, AK 99503-5823

Contract No. M09PG00016

August 2015

OCS Study BOEM 2015-034

This report has been reviewed by the Department of Interior and approved for publication. Approval does not signify that the contents necessarily reflect the views and policies of the Department, nor does mention of trade names or commercial products constitute endorsement or recommendation for use.

Chukchi Offshore Monitoring in Drilling Area (COMIDA): Factors Affecting the Distribution and Relative Abundance of Endangered Whales and Other Marine Mammals in the Chukchi Sea

Final Report of the Chukchi Sea Acoustics, Oceanography, and Zooplankton Study

Prepared for:

Environmental Studies Program
Alaska Outer Continental Shelf Region
Bureau of Ocean Energy Management
U.S. Department of Interior
3801 Centerpoint Drive, Suite 500
Anchorage Alaska 99503-5823



Submitted through:

National Marine Mammal Laboratory
Alaska Fisheries Science Center
National Marine Fisheries Service, NOAA
U.S. Department of Commerce
7600 Sand Point Way NE
Seattle, Washington 98115-6349



This study was initiated and supported by the U.S. Department of Interior, Bureau of Ocean Energy Management (BOEM), Alaska Outer Continental Shelf Region, Anchorage, Alaska, through an Interagency Agreement between BOEM and the National Marine Mammal Laboratory (M09PG00016), as part of the BOEM Alaska Environmental Studies Program.

REPORT AVAILABILITY

This document is available to the public through:

National Technical Information Service
5285 Port Royal Road
Springfield, Virginia 22161
FAX: (703) 605-6900
www.ntis.gov

CITATION

May be cited as: Berchok, C.L., J.L. Crance, E.C. Garland, J.A. Mocklin, P.J. Stabeno, J.M. Napp, B.K. Rone, A.H. Spear, M. Wang, and C.W. Clark. 2015. Chukchi Offshore Monitoring In Drilling Area (COMIDA): Factors Affecting the Distribution and Relative Abundance of Endangered Whales and Other Marine Mammals in the Chukchi Sea. Final Report of the Chukchi Sea Acoustics, Oceanography, and Zooplankton Study, OCS Study BOEM 2015-034. National Marine Mammal Laboratory, Alaska Fisheries Science Center, NMFS, NOAA, 7600 Sand Point Way NE, Seattle, WA 98115-6349.

Email of corresponding editors: Catherine.Berchok@noaa.gov and Jessica.Crance@noaa.gov

KEY PERSONNEL (IN ALPHABETICAL ORDER)

Catherine L. Berchok¹, Ph.D. – Program Coordinator, Passive acoustics P.I.

Christopher Clark⁵, Ph.D. – Noise Modeling and Auto-detection Buoy P.I.

Jessica L. Crance¹, M.S. – Project Manager

Ellen C. Garland⁷, Ph.D. – Statistical advisor

Julie A. Mocklin¹, M.S. – Final Report Editor

Sue E. Moore², Ph.D. – Science advisor (ecosystems)

Jeff Napp³, Ph.D. – Zooplankton P.I.

James E. Overland⁴, Ph.D. – Science advisor (climate)

Brenda K. Rone¹, M.S. – Visual Survey P.I.

Adam H. Spear³, M.S. – Zooplankton Acoustics

Phyllis Stabeno⁴, Ph.D. – Oceanography P.I.

Muyin Wang⁶, Ph.D. – Climate Modeling P.I.

¹ National Marine Mammal Lab (NMML), Alaska Fisheries Science Center, NOAA Fisheries Service, 7600 Sand Point Way NE, Seattle, WA 98115-6349

² National Marine Fisheries Service, Office of Science & Technology, 7600 Sand Point Way NE, Seattle, WA 98115-6349

³ Resource Assessment and Conservation Engineering (RACE) Division, Alaska Fisheries Science Center, NOAA Fisheries Service, 7600 Sand Point Way NE, Seattle, WA 98115-6349

⁴ Pacific Marine Environmental Laboratory (PMEL), Ocean Environment Research Division, 7600 Sand Point Way NE, Seattle, WA 98115-6349

⁵ Bioacoustics Research Program (BRP), Cornell University, 159 Sapsucker Woods Road, Ithaca, NY 14850

⁶ Joint Institute for the Study of the Atmosphere and Ocean (JISAO), University of Washington, 7600 Sandpoint Way NE, Seattle, WA 98195

⁷ School of Biology, University of St. Andrews, Fife, KY16 9TH, UK

I. LIST OF ACRONYMS

AB-2012: Auto-detection buoy deployed and operated in 2012

ACC: Alaska Coastal Current

ADCP: Acoustic Doppler Current Profiler

AFSC: Alaska Fisheries Science Center

AIC: Akaike Information Criterion

AMSR: Advanced Microwave Scanning Radiometer

ARCWEST: Arctic Whale Ecology Study

ARGOS: Advanced Research and Global Observation Satellite

ARS: Area Restricted Search

ARTS: Air Rocket Transmitter System

ASAMM: Aerial Surveys of Arctic Marine Mammals

AURAL: Autonomous Underwater Recorder for Acoustic Listening

AW: Anadyr Water

BCB: Bering-Chukchi-Beaufort

BOWFEST: Bowhead Whale Feeding Ecology Study

BS: Bering Sea

BW: Bering Water

BWASP: Bowhead Whale Aerial Survey Project

CCSM3: Community Climate System Model ver3

CCSM4: Community Climate System Model ver4

CDS: Conventional Distance Sampling

CESM: Community Earth System Model

CHAOZ: Chukchi Sea Acoustics, Oceanography, and Zooplankton Study

CHAOZ-X: Chukchi Sea Acoustics, Oceanography, and Zooplankton Study Extension

CMIP5: Coupled Model Intercomparison Project, phase 5

COMIDA: Chukchi Offshore Monitoring In Drilling Area

CPA: Closet Point of Approach

Cornell-BRP: Cornell-Bioacoustics Research Program

CSESP: Chukchi Sea Environmental Studies Program

CTD: Conductivity, Temperature, Depth sensor instrument package

CV: Coefficient of Variation
DBO: Distributed Biological Observatory
DELMA: Detection Classification and Machine Learning Algorithms
DiFAR: Directional Frequency Analysis and Recording
DTAG: Suction Cup Acoustic Tag
DVM: Diel Vertical Migration
DWBA: Distorted-wave Born Approximation
EcoFOCI: Ecosystems and Fisheries-Oceanography Coordinated Investigations
ECS: Eastern Chukchi Sea
ESW: Effective Strip Width
FFT: Fast Fourier Transform
FM: Frequency Modulated
GAM: Generalized Additive Model
GUI: Graphical User Interface
HEE: Hermes Electronics
HMM: Hidden Markov Model
IACUC: International Animal Care and Use Committee
JISAO: Joint Institute for the Study of the Atmosphere and Ocean
LFDCS: Low-frequency Detection and Classification System
MAG: Magnavox
MARU: Marine Autonomous Recording Unit
MGCV: Mixed GAM Computation Vehicle
MW: Melt Water
NCEP: National Centers for Environmental Prediction
NCAR: National Center for Atmospheric Research
NEPA: National Environmental Policy Act
NMML: National Marine Mammal Laboratory
NOAA: National Oceanic and Atmospheric Administration
NRC: National Research Council
NSF: National Science Foundation
NSIDC: National Snow and Ice Data Center
PAR: Photosynthetically Active Radiation

PCMDI: Program for Climate Model Diagnosis and Intercomparison
PMEL: Pacific Marine Environmental Laboratory
PRIEST: Pacific Right Whale Ecology Study
PTT: Platform Terminal Transmitter
RCP4.5: Representative Concentration Pathway4.5
RCP8.5: Representative Concentration Pathway8.5
RHIB: Rigid-Hulled Inflatable Boat
RMS: Root-mean-squared
ROC: Receiver Operating Characteristic
SBE 19plus: SeaBird SeaCAT CTD
SBE 49: SeaBird FastCAT CTD
SDA: Speed-Distance-Angle
SPOT 5: Smart POsition and Temperature tag ver5
SPW: Sparson sonobuoy
SSSM: Switching State-Space Model
TAPS6-NG: Tracor Acoustic Profiling System 6 - Next Generation
TEK: Traditional Ecological Knowledge
TFS: Truncated Fluid Sphere
TIROS: Television Infrared Observation Satellite
USS: Undersea Sensor Systems
UTC: Coordinated Universal Time
WARC: Western Alaska Resident Catalog
WATC: Western Alaska Transient Catalog
WHOI: Woods Hole Oceanographic Institution
WW: Winter Water

II. LIST OF FIGURES

Figure 1. Map showing general study area	3
Figure 2. Location of long-term passive acoustic recorder moorings	20
Figure 3. Bowhead whale calling activity.....	27
Figure 4. Gunshot call activity.....	28
Figure 5. Beluga whale calling activity	30
Figure 6. Gray whale calling activity.....	31
Figure 7. Walrus calling activity.....	34
Figure 8. Bearded seal calling activity.....	36
Figure 9. Seismic airgun noise activity.....	39
Figure 10. Vessel noise activity	40
Figure 11. Ice noise activity.....	41
Figure 12. Location of CHAOZ passive acoustic moorings off Icy Cape, AK in relation to those deployed by Hannay et al. (2013).....	43
Figure 13. Ice cover in northeastern Chukchi Sea	52
Figure 14. Location of passive acoustic recorders (red dots) in relation to areas of industrial activity. Figure modified from Blee et al.	59
Figure 15. Location of passive acoustic recorders (red dots) in relation to areas of industrial activity. Figure modified from Hartin et al.....	60
Figure 16. Modifications of a 77C sonobuoy	67
Figure 17. Sonobuoy monitoring station	68
Figure 18. Omnidirectional and Yagi antenna placement	69
Figure 19. Marine mammal observer using 25x “big-eye” binoculars.....	70
Figure 20. Summary of combined visual and acoustic effort, 2010-2012.....	71
Figure 21. Bowhead whale acoustic and visual detections.....	73
Figure 22. Gray whale acoustic and visual detections.....	74
Figure 23. Walrus acoustic and visual detections.....	74
Figure 24. Bearded seal acoustic and visual detections.....	75
Figure 25. Fin whale acoustic and visual detections.....	76
Figure 26. Humpback whale acoustic and visual detections	76
Figure 27. Miscellaneous cetacean acoustic and visual detections.....	77
Figure 28. Miscellaneous marine mammal acoustic and visual detections	77
Figure 29. An example of a SPOT 5 satellite transmitter that was deployed in 2012.....	87
Figure 30. Locations (red dots) of the gray whale tagged off Wainwright.....	88
Figure 31. Switching state-space modeled locations	89
Figure 32. Bathymetry in the study area, the three mooring sites, and the six hydrographic transects occupied	92
Figure 33. TAPS6-NG	95
Figure 34. Cross section of temperature and salinity at Icy Cape	97
Figure 35. Time series from the inshore mooring (C1), deployed August 2010-2011.....	99
Figure 36. Time series from the midshore mooring (C2), deployed August 2010-2011.....	100
Figure 37. Time series from the offshore mooring (C3), deployed August 2010-2011	101
Figure 38. Time series from the inshore mooring (C1), deployed August 2011-2012.....	102
Figure 39. Time series from the midshore mooring (C2), deployed August 2011-2012.....	103
Figure 40. Time series from the offshore mooring (C3), deployed August 2011-2012	104
Figure 41. Ice keel depth for both deployment years.....	105

Figure 42. Plots of daily bottom currents.....	106
Figure 43. Transport calculated at Icy Cape for deployments	107
Figure 44. Transport calculated at the Icy Cape line (Transect D) using the mooring data	108
Figure 45. The warmer, more saline Atlantic water is evident in the Temperature-Salinity (T-S) diagram	109
Figure 46. Percent areal ice cover on January 3, 2011	110
Figure 47. Temperature (A), salinity (B) measured in August 2011	111
Figure 48. Plots of temperature and salinity on a density grid	112
Figure 49. ADCP estimated zooplankton volume backscatter (S_v) late August to late September 2011.....	113
Figure 50. Wavelet analysis of 2010 - 2011 near surface data (7-8 m) zooplankton volume backscatter data from the Icy Cape transect	114
Figure 51. Wavelet analysis of 2010 - 2011 at depth data (27-28 m) zooplankton volume backscatter data from the Icy Cape transect	115
Figure 52. Wavelet analysis of 2011-2012 near surface data (11-12 m) zooplankton volume backscatter data from the Icy Cape transect	116
Figure 53. Wavelet analysis of 2011-2012 at depth data (28-32 m) zooplankton volume backscatter data from the Icy Cape transect	117
Figure 54. Estimated abundance at 25 m for two types of zooplankton scatterers.....	118
Figure 55. Estimated abundance at 10 m for two types of zooplankton scatterers.....	119
Figure 56. 1 m ² Tucker Sled on the icy deck of the F/V <i>Aquila</i>	125
Figure 57. Map of currents over the Chukchi shelf	127
Figure 58. Hydrographic measurements at Point Hope (Line A) in September 2010.....	129
Figure 59. Hydrographic measurements at Point Hope (Line A) in August 2011	130
Figure 60. Hydrographic measurements at Point Hope (line A) in August 2012.....	131
Figure 61. Hydrographic measurements at Cape Lisburne (Line B) in September 2010.....	132
Figure 62. Hydrographic measurements at Cape Lisburne (Line B) in August 2011	133
Figure 63. Hydrographic measurements at Cape Lisburne (Line B) in August 2012	134
Figure 64. Hydrographic measurements at Point Lay (Line C) in September 2010.....	135
Figure 65. Hydrographic measurements at Point Lay (Line C) in August 2011	136
Figure 66. Hydrographic measurements at Point Lay (Line C) in August 2012	137
Figure 67. Hydrographic measurements at Icy Cape (Line D) in September 2010.....	138
Figure 68. Hydrographic measurements at Icy Cape (Line D) in August 2011	139
Figure 69. Hydrographic measurements at Icy Cape (Line D) in August 2012	140
Figure 70. Hydrographic measurements at Wainwright (Line E) in September 2010	141
Figure 71. Hydrographic measurements at Wainwright (Line E) in August 2011	142
Figure 72. Hydrographic measurements at Wainwright (Line E) in August 2012.....	143
Figure 73. Hydrographic measurements at Barrow Canyon (Line F) in August 2011.....	144
Figure 74. Hydrographic measurements at Barrow Canyon (Line F) in August 2012.....	145
Figure 75. Trajectory of satellite-tracked drifters deployed in August 2011.....	146
Figure 76. Concentration of euphausiid calyptopae in the water column, 2010 - 2012.	149
Figure 77. Concentration of euphausiid furcilia in the water column, 2010 - 2012.	150
Figure 78. Concentration of euphausiid furcilia along the bottom, 2010 – 2012.	151
Figure 79. Concentration of euphausiid furcilia day and night, 2010 – 2012. Purple symbols indicate day, pink symbols indicate night.	152
Figure 80. Concentration of euphausiid juvenile and adults in the water column, 2010 – 2012.....	153

Figure 81. Concentration of euphausiid juvenile and adults in the bottom layer, 2010 – 2012.	154
Figure 82. Concentration of hyperiid amphipods in the water column, 2010 – 2012.	155
Figure 83. Concentration of gammarid amphipods in the water column, 2010 – 2012.	156
Figure 84. Concentration of gammarid amphipods near bottom, 2010 – 2012.	157
Figure 85. Concentration of <i>Pseudocalanus</i> spp. in the water column, 2010 – 2012.	158
Figure 86. Concentration of <i>Calanus glacialis</i> in the water column, 2010 – 2012.	159
Figure 87. Concentration of <i>Calanus glacialis</i> near bottom, 2010 – 2012.	160
Figure 88. Concentration of <i>Calanus hyperboreus</i> in the water column, 2010 – 2012.	161
Figure 89. Concentration of larvaceans in the water column, 2010 – 2012.	162
Figure 90. Concentration of pteropods in the water column, 2010 – 2012.	163
Figure 91. Concentration of pteropods along the bottom, 2010 – 2012.	164
Figure 92. Concentration of chaetognaths in the water column, 2010 – 2012.	165
Figure 93. Relationship between zooplankton displacement volume and mean water column volume backscatter in 2011	167
Figure 94. Relationship between zooplankton displacement volume and mean water column volume backscatter in 2012	168
Figure 95. Icy Cape 2010 transect sections of physical properties and zooplankton	169
Figure 96. Icy Cape 2011 transect sections of physical properties and zooplankton	170
Figure 97. Icy Cape 2012 transect sections of physical properties and zooplankton	171
Figure 98. Duration of ice cover at each grid point based on Hadley Sea Ice analysis	177
Figure 99. Time series of zonally averaged number of sea ice-free months	178
Figure 100. Time series of monthly sea ice extent for the Chukchi Sea	180
Figure 101. CESM1.0 simulated monthly ice thickness averaged over a small box around the moorings in the Chukchi Sea	182
Figure 102. Annual mean ocean current simulated by CESM.	183
Figure 103. Ocean current at 30 m depth.	184
Figure 104. Ocean temperature (left; °C) and salinity (right; psu) at 40 m depth	185
Figure 105. Model simulated ocean temperature (left; °C) and salinity.	186
Figure 106. Bowhead whale calling activity as it relates to oceanographic variables at the inshore location, 2010-2012	194
Figure 107. Bowhead whale calling activity as it relates to oceanographic variables at the midshore location, 2010-2012	195
Figure 108. Bowhead whale calling activity as it relates to oceanographic variables at the offshore location, 2010-2012	196
Figure 109. Marine mammal calling activity (blue line) vs. winds (m/s; black line) at the midshore location.	197
Figure 110. Gunshot calling activity as it relates to oceanographic variables at the inshore location, 2010-2012	199
Figure 111. Gunshot calling activity as it relates to oceanographic variables at the midshore location, 2010-2012	200
Figure 112. Gunshot calling activity as it relates to oceanographic variables at the offshore location, 2010-2012	201
Figure 113. Beluga whale calling activity as it relates to oceanographic variables at the inshore location, 2010-2012.	203
Figure 114. Beluga whale calling activity as it relates to oceanographic variables at the midshore location, 2010-2012	204

Figure 115. Beluga whale calling activity as it relates to oceanographic variables at the offshore location 2010-2012	205
Figure 116. Gray whale calling activity as it relates to oceanographic variables at the inshore location, 2010-2012	207
Figure 117. Barrow transect line oceanographic, zooplankton, and gray whale survey results, 2011.....	208
Figure 118. Point Hope transect line oceanographic, zooplankton, and gray whale survey results, 2012.....	209
Figure 119. Walrus calling activity as it relates to oceanographic variables at the inshore location, 2010-2012	212
Figure 120. Walrus calling activity as it relates to oceanographic variables at the midshore location, 2010-2012	213
Figure 121. Walrus calling activity as it relates to oceanographic variables at the offshore location, 2010-2012	214
Figure 122. Marine mammal calling activity (blue line) vs. winds (m/s; black line) at the midshore location.....	215
Figure 123. Wainwright transect line oceanographic, zooplankton, walrus, and bearded seal survey results, 2010	216
Figure 124. Wainwright transect line oceanographic, zooplankton, walrus, and bearded seal survey results, 2011	217
Figure 125. Wainwright transect line oceanographic, zooplankton, walrus, and bearded seal survey results, 2012	218
Figure 126. Icy Cape transect line oceanographic, zooplankton, walrus, and bearded seal survey results, 2010	219
Figure 127. Icy Cape transect line oceanographic, zooplankton, walrus, and bearded seal survey results, 2011	220
Figure 128. Icy Cape transect line oceanographic, zooplankton, walrus, and bearded seal survey results, 2012	221
Figure 129. Bearded seal calling activity as it relates to oceanographic variables at the inshore location, 2010-2012.....	224
Figure 130. Bearded seal calling activity as it relates to oceanographic variables at the midshore location, 2010-2012.....	225
Figure 131. Bearded seal calling activity as it relates to oceanographic variables at the offshore location, 2010-2012.....	226
Figure 132. Ice noise presence as it relates to oceanographic variables at the inshore location, 2010-2012	228
Figure 133. Ice noise presence as it relates to oceanographic variables at the midshore location, 2010-2012	229
Figure 134. Ice noise presence as it relates to oceanographic variables at the offshore location, 2010-2012	230
Figure 135. Water masses and circulation in the Chukchi Sea.....	244
Figure 136. Schematic of ecosystems and possible future scenarios.....	245
Figure 137. Detector performance curves as a function of different detection threshold settings	258
Figure 138. Relative classifier performance of training and test datasets.	259
Figure 139. Locations of the AB-2012 (red) and MARU-DB recorders.....	261

Figure 140. Diagram showing the schema and components of the Acoustic Ecology system...	264
Figure 141. Example of Noise Report Browser results	265
Figure 142. Example frame from one of the types of output movies computed by DELMA's spatial analyzer.....	266
Figure 143. Examples of another type of output from DELMA's communication space visualizer	267
Figure 144. Spectrogram example of a frequency-modulated sound automatically detected by AB-2012.....	268
Figure 145. Daily detections of potential bowhead whale sound clips transmitted from AB-2012	269
Figure 146. Examples of 12 bowhead sounds	270
Figure 147. Example of a long-term spectrogram	270
Figure 148. Example of time-varying median noise level plot from MARU-DB_2010-11.....	272
Figure 149. Three-panel plot for MARU-DB_2011-12 showing an example of noise from an ice movement event	273
Figure 150. Three-panel plot for MARU-DB_2013-14 which shows an example of noise from a ship passing close.....	274
Figure 151. Example of a diel plot of hourly median noise levels for the bowhead frequency band.....	275
Figure 152. Comparison of ambient noise level in the bowhead frequency band.....	277
Figure 153. Times-series of noise levels and surface wind speeds.....	278
Figure 154. Regressed wind speed plot: the linear regression of ambient noise level	279
Figure 155. Time series comparison of bowhead-band level noise.....	280
Figure 156. Monthly time series comparisons of daily bowhead-band level noise.....	281
Figure 157. On-effort transects and the area of analysis within Arctic waters to estimate relative abundance.	288

III. LIST OF TABLES

Table 1. List of all passive acoustic recorders	21
Table 2. Summary of results for bowhead, beluga, and gray whale, walrus, and bearded seal calling activity, 2010-2012.	24
Table 3. Key timing events for bowhead whale calling activity.....	25
Table 4. Key timing events for beluga whale calling activity.	29
Table 5. Key timing events for gray whale calling activity.....	31
Table 6. Key timing events for walrus calling activity.	33
Table 7. Key timing events of bearded seal calling activity.	35
Table 8. Key timing events of airgun, vessel, and ice noise activity.....	38
Table 9. Total number of sonobuoys deployed per year in the Arctic and the success rate, 2010-2012.....	71
Table 10. Summary of visual trackline effort	72
Table 11. Summary of sightings	78
Table 12. Summary of mooring locations and measurements taken	93
Table 13. Material properties and other parameters used in the scattering models	96
Table 14. Maximum keel depth measured at the mooring sites	98
Table 15. The number of hydrographic stations occupied in the Chukchi Sea	123
Table 16. The identifying number of the drifter and the latitude and longitude.....	123
Table 17. Net configuration and sampling strategy for all transect lines	124
Table 18. Temperature and salinity ranges for different water masses in the Chukchi Sea.	127
Table 19. Mean concentration of selected zooplankton taxa.....	147
Table 20. Measurements of ice thickness and bottom oxygen used in the GAM runs.....	190
Table 21. Summary of the top variables, AIC, % R-squared values, and sample size.....	192
Table 22. Bowhead whale results of the GAM model.....	193
Table 23. Gunshot call results of the GAM model	198
Table 24. Beluga whale results of the GAM model.....	202
Table 25. Gray whale results of the GAM model.....	206
Table 26. Walrus results of the GAM model.....	211
Table 27. Bearded seal results of the GAM model.....	223
Table 28. Ice noise results of the GAM model	227
Table 29. Summary of the effects of Scenario 1 on key marine mammal species.	249
Table 30. Summary of effects of Scenario 2 on key marine mammal species.	252
Table 31. Listing of the Cornell auto-detection buoy and MARU recording information.....	260
Table 32. The number of sightings (groups) used in the estimation of density (after truncation) of cetaceans within Arctic waters, 2010-2012.	289
Table 33. Estimates of encounter rate (groups/km) and CV (in parenthesis) across all years for cetaceans within Arctic waters, 2010-2012.	290
Table 34. Estimates of density (individuals/km ²) and CV (in parenthesis) across all years for cetaceans within Arctic waters, 2010-2012.	290

IV. TABLE OF CONTENTS

I. List of Acronyms.....	i
II. List of Figures	iv
III. List of Tables.....	ix
V. Executive Summary	1
VI. Introduction	16
A. Background	16
B. Objectives of study.....	17
C. Summary of research effort.....	18
D. Structure of report	18
VII. Marine mammal distribution.....	19
A. Moored Observations	19
1. Methods.....	19
2. Results.....	23
3. Discussion.....	42
4. Conclusions.....	62
5. Recommendations.....	64
B. Shipboard Observations	66
1. Methods.....	66
2. Results.....	70
3. Discussion	79
4. Conclusions.....	84
5. Recommendations.....	85
C. Photo-Identification.....	85
1. Methods.....	85
2. Results.....	85
3. Discussion	86
4. Conclusions.....	86
5. Recommendations.....	86
D. Satellite Telemetry	86
1. Methods.....	86
2. Results.....	88
3. Discussion	89

4. Conclusions.....	89
5. Recommendations.....	90
VIII. Biophysical Patterns and trends	91
A. Moored Observations	91
1. Methods.....	91
2. Results.....	96
3. Discussion	119
4. Conclusions.....	121
5. Recommendations.....	121
B. Shipboard Observations	122
1. Methods.....	122
2. Results.....	126
3. Discussion	172
4. Conclusions.....	173
5. Recommendations.....	174
IX. Climate modeling.....	175
1. Methods.....	175
2. Results.....	175
3. Discussion	185
4. Conclusions.....	186
5. Recommendations.....	187
X. Correlation of marine mammal distribution to biophysical parameters.....	188
1. Methods.....	188
2. Results.....	190
3. Discussion	231
4. Conclusions.....	241
5. Recommendations.....	242
XI. Long-range predictions of habitat use by arctic and subarctic marine mammal species.....	243
1. Discussion	243
2. Conclusions.....	252
3. Recommendations.....	253
XII. Noise modeling and impact mitigation	255
1. Methods.....	255
2. Results.....	268

3. Discussion	282
4. Conclusions.....	285
5. Recommendations.....	286
XIII. Estimating relative abundance of marine mammals	288
A. Visual.....	288
1. Methods.....	288
2. Results.....	289
3. Discussion	290
4. Conclusions.....	291
5. Recommendations.....	291
B. Acoustic.....	291
XIV. Summary	295
A. Overall summary	295
B. Recommendations for future work.....	295
XV. Literature cited.....	297
XVI. Acknowledgements	316
XVII. List of publications and presentations	317
XVIII. Appendices	321
A. Field survey summary table.	321
B. Mooring diagrams.	322
C. Long-term passive acoustic data by species.....	326
D. Sonobuoy and visual survey data	335
E. Passive acoustics table showing percentage of days with calls for each species by month.....	353
F. Photo-identification results within the Bering Sea and Gulf of Alaska.	354
G. Long-term passive acoustic data showing timespans included in the GAMs for each species or signal.....	356
H. GAM results including TAPS6-NG variables.....	360
I. List of attached electronic files	362

V. EXECUTIVE SUMMARY

The Chukchi Sea Acoustics, Oceanography, and Zooplankton (CHAOZ) study was initiated in September 2009 through an Interagency Agreement (formal title: *Chukchi Offshore Monitoring in Drilling Area (COMIDA): Factors Affecting the Distribution and Relative Abundance of Endangered Whales*) between the Bureau of Ocean Energy Management (BOEM) and the National Marine Mammal Laboratory (NMML). The goal of this study was to document the distribution and relative abundance of bowhead, humpback, right, fin, gray, and other whales in areas of potential seismic surveying, drilling, construction, and production activities and relate changes in those variables to oceanographic conditions, indices of potential prey density, and anthropogenic activities. The scope of this study was expanded to include more marine mammals than just the cetaceans listed above. The final list included bowhead, gray, beluga, killer, minke, humpback, right, and sperm whales, bearded and ribbon seals, and walrus. Not all the species in this study area are listed under the Endangered Species Act (i.e., gray, beluga, killer, and minke whales, ribbon and bearded seals, and walrus are not listed).

The study had ten principal objectives:

1. Assess the year-round seasonal occurrence of bowhead, gray, and other whale calls in the northeastern Chukchi Sea.
2. Estimate relative abundance of these whales.
3. Obtain two full years of biophysical measurements on the shallow Chukchi shelf utilizing moorings at three sites, and collect hydrographic and lower trophic level data during deployment/recovery of the moorings.
4. Evaluate the extent to which variability in environmental conditions such as sea ice, oceanic currents, water temperature and salinity, and prey abundance influence whale distribution and relative abundance.
5. Run the National Center for Atmospheric Research (NCAR) climate model (Community Earth System Model: CESM1.0) for future projections using the sea ice extents from 2007/2008 as initial conditions.
6. Analyze multiple ensemble members CESM as well as the group of CMIP5 models to assess the future variability of sea ice cover and extended sea ice free seasons during fall for the Chukchi Sea.
7. Evaluate whether changes in seasonal sea ice extent are resulting in a northward shift of Bering Sea cetacean species such as fin, humpback, and North Pacific right whales.
8. Provide long-term estimates of habitat use for large whale species and compare this with predictions about annual ice coverage to establish predictive variables that describe large whale occurrence.
9. Develop a quantitative description of the Chukchi Sea's noise budget, as contributed by biotic and abiotic sound sources, and continuous, time-varying metrics of acoustic habitat loss for a suite of arctic marine mammal species.

10. Develop a near-real-time passive acoustic monitoring system that can be used as an impact mitigation tool.

The objectives of CHAOZ were addressed using multiple research disciplines. The study area was mainly in the northeastern Chukchi Sea, but also included research in the Bering and western Beaufort Seas. Data were collected both over the short-term (roughly, one month), during ship surveys, and long-term, from year-round passive acoustic and oceanographic moorings. Data were collected in two year-long mooring deployments (2010-11 and 2011-12), as well as during three field surveys in August and September of 2010, 2011, and 2012. Research efforts during the field season included visual surveys, tagging studies, photo-identification studies, zooplankton and oceanographic sampling (CTD and Tucker sled zooplankton tows), passive acoustic monitoring (sonobuoys), drifter deployments, and a near-real-time auto-detection buoy (2012 only) that provided acoustic detections and ambient noise data via an Iridium satellite link. Research that occurred in the lab during the rest of the year, included long-term analysis from over-wintering moorings (passive acoustic and biophysical) located at 40, 70, and 120 nm off Icy Cape, noise modeling to establish baseline data and predictions on the low-frequency acoustic environment (<1 kHz), and climate modeling with a focus on future ice projections. Figure 1 depicts the general study area and the main locations for data collection among the various research disciplines; also shown are the study areas for the industry-sponsored Chukchi Sea Environmental Studies Program (CSESP) within the lease area.

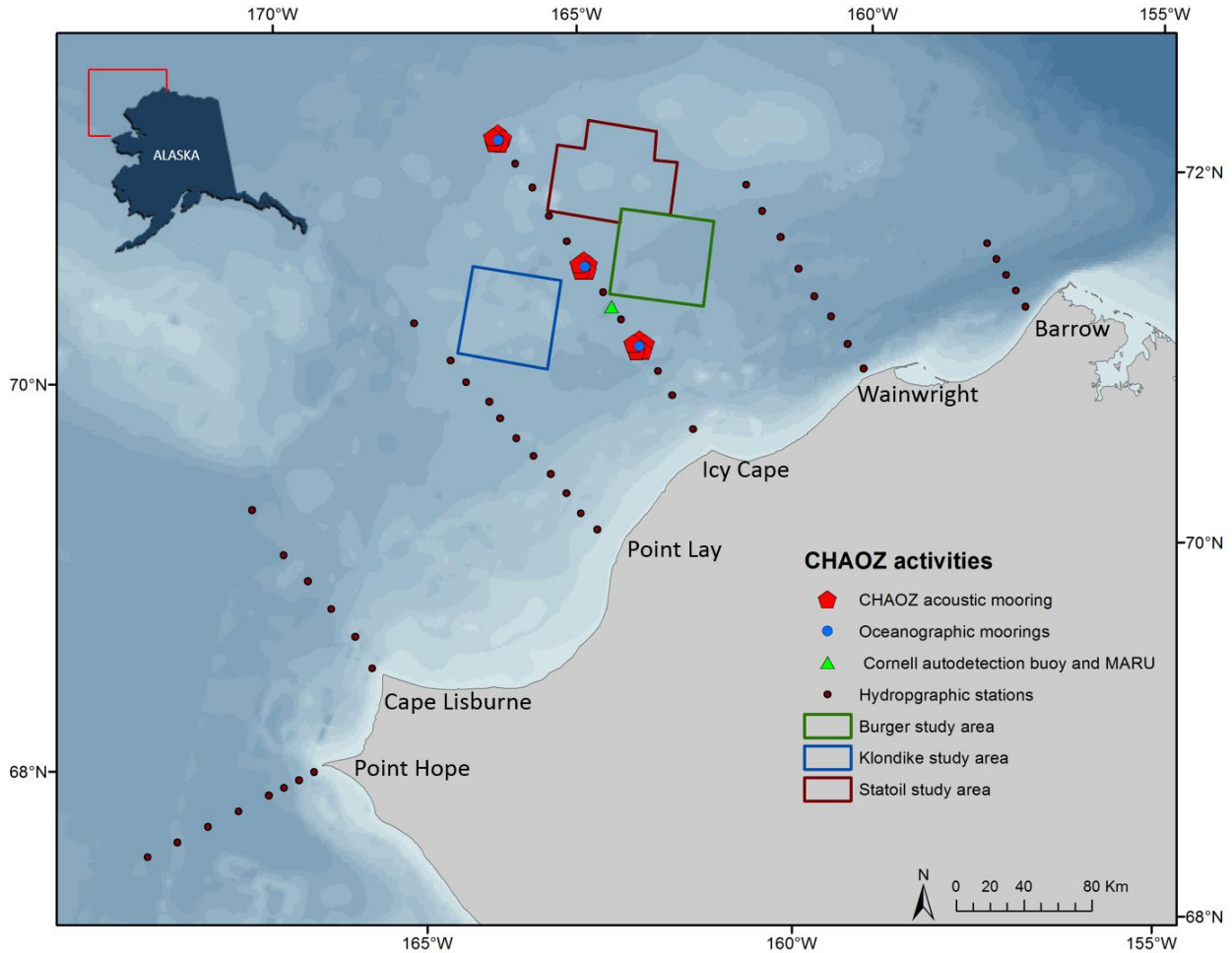


FIGURE 1. MAP SHOWING GENERAL STUDY AREA FOR THE CHAOZ PROJECT WITH CESP STUDY AREAS DISPLAYED.

Results of this research help explain the distribution of marine mammals in the Chukchi Sea Planning Area in relation to oceanographic conditions and potential prey availability. Important products of this work are the creation of integrated biophysical (including oceanography, zooplankton indices, and marine mammal distribution) databases, a near-real-time passive acoustic monitoring system which can be used as an impact mitigation tool in an increasingly noisy environment, and predictions on the variability of ice conditions in a warming Arctic, including an extended sea ice free season. Information from this study will be used by BOEM for pre- and post-lease analysis and documentation under the National Environmental Policy Act (NEPA) for Beaufort Sea and Chukchi Sea Lease Sales.

This report is organized into seven areas of research (Sections VII – XIII) which address the objectives; summaries for each section are presented herein. The major highlights and recommendations from this research precede the section summaries here.

Key Findings

The Chukchi Sea ecosystem is complicated: landscape ecology, and regional and local forcing all combine to determine whether or not there will be favorable conditions for both the permanent and transitory residents. The residents of interest in this study, marine mammals, belong to several different feeding guilds, further complicating our goal of understanding how climate change and other anthropogenic forcing will affect them. In this study, one species of interest is planktivorous (bowhead), another predominantly piscivorous (beluga), and two are obligate benthic feeders (walrus and bearded seal) and one is a facultative benthic feeder (gray whale). Another factor that challenges our comprehension of Chukchi Sea dynamics is the degree to which each species depends on or coexists with seasonal sea ice. Listed below are some key findings of this research.

- Dense, nutrient-rich Bering Sea water is advected into the Chukchi Sea shelf, together with warm, fresh water from the Alaska Coastal Current. Ice algal blooms occur below the ice and as the ice melts this production is exported to the bottom, where it continues to produce oxygen into the summer. During summer, subsurface phytoplankton blooms are common, and fuel secondary productivity.
- 30-50% of the transport through Bering Strait goes along the coast past Icy Cape, and variations in flow are highly correlated with local winds. Also, Atlantic water can be seen as far south as Icy Cape, indicating that slope water can intrude > 200 km onto the shallow Chukchi Sea shelf.
- There was large interannual variability, with 2010-11 having stronger flow, more polynyas, and more incidents of flow up from Barrow Canyon, than were observed in 2011-12 and 2012-13. Ice keels on the Icy Cape line often exceed 20 m in depth and some were greater than 25 m. Deep keels are usually found in the spring.
- High concentrations of ammonium can be seen on the Pt. Hope line and in Barrow Canyon, indicating an active microbial loop of converting detritus into ammonium. Ammonium is the preferred nitrogen form for many phytoplankton.
- In a shallow, benthic dominated system such as the Chukchi, sinking of the heavy refractory components of crude oil have the potential to impact food webs. Three of the six marine mammals in this study feed on the bottom; the species of krill fed upon by bowheads and Arctic cod may feed on detrital material in the nepheloid layer just above the bottom.
- Zooplankton community composition showed great variability among years and there was evidence for events such as on-shelf advection which introduced Arctic basin species to the shelf. There was also physical evidence for up-canyon transport along Transect E (Wainwright).
- Both bowhead and beluga whales undergo consistent, predictable seasonal migrations that are strongly correlated with both month and ice concentration. Bowhead calling activity showed a strong positive correlation with winds heading SSW. These winds could perhaps serve as a tailwind - helping them to conserve energy during their fall migration. These winds could also force ice into the area, and this may serve as a cue to start their migration. In the fall, bowhead calling ceased once ice thickness was > 0.5m.

- Bowhead whale calling activity during the fall 2010 migration was tri-modal, and may be the result of age/sex segregation. The gunshot call type occurred at end of these peaks, possibly suggesting its use as a migration cue to assemble and move. The gunshot calls were also strongly associated with the formation of ice. It is possible they use this call type to navigate through the ice and determine its thickness.
- Walrus were detected over winter at the offshore location, which was very unexpected, as most walrus overwinter on the Bering Sea pack ice. One ribbon seal call was also detected in April, when this species is said to be in the Bering Sea as well. In addition, vessels were also detected overwinter in both years, which we are attributing to Russian ice breakers.
- Gray whales were strongly correlated to prey availability, and were detected in large clusters either near the mouth of Barrow Canyon, or off Point Hope. Both of these locations showed large numbers of larvaceans and *Pseudocalanus* (proxies for high plankton biomass and productivity) as well as high amounts of nitrate and ammonium. Bearded seals and walrus tended to prefer the same shallow offshore locations near Hanna Shoal, an area known to have high biomass of benthic epifauna and infauna, but there were few overlapping sightings between the species.
- The photo-documentation of a cow/calf humpback pair within Arctic waters and the acoustic detection of fin whale calls (on sonobuoys) near Barrow Canyon were important achievements as they provided evidence of subarctic species in the Arctic. Also, satellite telemetry analysis of one gray whale indicated foraging behavior within a limited area during the tag's entire transmission period, providing insight into summer feeding ground habitat use.
- This study illustrates the importance of utilizing multiple survey methods. Comparison of visual survey versus passive acoustic monitoring during the fall cruises found comparable results for bowhead and beluga whales and walrus, better results visually for gray and minke whales, bearded seals, and Dall's and harbor porpoise, and better results acoustically for humpback, fin, and killer whales. Ringed and spotted seals were not differentiated acoustically and so comparisons cannot be made.
- Our results are consistent with recent publications predicting a shift in ecosystem regimes from a benthic-dominated system to a more pelagic-dominated system. That shift may already have begun.
- The first auto-detection buoy was successfully deployed in the Arctic approximately 55 nm off Icy Cape. From 01 September - 01 November 2012, the system detected and transmitted biotic and abiotic signals via satellite in near-real time.
- As a result of predicted increases in surface wind speeds, median minimum ambient noise levels in the 71-708 Hz frequency band (bandwidth utilized by most marine mammals) are predicted to increase by at least 10 dB, from approximately 85 dB to approximately 95 dB, with overall median noise level increasing from approximately 95 dB to approximately 105-110 dB, which is equivalent to levels in today's shipping lanes off Boston.
- Despite small sample sizes, results from the visual survey provided a measure of relative densities of four species (bowhead, fin, humpback and gray whale) in the Chukchi Sea during August and September.

- This study collected biophysical, marine mammal, and passive acoustic data in regions 3-5 (long-term for regions 4 and 5) of the Distributed Biological Observatory (DBO).

Section VII: Marine Mammal Distribution

Two year-long deployments of three long-term passive acoustic recorder arrays (moored AURALS) deployed off Icy Cape were made over the course of this study. A total of 8,054 days of acoustic data were collected from the long-term passive acoustic recorders. One recorder from each array (inshore, midshore, and offshore) for each year was analyzed fully for all species/signals (total of 1,744 days of acoustic data). Bowhead whales were regularly detected on the AURALS and both the fall and spring migrations were detected as pulses in the calling activity levels. The fall migration was captured on all three moorings and the spring migration was detected primarily at the inshore location, which is consistent with open leads in the nearshore ice in the spring and a fanning out of the fall migration over the Chukchi shelf. The fall 2010 migration pulse was trimodal, perhaps corresponding to age/sex segregation in the migration. Gunshot calls coincided with the end of most peaks in bowhead calling activity. This correlation may be useful for distinguishing between right whales and bowheads where their distributions overlap in the Bering Sea. Beluga whales also had strong calling peaks consistent with fall and spring migrations; both migrations are seen at all locations, with the highest levels of calling activity seen at the inshore location. Two populations of beluga whales migrate through the area at overlapping times; passive acoustics may be a useful tool for distinguishing between these populations. Very little calling activity was seen for gray whales, which is consistent with other research in the area and likely indicative of the placement of recorders outside their core summering areas and low calling rates, rather than an absence of gray whales in the study area. Fall and spring pulses in calling activity at the inshore location seem to suggest that those migrations were detected. Walrus were detected at all locations in both years, but limited to the summer/fall at the inshore and midshore locations. Calling activity was nearly year-round at the offshore location, with high peaks seen in February/March in both years; this was an unexpected finding and has not been described in any publication to date. Bearded seal calling activity was nearly ubiquitous for both years at all locations and showed slight differences in calling activity levels between locations and years. A large escalation to saturated calling levels coincided with the whelping/mating/molting season.

Killer whale calling activity was detected on several days, mostly inshore. Minke whale and ribbon seal calling activity were each detected on one day at the inshore location. The ribbon seal calling activity occurred in April which was outside the known range of this species in the Arctic. It is likely that spotted and ringed seals were detected, but we did not classify these to species. Instead they were categorized as unidentified pinnipeds, with calling activity occurring in both years and at all locations, with the majority at the inshore location. There was no calling activity for humpback, fin, right, and sperm whales from acoustic moorings; this was expected for the first two species given placement of the recorders (and expected in general for the latter two). The long-term distribution of vessel, airgun, and ice noise activity was also analyzed, with expected results. Two cases of vessel noise activity present in the middle of the winter are thought to be from distant Russian icebreakers.

In addition to moored AURALS, sonobuoys were deployed every three hours throughout the entire cruise to obtain an evenly sampled cross-survey census of marine mammal calling.

Concurrent with sonobuoy deployments, visual surveys, limited to daylight hours, were conducted to document the presence and distribution of all marine mammals encountered throughout the survey. A total of 630 sonobuoys were deployed and 4,250 nm of trackline were visually surveyed. Acoustic surveys detected six cetacean species (bowhead, gray, humpback, fin, minke, and killer whales) and two pinniped species (walrus and bearded seal). Visual surveys detected seven cetacean species (bowhead, gray, humpback, fin, minke, harbor porpoise, Dall's porpoise), five pinniped species (walrus, bearded, ringed, spotted, and northern fur seals) and a polar bear within the survey area. Photographs were opportunistically collected of humpback, killer, and gray whales, and North Pacific right whales (Bering Sea only) but no matches were made to existing catalogs. The most commonly sighted and/or acoustically detected species were bowhead whales, gray whales, walrus, and bearded seals. There were comparable visual and acoustic results for bowhead whales and walrus, (and a lack thereof for beluga whales). Gray whales and bearded seals were detected more often visually than acoustically, and believed to be a result of low calling rates at this time of year. Porpoise were only detected visually; frequency limitations of the sonobuoy system prevent their echolocation clicks from being detected. Fin, humpback, and killer whales were heard more often than they were seen. Fin whale calls were detected near the mouth of Barrow Canyon, which is at least 280 km farther north than the previous known record in the Alaskan Arctic. This study illustrates the importance of utilizing multiple survey methods, as certain methods are better at detecting certain species than others. Although limited in time, these data provide extensive spatial coverage to complement the long-term, but point sampled, data collected from the moored recorders.

The final method utilized to assess marine mammal distribution was satellite telemetry. One juvenile gray whale was embedded with a satellite tag which transmitted positional data for 48 days. The animal remained within 140 km of the deployment area and occupied relatively shallow waters (20-50 m in depth) to the south of Hanna Shoal. Models indicate it was most likely foraging in the area.

Section VIII: Biophysical Patterns and Trends

Each year, three, year-long biophysical moorings were deployed in the middle of the passive acoustic arrays at the three sites (inshore, midshore, offshore) off Icy Cape. To avoid ice keels, each mooring was only ~10 meters above the sea floor. These instruments collected data on over 15 different oceanographic parameters. Data were collected at least hourly and CTD and Niskin bottle casts were conducted following or preceding mooring recoveries and deployments to calibrate instruments on the moorings. Hydrographic surveys were also conducted yearly on six (five in 2010) hydrographic transect lines. CTD deployments measured water column properties, and Niskin bottles collected water samples at various depths to measure oxygen, chlorophyll, nutrients (nitrate, phosphate, silicate, nitrite and ammonium), and salinity.

Bottom currents were generally northeastward following bathymetry, and variability in currents was primarily wind-driven. Approximately 40% of the flow through Bering Strait passes the Icy Cape line. Bottom temperature ranged from approximately -1.8 to < 5.0 °C, with maximum temperatures occurring in late August or September. Salinity ranged from < 31 to ~34.5 psu and was highly variable, as a result of different water types, and the melting and freezing of sea ice. The highest turbidities occurred in fall when the winds began to increase and

before the sea ice areal coverage became >80%. The spring phytoplankton bloom was evident in each time series. Nitrate ranged from 0 – 20 μM ; concentrations decreased from mid-spring through July or August and then increased during late winter and early spring. During the time of the shipboard surveys, the surface was largely depleted of nutrients along all lines. Sea ice arrived in early to mid-November, increased quickly to near 100% areal coverage and then declined precipitously in late May or June. Ice thickness increases to an average of ~4 m in March, with the thickest ice generally seen late in spring. The position of the ice influenced the water properties; the Alaska Coastal Current and Winter Water appeared in both years, but Melt Water only appeared in 2012.

It was evident from the mooring deployments that there were more polynyas in 2010-2011 than 2011-2012. In addition, the transport was stronger in 2010-2011 than in 2011-2012 and 2012-2013. Ice arrived at approximately the same time in 2011 and 2012, but it retreated almost a month earlier in 2011 than 2012. This was reflected in the bottom mooring temperatures, which warmed to above -1.8 °C in early to mid-June in 2011 and in late June to late July in 2012. Shipboard transects showed that vertical stratification was strongest along the Point Hope transect (DBO3) in 2010, primarily due to lower surface salinities in 2010. Farther north at the Point Lay and Icy Cape lines, the ACC appeared to be more confined in a narrow band along the coast. The biggest difference between the years was at the Wainwright and Barrow Canyon lines. In 2012, intrusions of high silicate and nitrate were observed on the western Barrow Canyon and the shelf west of the canyon. We hypothesize that this is slope water intruding up the canyon and onto the shelf, perhaps a result of upwelling. This may have affected the ACC as well.

An Acoustic Doppler Current Profiler and a TAPS6-NG were used to estimate zooplankton volume backscatter and concentration. Inverse methods were used to estimate the abundance of scatterers as a function of size in two depth bins (near bottom and near surface). Near-bottom abundance estimates for euphausiid-shaped scatterers showed that the 14-18 mm size range had the highest concentrations (30-40 per m^3), with even higher concentrations of this class near the surface (100-200 per m^3). As expected, abundance was highest in the fall and declined during winter. Near-bottom abundance estimates for the 2-6 mm size range copepod-shaped scatterers were approximately 1500 per m^3 , and abundances did not decline with time from fall to winter. Adult and juvenile euphausiids had the highest concentration in the study area in the cold year, 2012. Concentrations of younger stages of euphausiids, principally furcilia, were at least an order of magnitude higher than adult and juvenile concentration with no consistent difference among cold and warm years. Low concentrations of the youngest euphausiid stage, calyptopis, were captured in 2010, the presence of which suggests recent spawning in the region. Net-based estimates of juvenile and adult euphausiid concentrations were low and did not yield evidence for the conveyor belt hypothesis. Concentrations of the furcilia stage were much higher, and in 2010 and 2011 were present at all stations across the shelf. In one warm year, evidence for euphausiid reproduction in the Chukchi was found. Hyperiid and gammarid amphipods were found in similar concentrations to euphausiids. Among the copepod taxa, *Oithona* spp. had the highest concentrations and *Pseudocalanus* spp., was very abundant in all years. Both net and acoustic estimates indicated that zooplankton concentrations are often as high or higher near the bottom than they are in the rest of the water column on the Chukchi shelf in summer.

Diel vertical migration by zooplankton was not regular (non-stationary) during the year. In the Chukchi Sea, a diel signal was not always detectable, but a semi-diurnal signal was often statistically significant at depth, particularly at the midshore and offshore moorings. Temporal patterns at the three mooring stations were often very different, indicating great variability in zooplankton behavior across this relatively broad, flat shelf. The shallow water column and difficulty predicting where the zooplankton spend most of their time may make it difficult to understand the exposure of plankton to oil, should there be an oil spill in the region. It is possible to moor single and multi-frequency instruments on the bottom to assess water column zooplankton throughout the year. As the instruments become more reliable, our knowledge of what happens during the winter and early spring will increase.

Section IX: Climate Modeling

The goal of the climate modeling component of the CHAOZ project was to provide projections of future sea ice and ocean conditions in the Chukchi Sea based on coupled climate models. There were two parts to the climate modeling aspect: conduct a climate model assessment, and study the impact of changing initial sea ice conditions on future projections. Based on evaluations, we found that all of the selected 12 CMIP5 models are doing decent jobs in terms of simulating the sea ice cover over the Chukchi Sea. According to these 12 models, the length of open water duration will be prolonged over the entire Chukchi Sea under the RCP8.5 emission scenario, although there is an evident north-south gradient. The changes in sea ice from 2010 to 2020 are small in the Alaskan Arctic, except near the coast in the Beaufort Sea and in the east Siberian Sea under the RCP8.5 (high) emission scenarios. From 2030 to 2040, the change is obvious with most of the northern Chukchi Sea (defined as 80° or north) and the Beaufort Sea having 11 months of ice coverage instead of 12. By the decade centered in 2050, the northern Chukchi Sea and the Beaufort Sea would have ice presence only up to 10 months. This implies that the northern Chukchi Sea (near latitude 80° N) would shift from current year-around sea ice cover to seasonal open water of 1-2 months. An acceleration of ice reduction can be inferred in the middle of the 21st century. In the southern Chukchi Sea (north of the Bering Strait to 70° N), sea ice cover will be reduced from 8-9 months coverage at present to 5-6 months of coverage by 2040, i.e., more than half a year of open water as predicted by these models. Currently there are 0-4 months of open water duration in the Chukchi Sea. As time progresses, the differences between the north and south will be reduced, and the entire Chukchi Sea will have more than 7 months of open water by the end of 21st century. Although the models indicate that ice can rebound from an extreme low condition within a year, in the past decade, we have been losing thick, multi-year sea ice in the Arctic, and therefore the quality of the ice has been reduced. Model simulations indicate that there is large interannual variability of ice thickness in the Chukchi Sea. At the beginning of ice formation, the averaged ice is less than 0.5 m thick (December), and ice gradually grows to 0.5-1 m thick in January. From February to June the average ice thickness is between 1-2 m thick with relatively large interannual variability. There is no significant trend in the next 20-30 years according to the CESM under the more moderate RCP6.0 emission scenario.

Besides sea ice condition, we also investigated the ocean conditions simulated by CESM1.0, and the modeling results are very encouraging. The monthly mean ocean currents at 30 m depth in the model agree well with observations. Both the directions and the magnitude of

ocean currents were well captured by the model runs. The ocean temperature and salinity from the CESM1.0 model runs and those observed at moorings were also compared. The model captured the seasonal variation of the ocean temperature well, but the models seem to show larger temperature gradients in the spring and fall seasons compared with the observations. The model results for salinity were less satisfactory; they underestimated salinity values year round at all three mooring locations. Running these models revealed that anthropogenic forcing is more important than the initial conditions on the decadal scales. The sea ice will remain at its current level up to 2040 in the Chukchi Sea in winter, but a larger decline in the fall is expected. This indicates that sea ice will arrive in the Southern Chukchi Sea later and later; this pattern has already been occurring in the past decade. Although the ice cover seems to be relatively stable in the spring as shown in the ensemble means, there are episodic events of early retreat. The increasing frequency of these early retreat events will especially become evident after 2050. The change of projected sea ice condition is consistent with model projected ocean temperature change, in that fall has the largest temperature increase compared with other seasons. We may see ice form later in the fall than at present, particularly in the southern Chukchi Sea. In any given year, the long-term ice thickness trend is overwritten by the large interannual variability, which is shown by our new, reduced ice cover initialized runs.

Section X: Correlation of Marine Mammal Distribution to Biophysical Variables

Generalized Additive Models (GAMs) were run to assess the effects of oceanographic conditions on the distribution of marine mammal calling activity. All possible combinations of the seven marine mammal species/sound sources at the three mooring locations and with the 19 biophysical variables were used in the GAM runs. In addition to the GAMs, calling presence for each species/sound source was plotted against eight oceanographic variables (ice concentration, ice thickness, chlorophyll, oxygen, nitrate, salinity, wind speed, and transport) at all three mooring locations to determine if any positive or negative correlations existed on a temporal scale. Furthermore, biophysical results from the shipboard transect lines were correlated with the visual and passive acoustic (sonobuoy) data. Measurements of temperature, salinity, nitrate, and ammonium were plotted with zooplankton (*Pseudocalanus*, *C. glacialis*, larvaceans, and pteropods) concentration. These were then plotted with sonobuoy effort and detections as well as visual sightings for gray whales, walrus, and bearded seals.

Both bowhead and beluga whales undergo consistent, predictable seasonal migrations that are strongly correlated with both month and ice concentration in the GAM models. Bowheads also showed a positive correlation with winds to the south-southwest in the fall, which may serve as a migration cue. Bowhead whale fall migrations were also found to be linked to several variables which may serve as proxies for prey availability. There was a strong correlation between gunshot call activity and both ice presence and thickness. We suggest that bowhead whales use this particular call type to assess ice thickness, to cue migration, or both. Beluga whales are positively correlated with the presence of polynyas. Because our recording system is frequency limited we are unable to detect the echolocation clicks beluga whales produce while feeding, however, our recorders were not placed in the prime beluga feeding area, and so a correlation with prey and calling activity was not expected.

Gray whale calling activity was sparse throughout the two years of long-term recordings most likely due to placement of the recorders along with low calling rates. This calling activity,

however, showed a significant correlation with ice concentration and a weak one (in 2011-12) with chlorophyll. There is also a tentative correlation between increased calling activity during the high transport deployment year. Gray whales were also sighted in large clusters near the mouth of Barrow Canyon and in the middle of the transect line off Point Hope; areas known to have high biomass of benthic infauna and epifauna. Both of these locations also showed high concentrations of zooplankton (larvaceans and *Pseudocalanus*) as well as high amounts of nitrate and ammonium at the Point Hope location.

Month, ice (thickness and concentration respectively), and several variables that can serve as proxies for prey availability, showed significant correlation with walrus and bearded seal calling activity. Possible presence of a polynya and prey availability make the surprising result of overwintering walrus in the northeastern Chukchi Sea plausible; we suggest these are juvenile males that did not migrate to the Bering Sea mating grounds. Results from the GAM analyses suggest prey availability might be the reason the ramp-up of bearded seal calling levels varies interannually and among locations. Both walrus and bearded seals were found along the Icy Cape and Wainwright transect lines near the shoals, an area known to have high biomass of benthic epifauna and infauna, but there were few overlapping sightings between the species. Ice noise activity levels were highest inshore and seemed to be influenced by wind direction. At all locations ice concentration was positively correlated and ice thickness was negatively correlated with ice noise activity levels.

Section XI: Long Range Predictions of Habitat Use by Arctic and Subarctic Marine Mammal Species

Currently, the Chukchi Sea shelf is a benthic-dominated ecosystem, with a large amount of nutrients being advected into the area from the highly productive Bering Sea. This dense water, modified by ice melt and summer heating, results in a highly stratified water column. In addition, near the coast, the warm low-salinity ACC overlays this denser Bering water, stratifying the coastal waters. Subsurface phytoplankton blooms are found at and below this interface, and fuel secondary productivity in the benthos. As a result, there is tight benthic-pelagic coupling that sustains the higher trophic levels.

We used the climate modeling results from this project to predict future changes in Arctic environmental conditions and the possible response of Arctic and subarctic marine mammals to these changes. The models predict an earlier retreat in seasonal sea ice and suggest that ice will form later in the fall season, creating longer open-water seasons. Based on these predictions, we would like to discuss two possible scenarios, both of which are dependent on the winds. If the winds remain strong as the ice retreats/melts, then the water column will be well mixed, delaying the spring phytoplankton bloom. This scenario will result in a loss of carbon flux to the benthos, and an increased volume of Bering Sea Summer Water and ACC into the Chukchi, and thus higher transport of nutrients into the system. However, an increase in ocean storms combined with weaker stratification will cause mixing of the water column, injection of nutrients into the sunlit surface waters, and result in a shift to a regime where more of the production remains in the water column. Our climate model predictions estimate that the magnitude and direction of the currents will remain similar to present day levels. If this holds true, then this scenario of shifting more production to the pelagic zone is highly likely.

The other scenario includes an earlier ice retreat/melt, a decrease in winds (e.g., weaker winds at the time of ice retreat), and continued warming of the atmosphere. This will result in early salinity stratification from the melting ice, supporting an early surface phytoplankton bloom which uses up all nutrients in that layer. This surface layer will warm via solar heating, resulting in a strong vertically stratified water column during the summer, which combined with a weakening of nutrient advection would limit surface blooms. However, the increased penetration of light below the pycnocline (due to low phytoplankton biomass) may allow subsurface phytoplankton blooms to form. This scenario will result in the early export of ice algae to the benthos, but the magnitude of that export will likely decrease with earlier ice retreats/melt. Thus, benthic secondary production will decrease unless the flux of phytoplankton carbon from the subsurface blooms is enough to compensate for the loss of carbon to the benthos when the ice retreats earlier. The amount of production in the subsurface layer under relatively low light, but high nutrient conditions remains unknown.

Bowhead, beluga, and gray whales are the most adaptive, and are best suited to adjust to a regime or ecosystem shift. However, ecosystem changes may result in population or migration re-distribution, which could have severe negative effects on native subsistence hunting. Walrus are predicted to be the most vulnerable to climate change or ecosystem shifts. They may be forced to haul out on the coast, which will impact population health; they may also just move out of the Chukchi Sea, which some studies show is already happening. Bearded seals are more adaptable than walrus, and will probably adjust accordingly. Finally, longer open-water seasons will result in more subarctic species (including pinnipeds) moving farther north into the Chukchi Sea and creating increased competition with resident Arctic species.

It is important to remember that regardless of which scenario actually occurs, most marine mammal species have innate migration patterns and reproductive cycles, as seen in the strong correlation between most of the marine mammals and month in the GAM integrative results. As such, migration timing and patterns either may not change significantly, or those changes may be considerably delayed. Furthermore, given their status in the highest trophic level, indirect effects of climate change on apex predators often involve several trophic levels and therefore have a delayed response on the population. This illustrates the importance of continued long-term passive acoustic monitoring, which is ideally suited to documenting migration patterns. Finally, both scenarios predict an increase in low-frequency ambient noise levels of about 10-15 dB, due to both natural causes as well as increased shipping traffic. This increase could have negative effects on acoustic communication with conspecifics, foraging, navigation, or evading predators.

Section XII: Noise Modeling and Impact Mitigation

This objective had two primary goals: a) develop methods to report occurrences of acoustically active marine species and ocean noise metrics in near-real-time; and b) quantify and assess the Chukchi Sea “noise budget” (including biotic and abiotic sound sources) and assess the influences of individual source types and the aggregate of multiple sources, including different source types, on the overall acoustic environment and on the acoustic habitats of selected marine mammal species. As a result we now have a method by which to quantify the acoustic contributions from vessels and seismic airgun surveys to the aggregate noise budget (see Clark et al., 2009; Hatch et al., 2012).

An auto-detection buoy was utilized to address the first objective. This was the first auto-detection buoy to be deployed in the Arctic. The buoy was deployed approximately 55 nm off Icy Cape between 01 September and 01 November 2012, and in that time detected and transmitted via satellite, 762 audio clips of possible bowhead whales. Of these 762 audio clips identified by the auto-detector as bowhead whales, 351 were confirmed as bowheads by experienced analysts (46%). In addition to bowhead whales, the auto-detection buoy detected a period of seismic airgun activity from approximately 12 - 18 September, 2012. A bidirectional communications feature was developed and successfully allowed analysts to request selected portions of data from the buoy. This enabled us to double check, in greater detail, any biotic or abiotic detection event recorded on the onboard data storage system. At this point, the AB's fundamental system infrastructure has been established and validated. One potential future utilization of this instrument would be to use this to monitor ambient noise levels in real-time for mitigation purposes.

In the summers of 2010 and 2011, a single marine autonomous recording unit (a.k.a., MARU) supplemented with a second glass sphere containing additional batteries was deployed in the Chukchi Sea between the inshore and midshore locations. The purpose of these instruments was to collect and utilize empirical data to determine current and predict future ambient noise levels in the Chukchi Sea. These MARU buoys recorded data throughout the year, on a 50% duty cycle in 2010, and continuously in 2011.

A computer analytical system called DELMA was used to process all recorded data and basic sound analyses were used to compute, illustrate, and compare a suite of acoustic measures for both the broadband and bowhead-band frequency ranges. Results were used to calculate the spatial-temporal-spectral variability of the acoustic environment. In particular, an effort was made to analyze the data for possible structure in the relationships between noise metrics, wind level, and percent ice coverage. This was undertaken in order to inform models to predict future ambient noise levels under reduced ice concentration conditions. Data on percent ice coverage and wind speeds were used to test for relationships between wind speed, percentage of ice cover, and ambient noise metrics.

A high negative correlation between noise and ice in the fall was discovered as the ice concentration is increasing, and a high positive correlation existed between noise and ice in late spring as the ice concentration is decreasing. In the future, with the expected decreases in ice concentration and the duration of the ice season, we expect an increase in ocean storms. The increase in the spatial and temporal extent of open water combined with the increase in storms will lead to a dramatic increase in ambient noise conditions. In terms of the spatio-temporal change, we should expect noise level increases to follow the seasonal and geographic decrease in loss of ice. A reasonable expectation is that median minimum noise levels in the 71-708 Hz frequency band will shift up by at least 10 dB from approximately 85 dB to approximately 95 dB and overall median noise level increase from approximately 95 dB to approximately 105-110 dB. These predicted median noise levels are equivalent to levels in today's shipping lanes off Boston (Hatch et al., 2012).

Section XIII: Estimating Relative Abundance of Marine Mammals

To estimate relative abundance within Arctic waters, encounter rates (groups/km) and densities (individuals/km²) from sightings collected during “on-effort” status were computed. The area of analysis (198,677 km²) was defined as U.S. waters just north of the Bering Strait to the easternmost extent of effort, east of Barrow, AK. Detection probability was estimated using the hazard-rate within Conventional Distance Sampling framework. Perpendicular distances were pooled across all “large whale” species (bowhead, fin, humpback, and gray whales). Pooling is beneficial in that it provides a greater sample size for fitting the detection function, it enables density to be computed for species with relatively low numbers of detections, and it improves the precision of these estimates. Modeling of perpendicular distance was conducted with ungrouped data truncated at 3 km for all whale species.

On-effort trackline used to estimate densities totaled 1,230 nm (2,278 km). Estimated parameters for the hazard rate model (the model most supported by AIC) across all species were: average detection probability (P) – 0.32, CV (P) – 0.23, and effective strip width (ESW) – 0.96 km. From 2010 to 2012, there were 16 sightings of bowhead whales (.0059 encounter rate; density = .0043), 5 sightings of fin whales (.0022 encounter rate; density = .0019), 2 sightings of humpback whales (.0007 encounter rate; density = .0004), and 15 sightings of gray whales (.0051 encounter rate; density = .0030). Visual estimates of relative abundance presented in this study assumed that no cetaceans were missed on the trackline ($g[0]=1$). Visual survey methods for this project differed from standard line-transect or abundance surveys due to constraints of the overall project. In the future we recommend conducting a dedicated shipboard survey if the goal is to compute densities in a relatively small area such as the lease area, or aerial transect surveys for large areas.

Recommendations

The data collected for this study demonstrate the utility and benefit of concurrent zooplankton, oceanography, and marine mammal/noise monitoring, combined with climate modeling. These data, along with those currently being collected for the ongoing BOEM-funded ARCWEST and CHAOZ-X projects represent the only long-term integrated dataset of its kind from the Chukchi Sea lease area and Alaskan Arctic in general. We therefore recommend continuation of the long-term mooring deployments. With current modifications to the moored TAPS6-NG instruments, we will be able to collect data for a full year, allowing for assessment of trophic interactions on an annual time scale. It will also be possible to establish multi-year patterns in marine mammal distributions as they relate to indices of zooplankton and oceanographic conditions. Moorings should be deployed not only in locations where the biggest changes in oceanographic and marine mammals and prey distribution are expected to occur, but also across a broad spatial range (as is the case with the ARCWEST/CHAOZ-X projects). This will ensure that critical migration timing and distribution patterns are fully documented.

We also recommend continuation of the integrated biophysical shipboard surveys conducted during this study. These surveys provide data on the fine-scale vertical resolution of zooplankton abundance as they correlate with oceanographic indices, nutrients, and distribution of marine mammals. To maximize marine mammal detections during shipboard surveys, it is essential to have both passive acoustic monitoring and visual survey components. Since each

method is well-suited to particular species, together they provide a more complete picture of marine mammal distribution. In addition, joint passive acoustic/visual survey focal follows enable future calculations of relative abundance. Addition of a benthic ecology component would help to address prey availability for those mammals that feed on benthic epifauna and infauna.

Because this area is predicted to undergo rapid climate change, it is critical to know what is happening to currents and ice cover during the crucial spring and fall months. Unfortunately, because of the ice cover these seasons are currently inaccessible with present technologies, excepting passive acoustic recorders. To help increase our understanding and knowledge of oceanographic conditions and to collect the necessary suite of data, investments in new technology are necessary, perhaps in the form of advanced moorings or autonomous subsurface gliders/AUVs. Furthermore, animal-borne sensors should be utilized to take advantage of real-time discrete sampling and gain valuable information on marine mammal habitat utilization during these dynamic seasons.

VI. INTRODUCTION

A. *Background*

The western Arctic physical climate is rapidly changing. The summer Arctic minimum sea ice extent in September 2012 reached a new record of 3.61 million square kilometers, a further 16% reduction from a record set in 2007 (4.30 million square kilometers), and a more than 50% reduction than that of two decades ago (Parkinson and Comiso, 2013). The speed of these changes was unexpected, as the consensus of the climate research community just a few years ago declared such changes would not occur for another thirty years (Wang and Overland, 2009). As sea temperature, oceanographic currents, and prey availability are altered by climate change, changes in marine mammal species composition, abundance, and distribution are expected (and evidenced already by local knowledge and opportunistic sightings). In addition, the observed northward retreat of the minimum extent of summer sea ice has the potential to create opportunities for the expansion of oil- and gas-related exploration and development into previously closed seasons and localities in the Alaskan Arctic. It may also open maritime transportation lanes across the Arctic adding to the ambient noise in the environment. Timing and location of whale migrations may play an important role in assessing where, when, or how exploration or access to petroleum reserves may be conducted to mitigate or minimize the impact on protected species. Moreover, several species are used, or potentially used, for subsistence by native communities in both Russia and the US. Whales form an important part of the diet and cultural traditions of most people in villages along the coasts of the Chukchi Sea. Detailed knowledge of large whale migration and movement patterns is essential for effective population monitoring. Because all marine mammal species are subjected to changes in environmental variables such as oceanographic currents, sea temperature, sea ice cover, prey availability, and anthropogenic impacts, more complete information on the year-round presence of these species as they relate to these variables is needed in the Chukchi Sea planning area.

Passive acoustic monitoring is currently the best tool for large scale population monitoring and assessment of baleen whales in Alaskan seas (Moore et al., 2006; Hannay et al., 2013). Specifically, acoustic detection has proven a key addition to the census of bowhead whales (*Balaena mysticetus*) during their spring migration past Barrow (Clark and Ellison, 2000; Blackwell et al., 2007; Delarue et al., 2009) and in relation to oil and gas development activities offshore of Prudhoe Bay (Greene et al., 2004; Blackwell et al., 2013). Gray whale (*Eschrichtius robustus*) calls have also been detected year-round near Barrow on long-term recorders deployed in collaboration with the NSF/Shelf-Basin Interaction Study (Stafford et al., 2007b). These long-term passive acoustic data, when integrated with data from concurrent monitoring of oceanographic conditions, can contribute strongly to explaining finer-scale variability in whale occurrence and relative abundance (e.g., Bluhm and Gradinger, 2008; Laidre et al., 2008; Stafford et al., 2013).

The CHAOZ study combined arrays of long-term passive acoustic recorders with collocated biophysical and oceanographic moorings deployed in the Chukchi Sea at 40, 70, and 120 nm off Icy Cape, AK over the course of two years (2010-11 and 2011-12). The passive acoustic arrays monitored for the presence of baleen whales, as well as odontocete whales, pinnipeds, and environmental and anthropogenic noise. The biophysical and oceanographic moorings estimated zooplankton size and abundance, ice concentration and thickness, fluorescence (chlorophyll), nitrate, oxygen, PAR, temperature, and salinity, as well as current

speed and direction. Moorings permit observations during long periods when ice covers the region, especially during the critical spring and early summer periods when spring phytoplankton blooms occur. Such measurements are virtually impossible to obtain from ships because of their limited ability to work in ice-covered seas. To complement these data and provide a more immediate assessment of whale presence, a short-term real-time auto-detection buoy was deployed during the summer of 2012 to monitor for bowhead whales; it transmitted data via satellite whenever a vocalization was detected. In addition, climate modeling was utilized to predict future sea ice and oceanographic conditions; results from these models were then used to predict future marine mammal distribution based on estimated sea ice and climate conditions. Noise modeling was also included to determine the current ambient noise levels in the Chukchi Sea based on anthropogenic and environmental sources, as well as predict increases in those levels due to sea ice retreat, increased shipping, or other factors. To complement and calibrate the long-term data, shipboard observations and measurements were collected during the fall field surveys. These included sampling stations that conducted CTD casts and zooplankton net tows, 24-hour passive acoustic monitoring using sonobuoys, opportunistic visual surveys for marine mammals, and satellite-tracked drifters.

B. Objectives of study

The overall goal of this multi-year, interdisciplinary study was to document the distribution and relative abundance of bowhead, humpback, right, fin, gray, and other whales in areas of potential seismic surveying, drilling, construction, and production activities and relate changes in those variables to oceanographic conditions, indices of potential prey density, and anthropogenic activities. This study had five component projects: marine mammal distribution (passive acoustics and visual methods), oceanography, zooplankton, climate modeling, and noise modeling/impact mitigation.

The specific objectives were:

1. Assess the year-round seasonal occurrence of bowhead, gray, and other whale calls in the Chukchi Sea.
2. Estimate relative abundance of these whales.
3. Obtain two full years of biophysical measurements on the shallow Chukchi shelf utilizing moorings at three sites, and collect hydrographic and lower trophic level data during deployment/recovery of the moorings.
4. Evaluate the extent to which variability in environmental conditions such as sea ice, oceanic currents, water temperature and salinity, and prey abundance influence whale distribution and relative abundance.
5. Run the National Center for Atmospheric Research (NCAR) climate model (Community Earth System Model: CESM1.0) for future projections using the sea ice extents from 2007/2008 as initial conditions.
6. Analyze multiple ensemble members CESM as well as the group of CMIP5 models to assess the future variability of sea ice cover and extended sea ice free seasons during fall for the Chukchi Sea.
7. Evaluate whether changes in seasonal sea ice extent are resulting in a northward shift of Bering Sea cetacean species such as fin, humpback, and North Pacific right whales.

8. Provide long-term estimates of habitat use for large whale species and compare this with predictions about annual ice coverage to establish predictive variables that describe large whale occurrence.
9. Develop a quantitative description of the Chukchi Sea's noise budget, as contributed by biotic and abiotic sound sources, and continuous, time-varying metrics of acoustic habitat loss for a suite of arctic marine mammal species.
10. Develop a near-real-time passive acoustic monitoring system that can be used as an impact mitigation tool.

C. *Summary of research effort*

The CHAOZ project consisted of three field seasons during the months of August and September on board three different vessels: the 2010 survey occurred from 24 August to 20 September 2010 on the F/V *Alaskan Enterprise*; the 2011 survey occurred from 12 August to 11 September 2011 on the F/V *Mystery Bay*; and the 2012 survey occurred from 8 August to 7 September 2012 on the R/V *Aquila*. Over the span of three field seasons, a total of 67 passive acoustic and 32 oceanographic moorings were deployed, a combined total of 190 hydrographic and 169 zooplankton sampling stations were conducted, and three drifters were deployed. A total of 630 sonobuoys were deployed during the 24-hour passive acoustic monitoring, and 4,250 nm were surveyed for marine mammal and bird observations. A total of 29 scientists from 15 organizations/institutions participated in the cruises.

D. *Structure of report*

This report is divided into a number of sections, each designed to be read as a stand-alone report. Sections VII-IX deal with the marine mammal (both Arctic and subarctic), oceanography and zooplankton, and climate modeling components, respectively. Section X integrates the first two of these individual components to examine how variability in environmental parameters and prey abundance affect marine mammal distribution. Future predictions of marine mammal distribution based on the predicted ice and climate conditions will then be provided in the form of two potential scenarios (Section XI); data from Sections VII-IX are used in this section. The report culminates with a section on noise modeling and impact mitigation (Section XII) and one on estimating relative abundance (Section XIII). Section XIV contains a summary of this study and recommendations for the future.

VII. MARINE MAMMAL DISTRIBUTION

A. *Moored Observations*

1. *Methods*

Equipment

Two deployments of three, long-term passive acoustic recorder arrays were made over the course of this study (Figure 2a, Table 1). The arrays were located at 40, 70, and 120 nm off Icy Cape, AK. The moorings for each array were arranged in a pentagonal shape, with 2-4 km spacing between units, and recorded for one year per deployment. These bottom-mounted moorings were comprised of an anchor, chain, acoustic release, passive acoustic recorder, and 30" steel subsurface float arranged in a linear configuration (Figure 2b, total length of mooring ~8 m; hydrophone ~6 m off the sea-floor). Autonomous Underwater Recorders for Acoustic Listening¹ (AURAL, Multi-Électronique, Rimouski, QC, Canada) were used on these subsurface moorings. The AURALS sampled at 16,384 Hz (nominal bandwidth from 10 Hz to 8 kHz), on a duty cycle of 95 min of recording every 5 hours in the 2010-2011 deployments (32% duty cycle). Upon retrieval of the 2010-2011 instruments, it was discovered that the recorders stopped three months early. To compensate for this extremely low battery life, the duty cycle was reduced to 85 min of recording every 5 hours for the 2011-2012 deployments (28% duty cycle). After the cruise, examination of the battery packs revealed a diode problem which limited their voltage output, and so only two of the 2011-2012 instruments recorded for a full year. A new model of battery pack was developed and has been successfully used for all AURAL deployments since 2012. In addition to the passive acoustic data, each AURAL has built-in sensors that measure temperature and pressure. Detection ranges, or the distance at which a calling animal or signal can be detected on a recorder, are highly variable. They depend on several factors, including the source level of the signal (how loud the call or noise is), ambient noise levels, and the sound speed profile of the water column. The sound speed profile varies depending on the oceanographic conditions (e.g., temperature, salinity, currents, fronts, etc.) at that time (Stafford et al., 2007a). Underwater sounds travel greater distances when the region is ice-covered (Urick, 1983); thus, we would expect greater detection ranges in the winter ice-covered months. However, if ice moves or shifts, this creates an increase in ambient noise levels (sometimes substantially), further illustrating the highly variable nature of detection ranges. Table 1 lists the deployment and recording information for these moorings.

¹ Reference to trade names does not imply endorsement by the National Marine Fisheries Service or NOAA.

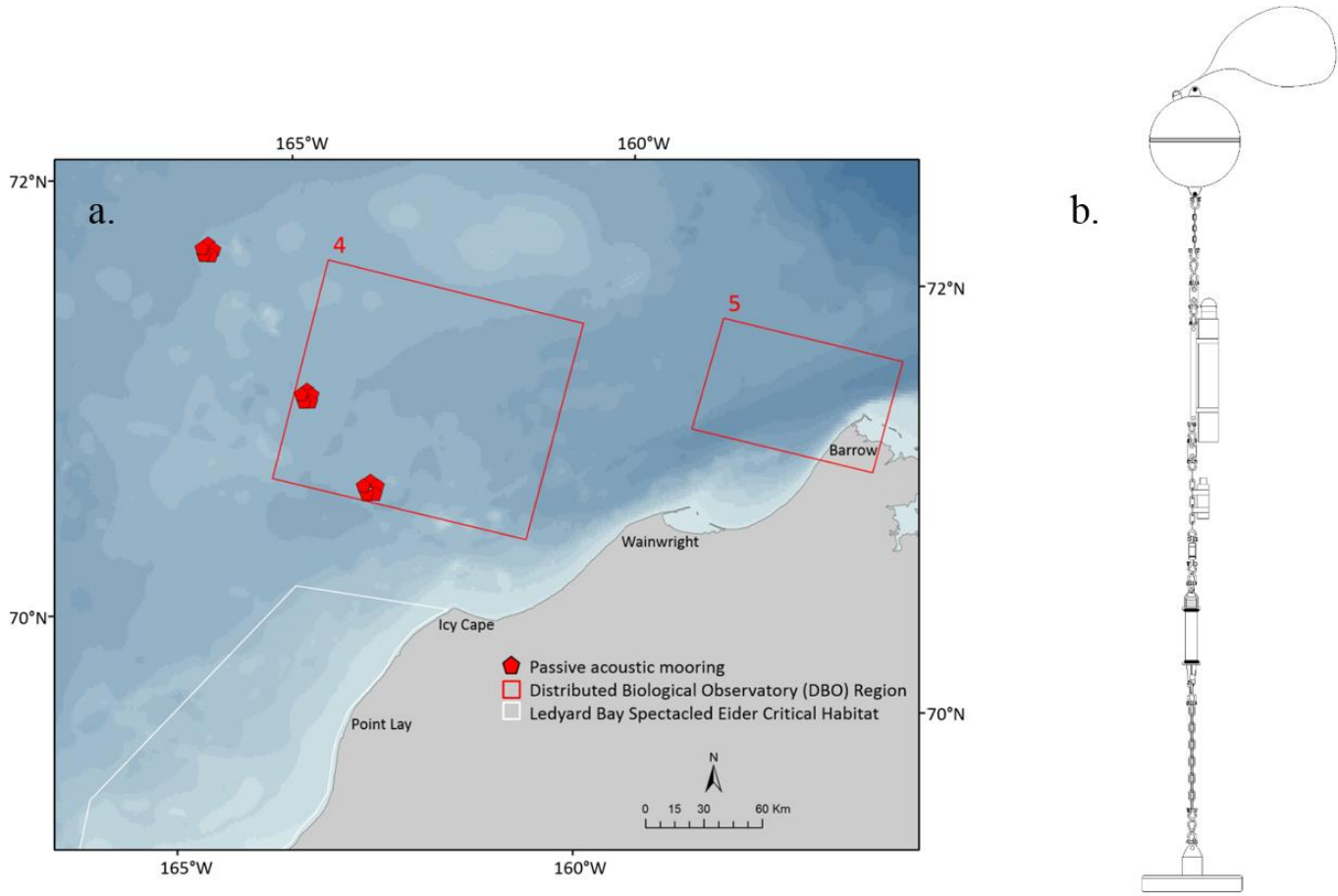


FIGURE 2. LOCATION OF LONG-TERM PASSIVE ACOUSTIC RECORDER MOORINGS IN THE CHUKCHI SEA (A). PASSIVE ACOUSTIC RECORDER MOORING DIAGRAM (B).

TABLE 1. LIST OF ALL PASSIVE ACOUSTIC RECORDERS AND DEPLOYMENT INFORMATION, 2010-2012. * = INSTRUMENT INCLUDED IN DETAILED ACOUSTIC ANALYSES.

Mooring	Mooring Cluster	Latitude	Longitude	Water depth (m)	Recorder Start Date	Recorder End Date	# Days with Data	Sampling Rate (Hz)	Duty Cycle (min on/5 hours)	Deployment Date	Retrieval Date
CZ10_AU_A01	Inshore	70.90715	-163.23940	42.5	9/10/2010	7/8/2011	302	16384	95	8/29/2010	8/25/2011
CZ10_AU_A02	Inshore	70.87172	-163.04417	44.3	9/10/2010	7/7/2011	301	16384	95	8/28/2010	8/25/2011
CZ10_AU_A03*	Inshore	70.79838	-163.08112	43.4	9/10/2010	6/27/2011	291	16384	95	8/28/2010	8/25/2011
CZ10_AU_A04	Inshore	70.78260	-163.28725	44.3	9/10/2010	6/10/2011	274	16384	95	8/29/2010	8/25/2011
CZ10_AU_A05	Inshore	70.85360	-163.36985	42.5	9/10/2010	6/8/2011	272	16384	95	8/29/2010	8/25/2011
CZ10_AU_B01	Midshore	71.25275	-164.27702	42.5	9/10/2010	6/7/2011	271	16384	95	8/29/2010	8/22/2011
CZ10_AU_B02	Midshore	71.23573	-164.18980	42.5	9/10/2010	6/11/2011	275	16384	95	8/29/2010	8/22/2011
CZ10_AU_B03*	Midshore	71.20203	-164.19223	42.5	9/10/2010	6/21/2011	285	16384	95	8/29/2010	8/22/2011
CZ10_AU_B04	Midshore	71.19615	-164.29698	43.4	9/10/2010	6/25/2011	289	16384	95	8/29/2010	8/22/2011
CZ10_AU_B05	Midshore	71.22858	-164.34443	43.4	9/10/2010	6/5/2011	269	16384	95	8/29/2010	8/22/2011
CZ10_AU_C01	Offshore	71.85340	-165.99580	44.3	9/10/2010	5/28/2011	261	16384	95	8/31/2010	8/22/2011
CZ10_AU_C02*	Offshore	71.83395	-165.90330	44.3	9/10/2010	6/8/2011	272	16384	95	8/31/2010	8/22/2011
CZ10_AU_C03	Offshore	71.80242	-165.92203	44.3	9/10/2010	5/23/2011	256	16384	95	8/31/2010	8/22/2011
CZ10_AU_C04	Offshore	71.79822	-166.03020	44.3	9/10/2010	6/3/2011	267	16384	95	8/31/2010	8/22/2011
CZ10_AU_C05	Offshore	71.82873	-166.07077	44.3	9/10/2010	5/23/2011	256	16384	95	8/31/2010	8/22/2011
CZ11_AU_A01	Inshore	70.87347	-163.22113	44.0	9/3/2011	4/22/2012	233	16384	85	9/1/2011	8/21/2012
CZ11_AU_A02	Inshore	70.85723	-163.11833	43.5	9/3/2011	4/22/2012	233	16384	85	9/1/2011	8/21/2012
CZ11_AU_A03*	Inshore	70.81677	-163.13612	43.5	9/3/2011	9/7/2012	371	16384	85	9/1/2011	8/21/2012
CZ11_AU_A04	Inshore	70.80977	-163.24780	43.7	9/3/2011	12/11/2011	100	16384	85	9/1/2011	8/21/2012
CZ11_AU_A05	Inshore	70.84755	-163.30945	43.8	9/3/2011	9/30/2012	394	16384	85	9/1/2011	8/21/2012
CZ11_AU_B01	Midshore	71.25242	-164.27443	43.5	8/29/2011	5/8/2012	254	16384	85	8/24/2011	8/22/2012
CZ11_AU_B02	Midshore	71.23530	-164.19293	43.9	8/29/2011	5/3/2012	249	16384	85	8/24/2011	8/22/2012
CZ11_AU_B03*	Midshore	71.20163	-164.19792	44.3	8/29/2011	5/19/2012	265	16384	85	8/24/2011	8/22/2012
CZ11_AU_B04	Midshore	71.19627	-164.29440	45.2	8/29/2011	5/24/2012	270	16384	85	8/24/2011	8/22/2012
CZ11_AU_B05	Midshore	71.22860	-164.34398	44.4	8/29/2011	5/4/2012	250	16384	85	8/24/2011	8/22/2012
CZ11_AU_C01	Offshore	71.85365	-165.99832	43.5	8/29/2011	5/29/2012	275	16384	85	8/26/2011	8/22/2012
CZ11_AU_C02*	Offshore	71.83190	-165.90055	42.6	8/29/2011	5/14/2012	260	16384	85	8/26/2011	8/22/2012
CZ11_AU_C03	Offshore	71.80225	-165.92727	42.7	8/29/2011	6/5/2012	282	16384	85	8/26/2011	8/22/2012
CZ11_AU_C04	Offshore	71.79858	-166.02878	43.3	8/29/2011	4/6/2012	222	16384	85	8/26/2011	8/22/2012
CZ11_AU_C05	Offshore	71.82903	-166.07145	43.7	8/29/2011	5/9/2012	255	16384	85	8/26/2011	8/22/2012

Data Processing

After the recorders were retrieved, the hard drives were removed and the raw data was immediately backed up onto an external hard drive. The original drives were saved as master copies of the data. The data were then processed in two steps. First the raw sound files were converted into ten-minute files, renamed with intuitive filenames containing mooring name, date, and time information. Image files (.png) of spectrograms were then pre-generated from recordings (FFT 1024, 0.85 overlap, Hamming window). These image files displayed either 300 s of data from 0 to 250 Hz (low-frequency signals), 225 s of data from 0 to 800 Hz (mid-frequency signals), or 90 s of data from 0 to 8.192 kHz (high-frequency signals).

Data Analysis

All acoustic data (100% of the image files) were analyzed manually for presence of the following: fin whales in the low frequency band; bowhead, right, humpback, gray, and minke whales, walrus, unidentified pinnipeds, as well as vessel noise and seismic airguns in the mid-frequency band; and beluga, killer whale, minke whale (boing call), bearded and ribbon seals, and environmental noise (ice) in the high frequency band. Bowhead whales were identified mainly by their frequency modulated moans and complex notes forming the basis of song, as per Hannay et al. (2013). Beluga vocalizations were classified as whistles, pulsed calls, noisy calls, combined calls, and echolocation clicks (Sjare and Smith, 1986). Generally, whistles and pulsed calls are easily identifiable; most echolocation clicks exceeded the frequency range that was recorded for this study. Gray whales were identified by their low-frequency moans, pulses, and bongo sounds (Cummings et al., 1968; Stafford et al., 2007b). Walrus were identified using their stereotypical knock and bell calls (Stirling et al., 1987) along with various grunts. Bearded seals were identified by their characteristic trills (Risch et al., 2007). Ribbon seals produce distinct vocalizations during the spring mating season, including downsweeps, roars, and grunts (Watkins and Ray, 1977). The call used to identify ribbon seals within this study was an intense downward frequency sweep. Representative repertoires obtained from literature were used for all other species included in the report.

An in-house, MATLAB-based program (SoundChecker) was used for the analysis. The SoundChecker program was developed in response to the sheer magnitude of the data, the enormous overlap of the acoustic repertoires of many Alaskan marine mammal species, and the lack of stereotyped calls for most species, which resulted in poor auto-detection performance. SoundChecker operates on the pre-generated image files, which reduces the computational time needed to generate spectrograms during analysis. The image files are indexed to allow for zoom and playback functioning during analysis. For each image file, the analyst selects one of four options: yes, no, maybe, and no-with-noise to indicate whether a species was detected in that file. The no-with-noise option is selected when the presence of high levels of noise mask potential calls from that species. It is important to note that analysts were highly conservative when assigning yes designations; if there was any doubt as to the source of the calls within an image file, that image file was marked as maybe. The results below use only those image files marked as yes. Furthermore 'maybe' was also used to mark any signals that could potentially be calls of that species; future studies using these data will be expedited as only the image files marked with yeses and maybes will need to be included and the full data set will not need to be re-analyzed.

For the 2011-2012 fin whale analysis, a low-frequency detection and classification system (LFDCS; Mark Baumgartner, WHOI) was used to automatically detect fin whale vocalizations. The LFDCS is an IDL-based program that uses manually created call libraries to apply discriminant function analysis across seven measurements, called call attributes, taken from each auto-detected call. The analyst selects exemplary calls, in this case fin whale calls, to create a call library. The LFDCS is then run on novel data sets and uses this comprehensive call library for comparison in discriminant function analysis to classify all of its auto-detections. Over two-hundred exemplars were carefully selected for the fin whale call library. The call library was then put through comprehensive and iterative logistical regression analysis, in order to determine its efficacy for application on novel data sets. Once the library was deemed robust enough for real application, the LFDCS was run on each mooring data set, and the resulting fin whale auto-detections were checked for accuracy by a manual analyst.

2. *Results*

Over the course of the CHAOZ study, a total of 8,054 days of acoustic data were collected from the long-term passive acoustic recorders. One recorder from each array (inshore, midshore, and offshore) for each year was analyzed fully for all species/signals (total of 1,744 days of acoustic data).

Because of the staggered duty cycle used for the recordings, there was differing sampling effort among days. This was normalized by dividing the number of image files with calls detected for that day by the number of available image files for that day. The results that follow are presented for each mooring as the percentage of time intervals with calls for each day. This will be referred to as *calling activity* for the remainder of this report. It is important to note that calling activity indicates the duration of sustained calling for that day, not the number of call detections or number of animals vocalizing. For example, if a day shows 100% beluga calling activity that means that 100% of the 335 ninety second time bins in that day contained at least one beluga call.

The percentage of days with calling for each species/signal by month is presented in Appendix E (see Section XVIII.E). The results for the species/signals analyzed were divided into those that had a lot of calling activity and those that had little to none. The species that had the greatest amount of calling activity were bowhead and beluga whales, bearded seals, and walrus. These species, along with gray whales, are good proxies for Arctic ecosystem change because they represent a variety of differing habitat and dietary niches. As such, this report will focus on these five species (Table 2). However, plots of the calling activity for all species analyzed are presented in Appendix C. In addition to all the species mentioned below, analysts also marked the presence of airgun, vessel, and ice noise.

TABLE 2. SUMMARY OF RESULTS FOR BOWHEAD, BELUGA, AND GRAY WHALE, WALRUS, AND BEARDED SEAL CALLING ACTIVITY, 2010-2012.

Species	Year	Mooring	First date with calling	Last date with calling	# days w/ calls	# days w/ recordings	% days w/ calls	# intervals w/ calls	# intervals w/ recordings	% intervals w/ calls
Bowhead whale	2010-2011	Offshore	9/22/2010	4/21/2011	62	272	22.8%	3278	36791	8.9%
		Midshore	9/14/2010	6/18/2011	85	285	29.8%	4186	38925	10.8%
		Inshore	9/14/2010	6/27/2011*	129	291	44.3%	7731	38175	20.3%
	2011-2012	Offshore	9/20/2011	12/3/2011	40	260	15.4%	2063	32498	6.3%
		Midshore	8/29/2011*	5/19/2012*	65	265	24.5%	3548	33114	10.7%
		Inshore	9/14/2011	8/14/2012	131	371	35.3%	5762	45919	12.5%
Beluga whale	2010-2011	Offshore	11/8/2010	4/21/2011	17	272	6.3%	128	87221	0.1%
		Midshore	10/20/2010	6/7/2011	29	285	10.2%	262	91510	0.3%
		Inshore	9/15/2010	6/19/2011	71	291	24.4%	3211	46222	6.9%
	2011-2012	Offshore	10/3/2011	5/7/2012	25	260	9.6%	340	74654	0.5%
		Midshore	10/10/2011	5/19/2012*	39	265	14.7%	763	76114	1.0%
		Inshore	10/5/2011	7/18/2012	81	371	21.8%	2827	106874	2.6%
Gray whale	2010-2011	Offshore	N/A	N/A	0	272	0.0%	0	36927	0.0%
		Midshore	10/8/2010	10/8/2010	1	285	0.4%	10	38915	0.0%
		Inshore	10/1/2010	11/9/2010	6	291	2.1%	71	38165	0.2%
	2011-2012	Offshore	N/A	N/A	0	260	0.0%	0	32498	0.0%
		Midshore	N/A	N/A	0	265	0.0%	0	33114	0.0%
		Inshore	9/20/2011	7/21/2012	15	371	4.0%	52	45919	0.1%
Walrus	2010-2011	Offshore	9/10/2010*	6/7/2011	107	272	39.3%	1984	36928	5.4%
		Midshore	9/10/2010*	6/21/2011*	41	285	14.4%	1149	38915	3.0%
		Inshore	9/10/2010*	6/27/2011*	87	291	29.9%	1781	38165	4.7%
	2011-2012	Offshore	8/29/2011*	5/10/2012	102	260	39.2%	2460	32498	7.6%
		Midshore	8/29/2011*	5/11/2012	67	265	25.3%	1178	33114	3.6%
		Inshore	9/3/2011*	8/13/2012	111	371	29.9%	5718	45922	12.5%
Bearded seal	2010-2011	Offshore	10/1/2010	6/8/2011*	157	272	57.7%	20485	87221	23.5%
		Midshore	9/10/2010*	6/21/2011*	222	285	77.9%	41473	91510	45.3%
		Inshore	9/25/2010	6/27/2011*	241	291	82.8%	38471	74044	52.0%
	2011-2012	Offshore	8/30/2011	5/14/2012*	222	260	85.4%	21610	74900	28.9%
		Midshore	8/29/2011*	5/19/2012*	222	265	83.8%	34610	76364	45.3%
		Inshore	9/8/2011	8/20/2012	279	371	75.2%	33636	106725	31.5%

*= Date recorder limited.

Bowhead whales

Bowhead whale fall migration was detected at all three locations in both deployment years (Figure 3, Table 3). In fall 2010, calling activity began in mid- to late September (inshore/midshore and offshore, respectively) and ended mid-December at all locations (Table 3). The main pulse of calling activity was divided into three distinct peaks centered on early October, early November, and early December for all three locations. In contrast, the main pulse of calling activity for the fall 2011 migration was more continuous, with no multiple calling peaks seen. For the inshore and offshore locations, calling activity began at approximately the same time as in 2010 (mid- to late September, respectively), but the midshore location saw calling activity in late August, two weeks earlier than in 2010. For all locations, calling activity ended within a few days of each other and approximately ten days earlier than in 2010.

TABLE 3. KEY TIMING EVENTS FOR BOWHEAD WHALE CALLING ACTIVITY.

Year	Mooring	Fall Migration		Spring Migration	
		Date Range	Peaks	Date Range	Peaks
2010-2011	Offshore	09/22/10-12/12/10	Three: early Oct, early Nov, early Dec	N/A	None, but recorder failed early
	Midshore	09/14/10-12/15/10	Three: early Oct, early Nov, early Dec	03/29/11-06/18/11	Small one mid-June, but recorder failed early
	Inshore	09/14/10-12/12/10	Three: early Oct, early Nov, early Dec	03/04/11-06/27/11*	Main: May; others mid-Apr, mid-Jun
2011-2012	Offshore	09/20/11-12/03/11	Main: late Nov; others: early Oct, early Nov	N/A	None, but recorder failed early
	Midshore	08/29/11*-12/01/11	One very broad: centered on early Nov; other early Oct	04/23/12-05/19/12*	One day: mid-May, but recorder failed on that day.
	Inshore	09/14/11-12/01/11	Main: early Nov.	04/11/12-08/14/12	Main: early May; others late May, mid-Jun.

* = Date recorder limited

Detection of the bowhead spring migration in both deployment years was greatest at the inshore and least at the offshore locations (Figure 3, Table 3). The spring 2011 pulse in calling activity at the inshore location began in late March, ending just before the recorder failed in late June. There is a slight indication of three peaks in calling activity in the spring of 2011, though these are less defined than the fall 2010 peaks. Very low levels of calling activity were present at the midshore locations from April through mid-June, with a small peak occurring right before the recorder stopped in mid-June. No calling activity was detected at the offshore location. The

spring calling activity in 2012 at the inshore location was more skewed. Although calling activity started much later (mid-April) than in 2011, the bulk of calling activity occurred in late April/early May, with scattered activity continuing until mid-August. Calling activity on the midshore recorder also began later than in 2011. There was one day with elevated calling activity at the midshore location (mid-May); however, this was also the day the recorder failed. As in 2011, there was no calling activity during the spring 2012 migration at the offshore location. There was no overwinter bowhead calling activity at any location in any study year.

Analysts also flagged image files containing gunshot calls, an impulsive call type produced by both bowhead and right whales (Clark, 1983; Würsig and Clark, 1993; Parks et al., 2005). Although it is attributed to bowhead whales in the Arctic, this call type is flagged separately from the other bowhead calls because of our ongoing effort in the Bering Sea to differentiate bowhead and right whale gunshot calls. Gunshot call activity (Figure 4, green) coincided with general bowhead calling activity, although there were considerably fewer days with gunshot call activity and lower levels of calling activity on those days. Interestingly, the peaks in gunshot call activity occur near the end of the peak in bowhead calling activity in nine out of fourteen cases. Gunshot call activity also coincided with the last days of general bowhead calling activity for both of the fall, and the 2011 spring, migrations.

In the fall of 2010, the offshore location showed generally higher and more sustained peaks in gunshot call activity than the midshore or inshore locations (Figure 4, green). In the fall of 2011, the opposite was true; the inshore location showed the highest peak in gunshot call activity. No gunshot call activity was detected at the midshore or offshore locations during the spring migrations of 2011 and 2012, although it is possible those migrations were missed due to recorder failure. For the inshore location, the 2012 spring calling activity was slightly greater than in 2011, and it aligned more closely with the end of the main pulse of calling activity.

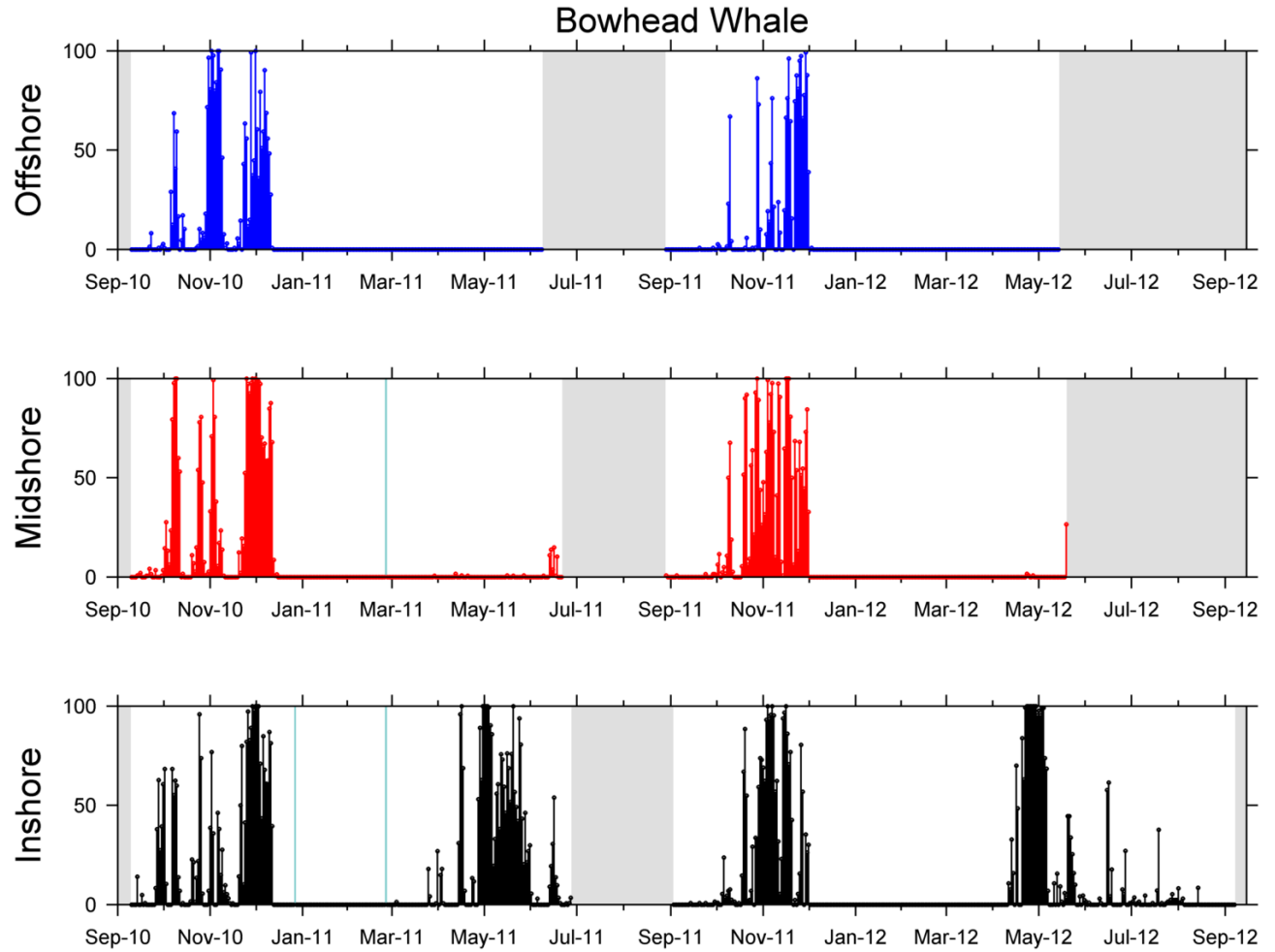


FIGURE 3. BOWHEAD WHALE CALLING ACTIVITY (PRESENTED AS THE PERCENTAGE OF TIME INTERVALS WITH CALLS) FOR INSHORE (LOWER PANEL), MIDSHORE (MIDDLE PANEL), AND OFFSHORE (UPPER PANEL) LOCATIONS, 2010-2012. DARK GRAY SHADING INDICATES NO DATA, AND TEAL SHADING INDICATES DAYS WHERE DETECTIONS WERE MASKED BY NOISE.

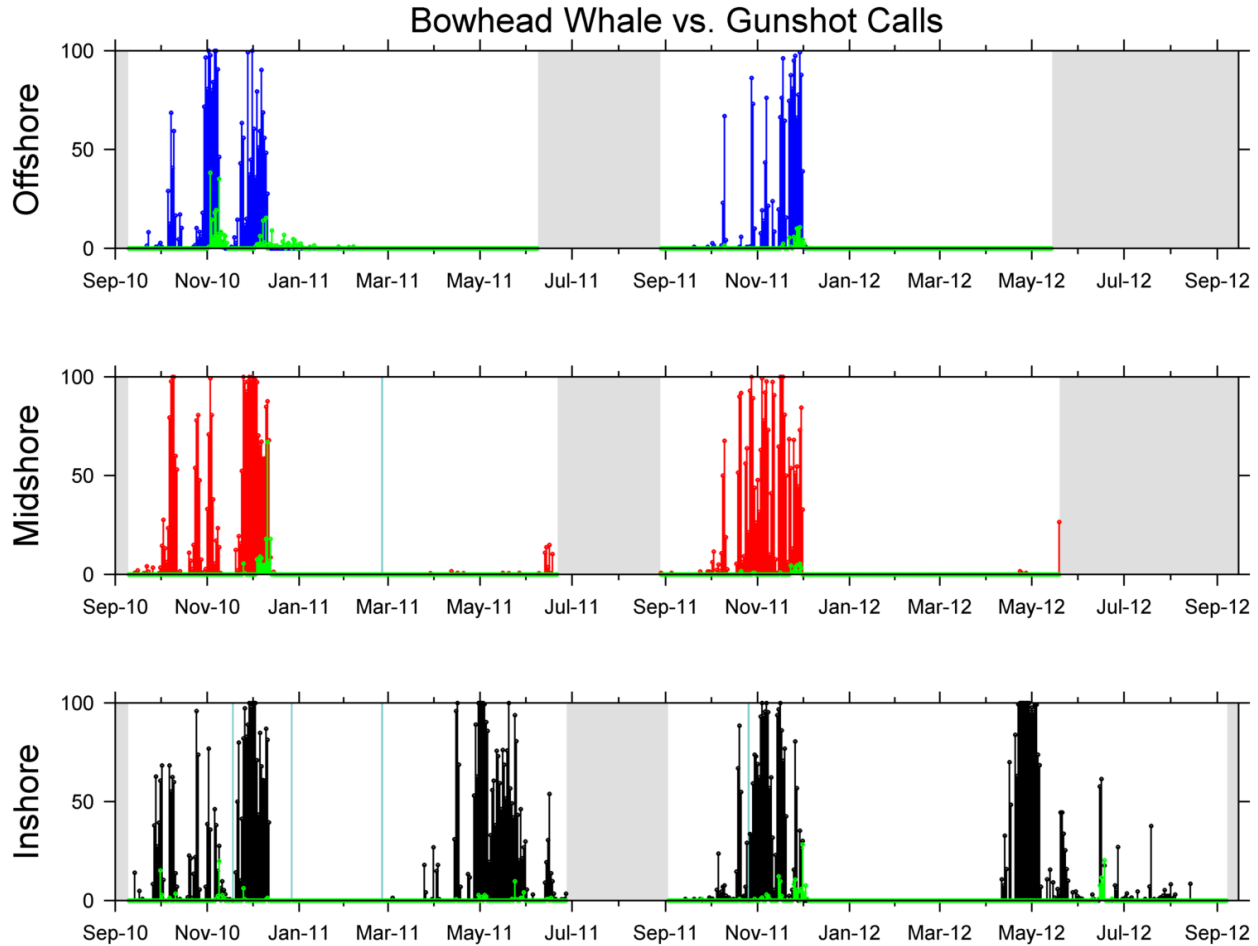


FIGURE 4. GUNSHOT CALL ACTIVITY (GREEN) OVERLAID ON BOWHEAD WHALE CALLING ACTIVITY. CALLING ACTIVITY IS PRESENTED AS THE PERCENTAGE OF TIME INTERVALS WITH GUNSHOT CALLS FOR INSHORE (LOWER PANEL), MIDSHORE (MIDDLE PANEL), AND OFFSHORE (UPPER PANEL) LOCATIONS, 2010-2012. DARK GRAY SHADING INDICATES NO DATA, AND TEAL SHADING INDICATES DAYS WHERE DETECTIONS WERE MASKED BY NOISE.

Beluga whales

Both the fall and spring beluga whale migrations were detected in both deployment years at all three locations, with higher and more sustained peaks in calling activity found inshore (Figure 5, Table 4). For the 2010 fall migration, calling activity began earliest inshore (mid-September), and latest offshore (early-November). The end of fall 2010 calling activity was also staggered the same way, ending in early December inshore, and mid-to-late December offshore. The peak in calling activity occurred in approximately late November at all three locations, although no peak exists at the offshore location. The fall 2011 migration showed a more uniform start of calling activity (early October in all locations); however, the end varied among locations, ranging from late November (offshore) to mid-December (inshore/midshore). The calling activity was also not as pronounced as in 2010, although it seems that the calling activity was distributed among locations in 2011, whereas it was more concentrated inshore in 2010. The peak in calling activity was slightly earlier (mid-November) in 2011 than in 2010.

TABLE 4. KEY TIMING EVENTS FOR BELUGA WHALE CALLING ACTIVITY.

Year	Mooring	Fall Migration		Spring Migration	
		Date Range	Peaks	Date Range	Peaks
2010-2011	Offshore	11/08/10-12/21/10	Very small cluster mid-Nov	04/03/11-04/21/11	Mid-Apr
	Midshore	10/20/10-12/15/10	Small one late Nov	03/04/11-06/07/11	Very small cluster mid-Apr
	Inshore	09/15/10-12/02/10	Late Nov	03/27/11-06/19/11	Two: early and late May
2011-2012	Offshore	10/03/11-11/23/11	Small one mid-Nov	04/12/12-05/07/12	Early May
	Midshore	10/10/11-12/12/11	Small one mid-Nov	04/02/12-05/19/12*	Early May
	Inshore	10/05/11-12/18/11	Early to mid-Nov	04/11/12-07/18/12	Two: early and mid-May

* = Date recorder limited

For all locations and years, there was generally more beluga whale calling activity in the spring than in the fall (with the exception of the midshore mooring in 2010-2011). As in the fall, there was considerably less calling activity at the midshore and offshore locations than at the inshore location. The start of spring 2011 calling activity varied among locations, the earliest being early March (midshore), and the latest being late-March/early April (inshore/offshore, respectively). Two large peaks in calling activity were seen at the inshore location (early and late May). The end of spring 2011 calling varied quite a bit among locations, ranging from late-April to mid-June. The spring pattern in 2012 was similar to that of the fall with calling activity less concentrated at the inshore location. The start of spring 2012 calling activity ranged from early to mid-April, and the end ranged from early May to mid-July, both similar to that of 2011, though this may be recorder-limited at the midshore and offshore locations. The peak in calling activity was early-May for all locations (although the inshore location had another peak in mid-May), slightly later than spring 2011. There were very few, scattered, overwinter instances of calling activity at all sites over both years.

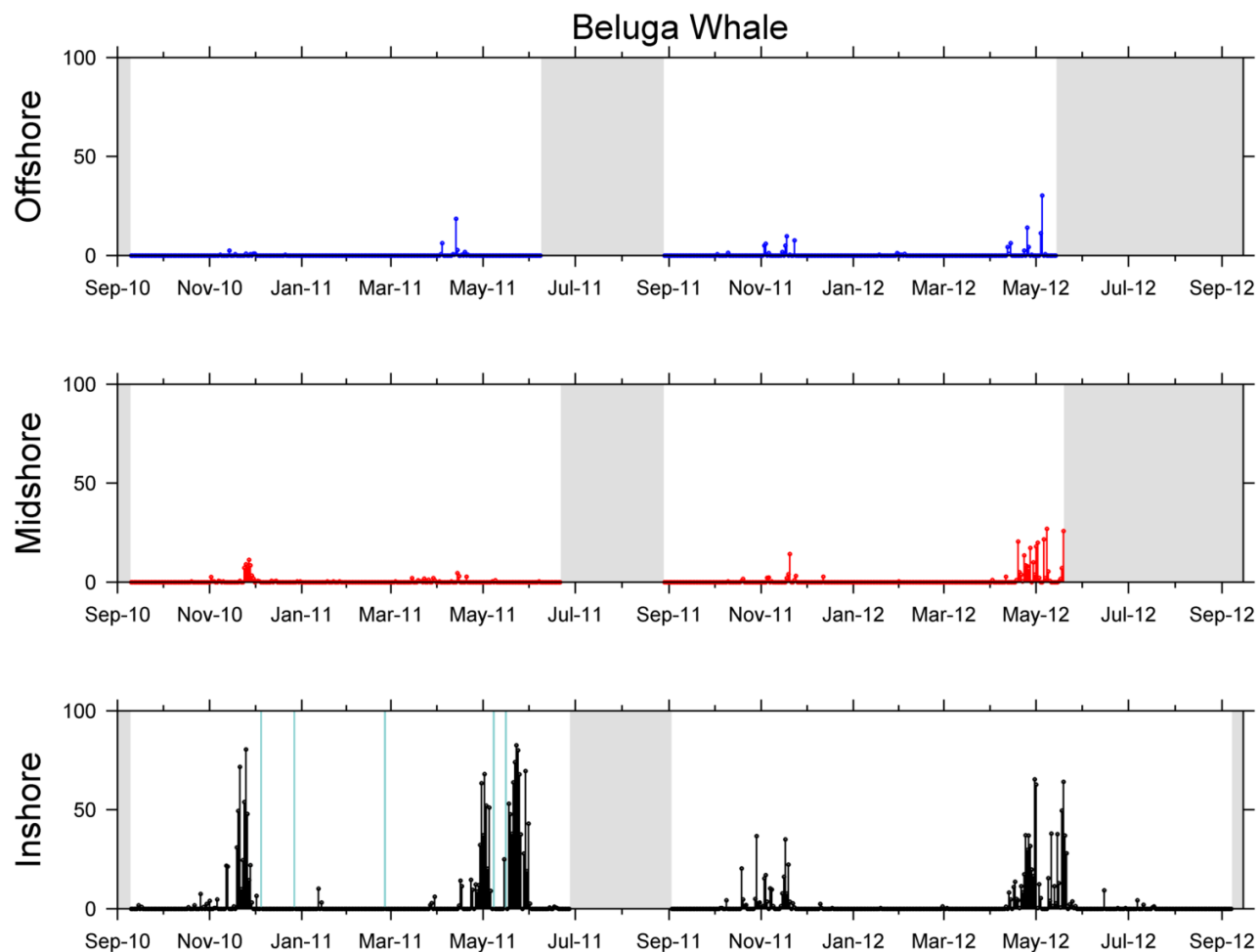


FIGURE 5. BELUGA WHALE CALLING ACTIVITY (PRESENTED AS THE PERCENTAGE OF TIME INTERVALS WITH CALLS) FOR INSHORE (LOWER PANEL), MIDSHORE (MIDDLE PANEL), AND OFFSHORE (UPPER PANEL) LOCATIONS, 2010-2012. DARK GRAY SHADING INDICATES NO DATA, AND TEAL SHADING INDICATES DAYS WHERE DETECTIONS WERE MASKED BY NOISE.

Gray whales

In contrast to bowhead and beluga whales, gray whale calls were detected infrequently in both years. With the exception of one day of calling activity at the midshore location, all calling activity was confined to the inshore location (Figure 6, Table 5).

For the 2010 fall migration, gray whale calling activity was detected on October 8th at the midshore location, and early October through early November, with a peak in early October, at the inshore location. The 2011 fall migration occurred approximately in the same time range (late September – early November). Calling activity was so low that no peak exists, although most of the calling activity is centered on early November.

No spring migration was detected at the midshore or offshore locations in either year, however the recorders ended early and it is possible that the migration was just missed. For the inshore location, the only location with year-round data, spring 2012 had calling activity from

mid-May through late July, with a very small peak in mid-July. There was no overwinter calling activity at any site during any year.

TABLE 5. KEY TIMING EVENTS FOR GRAY WHALE CALLING ACTIVITY.

Year	Mooring	Fall Migration		Spring Migration	
		Date Range	Peaks	Date Range	Peaks
2010-2011	Offshore	N/A	None	N/A	None
	Midshore	10/8/2010	One day: early Oct	N/A	None
	Inshore	10/01/10-11/19/10	Early Oct	N/A	None
2011-2012	Offshore	N/A	None	N/A	None
	Midshore	N/A	None	N/A	None
	Inshore	09/20/11-11/05/11	Very small cluster: early Nov	05/16/12-07/21/12	Very small one in mid-July

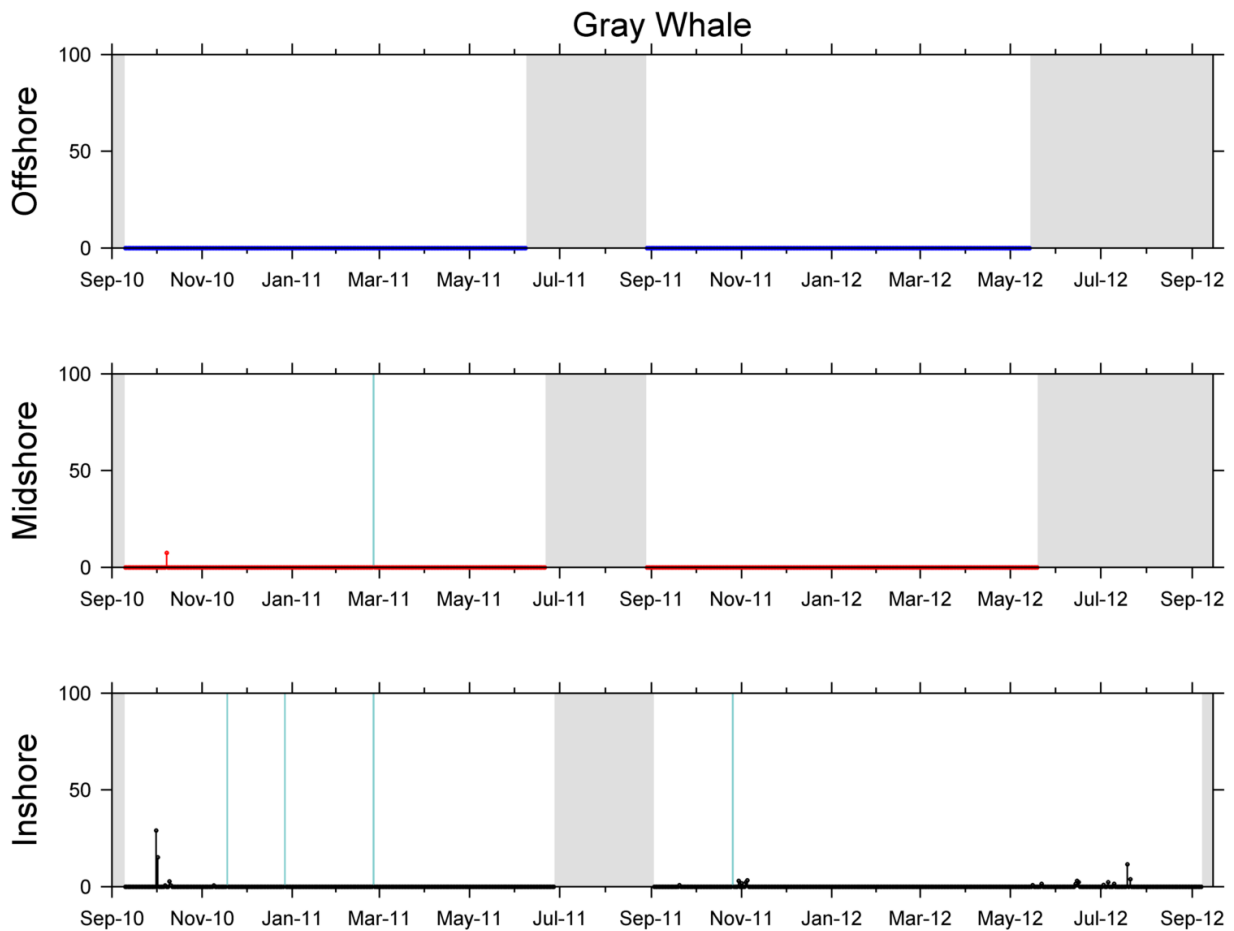


FIGURE 6. GRAY WHALE CALLING ACTIVITY (PRESENTED AS THE PERCENTAGE OF TIME INTERVALS WITH CALLS) FOR INSHORE (LOWER PANEL), MIDSHORE (MIDDLE PANEL), AND OFFSHORE (UPPER PANEL) LOCATIONS, 2010-2012. DARK GRAY SHADING INDICATES NO DATA, AND TEAL SHADING INDICATES DAYS WHERE DETECTIONS WERE MASKED BY NOISE.

Walrus

Walrus were detected at all locations in both years (Figure 7, Table 6). Their calling activity was nearly year-round at the offshore location, but limited to the summer/fall at the inshore and midshore locations. The lack in recording effort between June and September of 2011 makes clear interpretation of the results difficult. However, it seems likely, given the high percentages of calling activity immediately before and after this time period, especially at the inshore and midshore locations, that calling continued throughout this time period. Unlike the previous three species, with their distinct fall and spring migrations, walrus calling activity appears to have two time periods, over-summer (roughly May to November) and over-winter (November to May). Bouts of low level calling activity distributed throughout the year blurs the lines between these time periods, and so the date ranges presented in Table 6 should be considered approximate.

There are two complete sets of results for the overwinter time period: 2010-2011 and 2011-2012. In both cases there is extensive calling activity present at the offshore location, sporadic and low levels of calling activity at the inshore location, and minimal calling activity at the midshore location. This is contrary to the bowhead, beluga, and gray whale results where the offshore location had the least amount of calling activity. Walrus, unlike the cetaceans, had consistent calling activity detected overwinter. Peaks in the calling activity offshore occurred in mid-February 2011, and one month later (mid-March) in 2012. The calling activity in 2012 is more skewed than that in 2011. Inshore, the peaks were present for just a few days in late November 2010 and 2011 and mid-February 2012.

There are no complete sets of data for the over-summer time period. Calling activity was present from the start of the recordings at all three locations on September 10, 2010. This calling activity did end abruptly, however, in Mid-October at all three locations. For 2011, approximately two months of data is missing from the inshore and midshore locations. Calling activity is seen to increase to near-constant levels in June at both these locations before the recordings end. When the recordings for the subsequent deployment resume in early September, calling activity is still at high levels. It is impossible to know what the overall distribution in calling activity was during this time period, but it does appear that there is a peak in early November at both the inshore and midshore locations. The offshore recorder failed almost a month earlier than at the other locations and so there are not enough data in June to determine if a similar increase in calling activity occurred in that month. Again, there seems to be a peak in calling activity in early November at the offshore location. The 2012 May-November time period lasted only a couple of weeks in the midshore and offshore locations before those recorders failed. However, the recorder at the inshore location continued for the full deployment and data are available into September. Here, a very strong and lengthy pulse of calling activity was present, peaking in early July. No second peak in calling activity was seen. Determination of whether calling activity during the over-summer time period is typically bimodal will have to wait until analyses are completed on subsequent years.

TABLE 6. KEY TIMING EVENTS FOR WALRUS CALLING ACTIVITY.

Year	Mooring	Over-Summer		Over-Winter	
		Date Range	Peaks	Date Range	Peaks
2010-2011	Offshore	9/10/10* - 10/10/10	Maybe mid-Oct	11/18/10-4/22/11	Mid-Feb & late Apr
	Midshore	9/10/10*-10/10/10	Maybe mid-Oct	11/12/10-4/18/11	None
	Inshore	9/10/10*-10/17/10	-	11/8/10-4/27/11	One day: late Nov
2010-2011 & 2011-2012	Offshore	5/2/11** - 10/28/11**	Maybe early Oct	11/25/11 - 4/30/12	Mid-Mar
	Midshore	5/31/10** - 11/4/11**	Maybe mid-Jun & early Oct	11/20/11 - 4/27/12	Small ones late Nov & early Apr
	Inshore	5/7/11** - 11/3/11**	Maybe mid-Jun & early Oct	11/16/11 - 4/14/12	Late Nov & mid-Feb
2011-2012	Offshore	5/1/12-5/10/12*	-	-	-
	Midshore	5/11/12 - 5/11/12*	-	-	-
	Inshore	6/14/12 - 8/13/12	Early Jul	-	-

* = Date recorder limited

** = Dates missing in middle of range

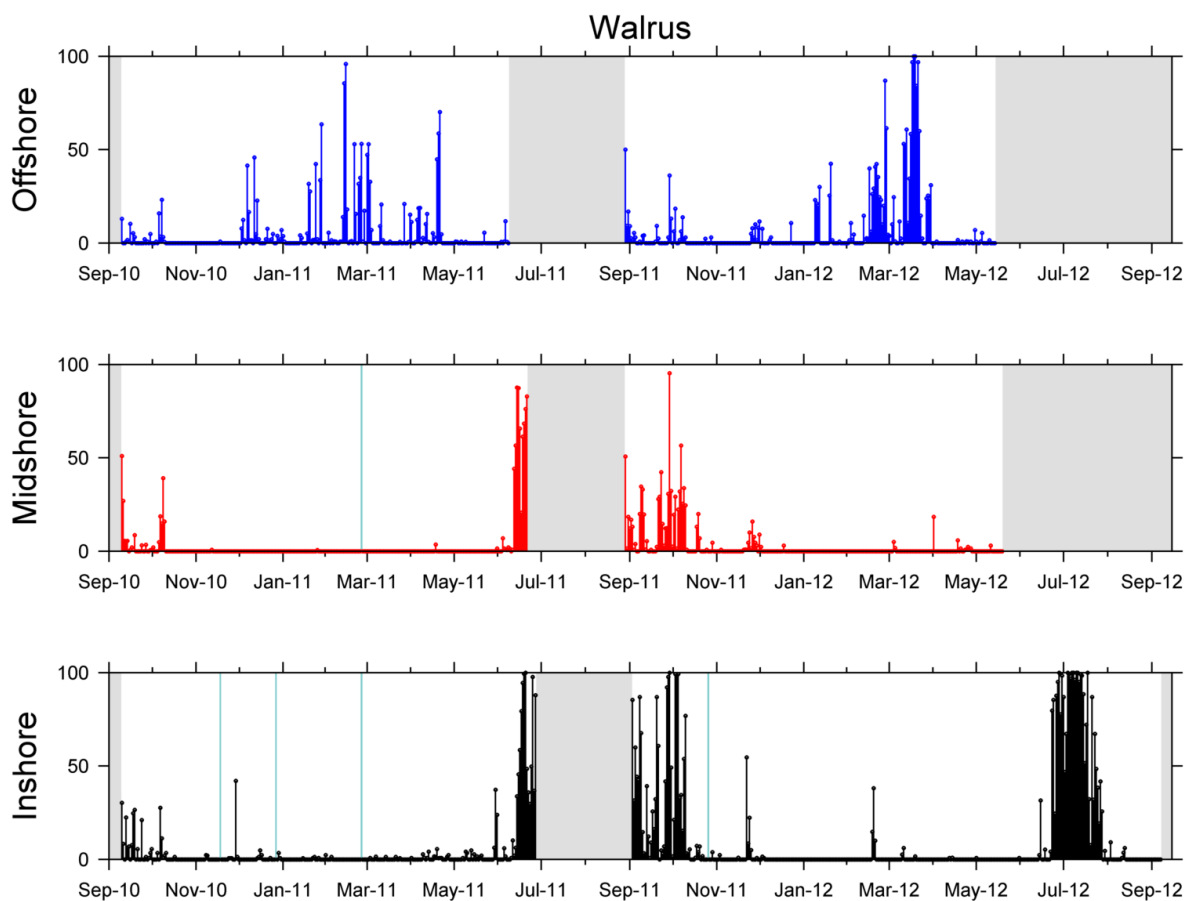


FIGURE 7. WALRUS CALLING ACTIVITY (PRESENTED AS THE PERCENTAGE OF TIME INTERVALS WITH CALLS) FOR INSHORE (LOWER PANEL), MIDSHORE (MIDDLE PANEL), AND OFFSHORE (UPPER PANEL) LOCATIONS, 2010-2012. DARK GRAY SHADING INDICATES NO DATA, AND TEAL SHADING INDICATES DAYS WHERE DETECTIONS WERE MASKED BY NOISE.

Bearded seals

Bearded seal calling activity was nearly ubiquitous for both years at all locations (Figure 8, Table 7). Low levels of calling activity were present throughout the year, gradually increasing from late fall through winter, reaching near saturated levels (calling present on 100% of time intervals per day) by late spring.

In 2010-2011, calling activity started earliest at the inshore location (late September), followed one to two weeks later at the offshore and midshore locations, respectively. Calling activity at the inshore location had the most gradual ramp-up, increasing from early October through early April. The ramp-up of calling activity at the midshore location occurred in a shorter timespan (early November through mid-March). At the offshore location, calling activity increased to saturated levels in just two months (early March to early April). Saturated calling levels lasted from early April through late June at the inshore location. It appears that the calling activity was beginning to decrease right before the recordings ended, but this cannot be known for certain. Saturated calling levels lasted somewhat longer at the midshore location (mid-March to mid-June), and again, it appears that calling activity may have begun to decline immediately

preceding the end of the recording. The offshore location has the shortest sustained period of saturated calling levels, but there was still 100% calling activity on the last day of the recordings, and so it looks like that calling activity period was truncated by the reduced recording effort.

Calling activity in the 2011-2012 data showed similar patterns; calls were detected year round, with calling activity increasing from the fall through the spring. Calling activity started earlier in 2011 than in 2010 with bearded seal calling activity present from the beginning of the recordings at all three locations. Ramp-up of calling was also more drawn out in 2011 and all three locations saw the start of this ramp-up in early October instead of the staggered start seen in 2010. Inshore, the increase continued until mid-April when extremely consistent and saturated levels of calling activity extended until late June, at which point they plummeted sharply, returning to low levels for the rest of the recording (early Sept.). The midshore location had a shorter ramp up period which extended until late February, when saturated calling activity levels were reached, albeit inconsistently at times. Saturated levels were artificially truncated by the early failure of the recorder. Offshore, the ramp up period was as long as the one inshore, however there was a less consistent (and more peaked) increase in calling activity offshore. Near saturation levels did not continue for long before the recorder stopped.

TABLE 7. KEY TIMING EVENTS OF BEARDED SEAL CALLING ACTIVITY.

Year	Mooring	Date Range	> 90% Calling Activity Range	Peaks
2010-2011	Offshore	10/1/10-6/8/11*	Mid-Apr to early Jun*	Late Dec
	Midshore	10/7/10-6/21/11*	Mid-Mar to mid-Jun	Late Jan
	Inshore	9/25/10-6/27/11*	early Apr to late Jun	Early Oct and late Dec
2011-2012	Offshore	8/30/11*-5/14/12*	mid-Apr to mid-May*	Early Oct and early Dec
	Midshore	8/29/11*-5/19/12*	late Feb to mid-May*	Early Oct
	Inshore	9/8/11*-6/23/12	mid-Apr to late Jun	Early Oct and mid-Jan

* = Date recorder limited

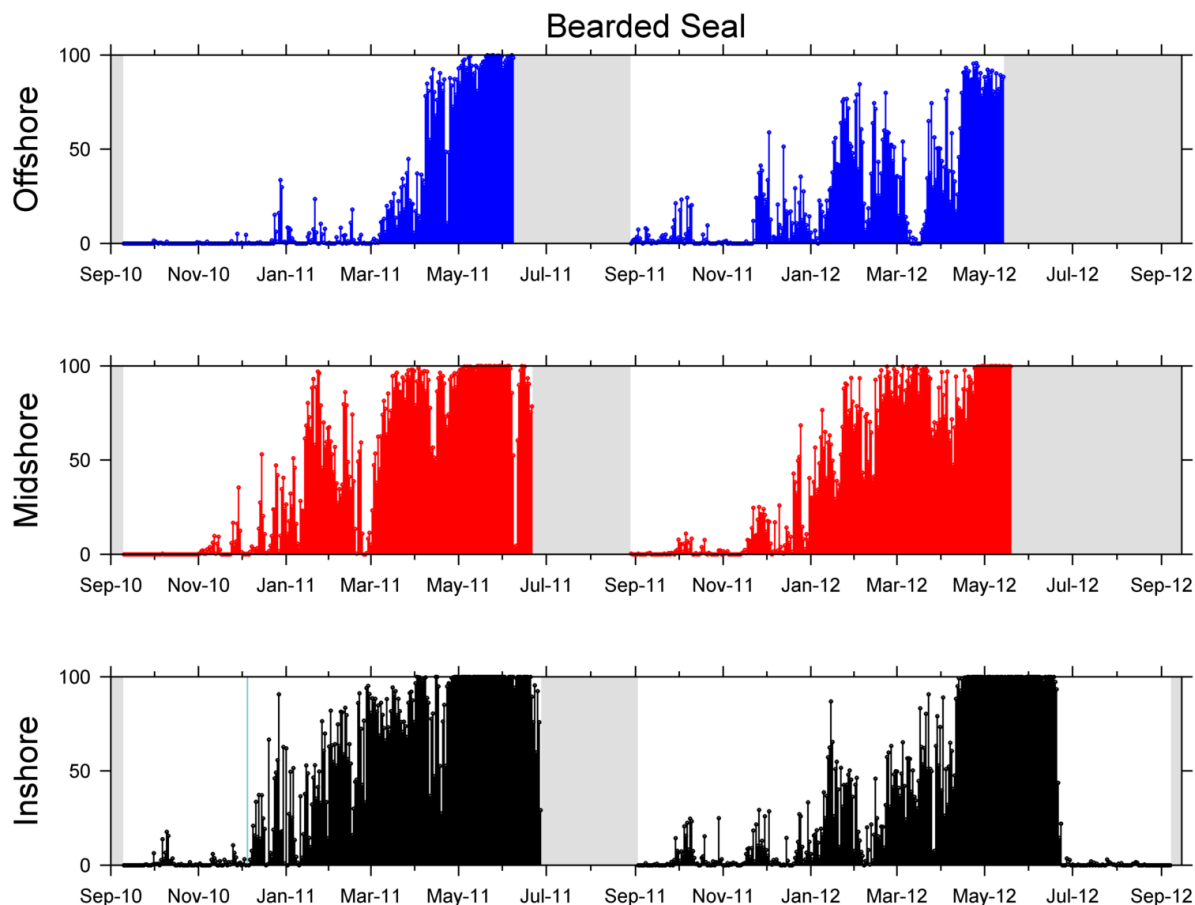


FIGURE 8. BEARDED SEAL CALLING ACTIVITY (PRESENTED AS THE PERCENTAGE OF TIME INTERVALS WITH CALLS) FOR INSHORE (LOWER PANEL), MIDSHORE (MIDDLE PANEL), AND OFFSHORE (UPPER PANEL) LOCATIONS, 2010-2012. DARK GRAY SHADING INDICATES NO DATA, AND TEAL SHADING INDICATES DAYS WHERE DETECTIONS WERE MASKED BY NOISE.

Other species

The rest of the species analyzed had little to no calling activity detected. Killer whales (Appendix C. 7) were detected on the 2011-2012 deployments at the inshore (6 days in September/October of 2011 and May/June of 2012) and midshore (1 day in April 2012) locations. Less than 10% of time intervals on those days had calling activity. Minke whale boing calls (Rankin and Barlow, 2005) were detected on the inshore location on only one day (19 October 2011; Appendix C. 8). No minke whale pulsed calls (Winn and Perkins, 1976) were detected at any location on any year (Appendix C. 9). A variety of pinniped grunts, yelps, and barks were detected but not identified to species (Appendix C. 10). These detections are lumped together as unidentified pinnipeds and most likely include species such as ringed and spotted seals as well as less common calls types from bearded and ribbon seals and walrus. These unidentified pinniped calls were detected most often at the inshore location, although there was sporadic low-level calling activity at the midshore location. Very sparse and low-level calling activity was present at the offshore location. The main peak in calling activity for these unidentified pinnipeds was in early December, with smaller peaks in early May and mid-June.

For all years, there was no calling activity at any location for the following species: humpback, right, fin, and sperm whales, and ribbon seals (Appendix C).

The LFDCS analysis for fin whales on the 2011-2012 data set flagged over 2,000 signals, all of which were checked manually and determined to be either mooring noise or airgun signals.

Environmental and anthropogenic sources

While reviewing the data for marine mammal calling activity, analysts also noted the presence of anthropogenic (seismic airguns and vessel) and environmental (ice) noise. Although not directly related to marine mammal presence, the results for these signals are reported here, as they were analyzed and presented in a similar manner. We use *noise activity* here as the equivalent of *calling activity* for these non-biological signal types. The presence of seismic airguns, vessel noise, and ice noise from the long-term AURAL recorders are shown in Figure 9-11.

Seismic airguns

Seismic airgun noise activity was ubiquitous at all three locations in the fall of 2010 and 2011 (Figure 9, Table 8). The start of the seismic airgun surveys in 2010 is unknown, as airgun noise activity was present on 100% of the time intervals for the first day of the recording period. This noise activity remained at high levels for most of September, decreasing in late September to zero on 25 September (offshore) or 26 September (inshore, midshore) before resuming the following day and quickly reaching 100% saturation. Shooting ceased abruptly on the last day of September at the offshore location, and the next day at the inshore and midshore locations. Due to recorder failure at the end of the 2010-2011 deployment, the start of the 2011 seismic surveys is again unknown. Airgun noise activity again was present on the first day of the recording period, although not at 100% saturation levels. In fact, airgun noise activity remained at much lower levels in fall of 2011 than in fall of 2010. Furthermore, the inshore location in 2011 had approximately one third the level of noise activity than at either the midshore or offshore locations. Airgun noise activity ceased in mid-September for approximately two weeks before resuming at the beginning of October. The last day with airgun noise activity differed among locations ranging from early (inshore) to mid-October (mid- and offshore).

TABLE 8. KEY TIMING EVENTS OF AIRGUN, VESSEL, AND ICE NOISE ACTIVITY.

Year	Mooring	Date Range Airguns	Date Range Vessel Noise	Date Range Ice Noise
2010- 2011	Offshore	9/10/10*-9/30/10	-	11/1/10-11/17/10 12/2/10-4/22/11
	Midshore	9/10/10*-10/1/10	10/11/10-10/12/10 2/14/11-2/18/11	11/4/10-11/21/10 12/3/11-3/4/11
	Inshore	9/10/10*-10/1/10	9/14/10-11/11/10	11/8/10-11/16/10 12/3/10-5/21/11**
2011- 2012	Offshore	8/29/11*- 9/17/11 10/3/11-10/10/11	8/29/11*-10/5/11 12/7/11-1/10/12	10/15/11-5/7/12
	Midshore	8/29/11*-9/17/11 10/3/11-10/13/11	8/29/11*-9/13/11 11/15/11-11/25/11	11/21/11-5/6/12
	Inshore	9/3/11*- 9/17/11 10/3/11-10/5/11	9/4/11*-10/6/11	11/21/11-7/22/12

* = Date recorder limited

** = Date bearded seal limited

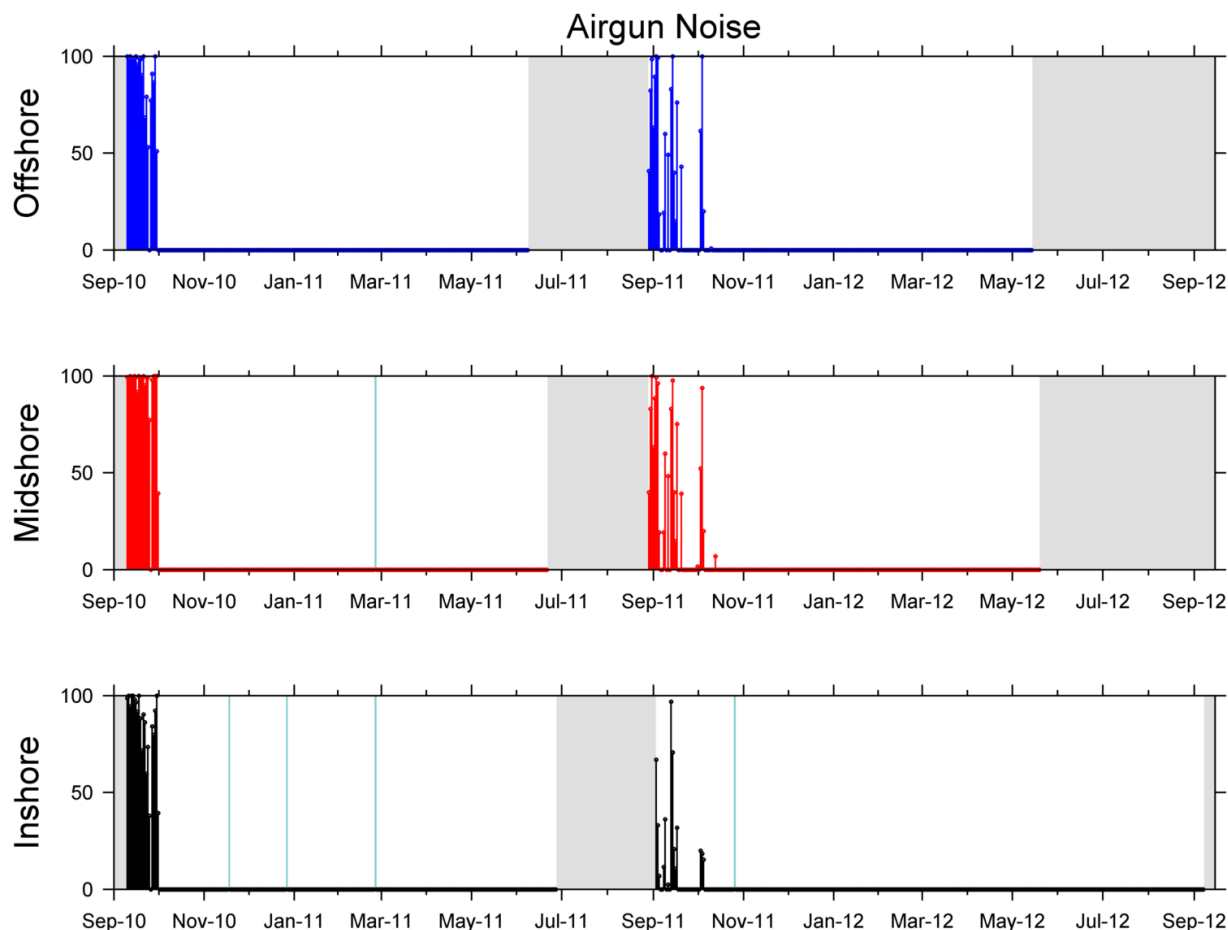


FIGURE 9. SEISMIC AIRGUN NOISE ACTIVITY (PRESENTED AS THE PERCENTAGE OF TIME INTERVALS WITH SIGNALS) FOR INSHORE (LOWER PANEL), MIDSHORE (MIDDLE PANEL), AND OFFSHORE (UPPER PANEL) LOCATIONS, 2010-2012. DARK GRAY SHADING INDICATES NO DATA, AND TEAL SHADING INDICATES DAYS WHERE DETECTIONS WERE MASKED BY NOISE.

Vessel noise

Vessel noise presence is shown in Figure 10 and Table 8. Vessel noise activity was present at only the inshore and midshore locations during the 2010-2011 deployment; starting mid-September and lasting for two months at the inshore location and starting mid-October and lasting for two days at the midshore location. In the spring there were low levels of vessel noise activity over four days in mid-February. Vessel noise activity was present at all three locations during the 2011-2012 deployment. The starting date of this noise activity in 2011 is unknown due to recorder failure at the end of the 2010-2011 deployment. Noise activity was detected on the first day of the 2011-2012 recordings at the midshore and offshore locations and on the second day at the inshore location. Noise activity continued for approximately one month at the inshore and offshore locations and a half-month at the mid-shore location. A second bout of vessel noise activity was seen at the midshore location the second half of November, and at the offshore location for about a month starting in early-December.

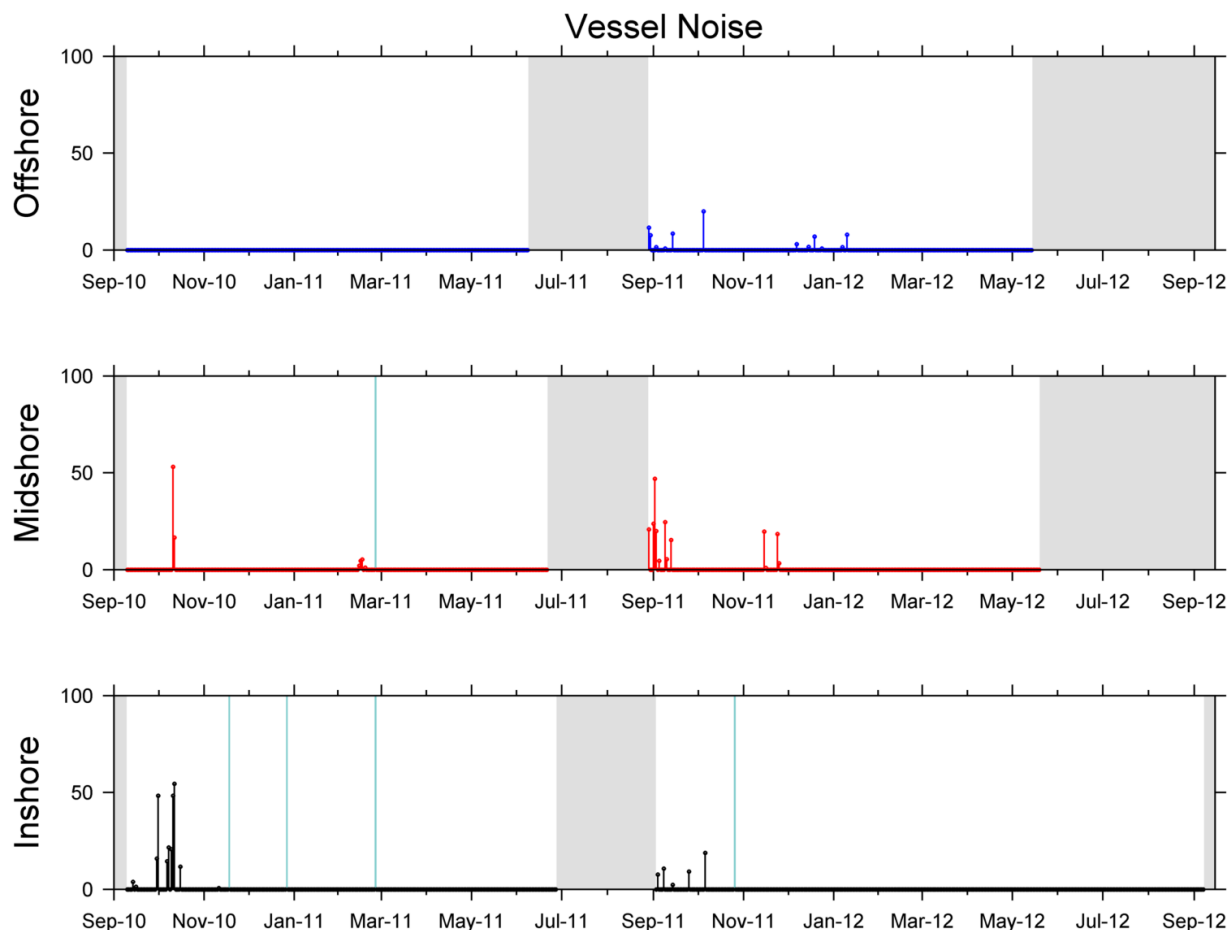


FIGURE 10. VESSEL NOISE ACTIVITY (PRESENTED AS THE PERCENTAGE OF TIME INTERVALS WITH SIGNALS) FOR INSHORE (LOWER PANEL), MIDSHORE (MIDDLE PANEL), AND OFFSHORE (UPPER PANEL) LOCATIONS, 2010-2012. DARK GRAY SHADING INDICATES NO DATA, AND TEAL SHADING INDICATES DAYS WHERE DETECTIONS WERE MASKED BY NOISE.

Ice noise

A substantial source of noise on the year-long recordings was from ice, primarily caused by cracking and rubbing (Xie and Farmer, 1992). Ice noise activity was present at all locations during both deployment years (Figure 11, Table 8). For the 2010-2011 deployment, ice noise activity occurred in two pulses: a small pulse of activity during approximately the first half of November followed about a half-month later by a long pulse of consistent, albeit varying, levels of noise activity throughout winter and the following spring. Ice noise activity was most prevalent at the inshore location, with several days in winter and early summer reaching 100% saturation levels. The last day with confirmed ice noise for the inshore location was in late May, however the actual end date may have been masked by other acoustic signals (e.g., bearded seals, Figure 8). Ice noise activity ended three months earlier at the midshore location, in early March, with levels staying below 50%. The offshore location showed the lowest levels of ice noise activity, not exceeding 25%. Noise activity at the offshore location ended in late April.

Overall, there were higher levels of ice noise activity at all three locations during the 2011-2012 deployment (Figure 11). Ice noise activity at the inshore location in 2011 started

nearly a month later than in 2010. It was also present two months longer, ending in late July, although there was no masking noise present like in 2010. In addition, even though the noise activity was present throughout this time period, there appears to be a main initial pulse ending in early-May, where levels frequently reached saturation, followed by a second pulse which contained more random presence and more random levels of noise activity. At the midshore location, noise activity began on the same day as the inshore location and continued at consistent moderate levels until early May, similar to the first pulse at the inshore location. Noise activity started the earliest at the offshore location (mid-October), and ended at a similar time to that at the midshore location. Both the mid- and offshore locations, however, had recorder failures that limit our ability to know the true end date of the noise activity.

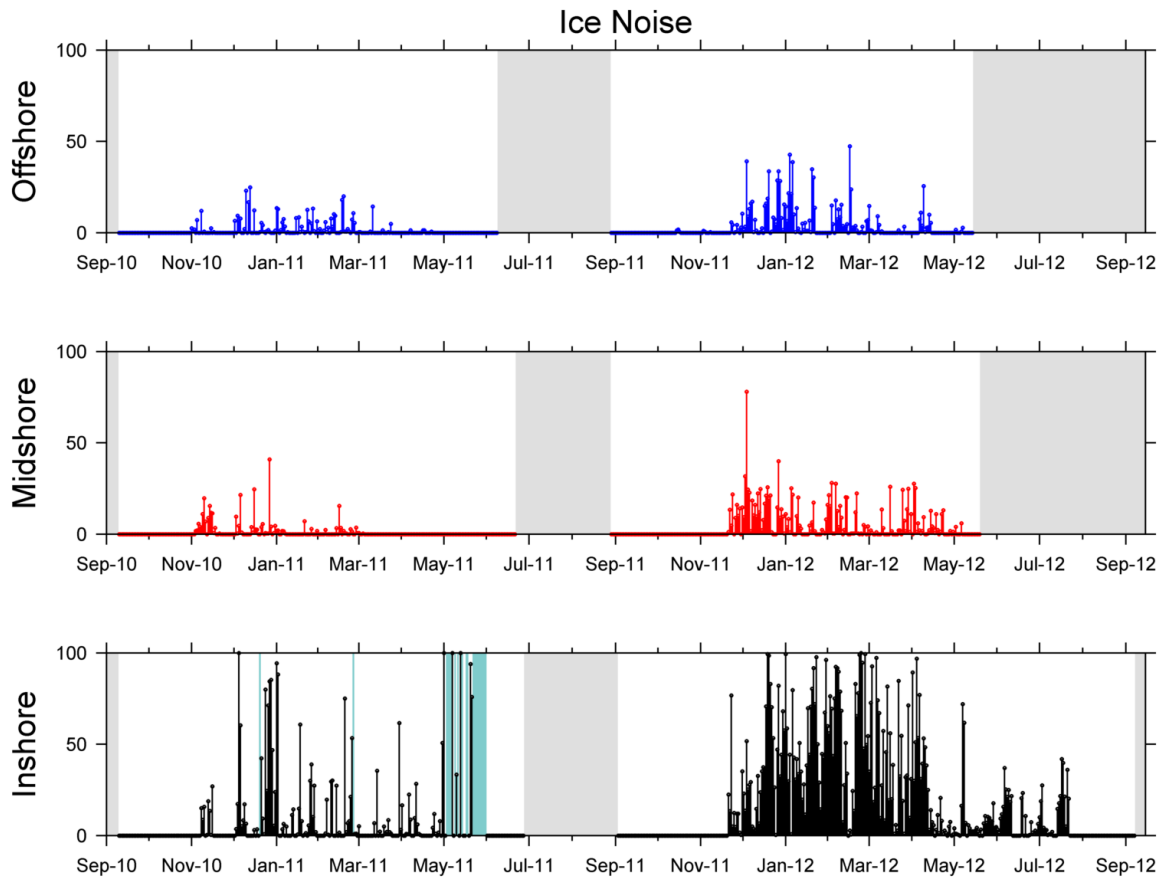


FIGURE 11. ICE NOISE ACTIVITY (PRESENTED AS THE PERCENTAGE OF TIME INTERVALS WITH SIGNALS) FOR INSHORE (LOWER PANEL), MIDSHORE (MIDDLE PANEL), AND OFFSHORE (UPPER PANEL) LOCATIONS, 2010-2012. DARK GRAY SHADING INDICATES NO DATA, AND TEAL SHADING INDICATES DAYS WHERE DETECTIONS WERE MASKED BY NOISE.

3. *Discussion*

Bowhead whales

The patterns of bowhead whale calling activity described in the results above complement what is currently known about their spatio-temporal distribution in the scientific literature. The bowhead whales detected on the long-term recorders are part of the Bering-Chukchi-Beaufort (BCB) stock that migrate through the Chukchi Sea annually between their wintering grounds in the Bering Sea and their summer feeding grounds in the Canadian Beaufort Sea (see Quakenbush et al., 2010 for an extensive literature review of this migration).

In both years of this study, the fall migration was detected as a strong pulse in calling activity between September and December. This is consistent with past studies (mainly aerial and some shipboard surveys) which have described the fall migration as beginning in September and continuing through November/December, when the whales pass through Bering Strait (Moore and Reeves, 1993). Current data from satellite tagging (Quakenbush et al., 2010) and other passive acoustic studies (Hannay et al., 2013) have described a similar time period. More specifically, the fall migration in 2010 ended in mid-December, the same as that reported by Hannay et al. (2013) at their central Chukchi mooring locations in 2007 and 2010 (Figure 12). In addition, our data show that the 2011 fall migration ended in late-November; although Hannay et al. (2013) do not report on the 2011 fall migration, this timing corresponds with what they found for the fall migrations of 2008 and 2009. The reasons for these interannual differences in timing will be discussed in Section X below.

The fall migration pulse in calling activity was seen at all recording locations, and at similar levels, suggesting an even distribution of bowhead whales across the Icy Cape line. The bowhead migration is known to diverge once past Point Barrow, AK; some whales head west toward Wrangel Island and others head southwest toward the northern Chukotka coast (Moore and Reeves, 1993; Moore and Laidre, 2006). In fact, the fall migration pathway in the Chukchi Sea fans out so much that it cannot be designated as a Biologically Important Area (BIA, Clarke et al., 2015) migratory corridor.

An interesting result of the bowhead whale call analysis was the presence of three distinct peaks in calling activity during the fall migration at all three sites in 2010 (Figure 3). Traditional Ecological Knowledge (TEK) asserts that bowheads are segregated by age class during their fall migration; smaller whales leading the migration, followed by large adults including cow/calf pairs (Braham et al., 1984). Recent work by Koski and Miller (2009) using calibrated vertical photography on bowhead whales during their fall migration in the Beaufort Sea, found that small subadults do precede the adults, with cow/calf pairs the last to leave. Ljungblad et al. (1987) also detected three peaks of calling activity in the fall from migrating bowhead whales. While they interpret the three peaks as representing aggregations or pulses of whales passing Barrow, they do not speculate as to the age/sex classes of the pulses.

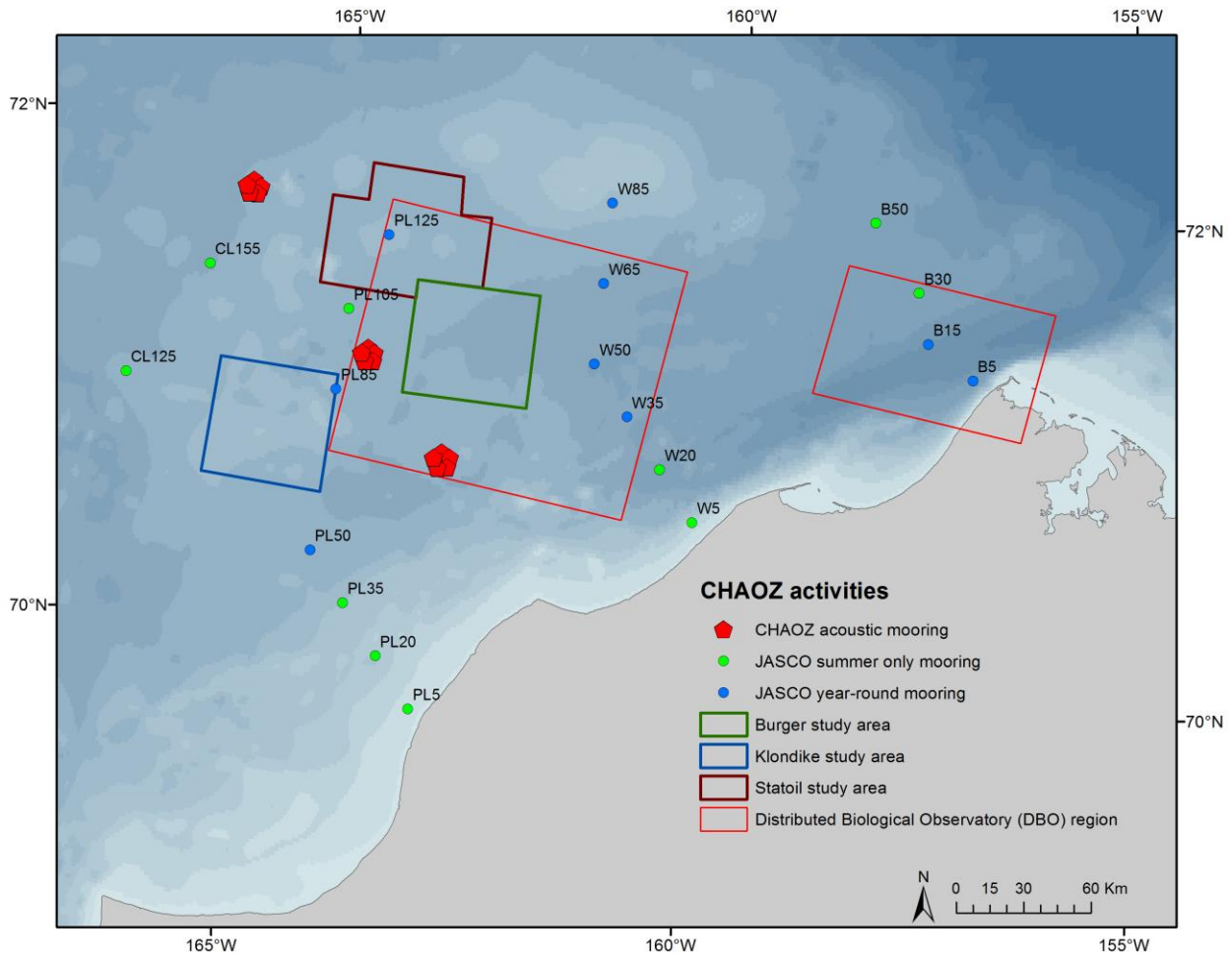


FIGURE 12. LOCATION OF CHAOZ PASSIVE ACOUSTIC MOORINGS OFF ICY CAPE, AK IN RELATION TO THOSE DEPLOYED BY HANNAY ET AL. (2013) AND THE CSESP STUDY AREAS. JASCO SUMMER MOORINGS RECORDED GENERALLY FROM AUGUST TO OCTOBER, AND WINTER MOORINGS RECORDED FROM OCTOBER TO AUGUST.

It is interesting that Hannay et al. (2013) state they did not find three distinct pulses of calling activity in their data set; however, it is unclear as to whether they intended this statement to apply to just the spring migration. There are several examples in their plot of bowhead whale daily call presence (Hannay et al., 2013, see their Figure 5) that show three pulses during the fall migration (e.g., W50, W35, CL50, PL85), and they do describe the bowhead calling as occurring in pulses. But it is clear that the triple pulse is not a consistent feature in the data collected throughout their study area. It was also not consistent throughout their study period, a result we also saw between our 2010 and 2011 fall migration data. Taken as a whole, these data suggest that if these pulses do represent temporal separation between age classes, this separation varies interannually. Barrow whalers report that the segregation of migration pulses in the fall is tenuous (Huntington and Quakenbush, 2009), which may explain the differences seen here.

A more detailed acoustic analysis of these three peaks is needed to determine whether there is a difference in call characteristics among them, which would suggest differences in calling among the age/sex classes. Results from this analysis could then be applied to the 2011 fall migration pulse to determine whether similar, but blurred, patterns exist in those data. We

have begun this finer scale analysis with the inclusion of the bowhead whale gunshot call. As shown in Figure 4, this call type occurs near the end of each of the fall migration pulses in calling activity for both 2010 and 2011. One definitive case of gunshot calls being produced during the spring ice census in Barrow could not be associated with any visible surface activity (Würsig and Clark, 1993); but current recollection of this event is that it was associated with adults and not cow/calf pairs (C. Clark, pers. comm.). Further discussion of the gunshot call and its potential function can be found in Section X.3.

In both years of this study, the spring migration was detected as a strong pulse in calling activity between April and July. This again agrees with past (Moore and Reeves, 1993) and current (Quakenbush et al., 2012; Hannay et al., 2013) literature, as well as from the TEK acquired from centuries of springtime bowhead whale subsistence hunts (Braham et al., 1980).

The calling activity detected during the spring migration was concentrated at the inshore location, with just low-level activity detected at the midshore, and none at the offshore locations. A very small possibility exists that the lack of spring calling activity at the midshore and offshore locations is due to early recorder failure at those locations, although the inshore recorder also failed early in the spring of 2011 and the spring pulse was still seen. Furthermore, this skewed spatial distribution of calling activity fits well with what is known about the spring migration of bowhead whales. In general, they remain close to shore and use leads in the ice to migrate northward from the northwestern Bering Sea along the Chukotka or Alaskan coasts through the Bering Strait, and then along the Alaskan coast toward their summering grounds in the Beaufort Sea (Braham et al., 1980; Moore and Reeves, 1993; Quakenbush et al., 2012). However, satellite tag data (Quakenbush et al., 2013) and passive acoustics (Clark et al., 1986) have shown that not all whales are confined to the lead system in the spring. The spring 2011 migration was detected in its entirety at the inshore location. Unlike the fall migration pulse in calling activity, there was no clear end to the spring calling pulse; rather, it gradually decreased starting mid-May with consistent calling activity until mid-August (Figure 3). Although the CHAOZ data are unable to determine if this gradual decline in calling activity is common across years, recorders deployed in the same locations for the subsequent BOEM-funded ARCWEST study have lasted a full year for several years, thus an answer will be available once those analyses are complete. In addition, Hannay et al. (2013) have reported similar decreases in detections after the main pulse of spring calling activity at other locations in the Chukchi Sea.

At the present (post-whaling era) time, the Chukchi Sea is used primarily as a migratory corridor by the BCB (Bering-Chukchi-Beaufort) stock. It is also identified as a Biologically Important Area (BIA) for reproduction (Clarke et al., 2015), but this is based on sightings of cow/calf pairs (including neonates) during the spring and fall migrations, and so it still has a migratory context.

Bowhead whales are planktivorous, feeding mainly on copepods and euphausiids, although they can also eat other crustaceans and fish (Lowry, 1993; Lowry et al., 2004). They can feed in the water column, at the surface, and epibenthically (Würsig et al., 1989). Recent work by Mocklin et al. (2012) has shown that epibenthic feeding is more prevalent than previously thought.

Whether bowhead whales use the Chukchi Sea to feed is unclear. As stated by Clarke et al. (2015), despite extensive aerial survey effort, very few observations of feeding bowhead whales exist for the northeastern Chukchi Sea to be designated as a BIA for feeding, although

they also mention the limitations in identifying feeding behavior during aerial surveys. Nevertheless, feeding has been observed in the Chukchi Sea (Lowry and Frost, 1984; Ljungblad et al., 1986), and old whaling catch records have shown that bowhead whales historically used the Chukchi Sea in the summer/fall months (Dahlheim et al., 1980). Several authors have also suggested feeding during the spring migration is more common than previously thought (Lowry et al., 2004; Moore and Laidre, 2006; Mocklin et al., 2012). Furthermore, recent data from satellite tags have shown that bowhead whales sometimes turn around mid-migration (Quakenbush et al., 2013), and so it is important to note that they most likely are influenced by multiple motivators while in the Chukchi Sea. Further investigation of this feeding behavior will be described in Section X.3.

Finally, as noted in Hannay et al. (2013) it is also possible that periods of low calling activity levels are due to low calling rates and not necessarily from low whale presence (Würsig and Clark, 1993). However, they also counter with the fact that periods with low calling rates also correspond to periods with low numbers of visual observations. The data presented here agree strongly with those obtained from visual observations, TEK, and satellite tag data, and so we conclude that calling activity is a good proxy for the spatio-temporal distribution of bowhead whales.

Beluga whales

Like bowheads, beluga whales are a migratory species that move between the Bering Sea and the Arctic annually. The story for beluga whales, however, is complicated by the fact that two populations of whales, the eastern Chukchi Sea (ECS) and eastern Beaufort Sea (BS), are migrating through the study area at overlapping times (Hauser et al., 2014). As summarized in Suydam et al. (2001), these populations were identified based on the areas that they use for calving, molting, and feeding, and confirmed through genetic analysis. The BS population concentrates in the Canadian Beaufort Sea, with core areas near the Mackenzie Delta and in Viscount Melville Sound, while the ECS population concentrates on the continental shelf and slope in the northeastern Chukchi and western Beaufort seas with core areas near Kasegaluk Lagoon and Barrow Canyon (Hauser et al., 2014).

Beluga whale acoustic presence was seen as pulses of calling activity in the late fall and spring at all locations and in both deployment years (Figure 5). This follows with what is known about ECS and BS beluga whale migration and their movements within the Arctic (Braham et al., 1984; Lowry et al., 1985; Moore et al., 2000; Suydam et al., 2001; Suydam, 2009; Delarue et al., 2011; Citta et al., 2013; Hauser et al., 2014; Clarke et al., 2015; Garland et al., 2015).

After overwintering in the northern Bering/southern Chukchi Seas, both populations begin their migration north to their feeding grounds in the Arctic. The spring migration occurs from March to early July. In the current study, calling activity was present on all three recorders from early March to mid-July, with peaks ranging from mid-April to late May, and with much greater levels occurring at the inshore location (Figure 5). The timing, location, and level of the inshore calling activity fits well with the migratory route of the larger BS population. These beluga whales begin their migration first, following leads in the ice until reaching their feeding grounds in the Canadian Beaufort Sea no later than July. They cross the Chukchi Sea in mid- to late April and the Beaufort Sea from May to June. Their migration corresponds well with that of

the bowhead whale, possibly because they might rely on the breathing holes left behind by the bowhead whales. However, the information on the BS population does not necessarily exclude the ECS population from contributing to the patterns of calling activity seen in this study. The smaller ECS population is thought to begin its migration later (D. Hauser, unpublished data). They arrive at Kasegaluk Lagoon by late June – early July, to calve, feed, and molt, and leave by mid- to late July as they spread out to feed further offshore of Kasegaluk Lagoon, near Barrow Canyon, or up to the ice edge (Hauser et al., 2014; Suydam et al., 2001). Although spring calling activity was highest at the inshore location, it was also detected at the mid- and offshore locations. This fits with results from other passive acoustic studies (Delarue et al., 2011; Moore et al., 2012; Hannay et al., 2013) that have also found high levels of beluga calling on offshore recorders in the Chukchi Sea in May, and suggests that not all beluga whales are traveling northeast along the inshore lead in the Chukchi Sea at this time of year. In fact, Suydam et al. (2001) have shown with satellite tags that beluga whales do not seem to be limited by high ice concentrations.

For both populations, calving and mating occur May-August, although young calves have been seen as early as March and as late as September in the Arctic. Braham et al. (1984) list Peard Bay (between Barrow and Wainwright) as a prime mating location, but there is no contemporary evidence to support this.

Only one recorder functioned during the summer (inshore 2011-2012), but only very low levels of calling activity were found into July. Results from aerial surveys place the inshore mooring far outside the core feeding area (Clarke et al., 2015), suggesting that our lack of calling activity is due to low whale densities. However, satellite tag results show that the summer core area for the ECS population off Kasegaluk Lagoon does extend to this inshore mooring (Hauser et al., 2014; Figure 1). It is unknown if belugas are feeding at the mooring locations, or while passing through the area toward the ice edge. Beluga whales are highly vocal during most behavior states (e.g. during social interactions, or directional swimming/migration), however, studies have shown that beluga whales rely almost entirely on echolocation clicks when foraging (Castellote et al., 2011; Panova et al., 2012; Castellote et al., in review); although see Stafford et al. (2013) for a summary of evidence to the contrary. Due to sampling rate limitations, the passive acoustic recorders used in this (and the Hannay et al., 2013) study would not be able to detect echolocation clicks, which have peak frequencies between 40-60 kHz (Au et al., 1985). However, there are instruments available (CPOD echolocation loggers, Chelonia Ltd., Cornwall, UK) that are designed to detect and record high frequency echolocation clicks. Although these instruments are currently unable to record for a full year, the addition of CPODs at our mooring locations would facilitate the identification of foraging behavior, possibly increasing both the number of detections (Castellote et al., 2013) and our knowledge of beluga whale spatio-temporal distribution.

Beluga whales are benthic and pelagic feeders (Seaman et al., 1982; Braham et al., 1984). The diet of the BS population has been said to be primarily Arctic cod, along with other fish, cephalopods, and shrimp (Moore et al., 2000). The diet of the ECS population is less well known but is thought to consist of saffron cod, cephalopods, crustaceans, and marine worms (Braham et al., 1984). Point Lay hunters have reported the stomachs of whales harvested in Kasegaluk Lagoon to contain shrimp, cephalopods, and small fish (Lowry et al., 1985). The most current data is from Quakenbush et al. (2015) who analyzed the stomach contents of 67 ECS whales and 62 BS whales. They found that shrimp were the predominant prey type of both

populations, with the most predominant fish species being saffron cod for the ECS and Arctic cod for the BS. Although other studies suggest that even the ECS population feeds on Arctic cod (Stafford et al., 2013; Hauser et al., 2014). Worms and octopus were still more common prey items than fish for the ECS and BS populations, respectively. It is important to note that the ECS whales analyzed by Quakenbush et al. (2015) were found near Point Lay in June and July, when they are concentrating in Kasegaluk for their molt/calving period. Most of the BS population were collected during their spring migration, presumably before they have reached their prime feeding grounds. Therefore, these results may not reflect the true composition of their diet. In fact, dive data from Citta et al. (2013) shows that the ECS beluga whales dive to depths of 200-300 m, where the boundary layer between water masses aggregates Arctic cod.

Beluga calling activity in the fall was less prominent than in the spring. This result follows that of Hannay et al. (2013). Belugas are distributed typically further offshore (Moore et al., 2000); it is not necessary for the whales to follow leads in the fall, since the waters are ice-free, and so they most likely fan out over a much wider area than during the spring migration. The fall migration has been said to split once past Point Barrow (Clarke et al., 1993), similar to the bowhead whale migration, with one migratory path continuing southwest through the Chukchi Sea and another remaining north of 72°N and heading west. In September, the BS population moves west past the ECS population and they hold this west-east positioning for the rest of the fall migration to the Bering Sea (Hauser et al., 2014). This bifurcation is the best explanation for the lack of calling activity at the mid- and offshore locations. In fact, the number of days in October with calling on a recorder located at 75°N (Moore et al., 2012) equaled that of the inshore mooring location of this study (Appendix E), and was 5-10 times greater than that of the mid- and offshore locations.

There were also a few instances of calling activity at all locations. This calling activity occurred when polynyas formed, creating leads in the ice. The association between belugas and ice conditions is discussed in detail in Section X.3.

In addition to the work on the seasonal distribution of beluga whales at the three locations, a separate study is currently being conducted to determine if the two populations of beluga whales can be discriminated based on passive acoustic techniques. Dr. Ellen Garland, an NRC post-doc at NMML from 2012-2014, analyzed the beluga acoustic data for the inshore and offshore recorders for 2010-2011 as part of a larger data set including archival data from two past BOEM –funded projects (PRIEST and BOWFEST). She determined that the different peaks in calling activity were indicative of distinct beluga stocks migrating through the Chukchi Sea at different times (Garland et al., 2015), which supports the current population stock delineation suggested by satellite telemetry, aerial surveys, and other acoustical studies (e.g., Suydam et al., 2001; Hauser et al., 2014; Clarke et al., 2015). Garland et al. (2015) concluded that the migration of beluga populations can be discriminated when temporal differences between calling peaks are large enough to be identified as independent events. She has begun to establish call repertoires for the two populations; see Garland et al. (2015) for the BS population repertoire. Alexandra Ulmke has taken over the analysis, under Dr. Garland's guidance and with NOAA S&T funding, and is to develop the call repertoire for the ECS population. When completed, the two repertoires will be compared and the results applied to the entire data set to hopefully differentiate between the two populations using call characteristics alone.

Note on spring migration of the BS and ECS populations of beluga whales:

Spring calling activity on the inshore recorder, as mentioned above, exhibited a bimodal pattern. This pattern was evident in both deployment years, and was also seen in the Hannay et al. (2013) data (e.g., their Figure 6, W35). This bimodal pattern might be caused by the two populations moving by at different times, it might also be due to sex/age segregation of the BS population (which was shown to occur in the fall migration (Hauser et al., 2014)). Braham et al. (1984) reported that beluga whales are in big groups in the winter, splitting into smaller groups of 2-4 animals during the spring migration (although bigger groups of 100+ are seen) that reform into large groups on the feeding grounds, dispersing once more into smaller groups as they migrate to the Bering Sea; the larger groups being led by large adult males followed by cow/calves along with subadults. It also could be due to just separate groups passing by at different times, or by oceanographic conditions temporally halting or diverting the migration. No bimodal pattern was seen in either the mid- or offshore spring data.

Although it is not clear from the literature how the two populations have been differentiated during the spring migration, unpublished satellite tag data support this population separation (D. Hauser, pers. comm.). Evidence from aerial surveys and passive acoustic recordings also seems to support that the BS population is the one passing through the Chukchi Sea at this time. Aerial surveys conducted during the spring migration have shown the whales swimming predominantly northeast in the Chukchi Sea and east in the Beaufort Sea (Moore et al., 1993). Timing of the spring bimodal peak in calling activity at the inshore location seems to align with a slightly delayed bimodal peak on a recorder (deployed through BOEM-funded BOWFEST project) located to the east off Barrow, AK (Garland et al., 2015). These again do not remove the ECS population from consideration, as there does not seem to be any evidence that the ECS whales always move directly from the Bering Sea to Kasegaluk Lagoon. They therefore could be part of the stream of whales moving to the northeast. In fact, the only ECS beluga with a functioning satellite tag during its spring migration left the Bering Sea and travelled NW into Russian waters off the Chukotka Peninsula then east toward Barrow Canyon and the ice edge before turning around and heading toward Icy Cape near Kasegaluk Lagoon (see tag #22149; <http://www.alaskafisheries.noaa.gov/protectedresources/whales/beluga/ptlay.htm>). As suggested by Delarue et al. (2011), it would seem logical for the migrating whales to replenish their energy stores before arriving in the lagoon, especially since they may not feed there.

Although Pt. Lay hunters have found evidence of feeding from whales taken within Kasegaluk Lagoon, they also say that whales taken from the large aggregations near the passes typically have empty stomachs (Lowry et al., 1985); new data from Quakenbush et al. (2015) also show a lack of feeding from whales harvested in the lagoon². In addition, the hunters assert that the beluga move back and forth between the lagoon for molting and the ice edge for feeding (Frost et al., 1993). Both Barrow Canyon and the ice edge are prime locations for foraging

² Quakenbush et al. (2015) do mention that beluga have the tendency to regurgitate food when being chased, so empty stomachs may not be a reliable indicator of feeding habits. They also cite evidence of fasting from tissue sample analysis (Woshner, 2000 in Quakenbush et al. (2015)); however, the lag times of the prey signatures in the tissue samples may be too great to be useful in determining whether beluga whales fast around Kasegaluk Lagoon.

(Delarue et al., 2011; Hauser et al., 2014), and so a direct migration path to Kasegaluk Lagoon seems unlikely.

Gray whales

The lack of gray whale calling activity at the three recording locations (Figure 6) was expected. The inshore location, where almost all the calling activity was detected, is still 40 nm off the coast, while aerial surveys have found that most gray whales remain within approximately 25 nm from shore between Point Barrow and Point Lay, AK or in the area between Wainwright, AK and Hanna Shoal which was to the east of our recording locations (Clarke and Ferguson, 2010). Our results also fit those from Hannay et al. (2013); although their recorders covered a much wider area they still found low levels of calling. Their results are even more surprising, however, because they had several recorders located right where the aerial surveys documented concentrations of gray whales.

The low levels of gray whale calls that Hannay et al. (2013) found in 2010 were limited to their recorder (hereafter referred to as *industry recorders*) locations within 35 nm of Point Lay and 5 nm of Wainwright. They detected calling in 2010 from late July to late August while we saw calling activity much later (between early-October to mid-November) on our inshore recorder. The timing of the two study results suggests that perhaps the calling heard on the industry recorders was from whales that shifted up to our inshore recorder location before migrating out of the Arctic. Our inshore location is ~75 km away from either their W50 or PL50 locations (Figure 12), so a small cluster of whales could make this move without being detected on either of the industry recorders. It is also possible that the migration happened along the coast (reaching our inshore location), after the inshore industry recorders were retrieved (last out mid-October). However, this does not explain why industry recorders the same distance from shore (e.g., W50, PL50) had no detections. It is likely that since only a small portion of the industry recorders were manually analyzed, gray whale calls, with their low calling rate, were missed.

The randomness of the spatial distribution of the calling activity is probably due to a combination of two factors: a low calling rate, and calling behavior that is context dependent. Crane and Lashkari (1996), found that gray whales do call along their migration route, but the calling rate is extremely low (mean: 20 hr. between calls). This means, assuming a swim speed of 6 km/hr (Rugh et al., 2001), that there could be ~65 nm between calls; so the chances that a recorder will be recording when a whale is calling nearby are low. We have found from the work we've done with joint visual and passive acoustic surveys (see Shipboard Observations below), that the same concentrations of whales in the same area at different times during a single cruise, can have vastly different calling rates, due to differences in behavior (the presence of courtship behavior in this case). Gray whales are in the Arctic to feed. They are typically benthic feeders, but will also feed in the water column (Swartz et al., 2006). Their prey include a variety of invertebrates including gammaridean amphipods (their preferred prey) which aggregate on the Chukchi and Bering shelves, worms, bivalves, pelagic mysids, crab larvae, and herring eggs (Nerini, 1984; Darling et al., 1998). Although there is information on gray whale calling behavior on their breeding grounds and during their migration, little exists on the sounds they make while feeding. We have noticed an interesting lack of gray whale calling behavior from sonobuoys during times when gray whales are obviously feeding, as evidenced by mud plumes.

The timing of the calling activity on our inshore recorder fits the timing of the migration. Eastern North Pacific gray whales make the long roundtrip migration from their feeding grounds in the Arctic to the breeding/calving lagoons off Baja California, Mexico annually (but note that not all whales migrate fully (see Rugh et al., 2001; Stafford et al., 2007b)). The start of the southbound migration varies; starting as early as mid-August, but the majority of whales start to leave during September/October, and most are out of northern waters mid-October to November (Rugh et al., 2001). The timing of this migration coincides with the breeding season, which is a three-week period from late November to early December when most females are in estrus (Swartz et al., 2006). Therefore, the fall peaks in calling, which occurred in early October 2010 and early November 2011, coincide with both this migration and breeding season. No gray whales were heard past November during this study or that of Hannay et al. (2013). This is in contrast to the results presented by Stafford et al. (2007b) who found that gray whale calls were present from October 2003 to May 2004 at a mooring located northeast of Barrow, AK.

The southbound migration takes about two months to complete (Rugh et al., 2001) and is segregated with pregnant females leading, mature adults next, with immature animals last (Swartz et al., 2006). In mid-February the migration shifts from southbound to northbound, a time period that has been relatively consistent since the 1960's (Rugh et al., 2001; Rugh et al., 2005; DeJesús et al., 2014). The northbound migration takes three months and occurs in two waves (Swartz et al., 2006). The first, in February, is made up of newly pregnant females followed two weeks later by adults; immature whales follow after another week. The second contains the cow/calf pairs that migrate between March and May arriving in the Arctic feeding grounds between May and June. Again, the calling activity seen at the inshore location in 2012 coincides with this spring migration. It seems plausible, therefore, to assume that the inshore mooring location is located in part of the migratory path taken by the gray whales in both the fall and spring. It remains to be seen whether there is a reason they are calling at that location instead of those with the overwintering industry recorders, or whether it was just a coincidence.

The last confounding factor that may influence both the calling behavior and the detection of those calls is the presence of ambient noise. As mentioned in both Crane and Lashkari (1996) and Hannay et al. (2013), ambient noise can make the low frequency calls of gray whales hard to detect. In addition, the latter paper describes improvements in recorder design that increased the detection of the gray whale calls by reducing noise generated by the recorder itself. Improvements were seen in their 2011 data, a year that saw a reduced amount of noise activity from airguns (Figure 9); however, this reduced presence of airgun noise did not result in more gray whale calling activity on our recorders (Figure 6). It is unknown what effect airgun noise has on the calling behavior of gray whales. Many studies exist (see Moore and Clarke, 2002 for summary) that show gray whales react to anthropogenic noise sources by changing their course to avoid it. Only one of these studies (Dahlheim, 1987) examined the effects of these noise sources on the calling behavior of gray whales. Its findings included increased calling rates with playback signals such as boat noise, gray whale calls, and pure tones, but a cessation of calling altogether when a test tone was played. It is possible that the presence of the impulsive signals from airguns might have an effect on gray whale calling rates, but no information is available from the literature to support or refute this.

Walrus

One of the biggest surprises of this study was the high level of mid-winter walrus calling activity at our offshore location, a result which was not found by Hannay et al. (2013). Calling was present from November through April in both deployment years and at all three locations, however, calling was most pronounced at the offshore location with peak levels reaching close to 100% saturation mid-February 2011 and mid-March 2012.

This is an unexpected result because of what is known about their migrations and subsequent seasonal distribution of Pacific walrus. Most winter on Bering Sea pack ice (Fay et al., 1984a), to the south of St. Lawrence Island (the majority of the population) and in outer Bristol Bay near Round Island, usually around some form of open water (e.g., polynyas). The mating season occurs mid-winter. Male fertility is highest between November and February; subadult males become fertile later in the year and may mate with the late ovulating females (Fay et al., 1984b). With ovulation occurring from December to May and fertilization occurring by March, the mating season is December through March. Because walrus calve on drifting ice, the males do their reproductive display (which includes acoustic displays (Miller, 1975)) in small areas near the nursing cow/calf pairs for short periods of time; it would be hard for a male to defend a herd in such an unstable environment (Van Opzeeland et al., 2008).

As described in Fay (1982) walrus begin to disperse from these wintering sites in April, and many move through Bering Strait in May (some reaching as far as Barrow, AK). However, historical sightings of walrus off Point Hope from January through April are not uncommon. It is not unreasonable to assume that the walrus heard overwintering on the offshore recorder are subadults that do not have any reason to expend the energy required to migrate to the breeding ground in the Bering Sea. Indeed, subadults seem ‘the most inclined to wander or to be diverted by irregular ice movements’ (Fay, 1982). In addition, young male walrus tend to remain at the periphery of the areas where the adults aggregate in the winter (Fay et al., 1984b). Miller (1975) describes instances of subadult males engaging in reproductive displays and suggests that practice sessions occur; this would explain the presence of calling activity if the animals are, in fact, subadults. At any rate, some form of open water (e.g., polynya, leads) has to be present throughout the time period with this calling activity. Jay et al. (2012) reported large amounts of open water accompanied by high numbers of walrus in the Chukchi Sea in November of 2008-2011, so it is not unreasonable to assume that some pockets of open water existed overwinter in the years of this study. A Modis ice image from mid-Feb 2011 shows evidence of leads offshore in the study area (Figure 13a). The Modis ice image from mid-March 2012 (Figure 13b) provides compelling evidence that cracks forming in the Bering Strait progressed toward the CHAOZ study area by mid-March, 2012.

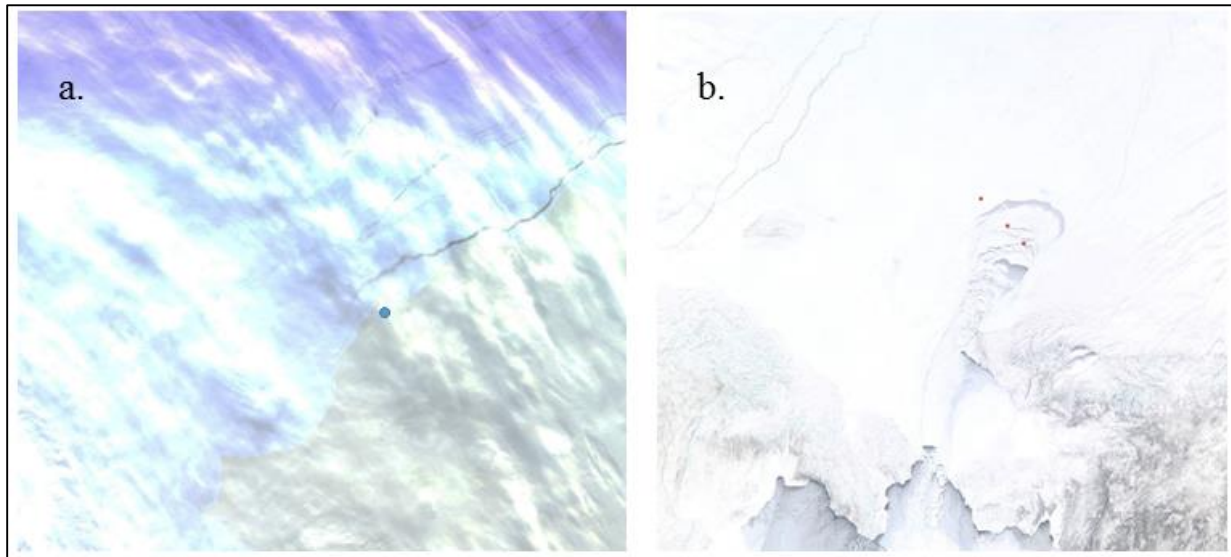


FIGURE 13. ICE COVER IN NORTHEASTERN CHUKCHI SEA. A) MODIS VISIBLE-BAND IMAGE WITH HEAVY CLOUD COVER FROM MID-FEBRUARY 2011. BLACK DOT SHOWS APPROXIMATE LOCATION OF ICY CAPE. B). MODIS INFRARED-BAND IMAGE FROM MID-MARCH 2012. THE THREE RED DOTS MARK THE LOCATIONS OF OUR INSHORE, MIDSHORE, AND OFFSHORE MOORING LOCATIONS.

Walrus time their northern migration based on ice movements from wind and sea surface currents – essentially hitching a ride on the moving icepack; however, they spend most of the migration swimming (Fay, 1982). They begin extending up into the northeastern Chukchi Sea starting in May. Most reach their summering grounds in July/August which corresponds to the beginning of the summer pulse of calling activity detected at all locations (Fay, 1982). The timing of the start of this pulse varies slightly between locations and deployment years, and also between our results and those from Hannay et al. (2013). Reasons for the differences seen within our data set will be discussed in Section X. Hannay et al. (2013) have shown that walrus are not uniformly distributed in the Chukchi Sea. They also found that areas of concentration shift throughout the summer season, with a gradual increase in detections near Hanna Shoal occurring in late July and August. For these reasons, variations in timing among locations are to be expected.

Females with calves are the most migratory, and tend to stay with the ice edge as it moves north in the Chukchi Sea. Jay et al. (2012) found that June/July is currently a time period with walrus ranging further north than in the past. Adult males are the least migratory, hauling out along the Chukchi coast in the summer. In addition, many thousands of males remain in the Bering Sea for the summer (Fay et al., 1984a). Walrus are benthic feeders and prefer to remain in areas where the water depth does not exceed 100 m (Fay, 1982). Their diet varies spatio-temporally, and they forage opportunistically (Seymour et al., 2014), but feed primarily on bivalve mollusks (Fay, 1982; Jay et al., 2014) and other invertebrates such as worms, snails, and crabs. The advantage for the walrus hauling out onto ice is that they can rest while it carries them around to new feeding grounds. Because of the high energetic demands of nursing (which lasts for approximately two years), it is logical that the females remain ice associated. It is unclear why males do not also remain with the ice, but Miller (1976) suggests it is because they do not have any high-energy demands in the summer, they save additional energy by lying closely in groups, and the extra heat generated from neighboring bodies aids with their molt. Their preference for haul out sites that are out of the wind further supports this argument. The

molting period is long, happening anywhere from March to October with a peak in July/August (Fay, 1982), it appears that it takes at least a month for an individual to completely molt. Trips into the water will impede the molt as that will cut off circulation to their skin, so the hair follicles cannot regenerate (Fay, 1982). It is important to note, however, that this model of age/sex class segregation is changing as a result of climate change. When the ice leaves Hanna Shoal early in the season, large aggregations of walrus of all ages and sex classes form enormous haul-outs (summarized in Hannay et al., 2013). These combined haul-outs are dangerous for young walrus who can get trampled and killed during stampedes; the resulting calf mortality can have compounding effects on the population (Udevitz et al., 2013).

It is assumed that underwater calls are produced by male walrus (Kastelein et al., 2002), so it would be expected that the largest levels of calling activity would occur closest to the coast where the males are hauled out. Although we are missing recording time in the middle of this summer pulse of calling activity, what remains seems to show a reduction in calling activity from the inshore to the offshore locations. However, the results from Hannay et al. (2013, their Figure 11) show the opposite result. It is possible that the assumption that these underwater calls can be produced only by males is incorrect, as Shusterman and Reichmuth (2008) have shown that females are capable of producing them as well. Analyses are currently underway for the BOEM-funded ARCWEST and CHAOZ-X projects; which have complete years of data and so can better describe the spatio-temporal trends in the data. Comparison with satellite tracks of tagged individuals might help determine if female walrus typically make underwater sounds in the wild, but tagging females with acoustic tags (e.g., DTAGs) would be, by far, the best method to quickly verify that the original, male-only, assumption is correct.

In the past, the southbound migration coincided with the rapid advance of the ice pack in October; possibly occurring in waves through the Bering Strait, with the animals that summered on the northern Chukotka coast preceding those that summered in Barrow and Wrangel Island. The pulse of calling activity seen from the start of the recordings until around 10 October at all three locations and in both years (Figure 7) might correspond to this fall migration. Most of the population remains south of the icepack, which reaches Bering Strait by November. The thin ice that develops in the fall is not strong enough to support the animals, and they swim ahead of it. The passive acoustic data from Hannay et al. (2013) and radio tag data from Jay et al. (2012) suggest that the walrus are moving out of the Chukchi Sea, not based on ice advance, but on the retreat of the ice edge. Also Jay et al. (2012) found that walrus are moving to the Chukotka coast prior to heading down through the Bering Strait. What has been known about walrus distribution is likely to continue to change as climate change progresses.

Bearded seals

Before the recent changes in sea ice extent, bearded seals spent a majority of their time in the Arctic and subarctic closely associated with the sea ice. This association still holds, but data from aerial surveys, tagging and passive acoustics show that many individuals now spend their summer in open water.

Braham et al. (1977), Burns and Eley (1978), and Allen and Angliss (2013) provide a thorough description of the past and current distribution and ecology of the Alaskan stock of the bearded seal (*Erignathus barbatus nauticus*) which is summarized below (with additional

references as needed). Bearded seals spend most of their time associated with the drifting pack ice, rarely hauling out on land (and even avoiding areas with continuous landfast ice). They can, but rarely do, maintain breathing holes, and so avoid areas with high ice concentrations, preferring areas where constantly moving ice helps to keep leads open. However, they also prefer heavier pack ice (70-90% ice cover) than other phocid seals and therefore tend to be distributed further north (they are most abundant 20-100 nm from shore, rather than within 20 nm from shore, with the exception of a group nearshore to Kivalina, AK). They are typically found in groups of 1-2, although groups of 30 seals have been seen during the molting season in the summer.

Like walrus, bearded seals tend to prefer areas where water depths are less than 200 m (Burns and Frost, 1979; Burns, 1981). They are primarily benthic feeders and eat mainly crustaceans, mollusks, cephalopods, worms, and fish. Their diet composition is strongly site-dependent. For example, crustaceans are the most common prey item near St. Lawrence Island, while bivalves and shrimp are the most common prey in Norton Sound. Males and females eat the same items, but a higher proportion of the diet is composed of shrimp for the younger seals (Lowry et al., 1980). Their ability to forage for a variety of organisms gives them an advantage over the more bivalve-centric walrus when feeding in the same areas (Lowry et al., 1980). However, as sea ice retreats farther away from the continental shelf into deeper waters, benthic foraging opportunities will diminish. This is most likely the reason for the recent uptick in bearded seal sightings and acoustic detections in the open water.

Bearded seals winter in the northern and central Bering Sea shelf and in the Strait. In the past they aggregated north of St. Lawrence Island in March, and began to disperse (both north and south) in April, crossing into the Arctic by June. Currently, it is thought that most of the north-bound seals pass through Bering Strait between April and June. They are widely distributed in the summer with some (mostly juveniles) remaining near the coast in the Bering and Chukchi Seas. Their whelping/mating/molting (in that order) seasons occur from March and late June (Burns and Eley, 1978). Pups are born in April on small drifting floes in shallow waters, and weaned in May. Male bearded seals produce long (> 1 min) trills (Ray et al., 1969) during the mating season which starts just prior to the weaning of pups in May. As summarized in Jones et al. (2014) these males return to the same breeding locations each year, and have been shown to use either a roaming or territorial mating strategy; the duration of the trill call used between the two strategies varies. Most seals head south through the Bering Strait in the fall, ahead of the advancing ice. This southbound migration is said to be less predictable and noticeable than the northbound leg. In late winter/early spring they are dispersed in the broken and drifting pack ice from the Chukchi Sea to the ice edge in the Bering.

Bearded seal calling vocalizations were ubiquitous throughout the study area for both years. The level of bearded seal calling activity increased in the fall to near saturated levels that started between late February and mid-April, depending on the deployment year, and location (Figure 8), which coincides with the start of the whelping/mating/molting time period. For most locations, the end of the peak calling could not be determined due to recorder failure. However, the inshore data for both years shows a sharp decrease in calling activity around the end of June, which matches well with the end of the whelping/mating/molting time period. These results are consistent with those reported by Hannay et al. (2013), who reported an increase in calling activity in fall-winter with a peak in April and an abrupt end of calling activity in late June. This

also fits with the results from Moore et al. (2012), who reported a pulse in calling activity May-July 2009 on a mooring located far north on the Chukchi Plateau.

The data collected for this study also shows that bearded seals are present in the northeastern Chukchi Sea year-round. Calling activity was seen year round, with low levels after the end of the whelping/mating/molting season until early October when a small peak was seen at all locations and in both years. Again, this is in agreement with the data presented by Hannay et al. (2013), as well as others (e.g., MacIntyre et al., 2013; Jones et al., 2014). From October to when calling activity reached near-saturated levels, calling activity levels fluctuated within each individual location/deployment and varied among locations/deployments. The environmental factors contributing to this variation will be discussed in Section X below.

Other species

The northward encroachment of subarctic species into habitats historically occupied solely by Arctic species is a serious concern. Clarke et al. (2013) suggest their intrusion into the Arctic may be due to either post-whaling population growth, or to climate change extending the open water season. Having the ability to monitor year-round for these species is important as we try to sort out what changes are happening and their subsequent effects on the Arctic species. For this reason, analysis of the passive acoustic recordings extended to a number of other subarctic marine mammal species. Some like fin, killer, minke, and humpback whales and ribbon seals, have been sighted or detected in the Arctic before, and therefore would be expected to have at least some calling activity. We will discuss each of these species below. Other species, such as right and sperm whales, are not expected to be present on the northeastern Chukchi shelf. Although we did analyze the data for these species, the fact that we did not find any calling activity is expected and therefore no discussion follows.

Fin whales

One surprising result was the lack of fin whale calling activity at any of the locations for either year. At first glance, this seems to be in direct contrast with the results from other passive acoustic studies (Delarue et al., 2013a; Hannay et al., 2013), as well as the short-term sonobuoy results (see Section VII.B.2; Crance et al., 2015) collected during the field season for this project. However, closer examination of the timing and locations for the detections made during these studies reveal that our effort was not comparable. Although the industry recorders, deployed by the two studies mentioned above, were spread throughout the northeastern Chukchi Sea, fin whale detections were limited to those to the southwest of our mooring line. These detections were rare, occurring on a handful of days per recorder in 2009 and 2010 (see Delarue et al., 2013a, Table 1), although 2007 saw a few recorders with approximately 30 days with calls detected. The majority of detections, in the years closest to those of our study, were made on a recorder that was ~100 nm away from our midshore location. The only detections made close to our mooring line, and in the same year as our study, were those from a recorder located ~35 nm away, and were made on 14 August 2010 and 3 October 2010. Given our recorders did not begin recording until 10 September 2010, only one day was missed. Fin whales detected on sonobuoys during the research cruises were also mainly concentrated in the area off Cape Lisburne and south. The one exception is a series of about 30 fin whale calls detected on a sonobuoy deployed

in late August 2012, approximately 50 nm off the coast near Barrow, AK (Crance et al., 2015). This detection, although to the east of the mooring line, was still made a long distance from our recorders, and it is much closer to the coast than our inshore mooring location, so it is possible the whale did not pass by any of our mooring locations.

The other possibility is that fin whales are present (albeit in low numbers), but are not vocalizing. However, it is generally not expected that fin whales would be present in large numbers in the Chukchi Sea. Fin whales are a subarctic species that, in Alaskan waters, are common throughout the Gulf of Alaska (Watkins et al., 2000; Stafford et al., 2007a) and Bering Sea shelf (Moore et al., 2002). Historically they ranged in these locations as well as in the Western Chukchi Sea (Mizroch et al., 2009). However, fin whale sightings in the southern Chukchi Sea from aerial surveys conducted since the 1980's have been rare (Moore et al., 2000; Clarke et al., 2013). Vessel surveys conducted since 2008 (Aerts et al., 2013) and 2010 (this study, see Section VII.B.2) have had no sightings of fin whales in the Arctic.

Although we did not have satisfactory performance from our attempts at fin whale auto-detection via the LFDCS, the full 2010-2011 dataset was analyzed manually, still without a single fin whale call detection. Further iterative testing and call library manipulation is underway to try and improve the LFDCS in correctly detecting fin whale calls.

Killer whales

Not much is known about killer whales in the Arctic other than it seems likely they are probably of the transient ecotype. See Clarke et al. (2013) for references that support this assumption. The transient ecotypes are the mammal eaters, who stalk their prey silently, and so it is unlikely that many calls would be detected in the study area. However, they are typically very noisy just after a kill (Deecke et al., 2005; C. Berchok pers. comm), so perhaps information on their feeding frequency might be able to be obtained from these data with additional analysis on the characteristics of post-meal calling bouts.

Killer whale calling activity was infrequent, occurring on only seven days out of the two years the recorders were in the water. All but one of these days occurred early September to early October and from mid-May to late June at the inshore mooring location. The first time period fits with the results from Hannay et al. (2013) who had occasional detections of killer whales in the Point Lay/Cape Lisburne recorders between late July and October annually. Their lack of call detections in the May/June time period is most likely due to the low calling rate of transient whales. In addition, sightings from shipboard (Aerts et al., 2013; this study - see Section VII.B.2) and aerial surveys (Clarke et al., 2013) are rare, so it is not just a matter of them being present and not heard, but rather a combination of low presence and low calling activity.

Humpback whales

Humpback whales are another subarctic species that is uncommon in the Arctic (Aerts et al., 2013; Clarke et al., 2013; this study - see Section VII.B.2). We detected no humpback whale calling activity on the long term moorings. Only two detections of humpback whale calls were reported by Hannay et al. (2013). These detections were made off Cape Lisburne in August 2010, ~100 nm from our mooring line, and a month before our recorders were deployed.

Minke whales

The story for the minke whale mirrors that of the humpback; they are sighted infrequently by visual and vessel surveys (Aerts et al., 2013; Clarke et al., 2013; this study - see Section VII.B.2), and passive acoustic detections are rare. We had only one day with calling activity from minke whales, 19 October 2011. The call type detected was the boing call (Rankin et al., 2005). Delarue et al. (2013b) found minke whale boing calls around the same time period in the same October/November time frame in 2009 and 2011 to the west of our moorings.

Ribbon seals

Although there was a lack of ribbon seal calling activity on our moorings, there was one detection found on 6 April 2011 (inshore). This is surprising due to what is currently known about their seasonal distribution in the Arctic. As summarized in Boveng et al. (2013), ribbon seals are strongly associated with sea ice in the Bering and Okhotsk Seas for reproduction (including whelping and nursing) and molting. The season for these activities extends from mid-March through June. Molting periods are segregated by age and reproductive status (Burns, 1981), with mature seals molting during the breeding season (beginning in late-April to early May and extending as late as July (Tikhomirov, 1961)). Ribbon seals do not form dense breeding aggregations, as females tend to be solitary and their breeding location is within the shifting ice front of the pack ice. They are not well adapted for maintaining breathing holes in the winter sea ice, and this restricts them to the part of the ice edge containing new, clean ice floes less than 20 m wide and of medium thickness. This part is never coastal but instead can extend up to 150 km from the southern edge of the ice. Ribbon seals are deep divers and prefer feeding on the continental shelf slope in the pelagic and demersal zones, when not limited by the distance of the ice edge from the slope. They prefer to feed on fish such as pollock and cod (Arctic, Pacific, and saffron), cephalopods such as squid and octopus, and crustaceans.

After they are finished with their reproductive/molting activities, ribbon seals leave the ice and spend the rest of their year at sea (Burns, 1981); remaining highly dispersed during the open-water season. To reiterate: ribbon seals do not remain on the ice until it recedes – they leave it once they are through with whelping, nursing, mating, and molting. There seems to be conflicting information as to where the ribbon seals go once the Bering and Okhotsk Seas are ice free. One view is that some of the seals move from the Bering into the southern Chukchi (with some of the Okhotsk seals moving into the Bering). Another view is that very few ribbon seals move through Bering Strait; they move instead to areas near the Bering Sea slope with high productivity such as the Pribilof Islands (Lowry, 1985). Recent satellite tagging efforts have found the real situation to be somewhere in between: about 30% of ribbon seals tagged in the central Bering Sea moved into the Arctic with the ice retreat and, during July-October, spent about 10% of their time budget there. Most of the tagged seals stayed in the Bering Sea, but not just near the slope: seals were tracked both on the shelf (including coastal areas) and in the basin, leading Boveng et al. (2013) to suggest that ribbon seals can thrive in a diversity of habitats and environmental conditions outside their ice-obligate activities time period.

Passive acoustics has detected ribbon seals on both the Bering Sea shelf and in the Arctic. Miksis-Olds and Parks (2011), found that the peak in ribbon seal calling in the southern half of

the Bering Sea shelf occurred from April to May, coinciding with the mating season. On both the Chukchi Sea shelf (Hannay et al., 2013) and basin (Moore et al., 2012) ribbon seal calling was detected in the late fall (October and November), which seems to fit timing-wise with their southbound return to the Bering Sea ice edge. Here we present calling activity in the northeastern Chukchi Sea that coincides with the timing of Bering Sea breeding season. As with the mid-winter walrus detection, it seems likely that the source of these calls are subadults that had no motivation to migrate down to the Bering Sea breeding grounds. As these calls are thought to be part of a reproductive/territorial display (Watkins and Ray, 1977), with this assumption it also seems likely that the presence of these sounds in the April Chukchi Sea are indicative of juvenile male practice sessions.

As for overall lack of ribbon seal calling activity on our recordings, if these calls are truly associated with reproductive displays, and these displays are limited to a small time period and limited to waters south of the Bering Strait, then it is logical to conclude that not many of these calls will be heard in the Arctic. In fact, Hannay et al. (2013) found only three ribbon seal detections between July and October over four years of recordings at 10-44 mooring locations per year. Although their overwinter detections of ribbon seals were greater, they were still confined to a small time window of less than ten days in 2008 and only four days in 2009. Their other two years (2007 & 2010) of overwinter recordings contained no detections of ribbon seals, the latter fitting within the time frame of the results presented here. Although Hannay et al. (2013) included puffing sounds in their analysis that we did not, Moore et al. (2012) also did not include puffing sounds, and so any differences in October/November call detections between studies is coincidental.

Other pinnipeds

Arctic pinnipeds make a variety of yelping, barking, grunting, growling, hissing, and roaring sounds (Jones et al., 2014). We did note the presence of these as unidentified pinniped, without unnecessarily delaying the rest of the analysis with trying to identify these sounds to species. Because these data are now flagged, it would not take much time to reprocess the data set and extract information on any of the additional pinniped species that may be of interest and have repertoires that are defined in the literature (i.e., ringed seals). The seasonal distribution of our unidentified pinniped sounds is near-year-round (see Figure C.10 in Appendix C), and occurred on all three mooring locations in both deployment years.

Environmental and anthropogenic sources

Seismic airguns

There were no surprises in the seasonal distribution of seismic airgun noise activity; these activities were confined to the open water season in both years of this study. In 2010 seismic airguns were detected on the long-term recordings at all three locations from the time the recordings started on 10 September to 1 October 2010. The timing of noise activity coincides with Statoil's 2D and 3D seismic exploration activities. The M/V *Geo Celtic*, under the direction of seismic contractor Fugro, completed almost 3,000 miles of seismic data acquisition (using a pair of 3000 in³ three-string arrays) in the Chukchi Sea in 2010, including participation in sound source verification trials (mitigation source gun: one 60 in³ airgun) conducted by JASCO

Research Ltd (Blees et al., 2010). The area they surveyed during these operations (Figure 14) was in very close proximity to our mooring line, and therefore the saturated levels of seismic airgun noise activity was expected. Shell did not conduct any deep water exploration in 2010 in either the Chukchi or Beaufort Seas, but did conduct some shallow hazard work in Harrison Bay in the Beaufort Sea September 13 through 9 October 2010, although some sound source verification work (again through JASCO Research Ltd) was conducted mid-August. It is not possible to distinguish between this survey and the one run on the M/V *Geo Celtic* with our current results; however, if doing so is of interest, this could be accomplished with further analysis. As with the unidentified pinniped, the data has already been flagged for the presence of seismic airgun noise, and so that time-consuming step in the process is already completed. There is a mention in Reiser et al. (2011) that the R/V *Mt Mitchell* conducted seismic airgun work in the Chukchi Sea from 10 October 2010 before reaching Dutch Harbor on 20 October 2010. This activity was not present on our recorders.

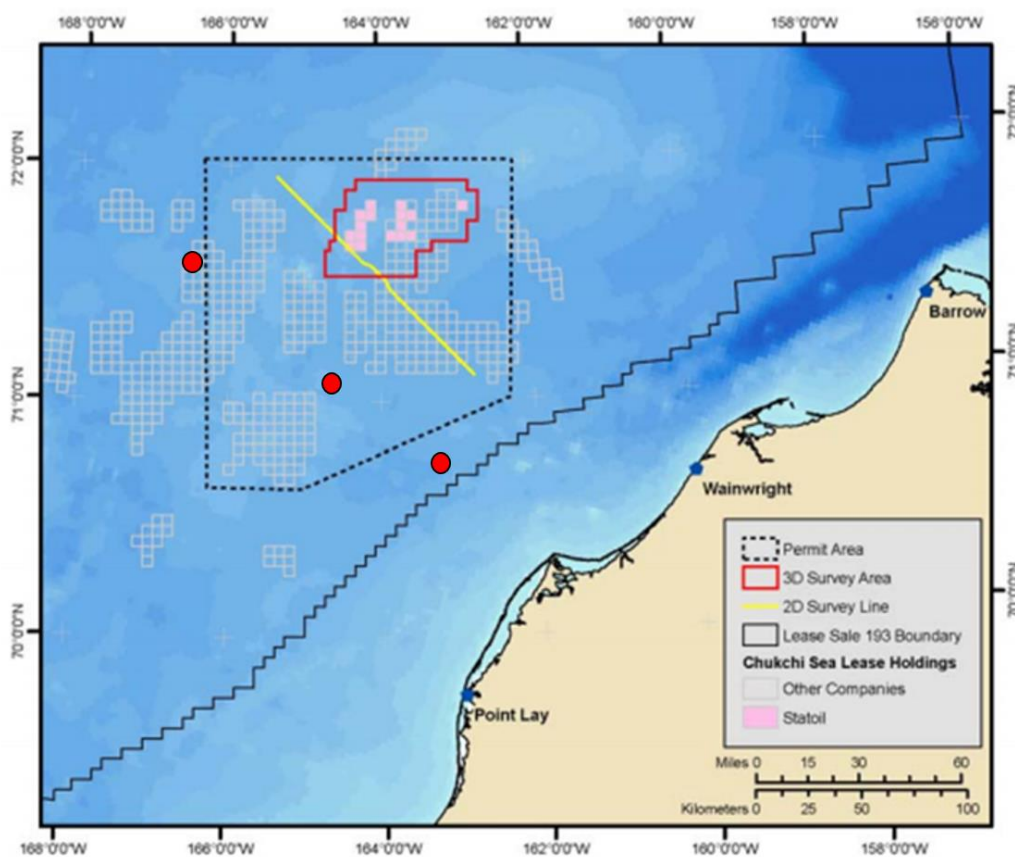


FIGURE 14. LOCATION OF PASSIVE ACOUSTIC RECORDERS (RED DOTS) IN RELATION TO AREAS OF INDUSTRIAL ACTIVITY. FIGURE MODIFIED FROM BLEES ET AL., 2010 (FIGURE 2.1).

Although the time period (beginning of recordings at beginning of September to mid-October) where airgun sounds were detected were the same between 2010 and 2011, the levels of seismic airgun noise activity in 2011 were much more sporadic and lower. The seismic surveying conducted in 2011 was limited to shallow hazard site surveys in the Statoil lease

blocks (Figure 15), to the northeast of our offshore and midshore recording locations (Hartin et al., 2011). The shallow hazards work was conducted using two clusters (one single and one 4-airgun) of 10 in³ airguns and covering nearly 3000 miles; this reduced effort explains the reduction in seismic airgun noise activity levels from 2010 to 2011, and also the higher levels at the offshore and midshore locations as compared with the inshore location. The second (smaller) pulse of airgun noise activity in early October 2011 cannot be explained by the timeline of Statoil activities, but could be due to other industry efforts in the Beaufort Sea or from scientific research efforts in the Chukchi or Beaufort Seas (Cameron et al., 2012).

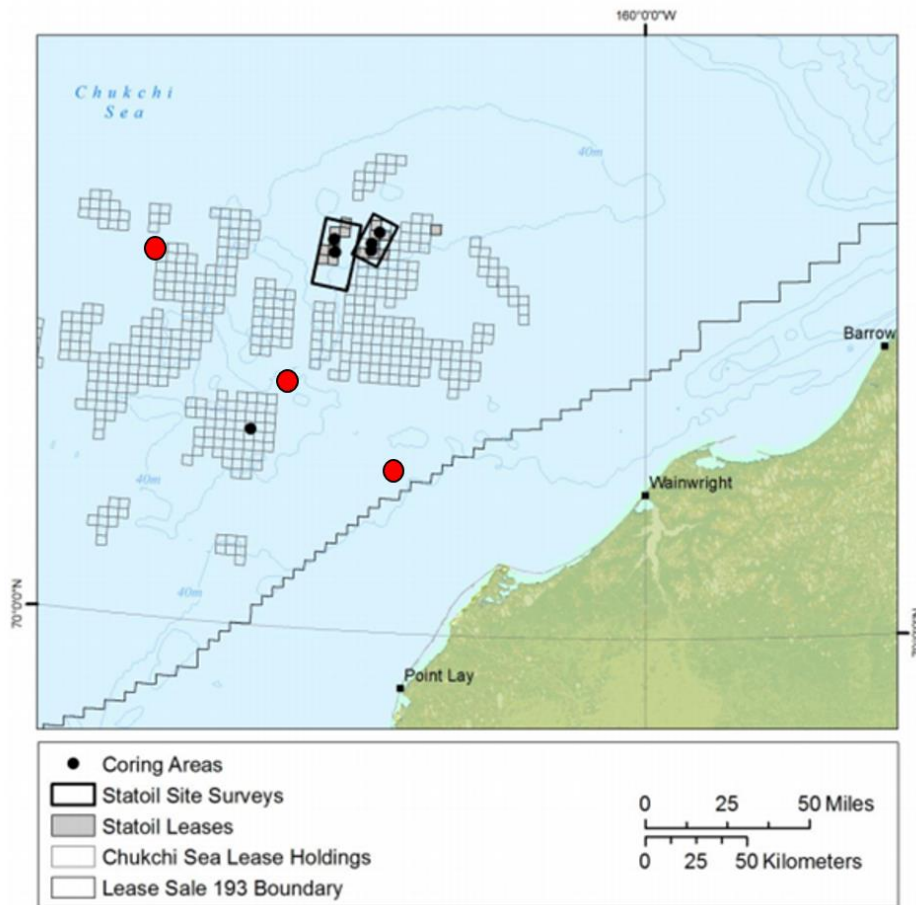


FIGURE 15. LOCATION OF PASSIVE ACOUSTIC RECORDERS (RED DOTS) IN RELATION TO AREAS OF INDUSTRIAL ACTIVITY. FIGURE MODIFIED FROM HARTIN ET AL., 2011 (FIGURE 2.1).

Vessel noise

The seasonal distribution of vessel noise coincides with the open water season, with a few notable exceptions. Most of the vessel noise occurred in September and October, consistent with the seismic airgun activities discussed above as well as with the field seasons of the various scientific studies (such as CHAOZ and CSESP) conducted in 2010 and 2011 (Hopcroft and Day, 2013). Vessel noise activity levels were much lower than those from the seismic activity, most likely because the lower level, less distinct, vessel noise signals were masked by the louder, more

ubiquitous, seismic noise. A second bout of vessel noise activity was seen at the midshore location the second half of November 2011, which corresponds to the presence of the USCGC *Healy* (C. Ashjian, pers. comm.).

There are two other instances with vessel noise activity detected outside of the expected open water season, 14-18 February 2011 at the midshore location and 7 December 2011 to 10 January 2012 at the offshore location. The first time period coincides with the peak in walrus calling activity at the offshore location. A Modis visible-band ice image (Figure 13a) shows the presence of long leads. Although no U.S. icebreakers were operating in the area at that time, the fact remains that there are 16 Russian icebreakers in operation (S. Moore, pers. comm.). The acoustic propagation conditions in the Arctic Ocean are well studied (Urick, 1983), with a surface duct present which permits long-distance propagation of sound, especially from sources near the surface. For these reasons, and from the fact that the sounds did not appear to be from nearby sources (C. Berchok opinion based on lack of distinct internal machinery sounds) we suspect that the vessel noise heard was from distant Russian icebreakers. As for the second bout of vessel noise at the end of 2011/beginning of 2012, there is no evidence to suggest this situation was any different.

Ice Noise

A very good summary of the characteristics of ambient noise from ice is provided in Urick (1983). Ice conditions, wind speed, snow cover, and air temperature are all factors that contribute to different qualities of the ice noise. For example, impulsive sounds are prominent during periods of cooling air temperature, while the noise has more of a Gaussian distribution during periods of warming air temperatures. Wind and currents can move the ice – causing collisions and sliding of the ice which can be impulsive or very tonal (e.g., Xie and Farmer, 1992). These tonal sounds may sometimes contain enough frequency modulation to be confused with bowhead and beluga whales unless care is taken to examine the sound within its full context – and by listening closely to the nuances in its character. Wind can also generate sound, even under full ice cover, through the pelting of ice granules on the ice surface.

In both deployment years, ice noise activity levels were highest at the inshore location. As this is the site closest to the fast ice boundary zone – a high energy area of constant upheaval between the landfast ice and the drifting pack ice. Other than a small pulse of ice noise activity in the first half of November, 2010, at all three locations, the rest of the seasonal distribution of the ice noise seems to be randomly patterned. Similar seasonal distributions were seen in both deployment years, with the ice noise typically starting in November and ending around May. Exceptions included an earlier end date at the midshore location in 2011 and a later end date at the inshore location in 2012. However the 2012 inshore recorder actually lasted for the entire deployment and may be better representative of the real seasonal patterning of the ice noise. Analysis of data from these locations from the BOEM-Funded ARCWEST and CHAOZ-X projects (with their full years of recordings) will help accurately determine this seasonal distribution. In addition to Section X.3, further discussion of ice noise can be found in the Noise Modeling Section (Section XII.3).

4. *Conclusions*

Generally, the seasonal and spatial distributions of sounds from the five main Arctic marine mammal species (bowhead, beluga, and gray whales, walrus, and bearded seals), the five subarctic species (fin, killer, humpback, and minke whales, and ribbon seals), anthropogenic sources (airguns and vessel), and environmental (ice) sources were within the expected ranges and were in agreement with past aerial survey and/or other passive acoustic results. The implication of this, for most of the biological sources, is that calling rates are sufficiently high enough that calling activity levels can be used as a proxy for species presence. The recording period for this study was September 2010 through September 2012.

The fall and spring migrations were detected for both bowhead and beluga whales. The fall bowhead migration was seen at equal levels of calling activity at all three recording locations, while calling activity from the spring migration was constrained mainly to the inshore location. Bowhead whales are known to follow leads as they migrate east toward their summer feeding grounds in the Canadian Arctic. Their westward migration in the fall is well known to fan out through the Chukchi shelf. In addition to describing this general migration timing we found two other aspects worth noting for the bowhead whales. First, we saw three distinct peaks in the fall migration that agree with the age/sex segregation of migrating bowheads known from traditional knowledge and aerial biometric studies. Second, our more fine-scale analysis of bowhead calling has revealed that the gunshot calling activity occurs near the end of each of the peaks of regular bowhead calling activity. Further analyses are planned to examine these results in more detail.

The fall and spring migrations for beluga whales were detected at all three recording locations. In general, calling activity levels for each recording location were slightly higher in the spring; higher levels were seen at the inshore location than at either the midshore or offshore locations. Beluga whales are known to associate with bowhead whales during the spring migration east, although the presence of calling activity at the midshore and offshore locations agrees with results from satellite tagging and other passive acoustic studies that show that they are not limited to the inshore leads in the spring. Calling activity from their fall migration is present at all three locations, but skewed to the inshore location, showing that although they do travel throughout the Chukchi shelf, they are not quite as evenly distributed across the shelf as are bowhead whales. Peaks in beluga calling activity have been noted and work is well underway to define the acoustic repertoires within each peak, with the eventual goal of using passive acoustics to discriminate between the eastern Beaufort Sea and eastern Chukchi Sea populations.

The very low calling rates of gray whales make them a difficult species to study using passive acoustic techniques. However, because we analyzed our data fully, we were able to see small pulses of low-level calling activity corresponding to their fall and spring migrations that were not seen on the results from the industry recorders. This calling activity was limited mostly to the inshore recording location, which was about 15 nm further offshore than the bulk of aerial survey sightings from the Chukchi Sea. We did not find any overwinter calling activity. With the placement of additional long-term recorders along the Chukchi coast for the BOEM-funded ARCWEST project, we should be able to build upon the results presented here and form a clearer picture of the movements of this species.

The high levels of walrus calling activity overwinter at our offshore location in both years was highly unexpected and have not been described in any published study to date. We suggest that the animals heard during this time period are subadults that remained in the Arctic for the winter instead of migrating to the mating grounds. Further investigation of ice images and walrus satellite tagging results will be pursued in the near future. Otherwise, the timing of the other calling activity on our recorders corresponds well with what is known about their spring and fall migrations.

Bearded seal calling activity was so ubiquitous and at such high levels that it occasionally masked other sounds and frankly was the bane of our analysts' existence, especially during the analysis of recordings for bowhead and beluga calling. Our results agree well with those from other passive acoustic studies. Year-round calling activity is present, with low levels in the summer, a small peak in the fall, and a large escalation to saturated levels between late February and mid-April (corresponding to the whelping/mating/molting season).

Several subarctic species had very low levels and short periods of calling activity, as was expected. Killer whale calling activity was found on seven days of recordings over the two years of this study. The timing of this calling activity, in early fall and late-spring, suggests a possible connection to migration. However, the ecotype most likely making these calls is the transient (marine mammal eating) ecotype, which is known to range throughout Alaskan waters, and so the timing found here might be tied to the gray whale migration. We had only one day with minke whale calling activity, the timing and location of which is in good agreement with that from other passive acoustic studies. Although we had only one day with ribbon seal calling activity, this activity occurred in April. This is surprising as this population should be south of the Bering Strait at this time of year. As with the walrus, it is most likely that this calling activity represents subadult animals that were not motivated to migrate south to breed.

No fin or humpback whale calling activity was detected during this study. Detections of these species, as reported from other passive acoustic studies, have been limited to the region off Cape Lisburne which is far to the west of our recorders. Aerial and ship-based studies have also found these species to be rare in the study area. We did not detect any calling activity from North Pacific right whales or sperm whales, as expected. Finally – we did not have any detections of ringed seals because we did not include that species in our analysis. We have, however, flagged results for unidentified seals in the data, and could produce seasonal distribution for this species with just a small amount of additional time.

This study illustrates the utility of passive acoustics to monitor marine mammal populations both spatially and temporally over large geographic regions. The results obtained from this study were in good agreement with those from aerial and vessel surveys, satellite tagging efforts, and other passive acoustic studies, as well as the natural history of these species obtained from TEK. The position of this mooring line between the Burger, Klondike, and Statoil lease areas, and relative to the industry recorders is optimal. The fact that we obtained such comparable results using just three mooring locations demonstrates the importance of this Icy Cape mooring line for monitoring marine mammals (as well as anthropogenic sources) in the Chukchi Sea lease area.

5. Recommendations

Long-term, year-round, monitoring of marine mammal populations is essential for understanding their distribution and behavioral ecology, particularly in the Alaskan Arctic where the environment is undergoing rapid modification as a result of climate change. Continuing to challenge what is currently known about marine mammal distribution in this area is vital, as assumptions - based on data obtained before the dramatic changes in sea ice extent were seen - may be outdated. Passive acoustic monitoring provides an excellent platform for monitoring marine mammals year-round, especially given the inaccessibility of the area for the majority of the year. Not only can we monitor year-round, we can (with careful placement of recorders) cover a large geographic region, allowing large-scale migration and movement patterns to be documented for the majority of marine mammal species present in the Arctic. Furthermore, the cost of supplies for turning around our recorders is incredibly inexpensive, making continued maintenance of this very valuable long-term dataset quite cost effective. Even if funds are not available for analysis at the current time, there is always the chance they will be in the future. Passive acoustic data do not have an expiration date; the more passive acoustic data that are available the better that trends can be identified. Therefore, our strongest recommendation is to continue to fund deployments and retrievals of these recorders, as well as facilitating vessel sharing to keep sea time costs at an equally reasonable level.

The addition of CPOD echolocation loggers to the passive acoustic moorings would allow us to detect echolocation clicks of foraging belugas. Although these instruments are currently unable to last a full year on a duty cycle, further advancements in their development may eventually allow for year-round recording. This would not only increase beluga whale detectability, but also enhance our knowledge of beluga habitat use.

One thing that was apparent during analyses of this data set, is that not much is known about the current ecology of these species in their wintering grounds in the Bering Sea. Recorders that have been deployed for the BOEM-funded ARCWEST project during our transits between Nome and Dutch Harbor, AK have collected a robust data set that can be analyzed to obtain more information from this area and season. We recommend making analysis of these data a priority so that better inferences can be made for the migratory patterns of these species.

We have developed a method for manually analyzing these acoustic data *fully*, and in as short a time period as possible. This effort is still time-consuming, but necessary, given the poor performance of auto-detection algorithms with the chaos³ of Arctic species sounds present in the Chukchi Sea. With the inevitable encroachment of subarctic species, the auto-detection problem becomes increasingly more difficult. Still, if auto-detectors can be developed that perform reasonably well, passive acoustic analyses will become orders of magnitude less expensive. These auto-detectors are also of critical importance for passive acoustic monitoring from other platforms such as auto-detection buoys (see Section XII) and autonomous gliders. For these reasons we recommend further funding of auto-detection techniques and equally importantly - comparison of these results with data sets fully reviewed by experienced analysts. We will continue to collaborate with M. Baumgartner (LFDCS, WHOI), C. Clark (Cornell Bioacoustics

³ This cacophony of Arctic sounds was the reason behind the naming of the CHAOZ project.

Research Program), and X. Mouy (JASCO Applied Sciences) to further develop our auto-detectors.

Great strides in the use of passive acoustics to determine the relative abundance of marine mammals have been made in the past several years (see Section XII). We recommend that these techniques be made a priority so that more information can be obtained from these archival passive acoustic recordings.

Finally, as mentioned in the conclusions above, there are a few interesting results from this study that should be examined further, namely, the multiple peaks seen in the bowhead and beluga whale migrations, and the timing of the bowhead gunshot call type within the main bowhead calling peaks. These analyses are either well underway for the BOEM-funded ARCWEST and CHAOZ-X projects, or they will be relatively soon.

B. Shipboard Observations

1. Methods

Sonobuoys

During the 2010-2012 CHAOZ field survey cruises, sonobuoys were deployed every three hours to obtain an evenly sampled cross-survey census of marine mammal calling. However, when in areas of high whale density, or when trying to localize on a calling species of interest, multiple sonobuoys were deployed more frequently to obtain near-continuous recording.

A sonobuoy is a free-floating, expendable, short-term passive acoustic listening device that transmits signals in real time via VHF radio waves to a receiver on a vessel or aircraft. The hydrophone is suspended down from the surface float at a programmable depth. Given that the minimum programmable deployment depth (61 m) of the sonobuoy exceeds that of the shallow Chukchi Sea shelf (~40 m), modifications were made by tying up sections of the sonobuoy housing to prevent the main wire spool from deploying (Figure 16). These modifications, which do not impact the signal transmission, resulted in a deployment depth of approximately 24 m, placing the hydrophone array at approximately 22 m, or mid-water column. Additional modifications involved replacement of the 9V display battery so that the sonobuoys could be programmed prior to deployment.



FIGURE 16. MODIFICATIONS OF A 77C SONOBUOY (TOP ROW, LEFT TO RIGHT): CUTTING OFF THE BOTTOM SECTION OF STRING AND REATTACHING IT TO THE WEIGHT; TAPING UP THE BOTTOM ARRAY OF SENSORS; A 77C SONOBUOY FULLY MODIFIED. (BOTTOM ROW) MODIFICATIONS OF 53E SONOBUOYS BY TYING UP CABLE TO SHORTEN THE DEPLOYMENT DEPTH: (LEFT) SPARTON 53E; (RIGHT) USS 53E.

Three types of sonobuoys were used over the three field seasons: omnidirectional only (57B), DiFAR only (77C), and programmable DiFAR/Omnidirectional (53D, 53E, 53F, 57B). DiFAR (Directional Frequency Analysis and Recording) capable sonobuoys transmit signal bearing information along with the acoustic signal. If two or more DiFAR sonobuoys are deployed, cross-fixes can be obtained on a calling animal to determine its location. When in DiFAR mode, the maximum frequency is limited to 2.5 kHz, thus the 53F sonobuoys were deployed occasionally in omnidirectional mode to achieve full bandwidth when it was not important to get a bearing to the calling animal.

The sonobuoy monitoring station (Figure 17a) was located in the bridge of the vessel, which allowed the acoustic technician to interact with the captain and visual observation team, and to make simultaneous visual and acoustic observations when needed. The signals transmitted from the sonobuoys were received by one of two preamplified antennas, an omnidirectional and a directional (Yagi) antenna. Both antennas (and preamps) were placed up

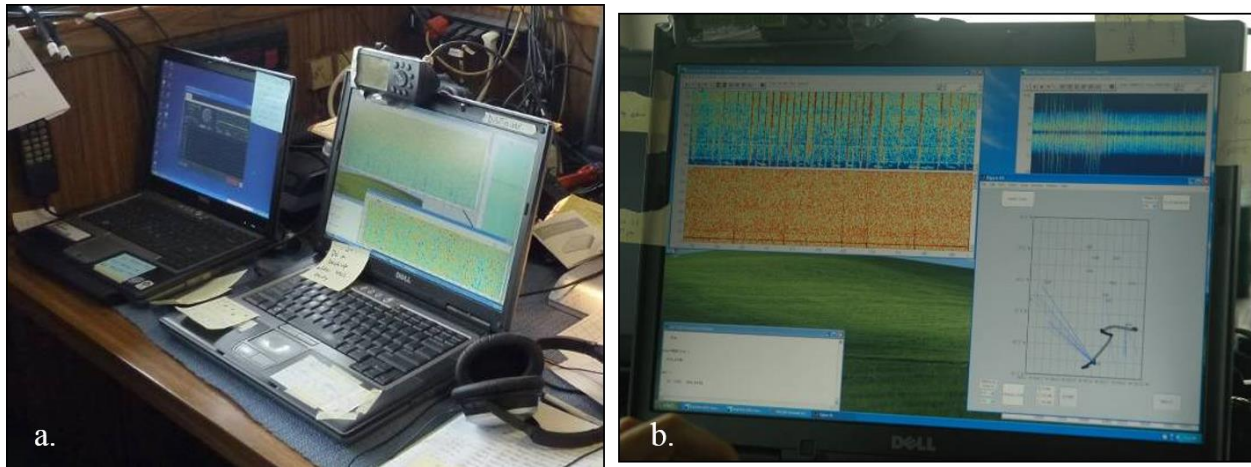


FIGURE 17. SONOBUOY MONITORING STATION (A). CUSTOM DESIGNED DIFAR TRACKING AND MONITORING PROGRAM (B).

in the crow's nest of the vessel with the directional antenna facing astern (Figure 18). The Yagi was used primarily during transit when the sonobuoy was guaranteed to be behind the vessel, and the omnidirectional antenna was used for monitoring multiple sonobuoys simultaneously, or when other shipboard scientific operations caused the sonobuoy to not be directly behind the vessel. A switch located in the bridge next to the acoustic station was used to alternate between antennas depending on the direction of travel. In-air reception range was approximately 10-12 miles when using the omnidirectional antenna. Reception range increased with the directional Yagi antenna, with an average of 14 miles, and a maximum of 18 miles. The age of the sonobuoy, its transmitting RF channel, and sea state ultimately determined reception range. It is important to note the difference between the in-air reception range (sonobuoy to antenna) and underwater sound propagation range (animal to sonobuoy). The underwater sound transmission range to the sonobuoy was estimated to be (at this time of year and in this study area) a radius of approximately 10-15 nm. Under the best conditions, with an average cruising speed of 9 kts, the 15 nm radius around the deployed sonobuoy could be monitored for up to an hour and a half. When the next sonobuoy was deployed three hours later, its 15 nm radius would just touch that of the previous one. So although there are temporal gaps in the sonobuoy coverage, the spatial coverage was near-complete.



FIGURE 18. OMNIDIRECTIONAL AND YAGI ANTENNA PLACEMENT (A) IN RELATION TO THE R/V *AQUILA* AND (B) IN RELATION TO EACH OTHER ON THE CROW'S NEST.

The signals received by the shipboard antennas were then pre-amplified (15dB; PV160VDA, Advanced Receiver Research, Burlington, VT), before being sent via cabling to up to three G39WSBe WinRadio sonobuoy receivers, then inputted into a MOTU brand Ultralite mk3 multi-channel external soundcard. The soundcard digitized the signal at a sampling rate of 48 kHz, which resulted in an audio frequency range up to 2.5 kHz for DiFAR and 24 kHz for omnidirectional sonobuoys. The external soundcard was connected to a laptop computer where the recordings were monitored in real-time using ISHMAEL (Mellinger 2001) software. Directional bearing information of calls was obtained using DiFAR demultiplexing software and a custom MATLAB interface (Greeneridge Sciences, Inc. and Mark McDonald, Whale Acoustics). A GPS feed into the computer provided the ship's position every minute, as well as the sonobuoy deployment location information, and time. A custom tracking and plotting program implemented in MATLAB (Catherine Berchok; Figure 17b) allowed for real-time plotting of the vessel and sonobuoy locations, as well as bearing and location coordinates of calling whales. All data were simultaneously recorded to an external hard drive.

Visual surveys

Vessel surveys were conducted in the Bering, Chukchi, and Beaufort Seas during the summers of 2010-2012. Visual operations were conducted to document the presence and distribution of all marine mammals encountered throughout the survey when transiting to mooring locations and sampling stations. Photographs were collected (namely North Pacific right, humpback, gray, and killer whales) on an opportunistic basis. Given the remote location and paucity of survey effort in a large portion of the areas, any information on distribution would provide an invaluable contribution to existing scientific knowledge.

Shipboard visual survey methods were applied during daylight hours and under acceptable survey conditions (Beaufort Sea state 5 or lower). A rotating team of three scientists (two on watch, one at rest position) collected sighting data using standard line-transect methods

during on-effort status. Operations began at 08:00 and ceased at 20:00, or as long as conditions would allow. A full observation period lasted 80 minutes (40 minutes in each position) and was followed by a 40 min rest period. One observer (port) was stationed on the ship's bridge wing. The observer used 25x 'big-eye' binoculars (Figure 19) with reticles to scan from 90° port to 90° starboard. The data recorder was positioned on the bridge and surveyed the trackline with 7x50 binoculars while scanning through the viewing area of the primary observer. When a sighting was detected, the primary observer conveyed to the recorder the horizontal angle and number of reticles from the horizon to the initial sighting. Additional information collected was sighting cue, course and speed, species identity, and best, low, and high estimates of group size. The computer program WINCRUZ (<https://swfsc.noaa.gov/uploadedFiles/Divisions/PRD/WinCruz.pdf>) was used to record all sighting and environmental data (e.g., cloud cover, wind speed and direction, and sea conditions).

On-effort status was defined as a visible horizon, Beaufort Sea state 5 or lower, and survey speed of ~9 knots. Under unacceptable weather conditions (no visible horizon and/or sea state 6 or greater), surveying continued in an off-effort status. When weather deteriorated (visibility ≤ 0.5 nautical miles (nm) and/or taking spray over the bow), off-effort watches were conducted on the bridge by one observer/recorder. This was mainly to monitor weather changes and notify when conditions improved as well as to record off-effort sightings.



FIGURE 19. MARINE MAMMAL OBSERVER USING 25X “BIG-EYE” BINOCULARS.

2. *Results*

A summary of the combined visual and passive acoustic effort during the 2010-2012 CHAOZ field surveys is shown in Figure 20 and Table 9-10. The results presented here are centered on the Alaskan Chukchi Sea, from Point Barrow, AK down to the Bering Strait. This area also extends slightly eastward into the western Beaufort Sea to Cape Halkett, AK. For full

survey coverage results, which include the visual and acoustic effort undertaken on the transit legs through the Bering Sea, please see Appendix D.

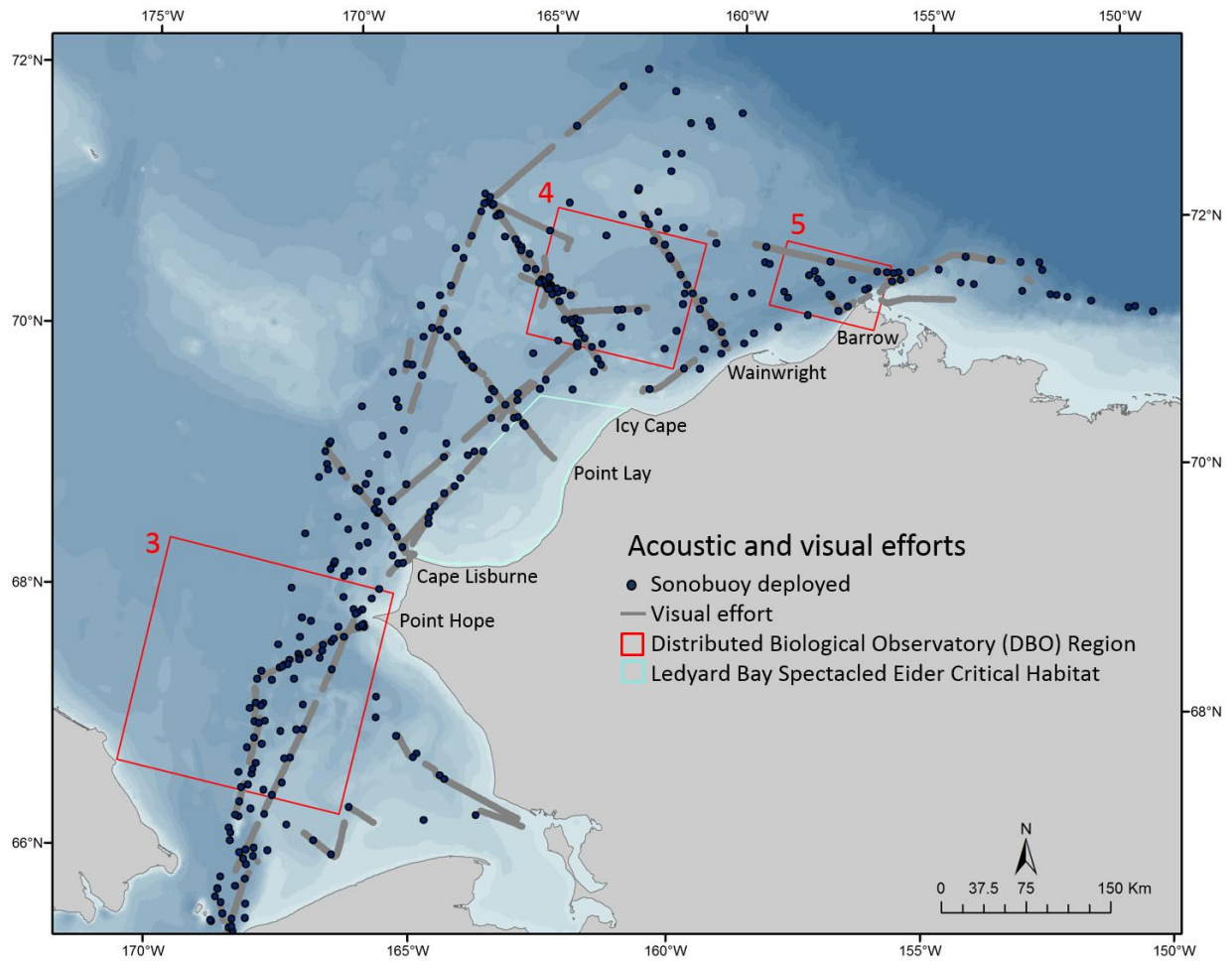


FIGURE 20. SUMMARY OF COMBINED VISUAL AND ACOUSTIC EFFORT, 2010-2012. GRAY LINES = VISUAL EFFORT, BLACK DOT = SUCCESSFUL SONOBUOY DEPLOYMENT.

TABLE 9. TOTAL NUMBER OF SONOBUOYS DEPLOYED PER YEAR IN THE ARCTIC AND THE SUCCESS RATE, 2010-2012.

Year	Deployed in Arctic	Successfully deployed	Success rate
2010	110	102	92.7%
2011	104	91	87.5%
2012	101	91	90.1%
Total	315	284	90.2%

TABLE 10. SUMMARY OF VISUAL TRACKLINE EFFORT FOR ARCTIC WATERS ONLY AND COMBINED ARCTIC WATERS AND BERING SEA, CHAOZ, 2010-2012.

Year	Arctic waters only		Arctic waters and Bering Sea	
	Km	Nm	Km	Nm
2010	1,061	573	1,582	854
2011	1,118	694	2,566	1,385
2012	549	296	1,226	662
Total	2,728	1,563	5,374	2,901

The total number of sonobuoys deployed per year and their success rate is shown in Table 9, and sonobuoy deployment locations and species detected are presented in Figure 20-28. A total of 259 sonobuoys were deployed during the 2010 cruise, of which 110 were deployed in the Arctic. Of these, 57 were modified (taped and tied) Sparton (SPW) 77C's, 48 were SPW 53F's, and 5 were 57B omnidirectional buoys. A total of 246 sonobuoys were deployed during the 2011 cruise, of which 104 were deployed in the Arctic. Of these, 19 were modified (taped and tied) SPW 77C's, 40 were SPW 53F's, 40 were modified (tied and battery replaced) Undersea Sensor Systems (USS) 53E's, and 5 were Hermes Electronics (HEE) 57B omnidirectional buoys. A total of 227 sonobuoys were deployed during the 2012 field survey, of which 101 were deployed in the Arctic. Of these, 22 were modified SPW 77C's, 23 were 53D's (21 USS, 1 SPW, 1 Magnavox [MAG]), 11 were 53E's (10 HEE, 1 SPW), 41 were UND 53F's, and 4 were 57B (3 MAG, 1 SPW). In total, six cetacean species (bowhead, gray, humpback, fin, minke, and killer whales), and two pinniped species (walrus and bearded seal) were detected in the study area (Figure 21-26; Appendices C, D).

Over the three year study, a total of 1,563 nm (2,728 km) of on-effort trackline was surveyed in Arctic waters and a total of 2,901 nm (5,374 km) for Arctic and Bering Sea combined (Table 10, Figure 20). Seven cetacean species, five pinniped species and a polar bear were documented within the survey area (Figure 20-26).

We present the results here in order of most commonly sighted to least commonly sighted. The most commonly sighted and/or acoustically detected species were bowhead whales, gray whales, walrus, and bearded seals (Figure 21-28). Bowhead whales were seen or acoustically detected in all three years, although there were no visual sightings in 2011 (Figure 21). There were no acoustic or visual detections south of Wainwright, and the majority of visual detections were concentrated around the Barrow Arch area. Gray whales were sighted in two main concentrations: off Barrow, AK in all years, and in the southern Chukchi in 2010 (Figure 22). Most acoustic detections of gray whales occurred between Icy Cape and the Barrow Arch, with one acoustic detection near the Bering Strait in 2010. Walrus were ubiquitous throughout the study area for all three years, with most sightings and acoustic detections in the northeastern Chukchi Sea, offshore of Icy Cape and Wainwright (Figure 23). Acoustic detections occurred as far south as the Bering Strait. In 2012, there was a concentration of walrus sightings off the Barrow Arch. Bearded seals were sighted regularly in all three years, although there were no

acoustic detections (Figure 24). Most sightings were in the northeastern Chukchi Sea between Icy Cape and the Barrow Arch, although there was a concentration of sightings in 2011 between Point Hope and the Bering Strait.

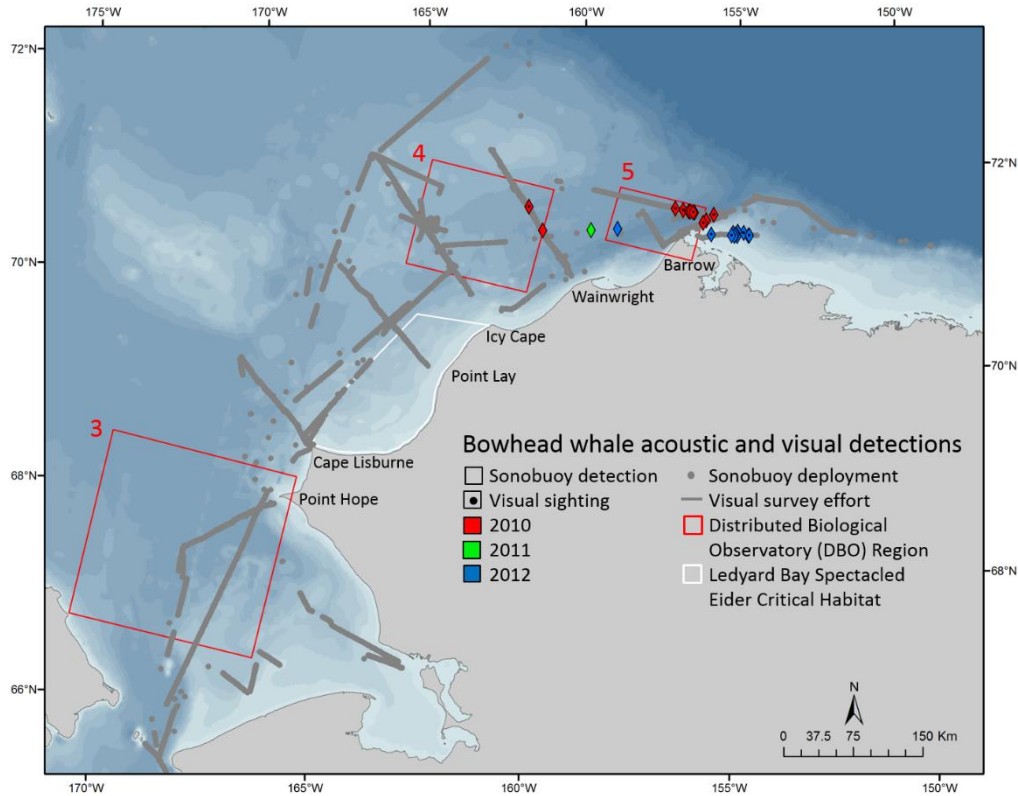


FIGURE 21. BOWHEAD WHALE ACOUSTIC AND VISUAL DETECTIONS DURING THE 2010-2012 CHAOZ SURVEYS.

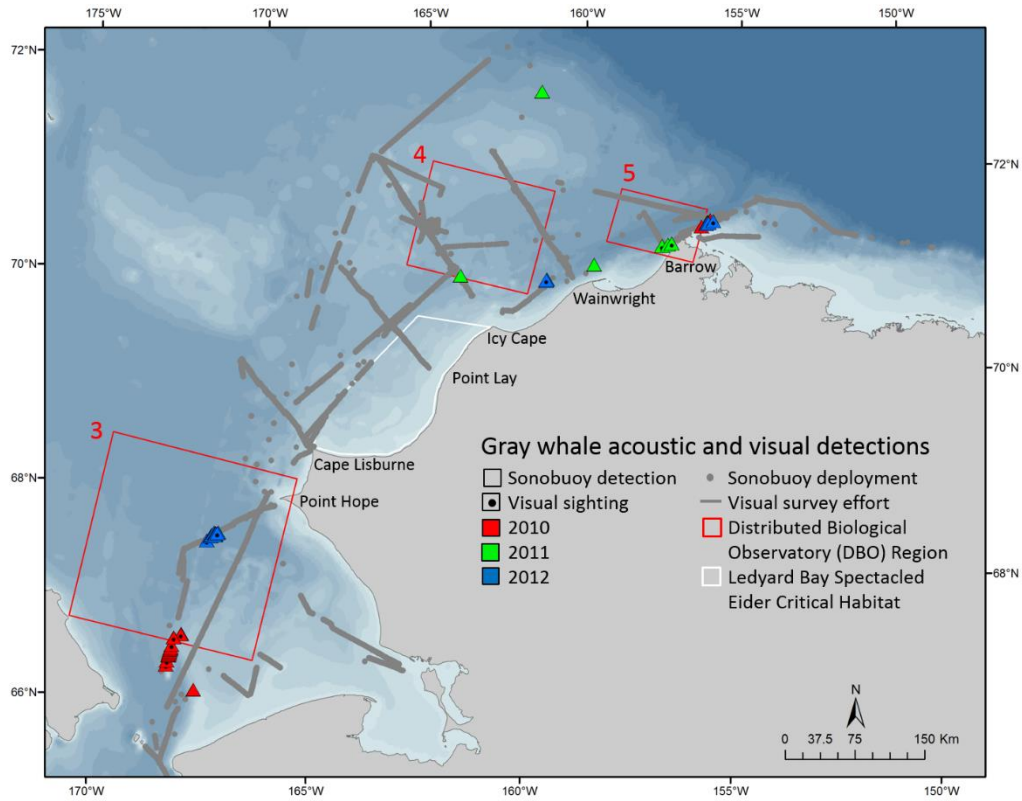


FIGURE 22. GRAY WHALE ACOUSTIC AND VISUAL DETECTIONS DURING THE 2010-2012 CHAOZ SURVEYS.

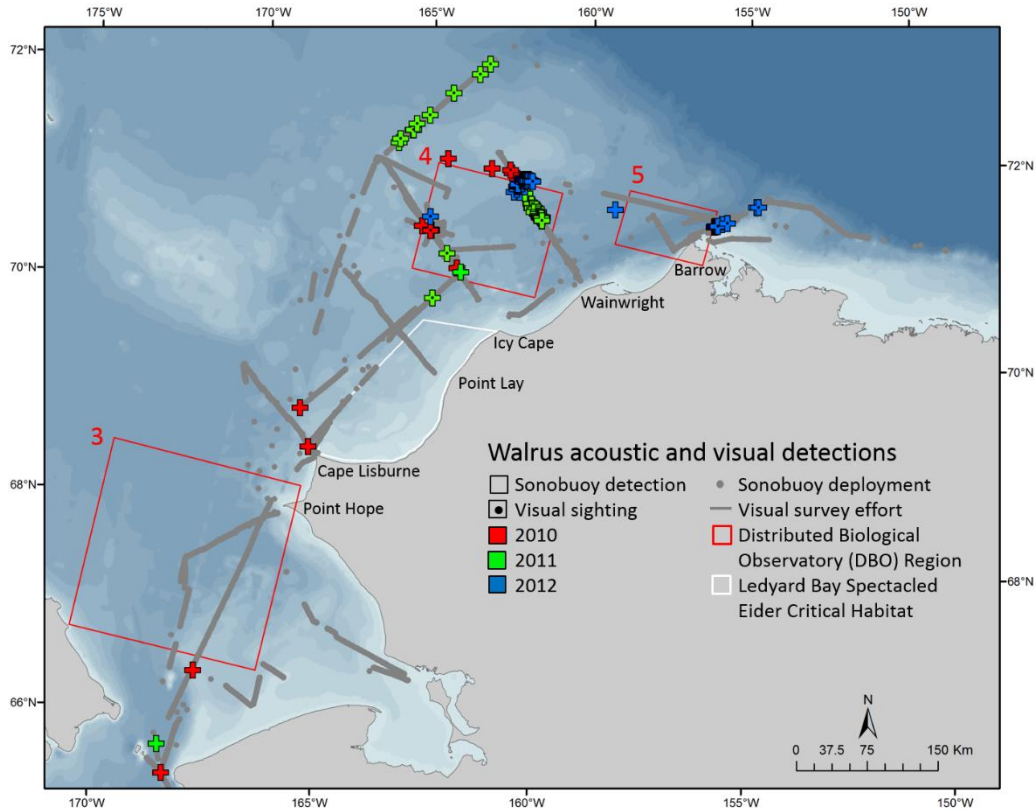


FIGURE 23. WALRUS ACOUSTIC AND VISUAL DETECTIONS DURING THE 2010-2012 CHAOZ SURVEYS.

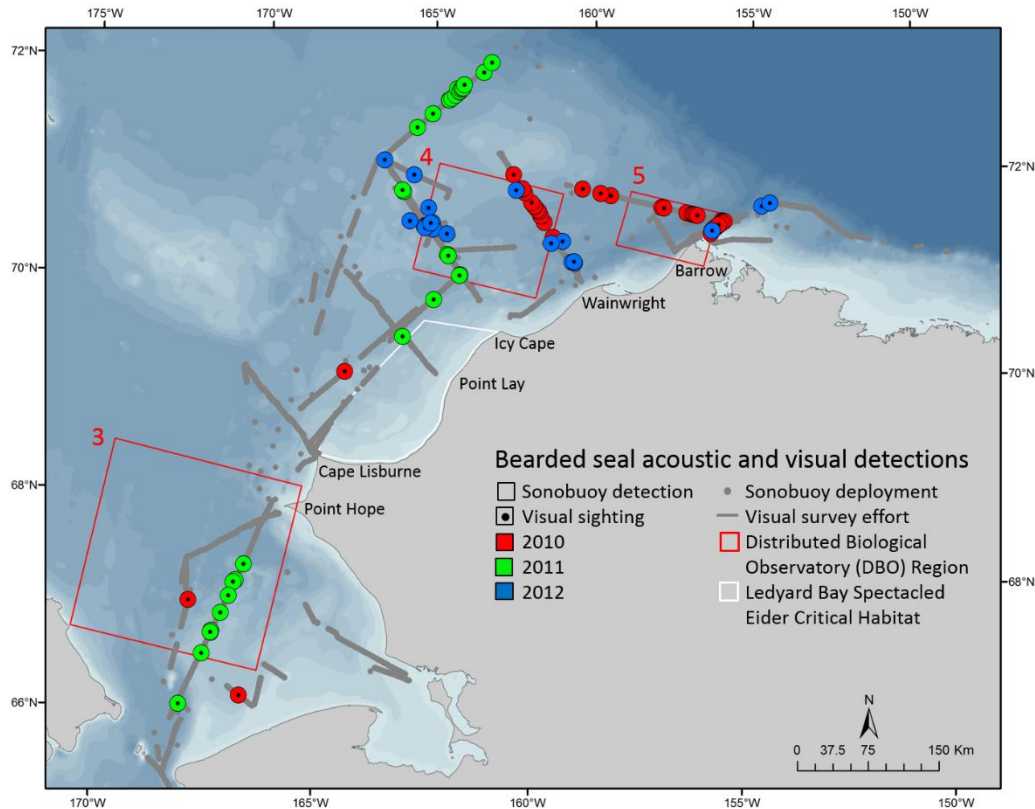


FIGURE 24. BEARDED SEAL ACOUSTIC AND VISUAL DETECTIONS DURING THE 2010-2012 CHAOZ SURVEYS.

Fin and humpback whales were often sighted and acoustically detected in the southern Chukchi; however, they were detected only acoustically north of Point Hope (Figure 25-26). One fin whale was detected acoustically off Barrow Canyon in 2012; this detection currently represents the farthest northeast report of a fin whale in the Alaskan Arctic (Figure 25; Crance et al., 2015). Killer whales were detected acoustically on two occasions: once in 2010 near Bering Strait, and once in 2012 off Point Hope (Figure 27, circles). They were never sighted in the Chukchi Sea in any of the three years of this study. Minke whales were sighted and acoustically detected on three occasions in 2010 in the southern Chukchi (two visual sightings, one acoustic detection), and were sighted only once in 2012 off Icy Cape (Figure 27, triangles). Harbor porpoise were sighted from the Bering Strait to north of Cape Lisburne in 2010, with one sighting off Icy Cape in 2011 and one off Barrow in 2011 (Figure 27, squares). There was one sighting of Dall's porpoise in 2010 near the Bering Strait. Harbor porpoise and Dall's porpoise were not acoustically detected; their only vocalization type, echolocation clicks, are too high in frequency (110-150 kHz) to be detected on sonobuoys.

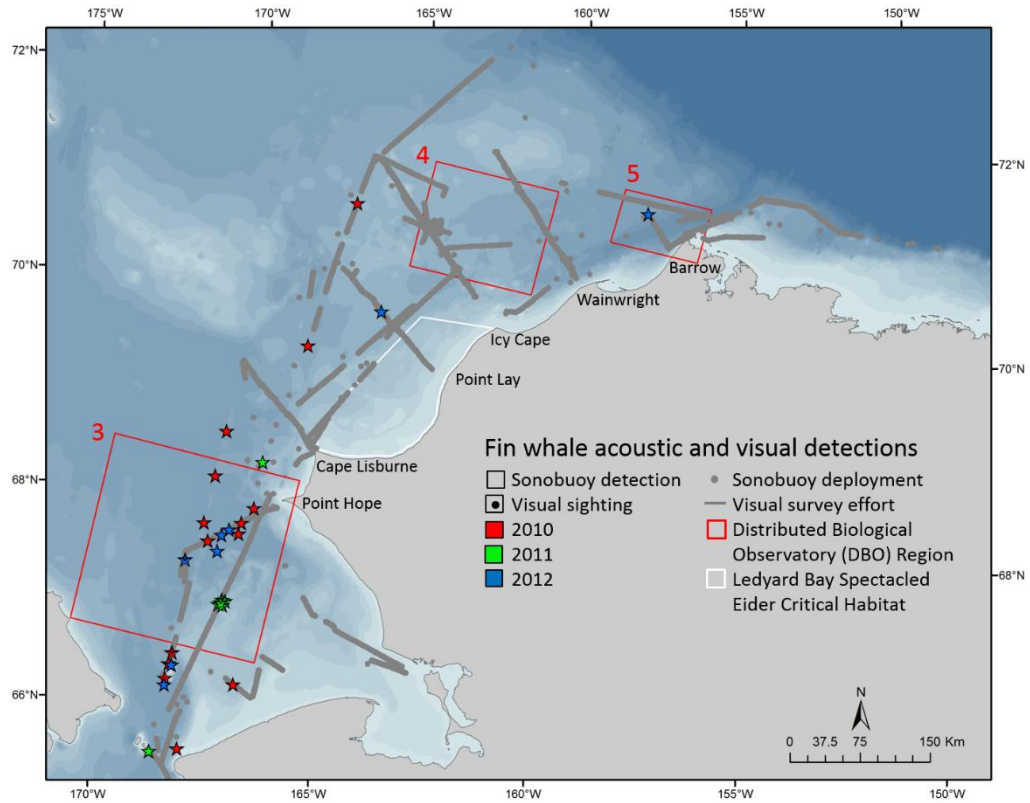


FIGURE 25. FIN WHALE ACOUSTIC AND VISUAL DETECTIONS DURING THE 2010-2012 CHAOZ SURVEYS.

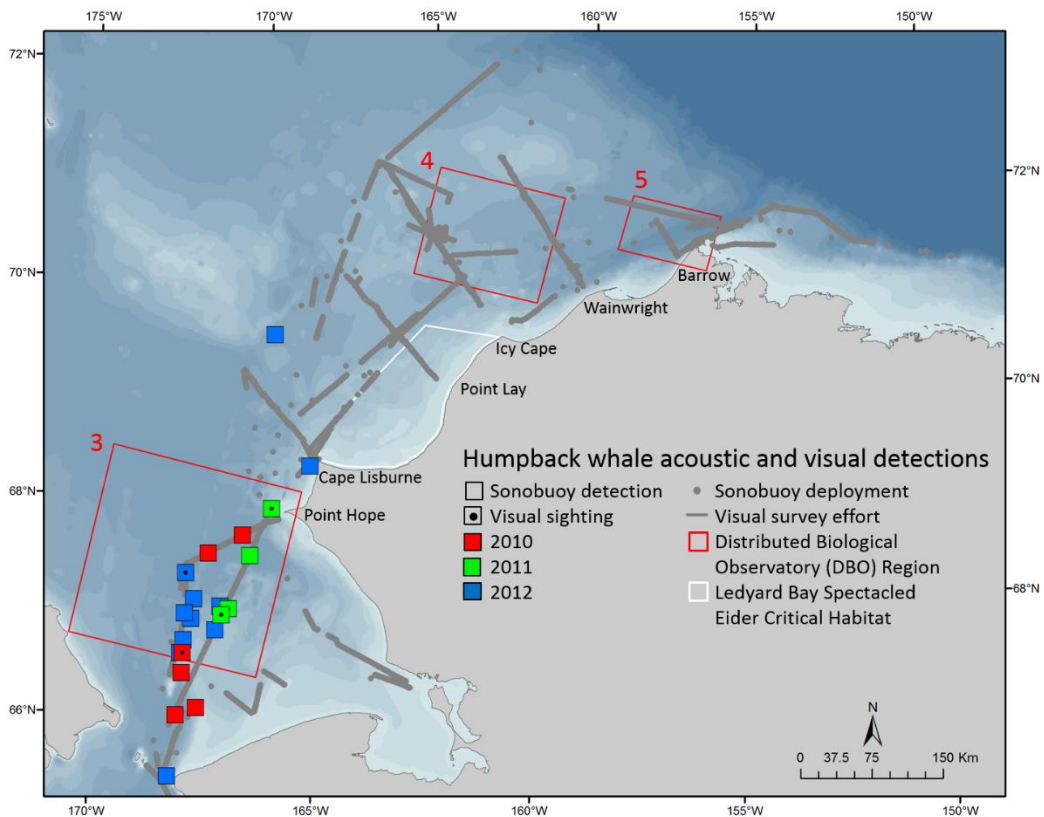


FIGURE 26. HUMPBACK WHALE ACOUSTIC AND VISUAL DETECTIONS DURING THE 2010-2012 CHAOZ SURVEYS.

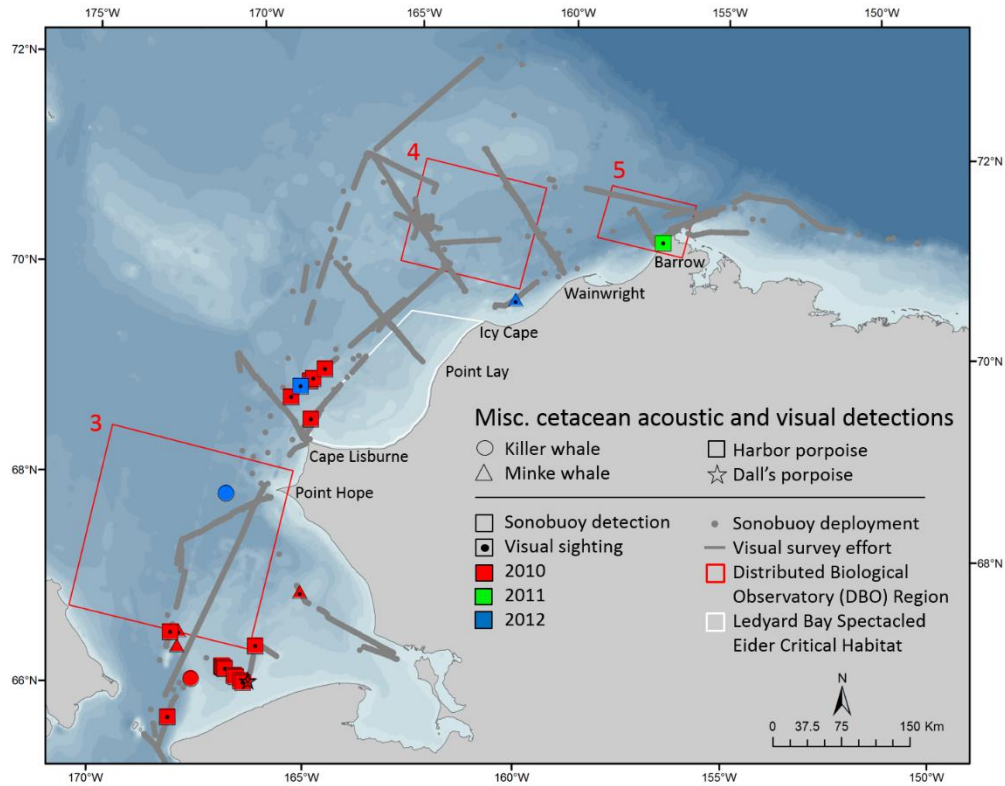


FIGURE 27. MISCELLANEOUS CETACEAN ACOUSTIC AND VISUAL DETECTIONS DURING THE 2010-2012 CHAOZ SURVEYS: KILLER AND MINKE WHALE, HARBOR AND DALL'S PORPOISE.

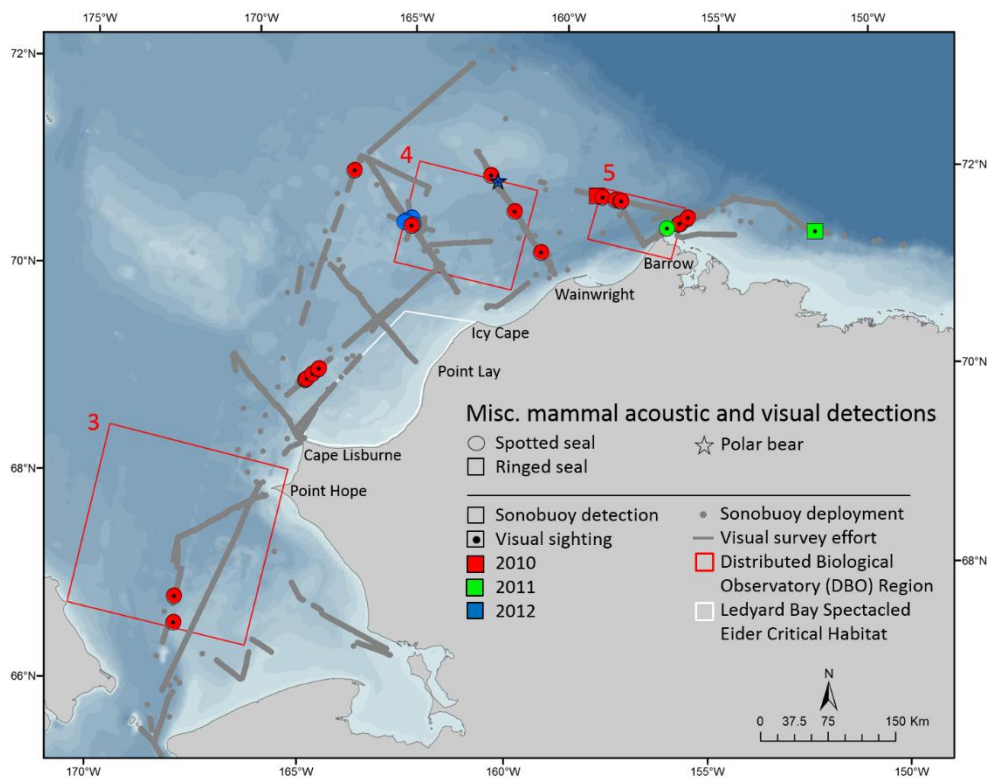


FIGURE 28. MISCELLANEOUS MARINE MAMMAL ACOUSTIC AND VISUAL DETECTIONS DURING THE 2010-2012 CHAOZ SURVEYS: SPOTTED SEAL, RINGED SEAL, AND POLAR BEAR.

Spotted seal visual sightings were ubiquitous throughout the study area in 2010, but were only sighted once in 2011 off Barrow and in one cluster off Icy Cape in 2012 (Figure 28, circles). There were only two sightings of ringed seals near Barrow, one in 2010 and one in 2011 (Figure 28, squares). However, a majority of the unidentified seals are likely either spotted or ringed; species identification was difficult to determine for animals in the water. One polar bear was sighted offshore of Wainwright in 2012 (Figure 28, star).

No belugas were detected either visually or acoustically, during any of the CHAOZ field surveys. There were also no sightings or acoustic detections of North Pacific right whales, ribbon seals, northern fur seals, or Stellar sea lions in the Alaskan Arctic.

TABLE 11. SUMMARY OF SIGHTINGS (NUMBER OF INDIVIDUALS) FOR ARCTIC WATERS, 2010-2012. ON, OFF = EFFORT STATUS.

	2010			2011			2012			<i>Grand Total</i>
	<i>On</i>	<i>Off</i>	<i>Total</i>	<i>On</i>	<i>Off</i>	<i>Total</i>	<i>On</i>	<i>Off</i>	<i>Total</i>	
Bowhead whale	7(12)	1(2)	8(14)	0	0	0	9(11)	1(3)	10(14)	18(28)
Bearded seal	36(39)	12(12)	48(51)	34(36)	0	34(36)	7(7)	4(4)	11(11)	93(98)
Dall's porpoise	1(1)	0	1(1)	0	0	0	0	0	0	1(1)
Fin whale	1(1)	0	1(1)	5(9)	0	5(9)	0	0	0	6(10)
Gray whale	15(17)	6(10)	21(27)	1(1)	2(3)	3(4)	0	4(4)	4(4)	28(35)
Harbor porpoise	15(20)	2(3)	17(23)	1(1)	0	1(1)	0	0	0	18(24)
Humpback whale	0	1(1)	1(1)	1(1)	2(2)	3(3)	0	0	0	4(4)
Minke whale	1(1)	1(1)	2(2)	0	0	0	0	0	0	2(2)
Northern fur seal	0(0)	1(1)	1(1)	0	0	0	0	0	0	1(1)
Polar bear	0	0	0	0	0	0	0	1(1)	1(1)	1(1)
Ringed seal	1(4)	0	1(4)	0	1(1)	1(1)	0	0	0	2(5)
Spotted seal	18(21)	5(5)	23(26)	0	1(1)	1(1)	1(1)	0	1(1)	25(28)
Walrus	2(4)	6(19)	8(23)	33(52)	0	33(52)	4(6)	52(340)	56(346)	97(421)
Unid large whale	10(12)	1(1)	11(13)	2(2)	0	2(2)	0	0	0	13(15)
Unid porpoise	2(2)	0	2(2)	0	0	0	0	0	0	2(2)
Unid seal	67(96)	10(11)	77(107)	36(36)	7(8)	43(44)	38(39)	10(10)	48(49)	168(200)
Unid small whale	2(2)	1(1)	3(3)	0	0	0	0	0	0	3(3)

3. Discussion

The three research cruises conducted for this study (2010-2012) took place in August and September; the survey results therefore represent just a snapshot of marine mammal distributions in the study area. However, the primary benefit of the survey data is the extensive spatial coverage they are able to achieve. These nicely complement the long-term, but point-sampled data, collected by the passive acoustic recorder moorings. In this section we will discuss results from the marine mammal data that was collected during the three survey cruises and how they tie in with the long-term passive acoustic recorder results. For this reason we will address the species in the order they were presented previously for the long-term recorder data. We will not repeat information already contained in the discussion for the long-term moorings (Section VII.A.3), and instead will refer the reader back to that section when needed.

Bowhead whales

There were comparable visual and acoustic results for bowhead whales, which suggests that their calls are a good proxy for presence, at least during this early fall time period. Clark et al. (1986) present results from multiple studies conducted during the spring ice survey off Barrow, AK that seem to suggest that comparable results are obtained from visual and acoustic survey methods when the visual observers had an unimpeded view of the area. Bowhead whale sightings and detections were concentrated near Barrow, AK, as is expected from numerous studies (e.g., Moore et al., 2000; Sheldon et al., 2013; Clarke et al., 2015). The field survey happened later in 2010 than in the other two years, and occurred the earliest in 2012. The distribution of the bowheads from these surveys, with whales seen/heard further to the east than in 2010, suggests that they were just beginning their fall migration south during this time period. In fact, these data were collected during the period with low calling activity preceding the first peak in bowhead whale calling activity seen on the long-term recorder. The lack of any sightings/detections along the Icy Cape line strengthen the argument that the bowhead whales were just not present that far west at that time of the year. Based on the long-term results (Figure 4) which show that the gunshot calling occurs within the pulses of regular bowhead calling activity, it would not be expected that any gunshot calls would be detected during any of the field seasons. Indeed, no gunshot calling was detected on the sonobuoys deployed on any of the cruises.

Beluga whales

There were no visual or acoustic detections of belugas during any of the three field seasons. This does not correspond with satellite tagging results that show that the Barrow Canyon area is a core area in August and September for both male and female beluga whales (Hauser et al., 2014). However, aerial survey data (summarized in Clarke et al., 2015) have found beluga whale sightings to be infrequent and widely distributed throughout the Chukchi Sea in the fall, with a sharp decline in sightings by September/October. This assumption is also supported by long-term passive acoustic recorder results from Hannay et al. (2013) and those from this study (Figure 5). Clarke et al. (2015) suggest that the beluga whales are north of our study area as they migrate west in the fall. This is supported by data from Moore et al. (2012)

that show a large pulse of beluga whale calling activity from May to August on a recorder located far north on the Chukchi Plateau. It is important to note that the satellite tagging results are from 40 BS whales and 24 ECS whales out of a total estimated population size of ~40,000 and 4,000 whales, respectively. Therefore, the data are not contradictory; all methods support the assumption that low numbers of animals are present in the Chukchi Sea in August and September. It is expected that these low densities would result in low sighting and detection rates during our surveys. Hannay et al. (2013), suggest that the lack of call detections in their data reflect a possible reduction in calling for the purpose of predator (i.e., killer whale) avoidance. Although these data cannot be used to link calling activity to whale presence, the lack of both call detections and visual sightings during our three years of field surveys suggests that the low levels of calling activity, for this highly vocal species, correspond to low beluga whale densities in that area.

Gray whales

Gray whales were more often detected visually than acoustically in August/September, a finding that supports the low calling rate reported by Crane and Lashkari (1996) for migrating gray whales and assumed throughout the discussion on the long-term recorder results (Section VII.A.3). The vast majority of sightings occurred in areas deemed gray whale Biologically Important Areas (BIAs) for feeding and reproduction for the summer and fall (Clarke et al., 2015). In the northeastern Chukchi/western Beaufort Seas, most sightings/detections occurred close to shore. This is expected from the narrow extent of the defined BIAs, and fits extremely well with the lack of gray whale calling activity along our Icy Cape mooring line (and the calling being mainly concentrated at the inshore location). Only two offshore occurrences of gray whales in the Arctic were found. One acoustic detection occurred close to Hanna Shoal, which used to be an area with high concentrations of feeding gray whales in the 1980s, but aerial surveys flown there since have not found many whales (Clarke and Ferguson, 2010). Low levels of acoustic detections, however, have been reported for the Hanna Shoal area by Hannay et al. (2013). The other acoustic detection occurred ~40nm off Icy Cape on August 28th, 2011. Although this calling activity was not detected at the inshore location because the recorder failed in late-June, no additional gray whale calling activity was found at this mooring location until late-September, further emphasizing the very low acoustic detectability and/or low densities of this species in the Chukchi Sea in the fall. In addition, studies have shown that gray whales are silent when feeding (Ljungblad et al., 1983), with sounds heard only when socializing was observed (S. Moore, pers. comm.). This was also observed during a 2013 field survey, in which gray whales that were feeding near Point Hope (evidenced by extensive mud plumes) were predominantly silent, while gray whales that were exhibiting presumed reproductive behavior were very vocal (C. Berchok, pers. observation). Given that the Chukchi is a known feeding ground, it is expected that the vocal activity of gray whales would be low. The other two areas of high gray whale concentrations were encountered in the southern Chukchi Sea off Point Hope and just north of Bering Strait. These areas are well known gray whale hotspots (Moore et al., 2003; Bluhm et al., 2007) and as such, are also designated as a BIA for gray whale feeding.

Walrus

There was good consistency between the visual and acoustic results for walrus detections in the northeastern Chukchi Sea, and also between the shipboard surveys and long-term mooring results (see Section VII.A.2). This supports the statement by Hannay et al. (2013) that walrus calling activity can serve as a proxy for walrus presence in the northeastern Chukchi Sea. The walrus reported from Cape Lisburne and south were detected acoustically but not visually sighted. The acoustic detections were made in high seas (2 sonobuoys), in the rain (1 sonobuoy), at night (2 sonobuoys), and while at station (1 sonobuoy) when visual operations cease; passive acoustic monitoring is a nice complement to traditional visual surveys in that it provides information on calling animals in a variety of unworkable visual survey conditions. Most sightings/detections occurred offshore between Icy Cape and Wainwright, near Hanna Shoal. Again, these results are consistent with what is currently known about walrus distribution (Jay et al., 2012). Walrus distributions determined from aerial survey data varied among the three field seasons of this study. In 2010 walrus were associated with sea ice in early August and moved to open water and coastal haul-outs near Pt. Lay and Cape Lisburne in late August and September (Clarke et al., 2011); the 2010 acoustics detections south of Cape Lisburne fall within this later time frame. In 2011 there was a larger walrus haul-out located near Pt. Lay that was discovered earlier (mid-August) and that lasted for a longer period of time (until early October) than in 2010 and contained 1,000 to 20,000 walruses at various times throughout the season (Clarke et al., 2012). Walrus sighted in open water offshore in 2011 showed a preference for the Hanna Shoal area in August/September. Indeed, our detections/sightings were predominantly offshore of Wainwright and near Hanna Shoal in 2011. In 2012, walruses were observed in the water and hauled out on ice, particularly near Hanna Shoal; walrus haul-outs on land were not seen in 2012 (Clarke et al., 2013). The walruses seen and heard during our 2012 research cruise were found further offshore than in the other two years of the study.

Bearded seals

Bearded seals, while commonly seen, were not acoustically detected during any of the three field seasons. This is consistent with the long-term results presented in Section VII.A.2, which had only sporadic detections in August and September. These also correspond with the results reported by Hannay et al. (2013) on their long-term recorders, who reported an abrupt decrease in detections from the end of June to late August. The authors suggested that this decrease was due to a lack of calling and not an absence of animals, which is supported by the visual and acoustic data presented here. This also agrees with aerial survey sightings in the Chukchi Sea in 2010-2012 of 25, 82, and 3 individuals respectively; bearded seals do not appear to be present in the northeastern Chukchi Sea in large numbers in the August/September time period.

Other species

There were several records of subarctic cetaceans detected and/or sighted during our survey cruises in the Chukchi Sea. Most were located in the southern Chukchi Sea, but a few (with the exception of the spotted seal) were found north of Point Hope. Two species, fin whales (Figure 25) and humpback whales (Figure 26), were both visually sighted and acoustically

detected; however, passive acoustic monitoring performed better than the visual surveys, while one species, minke whales (Figure 27), were seen more often than heard. Harbor and Dall's porpoise (Figure 27), had only visual sightings and killer whales (Figure 27) had only acoustic detections. This illustrates the importance of utilizing multiple survey methods, as certain methods are better at detecting certain species than others. For example, harbor and Dall's porpoise vocalizations are very high frequency, and therefore undetectable on sonobuoys due to sampling rate restrictions. On the other hand, fin whale calls are very low in frequency, and very loud; as a result, they have the potential to travel larger distances, and are therefore theoretically easier to detect acoustically. More generally, visual methods are restricted to good sea conditions, visibility, and daylight hours, while acoustic methods are limited to just the animals that are making calls. By combining visual and acoustic surveys, we can obtain a more complete picture of marine mammal distribution within the study area.

Fin whales

The low number of detections of fin and humpback whales in the northeastern Chukchi are consistent with results presented by other passive acoustic studies (Delarue et al., 2013a; Hannay et al., 2013), and from the results obtained from our long-term recorder data (Section VII.A.2). Most records of fin whale presence in the Chukchi Sea were obtained with passive acoustic monitoring instead of during the visual survey. All but one of the sightings were located to the west of the Icy Cape mooring line, and most of those were detected in the southern Chukchi Sea. Therefore, detections of fin whale calling activity at those three mooring locations were not expected (Section VII.A.2). There have been very few sightings of fin whales in the Chukchi Sea over the years from aerial survey efforts and none from vessel surveys. The increased presence of fin whales in the Arctic is most likely due to using passive acoustics to monitor for this species. Although it is not unreasonable to assume that there are increasing numbers of fin whales present in the Chukchi Sea, more long-term data is needed in more locations to determine if such a trend exists.

The acoustic detection of fin whale calling activity so far to the east (off Barrow Canyon) in 2012 suggests the possibility that this species may be encroaching on more northeasterly territories (Crance et al., 2015). This could be a result of post-whaling recovery, or it could be a response to the changing climate and ecosystem (Clarke et al., 2013; Crance et al., 2015). In either case, a greater presence of this species in the northeastern Chukchi could have potentially devastating impacts on the ecosystem (Moore and Huntington, 2008). Fin whales are opportunistic feeders, capable of thriving on zooplankton as well as fish (Mizroch et al., 1984; Perry et al., 1999; Flinn et al., 2002). The impact of this increased resource competition on feeding specialists such as bowhead whales could be substantial (Perry et al., 1999), particularly in this area where the zooplankton community is moderated by sea ice and temperature (Questel et al., 2013).

Humpback and minke whales

Like fin whales, humpback whales are another subarctic species that were detected infrequently during the survey cruise. Most of the detections/sightings occurred to the south of Cape Lisburne. None were close enough to the Icy Cape mooring line to have had any chance of

being detected on the long-term recordings, which fits with the lack of detections at those locations. As mentioned previously (Section VII.A.2), aerial survey efforts have also determined that humpback whales occur infrequently in the northeastern Chukchi Sea. However, they are opportunistic feeders, just like fin whales, and are currently well positioned to penetrate into the Biologically Important feeding areas of bowhead and gray whales, if conditions continue to change. There were only three records of minke whales during our field survey cruises, two in the southern Chukchi in 2010 and one just east of Icy Cape.

Killer whales

The only killer whale sightings were located south of Point Hope, in approximately the same areas as the concentrations of gray whales (Figure 27). As discussed in Section VII.A.2 above, these killer whales are most likely the transient ecotype, which eats marine mammals like gray whales. The transient ecotype tend to be more quiet than the other ecotypes (Deecke et al., 2005), likely as a means of reducing auditory cues to potential prey. Furthermore, they were found to be silent when chasing or hunting gray whales (Ljungblad and Moore, 1983). While the possibility that killer whales are present but not vocalizing cannot be eliminated, the lack of sightings/detections during the three years of survey cruises supports the long-term recorder findings that killer whales are rare in the northeastern Chukchi Sea.

Harbor and Dall's Porpoise

These small odontocete whale species were sighted in three areas: one close to Barrow Canyon (Harbor only), one cluster of sightings due north of Cape Lisburne (Harbor only), and another cluster to the northeast of Bering Strait (both species). The only sounds produced by porpoise are echolocation clicks that are too high to be detected on our sonobuoys or long-term recorders. Both species of porpoise are also difficult animals to identify during aerial surveys due to their small size; vessel surveys are therefore a good method for collecting information on their distribution. It is suggested that harbor porpoise are undergoing a range expansion and being seen more frequently in the Chukchi Sea (Aerts, 2012); more data should be collected so that these trends can be better identified.

Small ice seals

Spotted seals were sighted throughout the survey area, but the majority are concentrated from the Icy Cape line to the east. A few sightings of ringed seals were also made in the Beaufort Sea and in the eastern Chukchi Sea near Barrow Canyon. No sightings or acoustic detections of ribbon seals were made during the vessel surveys. It is difficult to distinguish between spotted and ringed seals during vessel surveys as they often rest vertically at the surface and have similar pelage. More often than not, they are lumped into a combination ringed/spotted seal category, or into the unidentified pinniped category. As such, their sightings do not appear on the species distribution maps. Like the two species of porpoise, small ice seals are difficult to sight during aerial surveys and these records are also saved as 'unidentified pinnipeds'. As mentioned with analysis of the long-term recorder data, Arctic pinnipeds make a variety of sounds in the snort/bark/yelp/etc. category. As the original objectives of this project did not

focus on ice seals, we just flagged any instances of this calling as ‘unidentified pinniped’. A combination of visual and acoustic survey methods should be used to help distinguish between the various species of ice seals in order to obtain a more accurate idea of distribution in the Chukchi Sea in the August/September time period.

Polar bears

One sighting of one polar bear was made up near the end of the Wainwright sampling line in 2012. 2012 was the only year in which we encountered ice during the survey, which may explain why there were no visual detections in the previous years. Polar bears do not make any underwater sounds that can be detected on passive acoustic recordings.

4. Conclusions

Shipboard visual and passive acoustic surveys conducted while the ship is underway provide an inexpensive way to leverage on the sea time needed to service the long-term moorings and conduct the biophysical sampling stations. The cruise track needed to complete this mooring/sampling work is extensive, covering a wide spatial area at an important time of the year for many of the marine mammal species. The results of this three year shipboard survey have shown that the northeastern Chukchi Sea is an important area for several resident species in the August/September time period, including bowhead and gray whales, walrus, and bearded seals. Although there was some interannual variability in detection locations, all four of these species were detected visually or acoustically in large numbers in all three years of surveys. The southern Chukchi Sea also appears to be an important area for both Arctic species (i.e., gray whales) and subarctic species (e.g., fin and humpback whales, and harbor porpoise). Clarke et al. (2013) suggest there may be an increase in these cetaceans within this region, which could be either a result of post-commercial whaling recovery and seasonal changes, a response to climate change, or both.

The combination of visual and acoustic surveys is essential to maximize the detection potential for each species. Either method alone runs the risk of missed detections and underestimating the importance of an area to a particular species. In addition, having this combination of methods on the same survey cruise allows comparisons to be made *in situ*. We have found that bowhead whales, fin whales, humpback whales, and walrus are equally likely (or for beluga and killer whales – equally unlikely) to be sighted or detected during the August/September time period of these cruises. For gray whales, bearded seals, minke whales, and the two porpoise species, call detections cannot be used as a proxy for presence of these species at this time of the year. It is important to note that the season over which these statements are valid must be defined so that the data are not misinterpreted during other times of the year.

In addition to the benefits listed above, having dedicated visual observers working concurrently with passive acoustics allows for focal follows to be conducted. These focal follows are crucial for several reasons. First, they allow for cross-validation of each method. They also are very important for attributing call types to species and to certain behaviors for those species,

adding to their known calling repertoire. Finally, they play a critical role in creating a database of call counts for each species which is necessary for eventually being able to estimate their relative abundance (see Section XIII). Information obtained on these call repertoires and call counts could then possibly be applied to the data collected from our long-term recorders, providing not only year-round seasonal distribution of the various species, but year-round seasonal distribution of their behaviors, and, eventually, accurate estimates of their year-round relative abundance.

5. *Recommendations*

While out at sea, we make every attempt to have a dedicated visual observation team working concurrently with someone using sonobuoys for real-time passive acoustic monitoring. In the event that we do not have a dedicated field season in the upcoming years, it is important that we ensure at least one visual observer and one passive acoustic technician are included in any opportunistic field surveys we may conduct. This ensures that we take full advantage of any opportunity to conduct combined visual/acoustic surveys, increase our knowledge of the calling repertoires of each marine mammal species, and increase the sample size of our database of call counts. Furthermore, the bearing information from the DiFAR sonobuoys will allow, with multiple sonobuoys deployed, the localization of calling animals (see Section VII.B.2). This then allows us to obtain estimates of call detectability that are necessary for calculations of relative abundance (XIII.B).

C. *Photo-Identification*

1. *Methods*

At the cruise leader's discretion, survey effort was temporarily suspended to allow closer approaches to sightings for photo-identification. Photographs were obtained to help evaluate the movements of animals during the survey and for comparison to existing catalogs. Photographs were taken using Canon 50D, 7D, and Nikon D200 digital cameras equipped with a 100-400 and 80-200 mm zoom lens set to autofocus. All photographs were reviewed, and the highest quality identification photograph(s) of each animal were selected to be compared to existing photo-identification catalogs.

2. *Results*

Over the three year study, opportunistic photographs were collected of humpback, killer, gray and North Pacific right whales. One humpback (mother/calf pair) and one juvenile gray whale were photographed in the Chukchi Sea in 2012. The humpback (mother) was compared to the NMML catalog. There was no match. The gray whale photographed in 2012 was a juvenile animal and not matched given the low likelihood of being in the catalog. All other photographs were collected in the Bering Sea and along the Alaskan Peninsula in the Gulf of Alaska (see Appendix F for plots of sighting and sonobuoy locations of these species detected outside the official study area).

3. *Discussion*

Photo-identification is an invaluable tool to understand seasonal and temporal habitat use and to understand population structure. Although there were no matches to date (ARCWEST or CHAOZ-X may still find matches), the documentation of a cow/calf humpback pair within Arctic waters was an important achievement as it provides insight into the distribution and habitat use of this crucial demographic for this species. Furthermore, with the changing climate, it is important to obtain visual documentation of species that are sighted infrequently within these waters.

4. *Conclusions*

Given the objectives of this project, we did not have sufficient time to dedicate to photo-identification studies. Only a few individuals were documented opportunistically, and there were zero matches to the catalogs.

5. *Recommendations*

Obtaining photographs for photo-identification purposes typically requires the survey to suspend operations when feasible and approach the animal(s). As a rule, we attempt to collect photographs opportunistically as the vessel continues on its course when we don't have time to stop. However, dedicated time would need to be allocated to conduct robust photo-identification studies.

D. *Satellite Telemetry*

1. *Methods*

In 2012, satellite tagging operations were conducted on an opportunistic basis to assess the feasibility of deploying tags on large whales in the Arctic for the BOEM-funded ARCWEST project that commenced in 2013⁴. Satellite telemetry was conducted at the discretion of the chief scientist after considering weather, time of day, and planned oceanographic operations. Once a tagging candidate (humpback, fin or gray whale) was located, a 24' rigid-hulled inflatable boat (RHIB) was launched with a coxswain, tagger, data recorder and photographer on board. Satellite transmitters were attached to the body of the whales using the Air Rocket Transmitter System (ARTS, Heide-Jørgensen et al., 2001), which is a modified marine safety pneumatic line thrower. Tagging took place from a bow platform with the RHIB positioned approximately 6-10 m perpendicular from the animal.

Whales were tagged with the implantable configuration of the SPOT 5 transmitters produced by Wildlife Computers (Redmond, WA) (Figure 29). These instruments are cylindrical

⁴ Although the satellite tags were paid for by ARCWEST funds, the ship time was paid for by CHAOZ funds and the results are included in this report.

in shape and contain an ARGOS satellite PTT. When deployed, approximately 4 cm of the tag remains external to the body of the whale, with an antenna extending out of the distal end of the tag. The tags were duty-cycled to record from 02:00-08:00 and 14:00-20:00 GMT daily in order to maximize battery life and transmission rate. This sampling design was expected to provide extensive data while the whales were on their feeding grounds. Beginning in November, when migration likely begins, transmitters were programmed to transmit every other day, following the same alternating 6 hr. on/off periods. Follow-up photo-documentation of tag placement and animal behavior was attempted for 20-30 min after deployment. Tag deployment and follow-up photo-documentation were performed according to regulations and restrictions specified in the existing permits issued by the National Marine Fisheries Service to the National Marine Mammal Laboratory (permit #14245) and the International Animal Care and Use Committee (IACUC) assurance issued to NMML.

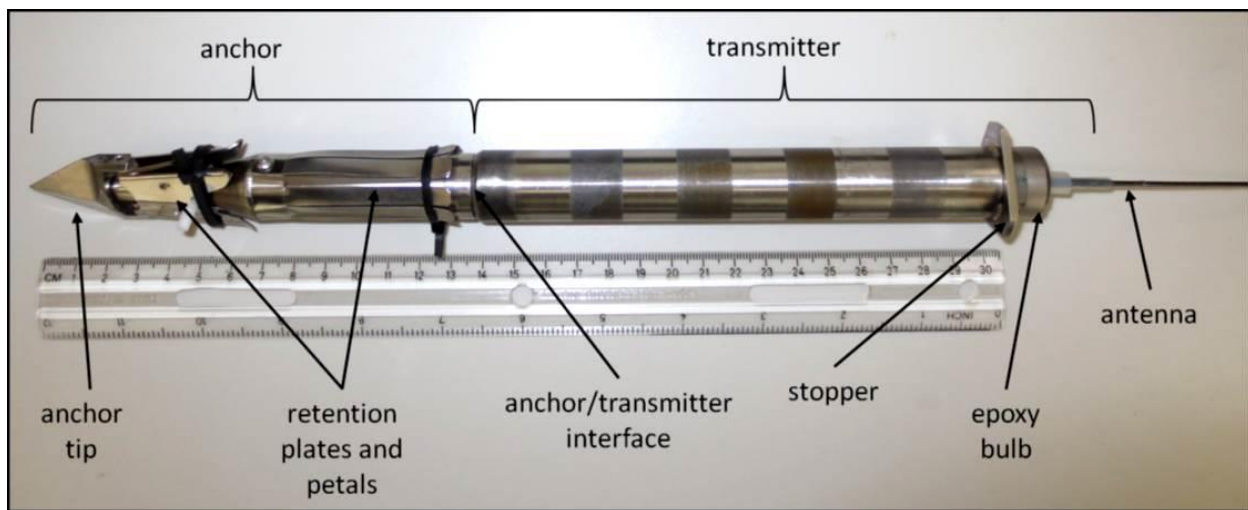


FIGURE 29. AN EXAMPLE OF A SPOT 5 SATELLITE TRANSMITTER THAT WAS DEPLOYED IN 2012.

Satellite tags were monitored by Argos Data Collection and Location Service receivers on NOAA TIROS-N weather satellites in sun-synchronous polar orbits (Argos, 1990). Locations were calculated by Argos from Doppler-shift data when multiple messages were received during a satellite's passage overhead. Argos codes locations into quality classes (LQ) labeled B, A, 0, 1, 2, 3, in order of increasing accuracy. Fadely et al. (2005) verified accuracies of 0.4 km (± 0.3) for LQ3, 0.7 km (± 0.6) for LQ2, 1.5 km (± 1.5) for LQ1, 4.9 km (± 5.3) for LQ0, 2.9 km (± 5.2) for LQA, and 17.4 km (± 26.2) for LQB.

The SDA Argos filter (Freitas et al., 2008) was applied to all location qualities in software R in order to remove locations that implied unlikely deviations from the track's path as well as unrealistic travel rates. This filter requires two main parameters: turning angles and maximum speed of travel. The default value of turning angles (Freitas et al., 2008) was used and the maximum speed was assumed to be 15 km/h. Exploratory analysis showed that the use of different maximum speed limits (12 and 18 km/h) did not influence the filter results. Distances between filtered locations were calculated assuming a great circle route. A Bayesian switching

state-space model was then applied to SDA filtered data to estimate a position and behavioral state every 6 hours (Jonsen et al., 2005; Kennedy et al., 2014).

2. Results

One gray whale was tagged during this study on 25 August, 2012. The deployment occurred 16 miles offshore from Wainwright, Alaska. The whale was judged to be a juvenile based on size. The tag transmitted for 48 days, until 11 October 2012 (Figure 30). The animal remained within 140 km of the deployment site for the duration of the tag and occupied relatively shallow waters (20-50 m in depth) to the south of Hanna Shoal. Results from the switching state-space model show that all positions fell within the area restricted search (ARS) criteria threshold (Figure 31).

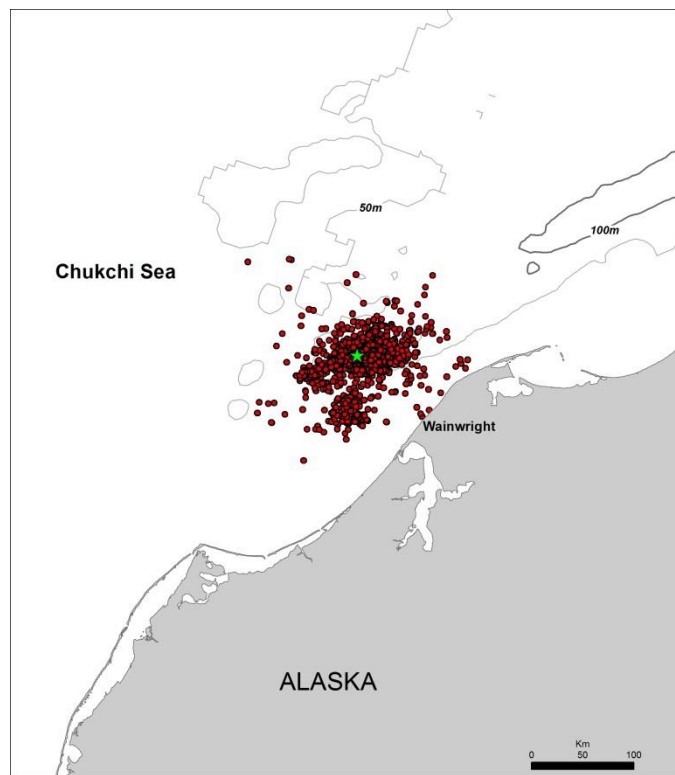


FIGURE 30. LOCATIONS (RED DOTS) OF THE GRAY WHALE TAGGED OFF WAINWRIGHT DURING 2012. THE GREEN STAR MARKS THE TAGGING LOCATION (70.8°N, 160.5°W).

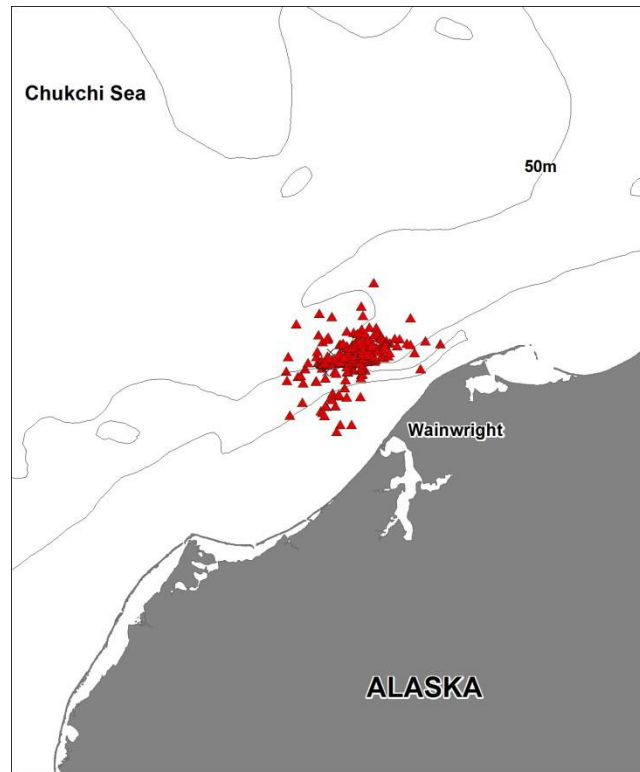


FIGURE 31. SWITCHING STATE-SPACE MODELED LOCATIONS (6 HOUR TIME-STEP) OF THE GRAY WHALE TAGGED OFF WAINWRIGHT DURING 2012. RED TRIANGLES INDICATE AREA RESTRICTED SEARCH (ARS). NO OTHER BEHAVIORAL STATES APPEARED IN THE MODEL RESULTS.

3. *Discussion*

Results from the gray whale satellite tagged off Wainwright, AK indicate the animal was most likely foraging in this area. Several gray whales were concentrated in the area and mud plumes were observed (indicative of foraging) (Rugh and Fraker, 1981). The switching state-space model showed that this animal was in ARS for the entire time the tag transmitted, which further suggests this animal was foraging. ARS is often synonymous with foraging behavior (Kareiva and Odell, 1987; Mayo and Marx, 1990; Kennedy et al., 2014). This animal will be included in a larger dataset of tagged individuals as part of ARCWEST which commenced in 2013.

4. *Conclusions*

Using a combination of visual surveys and satellite telemetry, results provided an understanding of the distribution of marine mammals during the months of August and September as well as information on habitat use within the summer feeding grounds during the summer and fall foraging periods.

5. *Recommendations*

Conducting satellite telemetry operations in Arctic waters is a challenging but not impossible endeavor. Inclement weather, locating concentrations of whales, and the approachability of the species, all factor into the amount of time needed to successfully deploy a satellite tag. From our experience, gray whales in the Arctic are highly sensitive to boat presence. Humpback and fin whales generally appear to be passing through the area, spending little time at the surface. Dedicated operations with sufficient time around large groups of whales are essential to successful telemetry projects in the Arctic.

VIII. BIOPHYSICAL PATTERNS AND TRENDS

A. *Moored Observations*

1. *Methods*

Mooring Sites and Instrument Configuration

Each year, three, year-long biophysical moorings were deployed at each of three sites (Figure 32; C1-inshore, C2-midshore, and C3-offshore). To avoid ice keels, the top of each mooring was only ~10 meters off the bottom (or ca. 30 m from the ocean surface). Mooring designs were identical for each year and the instruments which successfully collected data are listed in Table 12. Mooring deployment locations and parameters measured are presented in Table 12. Data were collected at least hourly and all instruments were calibrated prior to deployment. The physical and chemical data were processed according to manufacturers' specifications. All current time series were low-pass filtered with a 35 hour, cosine-squared, tapered Lanczos filter to remove tidal and higher-frequency variability, and re-sampled at 6 hour intervals. CTD and water bottle casts were conducted following or preceding mooring recoveries and deployments to provide quality control of the data collected by some of the instruments on the moorings (e.g., temperature, salinity, PAR, dissolved oxygen, and nitrate).

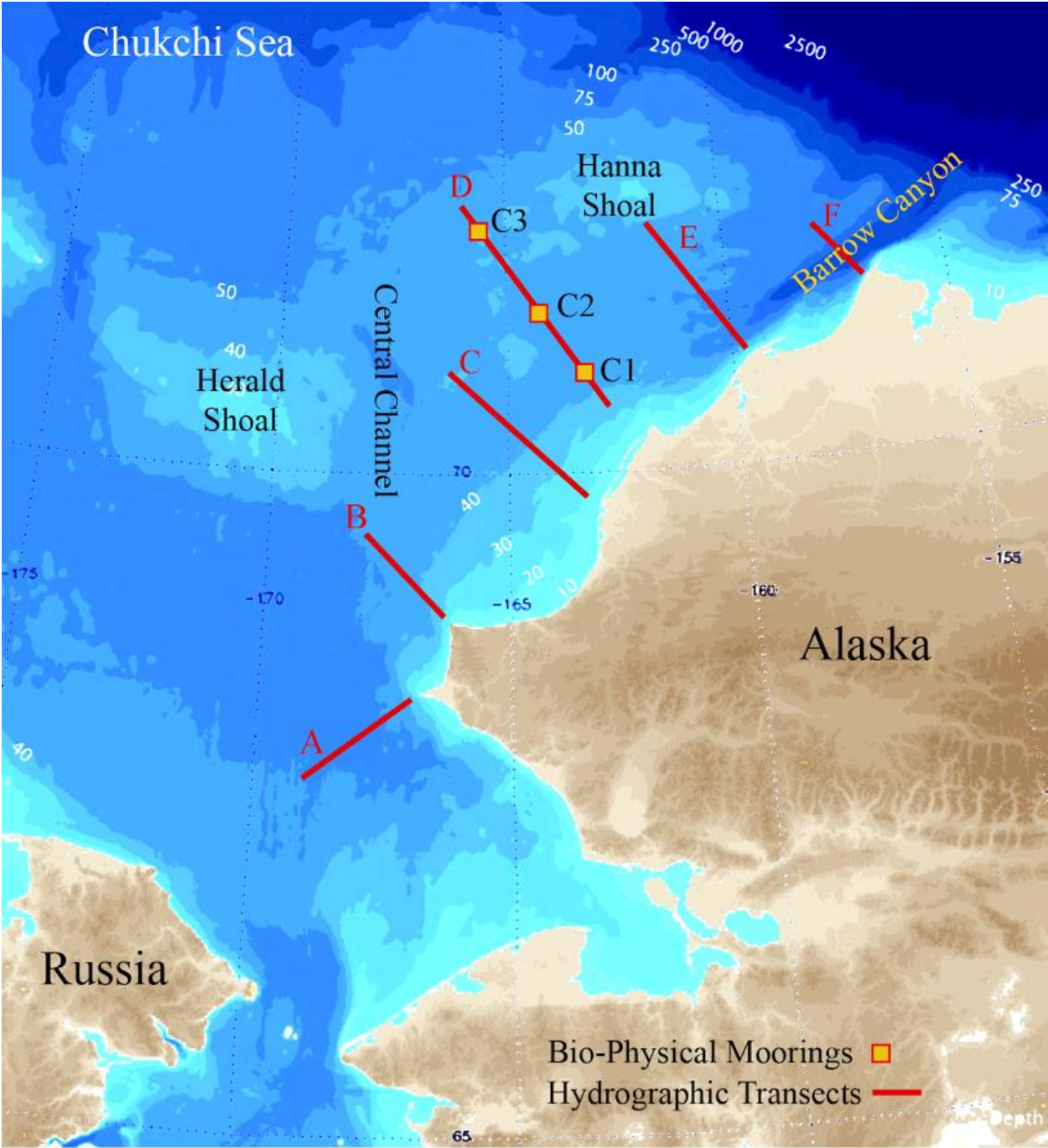


FIGURE 32. BATHYMETRY IN THE STUDY AREA, THE THREE MOORING SITES, AND THE SIX HYDROGRAPHIC TRANSECTS OCCUPIED.

TABLE 12. SUMMARY OF MOORING LOCATIONS AND MEASUREMENTS TAKEN FOR THE CHAOZ STUDY. ALL MOORINGS WERE TAUT-WIRE MOORINGS, MEASURING TEMPERATURE (SEACAT, RCM-9), SALINITY (SEACATS, RCM-9), CURRENTS (RCM-9, ACOUSTIC DOPPLER CURRENT PROFILER: ADCP) AND CHLOROPHYLL FLUORESCENCE (WETLABS ECO-FLUOROMETER). NITRATE CONCENTRATIONS WERE MEASURED USING SATLANTIC ISUS. OXYGEN WAS MEASURED USING AANDERAA OXYGEN OPTODE 3835 AND TURBIDITY WAS ALSO MEASURED ON THE RCM-9. THE ASL INSTRUMENT ACOUSTICALLY MEASURES ICE KEEL DEPTH. THE TAPS-8 (8 FREQUENCY TRACOR ACOUSTIC PROFILING SYSTEM) IS AN OLDER VERSION OF THE TAPS-6NG (TAPS-6 NEXT GENERATION) THAT WAS BUILT FOR SUBSEQUENT BOEM PROJECTS.

	Mooring name	Latitude	Longitude	Instrument	Parameters Measured	
2010	C1	10CKP-1A	70.839°N	163.197°N	600 KHz ADCP	T, PAR, FI, Currents (WC), Pres, Nitrate
		10CKIP-1A	70.840°N	163.205°N	RCM9, ASL	T, S, O2, Currents (B), Turb, Pres, Keel Depth
	C2	10CKP-2A	71.220°N	164.250°N	SeaCat, 600 KHz ADCP	T, S, PAR, FI, Currents (WC), Pres, Nitrate
		10CKIP-2A	71.223°N	164.252°N	RCM9, ASL	T, O2, Currents (B), Turb, Pres, Keel Depth
	C3	10CKP-3A	71.826°N	165.975°N	SeaCat, 600 KHz ADCP	T, S, PAR, Currents (WC), Pres
10CKIP-3A		71.820°N	165.982°N	RCM9, ASL	T, S, O2, Currents (B), Turb, Pres, Keel Depth	
2011	C1	11CKIP-1A	70.840°N	163.209°N	SeaCat, 600 KHz ADCP	T, S, PAR, FI, Currents (WC), Pres
		11CKP-1A	70.839°N	163.194°N	RCM9	T, O2, Currents (B), Turb, Pres
	C2	11CKP-2A	71.221°N	164.241°N	SeaCat, 600 KHz ADCP	T, S, PAR, FI, Currents (WC), Pres, Nitrate
		11CKIP-2A	71.223°N	164.257°N	RCM9, ASL	T, S, O2, Currents (B), Turb, Pres, Keel Depth
		11CKT-2A	71.218°N	164.248°N	TAPS-8	Zoop Biovolume
C3	11CKP-3A	71.825°N	165.975°N	SeaCat, 600 KHz ADCP	T, S, Par, FI, Currents (WC), Press, Nitrate	
	11CKIP-3A	71.819°N	165.982°N	RCM9, ASL	T, S, O2, Currents (B), , Press, Keel Depth	

Zooplankton Volume Backscatter Estimates Derived From ADCP Measurements

Estimates of zooplankton volume backscatter (S_v) were also derived from the upward looking, 600 kHz Teledyne RDI Workhorse Sentinel ADCP (Table 12). Measurements of echo counts from each bin and time point were used to estimate volume backscatter.

Matlab™ (R2012b) was used to process all data. The ADCP echo intensities (counts) were converted to S_v according to Gostiaux and van Haren's (2010) modified version of the commonly used Deines (1999) sonar equation:

$$S_v = C + 10\log_{10}((T_x + 273.16)R^2) - L_{DBM} - P_{DBW} + 2\alpha R + 10\log_{10}(10^{KcE/10} - 10^{KcEr/10}),$$

where C is a transducer/system noise constant provided by the manufacturer (-139.3 dB for the Workhorse Sentinel), T_x (°C) is the variable temperature at the transducers, L_{DBM} is the $10\log_{10}$ (transmit pulse length constant in meters), P_{DBW} is the $10\log_{10}$ (variable transmit power in Watts),

α (dB/m) is the sound absorption coefficient of seawater, R (m) is the slant range along the beam to the scatterers, E (counts) is the echo intensity, E_r (counts) is the reference noise level determined from the lowest echo intensity value over the whole water column during the entire deployment period, and K_c (dB/count) is the conversion factor provided by the manufacturer to convert ADCP counts to dB. S_v was calculated separately for each beam, then the average of all beams was computed in the linear domain before being converted back to log units.

Wavelet analysis (Torrence and Compo, 1998) was applied to standardized ADCP data $((x - \text{mean})/\text{standard deviation})$ to examine the dominant modes of temporal variation and to determine strength of these modes across the observation period. Software to accomplish the analyses was written in Python using information at <https://github.com/aaren/wavelets> as a resource. Wavelet transforms are similar to Fourier transforms in that they convert information in the time domain into the frequency domain. They are particularly informative when a signal is non-stationary, which is the case with our data. The orthogonal basis functions used here were sine and cosines. The rapid ascent and descent of zooplankton during diel vertical migration result in a “square” shaped migration. In addition, the length of time zooplankters remain in the upper water column also varies (see below).

Zooplankton Volume Backscatter Estimates Derived From Multi-Frequency Measurements

A 6-frequency (50, 78, 115, 200, 420, 735 kHz) Tracor Acoustic Profiling System - Next Generation (TAPS6-NG) was used to estimate the size and abundance of zooplankton from late August 2011, until late January 2012. Deployment of TAPS6-NG instruments in August 2010 was not possible due to the late arrival of funds and the difficulties of developing this new line of instruments. The new TAPS6-NG is comprised of a PVC block containing the 6 individual transducers (Transonics, Inc.) mounted on the top of an Acoustic Doppler Current Profiler (ADCP) syntactic foam float (Deep Water Buoyancy, Inc., Figure 33). The controller electronics case is clamped inside the float where the ADCP instrument would normally reside, and several pressure cases containing lithium ion batteries are mounted below the float in a custom-designed, stainless steel frame. The instrument collects measurements between the range of 1-35 m, with data bin centers every 0.37 m. Sample volumes for each frequency were from ca. 0.5-50 m³ at a range of 2-30 m, respectively, from the transducer faces. Raw data from each frequency of the TAPS6-NG were recorded during these intervals as mean integrated echo intensities (W/m²) computed over 24 individual pings per ensemble. System electronics optimization was obtained by tuning each transducer in the freshwater dive tank (30' x 15') at the NOAA Western Regional Center. System calibration consisted of determining the source and receiver levels for each frequency before and after deployments, using a standard calibrated transducer. Calibration was accomplished at the Hydroacoustic Technology Inc. calibration barge in Seattle, Washington.

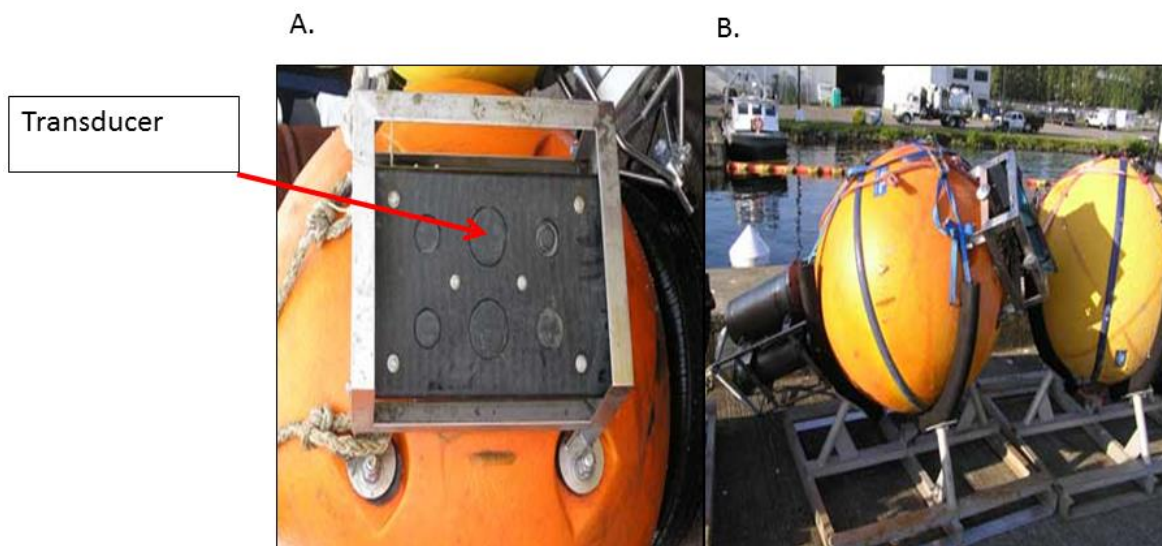


FIGURE 33. TAPS6-NG. A. A PVC BLOCK CONTAINING THE 6 INDIVIDUAL TRANSDUCERS IS MOUNTED ON THE TOP OF AN ACOUSTIC DOPPLER CURRENT PROFILER (ADCP) SYNTACTIC FOAM FLOAT. B. THE ENTIRE ASSEMBLY SHOWING THE TRANSDUCER BLOCK ABOVE THE FLOAT AND THE BATTERY CASES BELOW THE FLOAT.

Our first TAPS6-NG instrument was deployed at the midshore mooring site C2 in 2011 (Figure 32; Mooring 11CKT2B;) and successfully recovered one year later. The acoustic instrument was programmed to sample every 30 minutes April-September, and at 60 minute intervals October-March. This mooring was placed nearby two other moorings, one of which contained a 600 kHz ADCP, ISUS nitrate analyzer, chlorophyll fluorometer, CTD, and Photosynthetically Active Radiation (PAR) light meter (Table 12). The other mooring contained a mechanical current meter and an ice profiler (http://www.pmel.noaa.gov/foci/operations/mooring_plans/2011/aug2011_contVes_moorings.html).

Matlab™ (R2012b) was used to process the acoustic data. Background and instrument noise was defined as the weekly minimum intensities for each frequency. Those values were then subtracted from each measurement for that week. The intensities were then converted to volume-scattering strength (S_v , dB re 1 m^{-1}) followed by correction with calibration constants. Signal-to-noise ratios of <10 dB were used as a threshold to reject S_v values that were not used in further analyses.

Inverse methods were used to estimate the abundance of scatterers as a function of size (Holliday, 1977; Greenlaw, 1979; Greenlaw and Johnson, 1983). Abundances were estimated for near-bottom (10 meters from the transducer head) and near-surface (25 meters from the transducer head). Near-surface data were only analyzed until the end of September due the possibility of ice affecting the backscatter.

The truncated fluid sphere (TFS) and distorted-wave Born approximation (DWBA) scattering models were used in the inverse calculation to estimate scattering from small, spherical organisms (e.g., copepods, eggs, nauplii) and elongate organisms (e.g., euphausiids, mysids), respectively (Holliday, 1992; Holliday et al., 2003). The assumed values used in the models, included the animal orientation, sound speed (h) and density contrast (g), Levenberg-Marquardt factor, number of size classes, and size range, are provided in Table 13. Euclidian

norms were computed as a goodness-of-fit statistic between measured S_v and the inverse model fit to verify that the inversion could adequately explain the measured S_v values.

TABLE 13. MATERIAL PROPERTIES AND OTHER PARAMETERS USED IN THE SCATTERING MODELS AND INVERSE SOLUTIONS.

Parameter	TFS	DWBA
G	1.00	1.018
H	1.003	1.006
Levenberg-Marquardt	1.0×10^{-3}	1.0×10^{-3}
Orientation	random	broadside/horizontal
Size classes	48	48
Size Range	1.0-11.25 mm	10.0-24.0 mm

2. Results

Time Series of Physical and Chemical Data from Biophysical Moorings

Except for the ADCP (which measures throughout the water column) and the ice profiler (which measures keel depth), all measurements are in the bottom 10 meters of the water column. The inshore mooring (C1) was in Alaska Coastal Current (ACC) water, while ~ 70 km farther offshore the midshore mooring, C2, was in winter water (Figure 34).

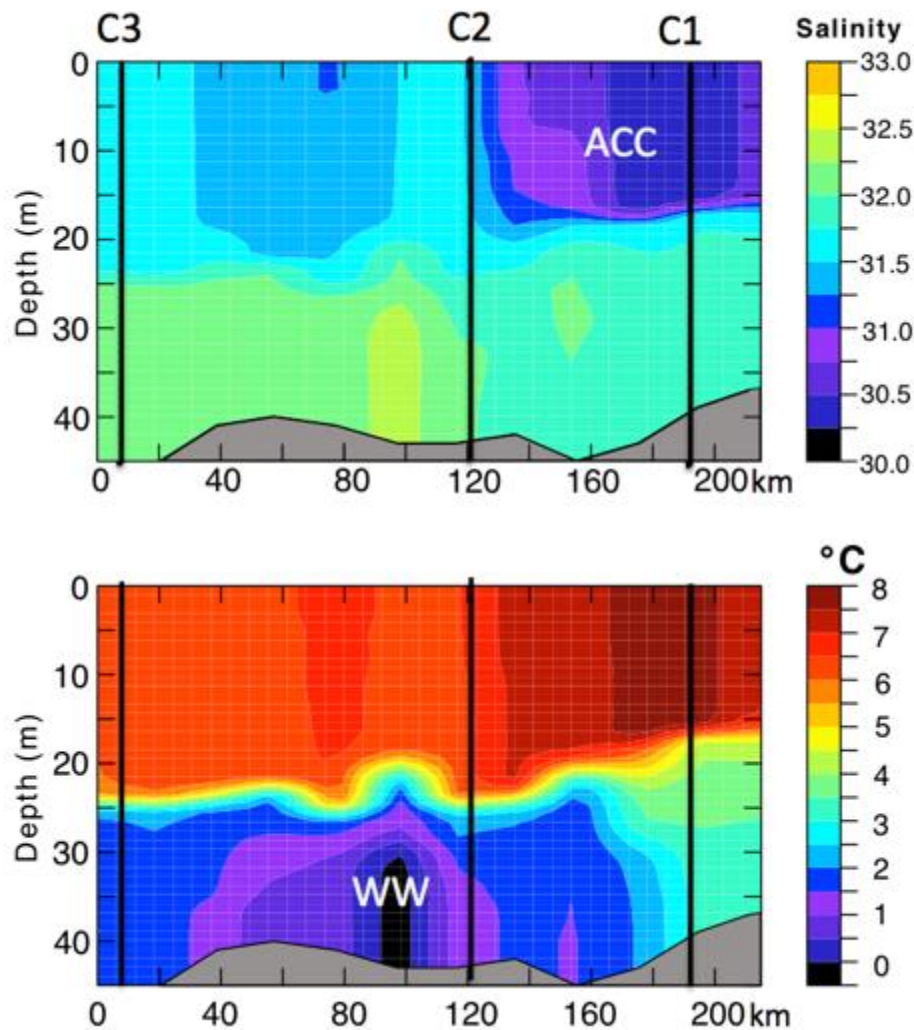


FIGURE 34. CROSS SECTION OF TEMPERATURE AND SALINITY AT ICY CAPE SHOWING THE LOCATIONS OF THE MOORINGS. NOTE THAT C1 IS IN THE ACC WATER.

Time series of all mooring data are shown in Figure 35-40. Only a few instruments failed completely, including the turbidity at the offshore location (C3, 2011-2012), the nitrate sensors at the offshore location (C3, 2010-2011) and inshore location (C1, 2011-2012), and after analysis, one fluorometer at the offshore location (C3, 2010-2011) proved to be inconsistent. The rest of the data are discussed below.

Bottom currents were generally northeastward following bathymetry. Daily net speeds were $< 45 \text{ cm s}^{-1}$. The low-pass filtered time series were variable, with reversals lasting typically 2-4 days. The variability in currents was forced by winds. Vertically, the currents were well correlated (typically $r > 0.7$; 95% significance level ~ 0.1 between surface and bottom currents).

Bottom temperature ranged from approximately -1.8 to < 5.0 °C, with maximum temperatures occurring in late August or September. Salinity ranged from < 31 to ~ 34.5 . The variability in salinity was the result of different water types, and the melting (and mixing) of sea ice, and the freezing of surface waters.

The highest turbidities occurred in fall when the winds began to increase and before the sea ice areal coverage became >80%. Evidence of wind mixing can be seen in the winter when polynyas occur (e.g., Figure 35).

The spring phytoplankton bloom is evident in each time series. The bloom (initially ice algae) likely occurs under and in the ice before evidence of it appears at the bottom of the water column where our fluorometer was located. This bloom consumes near-surface nutrients. Once the ice begins to melt, chlorophyll is exported to the benthos. Associated with the increase in primary production is an increase of percent oxygen saturation (e.g., Figure 35), suggesting that primary production continues at depth or that advection continually replenish oxygen (~40 m). PAR is an indication of how much light available for photosynthesis reaches the bottom of the water column. Typically, measureable light reaches the bottom from May through September. A common feature in the PAR time series is a decrease in PAR to almost zero during the height of the bloom (e.g., Figure 36 in June). This is likely a result of shading by phytoplankton above the instrument.

Nitrate ranges from 0 – 20 μM at depth. It decreases from mid-spring through July or August and then increases during late winter and early spring. The source of the water replenishing nutrients in the winter may be the continental slope or water originating in the Bering Sea and flowing up Central Channel joining the more coastal flow from Point Lay.

Sea ice arrives in early to mid-November, increasing quickly to near 100% areal coverage and declines precipitously in late May or June. The areal ice concentration was more variable in 2010-2011, than it was in 2011-2012; there were two periods of nearly open water occurring in 2010-2011, while none occurred in 2011-2012. Ice thickness (Figure 41) increases to an average of ~4 m in March. The thickest ice is generally seen late in spring (Table 14).

TABLE 14. MAXIMUM KEEL DEPTH MEASURED AT THE MOORING SITES. THE DATE OF MEASUREMENT IS GIVEN IN PARENTHESIS. THE ICE PROFILER SENSOR (ASL) AT C1 FAILED IN 2011/2012.

Maximum Keel Depth	C1 (m)	C2 (m)	C3 (m)
2010-2011	29.8 (April 1)	24.3 (June 4)	20.1 (April 19)
2011-2012	No data	27.6 (March 30)	28.7 (April 16)

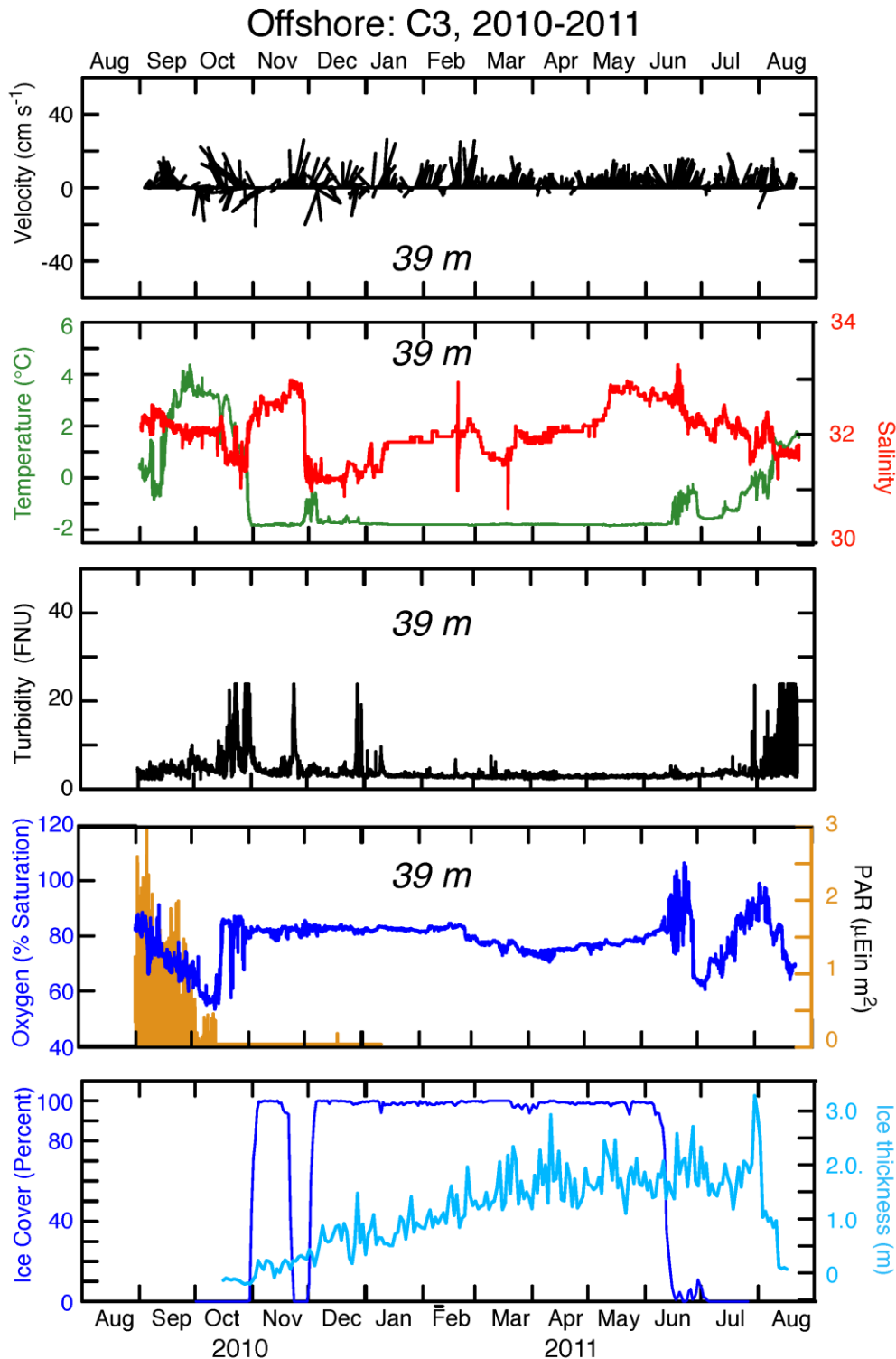


FIGURE 37. TIME SERIES FROM THE OFFSHORE MOORING (C3), DEPLOYED AUGUST 2010-2011. FROM TOP PANEL TO BOTTOM PANEL: NEAR-BOTTOM VELOCITY (ROTATED TO ALONG SHELF); TEMPERATURE (GREEN), SALINITY (RED); TURBIDITY; DISSOLVED OXYGEN PERCENT SATURATION (BLUE), PHOTOSYNTHETICALLY ACTIVE RADIATION (PAR, ORANGE); AND AREAL ICE CONCENTRATION IN A 50 KM X 50 KM BOX AROUND C3 (DARK BLUE), DAILY AVERAGE DEPTH OF THE ICE KEELS (LIGHT BLUE). NOTE: NITRATE IS MISSING IN THIS PLOT DUE TO FAILED SENSORS.

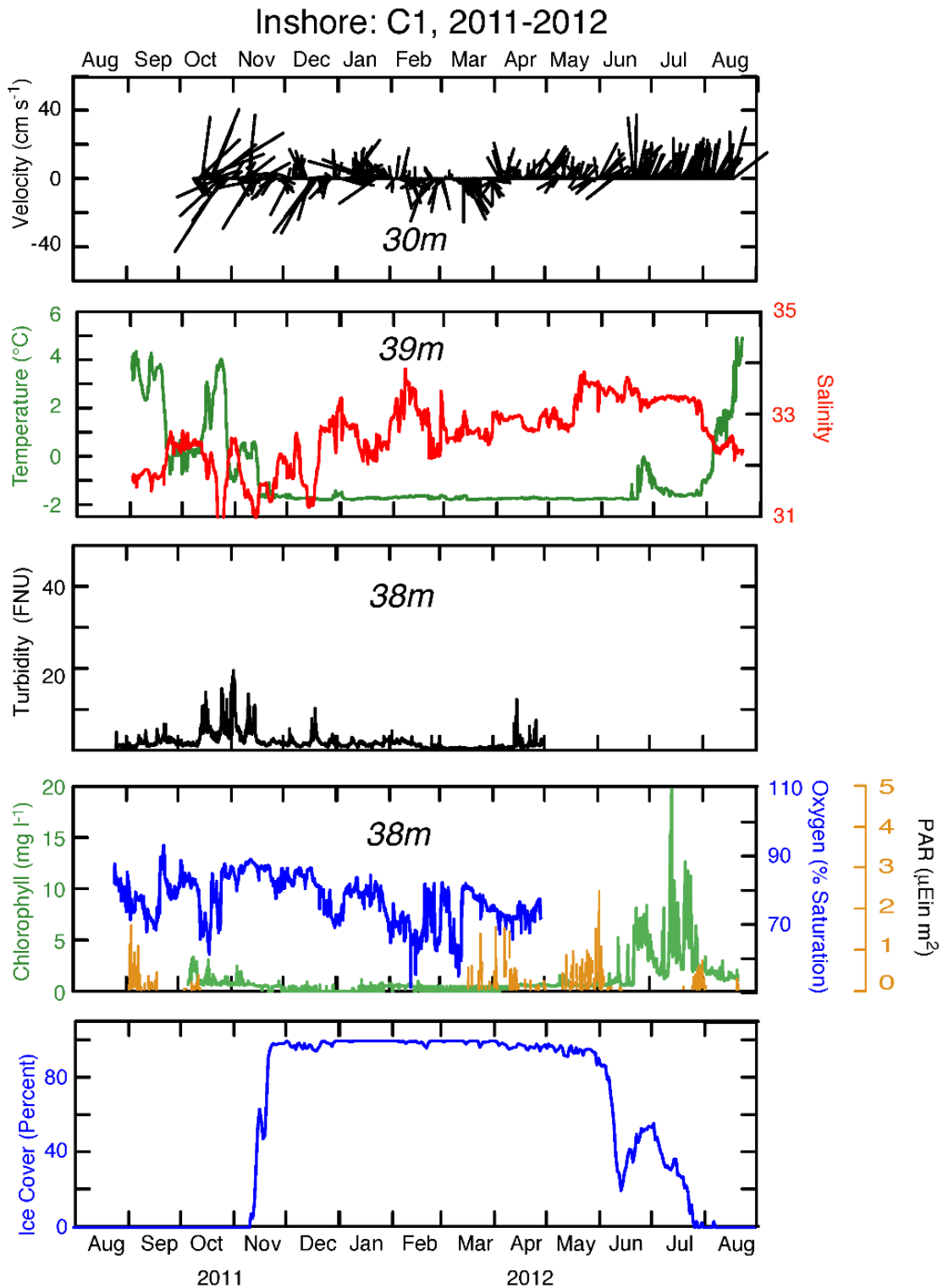


FIGURE 38. TIME SERIES FROM THE INSHORE MOORING (C1), DEPLOYED AUGUST 2011-2012. FROM TOP PANEL TO BOTTOM PANEL: NEAR-BOTTOM VELOCITY (ROTATED TO ALONG SHELF); TEMPERATURE (GREEN), SALINITY (RED); TURBIDITY; CHLOROPHYLL FLUORESCENCE CONCENTRATION (GREEN), DISSOLVED OXYGEN PERCENT SATURATION (BLUE), AND PHOTOSYNTHETICALLY ACTIVE RADIATION (PAR, ORANGE); AND AREAL ICE CONCENTRATION IN A 50 KM X 50 KM BOX AROUND C1 (DARK BLUE). NOTE: NITRATE IS MISSING IN THIS PLOT DUE TO FAILED SENSORS.

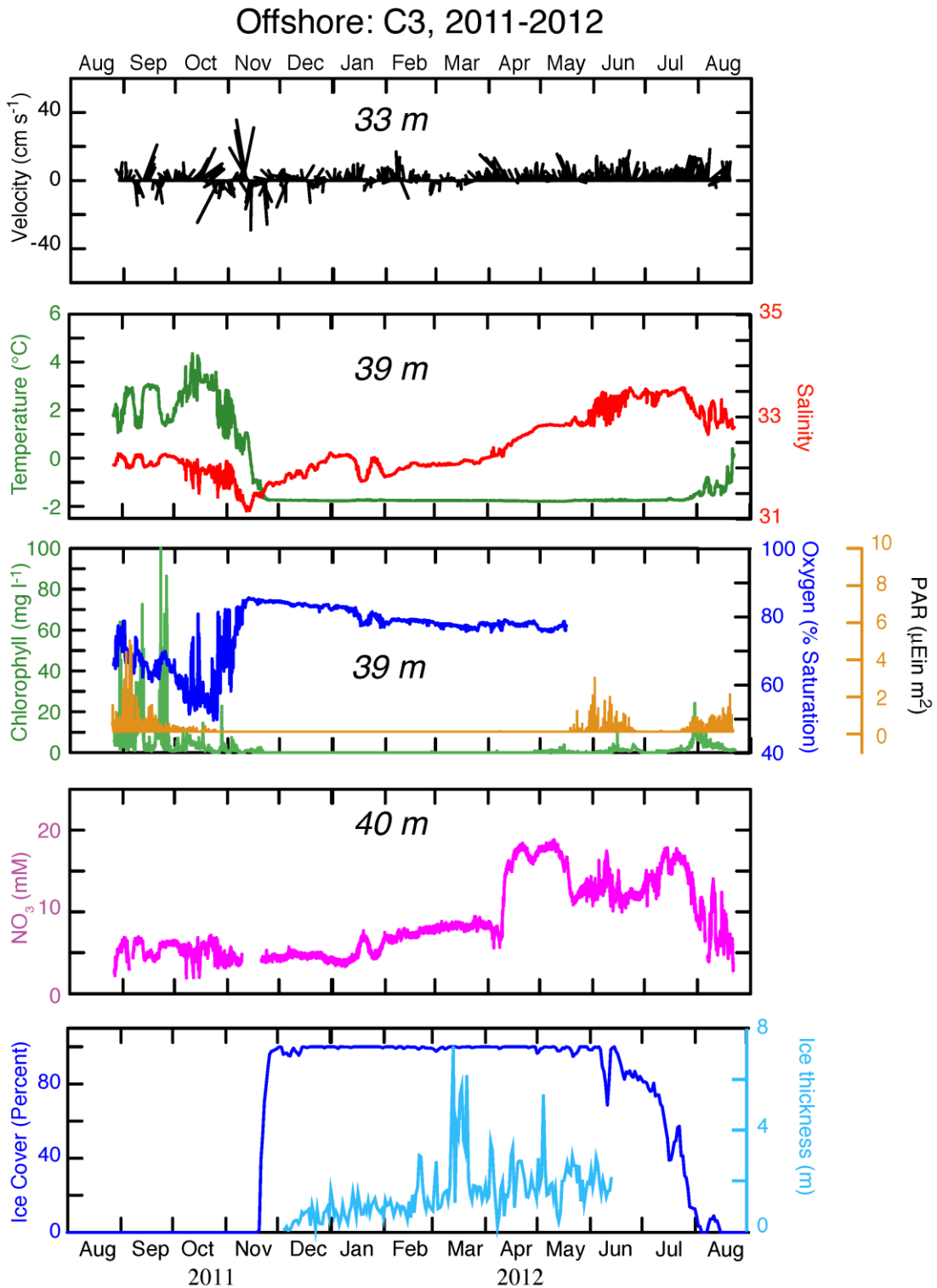


FIGURE 40. TIME SERIES FROM THE OFFSHORE MOORING (C3), DEPLOYED AUGUST 2011-2012. FROM TOP PANEL TO BOTTOM PANEL: NEAR-BOTTOM VELOCITY (ROTATED TO ALONG SHELF); TEMPERATURE (GREEN), SALINITY (RED); CHLOROPHYLL FLUORESCENCE CONCENTRATION (GREEN), DISSOLVED OXYGEN PERCENT SATURATION (BLUE), AND PHOTOSYNTHETICALLY ACTIVE RADIATION (PAR, ORANGE); NITRATE CONCENTRATION; AND AREAL ICE CONCENTRATION IN A 50 KM X 50 KM BOX AROUND C3 (DARK BLUE), DAILY AVERAGE DEPTH OF THE ICE KEELS (LIGHT BLUE). NOTE: TURBIDITY IS MISSING IN THIS PLOT DUE TO FAILED SENSORS.

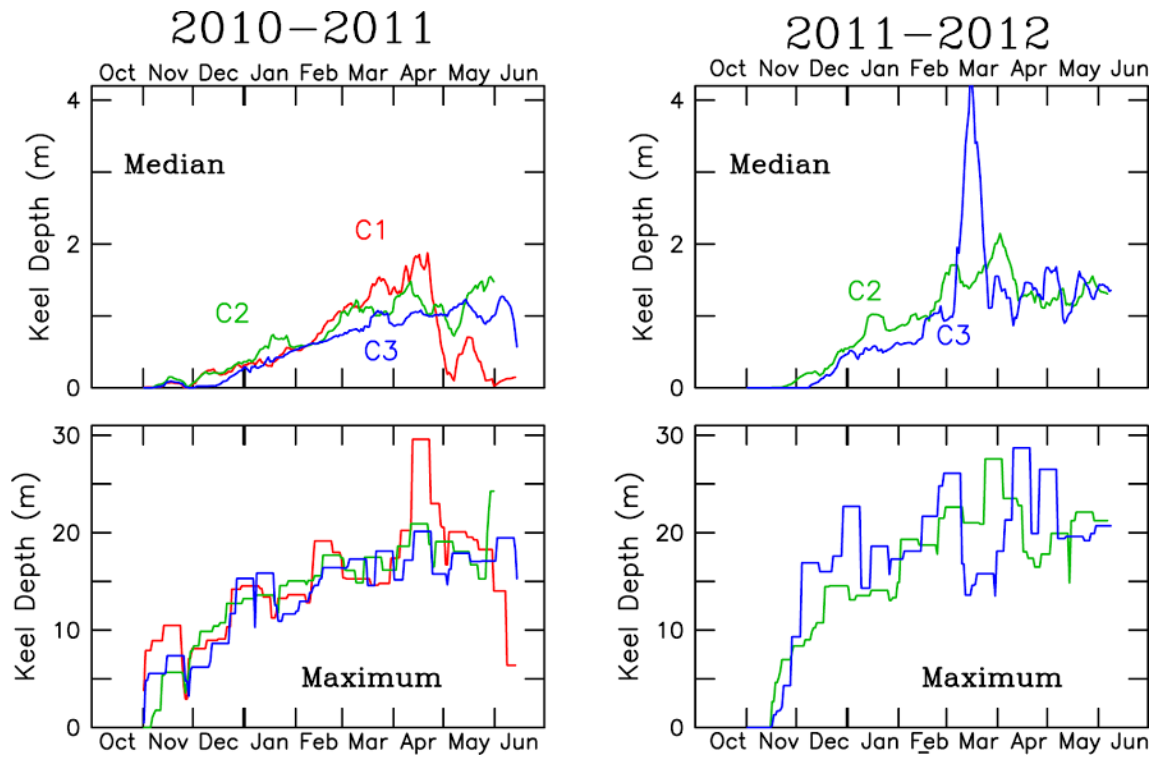


FIGURE 41. ICE KEEL DEPTH FOR BOTH DEPLOYMENT YEARS. THE TOP PANELS ARE THE MEDIAN ICE KEEL DEPTH WITH AN 11 DAY RUNNING FILTER. THE BOTTOM PANELS ARE THE MAXIMUM DEPTH OF THE ICE KEEL OVER AN 11 DAY PERIOD. THE ICE PROFILER FAILED ON THE INSHORE MOORING (C1) DURING THE 2011-2012 DEPLOYMENT.

Currents and Transport

The along shelf currents were well correlated for each deployment (Figure 42). The flow is strongest along the coast at the inshore mooring (C1), and weakens offshore, but does not go to zero at the offshore mooring (C3). In general the flow is toward the northeast, with multiple events of reversal in flow forced by wind events.

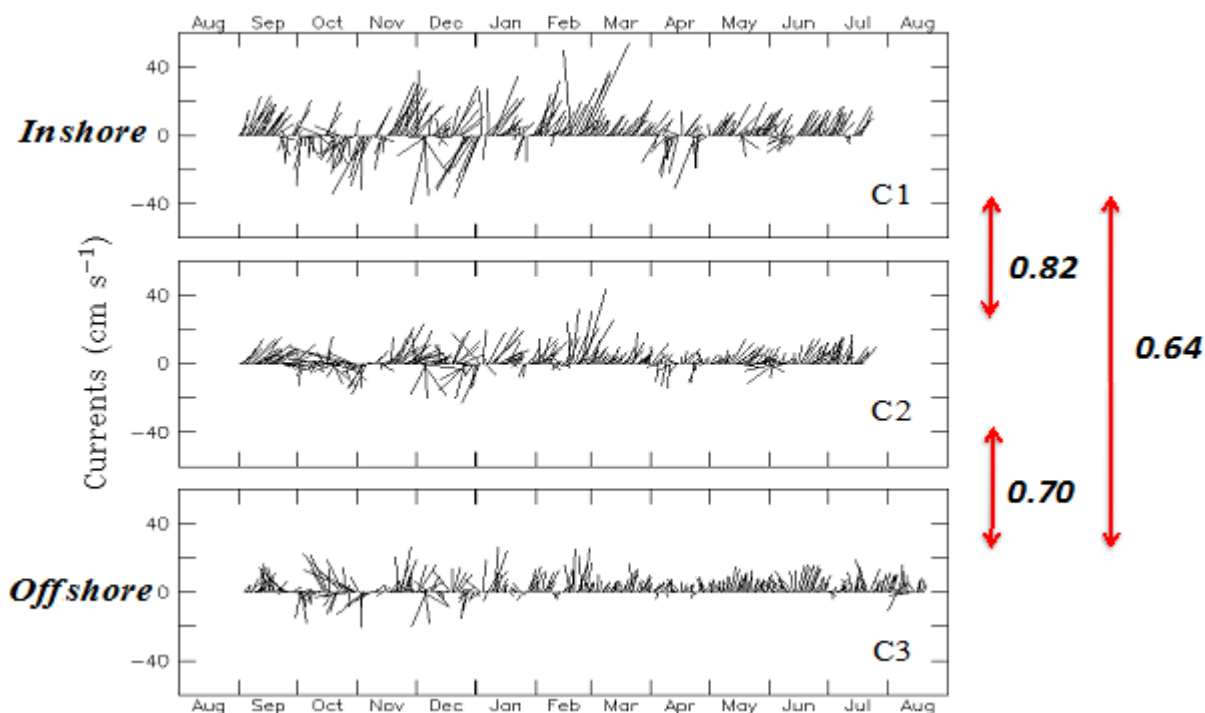


FIGURE 42. PLOTS OF DAILY BOTTOM CURRENTS (ROTATED TO ALONG SHORE) AT THE THREE MOORING SITES IN 2010-2011. THE TIME SERIES HAVE BEEN LOW PASS FILTERED. CORRELATIONS BETWEEN AND AMONG MOORING SITES REFLECTED BY RED ARROWS.

The current records can be integrated to obtain along shore transport (Figure 43). Since the flow at the offshore current meter does not go to zero, these estimates of transport may be an underestimation. The transports are significantly correlated with winds from the National Centers for Environmental Prediction (NCEP) ($r=0.68$, at 1 day lag) and dominated with 2-4 day variability. Mean transport for the 2010-2011 deployment was $0.42 \times 10^6 \text{ m}^3 \text{ s}^{-1}$, and in 2011-2012 it was $0.23 \times 10^6 \text{ m}^3 \text{ s}^{-1}$, indicating significant year-to-year variability (transport measured in 2012-2013 was similar to 2011-2012).

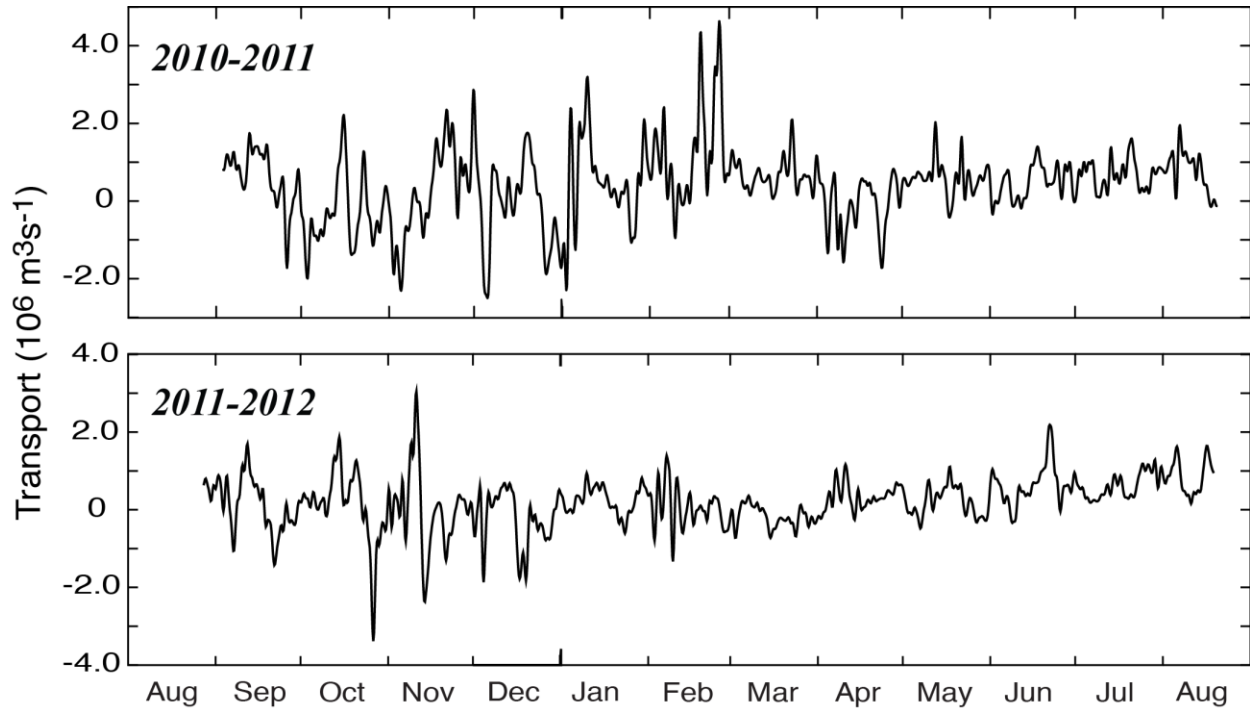


FIGURE 43. TRANSPORT CALCULATED AT ICY CAPE FOR DEPLOYMENTS IN 2010-2011 AND 2011-2012.

By calculating monthly averages of transport, the seasonal pattern of flow becomes clearer (Figure 44). The monthly mean transports during winter and fall were highly variable, but transport was northeastward with less variability in April through July. Using the measurements of transport through Bering Strait (Woodgate et al., 2005) indicates that the monthly mean transport on the Icy Cape line ranges from 25-50% of the transport through Bering Strait.

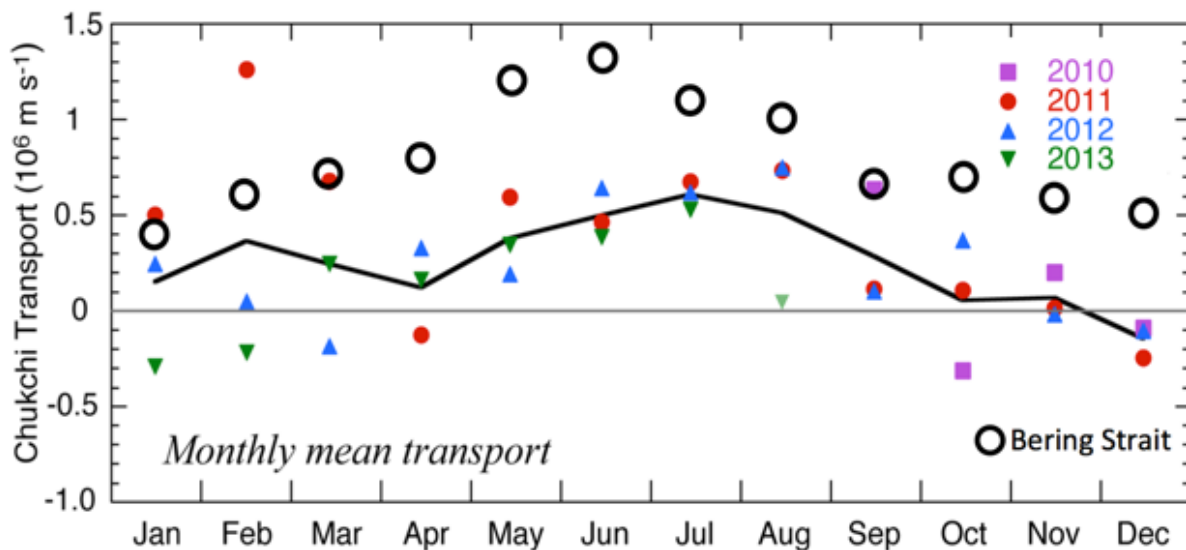


FIGURE 44. TRANSPORT CALCULATED AT THE ICY CAPE LINE (TRANSECT D) USING THE MOORING DATA. IN 2012-2013 ONLY THE MIDSHORE MOORING (C2) WAS DEPLOYED AND TRANSPORT WAS CALCULATED USING A REGRESSION DEVELOPED FOR THE 2010-2011 AND 2011-2012 DATA SETS. THE BLACK CIRCLES ARE THE LONG-TERM MONTHLY AVERAGE TRANSPORTS THROUGH BERING STRAIT (WOODGATE ET AL., 2005).

Upwelling Events and Intrusion of Atlantic Water onto the Shelf

Polynyas often occur on the eastern side of the Chukchi Sea. In 2010-2011, there were three events where the salinity increased markedly at the inshore mooring site (C1; Figure 35 and Figure 45). The first two events, which occurred in late-October and early January, respectively, were accompanied by an increase in temperature. The third event in mid-February, was associated with a slight decrease in temperature. Ice had not arrived at the mooring site at the time of the first event, but the second occurred when there was a reduction in areal ice cover. The open water is evident in Figure 46. Both events were associated with southwestward flow and a slight decrease in percent oxygen saturation, especially the second event (Figure 35). These two events are likely caused by intrusion of Atlantic water from Barrow Canyon. The third event is very different. It was associated with northeastward flow, and no apparent change in ice coverage. The slight cooling of temperature (Figure 45, green data) supports the conclusion that the event is a result of brine rejection.

In contrast, during the 2011 – 2012 deployment at the inshore mooring site (C1), salinity does not show the same extremes (>34.2), although there is some evidence of higher salinity and warmer water in and around January 1, 2012 (Figure 38).

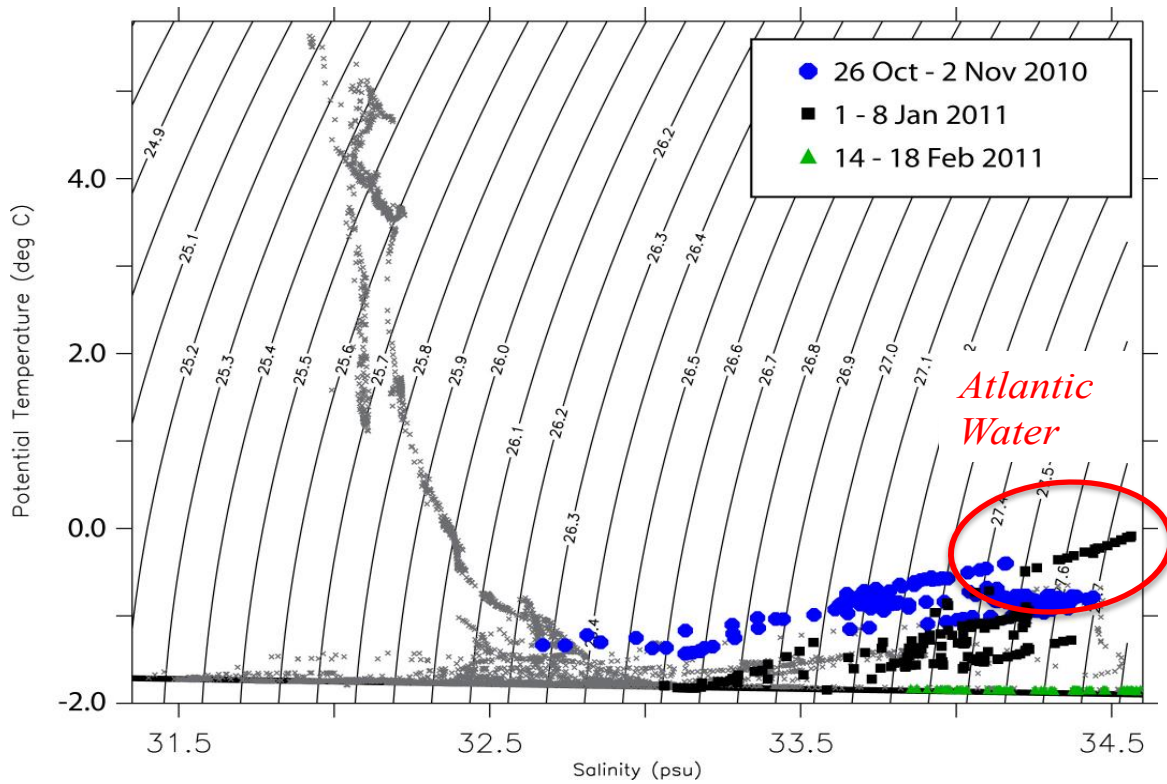


FIGURE 45. THE WARMER, MORE SALINE ATLANTIC WATER IS EVIDENT IN THE TEMPERATURE-SALINITY (T-S) DIAGRAM FROM THE TIME SERIES MEASURED AT THE INSHORE MOORING SITE, C1. THE COOLING OF THE FEBRUARY EVENT IS EVIDENT IN GREEN.

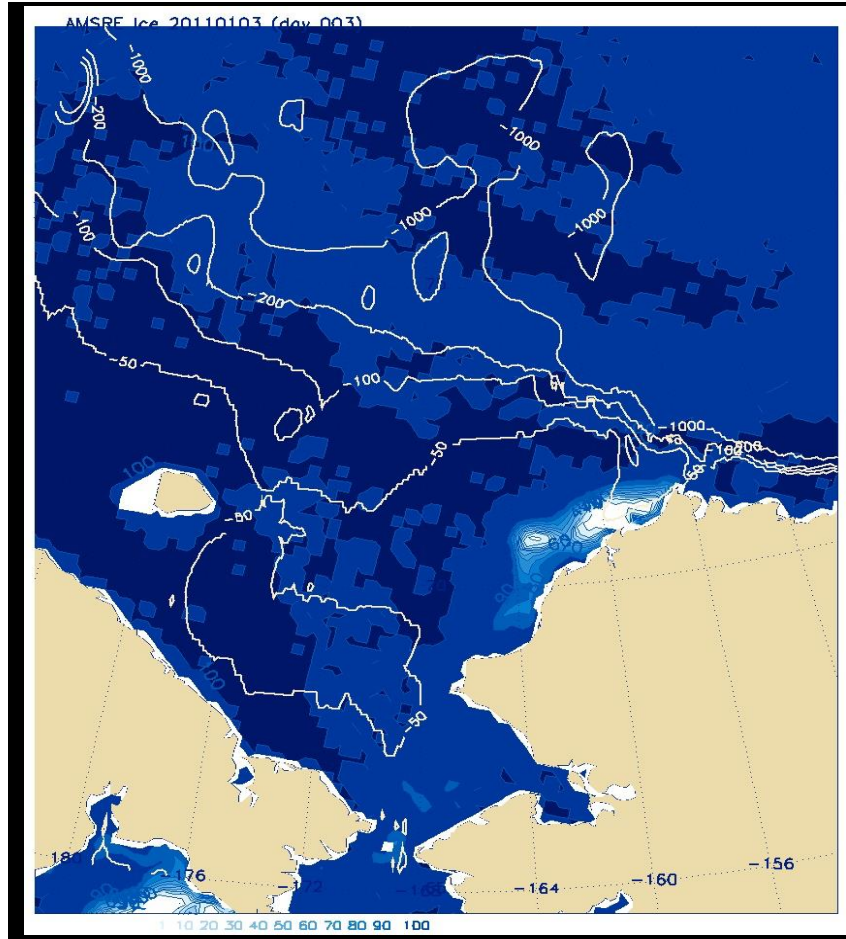


FIGURE 46. PERCENT AREAL ICE COVER ON JANUARY 3, 2011. THE DARK BLUE IS 100% ICE COVER, WHILE WHITE IS <10% COVER. ICE COVER SCALE IS AT THE BOTTOM OF THE PLOT.

Water Masses and year-to-year variability

Hydrographic data were collected in 2011 and 2012 along the Icy Cape line. In August 2011, the ice edge had retreated beyond the shelf break into the Beaufort Sea while in 2012 the ice persisted on the shelf, just to the north of the hydrographic transect. The position of the ice influences the water properties (Figure 47), with Alaska Coastal Current (ACC) and Winter Water (WW) appearing in both years. Melt Water (MW) only appeared in our 2012 data. The plots for 2010 are not shown (but see Figure 67) because in 2010 we were unable to collect deep data without a winch and real-time CTD. The presence/absence of melt water is even more clearly evident in the Temperature-Salinity (T-S) plot (Figure 48).

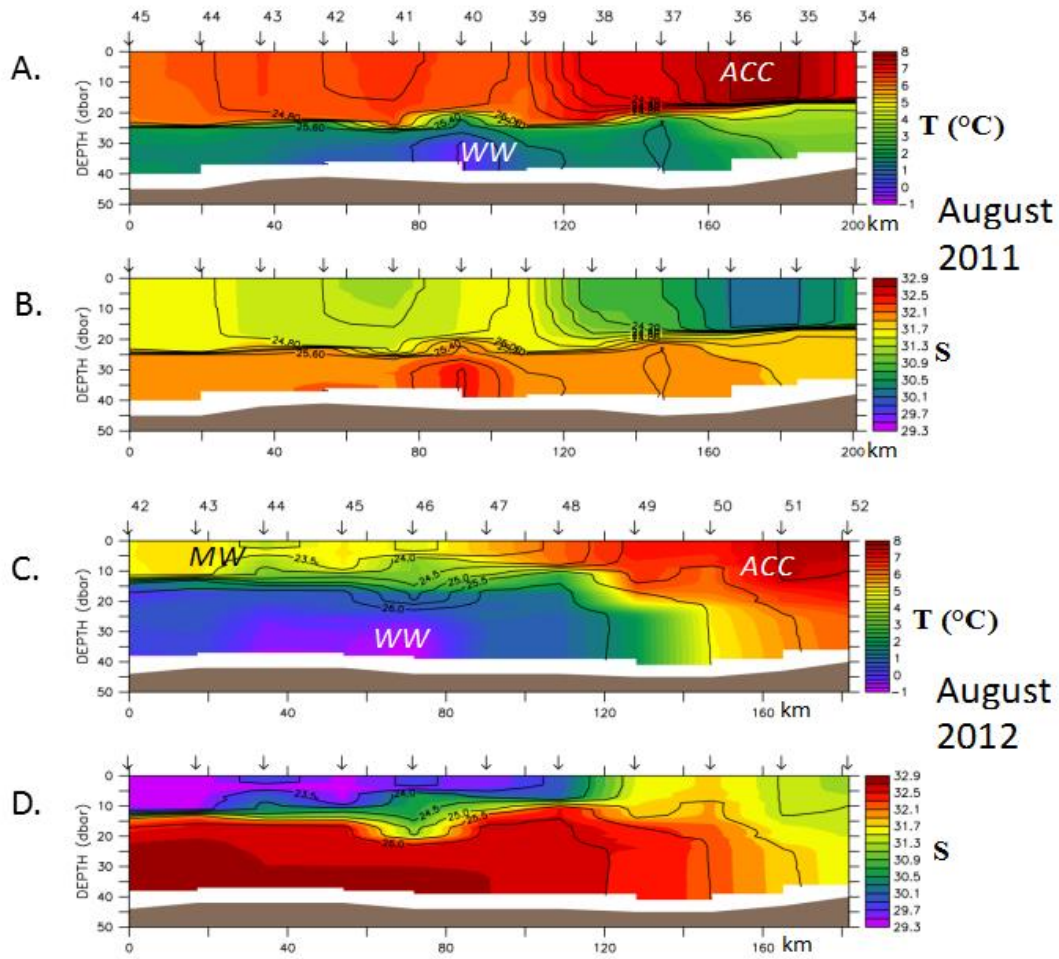


FIGURE 47. TEMPERATURE (A), SALINITY (B) MEASURED IN AUGUST 2011, TEMPERATURE (C), SALINITY (D) MEASURED IN AUGUST 2012 ALONG THE ICY CAPE TRANSECT. ACC, WW AND MW WATER ARE INDICATED IN THE TEMPERATURE PANEL.

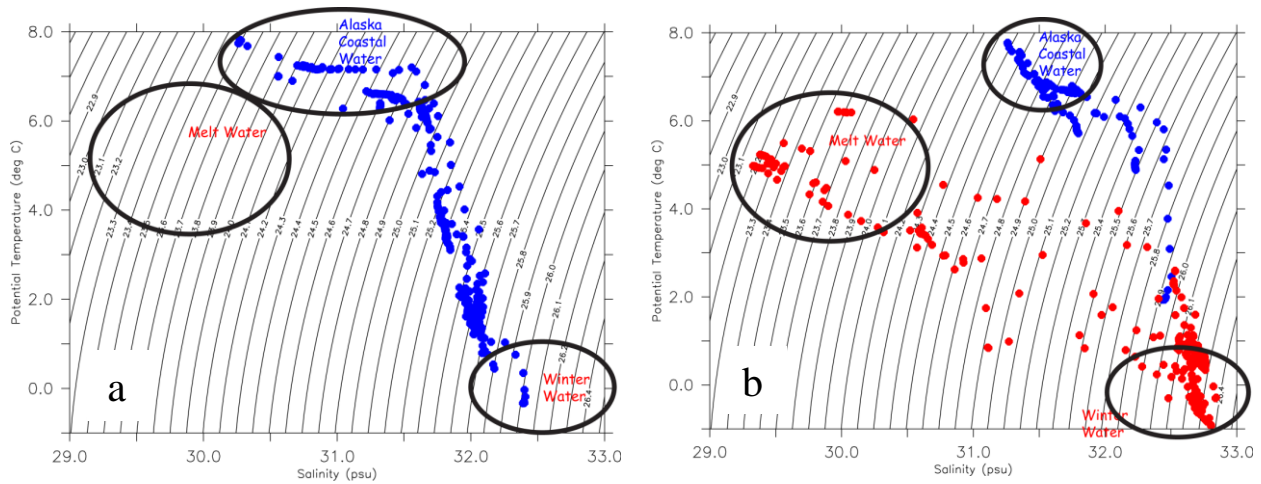


FIGURE 48. PLOTS OF TEMPERATURE AND SALINITY ON A DENSITY GRID FOR (A) AUGUST 2011 AND (B) AUGUST 2012. NOTE IN 2011 THERE WAS NO MELT WATER IN IN THE T-S PLOT (EMPTY OVAL WITHOUT POINTS).

Time Series of Zooplankton Backscatter Estimated From ADCP Instruments

We first examined the temporal patterns in ADCP-derived zooplankton volume backscattering from the fall 2011 echograms at the offshore (C3) and midshore (C2) moorings (Figure 49). One can see evidence for diel vertical migration (the cyclic banding of colors demonstrating daily highs and lows in volume backscatter) during this period as well as difference in S_v at the two sites along the same transect line.

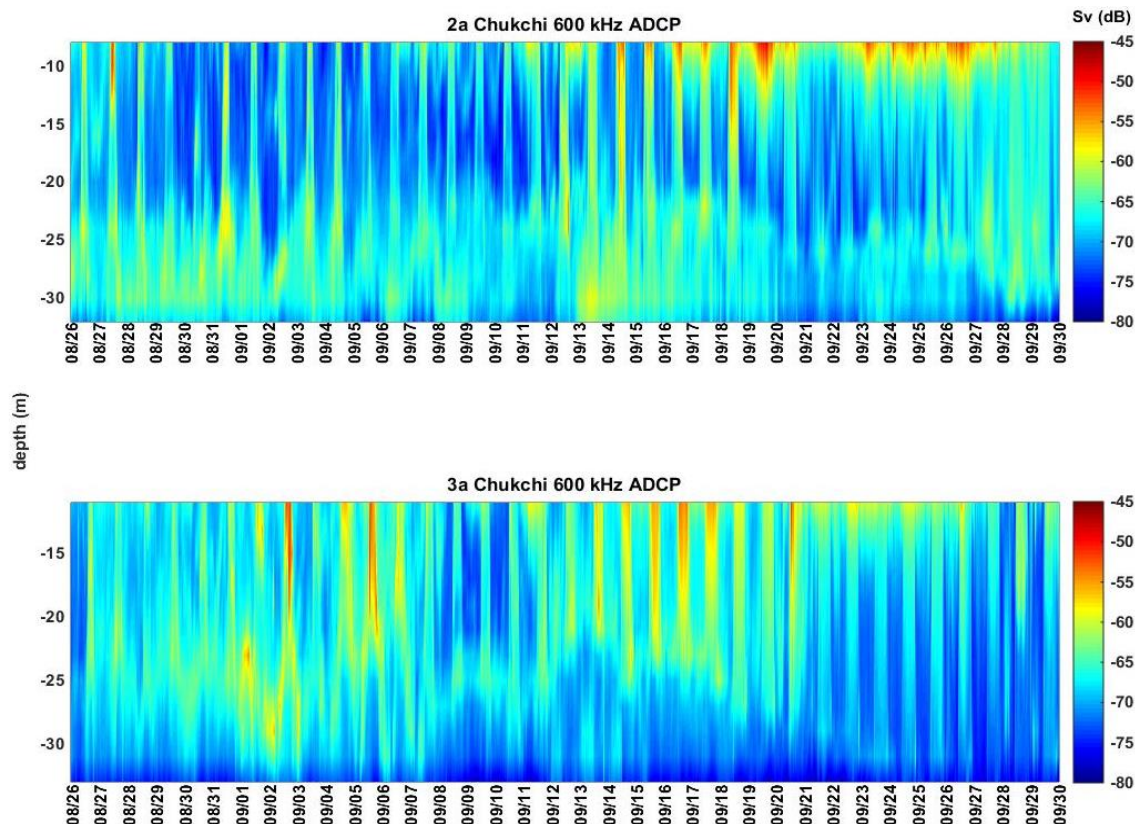


FIGURE 49. ADCP ESTIMATED ZOOPLANKTON VOLUME BACKSCATTER (S_v) LATE AUGUST TO LATE SEPTEMBER 2011. TOP PANEL = MIDSHORE MOORING; BOTTOM PANEL = OFFSHORE MOORING; MONTH/DAY IS ON ABSCISSA AND CENTERED AT 1300 HRS ALASKA DAYLIGHT SAVING TIME (ADT, GMT+8 HRS).

At the midshore location (Figure 49, top), S_v appears to be low in late August and high at the very end of September. The midshore station also has a layer of scattering that remains close to the bottom for most of the short time series. Zooplankton backscatter at the surface is very high in late September, but the signal may be contaminated by air bubbles. At the offshore station (C3) we see strong scattering in late August throughout the water column diminishing with time so that by late September, S_v has declined and there is a clear pattern in the diel vertical distribution.

We next examined the patterns of temporal variability near the surface (7 – 12 m depth) and at depth (27 – 31 m depth) during the 2010 and the 2011 deployments for each of the 3 sites (inshore C1, midshore C2, and offshore C3) to examine the strength of diel vertical migration and to learn if there were other strong temporal patterns in the data. In 2010-2011, near the surface there was very little evidence of any significant variability in either the diurnal or semi-diurnal periods (24- and 12-hr periods) in either the temporal plots (Figure 50, left panel) or the averages over the deployment (Figure 50, right panel). The contoured values of variability are highest for the longest period, > 64 hrs, however the averages over the entire deployments were not high enough to be statistically significant at any of the three mooring sites. The result was slightly different at depth. Again, the variability was highest at the longer periods in the contour plot (left panel > 64 hrs), however when averaged over the course of the entire deployment, there was statistically significant variability ($P < 0.05$) in the semi-diurnal (12-hr) period at the

midshore (C2) and offshore (C3) mooring sites and a peak in the variability at the diel (24-hr) period (Figure 51).

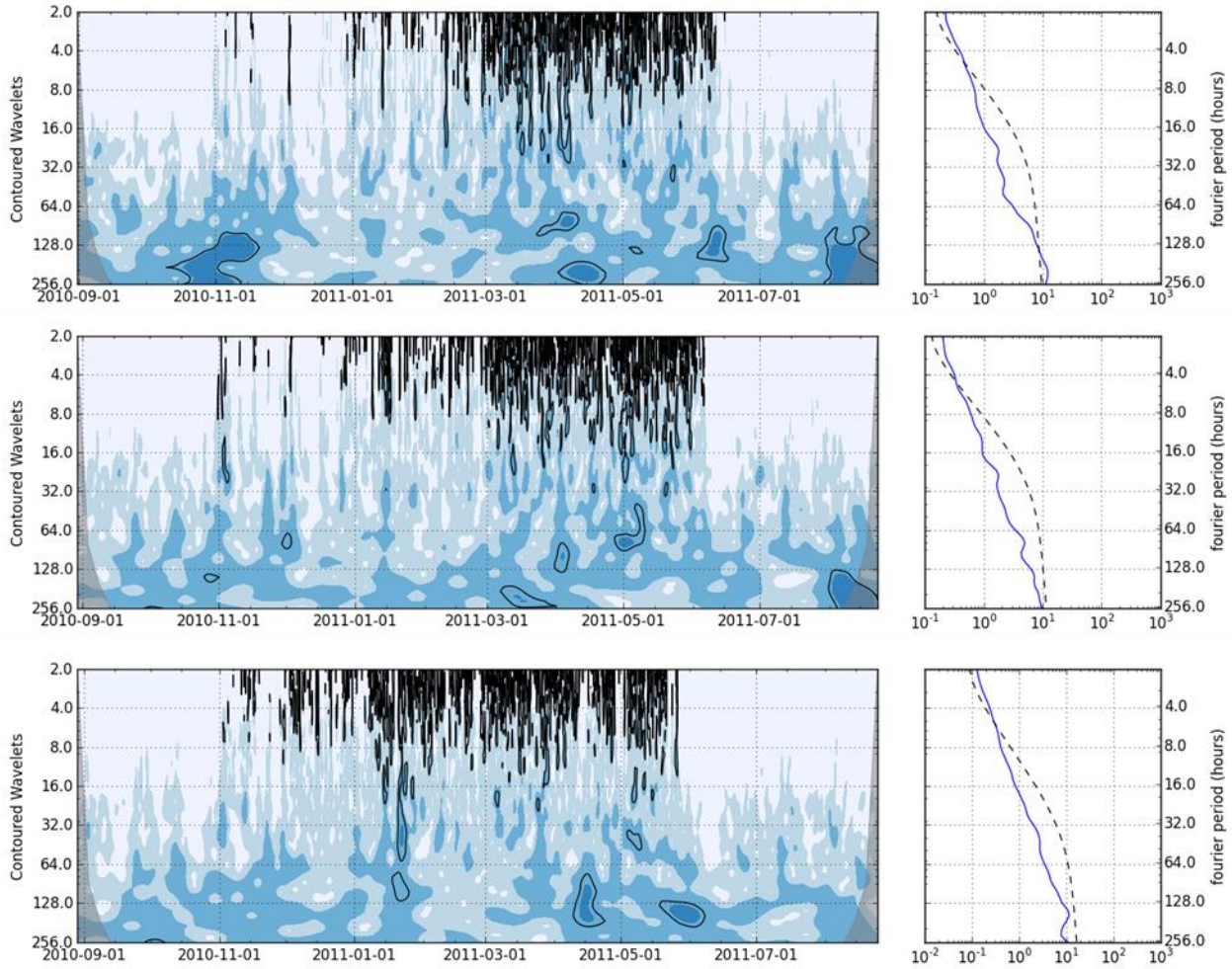


FIGURE 50. WAVELET ANALYSIS OF 2010 - 2011 NEAR SURFACE DATA (7-8 M) ZOOPLANKTON VOLUME BACKSCATTER DATA FROM THE ICY CAPE TRANSECT. FROM TOP PANEL TO BOTTOM PANEL: OFFSHORE, C3; MIDSHORE, C2; INSHORE, C1. LEFT PLOTS SHOW CONTOURED WAVELET VALUES AS A FUNCTION OF DATE. RIGHT PLOTS SHOW THE AVERAGE MAGNITUDE OF TEMPORAL SIGNAL AS A FUNCTION OF PERIOD. DOTTED LINE IS $P = 0.05$ SUCH THAT WHEN THE PEAKS ON THE BLUE LINE ARE TO THE RIGHT OF THE DOTTED LINE, VARIABILITY IN THAT PERIOD IS CONSIDERED TO BE STATISTICALLY SIGNIFICANT.

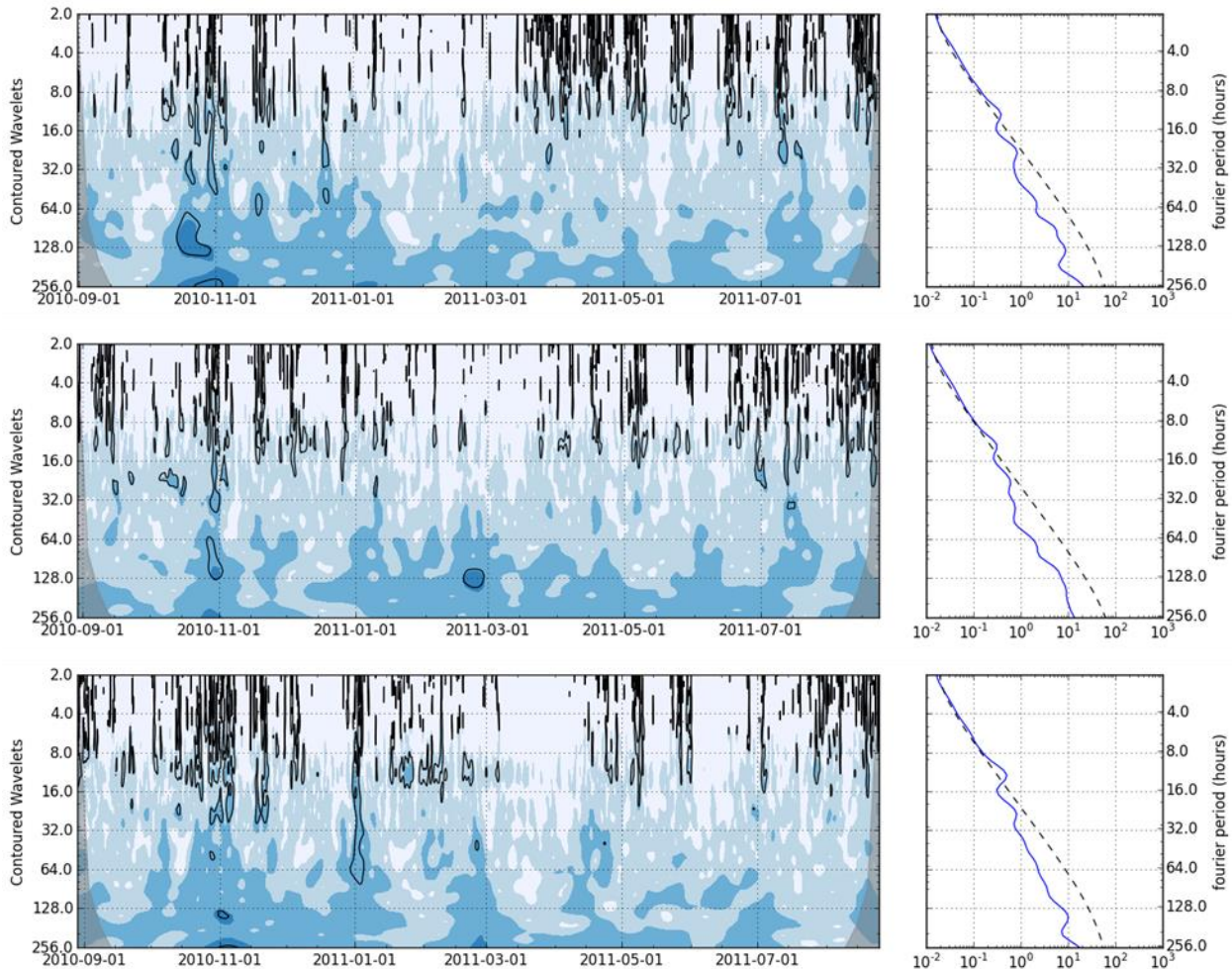


FIGURE 51. WAVELET ANALYSIS OF 2010 - 2011 AT DEPTH DATA (27-28 M) ZOOPLANKTON VOLUME BACKSCATTER DATA FROM THE ICY CAPE TRANSECT. FROM TOP PANEL TO BOTTOM PANEL: OFFSHORE, C3; MIDSHORE, C2; INSHORE, C1. DETAILS OF PLOTS ARE THE SAME AS IN THE PREVIOUS PLOT.

The temporal variability of zooplankton near the surface in 2011-2012 was somewhat similar to that observed during the previous year, although the peak diel variability was stronger at the midshore (C2) and offshore (C3) than it had been the previous year (Figure 52). Diel variability was still not significant ($P < 0.05$) when examined over the entire deployment. Results at depth were similar to the previous year with a significant ($P < 0.05$) amount of temporal variability at the semi-diurnal period and a non-significant peak in the diel period (Figure 52). Peaks in semi-diurnal variability occur at different times at the different locations. For example, much of the semi-diurnal signal occurred after May at the inshore mooring, while the levels of temporal variability were more evenly distributed over the time of deployment at the other two locations.

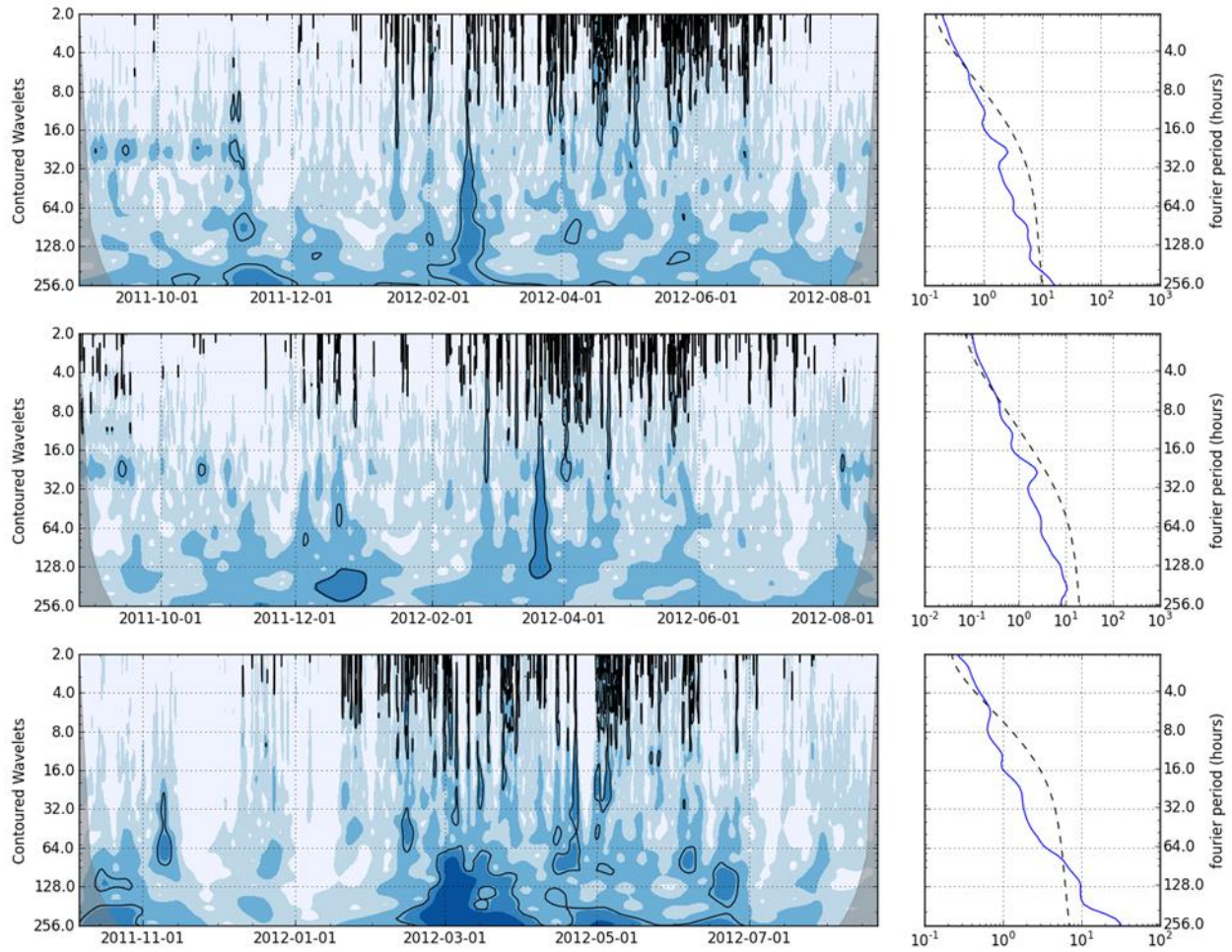


FIGURE 52. WAVELET ANALYSIS OF 2011-2012 NEAR SURFACE DATA (11-12 M) ZOOPLANKTON VOLUME BACKSCATTER DATA FROM THE ICY CAPE TRANSECT. FROM TOP PANEL TO BOTTOM PANEL: OFFSHORE, C3; MIDSHORE, C2; INSHORE, C1. DETAILS OF PLOTS ARE THE SAME AS IN THE PREVIOUS PLOT.

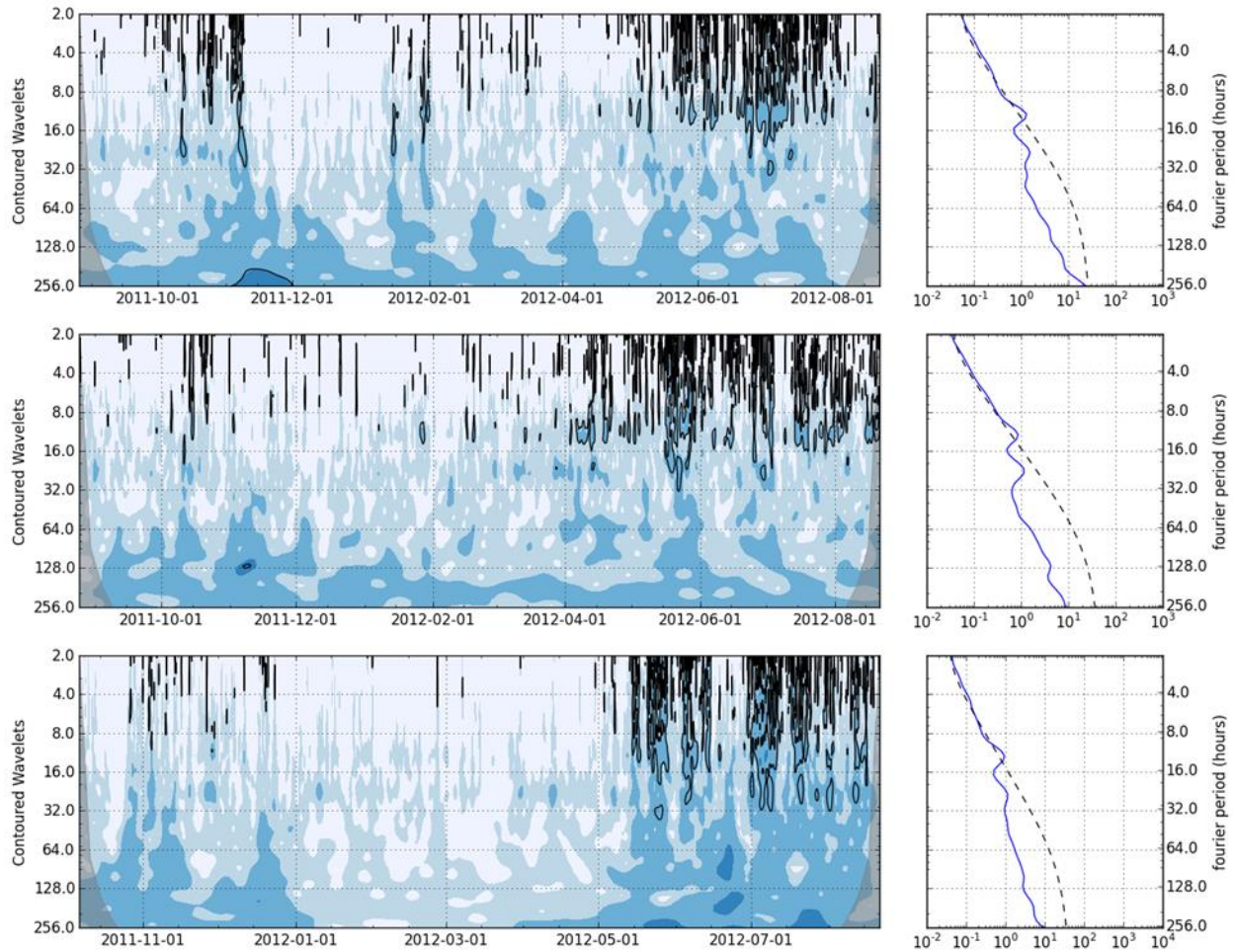


FIGURE 53. WAVELET ANALYSIS OF 2011-2012 AT DEPTH DATA (28-32 M) ZOOPLANKTON VOLUME BACKSCATTER DATA FROM THE ICY CAPE TRANSECT. FROM TOP PANEL TO BOTTOM PANEL: OFFSHORE, C3; MIDSHORE, C2; INSHORE, C1. DETAILS OF PLOTS ARE THE SAME AS IN THE PREVIOUS PLOT.

Time Series of Zooplankton Volume Backscatter Estimated From Multi-Frequency Acoustic Measurements (TAPS6-NG)

We successfully obtained measurements of echo intensity at all 6 frequencies from deployment until September 30th 2011 and then again from early December until late January 2012 at the midshore mooring, C2. The first interruption was due to an error in the instrument’s software code. The instrument ceased taking measurements after the attempt to change sample intervals from 30 to 60 minutes at the end of September (Figure 54-55; missing data indicated by red arrow on time axis). It started acquiring measurements again in early December and continued to operate until it depleted its batteries in late January 2012. Early depletion of battery power was corrected in later years by switching from alkaline to lithium batteries and increasing the capacity (amp hrs) of the battery packs.

Near-bottom abundance estimates for euphausiid-shaped scatterers showed that the 14-18 mm size range were most abundant at 30-40 per m³ (Figure 54A). Lower abundances for euphausiid-shaped scatterers of around 10 per m³ were apparent in the smaller (~10-11 mm) and

larger (>20 mm) size ranges. All size ranges, with the exception of the 20 mm individuals, were most abundant in the fall and declined in number in the winter months, consistent with expectations. Near-bottom abundance estimates for the 2-6 mm size range copepod-shaped scatterers were approximately 1500 per m³ (Figure 54B). Estimates of the abundance of copepod-shaped organisms did not decline with time from fall to winter.

Near-surface abundance estimates (25 m from transducer, ca 10 m depth) for euphausiid-shaped scatterers 14-18 mm were higher than those deeper in the water column (100-200 per m³ Figure 55A). Lower abundances of approximately 10-20 per m³ were estimated for the larger (>20 mm) sizes. Abundances stayed consistent throughout August and September. Near-surface abundances of approximately 1500 per m³ for the copepod-shaped, 2-6 mm size range were only briefly detected in early September (Figure 55B). Echo intensities during the remainder of the deployment were below the signal-to-noise ratio threshold used in our analyses.

A.

B.

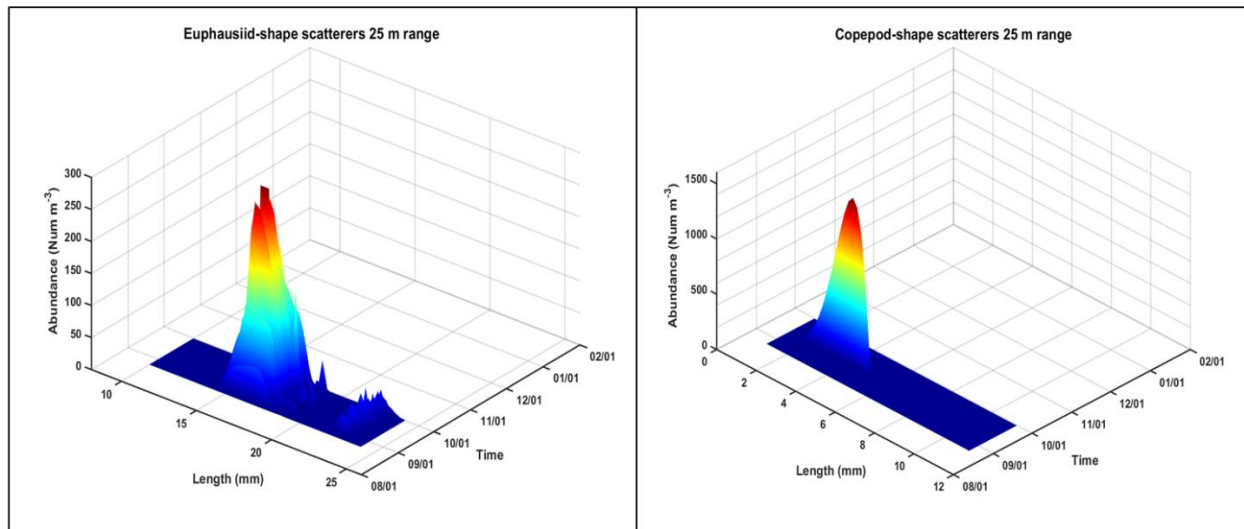
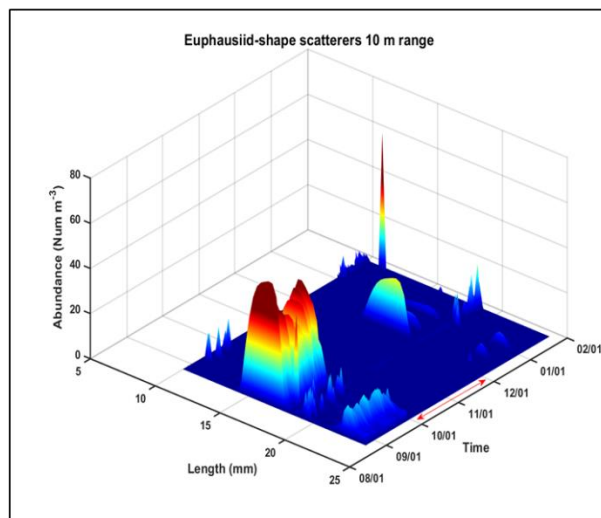


FIGURE 54. ESTIMATED ABUNDANCE AT 25 M FOR TWO TYPES OF ZOOPLANKTON SCATTERERS DERIVED FROM THE MULTI-FREQUENCY TAPS6-NG (A) EUPHAUSIIDS AND (B) COPEPODS. RED ARROW ON TIME AXIS INDICATES A GAP IN DATA COLLECTION CAUSED BY A PROBLEM WITH INSTRUMENT SOFTWARE.

A.



B.

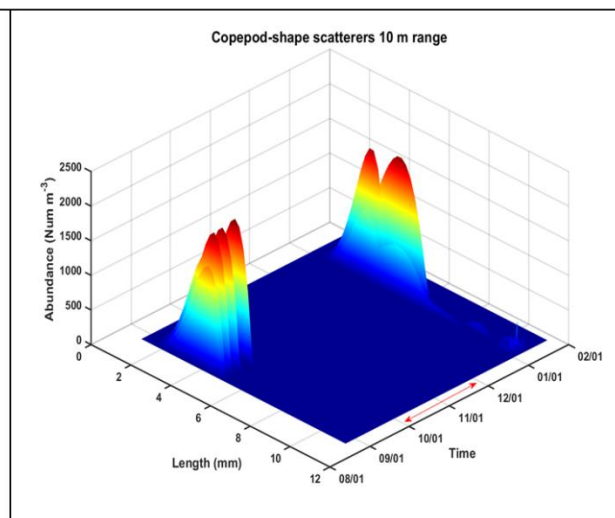


FIGURE 55. ESTIMATED ABUNDANCE AT 10 M FOR TWO TYPES OF ZOOPLANKTON SCATTERERS DERIVED FROM THE MULTI-FREQUENCY TAPS6-NG (A) EUPHAUSIIDS AND (B) COPEPODS.

3. Discussion

Time Series of Physical and Chemical Data from Biophysical Moorings

The Arctic has changed markedly in the last decade, entering a new phase sometimes referred to as the “new normal” - thinner ice, earlier ice retreat in spring and late ice arrival in the fall, warmer ocean temperatures during summer, and changes in weather patterns (Wood et al., 2015). These physical changes will continue to have profound impacts on this ecosystem. Long-term observations are necessary to quantify the changes in the ocean.

Time Series of Zooplankton Backscatter Estimated From ADCP Instruments

Single-frequency acoustic data does not allow users to attribute the volume backscattering (S_v) to specific components of the plankton community. Only multi- or broad-band acoustics can discriminate among the large diversity of sizes of plankton and target strengths of different types of scatterers in the plankton. However, ADCPs are a common tool of physical oceanographers and require little extra effort to capture the echo counts. These echo counts can be used to identify the period of maximum variability in zooplankton backscatter (e.g., diel, fortnightly, seasonal, etc.). Therefore, they are a useful tool for examining periodicity in bulk zooplankton and future investigations should include them.

The patterns of temporal variability in zooplankton volume backscatter were very different from what we’ve observed in the southeastern Bering Sea. In the southeastern Bering Sea, wavelet analysis of scattering at 18 m measured from spring to late summer, showed a strong diel periodicity. In that region it was strongest at the end of the summer in 2007 and 2009 and was strongest in the middle of the summer in 2010. In all three years, the strength of the diel

signal was much stronger than the semi-diurnal signal. In the Chukchi Sea, a diel signal was not always detectable, but a semi-diurnal signal was often statistically significant at depth, particularly at the midshore (C2) and offshore (C3) mooring sites. Temporal patterns at the three stations were often very different indicating great variability in zooplankton behavior across this relatively broad, flat shelf.

We attribute these results to differences in the zooplankton community and photoperiod between the Bering and Chukchi Seas. At mooring site M2 in the southeastern Bering Sea, the water column is much deeper than that of the Chukchi Sea (72 m versus 40 m) and the zooplankton biomass is dominated by late stage *Calanus* spp. and juvenile and adult *Thysanoessa* spp. In the Chukchi Sea there were very few adult or juvenile euphausiids.

In addition, the photoperiods (hours of sunlight) and sun angle vary affecting the light stimulus to the zooplankton. At M2 in the eastern Bering Sea there are a minimum of 6 3/4 hrs of sunlight in the winter and a maximum of almost 18 hrs at the summer solstice, while in the Chukchi Sea the zooplankton will experience 0 hrs of light from mid-November to mid-January and 24 hrs of light from mid-May to early August. Factors such as ice thickness and ice snow cover, further modify the light penetrating the surface waters and hinder or remove the light intensity cue. The intermittently detectable diel signal in the Chukchi Sea is consistent with previous Arctic research (Cottier et al., 2006; Berge et al., 2009; Wallace et al., 2010). Previous Arctic studies have confirmed that because of the extreme environment, DVM can become intermittently synchronized or even completely unsynchronized, where individuals vertically migrated in an uncoordinated way. Note that food cues and the onset of diapause may also modify migration behavior at high latitudes.

Time Series of Zooplankton Volume Backscatter Estimated From Multi-Frequency Measurements

The newly developed TAPS6-NG acoustics system was successful in obtaining two, short-term records of zooplankton volume backscatter at the midshore mooring site, C2 (August-September & December-January). Zooplankton backscatter from both copepod-shaped and elongate scatterers was detected during those periods. The size of the euphausiids resolved by the inverse method generally agreed with net samples collected in August which indicated that the number of adult euphausiids was very low and that most euphausiids were from much younger stages. The system software did not automatically take measurements of background electronic system noise as intended and we had to rely on using minimum echo intensities measured for each depth bin each week. This resulted in signal-to-noise ratio for many ensembles that were below our 10 dB cutoff, and is the likely reason why we were unable to detect more zooplankton scatters during winter in the near-surface estimates. Copepods are weak scatterers, thus may be difficult to detect above noise thresholds the further they are from the transducer face.

A net sampling program is important to help capture a near complete picture of the zooplankton community (minus the delicate jelly plankton), and can be used to guide which scattering models are appropriate to interpret zooplankton volume backscatter from acoustic instruments. Unfortunately, the amount of net sampling is currently limited to the ice-free periods and the times when an ice-breaker is in the area. Net samples also require a large

amount of analyst time to process. More effort should be expended on optical and other technologies with automated image analysis that can capture data on zooplankton community structure during times of the year when net sampling is not possible.

4. *Conclusions*

The currents in the Chukchi Sea are well correlated both horizontally and vertically, and are generally northeastward, but with events of southwestward flow. The currents are also well correlated with the local winds. The flow patterns on the shelf are fairly well known, and results from this study (hydrography, current measurements, and satellite-tracked drifter trajectories) contributed to the refinement of the map of currents shown in Figure 57.

Approximately 40% of the flow through Bering Strait passes the Icy Cape line. Furthermore, monthly mean total transport, measured from moorings, is highly variable in fall and winter, with less variability in summer. Transport was stronger as measured on the 2010-2011 mooring deployments than on those in 2011-2012 and 2012-2013. Intrusions of slope water up Barrow Canyon could be seen at Icy Cape. However, these intrusions have high interannual variability, as the two years differed markedly in the number and strength of the intrusions. Although average keel depth was ~4-5 m, deep ice keels (>27 m) occurred each year, generally in late spring. There were more polynyas seen on the 2010-2011 deployment than on the one from 2011-2012. Ice arrived at approximately the same time in 2011 and 2012, but it retreated almost a month earlier in 2011 than 2012. This was reflected in the bottom mooring temperatures, which warmed above -1.8°C in early to mid-June in 2011 and in late June to late July in 2012.

The Chukchi shelf is shallow and chlorophyll exported to the bottom continues to be productive, as evidenced by enhanced oxygen concentrations. At the end of summer, nitrate is usually low, indicating little or no nitrate on the shelf at that time. The bottom nitrate is replenished in September, but decreases in the fall likely because of dilution by vertical mixing. By May or June the nitrate supply has been replenished.

Diel vertical migration by zooplankton was not regular (non-stationary) during the year. The shallow water column and difficulty predicting where the zooplankton spend most of their time may make it difficult to understand the exposure of plankton to oil, should there be an oil spill in the region. Upward looking zooplankton acoustics holds promise for determining year-round abundance and distribution, however the instruments used for these measurements must be very robust.

5. *Recommendations*

It is critical that we continue to moor physical and biological instruments in close proximity to better conduct inter-disciplinary studies. Bio-physical moorings have been deployed each year since 2010 on the Icy Cape line (inshore, midshore, and offshore), thus it is essential that we maintain this long-term dataset. The measurements of currents provide an estimate of transport along the Alaskan coast in the Chukchi Sea. These, combined with measurements of

temperature, salinity, chlorophyll fluorescence, nutrients and PAR will provide indices to better understand how the ecosystem is changing, especially during the ice cover seasons.

We must work to improve the reliability of the TAPS6-NG controller board and update system memory so that individual ping data can be stored. Improvements will also include examining predicted signal to noise ratios to see if instrument performance for measurements far from the transducer face can be improved.

Ultimately, we must utilize new and emerging technologies to better sample this remote and harsh region. New instrumentation such as acoustic fish finders, new fluorometers which provide information on the health of phytoplankton, and “lab on a chip” which measures nitrate, phosphate, silicate, and ammonium are being developed to be deployed on moorings and vehicles. Furthermore, we need to collect or find better estimates of the material properties of euphausiids, particularly the relationship between lipid content and target strength. We also need to investigate ways to combine acoustic and optical methods so that analysts know which plankton scattering models to apply at different times of the year. Finally, it is important to conduct modeling and other experiments to arrive at methods to optimize our ability to detect plankton close to the underside of ice.

B. Shipboard Observations

1. Methods

Hydrography-- Physical and Chemical Variables

Hydrographic data were collected during cruises in 2010, 2011 and 2012 (Table 15). The primary design of the hydrographic survey was twofold: to collect samples of temperature, salinity, chlorophyll fluorescence, oxygen and PAR using a CTD, and to collect samples for analysis of oxygen, chlorophyll, nutrients (nitrate, phosphate, silicate, nitrite and ammonium), and salinity. Water samples were collected at selected depths on six hydrographic transect lines (Figure 32; A, B, C, D, E, F). Line F was not occupied in 2010. The primary purpose of the water samples collected for salinity and oxygen was to calibrate the instruments on the CTD.

In 2010, due to the failure of our winch and of the SeaBird SBE 911plus CTD deck unit, we were unable to complete hydrographic casts using our high resolution CTD and rosette. Therefore, the CTD/water bottle casts were conducted with a lower resolution SeaBird SeaCAT (SBE19plus) lowered on a mechanical (non-conducting) wire to 30 meters. Niskin bottles were attached to the wire at three depths (1, 20 and 30 meters). The bottles were tripped using messengers and the data were downloaded from the SBE 19 after each cast. In 2011 and 2012, sampling was fully successful, with a Sea-Bird SBE 911plus system with dual temperature and salinity sensors, and oxygen (SBE-43) sensors, a photosynthetically active radiation (PAR) sensor (Biospherical Instruments QSP-200 L4S or QSP-2300), and a chlorophyll fluorescence (WET Labs WETStar WS3S) sensor. Nutrients and chlorophyll samples were collected at the surface, at 10 meter intervals, and at the bottom of the cast.

Nutrients and chlorophyll samples were taken from each Niskin bottle, processed and frozen in the – 80°C freezer for analysis in the laboratories at PMEL and AFSC, respectively, in Seattle, Washington. Salinity calibration samples were taken on approximately half the casts and

analyzed using a laboratory salinometer at PMEL. Oxygen samples were taken on most casts and titrated using the Winkler method. The number of CTD stations and the number of nutrient and chlorophyll samples collected are shown in Table 15.

TABLE 15. THE NUMBER OF HYDROGRAPHIC STATIONS OCCUPIED IN THE CHUKCHI SEA (INCLUDING BERING STRAIT), TOGETHER WITH THE NUMBER OF NUTRIENT SAMPLES AND THE NUMBER OF CHLOROPHYLL SAMPLES COLLECTED AND PROCESSED.

	CTDs	Nutrients	Chl.
2010: 24 Aug – 20 Sep	57	159	176
2011: 12 Aug – 11 Sep	56	286	276
2012: 8 Aug – 7 Sep	55	297	276

Satellite-tracked drifters

In 2011, three satellite-tracked drifters were deployed (funded by NOAA) in the Chukchi Sea (Table 16). The drogues were “holey socks” centered at a depth of 25 m, which was below the summer mixed layer depth. Each drifter was instrumented with a temperature sensor at the bottom of a float (i.e., just below the sea surface). At these high latitudes, more than 14 position-fixes per day were obtained from Argos, until the drifter was caught in the ice at which time the fixes became erratic. Once the data were received from Argos, spurious data were deleted from the time series. Data collected after the drogue was lost or entered into ice (determined from maps of ice extent) were noted.

TABLE 16. THE IDENTIFYING NUMBER OF THE DRIFTER AND THE LATITUDE AND LONGITUDE WHERE IT WAS DEPLOYED.

Argos Drifter	Latitude	Longitude
106694	66.008°N	168.797°N
106699	67.776°N	168.580°N
106698	72.798°N	161.009°N

Satellite remote sensing and ice data

The Advanced Microwave Scanning Radiometer EOS (AMSR; <http://nsidc.org/data/amsre/>) was used in this report. AMSR is a data set of sea-ice extent and areal concentration, consisting of daily ice concentration data at 12.5 km resolution, which are available from the National Snow and Ice Data Center. The time series of percent areal coverage were calculated in a 50 km x 50 km box around each of the mooring sites.

Zooplankton Net Data

Zooplankton was collected on each cruise using a multiple-opening and closing 1 m² Tucker Sled trawl equipped with sled-like runners at the bottom so that samples could be taken in close proximity to the bottom (Dougherty et al., 2010; Figure 56). The majority of the

sampling was accomplished during daylight hours, however on several occasions we were unable to complete an entire transect during daylight and some stations were completed in darkness. The Tucker Sled was equipped with 1 m², 333 µm Nitex mesh nets for collection of “large” zooplankters and a 500 µm mesh drogue net that was open when the sled was deployed. Inside the mouths of the 333 µm mesh Tucker nets was a 20 cm diameter net of smaller mesh (153 µm) to capture the smaller-sized zooplankton species. A calibrated General Oceanics mechanical flowmeter was situated along the centerline of the 1 m² net to measure distance traveled and a small CTD was mounted just behind the top bar of the Tucker Sled to determine temperature, salinity, and depth during and after each cast. A SeaBird SeaCAT (SBE 19plus) or SeaBird FastCAT (SBE 49) was attached to the top of the frame immediately behind the net to telemeter depth data and record the *in situ* temperature and conductivity. Net configurations, sampling strategy, and instruments for individual years are described in Table 17.

When two 333 µm mesh nets were used, the bottom net was fished for 2 minutes along the bottom before being closed. At closure, the frame was retrieved at approximately 20 m/min so that the second net sampled the entire water column. Plankton captured by the nets was washed into the cod ends, sieved through identically-sized wire mesh screens and preserved in glass jars with sodium borate-buffered 5% Formalin. Samples were inventoried at the end of the cruise and then sent to the Polish Sorting Center in Szczecin, Poland for processing. During the first two years we used the standard FOCI zooplankton protocol (Napp et al., 1996). In the third year we instituted a revised protocol that provided better species-specific identifications of some of the non-copepod taxa and was more closely aligned with protocols used by other scientists working in the region. Taxa removed from the samples for enumeration were returned to Seattle in small glass vials. The remainder of the sample is archived at the Polish National Marine Fisheries Research Institute in Gdynia, Poland and will be archived there for 20 years from the date of sample collection, under an existing Joint Studies Agreement between the U.S. NOAA-Fisheries and the Polish National Marine Fisheries Research Institute. After 20 years the samples will be destroyed. Zooplankton data from this project are stored in the NOAA-Fisheries, Alaska Fisheries Science Center, Recruitment Processes Program relational database, EcoDAT.

TABLE 17. NET CONFIGURATION AND SAMPLING STRATEGY FOR ALL TRANSECT LINES EXCEPT THE BARROW CANYON LINE (TRANSECT F). ON THAT TRANSECT LINE NO ALONG-BOTTOM NET TOW WAS ATTEMPTED.

Year	Large Mesh Nets	Small Mesh Nets	CTD
2010	1, 333 µm mesh; double oblique tow	1, 153 µm mesh; double oblique tow	SBE 19plus
2011	2, 333 µm mesh nets; 1 towed along the bottom and 1 from bottom to the surface	2, 153 µm mesh nets; 1 towed along the bottom and 1 from bottom to the surface	SBE 19plus
2012	2, 333 µm mesh nets; 1 towed along the bottom and 1 from bottom to the surface	1, 153 µm mesh net; towed from bottom to the surface	SBE 49

Comparison of Zooplankton Estimates From the Tucker Net and a TAPS-6

An older, 6-frequency Tracor Acoustic Profiling System (TAPS-6) was used to estimate volume-scattering strength (S_v , dB re 1 m^{-1}) of zooplankton. The instrument and approach has been used in other subarctic and arctic ecosystems to examine patterns in the temporal and spatial distribution of zooplankton (Holliday et al., 2009). The six frequencies were: 265, 420, 700, 1100, 1850, and 3000 kHz. Note that the frequencies and instrument design are fundamentally different from the TAPS6-NG instruments designed and moored for this study and described in the previous section. The TAPS-6 was attached to the top of the epibenthic Tucker Sled, with the transducers angled towards the center of the net opening (Figure 56).



FIGURE 56. 1 M² TUCKER SLED ON THE ICY DECK OF THE R/V *AQUILA*. THE KNEELING SCIENTIST HAS HIS HEAD IN THE NET MOUTH. THE TAPS-6 (BLACK CANISTER) IS MOUNTED ON THE TOP BAR OF THE TUCKER FRAME AND IS POINTED DOWN INTO THE TOW PATH OF THE NET. THE TRANSDUCER FACES POINT TO THE RIGHT AND DOWN IN THIS PICTURE.

The instrument was used in a small volume (ca. 2.5 liters) measurement mode which collects S_v data at a range of 1.5-m from the transducer face. The TAPS-6 averages multiple ping cycles prior to storing the data. The number of ping cycles per average used during these deployments was 6, which gives a new data ensemble every 2.6 seconds. Since each ping averages 5 independent samples, each data set results in 30 degrees of freedom. TAPS-6 calibration was accomplished by determining the source and receiver levels for each frequency, before and after each field season, using a standard calibrated transducer.

For abundance comparisons of zooplankton between the nets and the TAPS-6, species abundance from the water column and bottom net samples were separated and then summed into copepod-shaped and elongate/euphausiid-shaped categories. For displacement volume comparisons, the water column Tucker large-mesh and 25-cm small-mesh net sample displacement volumes were summed for all species.

Matlab™ (R2012b) was used to process the TAPS-6 acoustic data. Raw data from each frequency of the TAPS-6 was recorded as S_v . Background noise was defined as the minimum intensities (W/m^2) for the entire cast for each frequency. Noise was then removed by subtracting it from each measurement. Signal-to-noise ratios of <10 dB were used as a threshold to reject S_v values that were not acceptable for further analysis.

Inverse methods were used to estimate the abundance of plankton scatterers in 1-m depth bins as a function of size (Holliday, 1977; Greenlaw, 1979; Greenlaw and Johnson, 1983). The truncated fluid sphere (TFS), distorted-wave Born approximation (DWBA) and hard elastic scattering models were used in the inverse calculation to estimate scattering from small, spherical organisms (e.g., copepods, eggs, nauplii), elongate organisms (e.g., euphausiids, mysids), and planktonic shelled molluscs, respectively (Holliday, 1992; Stanton, 1994; Holliday et al., 2003). Assumed values for the material properties and the assumed orientation of these scatterers are provided in Table 13. In this application, however, the Levenberg-Marquardt factors for the nonlinear regression was 1.0×10^{-3} as opposed to 1.0×10^{-4} that was used to process the moored acoustics data (Table 13). Euclidian norms were computed as a goodness-of-fit statistic between S_v and the inverse model, fit to verify that the inversion could adequately explain the measured S_v values.

Matlab™ (R2012b) was used for linear regression analysis. The TAPS-6 inverse-estimated abundance of copepods, pteropods, and euphausiids was compared to net sample estimates for those 3 taxonomic categories (copepods, euphausiids, and shelled molluscs) at all available stations in 2010, 2011, and 2012. Finally, mean volume backscatter in the water column for each of the 6 frequencies measured along Transect D (Icy Cape line) in 2011 and 2012 was compared to zooplankton displacement volume from the water column net from the same tows.

Contour section plots of zooplankton S_v at 420 kHz along transect D were created using Surfer Plot (Version 10.7.972) and compared to temperature and salinity data collected during the CTD casts at the same station.

2. *Results*

Hydrography -- Physical and Chemical Variables

The Chukchi Sea consists of a broad shallow shelf (Figure 32, Figure 57), which is incised by two major canyons at the slope – Barrow Canyon in the east and Herald Canyon in the west. The flow on the eastern part of the shelf is generally northward and follows bathymetry (Figure 57). Three types of water enter onto the shelf from Bering Strait: Alaska Coastal Current (ACC), Bering Water (BW) and Anadyr Water (AW). In addition, intrusions of water from the Bering Sea basin onto the shelf can occur either through Bering Canyon or over the shelf break to the west of Bering Canyon. Thus the physical, chemical, and biological properties over the shelf are the sum total of advective and in situ processes. Table 18 summarizes the range of properties expected for each water type. Data collected as part of CHAOZ provides insight into the magnitude of transport and flow pathways.

TABLE 18. TEMPERATURE AND SALINITY RANGES FOR DIFFERENT WATER MASSES IN THE CHUKCHI SEA. (FROM DANIELSON ET AL., SUBMITTED).

Water Mass	Temperature (°C)	Salinity
Alaska Coastal Water (ACW)	7 - 12	20 - 32
Winter Water (WW)	-2 - 0	30 - 33.5
Bering Shelf Summer Water (BSSW)	0 - 8	30 - 33.5
Atlantic Water (AtlW)	-2 - 1	33.5 - 35

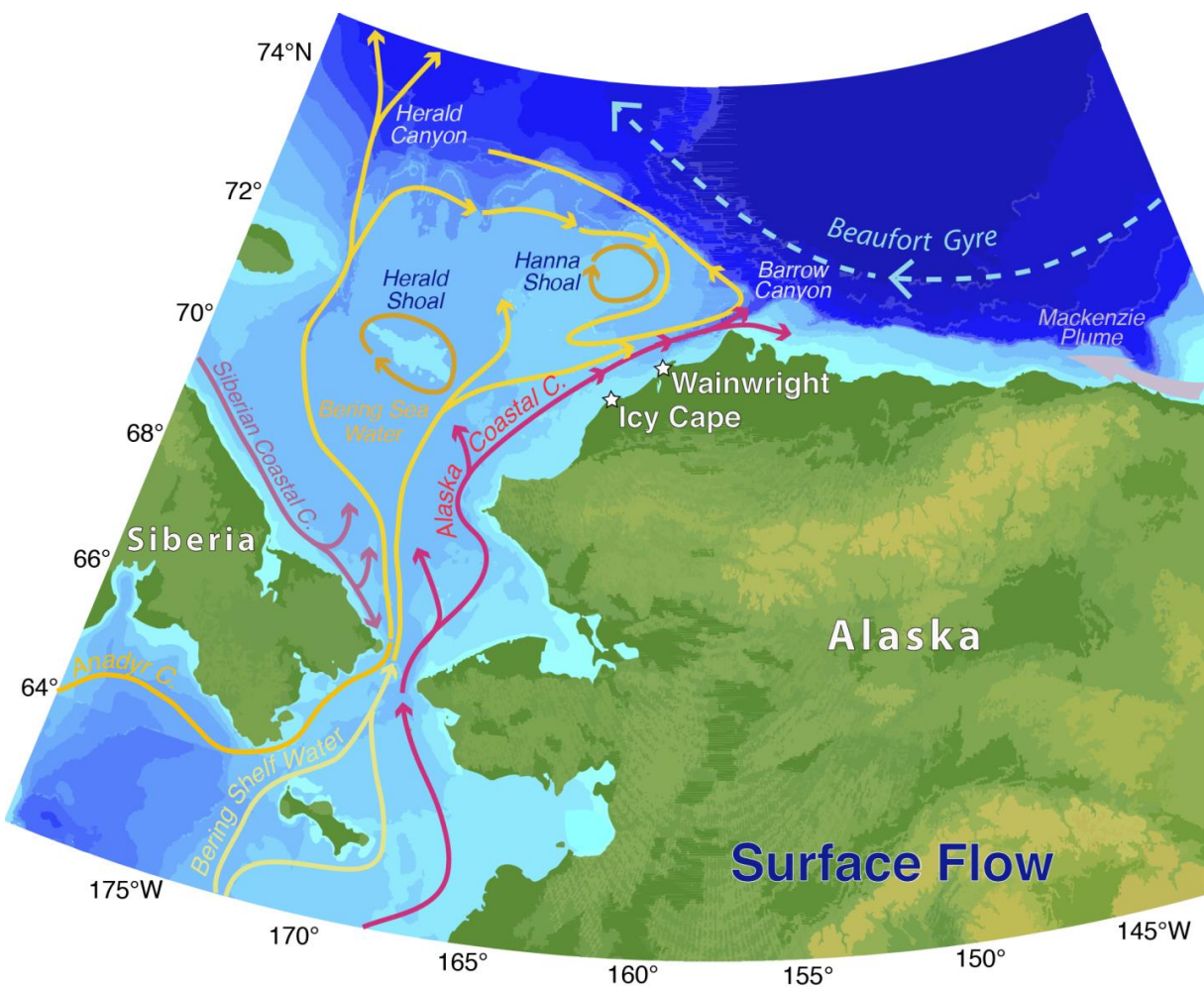


FIGURE 57. MAP OF CURRENTS OVER THE CHUKCHI SHELF (MODIFIED FROM WOOD ET AL., 2015).

Interannual and spatial variability among hydrographic sections

Line A: Point Hope (Figure 32, Figure 58-60)

The warmer, fresher water of the ACC was confined to the innermost and shallower 20 to 30-km, portions of this line. In 2010, waters of the ACC were vertically mixed to ~30-m, while in 2011, a shallow pycnocline was observed at 5-m. In 2012, waters of the ACC were weakly stratified. Nitrate tended to be low near shore both in the surface and at depth for all years.

In the offshore portion of this transect, the bottom layer was saltier and rich in nutrients (including ammonium), conditions that typify AW. Nitrite is an intermediate compound in several important biological reactions, and concentrations are generally low. While sections of nitrite are shown for completion, these will not be discussed. Bottom temperatures were $< 3^{\circ}\text{C}$ in 2012, and $> 3^{\circ}\text{C}$ in 2011. In 2010, offshore water was weakly stratified, and the pycnocline was $> 10\text{-m}$ thick, while in 2011 and 2012, there was a strong two-layer system with a sharp pycnocline between 5-10 m. Continuous depth distributions of chlorophyll and oxygen were not measured in 2010 due to the failure of the winch and SeaBird 911plus CTD deck unit. In 2011, maximum chlorophyll was confined to the coast, while in 2012 there was a sub-surface chlorophyll maximum farther offshore. In both years, surface waters were generally supersaturated with oxygen, while deeper waters were undersaturated, likely due to respiration.

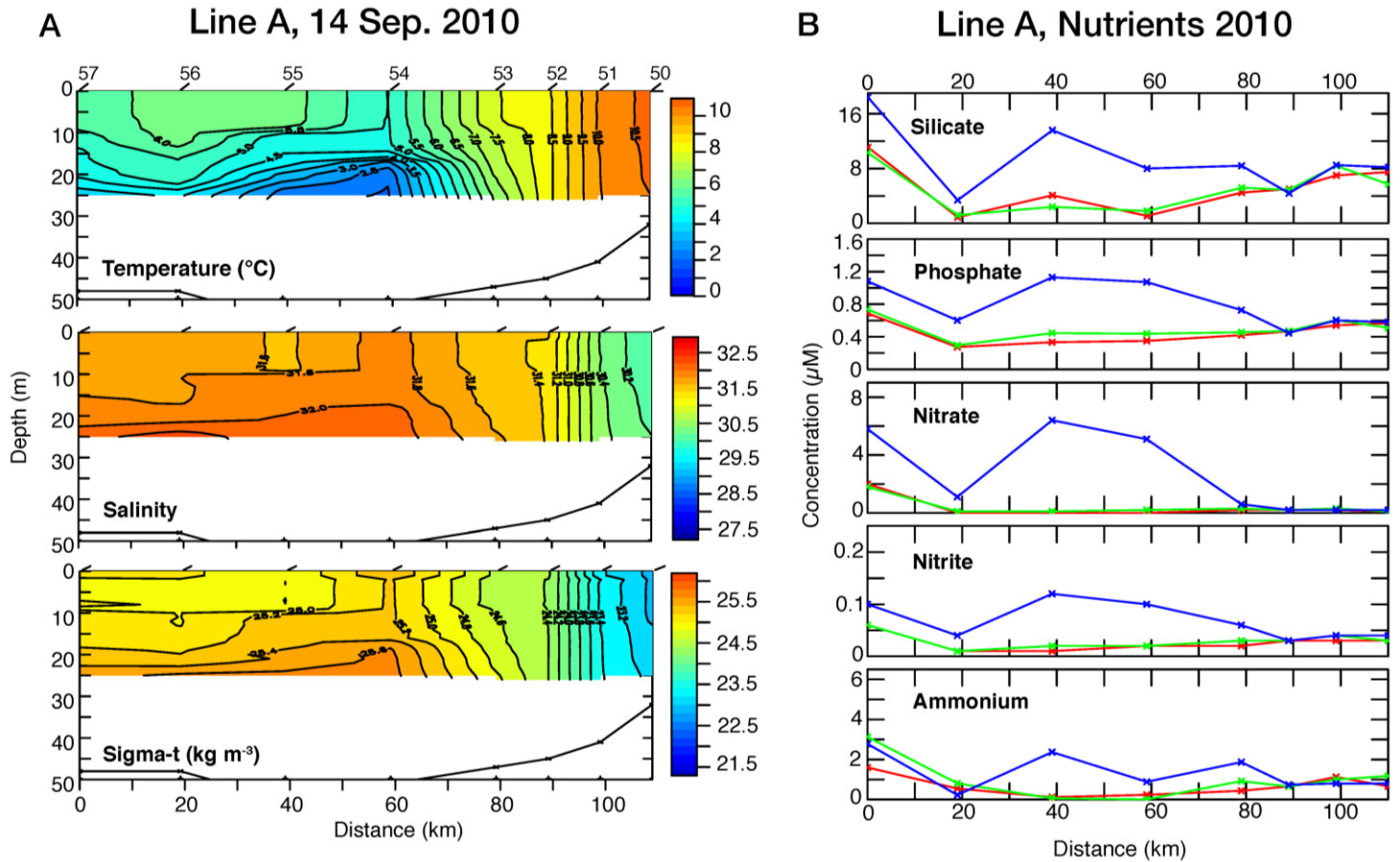


FIGURE 58. HYDROGRAPHIC MEASUREMENTS AT POINT HOPE (LINE A) IN SEPTEMBER 2010. (A.) CONTOURS OF TEMPERATURE, SALINITY, SIGMA-T, AND BOTTOM DEPTH. (B.) LINE PLOTS OF NUTRIENTS (SILICATE, PHOSPHATE, NITRATE, NITRITE AND AMMONIUM) MEASURED AT THREE DEPTHS (1 M; RED, 20 M; GREEN AND 30 M; BLUE). THE COASTLINE IS ON THE RIGHT SIDE OF EACH PLOT.

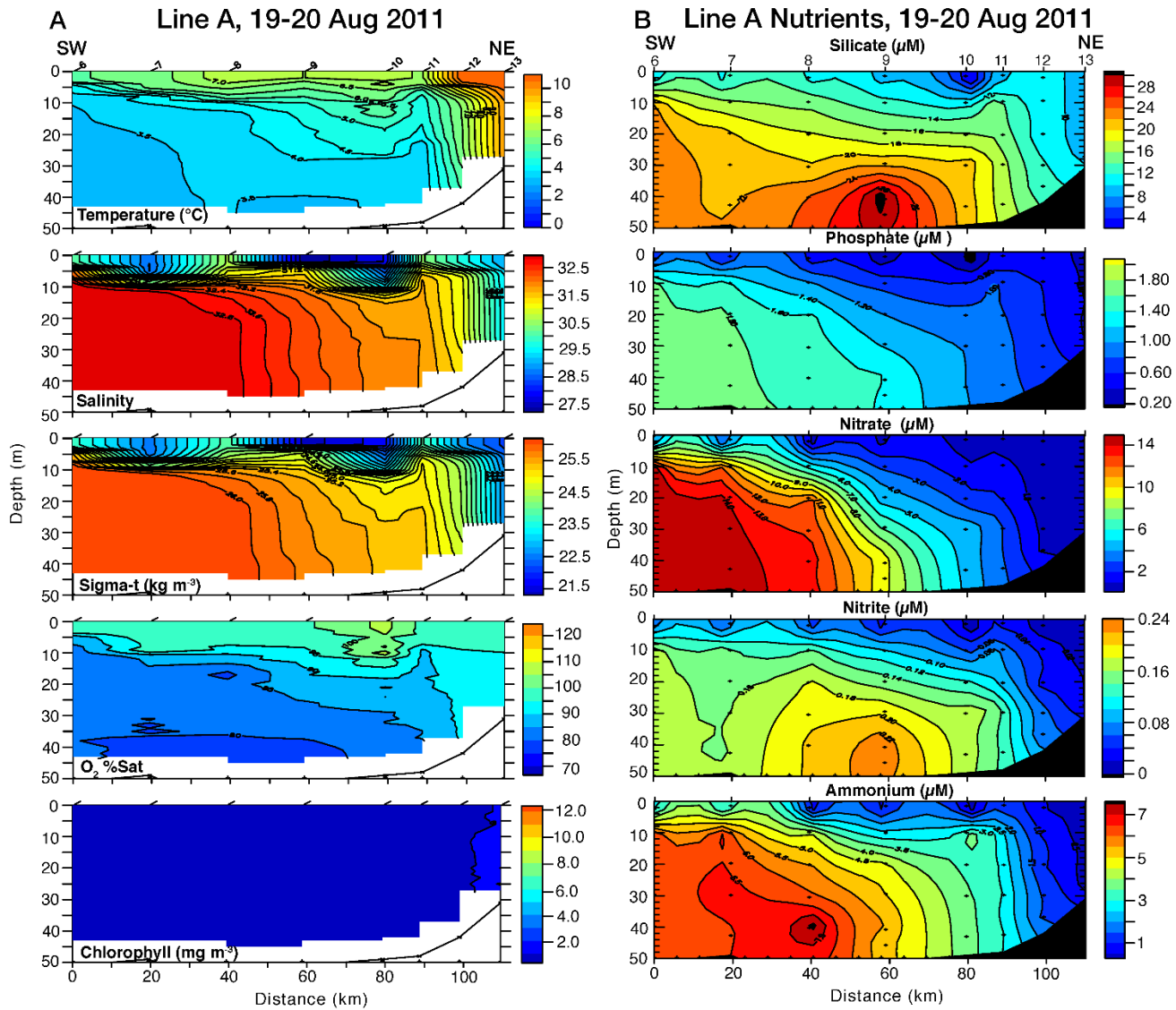


FIGURE 59. HYDROGRAPHIC MEASUREMENTS AT POINT HOPE (LINE A) IN AUGUST 2011. (A.) TEMPERATURE, SALINITY, SIGMA-T OXYGEN (PERCENT SATURATION) AND CHLOROPHYLL FLUORESCENCE. (B.) THE FIVE NUTRIENTS (SILICATE, PHOSPHATE, NITRATE, NITRITE AND AMMONIUM).

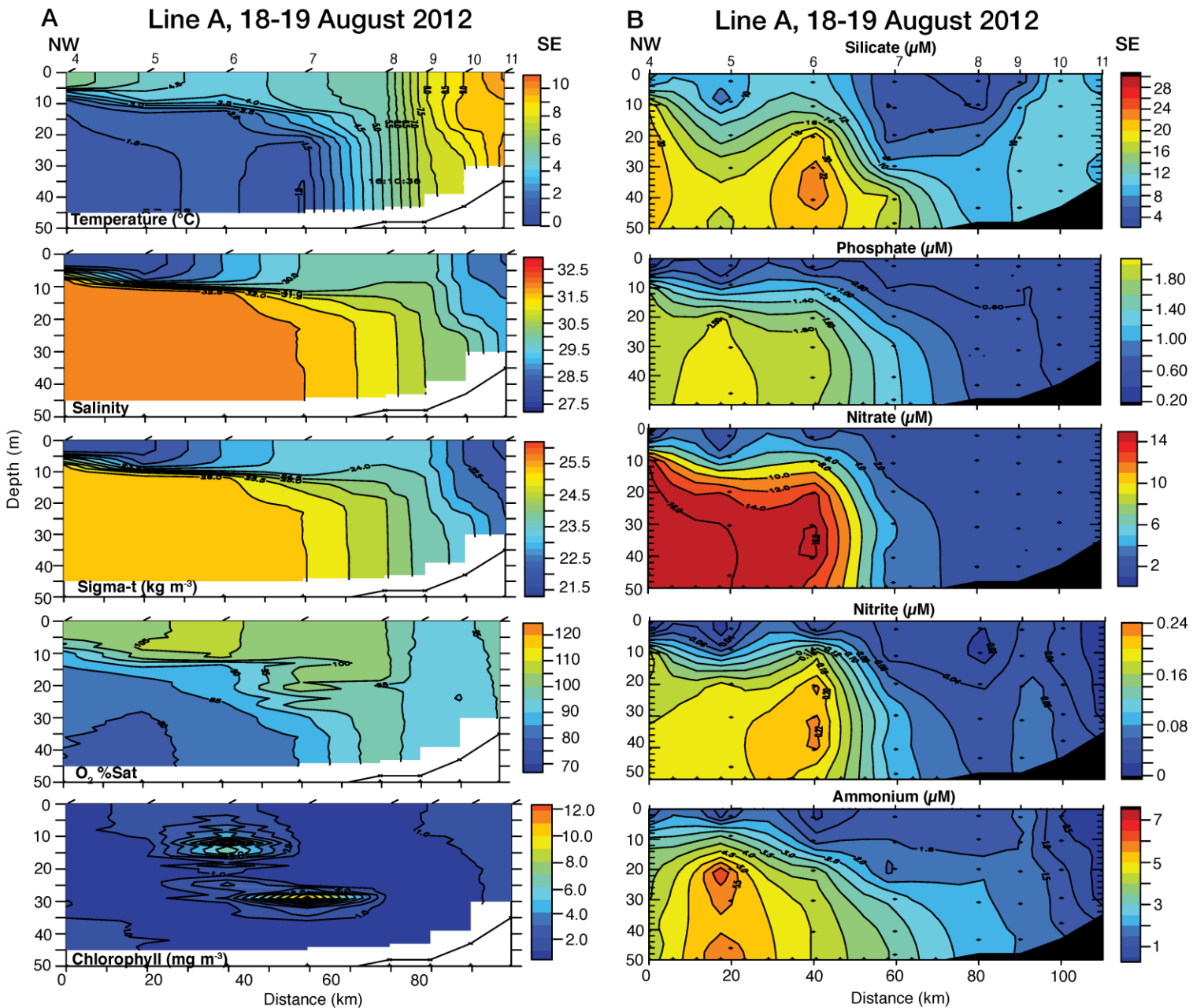


FIGURE 60. HYDROGRAPHIC MEASUREMENTS AT POINT HOPE (LINE A) IN AUGUST 2012. LEFT: TEMPERATURE, SALINITY, SIGMA-T OXYGEN (PERCENT SATURATION) AND CHLOROPHYLL FLUORESCENCE. RIGHT: THE FIVE NUTRIENTS (SILICATE, PHOSPHATE, NITRATE, NITRITE AND AMMONIUM).

Line B: Cape Lisburne (Figure 32, Figure 61-63)

While warmer, fresher water of the ACC was still observed along the inner portions of this hydrographic line, the saltier nutrient rich Anadyr water was no longer evident on the offshore portion of the line. Thus, horizontal gradients in physical and chemical properties were relatively weak. Once again, in 2011, bottom temperatures were warmer and stratification was stronger than in 2012. In 2011 and 2012, the pycnocline was deeper than, and not as sharp as,

the pycnocline observed along Line A. An offshore lens of fresher water was evident in 2010 resulting in an upper stratified layer. Nutrients were generally low, but in 2011 and 2012, higher silicate was observed along the coast, and nutrients were elevated offshore in association with higher salinities at depth. This may be an indication of water from the Pt. Hope transect entering the shelf through Central Channel. A sub-surface chlorophyll maximum was observed in 2011 and 2012; however, in 2011 oxygen remained undersaturated (perhaps indicating that a bloom was in an early stage or that the cells at depth had higher chlorophyll/biomass ratios than the cells near the surface), while in 2012 large portions of the water column were supersaturated.

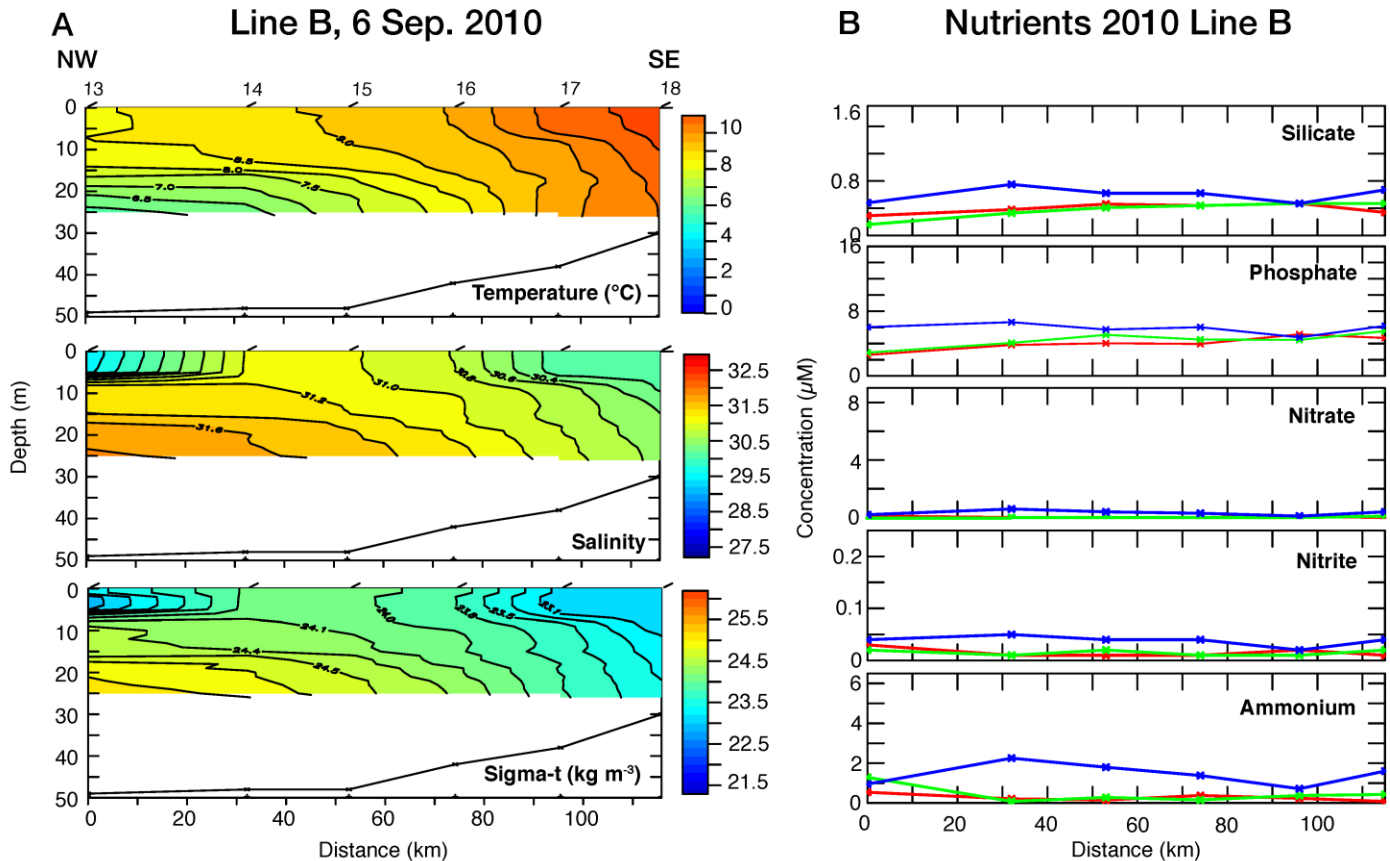


FIGURE 61. HYDROGRAPHIC MEASUREMENTS AT CAPE LISBURNE (LINE B) IN SEPTEMBER 2010. (A.) CONTOURS OF TEMPERATURE, SALINITY AND SIGMA-T. (B.) LINE PLOTS OF NUTRIENTS (SILICATE, PHOSPHATE, NITRATE, NITRITE AND AMMONIUM) MEASURED AT THREE DEPTHS (1 M; RED, 20 M; GREEN AND 30 M; BLUE).

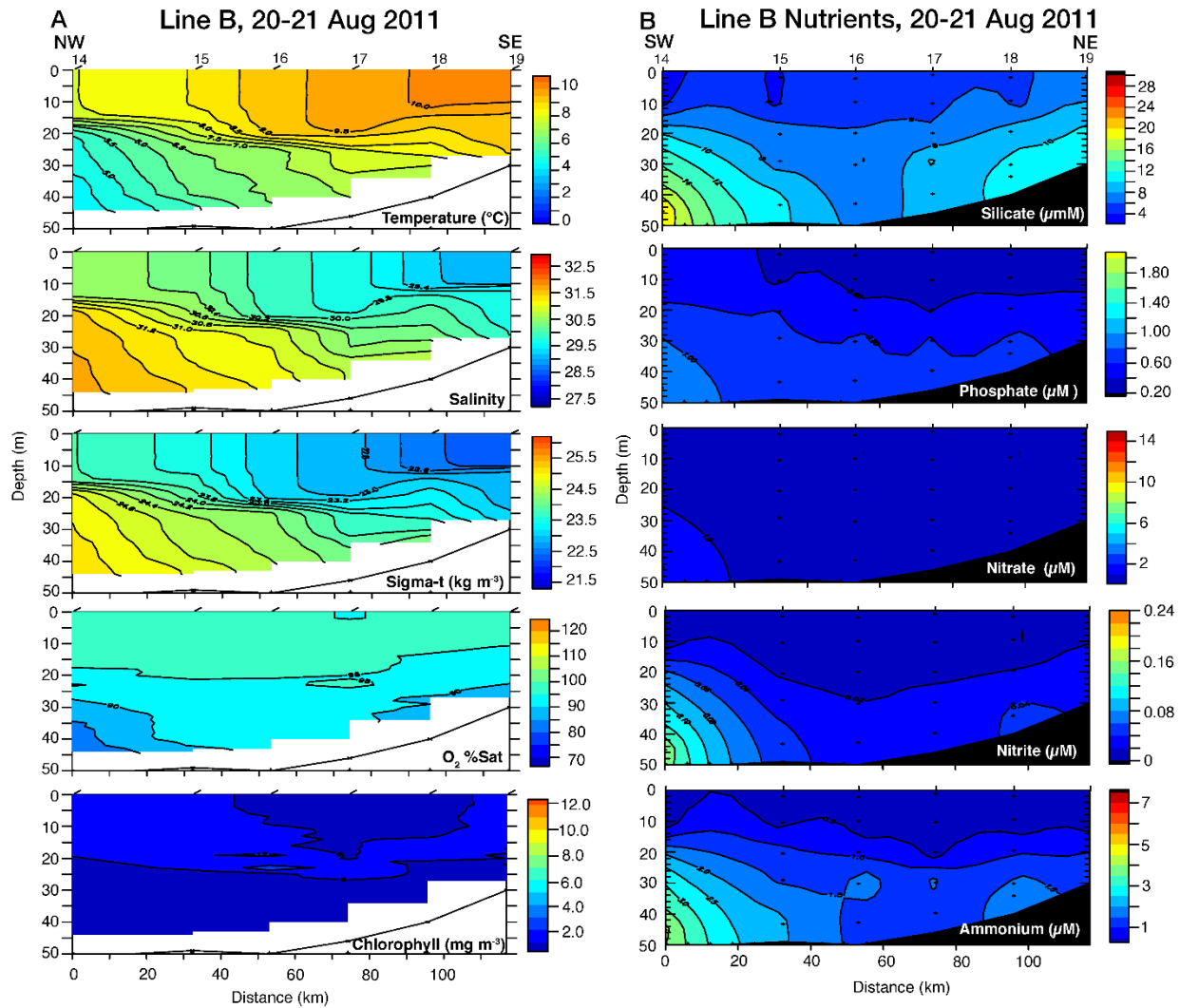


FIGURE 62. HYDROGRAPHIC MEASUREMENTS AT CAPE LISBURNE (LINE B) IN AUGUST 2011. (A.) TEMPERATURE, SALINITY, SIGMA-T OXYGEN (PERCENT SATURATION) AND CHLOROPHYLL FLUORESCENCE. (B.) THE FIVE NUTRIENTS (SILICATE, PHOSPHATE, NITRATE, NITRITE AND AMMONIUM).

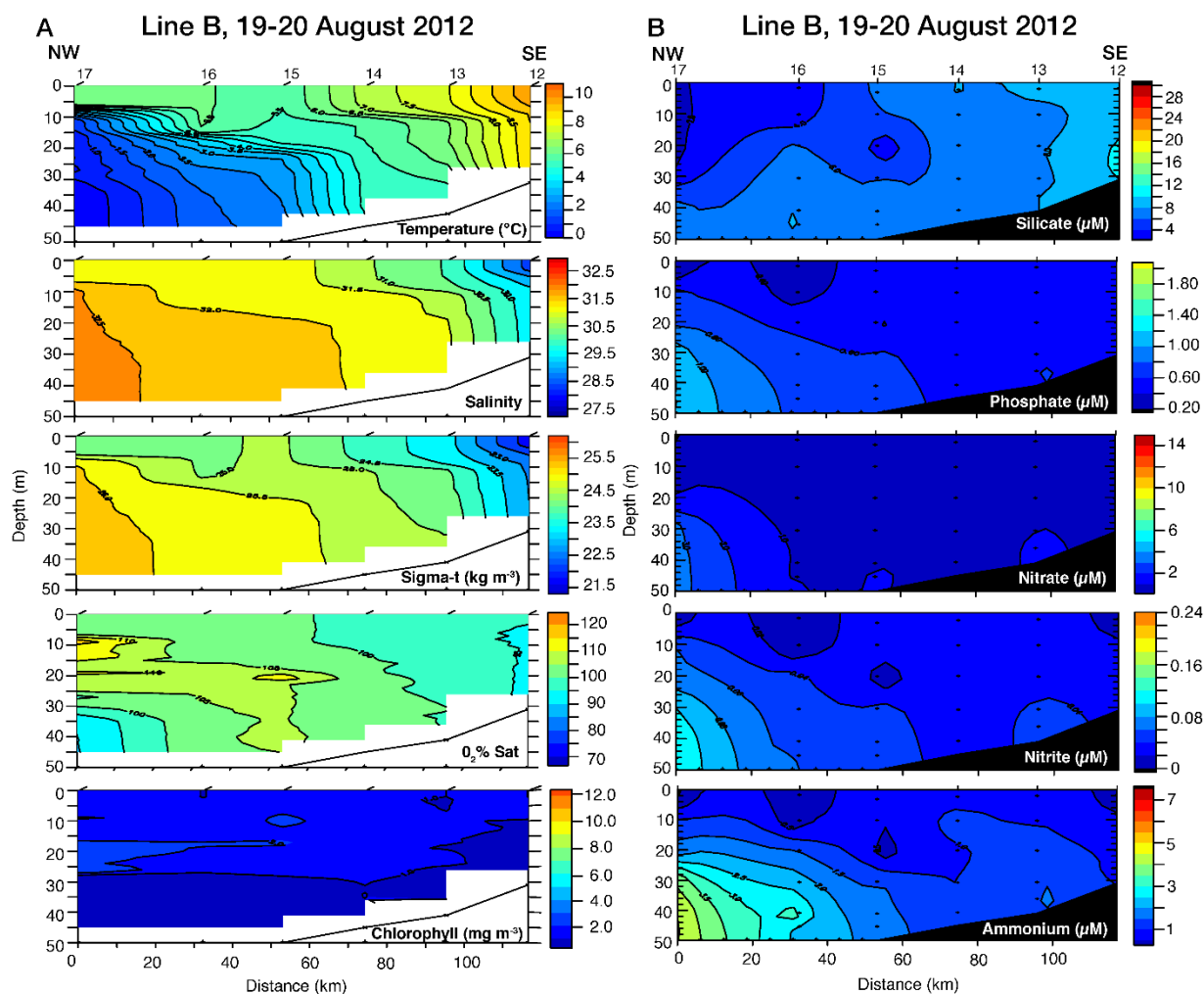


FIGURE 63. HYDROGRAPHIC MEASUREMENTS AT CAPE LISBURN (LINE B) IN AUGUST 2012. (A.) TEMPERATURE, SALINITY, SIGMA-T OXYGEN (PERCENT SATURATION) AND CHLOROPHYLL FLUORESCENCE. (B.) THE FIVE NUTRIENTS (SILICATE, PHOSPHATE, NITRATE, NITRITE AND AMMONIUM).

Line C: Point Lay (Figure 32, Figure 64-66)

In 2010 and 2011, the ACC was slightly cooler and saltier at line C than on Lines A and B. In 2012, the ACC had a larger seaward extent, and was vertically mixed along the coast. Most notably in 2012, the deeper, offshore water was less saline than in 2010 and 2011. Silicate and ammonium concentrations were generally higher in bottom water at Line C than at Line B indicating remineralization and nutrient regeneration, while nitrate and phosphate remained low. A subsurface chlorophyll maximum was observed in 2011; however, oxygen remained undersaturated.

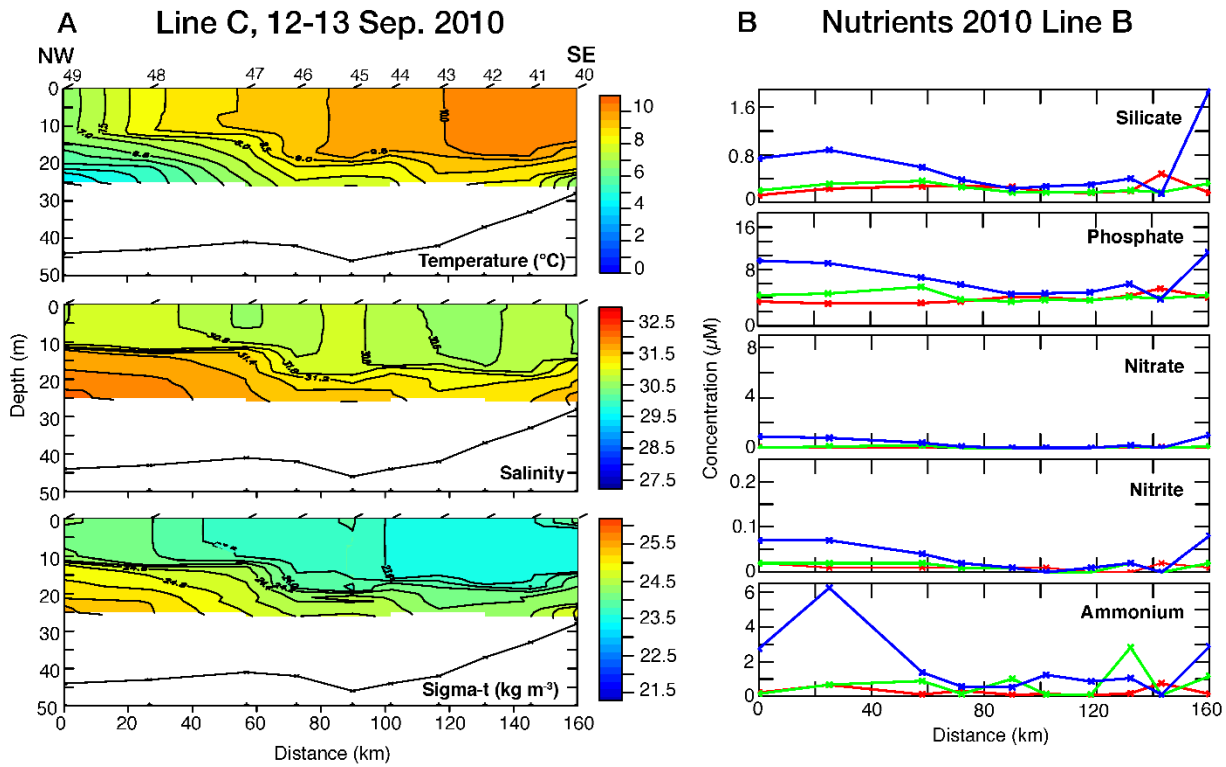


FIGURE 64. HYDROGRAPHIC MEASUREMENTS AT POINT LAY (LINE C) IN SEPTEMBER 2010. (A.) CONTOURS OF TEMPERATURE, SALINITY AND SIGMA-T. (B.) LINE PLOTS OF NUTRIENTS (SILICATE, PHOSPHATE, NITRATE, NITRITE AND AMMONIUM) MEASURED AT THREE DEPTHS (1 M; RED, 20 M; GREEN AND 30 M; BLUE).

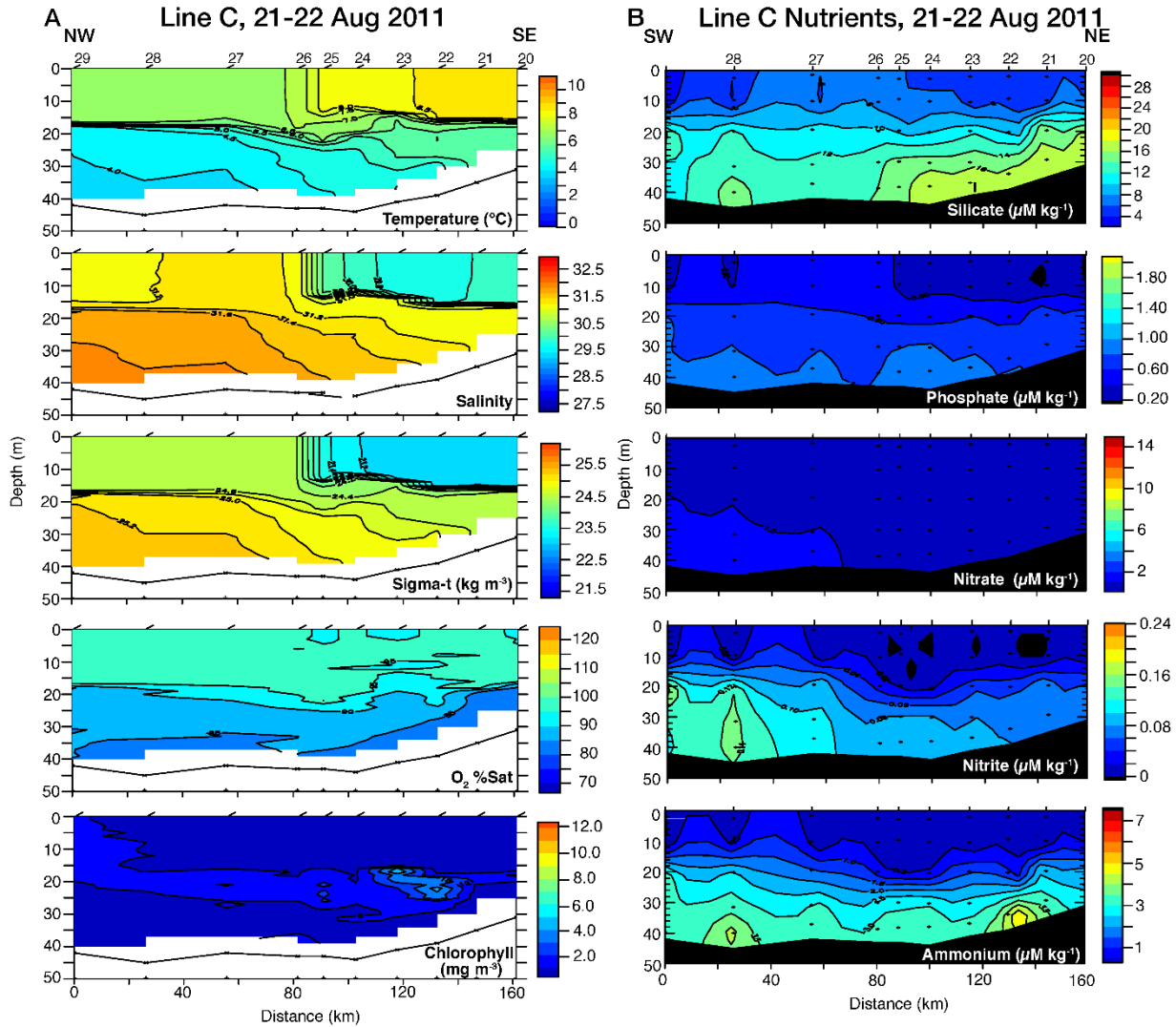


FIGURE 65. HYDROGRAPHIC MEASUREMENTS AT POINT LAY (LINE C) IN AUGUST 2011. (A) TEMPERATURE, SALINITY, SIGMA-T OXYGEN (PERCENT SATURATION) AND CHLOROPHYLL FLUORESCENCE. (B) THE FIVE NUTRIENTS (SILICATE, PHOSPHATE, NITRATE, NITRITE AND AMMONIUM).

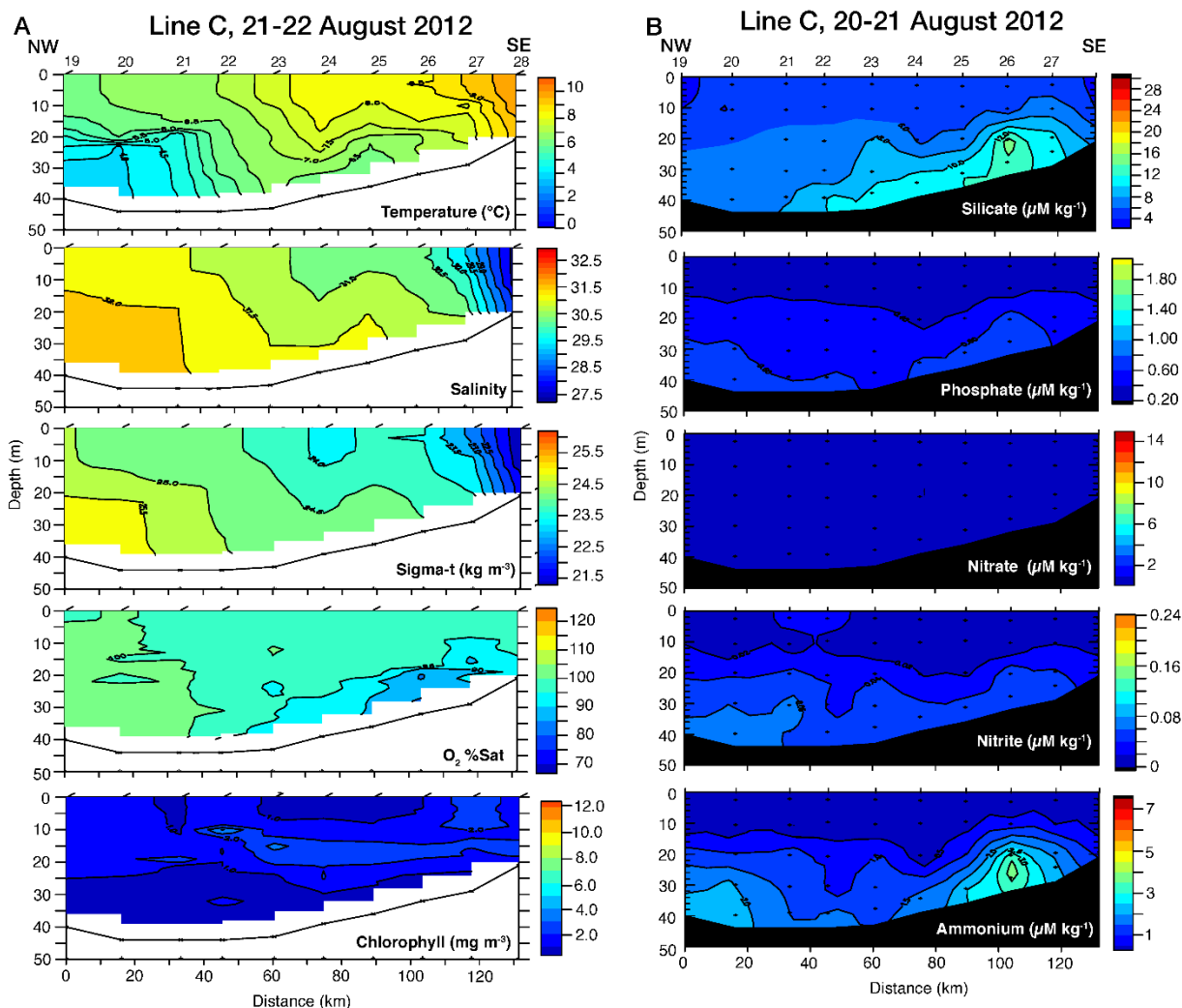


FIGURE 66. HYDROGRAPHIC MEASUREMENTS AT POINT LAY (LINE C) IN AUGUST 2012. (A) TEMPERATURE, SALINITY, SIGMA-T OXYGEN (PERCENT SATURATION) AND CHLOROPHYLL FLUORESCENCE. (B) THE FIVE NUTRIENTS (SILICATE, PHOSPHATE, NITRATE, NITRITE AND AMMONIUM).

Line D: Icy Cape (Figure 32, Figure 67-69)

Along this transect, the warmer fresher signature of the ACC observed to the southwest continued to weaken. Along the bottom, there was colder and saltier water than along Line C, except for the nearshore stations in 2012 where stratification was weak. In each year at the bottom near the middle of the hydrographic line was a small concentration of winter water. Not only was silicate and ammonium elevated along the bottom as observed along Line C, but nitrate and phosphate concentrations were also higher in association with elevated salt content along the bottom. There were strong subsurface chlorophyll maximums in 2011 and 2012, with oxygen supersaturation at or above these features, and undersaturation and high ammonium concentrations below.

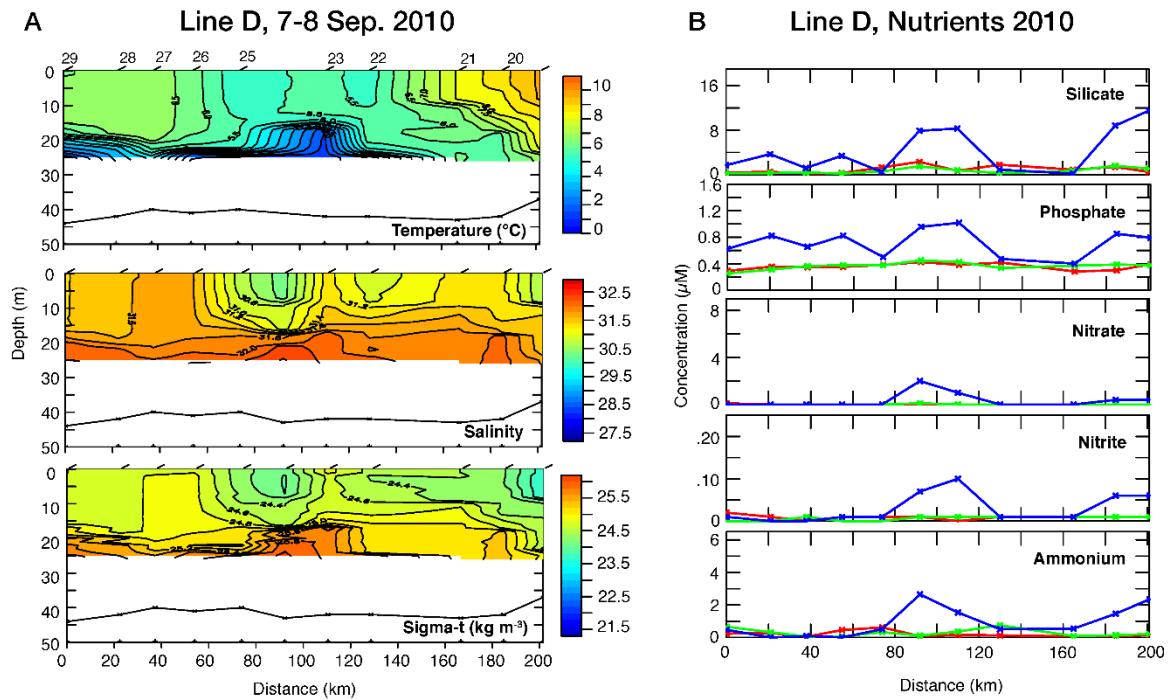


FIGURE 67. HYDROGRAPHIC MEASUREMENTS AT ICY CAPE (LINE D) IN SEPTEMBER 2010. (A.) CONTOURS OF TEMPERATURE, SALINITY AND SIGMA-T. (B.) LINE PLOTS OF NUTRIENTS (SILICATE, PHOSPHATE, NITRATE, NITRITE AND AMMONIUM) MEASURED AT THREE DEPTHS (1 M; RED, 20 M; GREEN AND 30 M; BLUE).

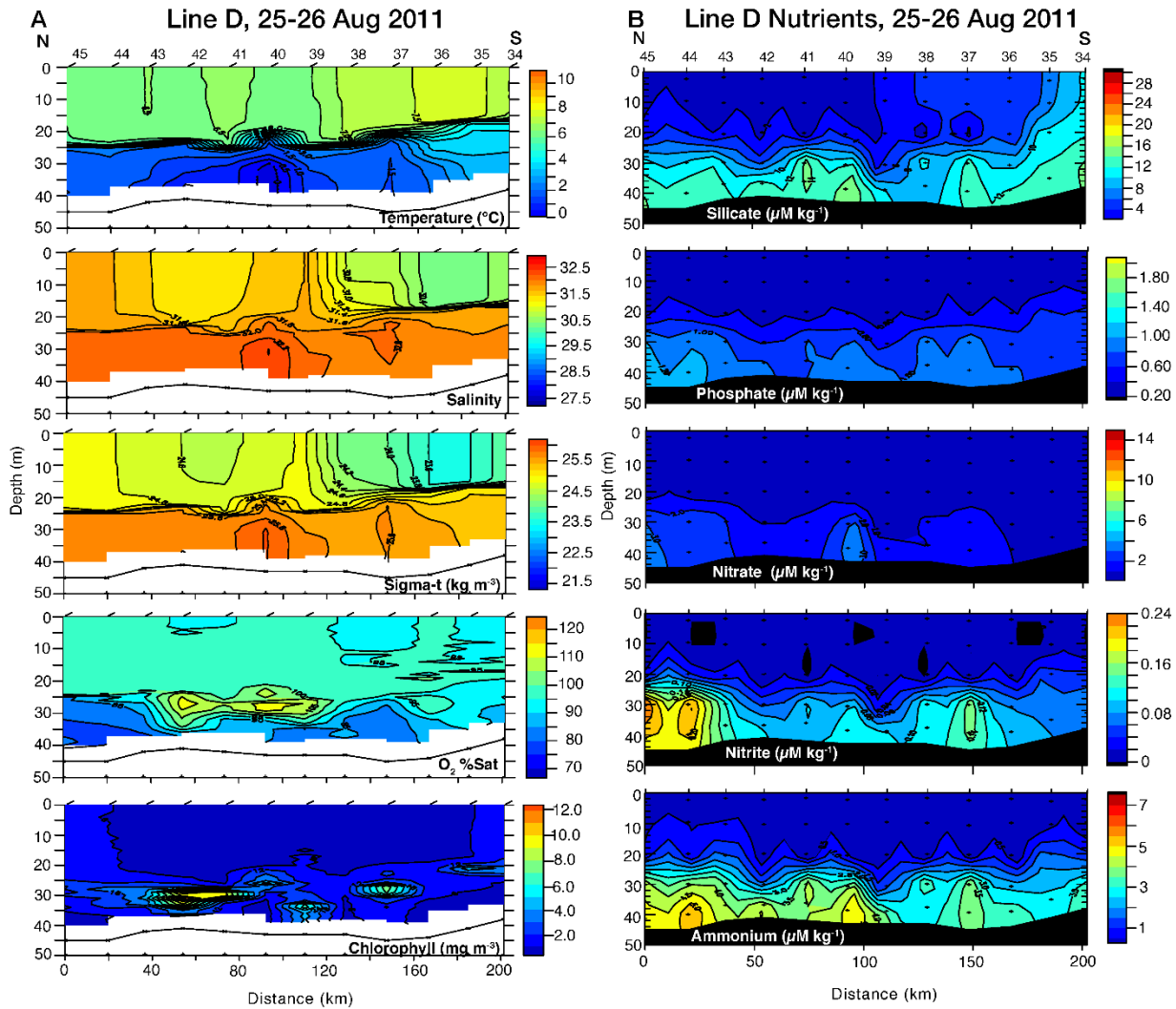


FIGURE 68. HYDROGRAPHIC MEASUREMENTS AT ICY CAPE (LINE D) IN AUGUST 2011. (A) TEMPERATURE, SALINITY, SIGMA-T OXYGEN (PERCENT SATURATION) AND CHLOROPHYLL FLUORESCENCE. (B) THE FIVE NUTRIENTS (SILICATE, PHOSPHATE, NITRATE, NITRITE AND AMMONIUM).

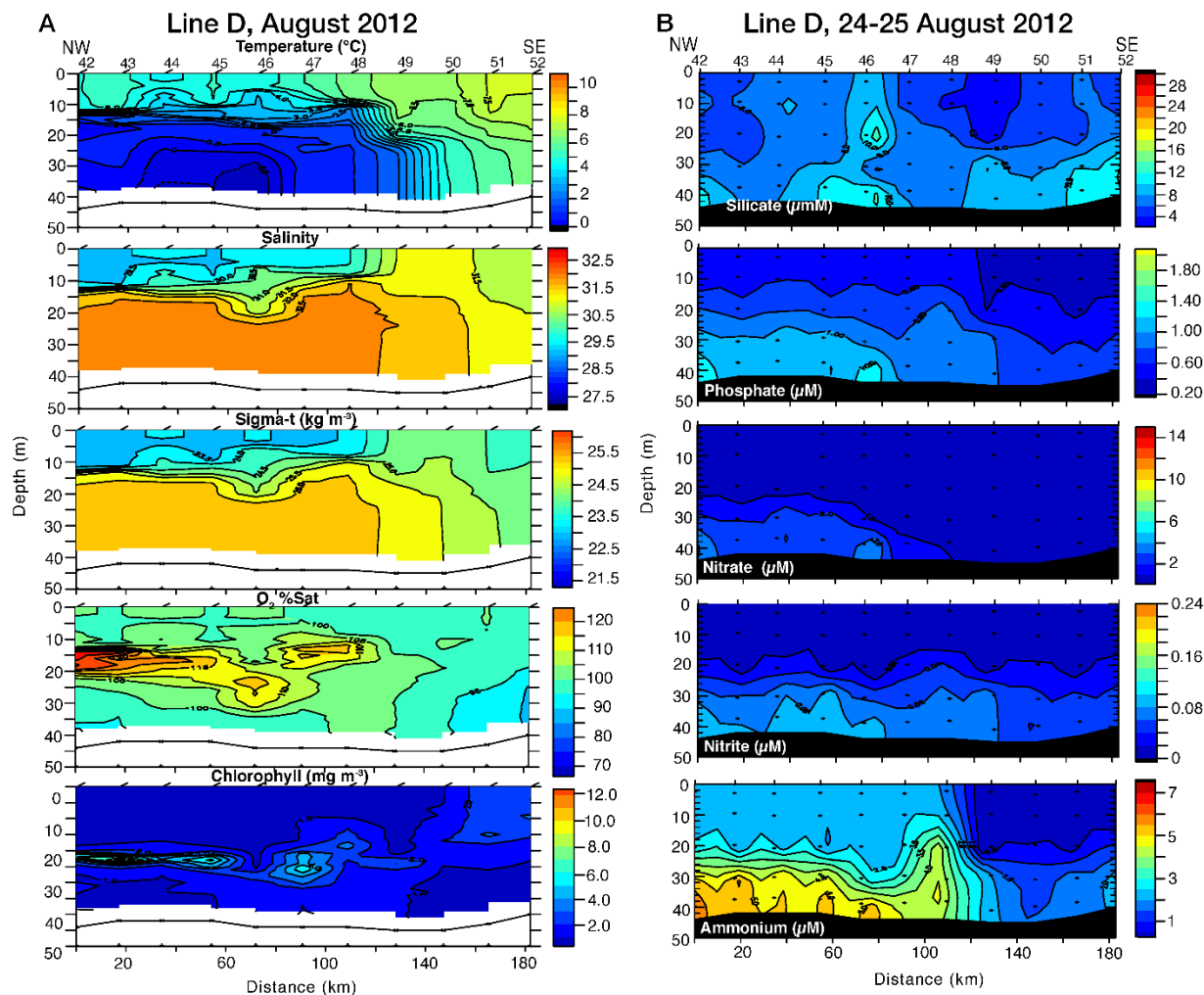


FIGURE 69. HYDROGRAPHIC MEASUREMENTS AT ICY CAPE (LINE D) IN AUGUST 2012. (A) TEMPERATURE, SALINITY, SIGMA-T OXYGEN (PERCENT SATURATION) AND CHLOROPHYLL FLUORESCENCE. (B) THE FIVE NUTRIENTS (SILICATE, PHOSPHATE, NITRATE, NITRITE AND AMMONIUM).

Line E: Wainwright (Figure 32, Figure 70-72)

Warmer fresher water, (the ACC), was observed at the innermost portion of Transect E each year. In 2011, the region of warmer fresher water separated from the coast and was found over the center of the canyon. Further inshore, cooler, saltier water in the canyon is consistent with upwelling along the edge of the canyon. This transect was well stratified, especially in 2010 and 2011, with weaker stratification in 2012. Bottom salinities were relatively high, with the highest salinities observed in 2012. These salinities were comparable to Line A and higher than at Lines B, C and D. Nutrient concentrations were moderate in 2010 and 2011, but in 2012, concentrations were high, and resembled concentrations in AW that were observed along Line A. The cold temperatures (<0°C) and salinities (>33) is indicative of either onshore flow of slope water or AW/WW that was transported to the region. Once again a subsurface bloom is evident (especially in 2012) and the oxygen was supersaturated near the thermocline in both 2011 and 2012. Percent oxygen saturation was highest in the middle of the water column in 2011 and

2012 and extended for most of the length of the transect. In 2012 the supersaturated oxygen layer was shallower than the fluorescence maximum.

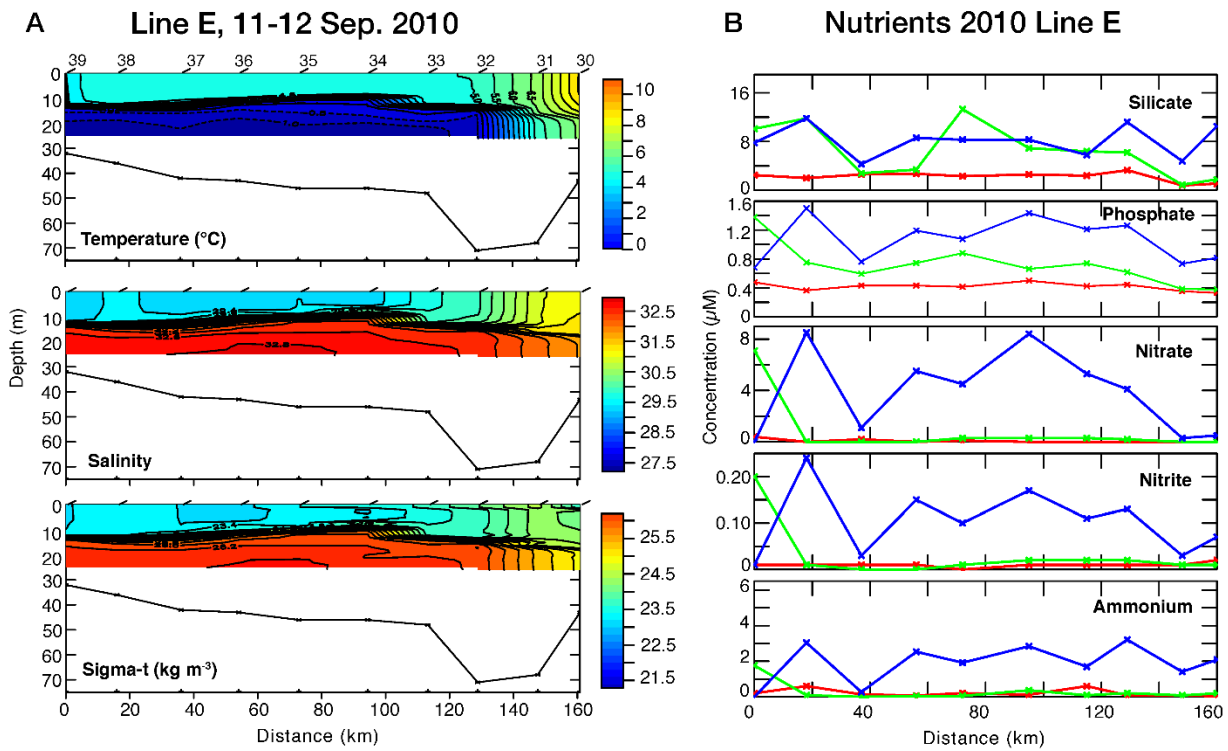


FIGURE 70. HYDROGRAPHIC MEASUREMENTS AT WAINWRIGHT (LINE E) IN SEPTEMBER 2010. (A.) CONTOURS OF TEMPERATURE, SALINITY, AND SIGMA-T. (B.) LINE PLOTS OF NUTRIENTS (SILICATE, PHOSPHATE, NITRATE, NITRITE AND AMMONIUM) MEASURED AT THREE DEPTHS (1 M; RED, 20 M; GREEN AND 30 M; BLUE).

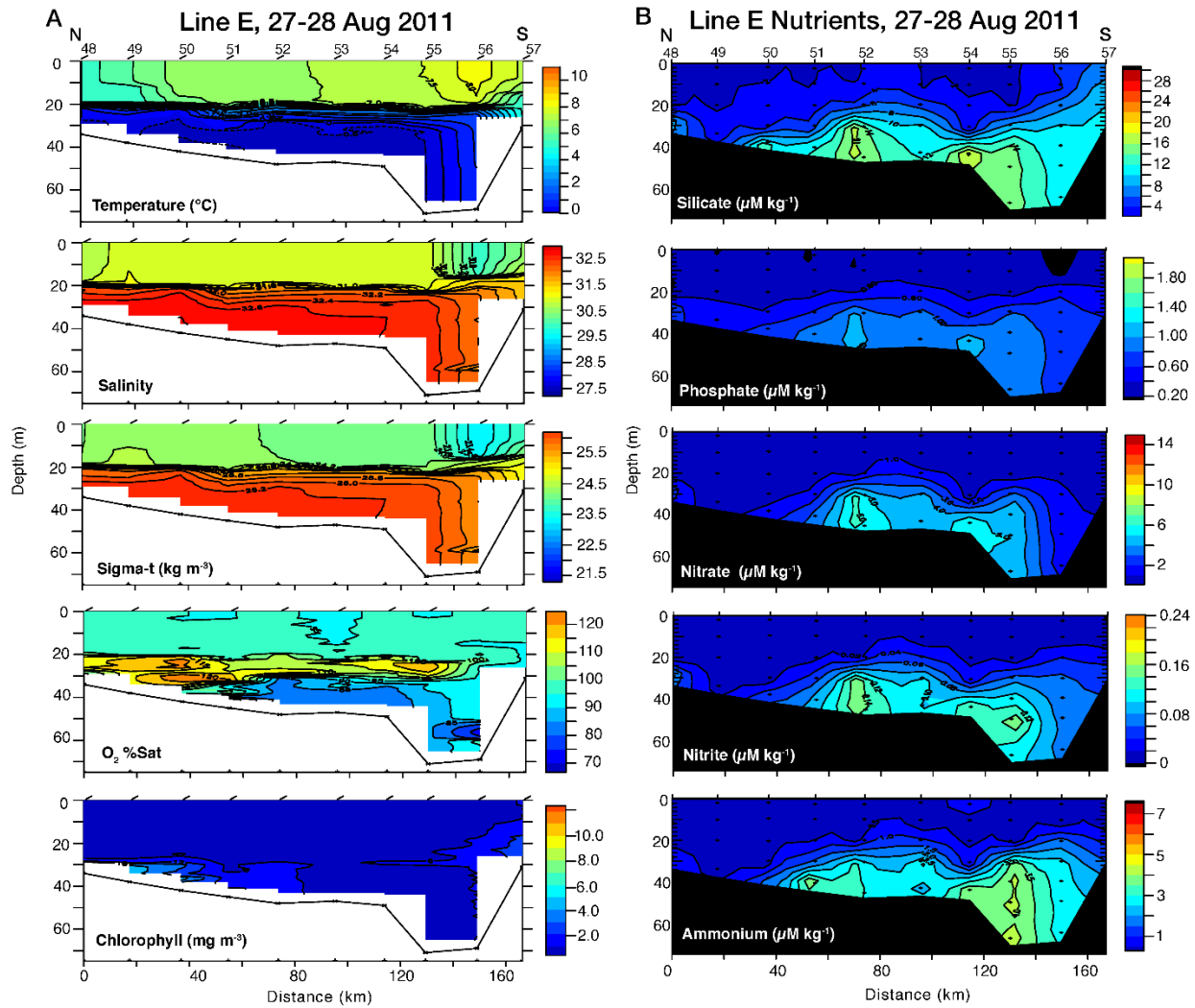


FIGURE 71. HYDROGRAPHIC MEASUREMENTS AT WAINWRIGHT (LINE E) IN AUGUST 2011. (A) TEMPERATURE, SALINITY, SIGMA-T OXYGEN (PERCENT SATURATION) AND CHLOROPHYLL FLUORESCENCE. (B) THE FIVE NUTRIENTS (SILICATE, PHOSPHATE, NITRATE, NITRITE AND AMMONIUM).

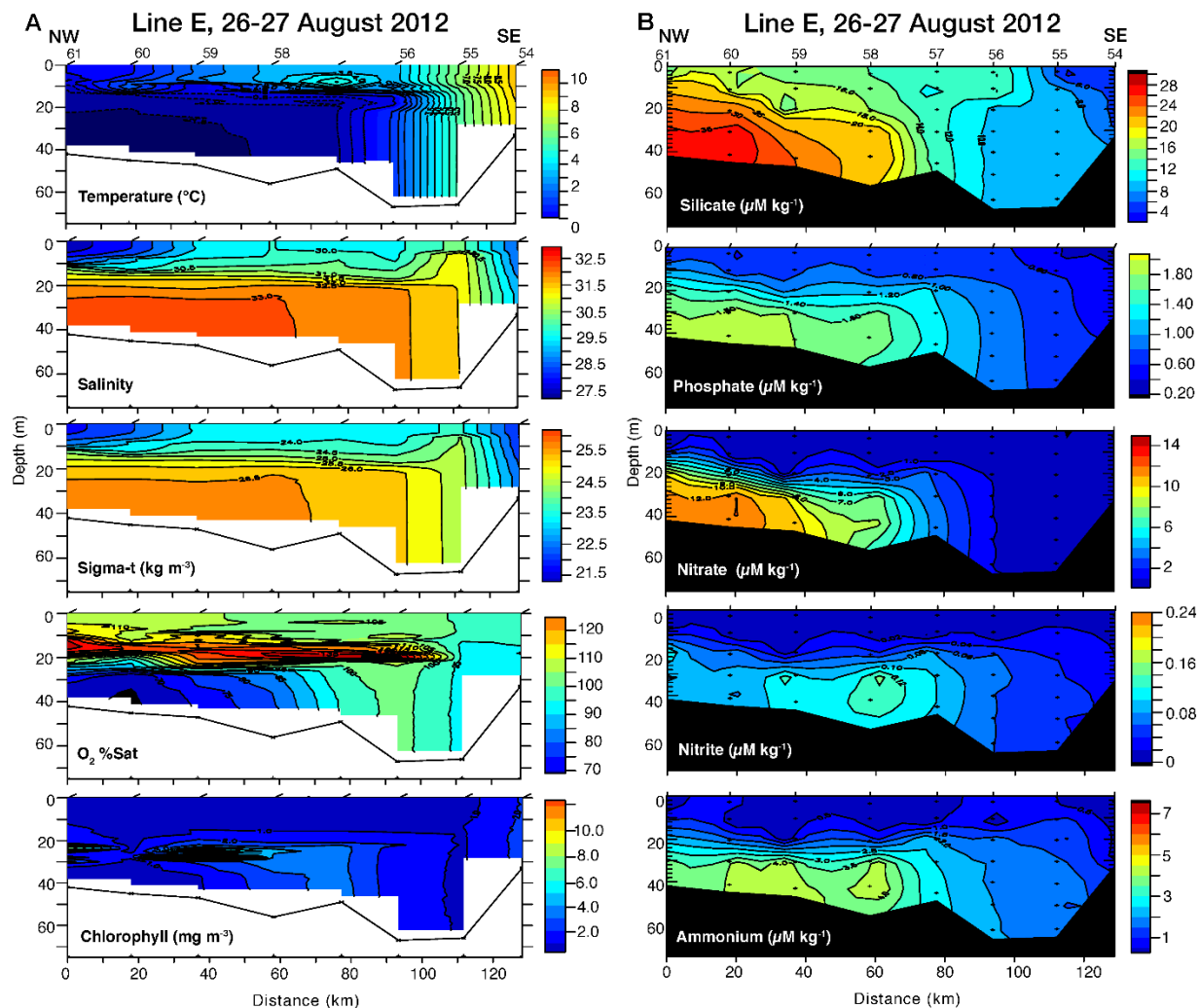


FIGURE 72. HYDROGRAPHIC MEASUREMENTS AT WAINWRIGHT (LINE E) IN AUGUST 2012. (A) TEMPERATURE, SALINITY, SIGMA-T OXYGEN (PERCENT SATURATION) AND CHLOROPHYLL FLUORESCENCE. (B) THE FIVE NUTRIENTS (SILICATE, PHOSPHATE, NITRATE, NITRITE AND AMMONIUM).

Line F: Barrow Canyon (Figure 32, Figure 73-74)

This Distributed Biological Observatory (DBO) transect was occupied in 2011 and 2012. On the northern side of the canyon, bottom waters were very cold, salty, and relatively high in nutrient concentrations. In 2011, stratification was relatively weak, and the cold, saltier, nutrient-rich waters were confined to depths > 50 m. In 2012, stratification was stronger, and the base of the pycnocline was ~20 m; hence the cold, saltier and nutrient-rich bottom waters occupied the bottom ~40 m of the water column. As observed on Line E, salinities and nutrients were higher in 2012 than in 2011. Along the northern flank of the canyon, there was a chlorophyll fluorescence maximum and regions of oxygen supersaturation. As in previous years the area of oxygen supersaturated was shallower than the region of high chlorophyll fluorescence. On the southern portion of the transect, stratification weakened, and nutrients were depleted throughout the water column. In 2011, ammonium concentrations were elevated in

bottom waters, with the concentration gradient shoaling at the southern end of the transect. In 2012, the ammonium maximum was confined to the northern portion of the transect.

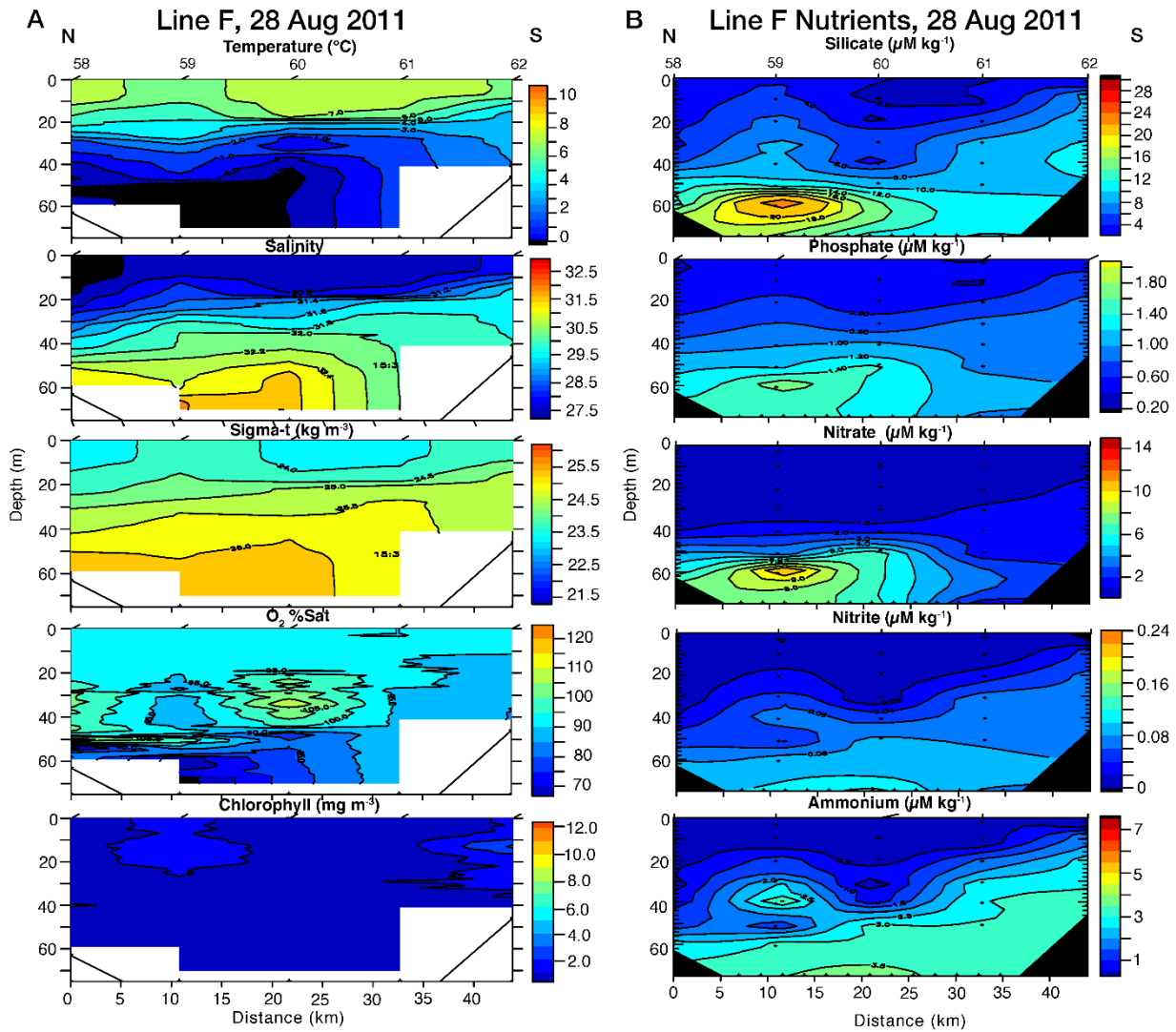


FIGURE 73. HYDROGRAPHIC MEASUREMENTS AT BARROW CANYON (LINE F) IN AUGUST 2011. (A) TEMPERATURE, SALINITY, SIGMA-T OXYGEN (PERCENT SATURATION) AND CHLOROPHYLL FLUORESCENCE. (B) THE FIVE NUTRIENTS (SILICATE, PHOSPHATE, NITRATE, NITRITE AND AMMONIUM) AT THE DISTRIBUTED BIOLOGICAL OBSERVATORY LINE.

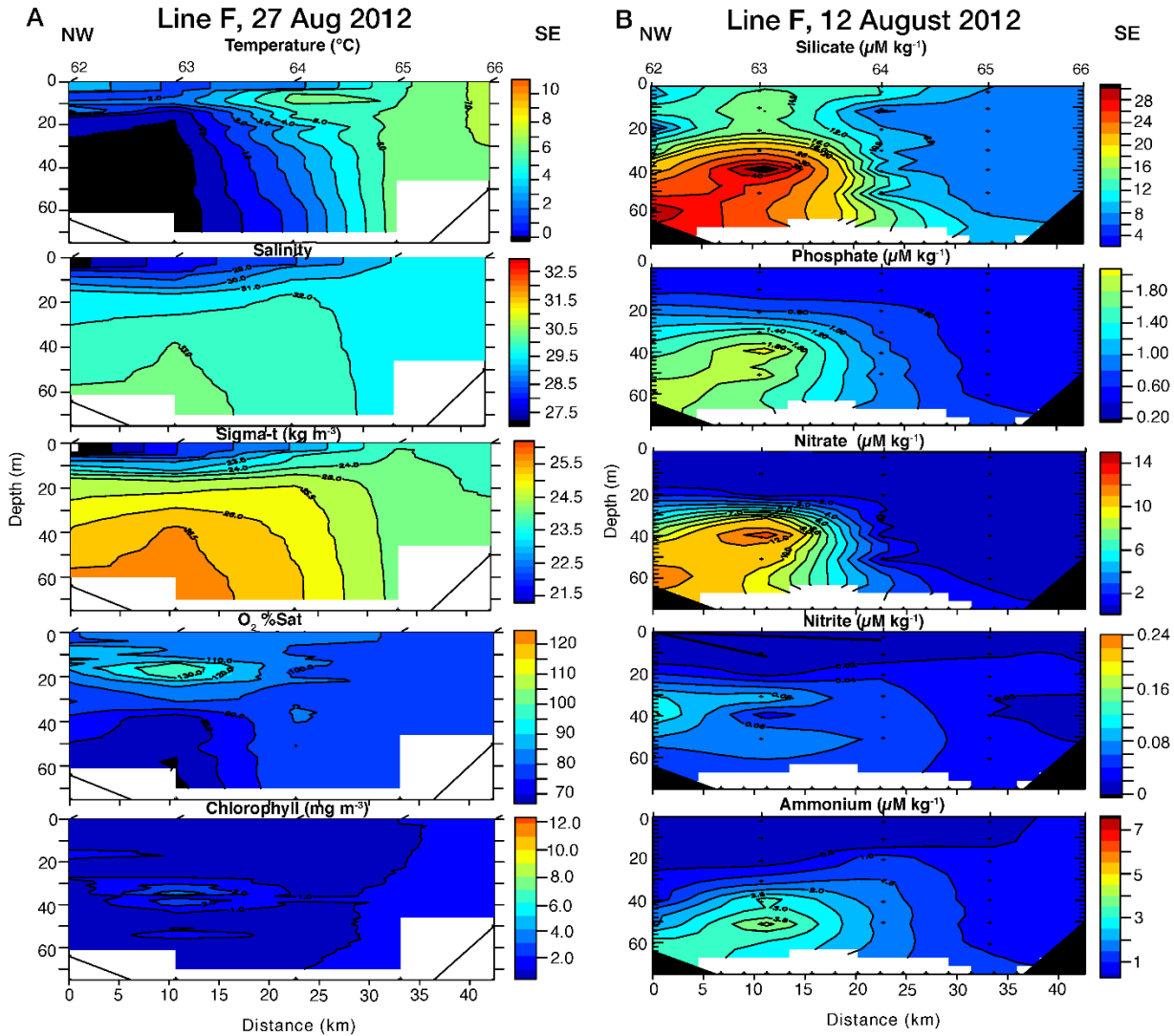


FIGURE 74. HYDROGRAPHIC MEASUREMENTS AT BARROW CANYON (LINE F) IN AUGUST 2012. (A) TEMPERATURE, SALINITY, SIGMA-T OXYGEN (PERCENT SATURATION) AND CHLOROPHYLL FLUORESCENCE. (B) THE FIVE NUTRIENTS (SILICATE, PHOSPHATE, NITRATE, NITRITE AND AMMONIUM) AT THE DISTRIBUTED BIOLOGICAL OBSERVATORY LINE.

Satellite-tracked drifters

Three satellite-tracked drifters were deployed in collaboration with EcoFOCI/PMEL (Figure 75). Their drogue was centered below the wind mixed layer, so until the beginning of the fall mixing period the drifters were not strongly influenced by the winds. The trajectories of the two drifters released between Bering Strait and Pt. Hope showed generally northward flow. The other drifter, released near Hanna Shoal, traveled counterclockwise and then to the west. After being caught in the ice field (and likely losing their drogues) the drifter trajectories showed limited movement indicating that at least through December the ice was resident over the Chukchi Sea.

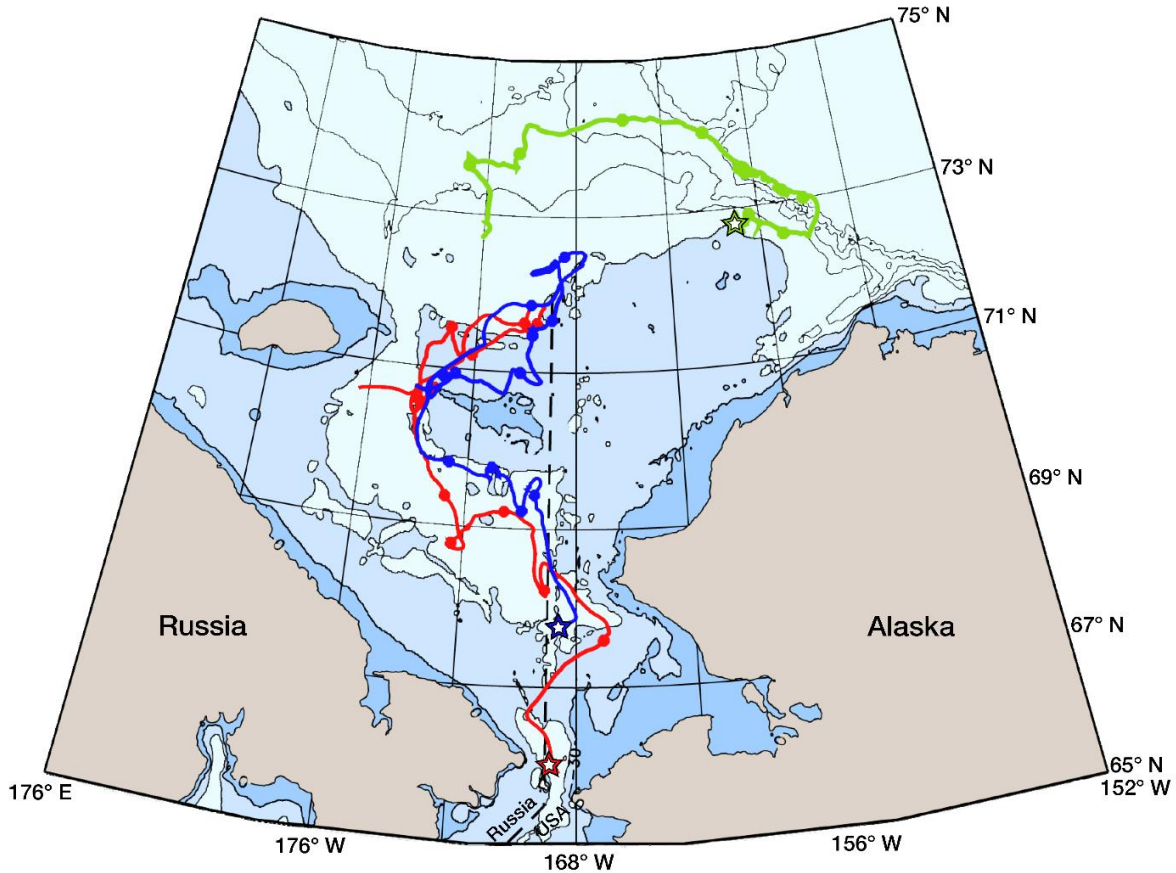


FIGURE 75. TRAJECTORY OF SATELLITE-TRACKED DRIFTERS WITH 25-M-DEEP DROGUES DEPLOYED IN AUGUST 2011. THE STARS INDICATE THE STARTING LOCATIONS, AND CIRCLES ARE PLOTTED EVERY 10 DAYS. THE DRIFTER-TRACK COLORS AND TIME SPANS ARE AS FOLLOWS: DRIFTER 106694, RED, 19 AUGUST–12 DECEMBER 2011; DRIFTER 106698, GREEN, 27 AUGUST–27 NOVEMBER 2011; DRIFTER 106699, BLUE, 19 AUGUST–11 DECEMBER 2011. ENDING DATES INDICATE THE LAST TRANSMISSION OR WHEN THE DRIFTER WAS CAUGHT IN SEA ICE. THE DEPTH CONTOURS ARE AT 30, 50, 100, 200, 500 AND 1000 M.

Zooplankton Net Data

The mean net-estimated concentration of adult and juvenile euphausiids was below 1 m^{-3} with the highest mean concentration occurring during the cold year, 2012 (Table 19). Concentrations of younger stages of euphausiids, principally furcilia, were at least an order of magnitude higher than adult and juvenile concentrations with no consistent difference among cold and warm years. The concentrations of the youngest euphausiid stage captured, calyptopis, were low in all years, but in the first year the concentrations were on the order of 1 m^{-3} . The presence of calyptopis stage euphausiids suggests recent spawning in the region. Other plankters whose acoustic scattering would also be approximated by the elongate scattering model, hyperiid and gammarid amphipods, were found in similar concentrations to euphausiids. The mean concentration of gammarid amphipods was also highest during 2012, the coldest year; the highest concentration of hyperiid amphipods was in 2011.

Among the copepod taxa, *Oithona* spp. (not shown) had the highest concentrations. *Pseudocalanus* spp., was very abundant in all years ($O 10^2$ - 10^3 individuals m^{-3} , but the mean concentration in the cold year (2012) was about 70% that in the two warmer years). This species

complex is often identified as important for producing prey for larval fish. *Pseudocalanus* spp. production is thought to be more closely tied to temperature than food availability. *Calanus glacialis*, a “medium-sized” copepod (females 3.5 – 5.2 mm), was found at lower concentrations than *Pseudocalanus* spp. ($10^1 - 10^2$ individuals m^{-3}), and had its highest concentrations during the final cold year, 2012. A congener, *Calanus hyperboreus*, which is significantly larger and normally found in deeper water, was present only in 2011.

We also examined trends in three non-copepod taxa: planktonic molluscs (pteropods) for their high acoustic reflectance, chaetognaths for their predatory impact on the younger copepod and euphausiid stages, and larvaceans. Under the initial protocol, shelled and naked pelagic molluscs were counted together. In 2012, however, they were separated and the shelled pteropods dominated. Concentrations of chaetognaths were $O 10^1$, and somewhat lower in 2012 than the other two years. Larvaceans are often considered important for transferring energy from small-sized phytoplankton to higher trophic levels. Their mean concentrations spanned three orders of magnitude ($10^1 - 10^3$) with the highest concentrations observed during the first two years. Barnacle nauplii (not shown) were the most abundant taxa captured by our nets.

TABLE 19. MEAN CONCENTRATION OF SELECTED ZOOPLANKTON TAXA (NUMBER PER M^3).

Mean No. Per M^3 Taxon	Year		
	2010	2011	2012
Euphausiids			
calytopis stage	1.18	0.03	0.04
furcilia stage	9.75	6.61	8.38
juvenile and adult stages	0.19	0.22	0.95
Organisms with similar acoustic scattering as euphausiids			
Hyperiid amphipods	0.12	2.68	0.52
Gammarid amphipods	0.11	0.01	1.76
Copepods			
<i>Pseudocalanus</i> spp.	1052.69	1025.19	737.56
<i>Calanus glacialis</i>	82.08	63.25	290.48
<i>Calanus hyperboreus</i>	0.00	2.71	0.00
Other non crustacean taxa			
Larvaceans	781.22	1096.01	8.10
Pteropods (with and without shells)	126.95	11.64	5.05 (4.89 T)
Chaetognaths	46.71	47.00	27.57

Areal distribution of selected taxa

The distribution of euphausiid calytopae was very patchy in space and time (Figure 76). The highest concentrations were sampled in 2010 and were most often located in the eastern portion of the Chukchi shelf. Despite one large sample at the end of Transect A (Pt. Hope line), most of the youngest stage of euphausiids were found on either Transect D (Icy Cape) or Transect E (Wainwright). In 2011 and 2012, calytopae were found either in or adjacent to

Transect F (Barrow Canyon). The distribution of the furcilia stage was much less patchy with individuals found along each transect in 2010 and 2011 (Figure 77). In 2012, individuals were absent from the entire Transects E & F and mostly absent from Transect D. This latter observation could be an indication of lower physical transport during the cold year. Concentrations of furcilia along the bottom layer were determined in 2011 and were found to be comparable and sometimes higher in magnitude to those found throughout the water column (Figure 78). Concentrations of furcilia captured at night were not appreciably higher than those captured during the day along the same transect lines (Figure 79). The distribution of juvenile and adult euphausiids was also very patchy, particularly in the first two years (Figure 80). A higher proportion of stations had non-zero concentrations in 2012, with the highest concentrations found at the western (Transect A) and eastern (Transect F) extremes of the region. Concentrations along the bottom were of the same magnitude as those in the water column, but they were found in the bottom layer less often than in the water column (Figure 81).

The distributions of both hyperiid and gammarid amphipods was also very patchy. The number of stations at which we found hyperiids was much greater than that for gammarids. In 2010, hyperiids were most often found at the offshore extent of our transects (Figure 82). They were found both inshore and offshore in other years. Gammarid amphipods were much more frequently encountered in 2012, with the highest concentrations along Transect E (Wainwright line) and one station on each of Transects A & C (Figure 83). They were frequently found in the net fished near the bottom (Figure 84).

Copepods were ubiquitous across the shelf. *Pseudocalanus* spp. was found at almost every station in every year (Figure 85). In 2010, the concentrations were somewhat higher in the eastern part of the region on Transects D & E. In 2011 it appeared that the concentrations at the western and eastern edges of the sampling region were comparable. In 2012, we found high concentrations along Transect E, but much lower concentrations along the other lines. *Calanus glacialis* was also found at almost every station in all years (Figure 86). The lowest concentrations were often found in the central transect lines (B & C). The concentrations in 2012 were higher and much more uniform across the sampling region. *Calanus glacialis* was also found along the bottom, but in lower concentrations than in the water column (Figure 87). *C. hyperboreus* was found only in 2011 and only along Transects E & F in the water column (Figure 88). This indicates an intrusion of oceanic waters onto the shelf. During that one year, *C. hyperboreus* was found more frequently along the bottom on Transect E than it was found in the water column, however, the concentrations were much lower along the bottom.

The non-copepod taxa also had patchy distributions. Larvaceans were abundant and more frequently captured in the first two years of the study (Figure 89). They were present at almost every station in those years, although their concentrations were low along Transects B & C in 2010. In 2012, they were infrequently encountered and their concentrations were low with few positive stations in the middle of the region (Transects B, C, and D). Pteropods were most frequently encountered in the first year of the study when we also had the highest concentrations (Figure 90). 2011 had low concentrations and a low frequency of occurrence. Two of the three years they were found along Transect D where our acoustic instruments were deployed. They were rarely encountered in the net towed along the bottom (Figure 91; data only for 2012). Chaetognaths were also ubiquitous and found at all stations in all years (Figure 92). They had high concentrations along Transects A & D in 2010, Transects E & F in 2011, and Transect C in 2012. In 2012, after changing our protocol, we determined that the majority of the chaetognaths

were of the genus *Parasagitta*. *Eukrohnia* spp. were only found along the western-most line (Transect A), except for a single station at the end of Transect B (Cape Lisburne) and in the middle of Transect E (not shown).

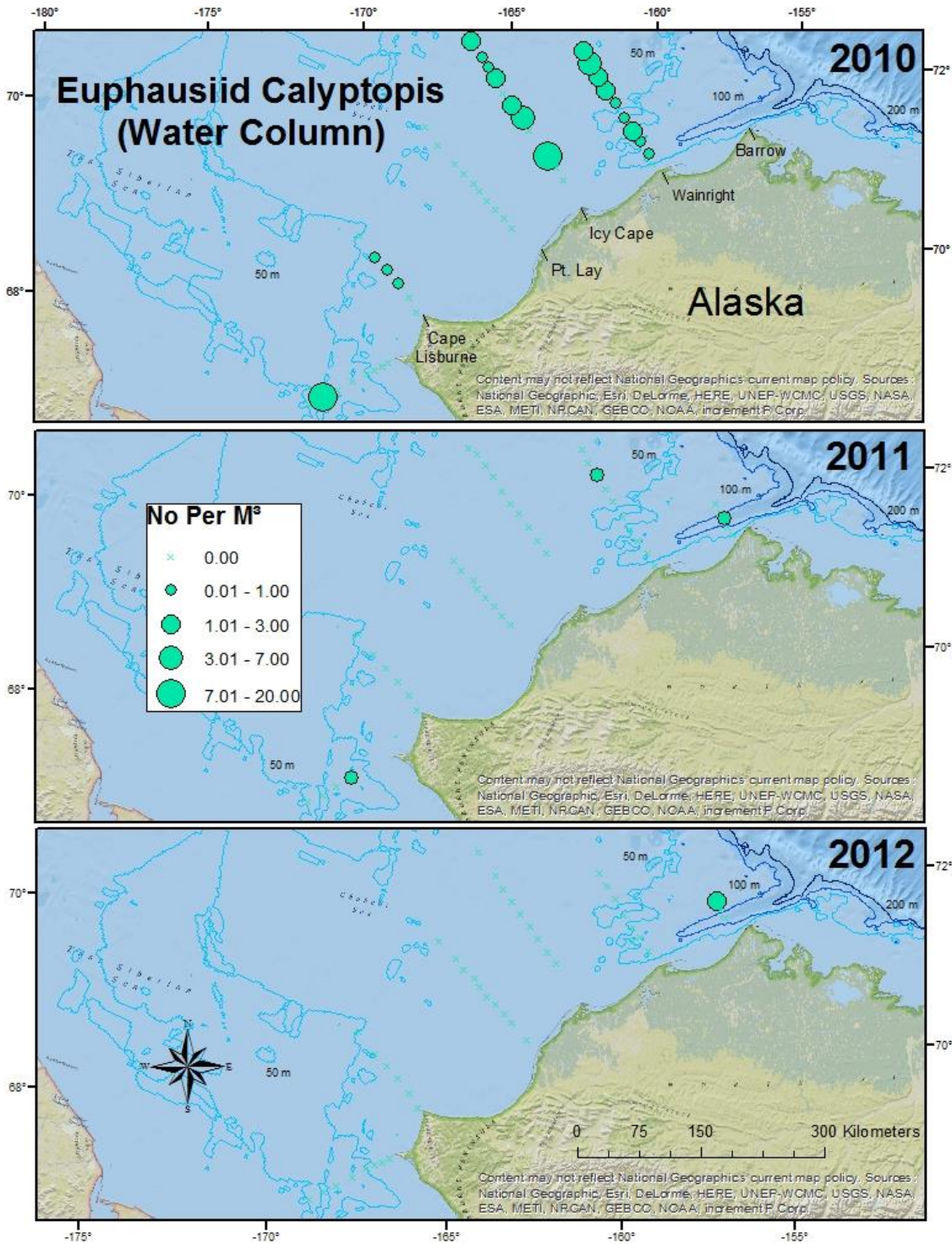


FIGURE 76. CONCENTRATION OF EUPHAUSIID CALYPTOPAE IN THE WATER COLUMN, 2010 - 2012.

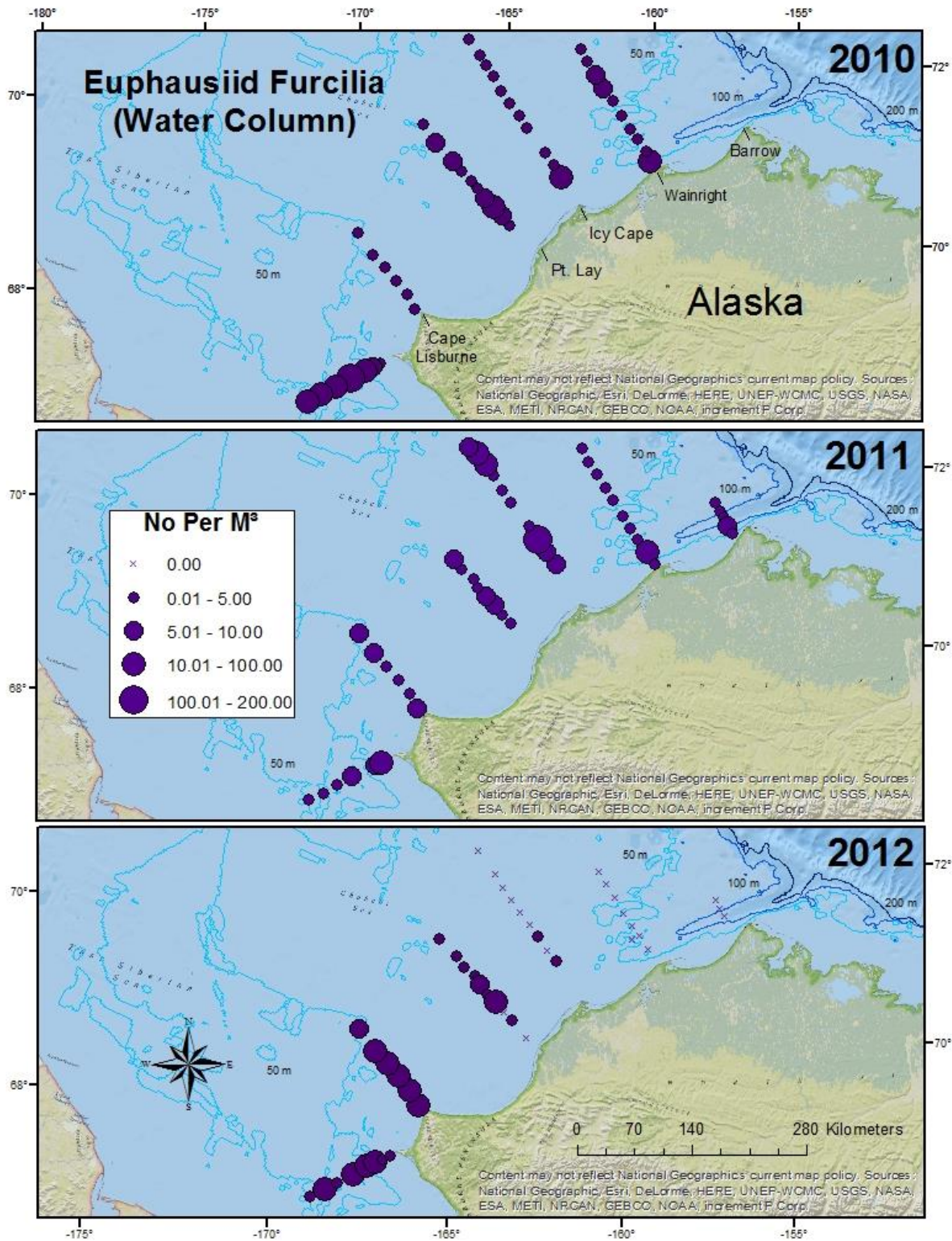


FIGURE 77. CONCENTRATION OF EUPHAUSIID FURCILIA IN THE WATER COLUMN, 2010 - 2012.

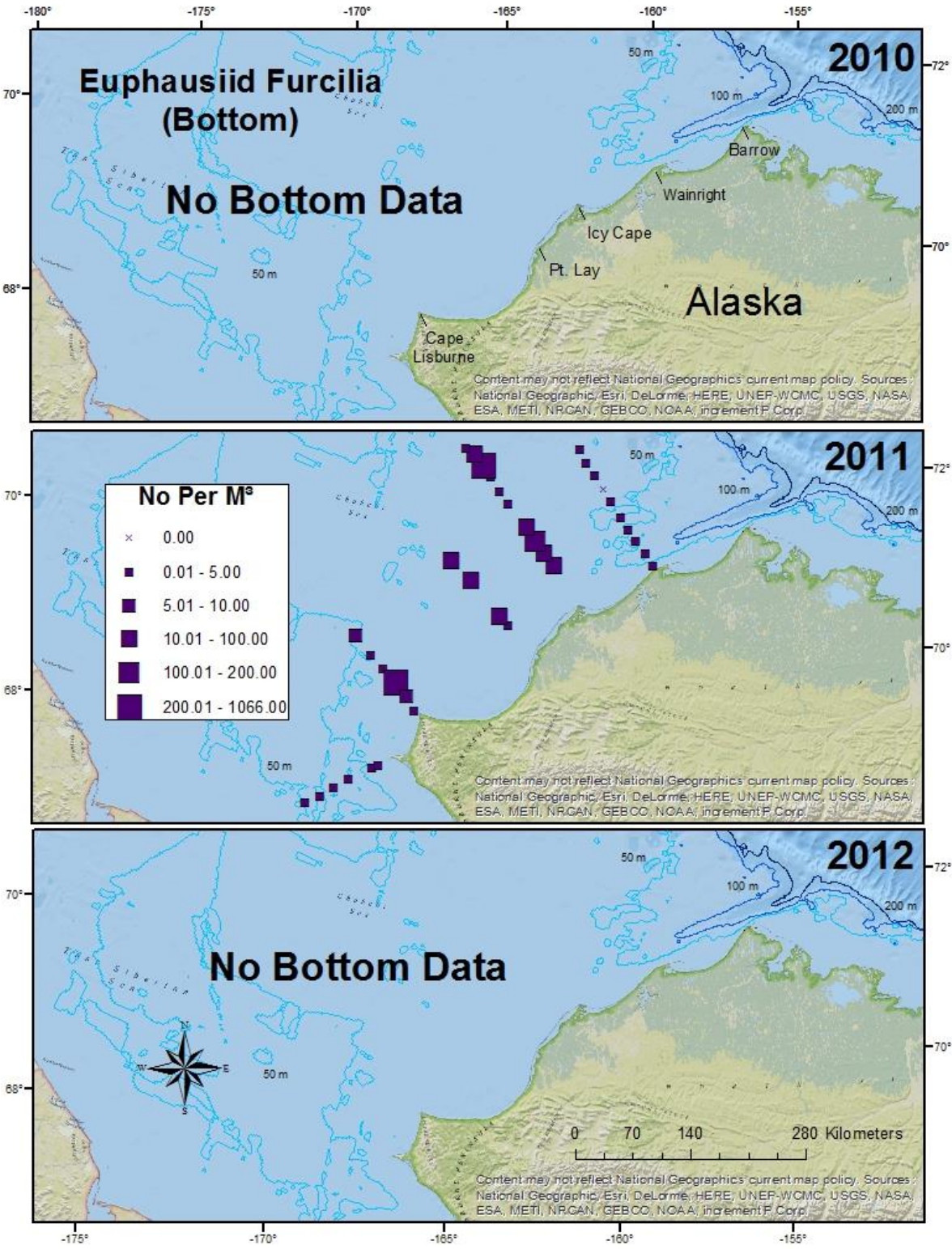


FIGURE 78. CONCENTRATION OF EUPHAUSIID FURCILIA ALONG THE BOTTOM, 2010 – 2012.

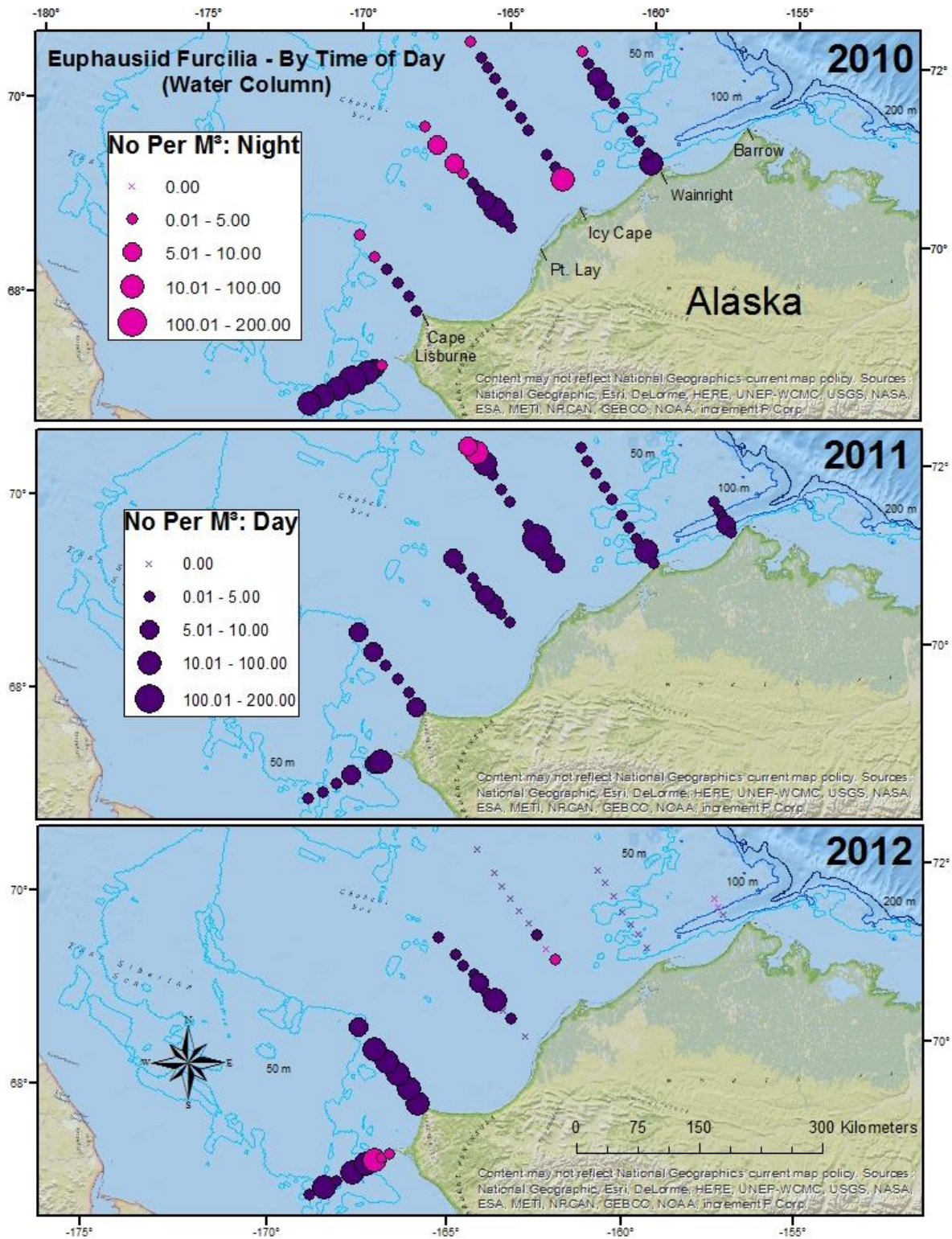


FIGURE 79. CONCENTRATION OF EUPHAUSIID FURCILIA DAY AND NIGHT, 2010 – 2012. PURPLE SYMBOLS INDICATE DAY, PINK SYMBOLS INDICATE NIGHT.

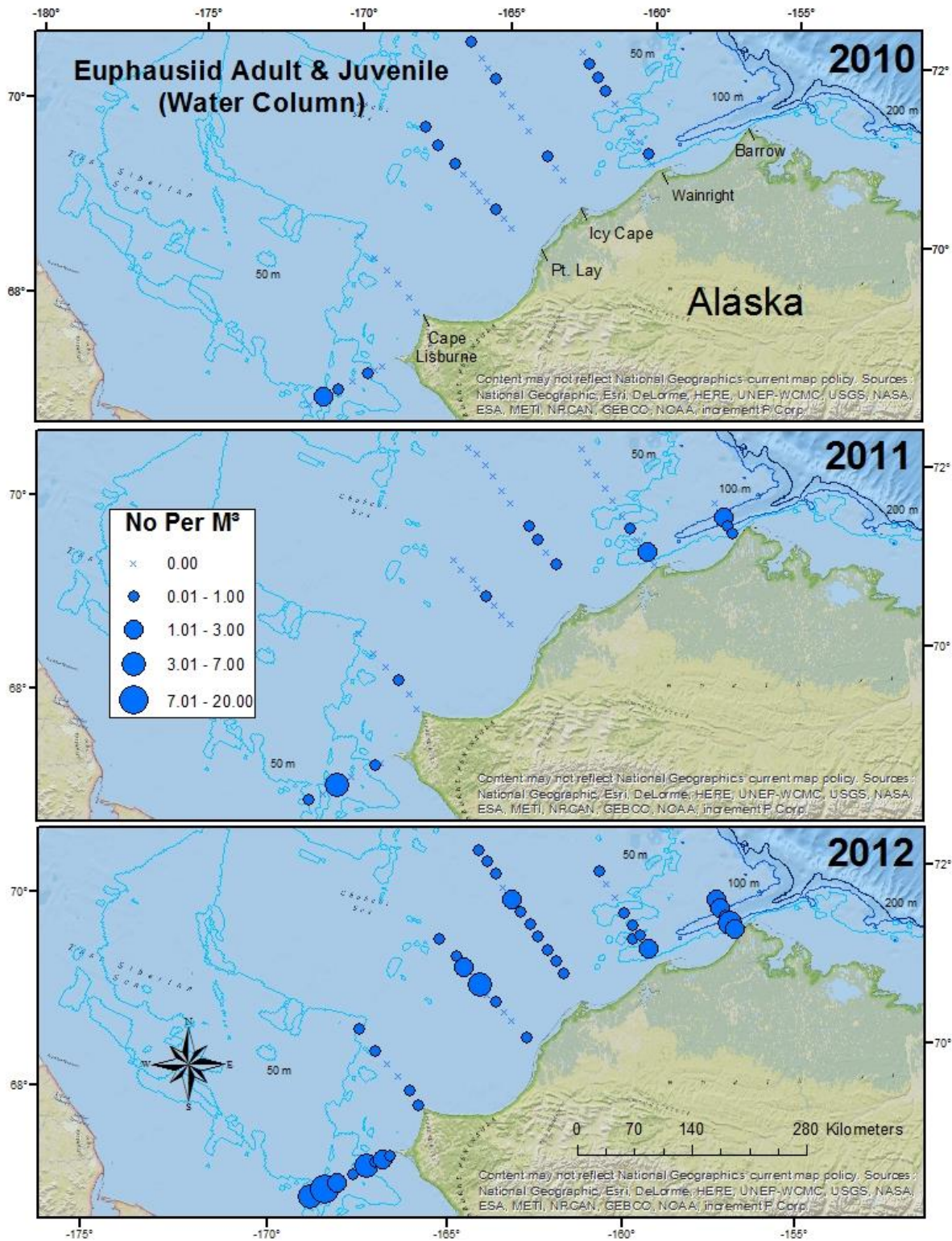


FIGURE 80. CONCENTRATION OF EUPHAUSIID JUVENILE AND ADULTS IN THE WATER COLUMN, 2010 – 2012.

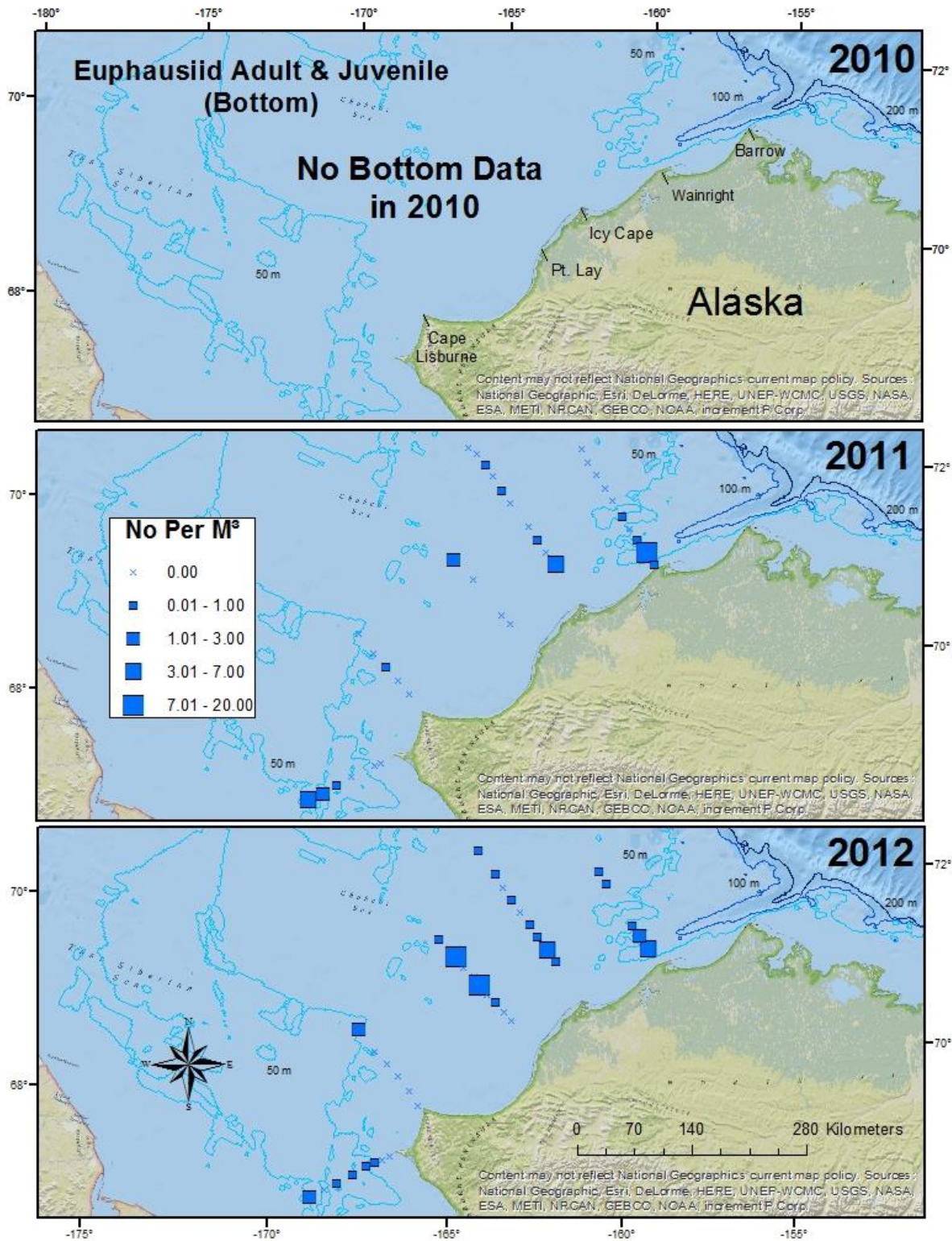


FIGURE 81. CONCENTRATION OF EUPHAUSIID JUVENILE AND ADULTS IN THE BOTTOM LAYER, 2010 – 2012.

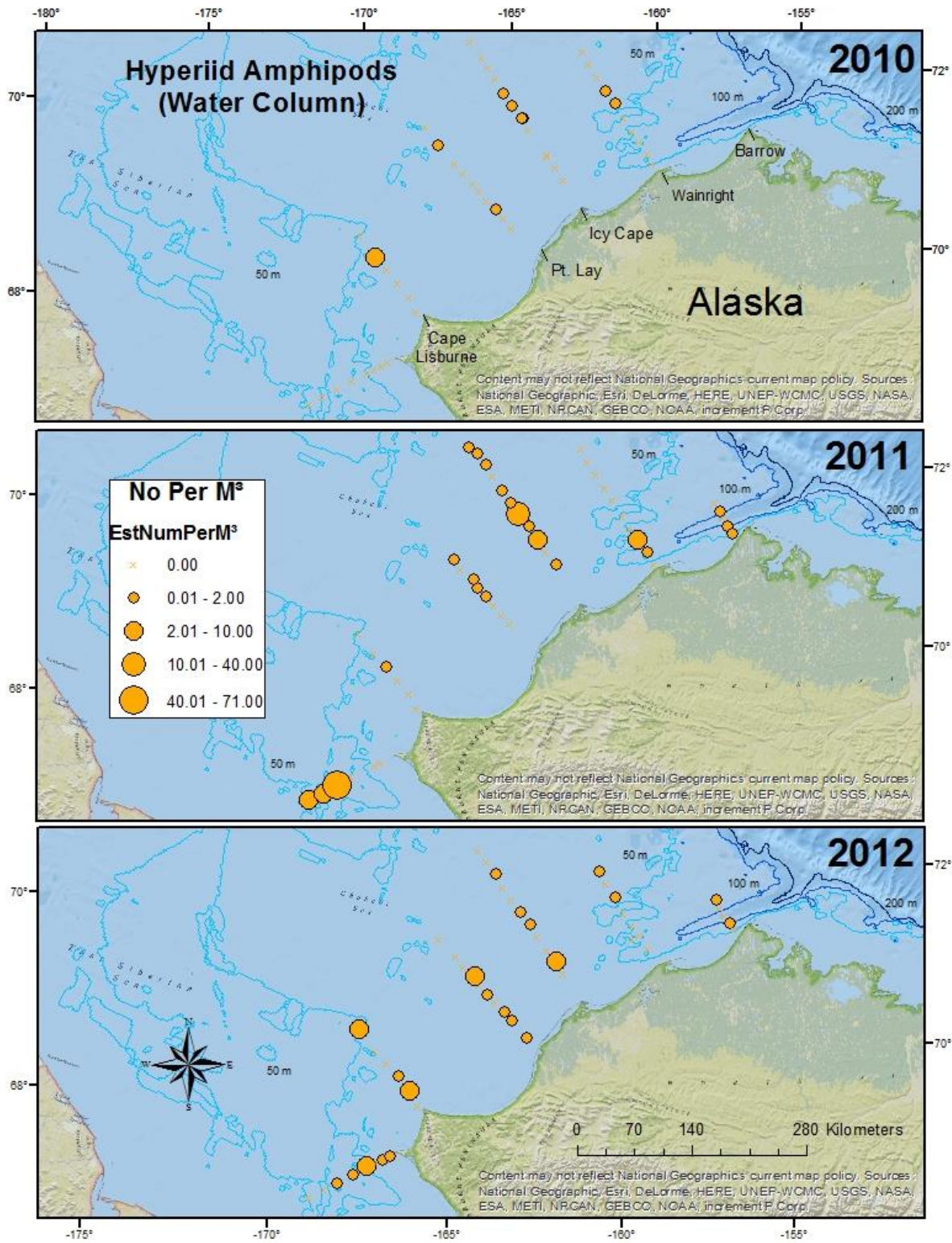


FIGURE 82. CONCENTRATION OF HYPERIID AMPHIPODS IN THE WATER COLUMN, 2010 – 2012.

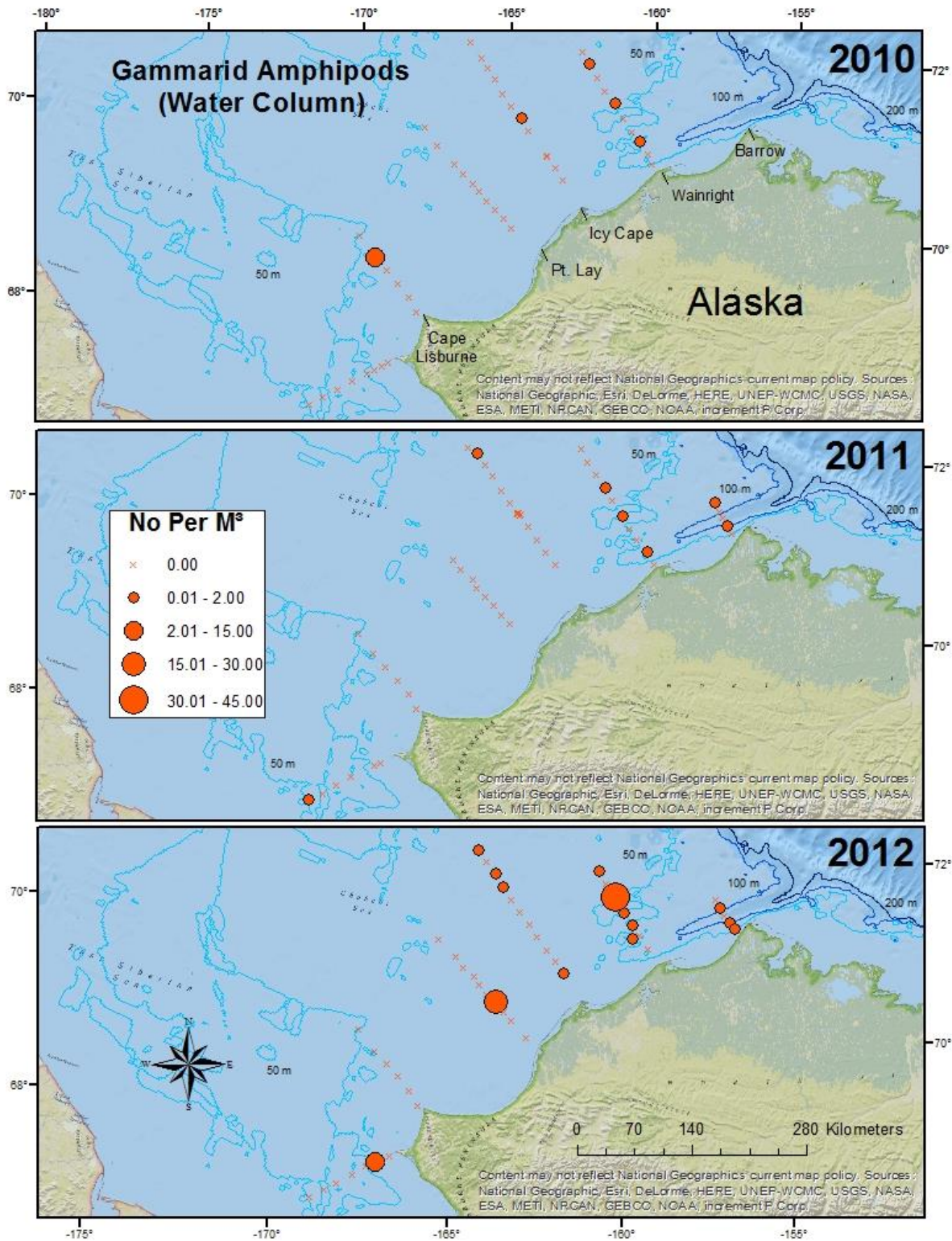


FIGURE 83. CONCENTRATION OF GAMMARID AMPHIPODS IN THE WATER COLUMN, 2010 – 2012.

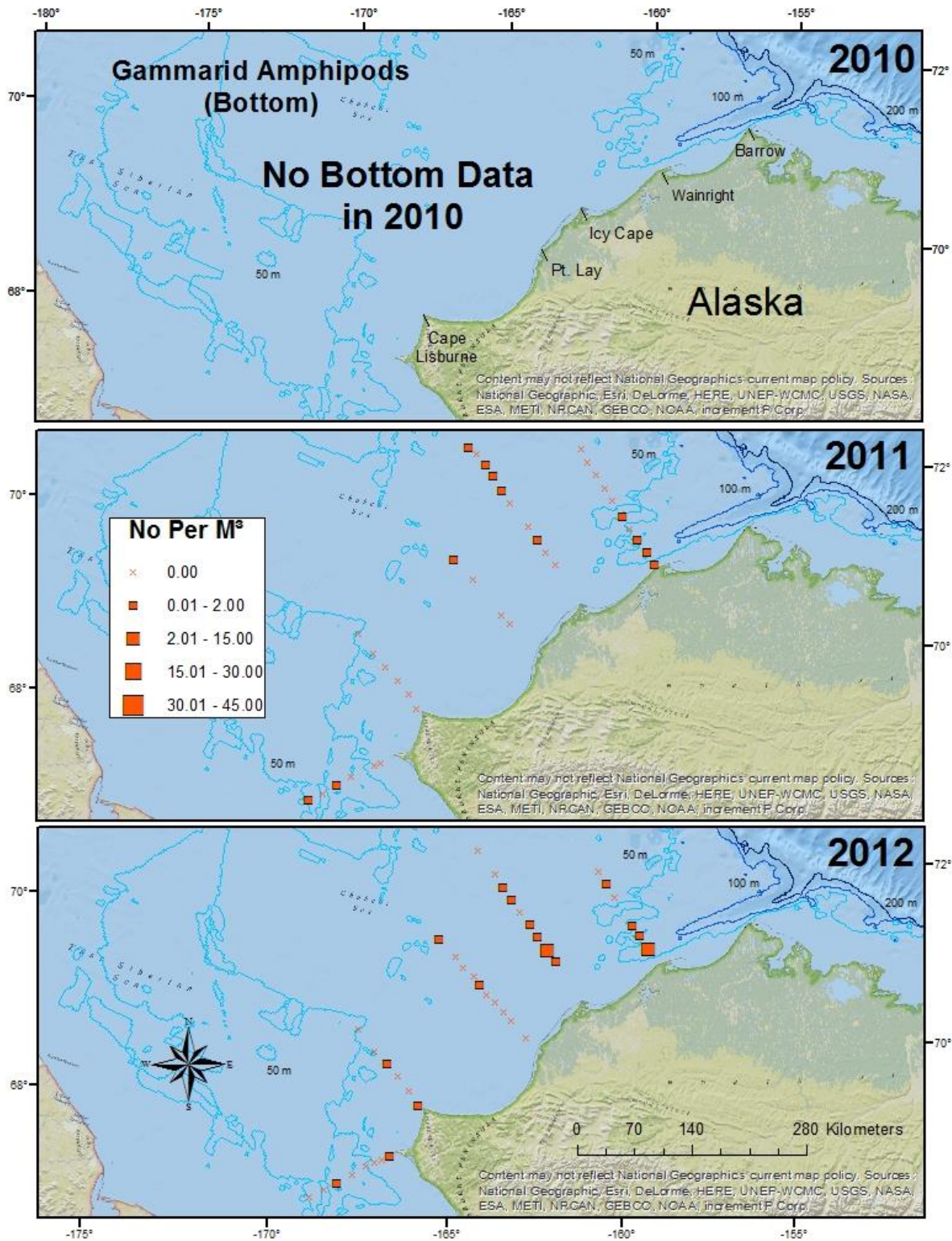


FIGURE 84. CONCENTRATION OF GAMMARID AMPHIPODS NEAR BOTTOM, 2010 – 2012.

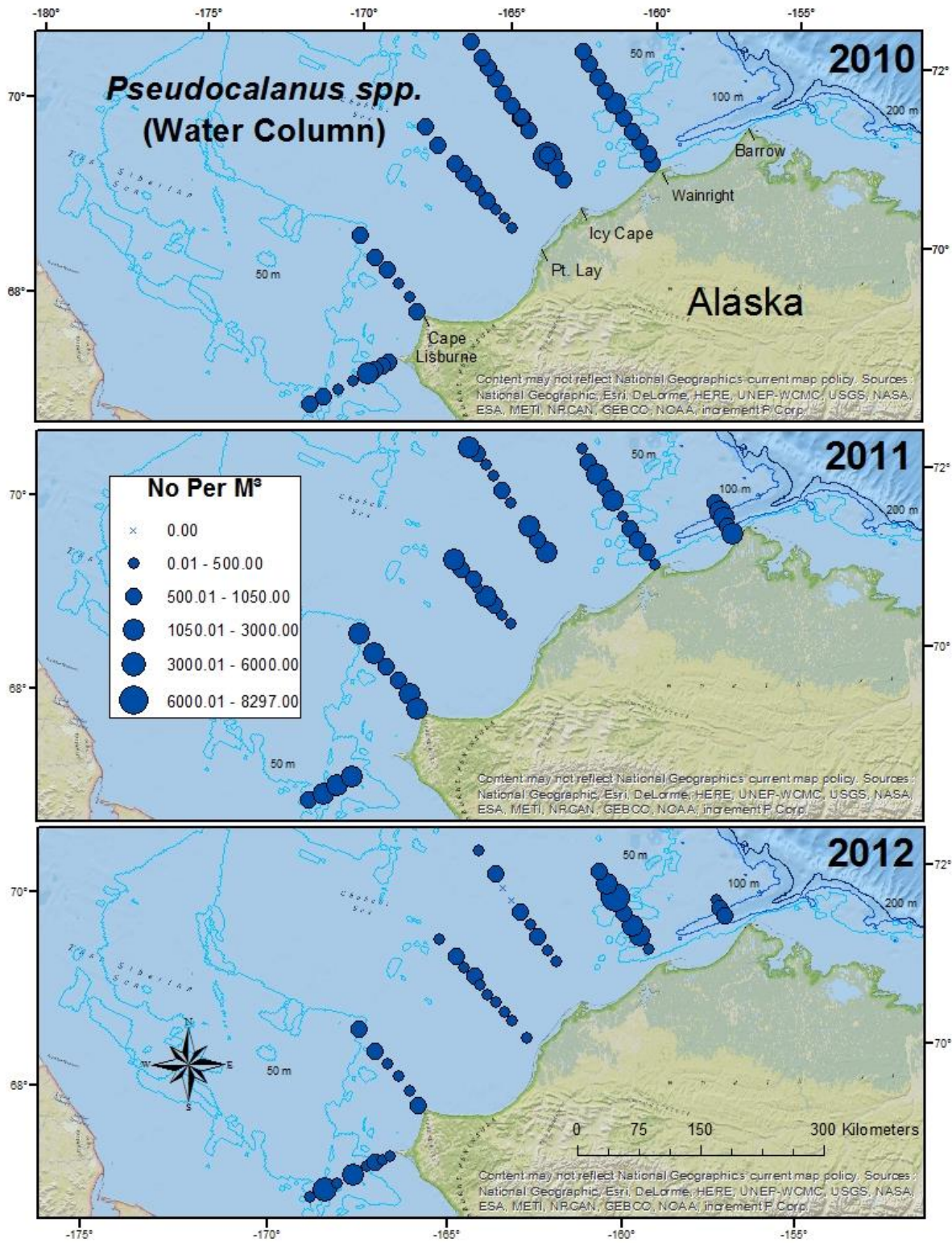


FIGURE 85. CONCENTRATION OF *PSEUDOCALANUS* SPP. IN THE WATER COLUMN, 2010 – 2012.

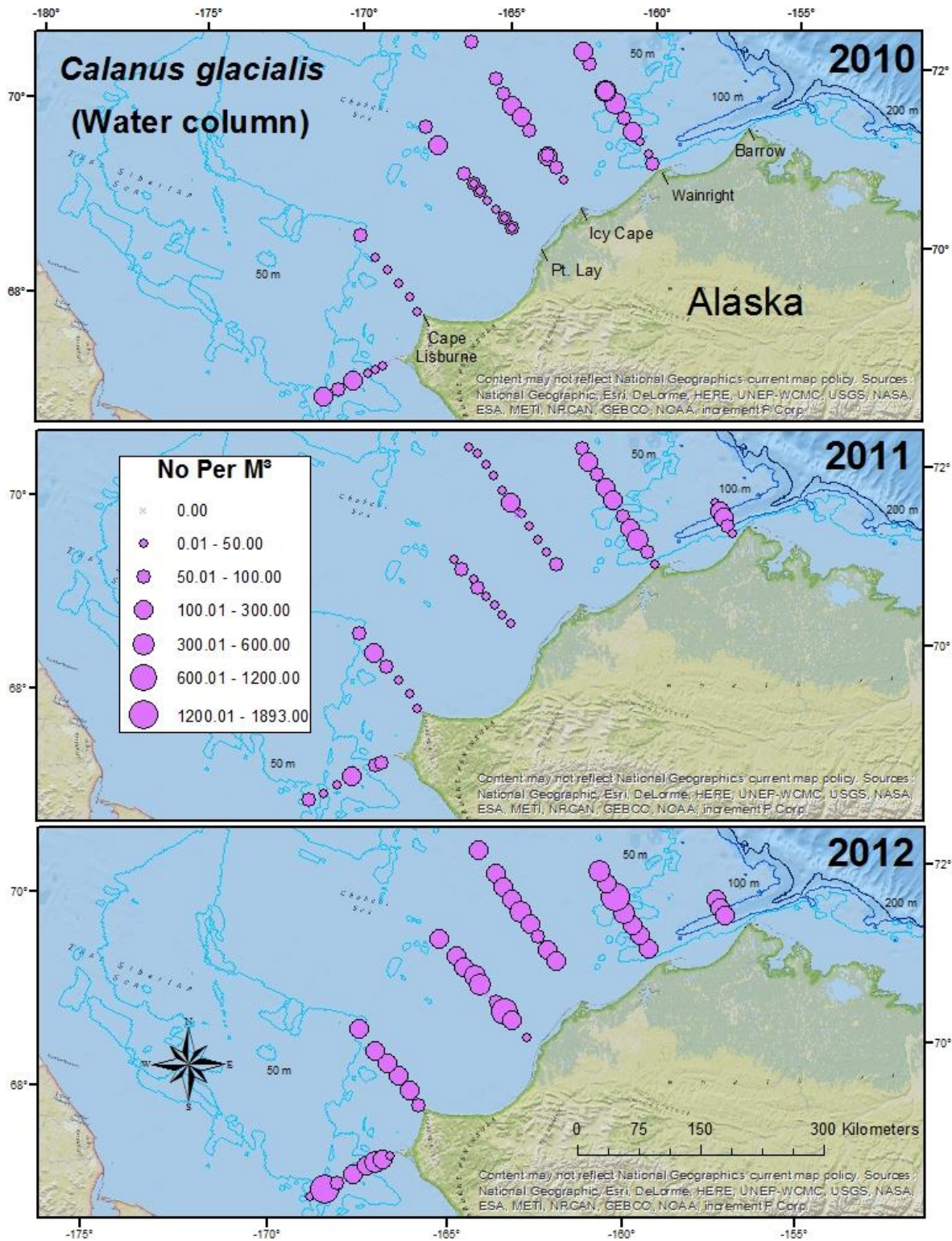


FIGURE 86. CONCENTRATION OF *CALANUS GLACIALIS* IN THE WATER COLUMN, 2010 – 2012.

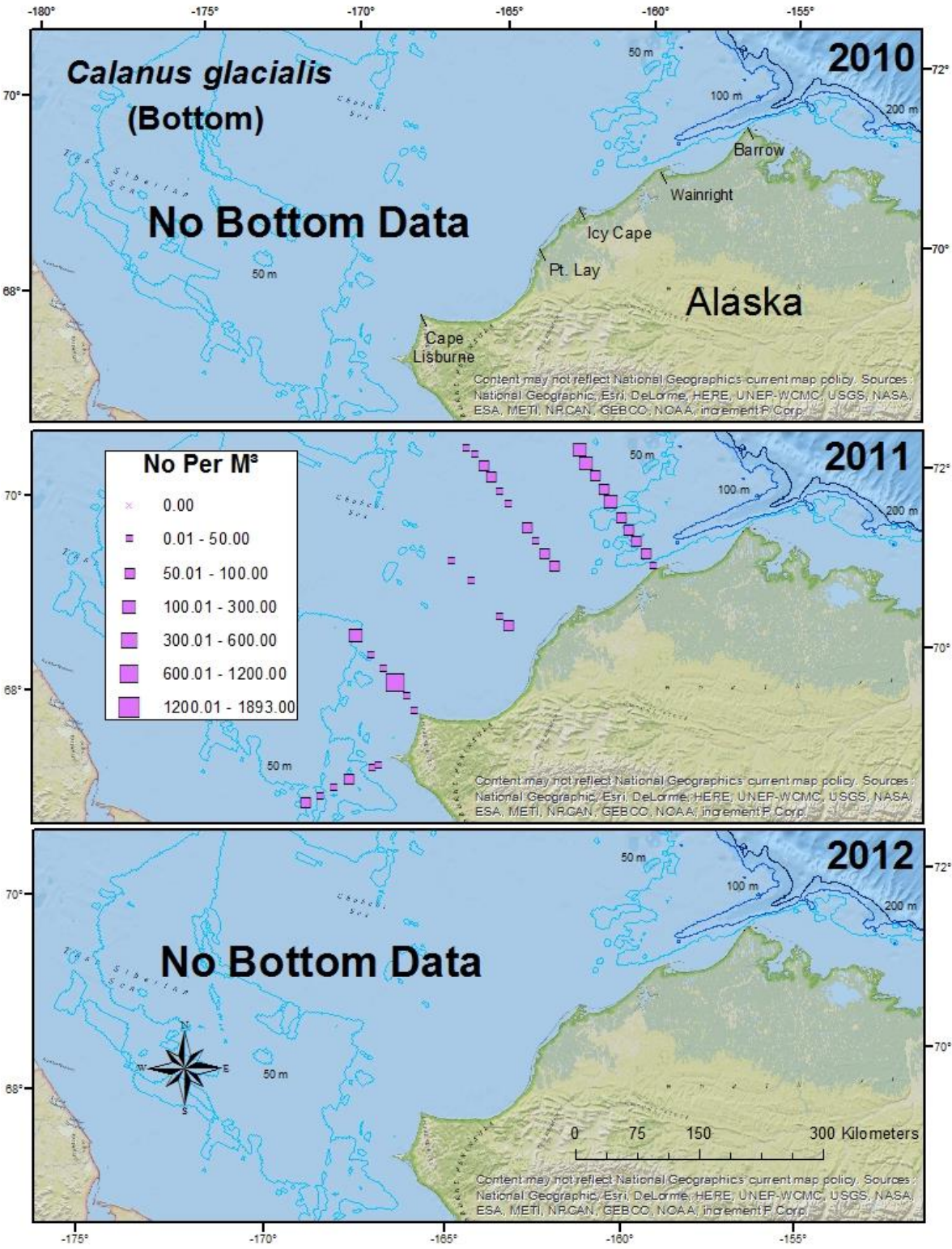


FIGURE 87. CONCENTRATION OF *CALANUS GLACIALIS* NEAR BOTTOM, 2010 – 2012.

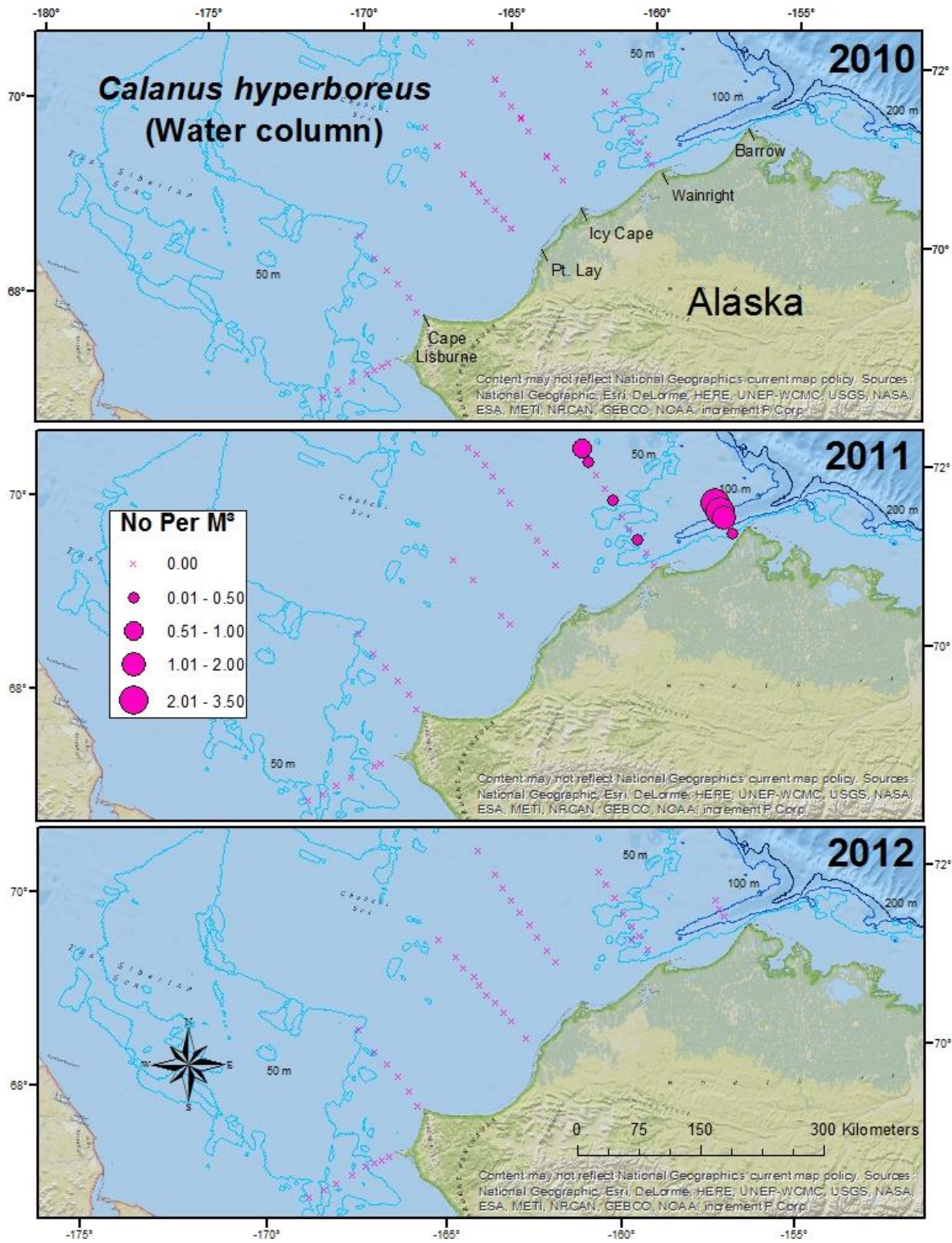


FIGURE 88. CONCENTRATION OF *CALANUS HYPERBOREUS* IN THE WATER COLUMN, 2010 – 2012.

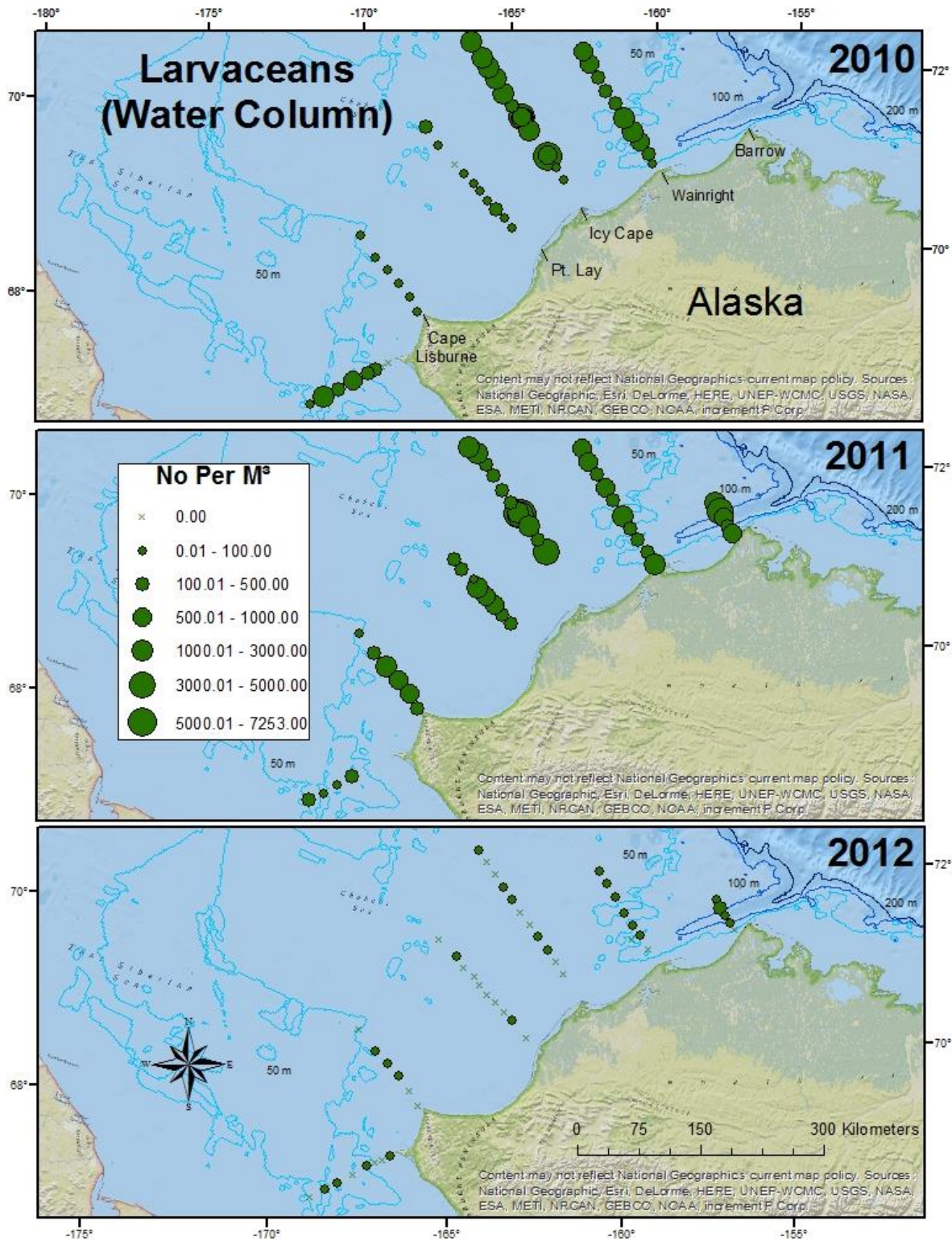


FIGURE 89. CONCENTRATION OF LARVACEANS IN THE WATER COLUMN, 2010 – 2012.

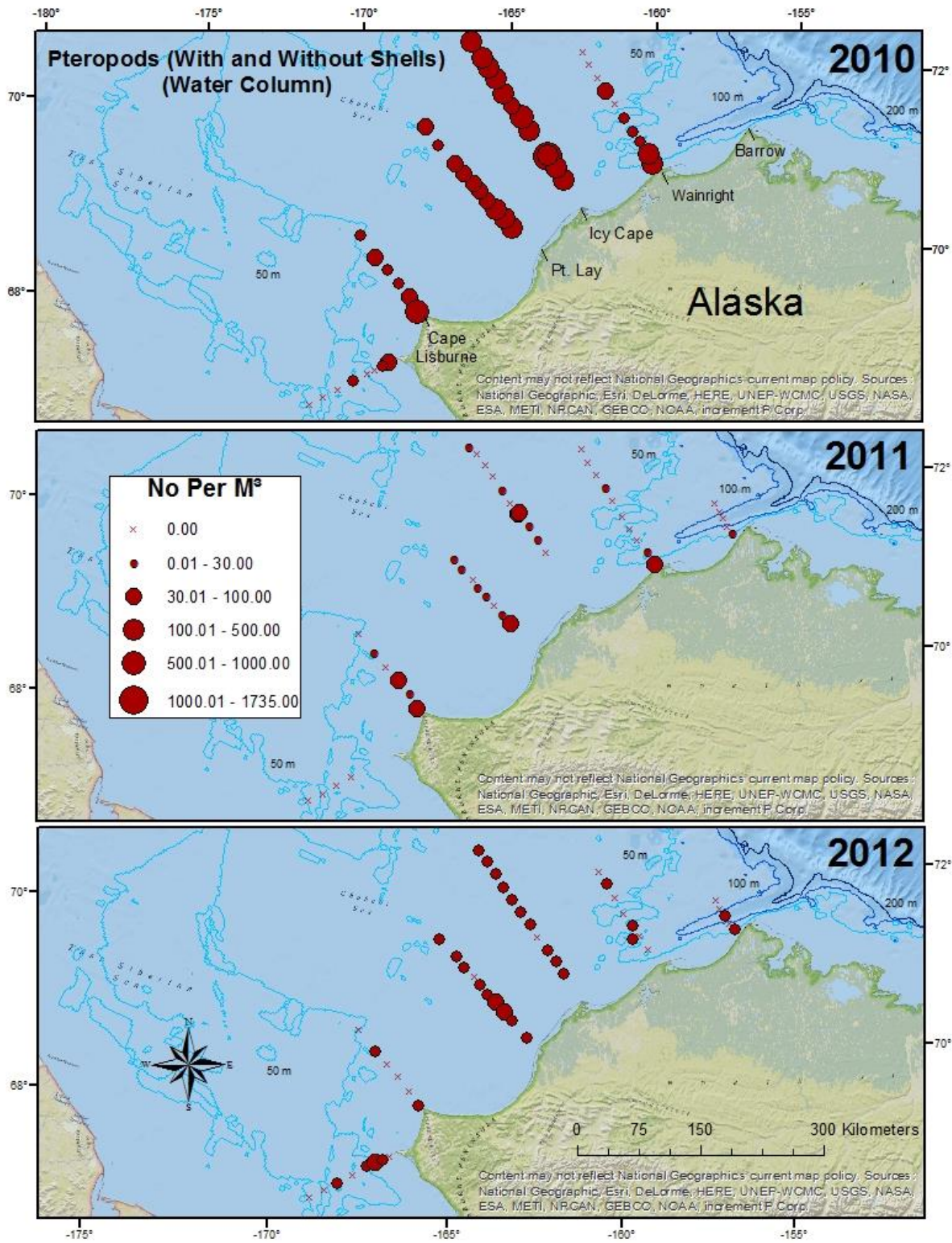


FIGURE 90. CONCENTRATION OF PTEROPODS IN THE WATER COLUMN, 2010 – 2012.

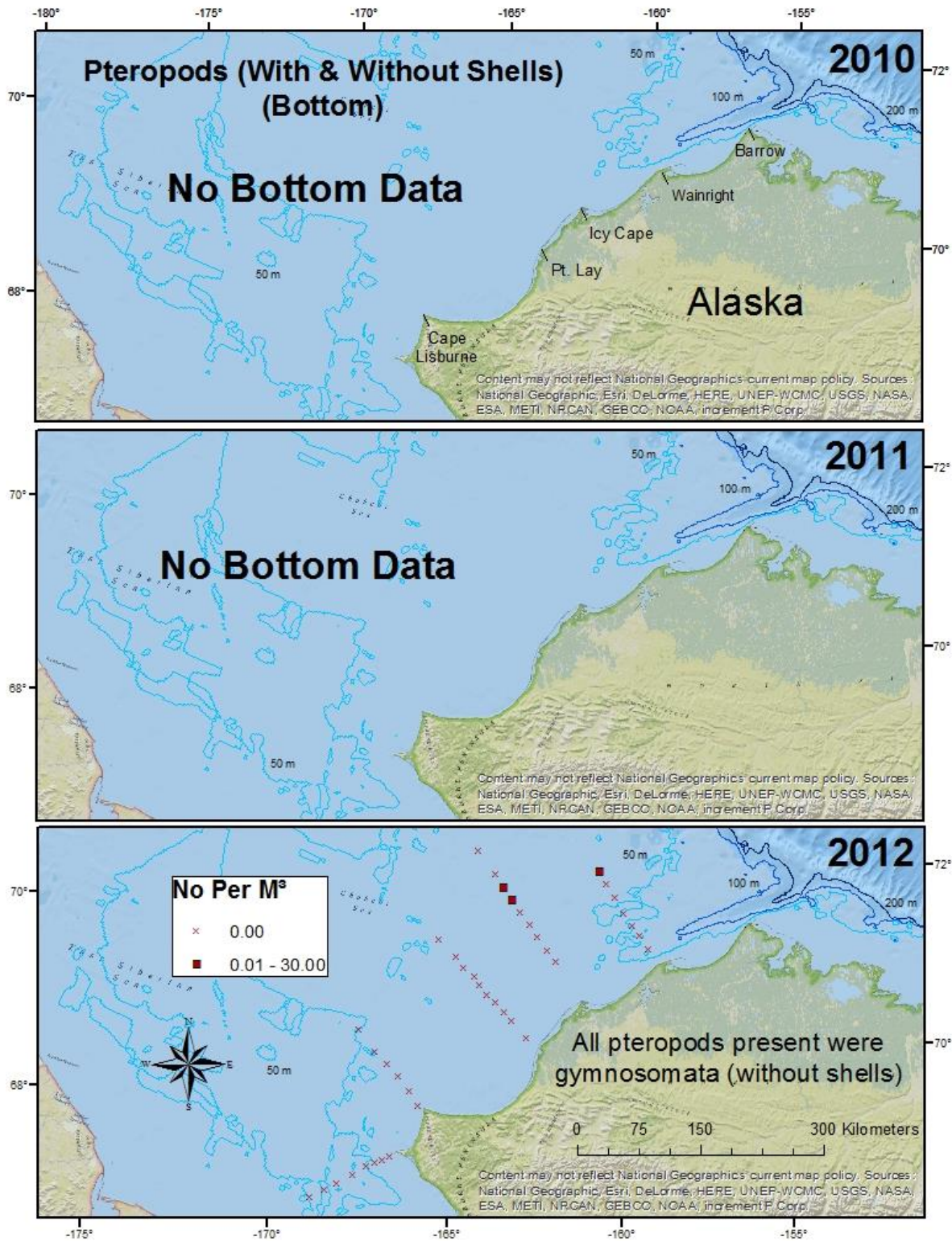


FIGURE 91. CONCENTRATION OF PTEROPODS ALONG THE BOTTOM, 2010 – 2012.

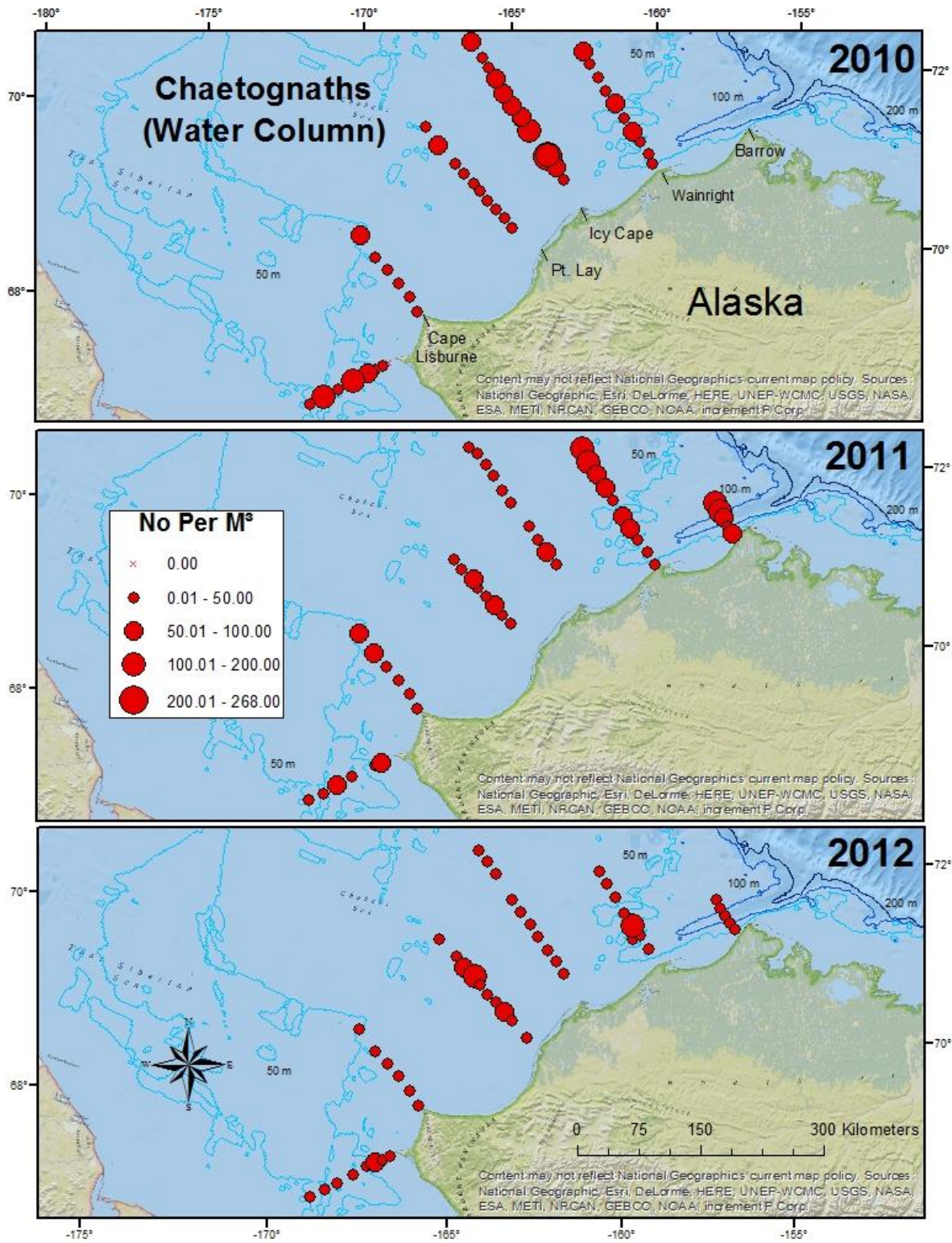


FIGURE 92. CONCENTRATION OF CHAETOGNATHS IN THE WATER COLUMN, 2010 – 2012.

Comparison of Zooplankton Estimates From the Tucker Net and a TAPS-6

There was a modest relationship between S_v and zooplankton displacement. Data from four of the six frequencies showed a positive relationship between the two variables (Figure 93-94). The variance, explained by a linear relationship, was highest for the three lowest frequencies (r^2 values ~0.5-0.7, p-values ~ 0.003-0.03) for the 265, 420, and 700 kHz frequencies. The amount of variation explained for the three highest frequencies: 1100, 1850, and 3000 kHz, was poor.

This may have been due, in part, to the presence of pteropods in the samples. Shelled pelagic molluscs, are hard elastic scatterers and have much higher target strength relative to their displaced volume compared to other organisms. An example of this can be seen in Figure 93 and Figure 94, as indicated by outlier points circled in red on the 1850 and 3000 kHz plots. These plots show a large increase in S_v values without a commensurate change in displacement volume.

The inverse-estimated zooplankton abundance from TAPS-6 data using data from all six frequencies did not show a significant correlation with the net sample abundance (not shown). The inverse-estimated abundance was also several orders of magnitude greater than net abundance. This could be the result of incorrect model assumptions, or the inability to model all types of scatterers that are captured by the nets. For example, the calcareous-shelled pteropod has much stronger target strength as opposed to a fluid-like copepod. Larvaceans were also present in high numbers, but are difficult to model because they may or may not be surrounded by a mucous mesh house. Additionally, there was no significant correlation between inverse-estimated zooplankton abundance and net abundance after the 1100, 1850 and 3000 kHz frequencies were removed from inverse analysis. Removing these frequencies showed a decrease in estimated abundance with the final result being that the estimated and net caught abundances were of the same order of magnitude, but the correlation between the variables was still poor.

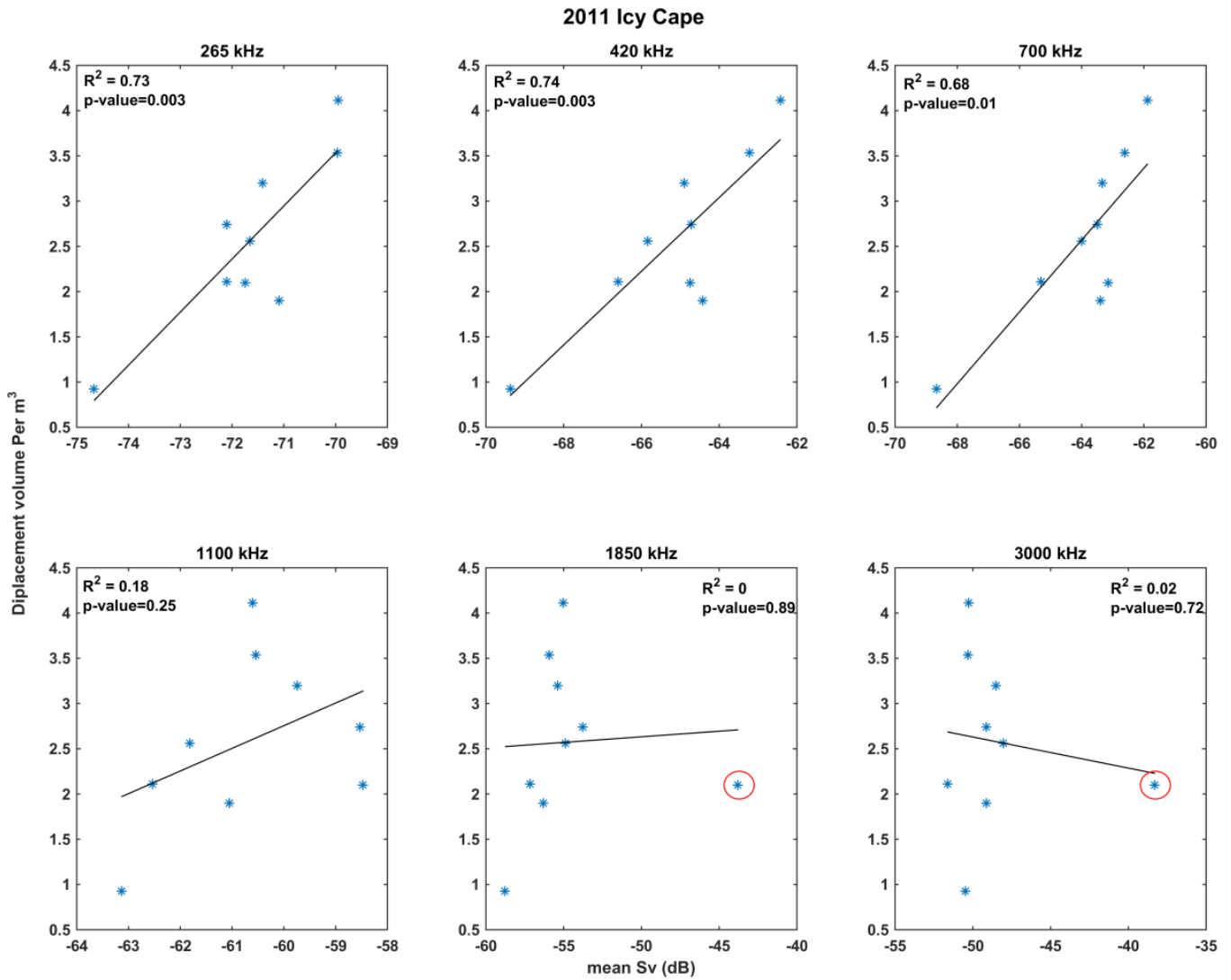


FIGURE 93. RELATIONSHIP BETWEEN ZOOPLANKTON DISPLACEMENT VOLUME AND MEAN WATER COLUMN VOLUME BACKSCATTER IN 2011 AT DIFFERENT FREQUENCIES ALONG THE ICY CAPE TRANSECT. RED CIRCLES INDICATE OUTLIERS DUE TO THE PRESENCE OF SHELLED PTEROPODS.

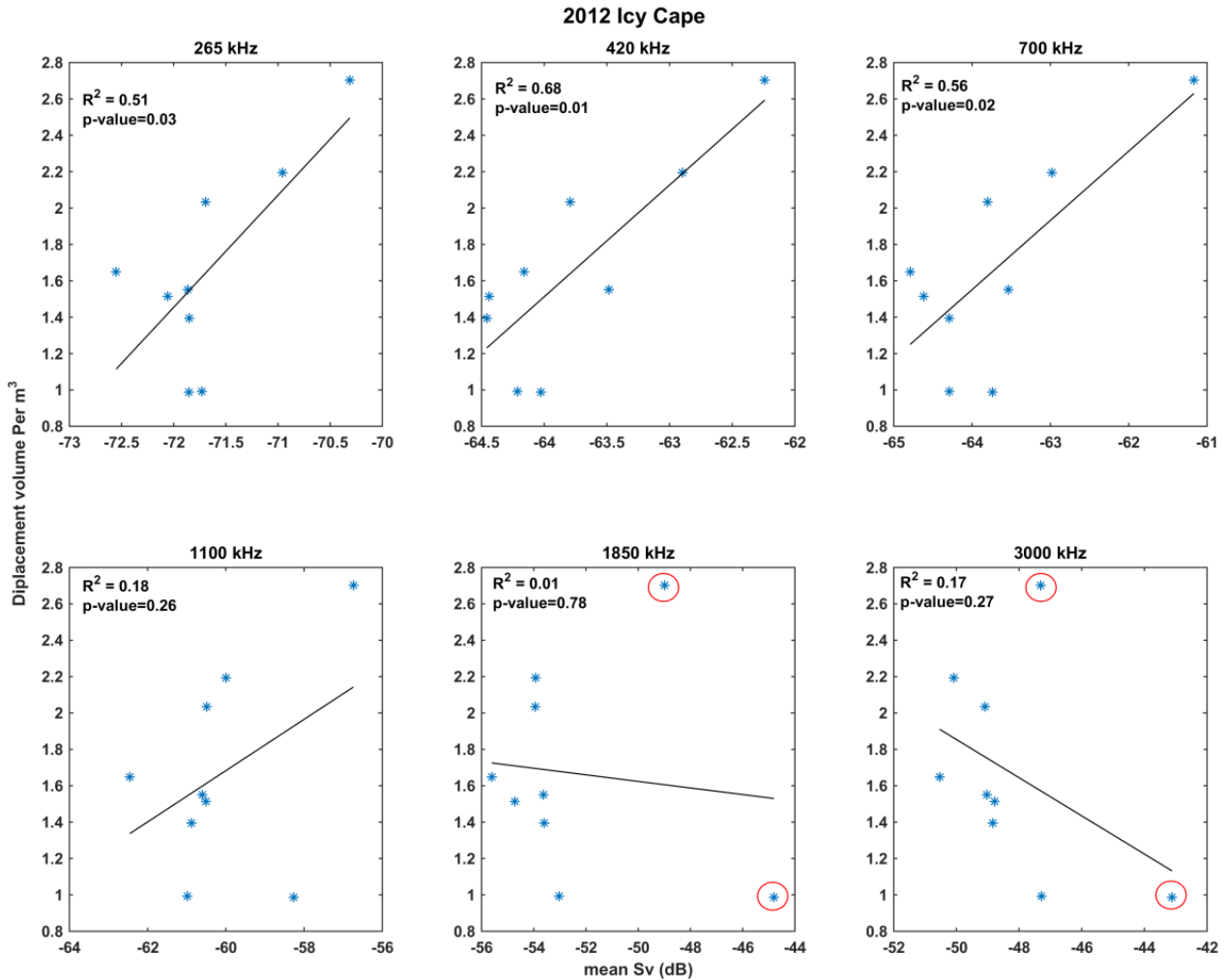


FIGURE 94. RELATIONSHIP BETWEEN ZOOPLANKTON DISPLACEMENT VOLUME AND MEAN WATER COLUMN VOLUME BACKSCATTER IN 2012 AT DIFFERENT FREQUENCIES ALONG THE ICY CAPE TRANSECT. RED CIRCLES INDICATE OUTLIERS DUE TO THE PRESENCE OF SHELLED PTEROPODS.

We used the acoustic volume backscatter at 420 kHz as a proxy or index for zooplankton biomass and contoured S_v at 420 kHz as a function of depth along the Transect D (Icy Cape) for each year. The daytime sections of acoustically estimated zooplankton biovolume were plotted along with temperature and salinity (Figure 95-97). In 2010 and 2011, the highest volume backscatter was observed within 10-15 m of the bottom where the coldest, most saline waters were found.

In 2012, high values of volume backscatter were found in the pycnocline (Figure 97). The pycnocline was strongest that year along this transect and zooplankton values decreased inshore of a front that separated stratified and well mixed waters. Inshore values of volume backscatter in 2010 and 2011 tended to be lower than other parts of the transect, although the structure of the water column in those years was very different. In 2010 and 2011, the thickness of the bottom layer of zooplankton between 80 and 150 km from the transect origin was greater than it was during 2012.

2010 Icy Cape TAPS-6

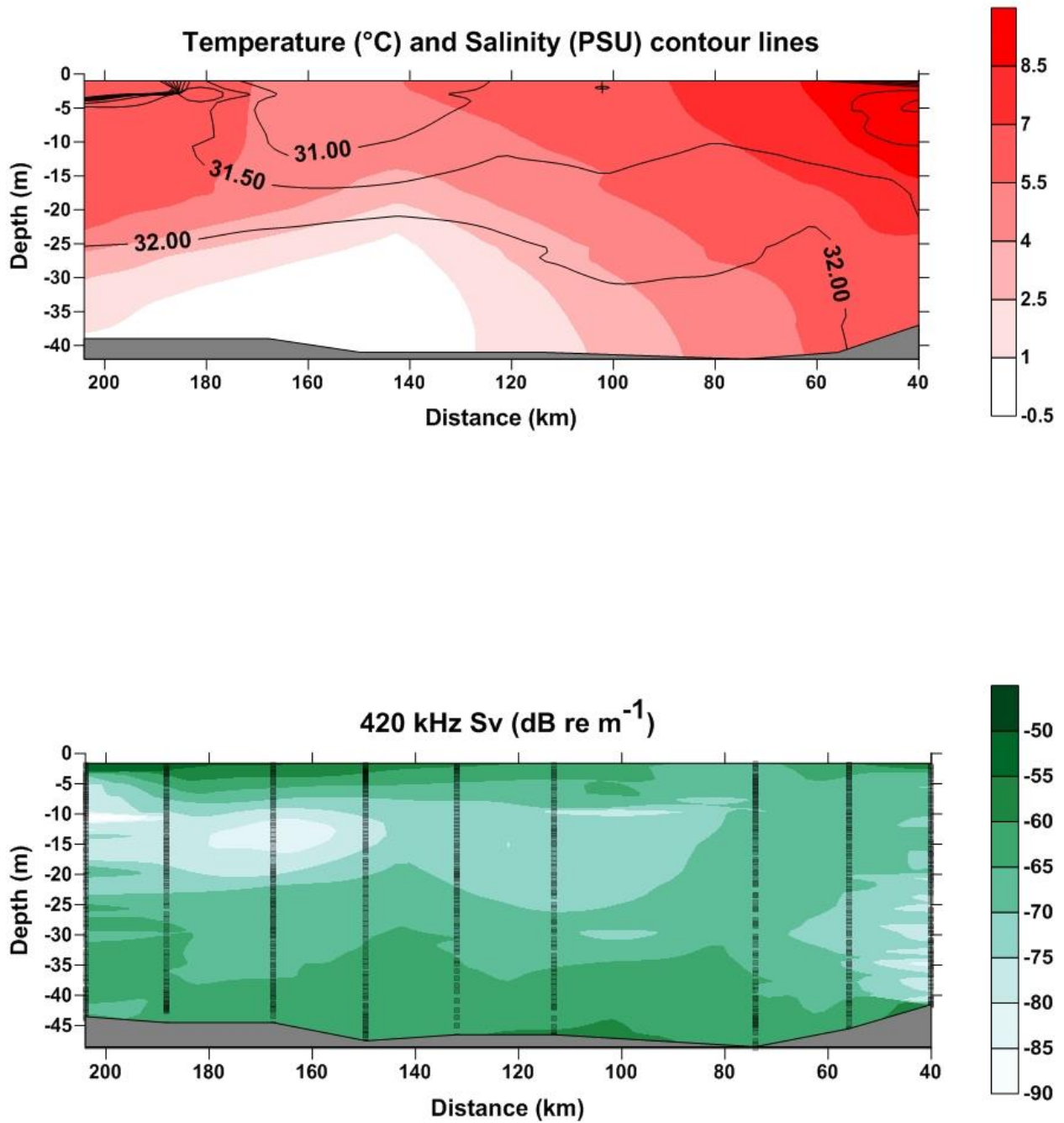


FIGURE 95. ICY CAPE 2010 TRANSECT SECTIONS OF PHYSICAL PROPERTIES AND ZOOPLANKTON. DISTANCE (KM) FROM SHORE. TOP – TEMPERATURE (°C, COLOR CONTOURS) AND SALINITY (PSU, LINE CONTOURS); BOTTOM – ZOOPLANKTON VOLUME BACKSCATTER (Sv).

2011 Icy Cape TAPS-6

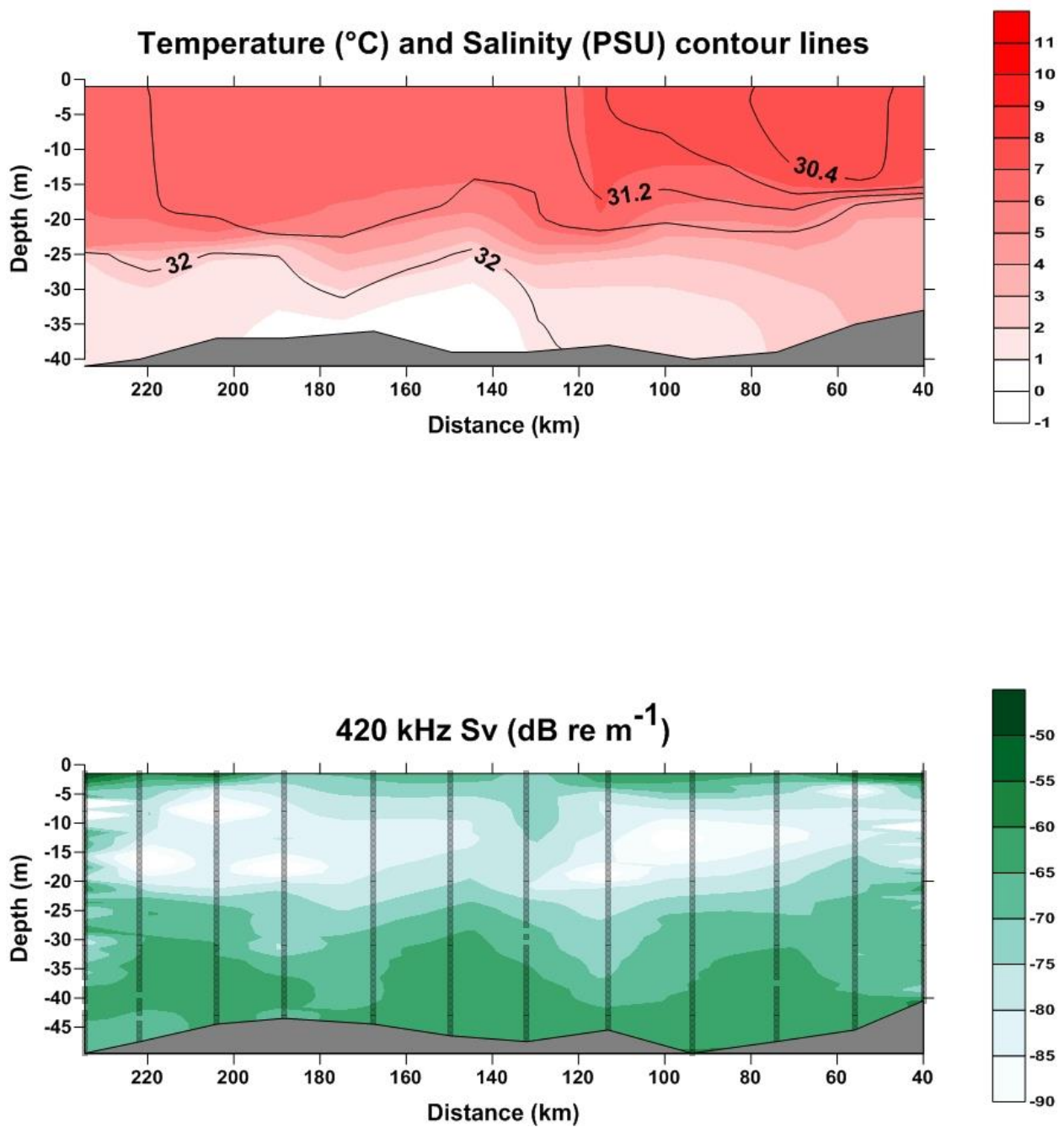


FIGURE 96. ICY CAPE 2011 TRANSECT SECTIONS OF PHYSICAL PROPERTIES AND ZOOPLANKTON. DISTANCE (KM) FROM SHORE. TOP – TEMPERATURE (°C, COLOR CONTOURS) AND SALINITY (PSU, LINE CONTOURS); BOTTOM – ZOOPLANKTON VOLUME BACKSCATTER (S_V).

2012 Icy Cape TAPS-6

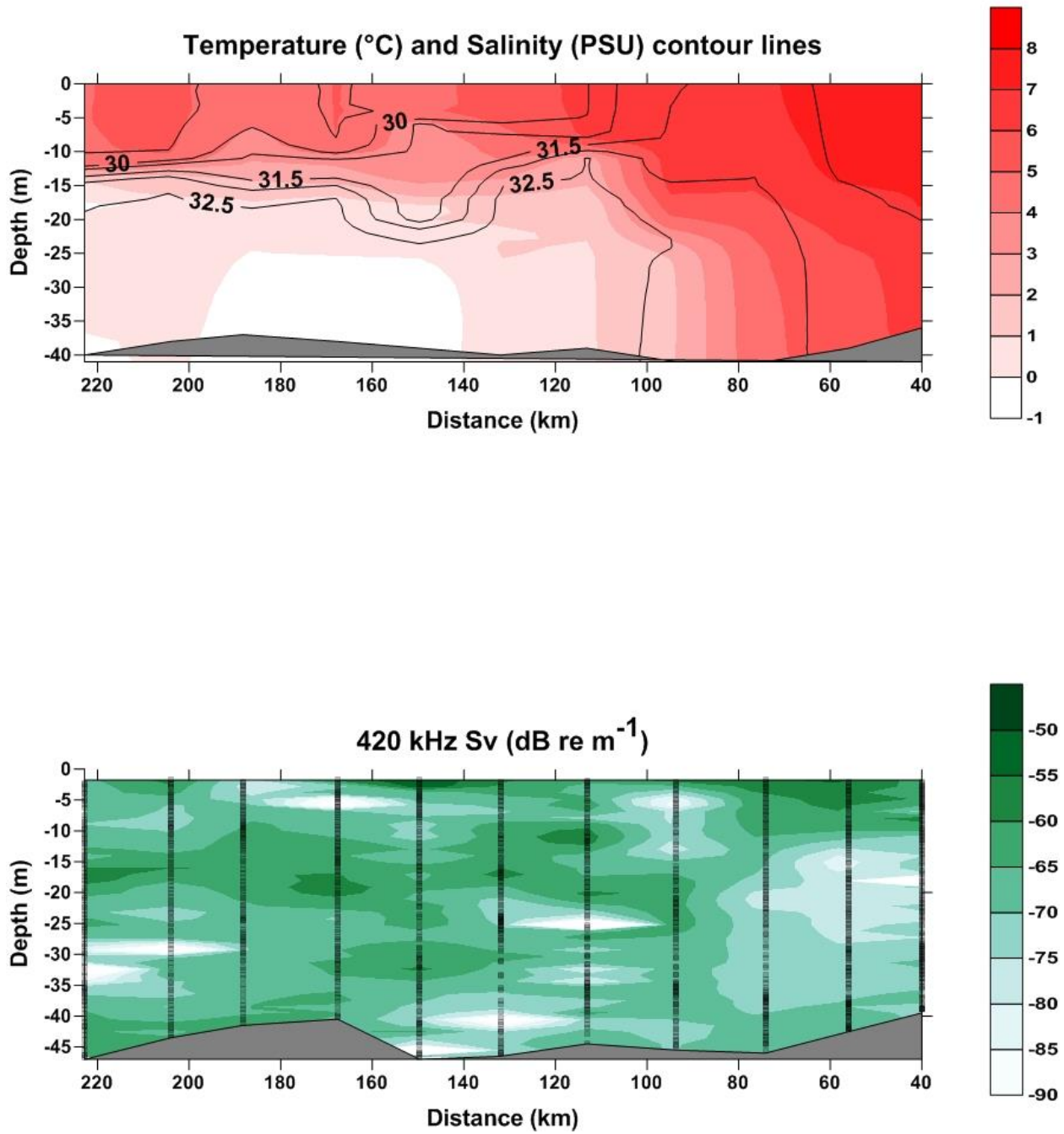


FIGURE 97. ICY CAPE 2012 TRANSECT SECTIONS OF PHYSICAL PROPERTIES AND ZOOPLANKTON. DISTANCE (KM) FROM SHORE. TOP – TEMPERATURE (°C, COLOR CONTOURS) AND SALINITY (PSU, LINE CONTOURS); BOTTOM – ZOOPLANKTON VOLUME BACKSCATTER (S_v).

3. Discussion

Our hydrographic data set with transects normal to the coast line provide new insight into the physical and chemical oceanography of the Chukchi shelf. These data and those from the moorings enable us to refine previous summaries of Chukchi shelf currents, and in particular those waters that flow over the lease area. They also allow us to quantify transport and flux of heat, salt, and nutrients during the sampling period. For example, we determined that between 30 - 50% of the transport through Bering Strait, eventually travels along the coast past Icy Cape. Variations in flow were highly correlated with the winds. With three years of data we can begin to look at variability across the shelf; however, more years of data will be necessary to fully capture the inherent variability in the system. The years 2010-2011 had stronger flow, more polynyas, more incidents of flow up Barrow Canyon, than were observed in 2011-2012 and 2012-2013. Hydrographic data also revealed that Atlantic water can be seen as far south and west as Icy Cape, indicating that slope water can intrude > 200 km onto the shallow Chukchi shelf. The Atlantic water was the source of the *C. hyperboreus* present only in 2011. Of particular interest from the hydrographic data were the pools of nutrient-rich waters often found offshore in the Bering Shelf waters and other non-Alaska Coastal Current waters. High ammonium concentrations between Pt. Hope and Barrow Canyon indicate the effects of active remineralization and regeneration of nutrients in the cold Arctic. Subsurface maxima of chlorophyll fluorescence were common during the late summer cruises. It was not determined whether or not these regions were due to higher fluorescence per cell (photo-adaptation) or if there was increased phytoplankton biomass there. However these regions were sometimes associated with high percent saturation of oxygen. In those cases it is presumed that the cells were actively photosynthesizing and contributing to the total primary production. Sinking cells from this subsurface region would continue to seed the benthos and add carbon to support secondary production.

Zooplankton Net Data

The Tucker Sled data showed great interannual and spatial variability. The hydrography (temperature, salinity, and location of different water masses) varied among years and the zooplankton distributions may reflect this to a large degree. Our data also provided insight into “event-scale” phenomena. For example, the warmest year, 2010, had low, but detectable concentrations of an early developmental stage of euphausiids, indicating reproduction over the Chukchi Sea shelf. Previous work hypothesized that euphausiids in the Chukchi are expatriate populations that do not reproduce. Similarly, the presence of low, but detectable concentrations of *C. hyperboreus*, an arctic basin species, are indicative of a major advective event that delivered water and organisms onto the Chukchi shelf. The documented variability in zooplankton community indicates that the arctic strongly responds to those forces that drive the summer physics, chemistry, and biology of this region.

The lack of high concentrations of juvenile and adult euphausiids away from Barrow canyon is puzzling. Bowhead and other baleen whales transit through this region in spring and fall, and our expectation was that we would find concentrations of euphausiids over the continental shelf. While the concentrating mechanism around Barrow Canyon is now well described (Ashjian et al., 2010), previous authors hypothesized that there was a “conveyor belt”

of euphausiids that originated in the Bering Sea and were transported into the Chukchi Sea (Berline et al., 2008). Net-based estimates are known to underestimate actual euphausiid abundance due to avoidance of the sampler (e.g., Clutter and Anraku, 1968; Sameoto et al., 1993). Although we did not include a light to “blind” the targets, we did tow our nets on the bottom in anticipation that euphausiids would be hard on bottom as observed in the eastern Bering Sea (Napp, unpublished data). While many of the taxa we captured had abundances on bottom that were greater than or equal to water column abundance, there was no clear evidence of a euphausiid conveyor belt.

Comparison of Zooplankton Estimates From the Tucker Net and a TAPS-6

This exercise was a valuable test to see what, if any, information the older TAPS-6 units could provide on plankton abundance, biovolume, and size distribution in an Arctic environment. The older TAPS-6 instruments were designed with relatively high acoustic frequencies and low sample volume for vertical casts or moored deployment in regions where scattering was dominated by relatively small (down to 1 mm ESR), highly abundant, taxa like copepods. In our use of the instrument, the inverse-modeling analytical approach using two or three, simple scattering models (copepod, euphausiid, and pteropod) did not provide estimates of taxon-specific plankton abundance that closely approximated net caught plankton abundance. We attribute this to multiple factors: 1. the complexity of the zooplankton community that includes high abundances of organisms such as shelled molluscs, appendicularia, and chaetognaths that are difficult to model; 2. the potential contribution of marine snow; 3. the instrument configuration which averages multiple pings and saves the average value rather than the raw pings; 4. lack of true noise measurements. Comparison of the TAPS-estimated biovolume with net-captured biomass was not possible because we lacked wet weight information on the species retained by the net.

There was, however, good agreement between the number of organisms captured by the net and the S_v at 420 kHz ($R^2 = 74$; 0.68). Although the water column is shallow throughout most of the Chukchi shelf (30-40 m) there is physical structure to the water column with the interleaving of different water masses. The structure was different among years with 2012 showing the highest degree of stratification. Zooplankton can recognize the differing temperatures and salinities of these water masses and may align themselves according to their preferences. Thus, in the absence of other information, using the S_v at 420 kHz may provide insight into the vertical distribution of the zooplankton community, in general, in ways that could not be observed with the Tucker sled where a single sample is collected over the entire water column.

4. Conclusions

There was no evidence of Bering Sea Water or Anadyr Water along Cape Lisburne (Transect B), but some evidence of it at the seaward edge of Point Lay and Icy Cape (Transects C & D). The greatest interannual variability was along the Wainwright line (Transect E). Subsurface (sub-pycnocline) blooms of phytoplankton were common, but the waters were not always supersaturated. Oxygen saturations are likely confounded by rates of primary production, respiration, vertical mixing, and warming of the water column. During the time of our surveys,

the surface was largely depleted of nutrients along all lines. Ammonium concentrations along the bottom were often $>2 \mu\text{M}$. Ammonium is the result of decomposition of organic matter, and is the preferred nitrogen source (over nitrate) for some phytoplankton. It can also be converted into nitrate through nitrification (ammonium \rightarrow nitrite \rightarrow nitrate). Nitrite as an intermediary product is usually found at low concentrations, as is observed in this data set.

At the Point Hope transect line (Transect A; which is the same as the Distributed Biological Observatory [DBO] Line 3) the high concentrations of ammonium could be regionally formed or advected from the Bering Sea where high ($>6 \mu\text{M}$) concentrations are observed during summer and fall. Further investigation is necessary to examine timing of the bloom, rates of ammonification and regional advection to quantify the sources of ammonium. Vertical stratification along this line was strongest in 2010, primarily due to lower surface salinities in 2010. Farther north on the Chukchi plateau at lines C and D, the ACC appeared to be more confined in a narrow band along the coast. The biggest difference between the years was at Lines E and F. In 2012, intrusions of high silicate and nitrate were observed on the western Barrow Canyon and the shelf west of the canyon. We hypothesize that this is slope water intruding up the canyon and onto the shelf, perhaps a result of upwelling; perhaps affecting the ACC as well.

Zooplankton community composition showed great variability among years, as well as evidence for physical events such as advection, which introduced Arctic basin species to the shelf. Net-based estimates of juvenile and adult euphausiid concentrations were low and did not yield evidence for the conveyor belt hypothesis. Concentrations of the furcilia stage were much higher, and in 2010 and 2011 were present at all stations across the shelf. In warm years with low summer areal ice extent, euphausiids may reproduce. However, the fate of those progeny is not known, and the question of endemic versus expatriate populations still exists. Finally, both net and acoustic estimates indicated that zooplankton concentrations are often as high or higher near the bottom than they are in the rest of the water column on the Chukchi shelf in summer.

5. *Recommendations*

It is important to utilize new and varied technologies to better sample this remote and difficult region. These include towed vehicles, and autonomous and semi-autonomous vehicles such as wave gliders and profiling gliders. The use of multiple-frequency, hull mounted acoustic transducers during spring and summer would help us to better map distribution and biomass of euphausiids (e.g., De Robertis et al., 2010; Ressler et al., 2012). At the end of ARCWEST, when we have additional years of zooplankton data, we should use multi-variate statistical analyses to examine variability in zooplankton community composition and the relationship among different taxa and the water masses present at the time of sampling. Further investigation is necessary to examine timing of the phytoplankton blooms, rates of ammonification, and regional advection to quantify the sources of ammonium

IX. CLIMATE MODELING

1. *Methods*

The speed of changes in Arctic sea ice cover in the last decade were unexpected, as the consensus of the climate research community just a few years ago was that such changes would not be seen for another thirty years. The modeling component of this project aims to provide projections of future sea ice and ocean conditions in the Chukchi Sea based on coupled climate models. There are two parts to the climate modeling aspect in this study.

The first part is climate models assessment. Models that contributed to the Coupled Model Intercomparison Project, Phase 5 (CMIP5) were used in this study. We obtained all available sea ice concentration simulations from the Program for Climate Model Diagnosis and Intercomparison (PCMDI) at the Lawrence Livermore National Laboratory. Model simulations of historical sea ice extent were used for assessment purposes. We compared the climatological mean and the magnitude of the seasonal cycle of the Arctic sea ice extent with observations following Wang and Overland (2009, 2012). Models that passed both criteria were further evaluated for the Chukchi Sea region, and used for future projections. Projections under two emission scenarios, named Representative Concentration Pathways (RCP4.5 and RCP8.5) are used for future projections. These represent low and high emission scenarios, respectively. The reason we did not include the RCP6.0 in the ensemble discussion is because not all the models submitted their RCP6.0 simulations, and we wanted to keep the number of models consistent.

The second part is to study the impact of changing initial sea ice conditions to the future projections. One of the better CMIP5 models, the National Center for Atmospheric Research (NCAR) CESM1.0 (a newer version of CCSM4) was used in this part of the study. From CCSM4 (RCP6.0) future runs, we selected one September with low sea ice extent in the Arctic resembling the lowest value observed (4.23 million km² in model) in recent years. Taking this as current sea ice condition (year 2011), we then re-ran CESM1 for another 30 years under the RCP6.0 emission scenario starting from Sept. 1, 6, and 11, 2011, respectively. One of the reasons to choose the RCP6.0 scenario is because this is a medium emission scenario. The new 30-year CESM runs (2010-2040) represent projections of the ice conditions after the new record low was reached.

2. *Results*

Based on our careful evaluations, we found that all of the selected 12 CMIP5 models are doing decent jobs in terms of simulating the sea ice cover over the Chukchi Sea (Wang and Overland, 2015). According to these 12 models, the length of open water duration will be prolonged over the entire Chukchi Sea, under the RCP8.5 emission scenario, although there is an evident north-south gradient. As shown in Figure 98, the shading indicates the number of months with sea ice present at each grid point within a calendar year averaged over the 12 selected models. A grid box is considered to be ice-covered when its sea ice concentration is more than 15%, following normal convention. In the past decade (2004 – 2013) north of 75° N, there were 12 months of ice cover at almost all grid points in the Alaskan Arctic based on Hadley

sea ice analysis (<http://www.metoffice.gov.uk/hadobs/hadisst/data/download.html>). Near the Bering Strait, the average sea ice cover lasted about 7 months/year in the last decade. The mean sea ice durations for the decade centered on 2010 from the selected 12 climate models (all interpolated to the same $0.5^\circ \times 1^\circ$ resolution latitude-longitude grid; Figure 98), show similar structure compared with observations (i.e., the overall feature of ice presence is well captured by these models). As time progresses, the changes from 2010 to 2020 are small in the Alaskan Arctic, except near the coast in the Beaufort Sea and in the east Siberian Sea under the RCP8.5 (high) emission scenarios. From 2030 to 2040, the change is obvious with most of the northern Chukchi Sea and the Beaufort Sea having 11 months of ice coverage instead of 12 (Figure 98). By the decade centered in 2050, the northern Chukchi Sea and the Beaufort Sea would have ice presence only up to 10 months (Figure 98). This implies that the northern Chukchi Sea (near latitude 80° N) would shift from current year-round sea ice cover to seasonal open water of 1-2 months. An acceleration of ice reduction can be inferred from these plots in the middle of the 21st century. In the southern Chukchi Sea, north of the Bering Strait to 70° N, sea ice cover will be reduced from eight to nine months coverage at present to five to six months of coverage by 2040 (Figure 98), i.e., more than half a year of open water as predicted by these models.

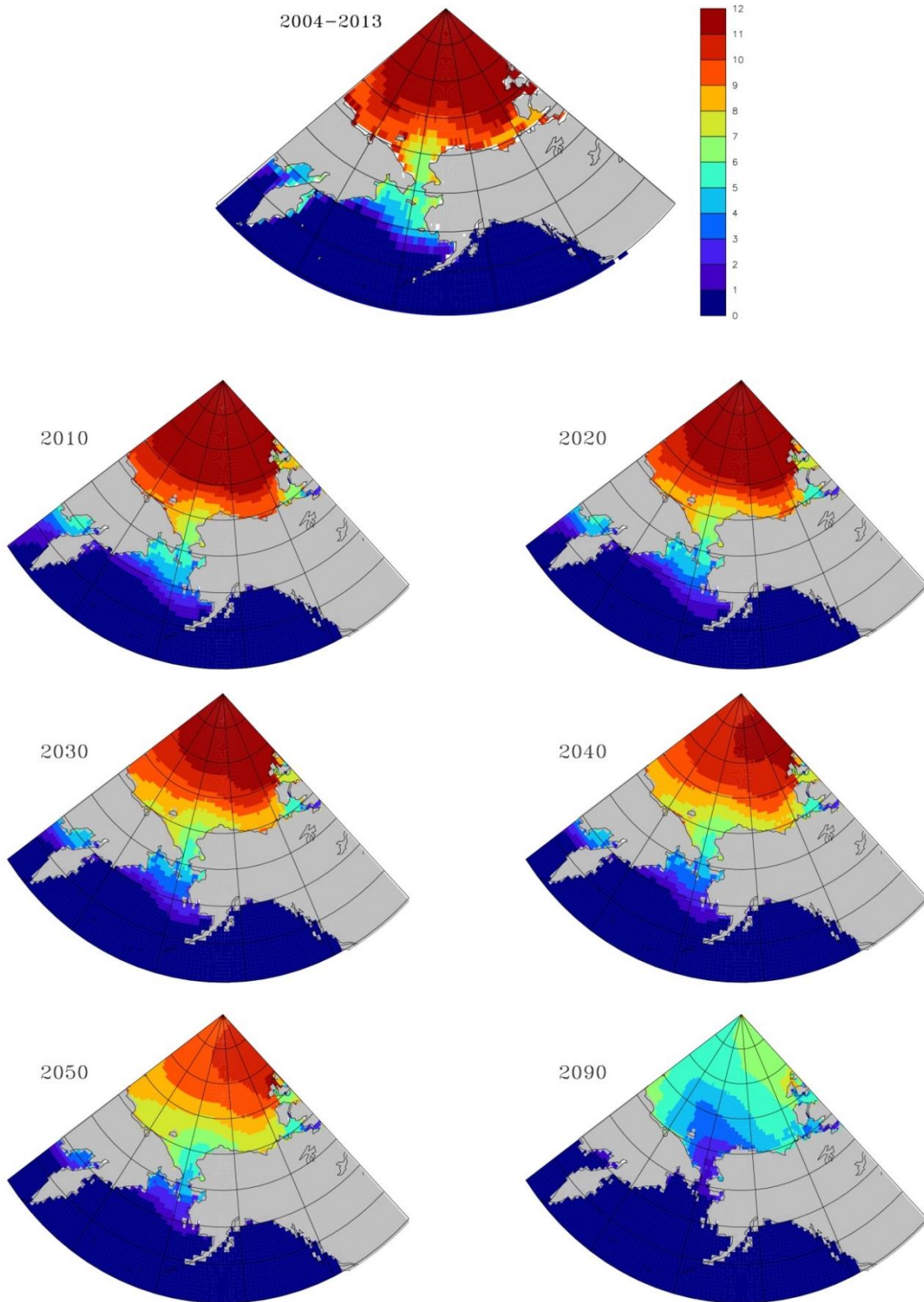


FIGURE 98. DURATION OF ICE COVER AT EACH GRID POINT BASED ON HADLEY SEA ICE ANALYSIS (TOP PANEL) AND MODEL SIMULATIONS FOR PRESENT (2010) AND FUTURE UNDER RCP8.5 EMISSION SCENARIOS (REMAINING PANELS). RESULTS ARE SMOOTHED WITH A 9-YR MEAN WITH THE LABELED YEAR INDICATING THE CENTER OF THE DECADE. MODEL RESULTS ARE BASED ON THE ENSEMBLE MEANS OF THE 12 SELECTED MODELS.

The change in the north-south gradients of the open water duration can be clearly seen from Figure 99, which shows the zonally averaged length of open water duration at each latitude. Currently there are 0-4 months of open water duration in the Chukchi Sea. As time progresses, the difference between the north and south will reduce, and the entire Chukchi Sea will have more than 7 months of open water by the end of the 21st century. Around the 2040s, we may see one month of open water in the northern Chukchi Sea by 80° N, where there is none at present. Similarly, there is one more month of open water duration in the Chukchi Sea from north to south at other latitudes.

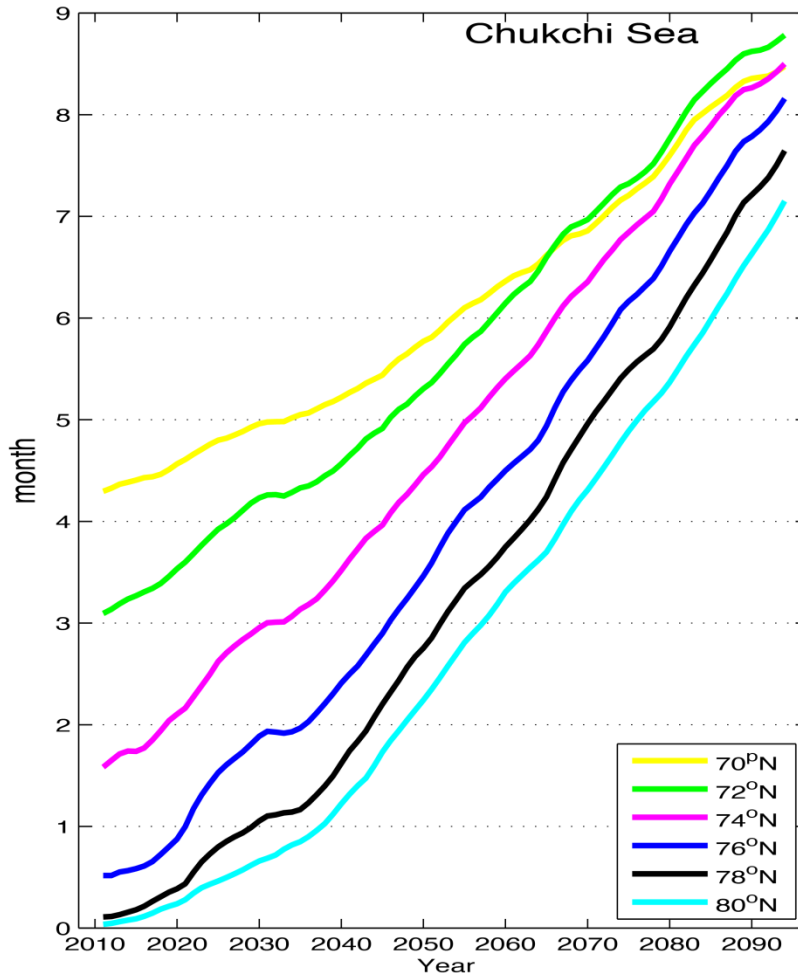


FIGURE 99. TIME SERIES OF ZONALLY AVERAGED NUMBER OF SEA ICE-FREE MONTHS OVER THE CHUKCHI SEA BASED ON THE 12 MODELS' PROJECTIONS UNDER EMISSION SCENARIO RCP8.5.

Figure 100 shows the historical and future projected monthly sea ice extent time series averaged over the Chukchi Sea (bounded by 65° - 80° N, and 175° E - 157° W). As shown in the historical time series, the Chukchi Sea is now completely covered by sea ice for nearly seven months of the year, from December to June. Sea ice starts to retreat in June, though more than 90% of the Chukchi Sea is still covered by sea ice during that month. This retreat progresses slowly, and by August, the ice cover can still be as much as 60% of the Chukchi Sea (except in 2007, which had record low ice cover). The mean sea ice cover in September has had a large

reduction in recent years (2007-2012), with some recovery in 2013 (Figure 100; the black curve in right panel of 3rd row). In recent years, there has been ice cover only up to 21% of its climatological mean of 0.60 million km². As a result, the following October also shows ice reduction in recent years, as severe as September. The Chukchi Sea was nearly ice free during September 2007 and 2012 in the observed sea ice extents, but the recovery in October 2012 was faster than 2007. Some of the individual runs from these 12 models seem to catch this kind of sudden drop. Since what actually happened is only one single realization of the model, we should not expect the ensemble mean to represent the observed time-series. At the beginning of the 21st century, the slope of the ensemble mean (red and blue) is relatively flat, but it shows increased decline near the middle of the 21st century. Near the end of the 21st century, a clear departure between the ensemble mean of the selected 12 models (red/blue) and the mean of all members of 37 models (magenta/green) is seen. The selected models show faster decline under both emission scenarios (red for RCP8.5 and blue for RCP4.5).

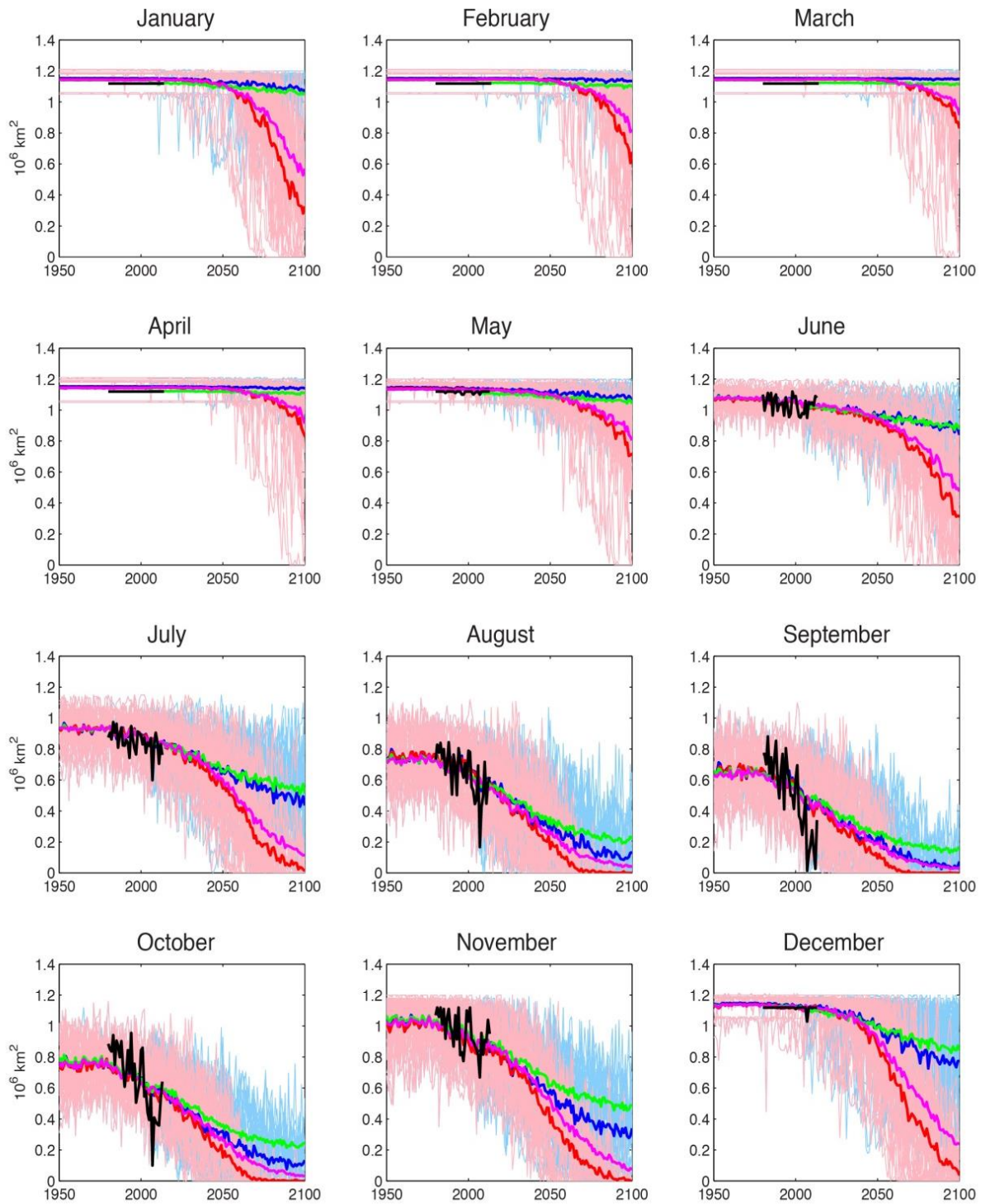


FIGURE 100. TIME SERIES OF MONTHLY SEA ICE EXTENT FOR THE CHUKCHI SEA (65° - 80° N, AND 175° E - 157° W). THE THIN COLORED CURVES ARE COMBINATIONS OF HISTORICAL RUNS AND PROJECTIONS UNDER EMISSION SCENARIOS RCP4.5 (LIGHT BLUE), AND RCP8.5 (PINK). THE SOLID BLACK CURVES ARE BASED ON THE HADLEY SEA ICE ANALYSIS, HADISST_ICE. THE THICK SOLID RED/MAGENTA CURVES ARE THE ENSEMBLE MEANS OF THE SELECTED 12 MODELS (ALL MODELS) UNDER EMISSIONS SCENARIOS RCP8.5, AND THE SOLID BLUE/GREEN CURVES ARE CORRESPONDING MEANS UNDER EMISSIONS SCENARIO RCP4.5.

The CCSM4 (slightly older version of CESM1.0) sea ice simulation shows some improvement compared to its precursor, CCSM3 (part of CMIP3), as we found at the beginning of the project. This is rather encouraging. By the time we were ready to execute our own simulations with the computational support obtained from the NCAR super computer, NCAR had upgraded their model to CESM version 1.0 and removed the support of CCSM4. We therefore did our simulations using the most updated version, CESM1.0. Three runs were carried out and each lasted 30 years under the emission scenarios RCP6.0. Even though we started with low sea ice cover at the beginning of the simulation (September 2010), soon there were no differences between our runs (blue dashed lines) and the original CCSM4 runs (purple lines) as shown in the ice thickness time series in Figure 101. This indicates that ice can rebound from an extremely low condition within a year. However, as several studies have pointed out, in the past decade, we have been losing thick, multi-year sea ice in the Arctic (Kwok et al., 2009; Kwok and Untersteiner, 2011). In other words, the quality of the ice has been reduced. Although the overall ice thickness has been reduced, the projected ice thickness in the small region around the mooring locations seems to be relatively stable as projected by CESM1, shown in Figure 101. In order to validate the model results, ice thickness obtained from C1-C3 moorings deployed in the Chukchi Sea (C1: 70.8°N, 163.2°W, C2: 71.2°N, 164.2°W, and C3: 71.8°N, 166.0°W) are also plotted in Figure 101 for a comparison. By converting ice draft observed to ice thickness (colored squares/circles in Figure 101), we found that the CESM1.0 model actually simulated the ice thickness reasonably well (Figure 101). Model simulations indicate that there is quite large interannual variability of ice thickness in the Chukchi Sea. At the beginning of ice formation, the averaged ice is less than a half-meter thick (December), and ice gradually grows to 0.5-1 m thick in January. From February to June the average ice thickness is between 1-2 m thick with relatively large interannual variability. There is no significant trend in the next 20-30 years according the CESM under RCP6.0 emission scenario.

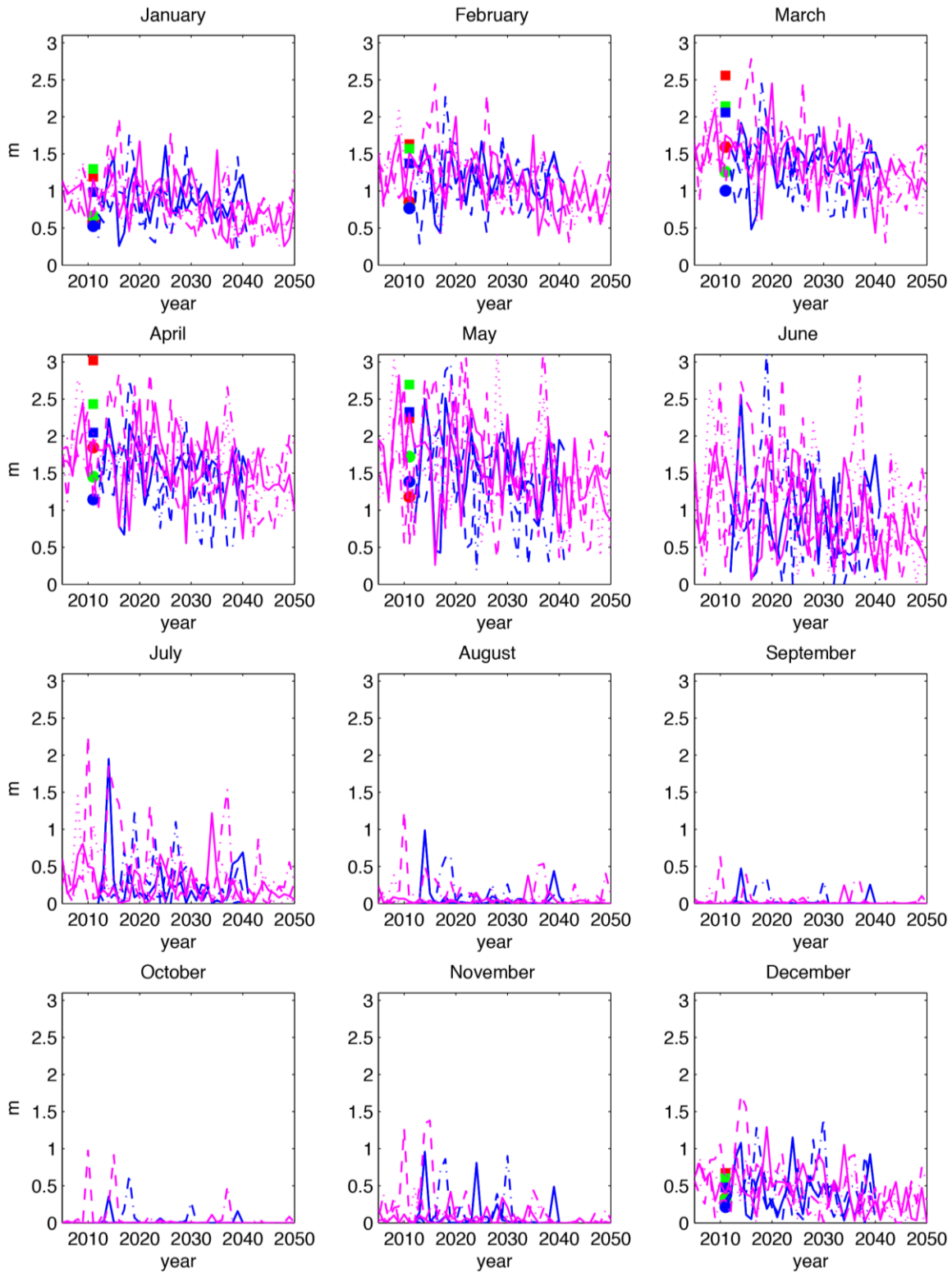


FIGURE 101. CESM1.0 SIMULATED MONTHLY ICE THICKNESS AVERAGED OVER A SMALL BOX AROUND THE MOORINGS IN THE CHUKCHI SEA. COLORED CIRCLES ARE OBSERVED MEDIAN ICE THICKNESS AND COLORED SQUARES ARE OBSERVED MEAN ICE THICKNESS AT THE 3 CHUKCHI SEA MOORINGS (C3-OFFSHORE, BLUE; C2-MIDSHORE, GREEN; AND C1-INSHORE, RED).

Besides sea ice conditions, we also investigated the ocean conditions simulated by CESM1.0, and the results are very encouraging. Figure 102 shows the spatial distribution of annual mean ocean currents simulated by the model. The broad features of the northward flow through the Bering Strait, as well as the splits of the currents into the Chukchi Sea are clearly seen from Figure 102.

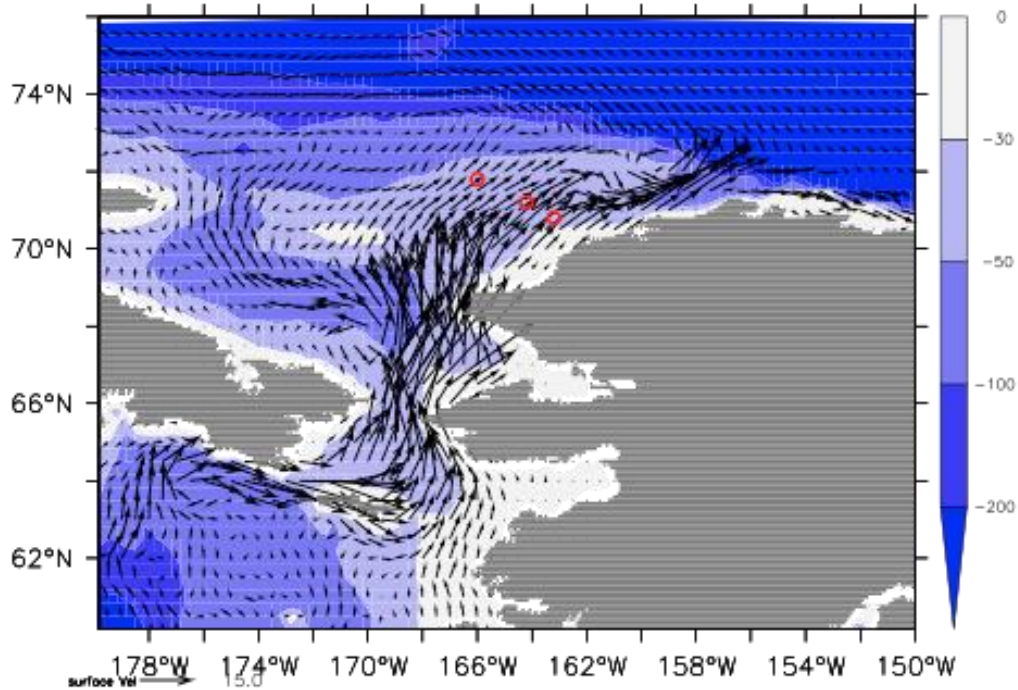


FIGURE 102. ANNUAL MEAN OCEAN CURRENT SIMULATED BY CESM. RED CIRCLES ARE THE C1-INSHORE, C2-MIDSHORE, AND C3-OFFSHORE MOORING LOCATIONS.

The monthly mean ocean currents at 30 m depth agree well with observations as shown in Figure 103. The closest points of the model simulated ocean currents are chosen to be compared with those observed at the three mooring locations. Apparently, both the directions and the magnitude of ocean currents are well captured by the model runs.

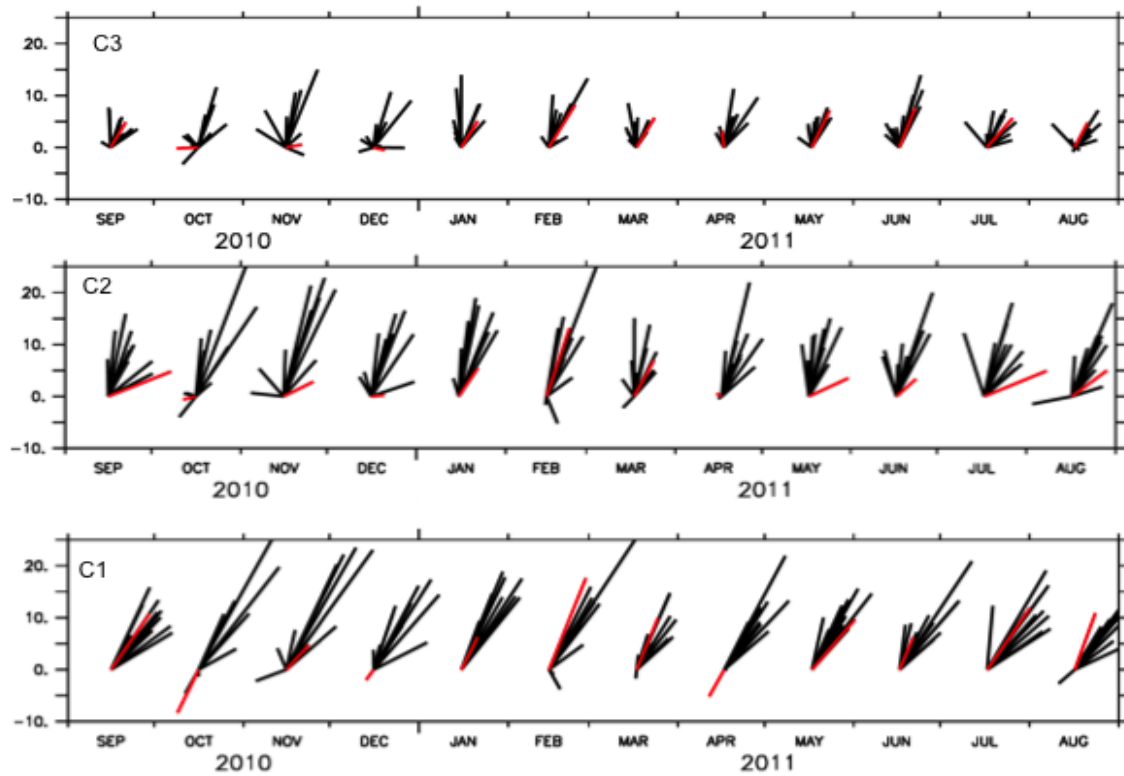


FIGURE 103. OCEAN CURRENT AT 30 M DEPTH FROM OBSERVATION (RED) AND MODEL SIMULATION (BLACK). EACH BLACK STICK REPRESENTS 1-YR SIMULATION FROM THE FIRST DECADE RUN (2010-2020). TOP PANEL CORRESPONDS WITH THE C3-OFFSHORE; C2-MIDSHORE; C1-INSHORE MOORINGS.

The ocean temperature and salinity from the CESM1 model runs and those observed at moorings were also compared. Figure 104 shows that the model captures the seasonal variation of the ocean temperature well, especially at the C3 mooring (top left panel of Figure 104). Close to shore, the temperature variations are also captured well by the model runs, but the summer temperature is higher than the observed (left middle panel). Models seem to show larger temperature gradients in the spring and fall seasons compared with the observations. As for the salinity, the model results are less satisfactory. The model underestimates the salinity values year round at all three mooring locations (right panels of Figure 104), and the twin peak feature of the seasonal salinity variation is missed by the model runs. Yet, the model is able to capture the May salinity peak even though the value is still less than the observations.

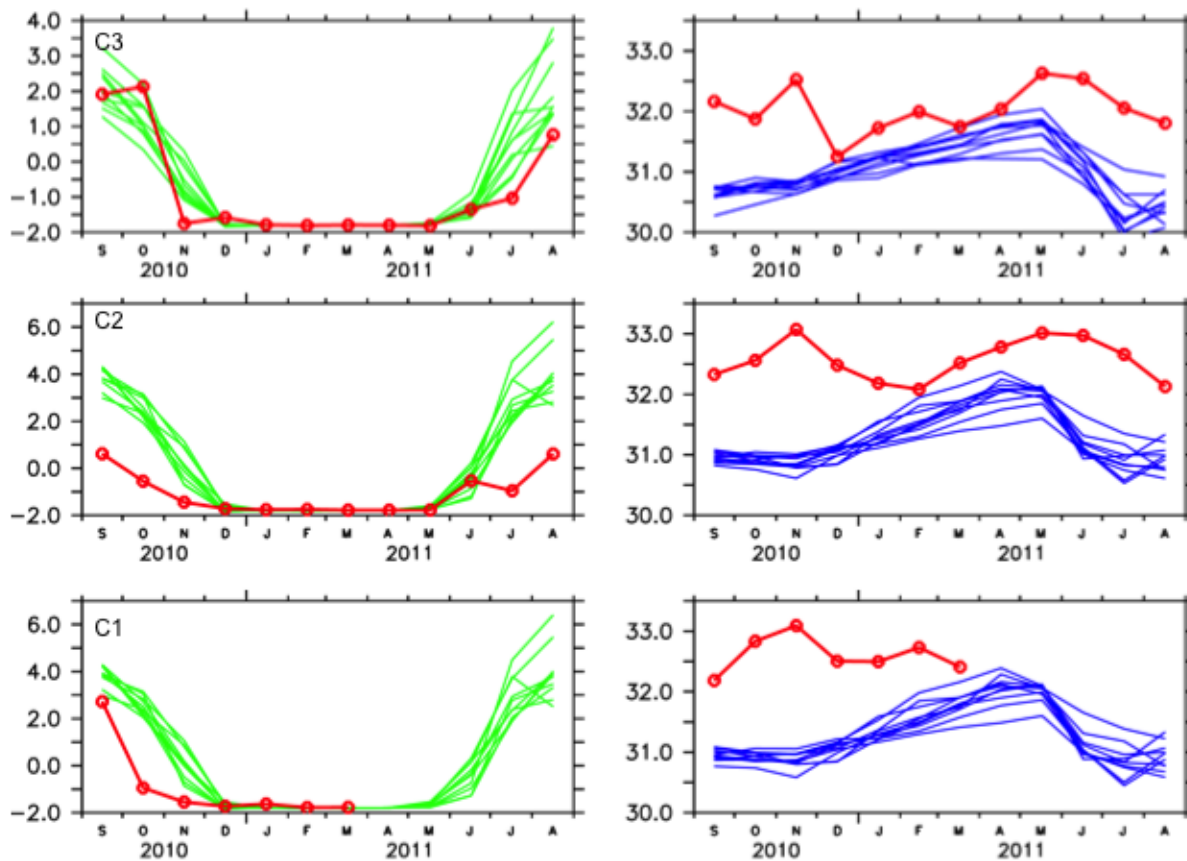


FIGURE 104. OCEAN TEMPERATURE (LEFT; °C) AND SALINITY (RIGHT; PSU) AT 40 M DEPTH FROM OBSERVATION (RED) AND MODEL SIMULATION (GREEN/BLUE) AT THE C3-OFFSHORE MOORING (TOP); C2-MIDSHORE MOORING (MIDDLE); AND C1-INSHORE MOORING (BOTTOM).

3. Discussion

Over the past decade there has been rapid decline of Arctic sea ice cover, yet the largest changes happened in the Alaskan Arctic, i.e., the Chukchi Sea and the Beaufort Sea (Wang and Overland, 2015). The reduced sea ice cover will impact not only the climate system, but also the components of the ecosystem in the region, and people who live along its shores. Climate model simulations show that there will be reduced ice cover, particularly in the fall season in the southern Chukchi Sea. This is consistent with the model projected ocean temperature changes in the next 20 years, shown in Figure 105. Generally speaking, the ocean temperature in the 2020s (magenta dashed lines; left panels) will be higher than that in the 2010s (green solid lines; left panels, Figure 105). As discussed earlier, the CESM1 model generally captures the seasonal cycle of the ocean temperature changes at the three moorings (C1-C3) near Icy Cape. Yet it shows that the temperature in the second decade is slightly higher, although there is quite large interannual variability. As for the salinity (right panels of Figure 105), there are no obvious changes from the 2010s to 2020s as all the magenta lines and green lines overlaid each other. We also found that the direction and magnitude of ocean currents will stay about the same at

these locations (figure is not shown) compared to present day. Large interannual variability dominates the flow in the region.

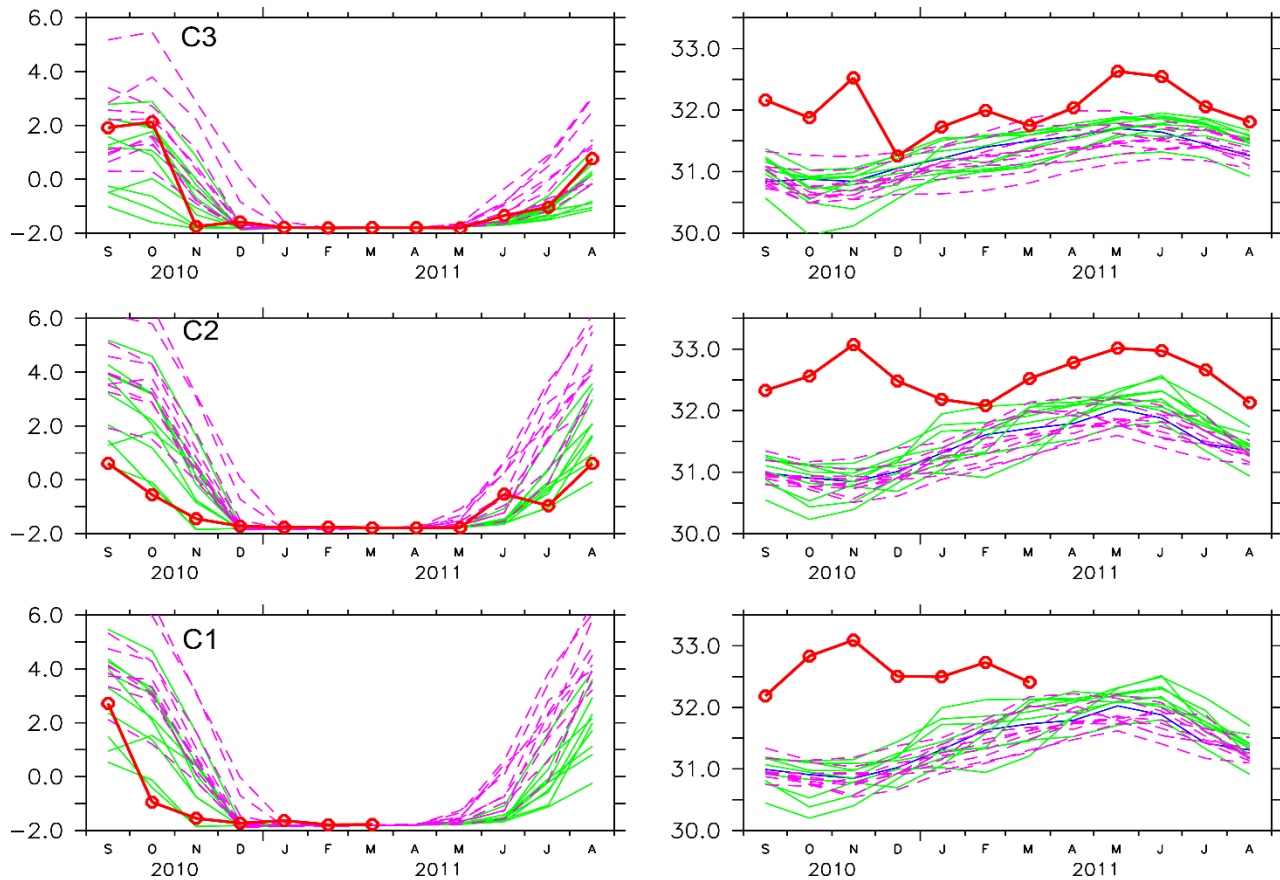


FIGURE 105. MODEL SIMULATED OCEAN TEMPERATURE (LEFT; °C) AND SALINITY (PSU; RIGHT) IN CURRENT DECADE, 2010-2019 (GREEN) AND NEAR FUTURE, 2020-2029 (MAGENTA) BASED ON CESM1 UNDER EMISSION SCENARIO RCP6.0. SOLID RED LINES ARE OBSERVED VALUES OBTAINED FROM ICY CAPE MOORINGS: TOP = C3-OFFSHORE, MIDDLE = C2-MIDSHORE, BOTTOM = C1-INSHORE.

4. Conclusions

We discovered that the anthropogenic forcing is more important than the initial conditions on the decadal scales. The sea ice extent declines fast in the fall (August to November) and will continue to decline in the future as simulated by the models. This indicates that sea ice will arrive the Southern Chukchi Sea later and later. This pattern has already been occurring in the past decade or so (Wood et al., 2015). Although the ice cover seems to be relatively stable in the spring (May-June) as shown in the ensemble means, there are episodic events of early retreat (e.g., the thin red lines in Figure 100, in June). The increasing frequency of these early retreat events will especially become evident after 2050.

There is a weak declining trend in the simulated Chukchi sea ice extent in the fall, but not in the spring in the next 20-30 years. The sea ice will remain at its current level up to 2040 in the Chukchi Sea in winter, but a larger decline in the fall is expected. The change in projected sea ice conditions is consistent with model projected ocean temperature change; that is, fall has the

largest temperature increase compared with other seasons. We may see ice form later, particularly in the southern Chukchi Sea. Based on selected CMIP5 models, the future duration of the open water season will be longer by about 1-month around the 2040s in the Chukchi Sea, and the gradients of the length of the open water season will be reduced between north and south. For the ice thickness, at any given year, the long term trend is overwritten by the large interannual variability, which is shown by our new, reduced ice cover initialized runs. We found that they are almost indistinguishable between our new CESM1 runs and CCSM4 runs. The CESM1.0 model is able to capture the ocean current well in both direction and magnitude. The ocean temperature was simulated well by CESM1, yet improvements are needed in the ocean salinity simulations, as the model missed the fall peak at all three mooring locations.

5. *Recommendations*

Models are built upon physical rules and are the only tools we have to make objective projections for the future climate state. Although not perfect, models are able to capture the main features of the ocean circulation, ocean temperature, and the sea ice cover and thickness in good agreement with observations. The ice-ocean-atmosphere is a dynamically coupled system, and we need to rely on models to help us understand the physical processes. *In situ* observations are important sources for us to validate model results, and can help us to further improve our models. We need to keep both teams working together.

X. CORRELATION OF MARINE MAMMAL DISTRIBUTION TO BIOPHYSICAL PARAMETERS

1. Methods

Moored observations

Gaussian distribution Generalized Additive Models (GAMs) were utilized to assess the effects of oceanographic conditions on marine mammal distribution and the presence of ice noise. GAMs were chosen because they are particularly well suited to multi-variate, non-normally distributed and nonparametric datasets, and because of their flexibility with non-linear relationships. Our data contain a considerable amount of zero values (especially for calling activity) making the use of GAMs a necessity. One drawback of GAMs, however, is that their interpretation is not as straightforward as that from linear models.

Analyses were run in the R programming language (R Development Core Team 2012), and the models were fitted using the *gam* function from the *mgcv* package (Wood 2006). Large differences in calling/noise activity were seen among the three mooring locations (Section: VII.A.2), indicating each location should be analyzed separately. For each of the three locations – inshore, midshore, and offshore – a GAM was fit to seven passive acoustic data results: the seasonal calling activity data for each of the five key Arctic marine mammal species, to the seasonal calling activity data specific to bowhead whale gunshot calls, and to the seasonal ice noise activity data. This resulted in 21 full GAM runs in total.

There were 32 different biophysical measurements available to include for each GAM run (XVIII.H), which would have resulted in the generation of 4.3 billion models for each of the 21 runs. To reduce this to a more practical and manageable (i.e., non-supercomputer) size, a number of assumptions and protocols were enacted to keep the process consistent and logical.

First, we eliminated the 8 TAPs measurements from the base set of runs. There was only one mooring location (midshore) where these data were collected and at that location the instruments operated for just 36 days. This TAPS6-NG data set was run separately: 36 days at midshore location for the 7 sound sources, including the following additional variables (full column and bottom for each): total zooplankton biovolume (mm^3/m^3), euphausiid abundance ($\text{No.}/\text{m}^3$), total volume backscatter (420 kHz, S_v , full column: dB re 1 ($\text{m}^2 \text{m}^{-2}$); bottom: dB re 1 m^{-1}), and total volume backscatter (50kHz, S_v , full column: dB re 1 ($\text{m}^2 \text{m}^{-2}$); bottom: dB re 1 m^{-1}). Further details on the methods, and the results are presented in Appendix H (see Section XVIII.H).

Second, we eliminated the two measurements of surface currents (u-vector and v-vector) because of the near-uniformity of the currents throughout the water column, and the strong correlation between the winds and surface currents (Stabeno et al., in prep). To ensure this assumption was valid, we completed a third set of runs replacing bottom currents with surface currents; the results of this comparison are included in Section X.2 below.

Lastly, there were two sets of variables, ice thickness and bottom oxygen levels, where the differences among the variables were just differences in measurement type, not in the variables themselves. That is, the three measures of ice thickness, for example, were directly correlated and would bias the model outcome if all three were included in the GAM runs. To

eliminate this bias, we ran a set of single-variable GAM runs for each of the location/sound source combinations. For each combination we selected the measurement type that provided the highest explanatory power for the variance in seasonal calling (or noise) activity based on the lowest AIC (Akaike's Information Criterion) value. The measurements selected for each of the 21 location/sound source combinations are listed in Table 20.

These steps reduced the number of variables to a total of 19. In addition to the ice thickness (m) and oxygen (either % saturation or mMol kg^{-1}) variables selected from Table 20, the following 17 variables (with their units in parentheses) were included: month, year, zooplankton volume backscattering [bottom- ADCP, S_v], zooplankton volume backscattering [full column-ADCP, S_v], ice concentration (%), chlorophyll ($\mu\text{g/L}$), PAR ($\text{mEin cm}^{-2}\text{s}^{-1}$), temperature ($^{\circ}\text{C}$), salinity (psu), bottom currents (u-vector, m/s), bottom currents (v-vector, m/s), transport (S_v), bottom nitrate, turbidity (FNU), winds (u-vector, m/s), winds (v-vector, m/s), and windspeed (m/s). For the u and v vectors listed above, u is in the east/west direction and v is in the north/south direction. These 19 variables resulted in the generation of a more manageable 500,000 models for each of the 21 GAM runs.

For each of the 21 GAM runs, we ranked the resulting half-million models as follows. First, we sorted the models using their AIC values (lowest to highest) and their R-squared values (highest to lowest). Then we looked at sample size used for each model (i.e., the number of days included in that model), and eliminated any that were less than 100 on the assumption that these models were not representative of the data. Finally, we chose the top AIC and top R-squared models from those remaining on these lists. These are identified in Table 21, along with their R-squared values (%) and the sample size of data used for that model. The best model for each GAM run provided the best fit to the data (AIC) *and* explained the most variance in the data (R-squared).

The differences in sample size are the result of the GAM protocol: any instance of an "NA" in the dataset (meaning data are not available for that variable for that day) led to the removal of that entire day from the GAM. Because our dataset is made up of measurements collected from multiple instruments at multiple locations with various failure dates, some models contained larger datasets than others. A caveat of our analysis is that the overlap between the passive acoustic results and the oceanographic measurements is sometimes patchy (especially at the inshore and offshore locations); as a result the top models selected may not be the best suited to explain the variability seen in the calling activity distributions, but they are the best models for these data at this time. As the BOEM-funded ARCWEST and CHAOZ-X data are added to the dataset, this patchiness will be reduced and the GAM results can then be updated. The actual time periods of data used in the top AIC model for each of the location/sound source runs are included as yellow bars in the figures included in Appendix G, Section XVIII.G.

Because of the large number of possible models for each GAM run (i.e., a half-million), we also wanted to look at what variables consistently came out on top, not necessarily just in the top AIC model. To this end, we selected the top five models from the AIC and R-squared lists (Cerchio et al., 2014), and compiled a list of variables which had P-values that were significant to < 0.01 and those that had P-values that were significant to < 0.05 . To make these lists, a variable had to show that level of significance for three or more of the top AIC models as well as three or more of the top R-squared models.

For the results that follow, we've included a table that shows both the variables that contributed to the top AIC model, color-coded by significance, and the common significant variables for that location/sound source combination (Table 22-27).

In addition to the GAMs, calling presence for each species was plotted against eight oceanographic variables (ice concentration, ice thickness fluorescence, oxygen, nitrate, salinity, wind speed, and transport) to determine any positive or negative correlations on a temporal scale. When individual variables had more than one possible measurement (e.g., ice thickness: average, median, or standard deviation), the measurement that was included in the GAM was the measurement plotted with marine mammal calling presence. Also indicated on these plots (e.g., Figure 106) are times where there were no data.

TABLE 20. MEASUREMENTS OF ICE THICKNESS AND BOTTOM OXYGEN USED IN THE GAM RUNS

	Inshore		Midshore		Offshore	
	Ice Thickness	Oxygen	Ice Thickness	Oxygen	Ice Thickness	Oxygen
Gunshot Call	Average	% Sat.	Average	% Sat.	Median	% Sat.
Bowhead	Median	% Sat.	Average	% Sat.	Average	mMol kg-1
Gray	Std. Dev.	% Sat.	Std. Dev.	% Sat.	Average	% Sat.
Walrus	Std. Dev.	mMol kg-1	Std. Dev.	mMol kg-1	Average	% Sat.
Beluga	Median	% Sat.	Std. Dev.	% Sat.	Median	mMol kg-1
Bearded	Std. Dev.	% Sat.	Average	% Sat.	Median	% Sat.
Ice Noise	Std. Dev.	mMol kg-1	Average	% Sat.	Median	mMol kg-1

Shipboard observations

Oceanographic and zooplankton results from the shipboard transect lines were correlated with the visual and passive acoustic (sonobuoy) data. Measurements of temperature, salinity, nitrate, and ammonium were plotted with zooplankton (*Pseudocalanus*, *C. glacialis*, larvaceans, and pteropods) concentration. These were then plotted with sonobuoy effort and detections as well as visual sightings for gray whales, walrus, and bearded seals. Only those transects and years where marine mammal species were detected on transect were included, thus some species may not have plots of transect line summaries (e.g., bowhead, beluga). As noted earlier, CTD data collected in 2010 were a more coarse spatial resolution than the two following years, with data collected only in the upper 30 m, and discrete samples collected at three depths: surface (1 m), 20 m, and 30 m.

2. *Results*

While the results of the GAM models were run for all three locations, the midshore data had the largest sample sizes spanning the longest timeframes, and had the most consistent R-Squared values between the top AIC and top R-Squared models for each run. Furthermore, the midshore location is positioned between the Burger and Klondike study areas, and as such is best suited for representing the area of interest for this study. Therefore, the GAM results for all locations will be listed in the tables below, but the description of these results will focus on the

midshore location unless otherwise stated; any significant differences between the three locations will be described. It is also important to note that reference to any correlations regarding the long term plots are qualitative in nature, winds were estimated from the midshore location only, and transport was averaged between the three locations.

Table 21 represents a summary of the top models (lowest AIC and greatest R-squared), their AIC and R-squared values and sample size, as well as the variables with significant (i.e. $P < 0.01$ and $P < 0.05$) values that were consistent between the top five AIC and top five R-squared models. As mentioned in the methods section above, because of the patchiness in the available passive acoustic and biophysical data sets, it is important to understand which time periods were used for the top AIC models selected by the GAMs. Plots indicating these time periods in the long-term passive acoustic data are included in Appendix G, Section XVIII.G.

The results below are organized by species/sound source. For each species/sound source we present the GAM results, followed by the long-term qualitative comparison plot, and the short-term transect line qualitative comparison plot (if applicable). Finally, the GAM results for the surface vs. bottom current comparison and TAPS6-NG-only runs are briefly described.

Bowhead whale

Table 22 presents the results of the GAM runs for bowhead whales. For all three locations, month and ice concentration were significant, with month extremely significant. At the midshore location, which had the highest sample size included in the GAM, month was significant to $p < 5.16 E^{-29}$. The common significant variables between the top AIC and top R-Squared models were chlorophyll, bottom currents (V), ice concentration, month, turbidity, and wind speed for the midshore location. The best model for the midshore GAM run included ten variables, of which chlorophyll, bottom currents (V), ice concentration, month, turbidity, and wind speed were all highly significant. It is important to note that because the GAM models exclude all days where data is missing for any variable, only certain time spans were included for each of the GAM runs. While most of the midshore bowhead calling activity data were included, the two spring peaks were excluded for both years. Only the fall migration was included for both the inshore and offshore data, a result of large gaps among oceanographic variables (See Appendix G, Section XVIII.G, for time spans included).

Bowhead whale calling activity as it relates temporally to ice, oceanographic variables, nutrients, transport, and wind speed is presented in Figure 106-108. There was a strong association with ice; calling activity would peak just before the ice concentration reached 100% and while ice thickness was less than 0.5 m. However, bowhead whale calling activity at the inshore location in the spring began when ice concentration started to decrease, even when ice thickness was still over 1 m (Figure 106). Furthermore, calling activity would also increase when polynyas formed (Figure 106). There is a strong correlation between bowhead whale calling activity and chlorophyll, most notably at the midshore location (Figure 107). There is also a strong correlation between bowhead whale calling activity and wind speeds, with high winds in fall and low winds in spring. This is most evident when bowhead whale calling activity is plotted against wind vectors for the midshore location (Figure 109). In the fall of both years, bowheads have an association with strong winds to the SSW, with the one exception of the third pulse in the fall 2010 migration.

TABLE 21. SUMMARY OF THE TOP VARIABLES, THE AIC AND % R-SQUARED VALUES, AND THE SAMPLE SIZE, FOR BOTH THE TOP AIC MODEL AND THE TOP R-SQUARED MODEL, AND THE COMMON SIGNIFICANT VARIABLES AMONG THE TOP FIVE AIC AND R-SQUARED MODELS FOR EACH SPECIES OR SIGNAL.

		Inshore	Midshore	Offshore	
Bowhead Whale	Top 1 Models	Top AIC AIC, % R ² , n	I + S + U + R + N + t + n + M + G 1664, 39.8%, 182	A + I + F + P + S + V + N + C + n + M 3926, 50.0%, 452	A + I + P + C + t + M + H + O 961, 46.8%, 103
		Top R ² AIC, % R ² , n	Q + I + F + T + U + R + C + n + M + G 1788, 56.9%, 200	Q + I + F + V + N + C + u + n + M + H + G 4283, 50.3%, 492	Q + I + T + S + U + N + u + n + M + O 1832, 74.2%, 246
	Top 5 Models: Common Vars*	Sig < 0.01 Sig < 0.05	I n M I R n M	I V C n M I F V C n M	M I M
Gunshot Call	Top 1 Models	Top AIC AIC, % R ² , n	P + N + n + G 750, 8.7%, 182	A + S + N + C + n + M 2398, 7.0%, 452	I + U + V + N + M 549, 70.0%, 247
		Top R ² AIC, % R ² , n	I + S + V + C + n + M 1064, 12.5%, 235	A + S + V + N + C + n + M 2399, 7.0%, 452	I + S + U + V + N + M 549, 70.0% 247
	Top 5 Models: Common Vars*	Sig < 0.01 Sig < 0.05	- -	S M S n M	I M I U V M
Beluga Whale	Top 1 Models	Top AIC AIC, % R ² , n	I + F + T + C + n + M 1279, 21.9%, 200	A + I + F + P + T + S + N + C + n + M 2180, 15.1%, 452	A + I + P + S + C 37, 9.3%, 103
		Top R ² AIC, % R ² , n	A + I + T + U + N + u + n + M 2261, 46.1%, 288	A + I + F + P + T + S + N + M 2271, 17.8%, 460	A + I + P + S + N + n 1109, 12.3%, 247
	Top 5 Models: Common Vars*	Sig < 0.01 Sig < 0.05	M I T M	F P M F P T M N	A A
Gray Whale	Top 1 Models	Top AIC AIC, % R ² , n	I + F + T + S + C + t + n 148, 17.2%, 200	I + T 303, 0.6%, 550	No suitable models -
		Top R ² AIC, % R ² , n	T + S + R + N + u + n + M 811, 20.7%, 182	I + T + S + U + V + R + N + C + G 335, 2.7%, 453	No suitable models -
	Top 5 Models: Common Vars*	Sig < 0.01 Sig < 0.05	T T	- I	- -
Walrus	Top 1 Models	Top AIC AIC, % R ² , n	P + T + N + n + K 1097, 26.8%, 182	A + Q + F + P + S + N + u + n + M + O 2882, 41.5%, 452	P + C + M 696, 12.5%, 103
		Top R ² AIC, % R ² , n	I + F + T + S + u + t + n + M 3921, 66.5%, 497	A + Q + I + T + S + t + n + M + O 3521, 50.4%, 495	Q + R + N + M + H + G 2053, 32.5%, 246
	Top 5 Models: Common Vars*	Sig < 0.01 Sig < 0.05	n n	Q n O Q S M n O	M M
Bearded Seal	Top 1 Models	Top AIC AIC, % R ² , n	Q + P + S + U + V + N + t + n + M 1492, 79.4%, 182	A + Q + I + S + V + R + N + C + n + M + G 3771, 85.0%, 452	A + Q + I + P + C + t + M 215, 14.2%, 103
		Top R ² AIC, % R ² , n	Q + V + R + N + n + M + K 2273, 88.9%, 279	Q + I + T + R + t + n + M + H 4380, 86.7%, 530	A + S + V + C + t + M + J 2063, 92.0%, 272
	Top 5 Models: Common Vars*	Sig < 0.01 Sig < 0.05	V n M V n M	Q R n M Q I R n M	- A M
Ice Noise	Top 1 Models	Top AIC AIC, % R ² , n	Q + I + S + U + R + N + u + n 1539, 33.6%, 182	A + I + F + P + S + N + C + u + t + n + M 3002, 24.1%, 452	I + P + S + C + J 568, 25.6%, 103
		Top R ² AIC, % R ² , n	S + U + R + C + u + n + M 2152, 48.5%, 235	A + I + F + P + U + N + C + u + t + n + M + H 3243, 25.9%, 491	I + P + C + M + J 569, 26.1%, 103
	Top 5 Models: Common Vars*	Sig < 0.01 Sig < 0.05	- U	I F M I F M	- J

* To be included, variable had to be in at least 3 of each set of models. I = ice concentration (%); S = salinity (psu); U = U bottom currents (cm s⁻¹); R = transport (Sv, averaged across all locations); N = nitrate (bottom); t = V winds at midshore location; n = wind speed at midshore location; M = month; G = bottom O₂ (mMol kg⁻¹); A = ADCP (600) column Sa (area backscattering dB re 1 m⁻¹); F = chlorophyll (fluorescence); P = PAR (mE in cm⁻² s⁻¹); V = V bottom currents (cm s⁻¹); C = Turbidity (FNU); H = average ice thickness; O = % oxygen saturation; Q = ADCP (600 kHz) bottom Sv (volume backscattering dB re 1 m⁻¹); T = temperature (°C); u = U winds at midshore location; K = standard deviation ice thickness; J = median ice thickness

While no clear associations are present with the salinity and nitrate data, it is interesting to note that both salinity and nitrate were increasing during the fall 2010 migration, and decreasing in the fall 2011 migration. It is possible this may have some relationship with the three migration pulses that are evident in fall 2010 but not 2011; however, more data are needed to determine this. Only two reports of bowhead whales occurred along the transect lines, one visual sighting and one acoustic detection along Wainwright in 2010. As a result, bowheads were not included in the transect line plots.

TABLE 22. BOWHEAD WHALE RESULTS OF THE GAM MODEL. RESULTS REPRESENT THE TOP AIC MODEL (LOWEST AIC VALUE), AND THE COMMON SIGNIFICANT (P<0.05) VARIABLES AMONG THE TOP AIC AND THE TOP R-SQUARED MODELS. GREEN = HIGHLY SIGNIFICANT, P<0.01. YELLOW = SIGNIFICANT, P<0.05. RED = NOT SIGNIFICANT.

	Inshore	Mid-Shore	Offshore
Top AIC model		ADCP_colSa	ADCP_colSa
		Chlorophyll	
	Currents_botU		
		Currents_botV	
	Ice_conc	Ice_conc	Ice_conc
			IceThick_avg
	Month	Month	Month
	Nitrate	Nitrate	
	O2_mmol		
			O2_%sat
		PAR	PAR
	Salinity	Salinity	
	Transport		
		Turbidity	Turbidity
Wind_spd	Wind_spd		
Wind_v		Wind_v	
Common sign. variables		Chlorophyll	
		Currents_botV	
	Ice_conc	Ice_conc	Ice_conc
	Month	Month	Month
	Transport		
	Turbidity		
	Wind_spd		

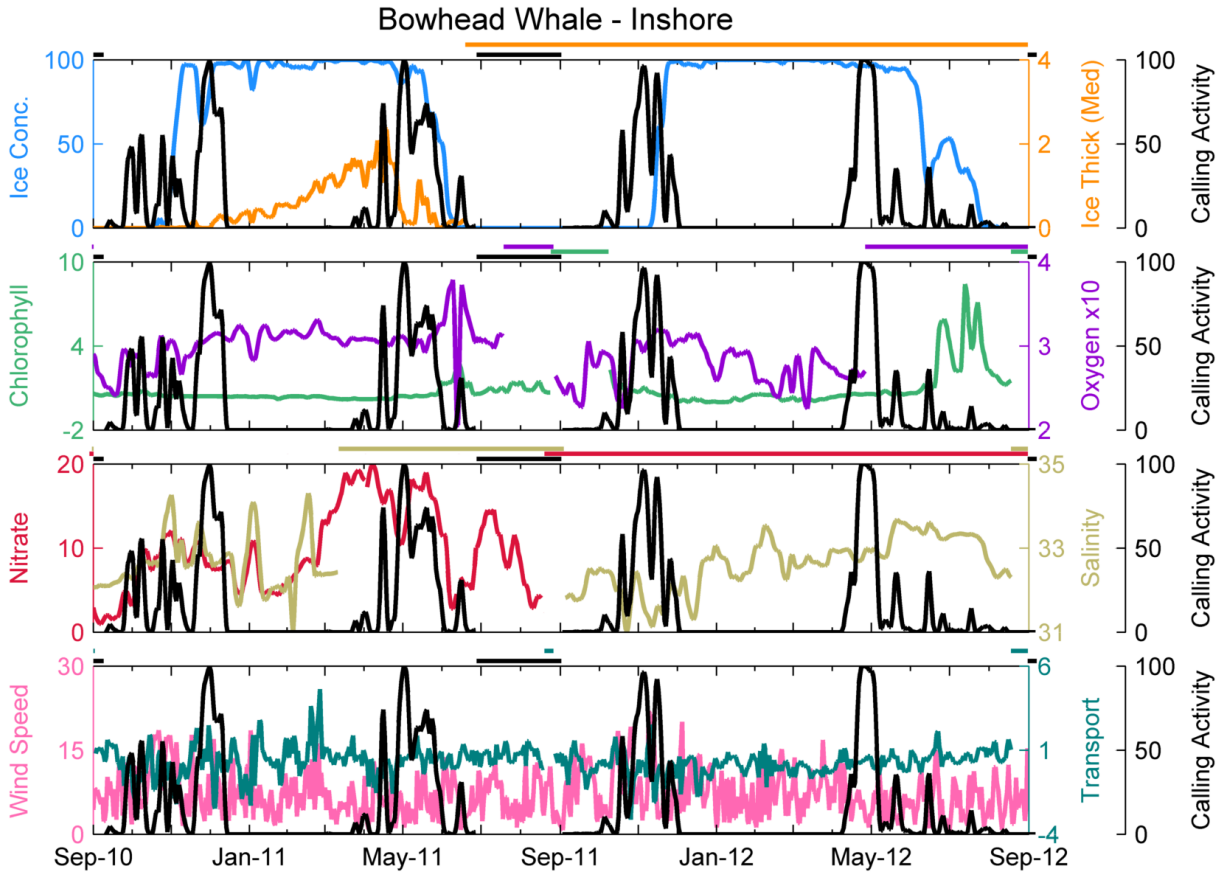


FIGURE 106. BOWHEAD WHALE CALLING ACTIVITY AS IT RELATES TO OCEANOGRAPHIC VARIABLES AT THE INSHORE LOCATION, 2010-2012. BLACK LINE = PERCENT OF TIME INTERVALS WITH CALLS. TOP ROW: PERCENT ICE CONCENTRATION (BLUE LINE) AND ICE THICKNESS (M; ORANGE LINE). SECOND ROW: CHLOROPHYLL ($\mu\text{G/L}$; GREEN LINE) AND OXYGEN ($\text{M} \times 10$; PURPLE LINE). THIRD ROW: NITRATE (μM ; RED LINE) AND SALINITY (PSU; TAN LINE). BOTTOM ROW: WIND SPEED (M/S; PINK LINE) AND TRANSPORT (SV; TEAL LINE). HORIZONTAL BARS ABOVE EACH ROW INDICATE TIMES WITH NO DATA. ALL DATA EXCEPT WIND SPEED ARE PRESENTED AS A 3-DAY MOVING AVERAGE.

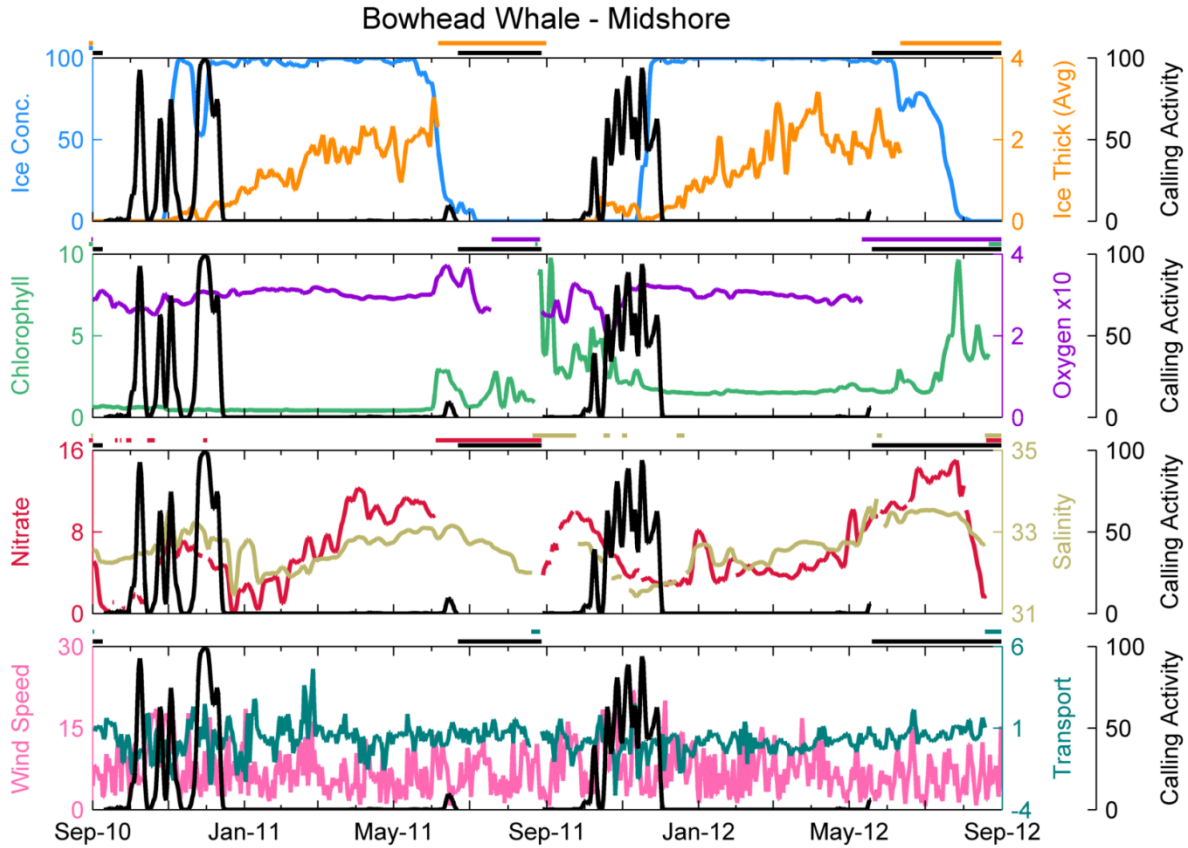


FIGURE 107. BOWHEAD WHALE CALLING ACTIVITY AS IT RELATES TO OCEANOGRAPHIC VARIABLES AT THE MIDSHORE LOCATION, 2010-2012. BLACK LINE = PERCENT OF TIME INTERVALS WITH CALLS. TOP ROW: PERCENT ICE CONCENTRATION (BLUE LINE) AND ICE THICKNESS (M; ORANGE LINE). SECOND ROW: CHLOROPHYLL ($\mu\text{g/L}$; GREEN LINE) AND OXYGEN ($\text{M} \times 10$; PURPLE LINE). THIRD ROW: NITRATE (μM ; RED LINE) AND SALINITY (PSU; TAN LINE). BOTTOM ROW: WIND SPEED (M/S; PINK LINE) AND TRANSPORT (SV; TEAL LINE). HORIZONTAL BARS ABOVE EACH ROW INDICATE TIMES WITH NO DATA. ALL DATA EXCEPT WIND SPEED ARE PRESENTED AS A 3-DAY MOVING AVERAGE.

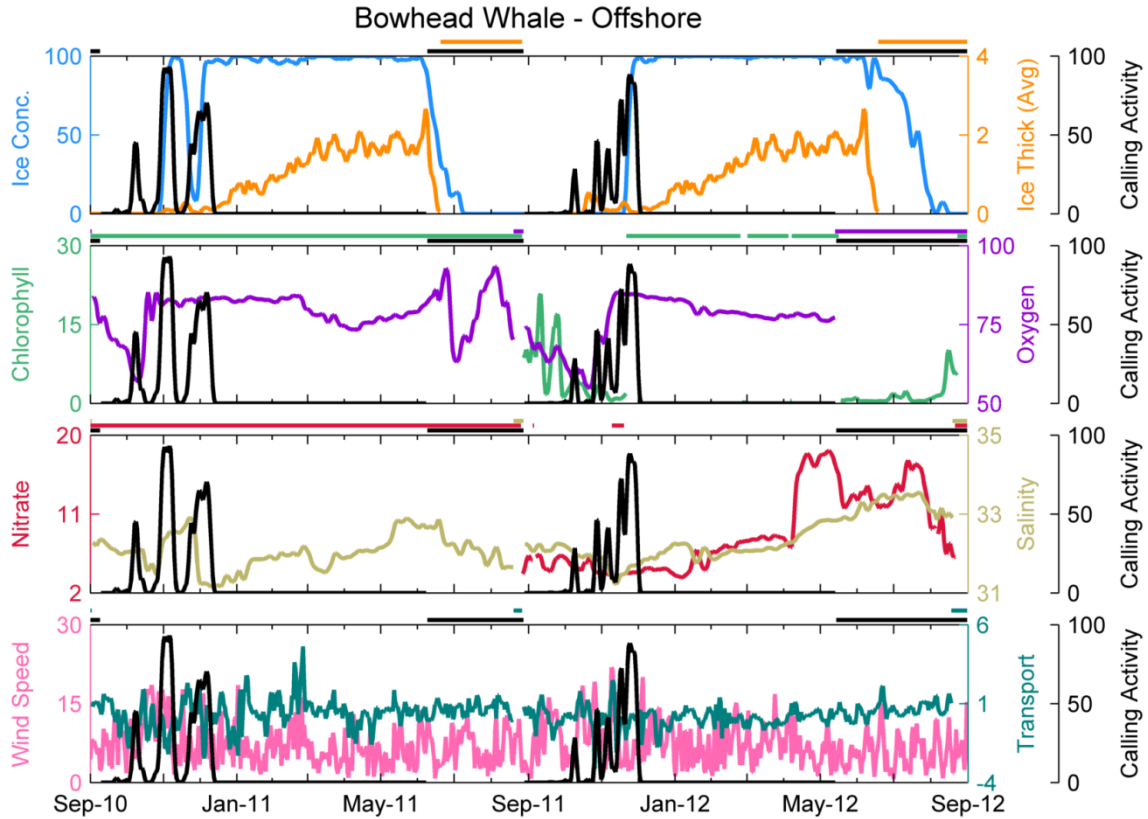


FIGURE 108. BOWHEAD WHALE CALLING ACTIVITY AS IT RELATES TO OCEANOGRAPHIC VARIABLES AT THE OFFSHORE LOCATION, 2010-2012. BLACK LINE = PERCENT OF TIME INTERVALS WITH CALLS. TOP ROW: PERCENT ICE CONCENTRATION (BLUE LINE) AND ICE THICKNESS (M; ORANGE LINE). SECOND ROW: CHLOROPHYLL ($\mu\text{G/L}$; GREEN LINE) AND OXYGEN ($\text{M} \times 10$; PURPLE LINE). THIRD ROW: NITRATE (μM ; RED LINE) AND SALINITY (PSU; TAN LINE). BOTTOM ROW: WIND SPEED (M/S; PINK LINE) AND TRANSPORT (SV; TEAL LINE). HORIZONTAL BARS ABOVE EACH ROW INDICATE TIMES WITH NO DATA. ALL DATA EXCEPT WIND SPEED ARE PRESENTED AS A 3-DAY MOVING AVERAGE.

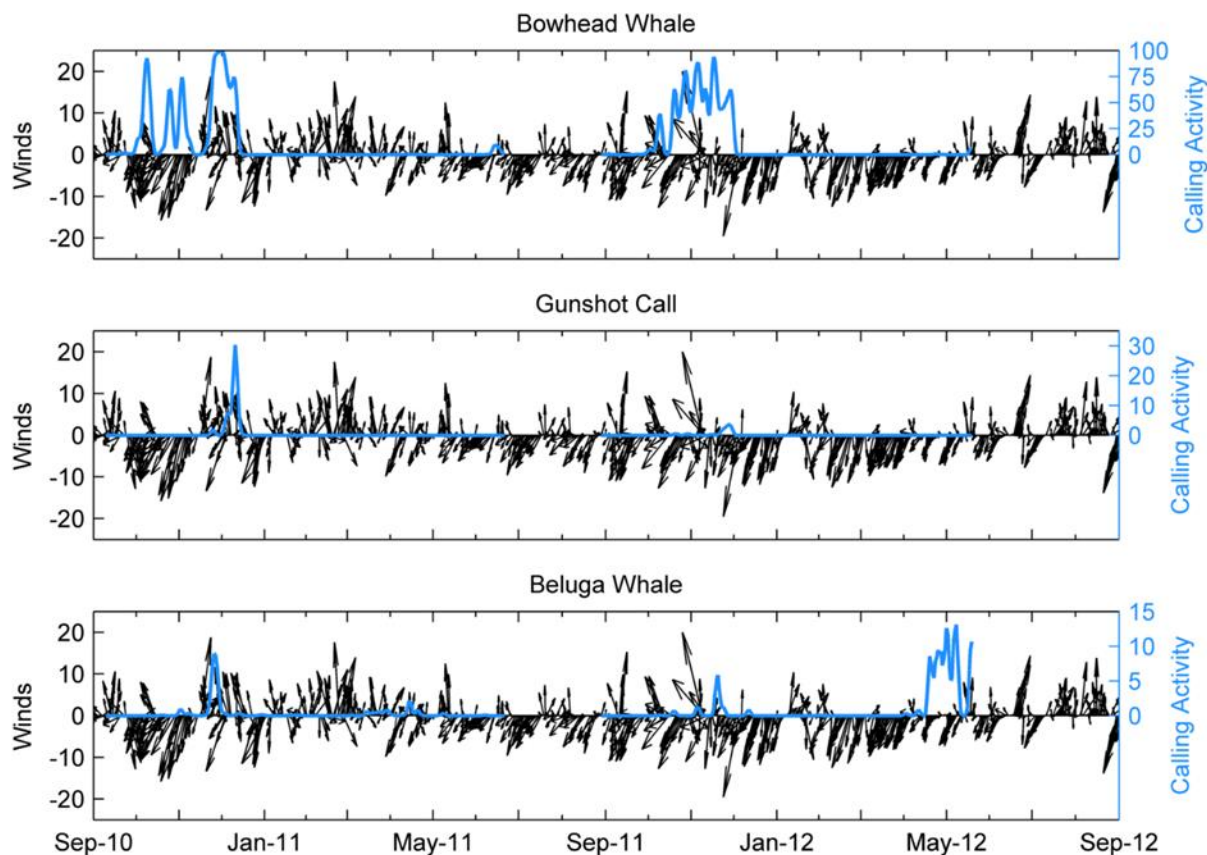


FIGURE 109. MARINE MAMMAL CALLING ACTIVITY (BLUE LINE) VS. WINDS (M/S; BLACK LINE) AT THE MIDSHORE LOCATION, 2010-2012. ARROWS (USING THE OCEANOGRAPHIC CONVENTION) INDICATE THE DIRECTION THE WINDS ARE BLOWING TOWARD, (I.E., AN ARROW POINTING TO THE TOP OF THE PAGE INDICATES WINDS BLOWING FROM THE SOUTH AND TO THE NORTH). LENGTH OF WIND VECTOR INDICATES SPEED. TOP ROW: BOWHEAD WHALE. MIDDLE ROW: GUNSHOT CALL. BOTTOM ROW: BELUGA WHALE. NOTE CALLING ACTIVITY Y-AXIS IS NOT ON THE SAME SCALE.

Gunshot calls (Bowheads)

Gunshot calling activity occurred near the end of most of the peaks in regular bowhead whale calling activity (Figure 4). It was therefore expected that gunshot calls would be correlated with similar variables as bowhead whales, however this was not the case. The results for the GAM runs for gunshot calls are presented in Table 23. There were no consistent significant variables in the best models across the three locations, although nitrate appeared in all three top models. The common significant variables were month, salinity, and wind speed for the midshore location. Six variables were included in the best model for the midshore location, of which three (month, salinity, and wind speed) were significant. Only four significant variables were shared between bowheads and gunshot calls: ice concentration (offshore only), month (highly significant, midshore and offshore), oxygen (inshore only) and wind speed (inshore and midshore). While most of the midshore calling activity data were included in the GAMS (spring missing in both years), only 2010-11 fall data were included for the inshore location, and only 2011-12 data were included for the offshore location due to a lack of coincidental oceanographic data (see Appendix G, Section XVIII.G).

Gunshot call presence was correlated with ice presence at all locations (Figure 110-112). Gunshot calling would peak immediately after ice concentration hit 100%, but while thickness was still less than 0.5 m. They are also strongly associated with polynyas, with increased calling activity occurring during polynyas. In the spring, gunshot calling resumes as the ice retreats. Like the general bowhead whale calling activity, gunshot calling activity is also slightly associated with wind speed, albeit to a lesser degree (Figure 110-112). For the midshore location, gunshot calling activity was slightly correlated with winds to the NNW in 2010-11, whereas they were associated with consistent winds to the SSW in 2011-12 (Figure 109, middle panel).

TABLE 23. GUNSHOT CALL RESULTS OF THE GAM MODEL. RESULTS REPRESENT THE TOP AIC MODEL (LOWEST AIC VALUE), AND THE COMMON SIGNIFICANT (P<0.05) VARIABLES AMONG THE TOP AIC AND THE TOP R-SQUARED MODELS. GREEN = HIGHLY SIGNIFICANT, P<0.01. YELLOW = SIGNIFICANT, P<0.05. RED = NOT SIGNIFICANT.

	Inshore	Mid-Shore	Offshore
Top AIC model		ADCP_colSa	-
			Currents_botU Currents_botV
		Month	Ice_conc Month
	Nitrate	Nitrate	Nitrate
	O2_mMol		
	PAR		
		Salinity	
		Turbidity	
	Wind_spd	Wind_spd	
	Common sign. variables		Month Salinity Wind_spd

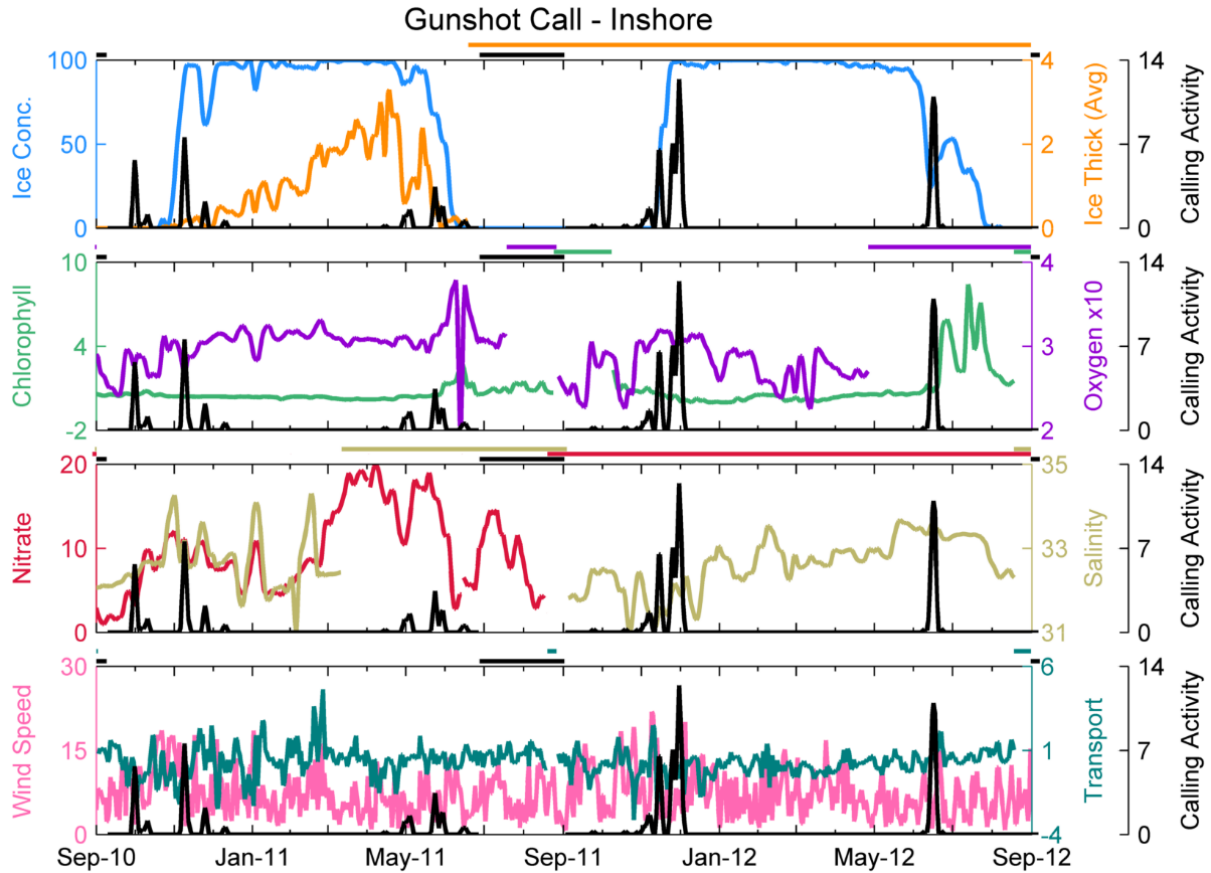


FIGURE 110. GUNSHOT CALLING ACTIVITY AS IT RELATES TO OCEANOGRAPHIC VARIABLES AT THE INSHORE LOCATION, 2010-2012. BLACK LINE = PERCENT OF TIME INTERVALS WITH CALLS. TOP ROW: PERCENT ICE CONCENTRATION (BLUE LINE) AND ICE THICKNESS (M, ORANGE LINE). SECOND ROW: CHLOROPHYLL ($\mu\text{G/L}$; GREEN LINE) AND OXYGEN ($\text{M} \times 10$; PURPLE LINE). THIRD ROW: NITRATE (μM ; RED LINE) AND SALINITY (PSU; TAN LINE). BOTTOM ROW: WIND SPEED (M/S; PINK LINE) AND TRANSPORT (SV; TEAL LINE). HORIZONTAL BARS ABOVE EACH ROW INDICATE TIMES WITH NO DATA. ALL DATA EXCEPT WIND SPEED ARE PRESENTED AS A 3-DAY MOVING AVERAGE.

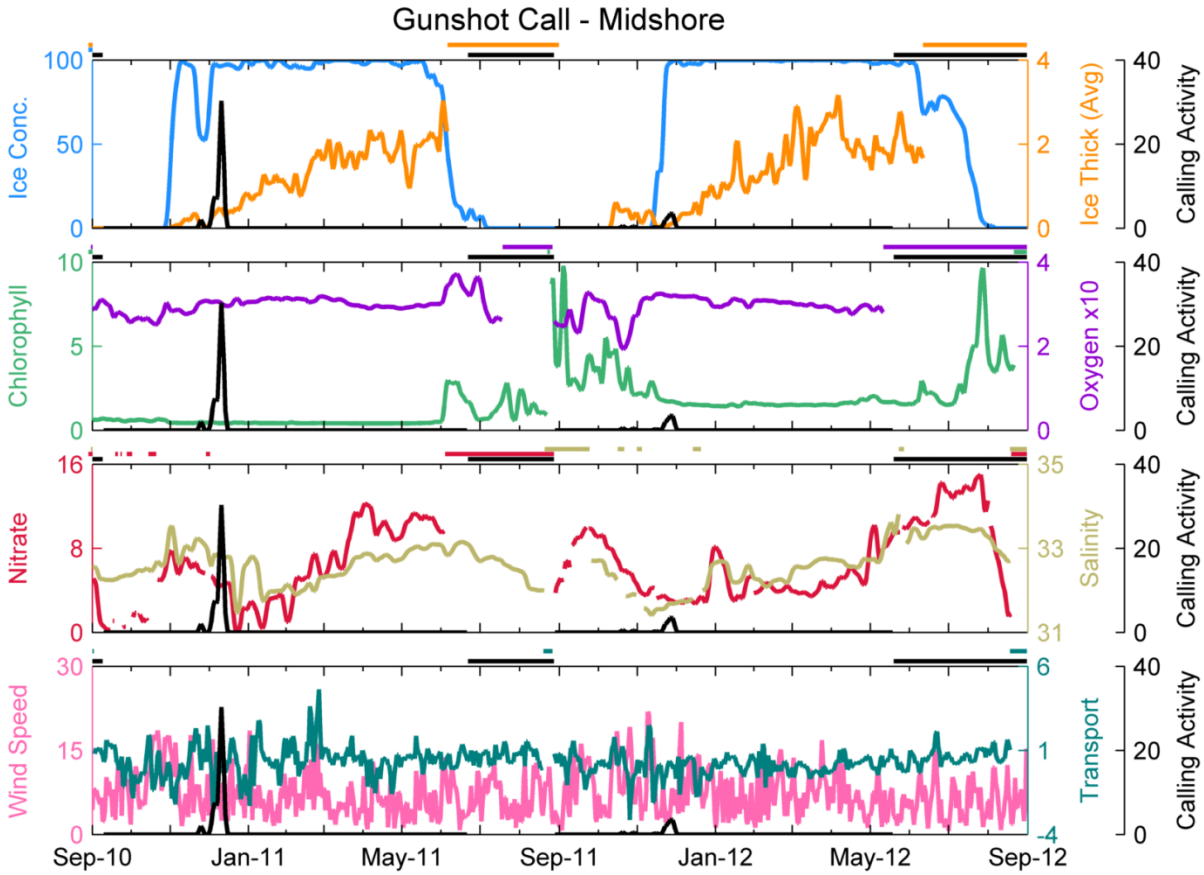


FIGURE 111. GUNSHOT CALLING ACTIVITY AS IT RELATES TO OCEANOGRAPHIC VARIABLES AT THE MIDSHORE LOCATION, 2010-2012. BLACK LINE = PERCENT OF TIME INTERVALS WITH CALLS. TOP ROW: PERCENT ICE CONCENTRATION (BLUE LINE) AND ICE THICKNESS (M; ORANGE LINE). SECOND ROW: CHLOROPHYLL ($\mu\text{G/L}$; GREEN LINE) AND OXYGEN ($\text{M} \times 10$; PURPLE LINE). THIRD ROW: NITRATE (μM ; RED LINE) AND SALINITY (PSU; TAN LINE). BOTTOM ROW: WIND SPEED (M/S; PINK LINE) AND TRANSPORT (SV; TEAL LINE). HORIZONTAL BARS ABOVE EACH ROW INDICATE TIMES WITH NO DATA. ALL DATA EXCEPT WIND SPEED ARE PRESENTED AS A 3-DAY MOVING AVERAGE.

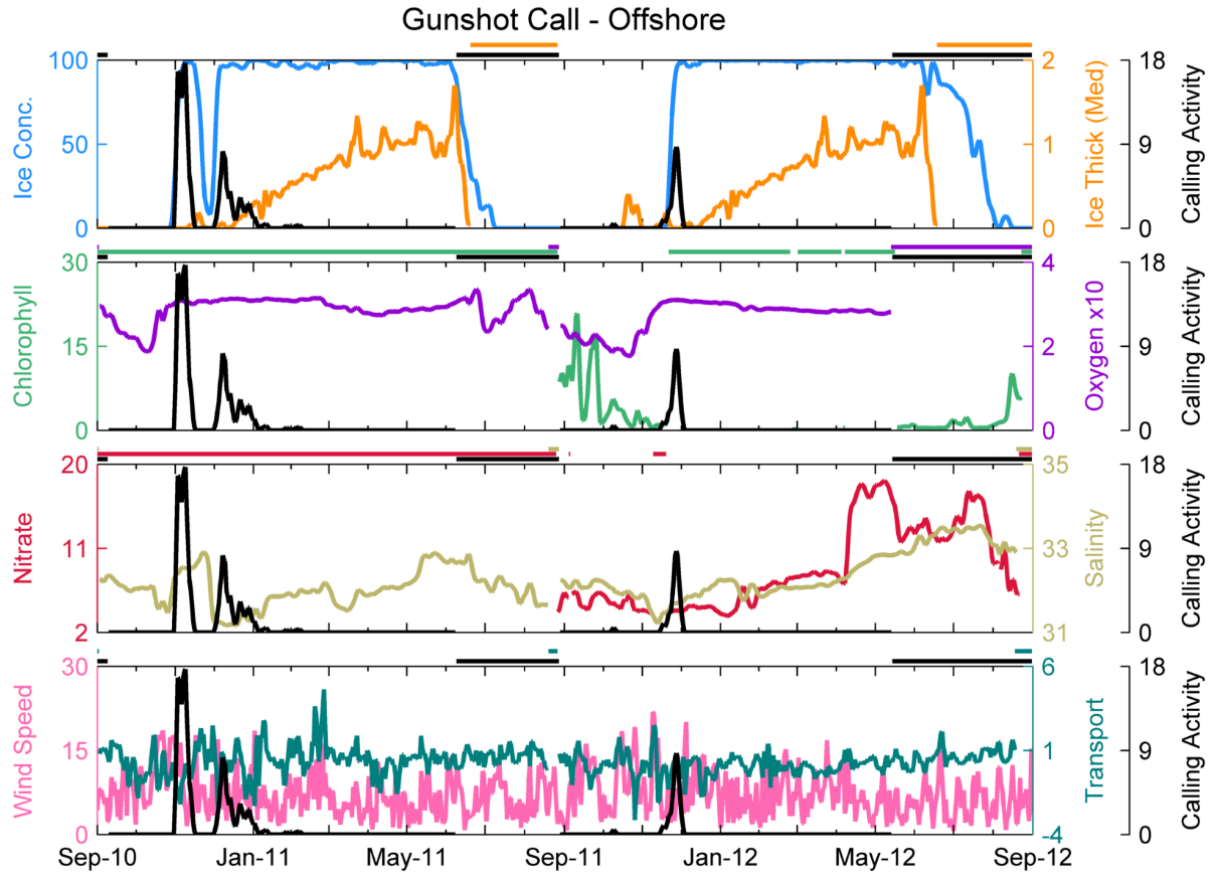


FIGURE 112. GUNSHOT CALLING ACTIVITY AS IT RELATES TO OCEANOGRAPHIC VARIABLES AT THE OFFSHORE LOCATION, 2010-2012. BLACK LINE = PERCENT OF TIME INTERVALS WITH CALLS. TOP ROW: PERCENT ICE CONCENTRATION (BLUE LINE) AND ICE THICKNESS (M; ORANGE LINE). SECOND ROW: CHLOROPHYLL ($\mu\text{G/L}$; GREEN LINE) AND OXYGEN ($\text{M} \times 10$; PURPLE LINE). THIRD ROW: NITRATE (μM ; RED LINE) AND SALINITY (PSU; TAN LINE). BOTTOM ROW: WIND SPEED (M/S; PINK LINE) AND TRANSPORT (SV; TEAL LINE). HORIZONTAL BARS ABOVE EACH ROW INDICATE TIMES WITH NO DATA. ALL DATA EXCEPT WIND SPEED ARE PRESENTED AS A 3-DAY MOVING AVERAGE.

Beluga whale

The results of the GAM runs for beluga whales are represented in Table 24. The common significant variables among the top AIC and top R-Squared models selected by the GAM runs were ice concentration, month, and temperature at the inshore location, chlorophyll, month, nitrate, PAR, and temperature for the midshore location. The midshore model included ten different variables, of which seven (ADCP volume backscatter (full column), chlorophyll, month, nitrate, PAR, temperature, wind speed) were significant. It is important to note that while the midshore location included most of the calling activity in the GAMs, the inshore location only included the 2011-12 data (about 75%), and only the fall of 2010 for the offshore location, again a result of insufficient data in the oceanographic variables dataset.

Plotting beluga calling activity with ice conditions and nutrients revealed a strong association with ice at the inshore and midshore, but not the offshore, locations (Figure 113-115). Peak vocal activity occurred when ice was forming in the fall, and as it began breaking up (decreased ice concentration and decreasing thickness) in the spring. Belugas are also strongly

associated with polynyas, where a sharp decrease in ice concentration is correlated with a peak in vocal activity. There may be a slight association with nitrate levels in the spring, however more data are needed for confirmation. Belugas were only marginally associated with winds (Figure 109, bottom row), with a slight correlation between calling activity and moderate winds to the SSW, most notably in 2011-12. There were no visual or acoustic detections of beluga during the shipboard surveys, therefore they are not included in the transect line plots.

TABLE 24. BELUGA WHALE RESULTS OF THE GAM MODEL. RESULTS REPRESENT THE TOP AIC MODEL (LOWEST AIC VALUE), AND THE COMMON SIGNIFICANT (P<0.05) VARIABLES AMONG THE TOP AIC AND THE TOP R-SQUARED MODELS. GREEN = HIGHLY SIGNIFICANT, P<0.01. YELLOW = SIGNIFICANT, P<0.05. RED = NOT SIGNIFICANT.

	Inshore	Mid-Shore	Offshore
Top AIC model		ADCP_colSa	ADCP_colSa
	Chlorophyll	Chlorophyll	
	Ice_conc	Ice_conc	Ice_conc
	Month	Month	
		Nitrate	
		PAR	PAR
		Salinity	Salinity
	Temperature	Temperature	
	Turbidity	Turbidity	Turbidity
Wind_spd	Wind_spd		
Common sign. variables			ADCP_CoIA
	Ice_conc	Chlorophyll	
	Month	Month	
	Temperature	Nitrate	
	PAR		
	Temperature		

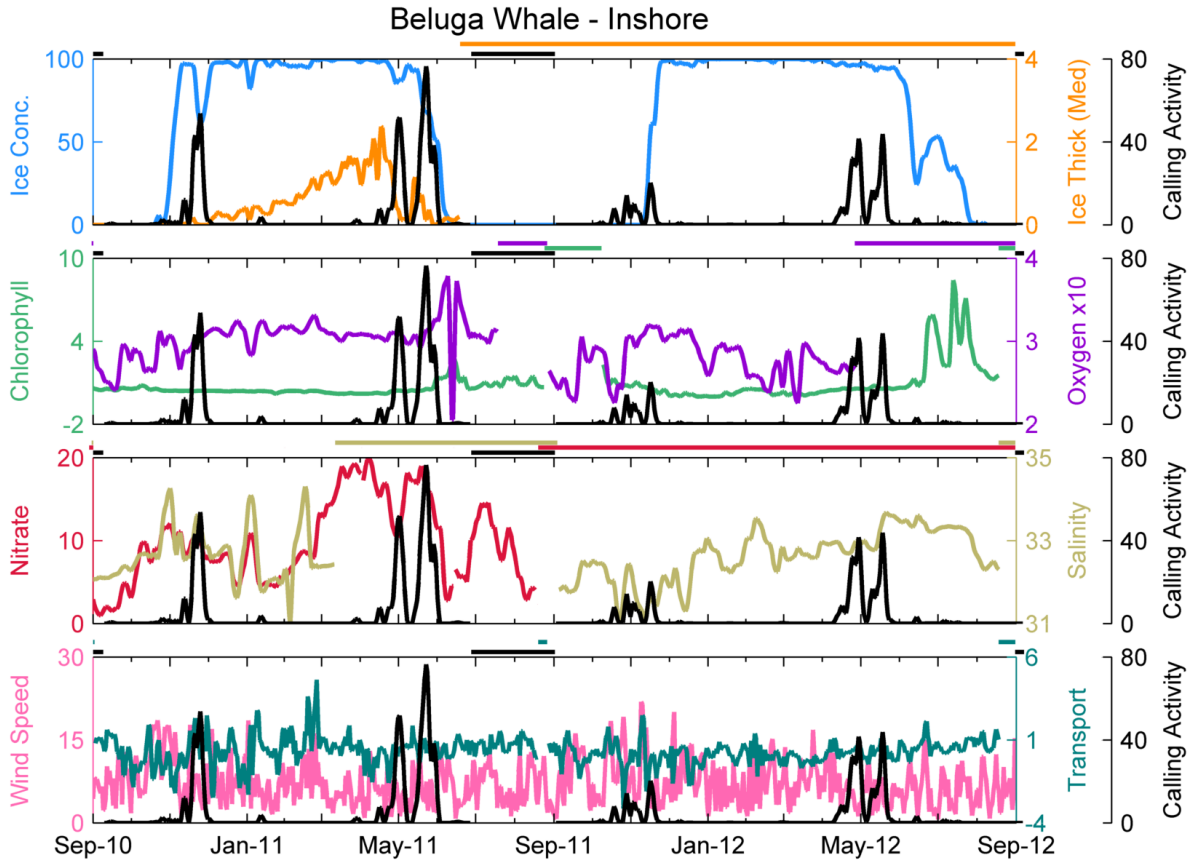


FIGURE 113. BELUGA WHALE CALLING ACTIVITY AS IT RELATES TO OCEANOGRAPHIC VARIABLES AT THE INSHORE LOCATION, 2010-2012. BLACK LINE = PERCENT OF TIME INTERVALS WITH CALLS. TOP ROW: PERCENT ICE CONCENTRATION (BLUE LINE) AND MEDIAN ICE THICKNESS (M; ORANGE LINE). SECOND ROW: CHLOROPHYLL ($\mu\text{G/L}$; GREEN LINE) AND PERCENT OXYGEN SATURATION (PURPLE LINE). THIRD ROW: NITRATE (μM ; RED LINE) AND SALINITY (PSU; TAN LINE). BOTTOM ROW: WIND SPEED (M/S; PINK LINE) AND TRANSPORT (SV; TEAL LINE). HORIZONTAL BARS ABOVE EACH ROW INDICATE TIMES WITH NO DATA. ALL DATA EXCEPT WIND SPEED ARE PRESENTED AS A 3-DAY MOVING AVERAGE.

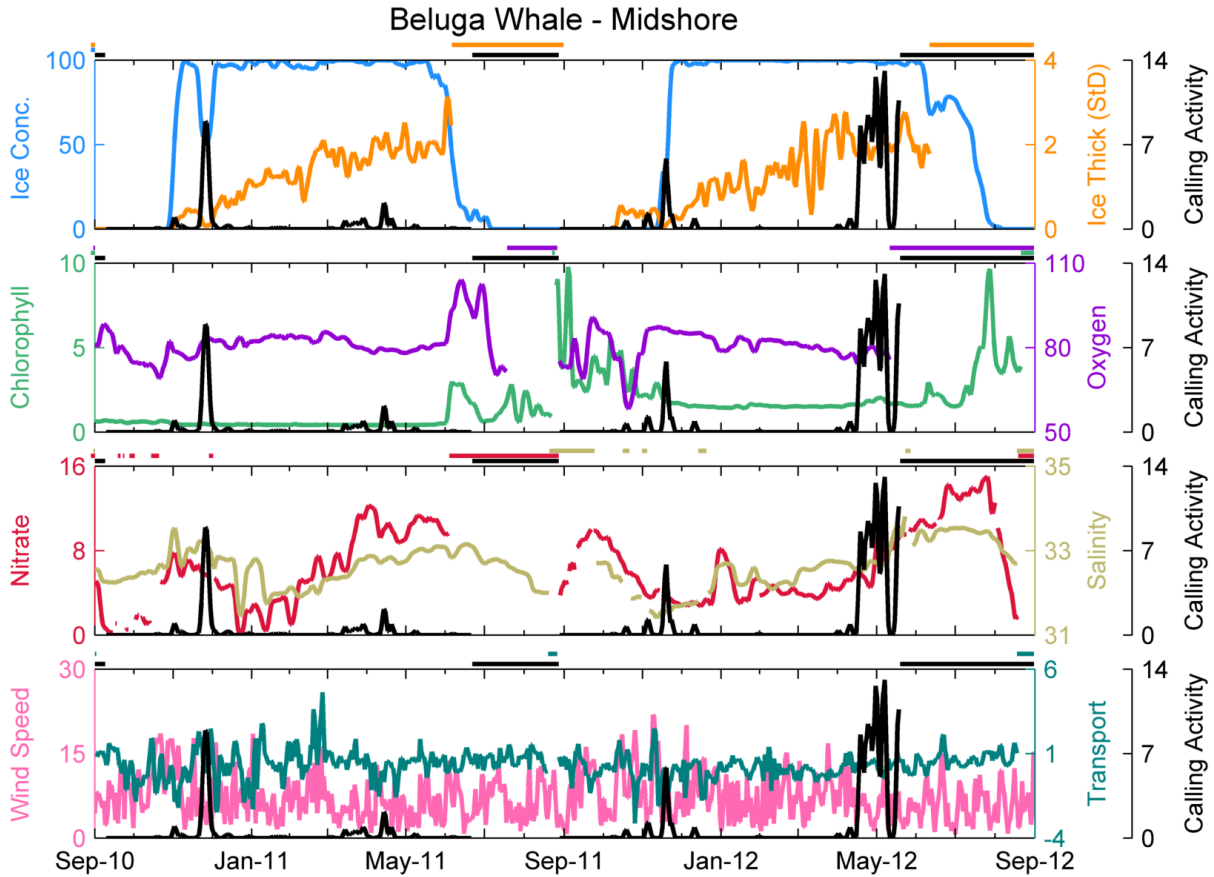


FIGURE 114. BELUGA WHALE CALLING ACTIVITY AS IT RELATES TO OCEANOGRAPHIC VARIABLES AT THE MIDSHORE LOCATION, 2010-2012. BLACK LINE = PERCENT OF TIME INTERVALS WITH CALLS TOP ROW: PERCENT ICE CONCENTRATION (BLUE LINE) AND STANDARD DEVIATION ICE THICKNESS (M; ORANGE LINE). SECOND ROW: CHLOROPHYLL ($\mu\text{G/L}$; GREEN LINE) AND PERCENT OXYGEN SATURATION (PURPLE LINE). THIRD ROW: NITRATE (μM ; RED LINE) AND SALINITY (PSU; TAN LINE). BOTTOM ROW: WIND SPEED (M/S; PINK LINE) AND TRANSPORT (SV; TEAL LINE). HORIZONTAL BARS ABOVE EACH ROW INDICATE TIMES WITH NO DATA. ALL DATA EXCEPT WIND SPEED ARE PRESENTED AS A 3-DAY MOVING AVERAGE.

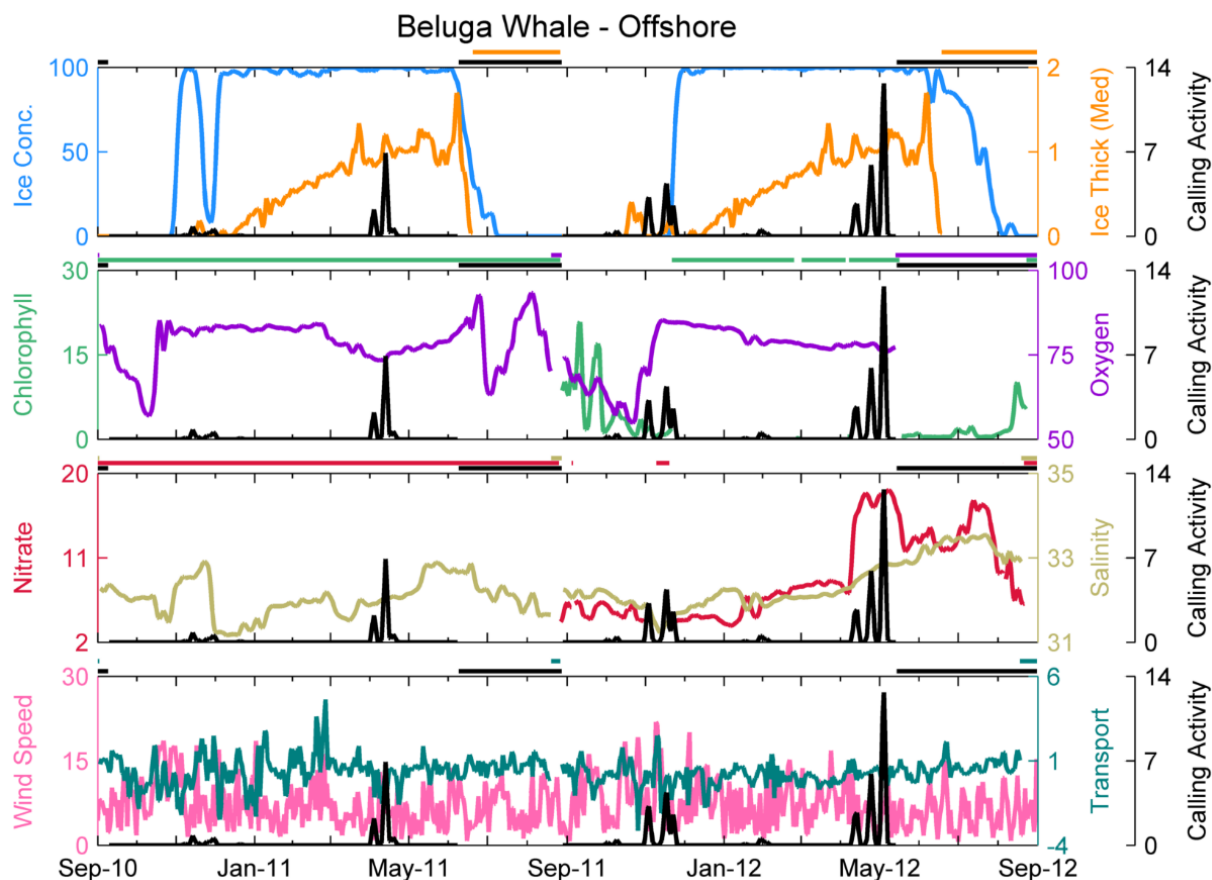


FIGURE 115. BELUGA WHALE CALLING ACTIVITY AS IT RELATES TO OCEANOGRAPHIC VARIABLES AT THE OFFSHORE LOCATION 2010-2012. BLACK LINE = PERCENT OF TIME INTERVALS WITH CALLS; TOP ROW: PERCENT ICE CONCENTRATION (BLUE LINE) AND STANDARD DEVIATION ICE THICKNESS (M; ORANGE LINE). SECOND ROW: CHLOROPHYLL ($\mu\text{G/L}$; GREEN LINE) AND PERCENT OXYGEN SATURATION (PURPLE LINE). THIRD ROW: NITRATE (μM ; RED LINE) AND SALINITY (PSU; TAN LINE). BOTTOM ROW: WIND SPEED (M/S; PINK LINE) AND TRANSPORT (SV; TEAL LINE). HORIZONTAL BARS ABOVE EACH ROW INDICATE TIMES WITH NO DATA. ALL DATA EXCEPT WIND SPEED ARE PRESENTED AS A 3-DAY MOVING AVERAGE.

Gray whale

Results for the gray whale GAM runs are presented in Table 25. Ice concentration, temperature and wind speed were the only significant variables in the best model selected from the inshore GAM run. The only consistent significant variable among the top AIC and top R-Squared models from the inshore GAM run was temperature. Gray whale calling activity was limited to the inshore location; the midshore location had only one day of calling activity, and the offshore location had none. It is important to note that only the fall 2011 gray whale calling peak was included in the GAM for the inshore location; no data were included for 2010-11 at the inshore location, a result of the low number of coincident data from the oceanographic variables dataset.

Only the inshore calling activity data were plotted with the other variables (Figure 116). Gray whale calling activity showed a negative correlation with ice presence. Calling activity in the fall ceased before the ice formation began, and did not resume in spring until the concentration started to decrease. There was an association with chlorophyll in 2011-2012,

though not in 2010-2011. It is possible that gray whales are associated with either low nitrate levels, or occur just before a peak in nitrate levels. Unfortunately, there are no nitrate data for 2011-2012, so we cannot confirm this association.

Gray whale visual and acoustic detections during the shipboard survey were plotted against results from the transect line sampling (zooplankton concentration), temperature, salinity, nitrate, and ammonium), the results of which are presented in Figure 117. Overall, gray whales were associated with high levels of *Pseudocalanus*, *C. glacialis*, and larvaceans, as well as nitrate and ammonium. In 2011 along the Barrow transect (Line F), all gray whale sightings were inshore near the start of the transect line. There were no acoustic detections. The location of the gray whale sightings corresponds with high levels of *Pseudocalanus* and moderate levels of larvaceans, though there were no obvious correlations between gray whales and the other variables. Generally, there were high levels of larvaceans and *Pseudocalanus* associated with high levels of salinity, nitrate, and ammonium. In 2012 at the Point Hope line (Line A), there were high numbers of gray whale sightings near high levels of *Pseudocalanus* and *C. glacialis*. These were also associated with high levels of nitrate and ammonium.

TABLE 25. GRAY WHALE RESULTS OF THE GAM MODEL. RESULTS REPRESENT THE TOP AIC MODEL (LOWEST AIC VALUE), AND THE COMMON SIGNIFICANT (P<0.05) VARIABLES AMONG THE TOP AIC AND THE TOP R-SQUARED MODELS. GREEN = HIGHLY SIGNIFICANT, P<0.01. YELLOW = SIGNIFICANT, P<0.05. RED = NOT SIGNIFICANT.

	Inshore	Mid-Shore	Offshore
Top AIC model	Chlorophyll		
	Ice_conc	Ice_conc	
	Salinity		
	Temperature	Temperature	
	Turbidity		
	Wind_spd		
	Wind_v		
Common sign. variables	Temperature	Ice_conc	

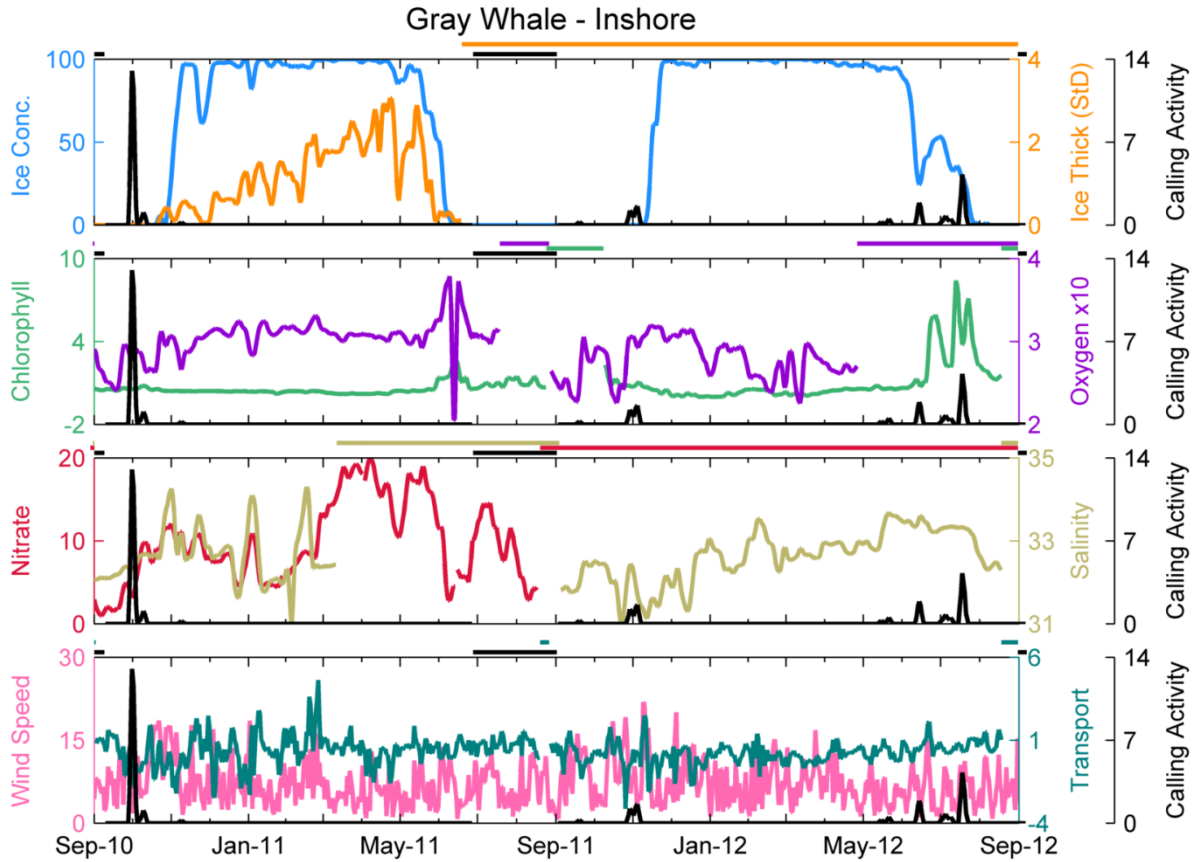


FIGURE 116. GRAY WHALE CALLING ACTIVITY AS IT RELATES TO OCEANOGRAPHIC VARIABLES AT THE INSHORE LOCATION, 2010-2012. BLACK LINE = PERCENT OF TIME INTERVALS WITH CALLS. TOP ROW: PERCENT ICE CONCENTRATION (BLUE LINE) AND AVERAGE ICE THICKNESS (M; ORANGE LINE). SECOND ROW: CHLOROPHYLL ($\mu\text{G/L}$; GREEN LINE) AND PERCENT OXYGEN SATURATION (PURPLE LINE). THIRD ROW: NITRATE (μM ; RED LINE) AND SALINITY (PSU; TAN LINE). BOTTOM ROW: WIND SPEED (M/S; PINK LINE) AND TRANSPORT (SV; TEAL LINE). HORIZONTAL BARS ABOVE EACH ROW INDICATE TIMES WITH NO DATA. ALL DATA EXCEPT WIND SPEED ARE PRESENTED AS A 3-DAY MOVING AVERAGE.

Barrow Canyon, 2011

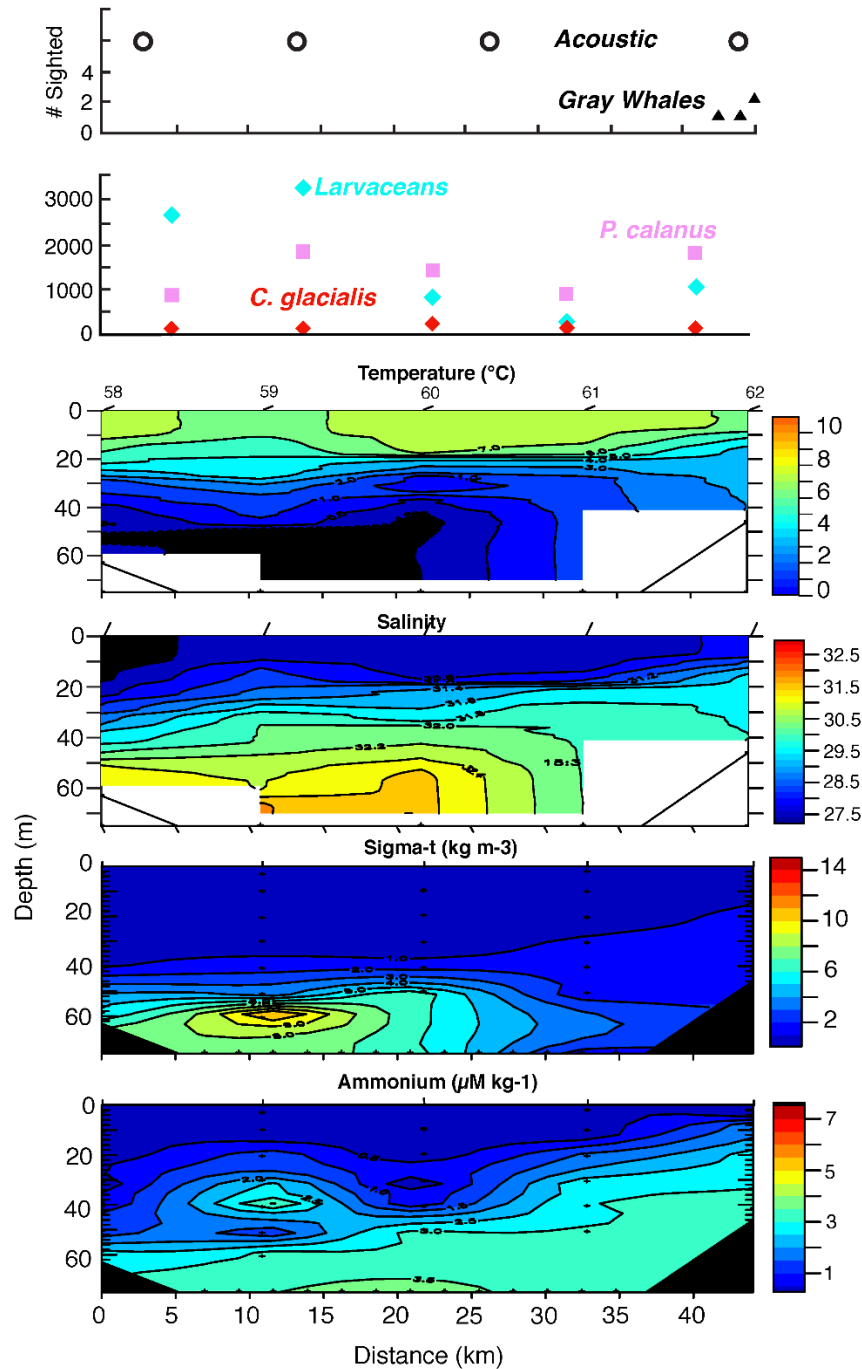


FIGURE 117. BARROW TRANSECT LINE OCEANOGRAPHIC, ZOOPLANKTON, AND GRAY WHALE SURVEY RESULTS, 2011. X-AXIS REFERS TO DISTANCE ALONG TRANSECT, WHERE 0 KM = STATION 1 ALONG TRANSECT. TOP ROW = SONOBUOY EFFORT AND DETECTIONS AND VISUAL SIGHTINGS (INCLUDING # INDIVIDUALS) ALONG TRANSECT LINE; OPEN CIRCLE = SONOBUOY DEPLOYED BUT NO DETECTIONS, CLOSED CIRCLE = ACOUSTIC DETECTION, BLACK DIAMOND = SIGHTING. SECOND ROW = ZOOPLANKTON DENSITY AT EACH TRANSECT STATION; *PSEUDOCALANUS* (ABBREVIATED *P. CALANUS*) = PINK SQUARE, *C. GLACIALIS* = RED DIAMOND, LARVACEANS = TURQUOISE DIAMOND. THIRD ROW = TEMPERATURE (°C). FOURTH ROW = SALINITY (PSU). FIFTH ROW = NITRATE (μM). BOTTOM ROW = AMMONIUM (μM).

Pt. Hope 2012

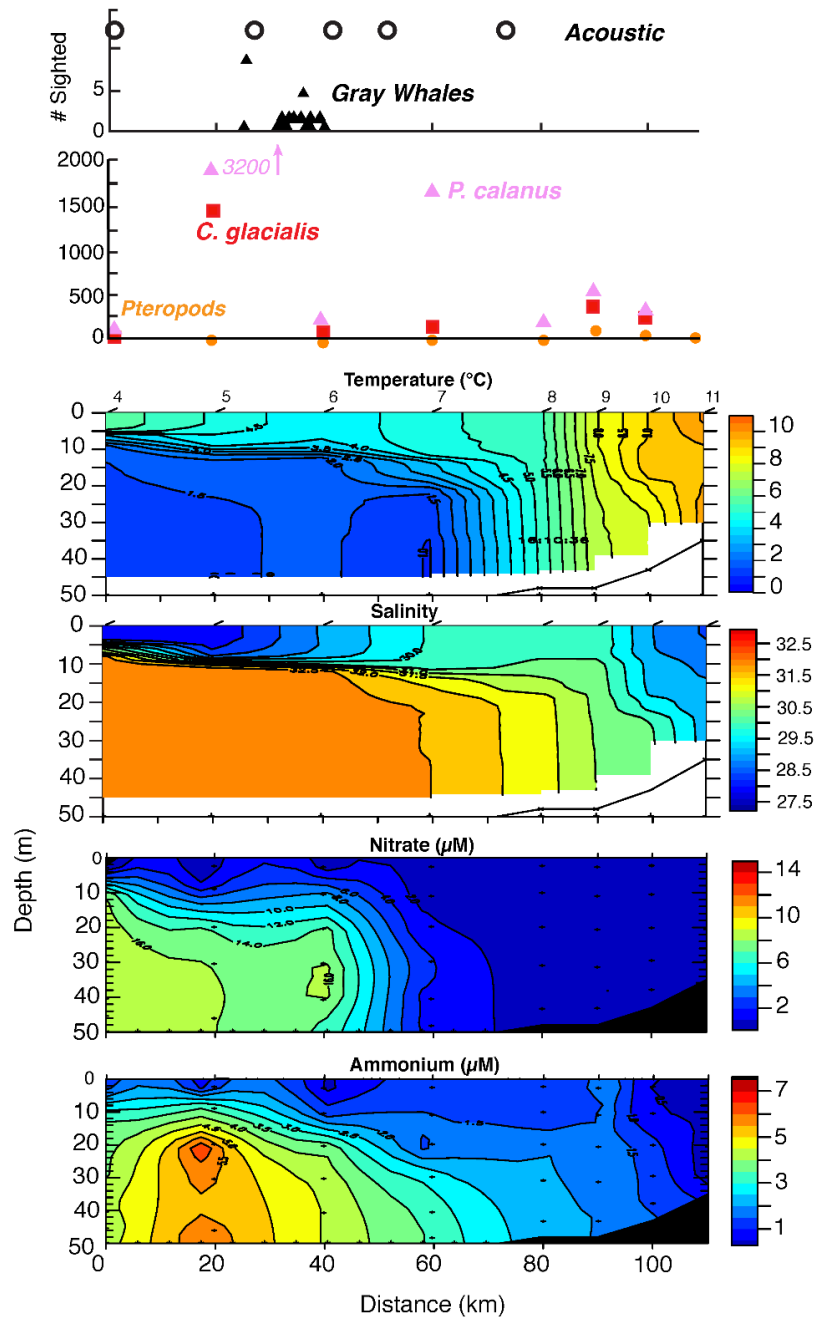


FIGURE 118. POINT HOPE TRANSECT LINE OCEANOGRAPHIC, ZOOPLANKTON, AND GRAY WHALE SURVEY RESULTS, 2012. X-AXIS REFERS TO DISTANCE ALONG TRANSECT, WHERE 0 KM = STATION 1 ALONG TRANSECT. TOP ROW = SONOBUOY EFFORT AND DETECTIONS AND VISUAL SIGHTINGS (INCLUDING # INDIVIDUALS) ALONG TRANSECT LINE; OPEN CIRCLE = SONOBUOY DEPLOYED BUT NO DETECTIONS, CLOSED CIRCLE = ACOUSTIC DETECTION, BLACK DIAMOND = SIGHTING. SECOND ROW = ZOOPLANKTON DENSITY AT EACH TRANSECT STATION; *PSEUDOCALANUS* (ABBREVIATED *P. CALANUS*) = PINK TRIANGLE, *C. GLACIALIS* = RED SQUARE, PTEROPODS = ORANGE CIRCLE. THIRD ROW = TEMPERATURE ($^{\circ}\text{C}$). FOURTH ROW = SALINITY (PSU). FIFTH ROW = NITRATE (μM). BOTTOM ROW = AMMONIUM (μM).

Walrus

The results of the GAM runs for walrus calling activity are presented in Table 26. The common significant variables for the top AIC models and the top R-Squared models are ADCP volume backscatter (bottom), month, oxygen saturation, salinity, and wind speed for the midshore location. Ten variables contributed to the best model selected by the GAM run at the midshore location, of which six (ADCP volume backscatter (bottom), chlorophyll, month, oxygen saturation, salinity, wind speed) were highly significant. It is important to note that only very little of the main peaks in walrus calling activity were included in the GAM runs. Just the fall end of the summer pulse in calling activity was included for all locations in 2010 and at the midshore location in 2011-12. There was just one instance (2010-11; offshore) where the beginning portion of the winter pulse in calling activity was included (Appendix G., Section XVIII.G).

When plotted with ice and nutrients, a strong negative correlation with ice was evident at the inshore and midshore locations, though not at the offshore location (Figure 119-121). For the inshore and midshore locations, walrus calling activity began to increase when the ice was breaking up in the early summer, peaked during the ice-free summer months, and decreased when the ice began forming again; however, there was low levels of calling activity overwinter at both of these locations. The offshore location had two calling peaks, one during the ice-free summer months, and one over winter when ice was present. There was a strong correlation with chlorophyll in 2011-2012. Peak calling activity followed the peak in chlorophyll at the midshore and offshore locations in fall 2011, and aligned well in spring 2012 at the inshore location. There is also a possible association with oxygen saturation at the inshore and midshore locations.

The results correlating the shipboard walrus visual and acoustic detections with the transect line data are presented in Figure 123-128. Generally, walrus were strongly associated with high levels of nitrate and ammonium, as well as high concentrations of *Pseudocalanus* and larvaceans. At the Wainwright transect line, walrus were consistently sighted in areas that had high concentrations of *Pseudocalanus* and larvaceans. These also corresponded with areas of high nitrate and ammonium levels (Figure 123-128). In 2012, interestingly, walrus were not associated with high zooplankton levels, although there were still high nitrate levels (Figure 125). Even though walrus do not eat zooplankton, high zooplankton concentrations are usually indicative of high productivity, and high benthic biomass. At the Icy Cape transect line, walrus were again associated with high levels of nitrate and ammonium (Figure 126-128). In 2010, walrus were also strongly associated with salinity (Figure 126). In 2011 there was a strong correlation with zooplankton, though this was less obvious in the other years (Figure 127). Overall, there were many visual sightings of walrus, though only a handful of acoustic detections.

TABLE 26. WALRUS RESULTS OF THE GAM MODEL. RESULTS REPRESENT THE TOP AIC MODEL (LOWEST AIC VALUE), AND THE COMMON SIGNIFICANT (P<0.05) VARIABLES AMONG THE TOP AIC AND THE TOP R-SQUARED MODELS. GREEN = HIGHLY SIGNIFICANT, P<0.01. YELLOW = SIGNIFICANT, P<0.05. RED = NOT SIGNIFICANT.

	Inshore	Mid-Shore	Offshore
Top AIC model		ADCP_botSv	
		ADCP_colSa	
		Chlorophyll	
	IceThick_std		
		Month	Month
	Nitrate	Nitrate	
		O2_%sat	
	PAR	PAR	PAR
		Salinity	
	Temperature		
			Turbidity
	Wind_spd	Wind_spd	
		Wind_u	
Common sign. variables		ADCP_botV Month O2_%sat Salinity Wind_spd	Month

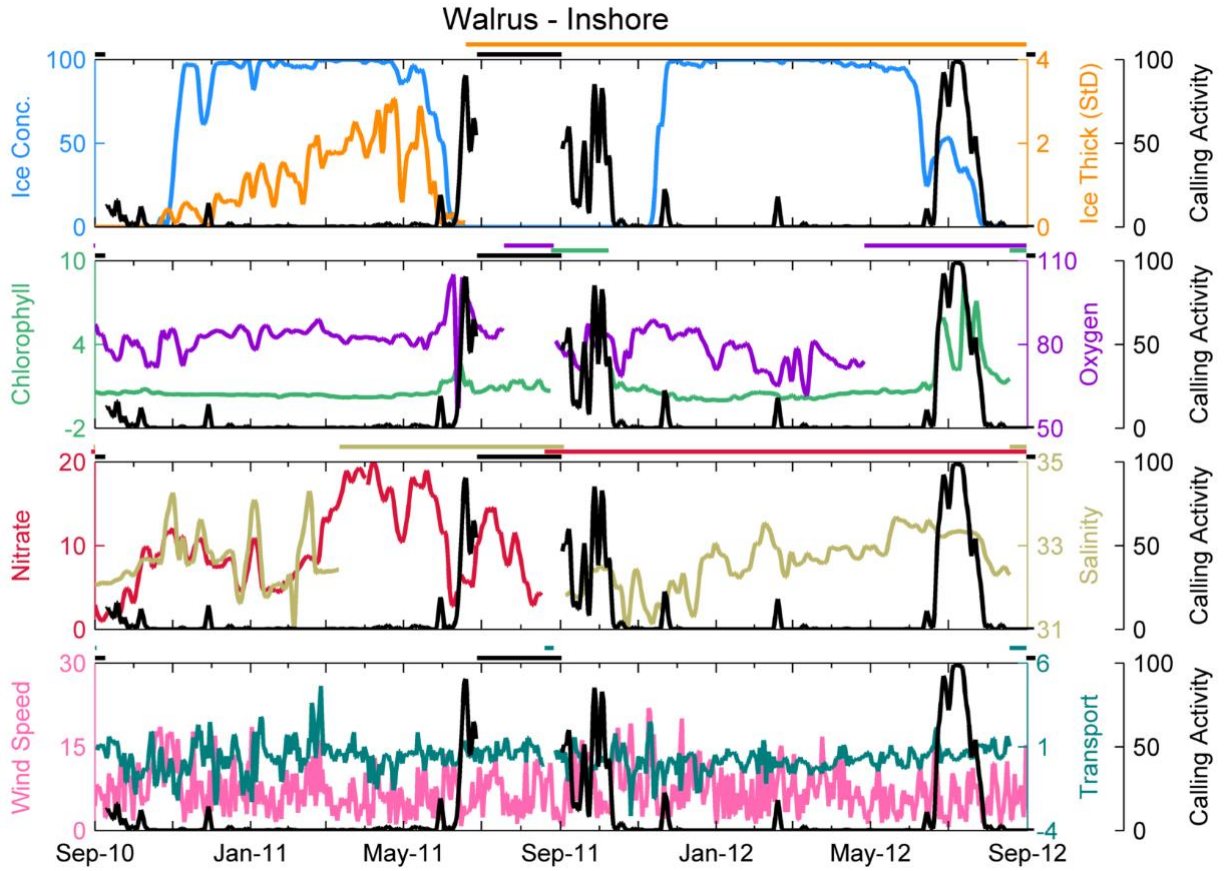


FIGURE 119. WALRUS CALLING ACTIVITY AS IT RELATES TO OCEANOGRAPHIC VARIABLES AT THE INSHORE LOCATION, 2010-2012. BLACK LINE = PERCENT OF TIME INTERVALS WITH CALLS. TOP ROW: PERCENT ICE CONCENTRATION (BLUE LINE) AND STANDARD DEVIATION ICE THICKNESS (M; ORANGE LINE). SECOND ROW: CHLOROPHYLL ($\mu\text{G/L}$; GREEN LINE) AND PERCENT OXYGEN SATURATION (PURPLE LINE). THIRD ROW: NITRATE (μM ; RED LINE) AND SALINITY (PSU; TAN LINE). BOTTOM ROW: WIND SPEED (M/S; PINK LINE) AND TRANSPORT (SV; TEAL LINE). HORIZONTAL BARS ABOVE EACH ROW INDICATE TIMES WITH NO DATA. ALL DATA EXCEPT WIND SPEED ARE PRESENTED AS A 3-DAY MOVING AVERAGE.

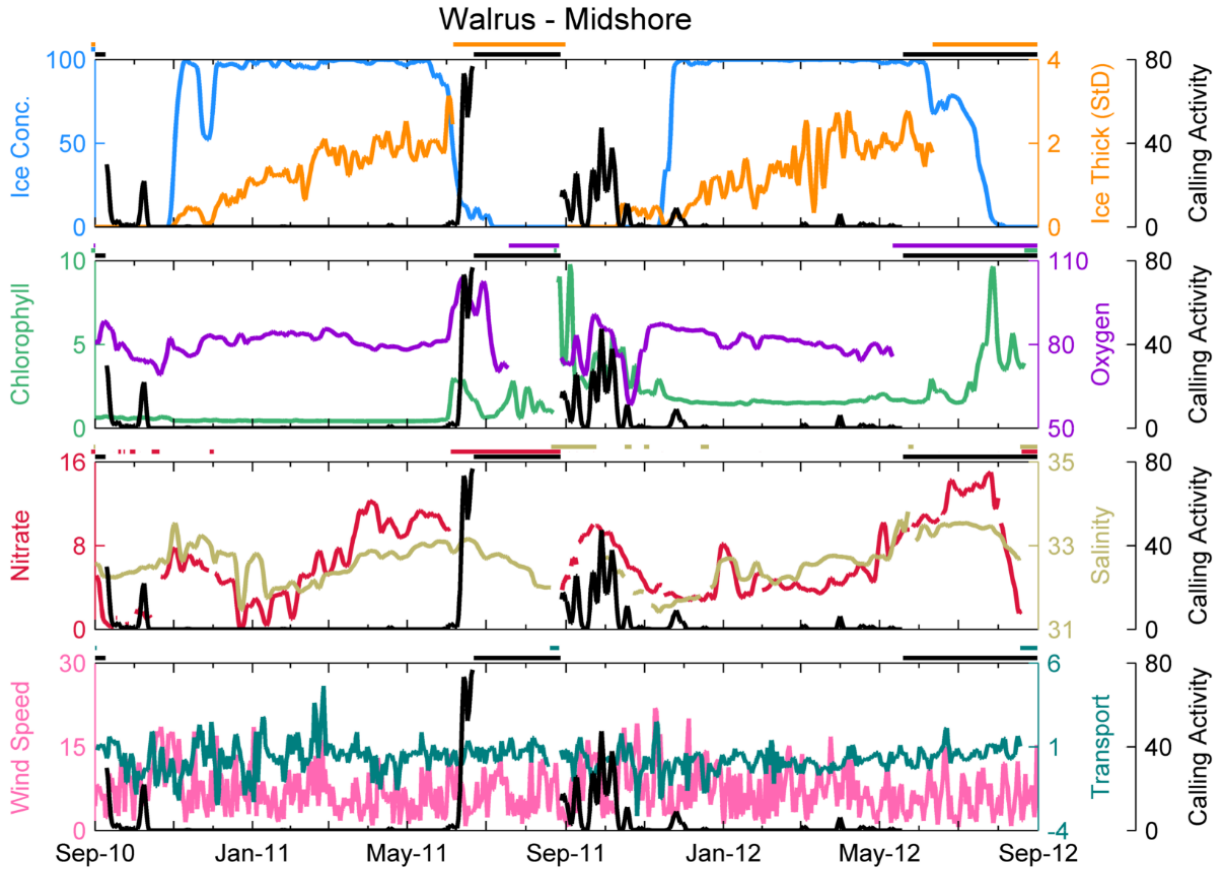


FIGURE 120. WALRUS CALLING ACTIVITY AS IT RELATES TO OCEANOGRAPHIC VARIABLES AT THE MIDSHORE LOCATION, 2010-2012. BLACK LINE = PERCENT OF TIME INTERVALS WITH CALLS. TOP ROW: PERCENT ICE CONCENTRATION (BLUE LINE) AND STANDARD DEVIATION ICE THICKNESS (M; ORANGE LINE). SECOND ROW: CHLOROPHYLL ($\mu\text{G/L}$; GREEN LINE) AND PERCENT OXYGEN SATURATION (PURPLE LINE). THIRD ROW: NITRATE (μM ; RED LINE) AND SALINITY (PSU; TAN LINE). BOTTOM ROW: WIND SPEED (M/S; PINK LINE) AND TRANSPORT (SV; TEAL LINE). HORIZONTAL BARS ABOVE EACH ROW INDICATE TIMES WITH NO DATA. ALL DATA EXCEPT WIND SPEED ARE PRESENTED AS A 3-DAY MOVING AVERAGE.

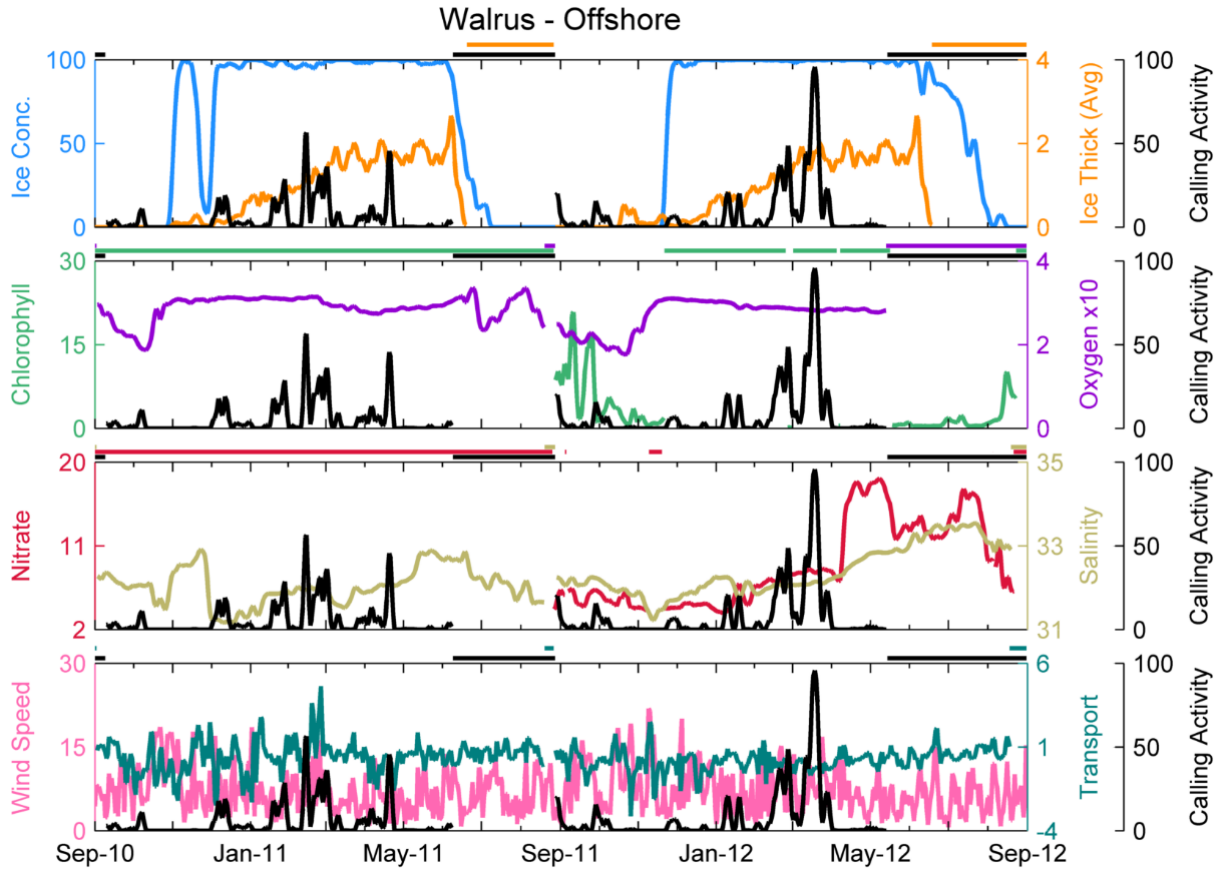


FIGURE 121. WALRUS CALLING ACTIVITY AS IT RELATES TO OCEANOGRAPHIC VARIABLES AT THE OFFSHORE LOCATION, 2010-2012. BLACK LINE = PERCENT OF TIME INTERVALS WITH CALLS. TOP ROW: PERCENT ICE CONCENTRATION (BLUE LINE) AND AVERAGE ICE THICKNESS (M; ORANGE LINE). SECOND ROW: CHLOROPHYLL ($\mu\text{G/L}$; GREEN LINE) AND PERCENT OXYGEN SATURATION (PURPLE LINE). THIRD ROW: NITRATE (μM ; RED LINE) AND SALINITY (PSU; TAN LINE). BOTTOM ROW: WIND SPEED (M/S; PINK LINE) AND TRANSPORT (SV; TEAL LINE). HORIZONTAL BARS ABOVE EACH ROW INDICATE TIMES WITH NO DATA. ALL DATA EXCEPT WIND SPEED ARE PRESENTED AS A 3-DAY MOVING AVERAGE.

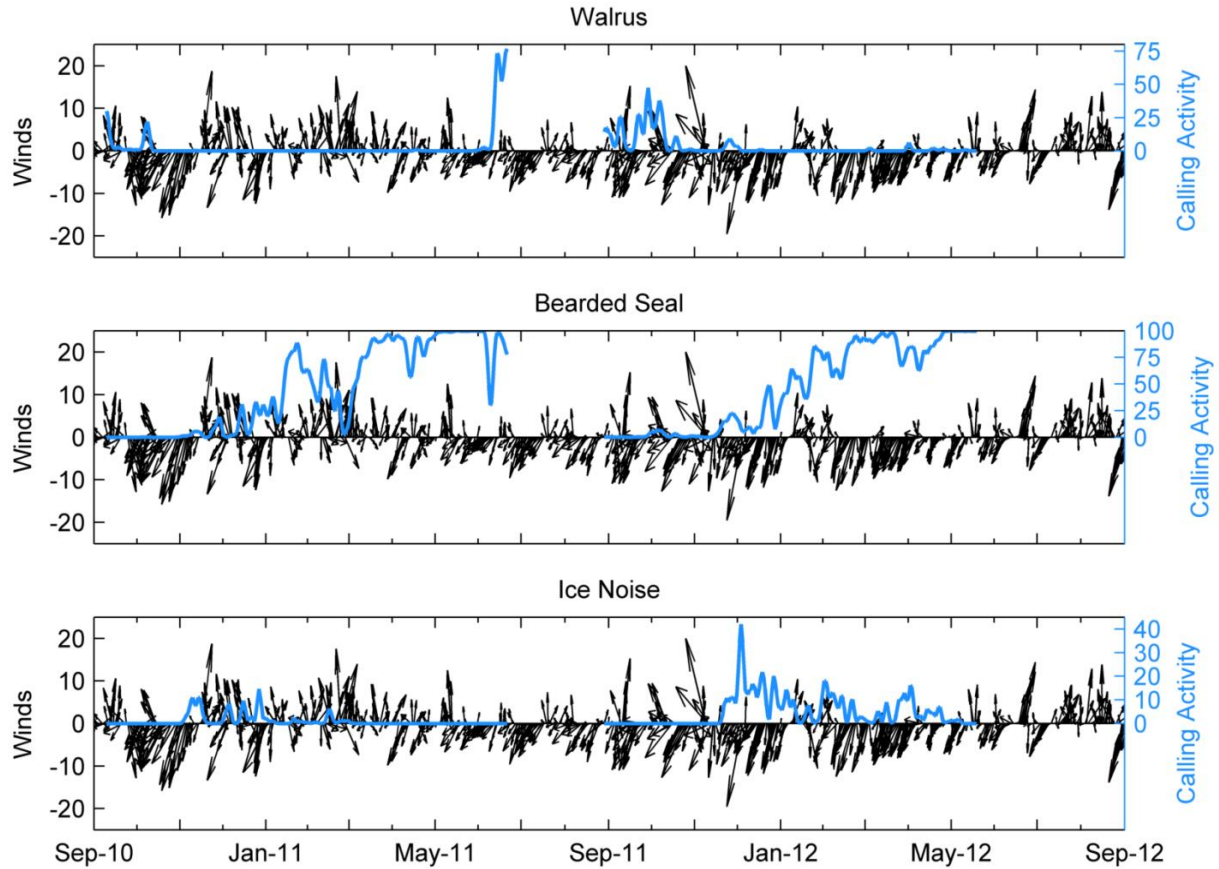


FIGURE 122. MARINE MAMMAL CALLING ACTIVITY (BLUE LINE) VS. WINDS (M/S; BLACK LINE) AT THE MIDSHORE LOCATION, 2010-2012. ARROWS (USING THE OCEANOGRAPHIC CONVENTION) INDICATE THE DIRECTION THE WINDS ARE BLOWING TOWARD, (I.E., AN ARROW POINTING TO THE TOP OF THE PAGE INDICATES WINDS BLOWING FROM THE SOUTH AND TO THE NORTH). LENGTH OF WIND VECTOR INDICATES SPEED. TOP ROW: WALRUS. MIDDLE ROW: BEARDED SEAL. BOTTOM ROW: ICE NOISE. NOTE CALLING ACTIVITY Y-AXIS IS NOT ON THE SAME SCALE.

Wainwright, 2010

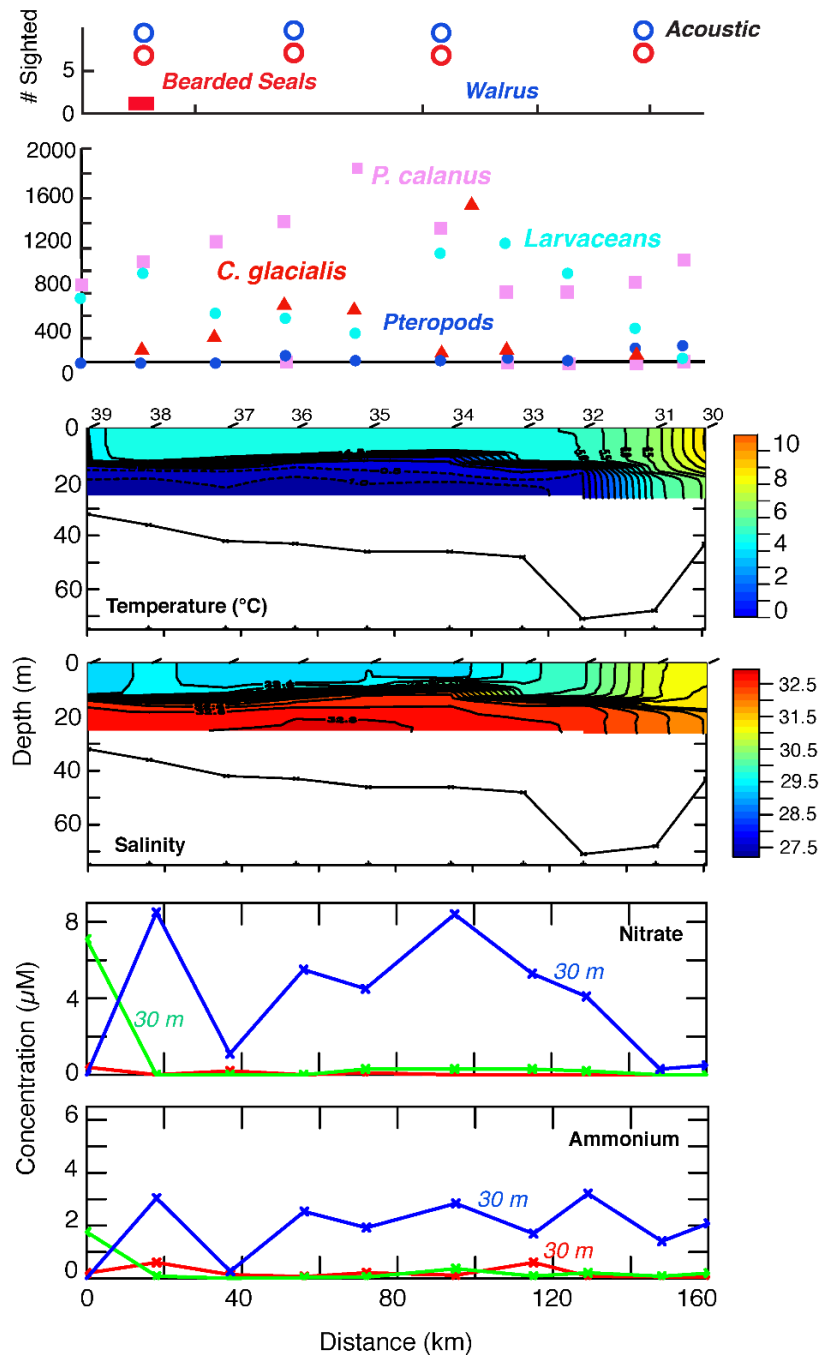


FIGURE 123. WAINWRIGHT TRANSECT LINE OCEANOGRAPHIC, ZOOPLANKTON, WALRUS, AND BEARDED SEAL SURVEY RESULTS, 2010. X-AXIS REFERS TO DISTANCE ALONG TRANSECT, WHERE 0 KM = STATION 1 ALONG TRANSECT. TOP ROW = SONOBUOY EFFORT AND DETECTIONS AND VISUAL SIGHTINGS (INCLUDING # OF INDIVIDUALS) OF WALRUS AND BEARDED SEALS; OPEN CIRCLE = SONOBUOY DEPLOYED BUT NO DETECTIONS, CLOSED CIRCLE = ACOUSTIC DETECTION, BEARDED SEALS = RED SQUARE. SECOND ROW = ZOOPLANKTON DENSITY AT EACH TRANSECT STATION; *PSEUDOCALANUS* (ABBREVIATED *P. CALANUS*) = PINK SQUARE, *C. GLACIALIS* = RED TRIANGLE, LARVACEANS = TURQUOISE CIRCLE, PTEROPODS = BLUE CIRCLE. THIRD ROW = TEMPERATURE (°C). FOURTH ROW = SALINITY (PSU). FIFTH ROW = NITRATE (μM). BOTTOM ROW = AMMONIUM (μM).

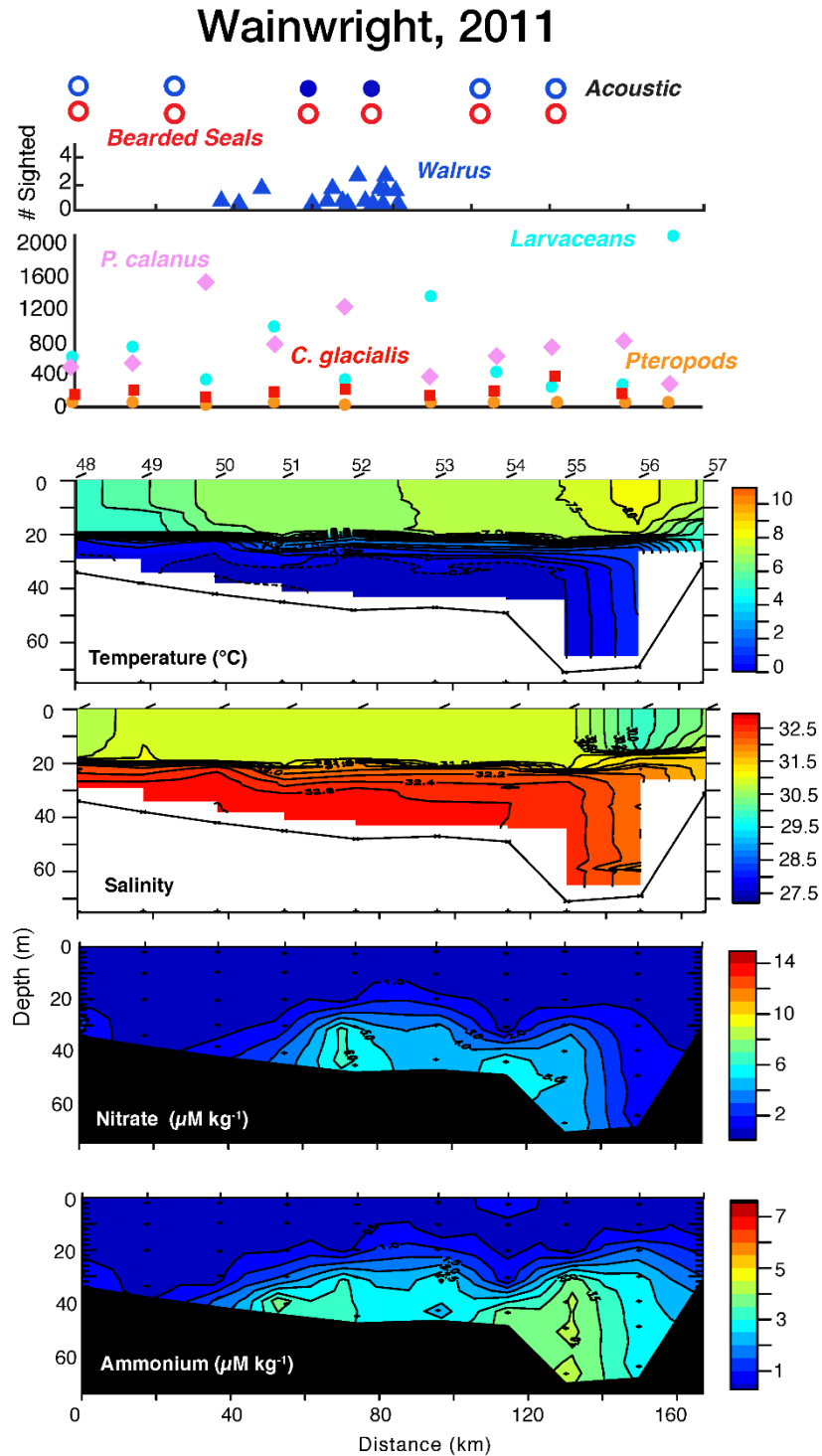


FIGURE 124. WAINWRIGHT TRANSECT LINE OCEANOGRAPHIC, ZOOPLANKTON, WALRUS, AND BEARDED SEAL SURVEY RESULTS, 2011. X-AXIS REFERS TO DISTANCE ALONG TRANSECT, WHERE 0 KM = STATION 1 ALONG TRANSECT. TOP ROW = SONOBUOY EFFORT AND DETECTIONS AND VISUAL SIGHTINGS (INCLUDING # OF INDIVIDUALS) OF WALRUS AND BEARDED SEALS; OPEN CIRCLE = SONOBUOY DEPLOYED BUT NO DETECTIONS, CLOSED CIRCLE = ACOUSTIC DETECTION, WALRUS = BLUE TRIANGLES. SECOND ROW = ZOOPLANKTON DENSITY AT EACH TRANSECT STATION; *PSEUDOCALANUS* (ABBREVIATED *P. CALANUS*) = PINK DIAMOND, *C. GLACIALIS* = RED SQUARE, LARVACEANS = TURQUOISE CIRCLE, PTEROPODS = ORANGE CIRCLE. THIRD ROW = TEMPERATURE (°C). FOURTH ROW = SALINITY (PSU). FIFTH ROW = NITRATE (μM). BOTTOM ROW = AMMONIUM (μM).

Wainwright , 2012

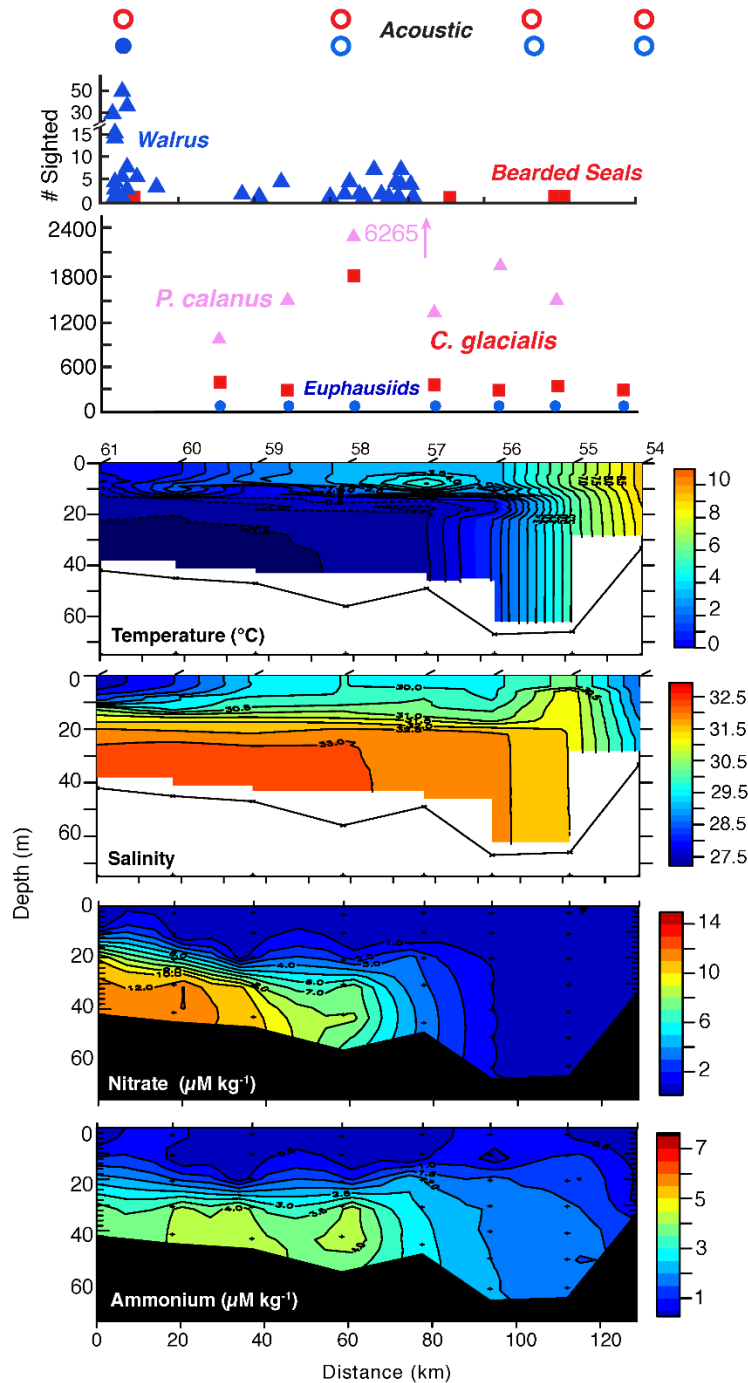


FIGURE 125. WAINWRIGHT TRANSECT LINE OCEANOGRAPHIC, ZOOPLANKTON, WALRUS, AND BEARDED SEAL SURVEY RESULTS, 2012. X-AXIS REFERS TO DISTANCE ALONG TRANSECT, WHERE 0 KM = STATION 1 ALONG TRANSECT. TOP ROW = SONOBUOY EFFORT AND DETECTIONS AND VISUAL SIGHTINGS (INCLUDING # OF INDIVIDUALS) OF WALRUS AND BEARDED SEALS; OPEN CIRCLE = SONOBUOY DEPLOYED BUT NO DETECTIONS, CLOSED CIRCLE = ACOUSTIC DETECTION, WALRUS = BLUE TRIANGLES, BEARDED SEALS = RED SQUARES. SECOND ROW = ZOOPLANKTON DENSITY AT EACH TRANSECT STATION; *PSEUDOCALANUS* (ABBREVIATED *P. CALANUS*) = PINK TRIANGLE, *C. GLACIALIS* = RED SQUARE, EUPHAUSIIDS = BLUE CIRCLE. THIRD ROW = TEMPERATURE (°C). FOURTH ROW = SALINITY (PSU). FIFTH ROW = NITRATE (μM). BOTTOM ROW = AMMONIUM (μM).

Icy Cape, 2010

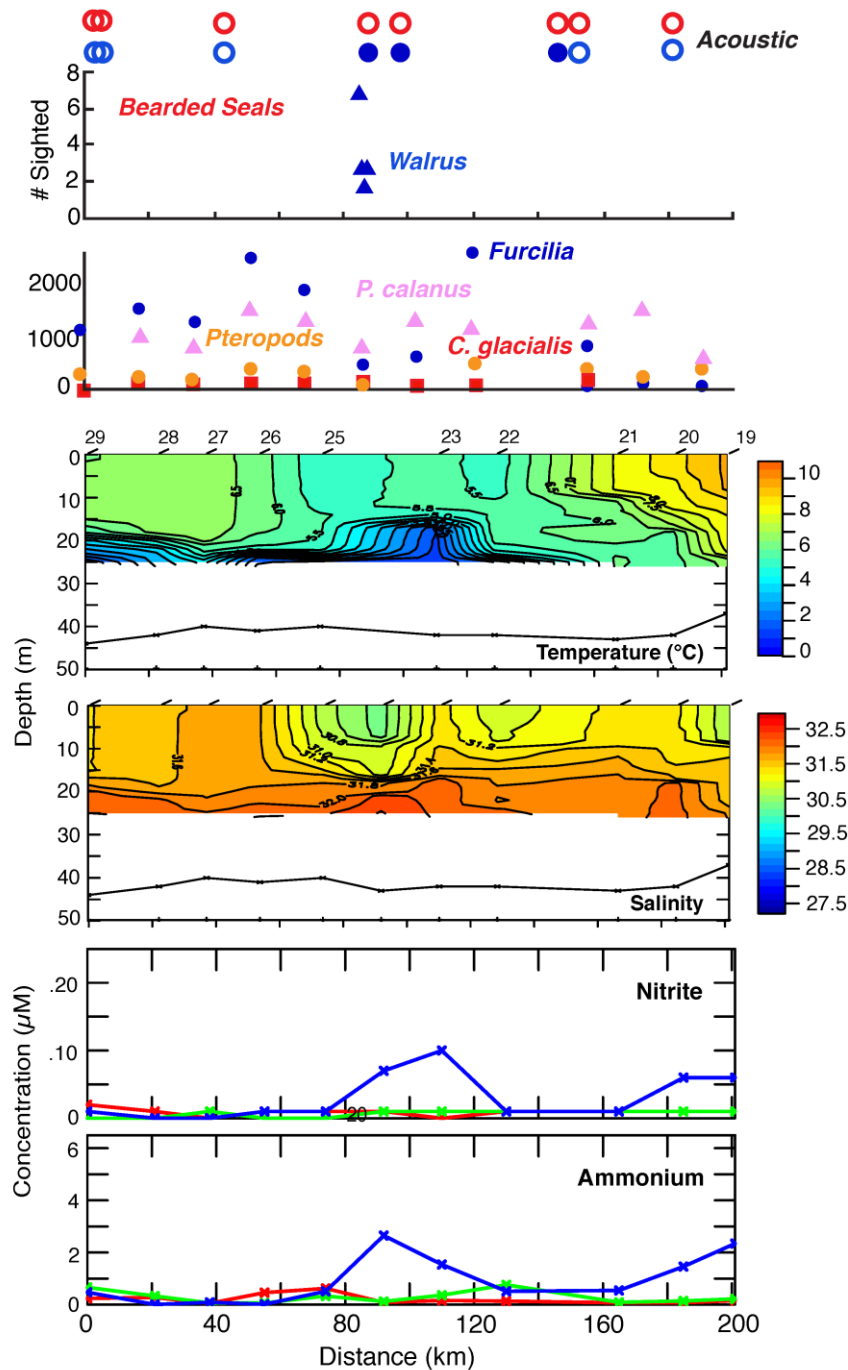


FIGURE 126. ICY CAPE TRANSECT LINE OCEANOGRAPHIC, ZOOPLANKTON, WALRUS, AND BEARDED SEAL SURVEY RESULTS, 2010. X-AXIS REFERS TO DISTANCE ALONG TRANSECT, WHERE 0 KM = STATION 1 ALONG TRANSECT. TOP ROW = SONOBUOY EFFORT AND DETECTIONS AND VISUAL SIGHTINGS (INCLUDING # OF INDIVIDUALS) OF WALRUS AND BEARDED SEALS; OPEN CIRCLE = SONOBUOY CIRCLE = SONOBUOY DEPLOYED BUT NO DETECTIONS, CLOSED CIRCLE = ACOUSTIC DETECTION, WALRUS = BLUE TRIANGLES. SECOND ROW = ZOOPLANKTON DENSITY AT EACH TRANSECT STATION; *PSEUDOCALANUS* (ABBREVIATED *P. CALANUS*) = PINK TRIANGLE, *C. GLACIALIS* = RED SQUARE, FURCILIA = BLUE CIRCLE, PTEROPODS = ORANGE CIRCLE. THIRD ROW = TEMPERATURE (°C). FOURTH ROW = SALINITY (PSU). FIFTH ROW = NITRATE (µM). BOTTOM ROW = AMMONIUM (µM).

Icy Cape, 2011

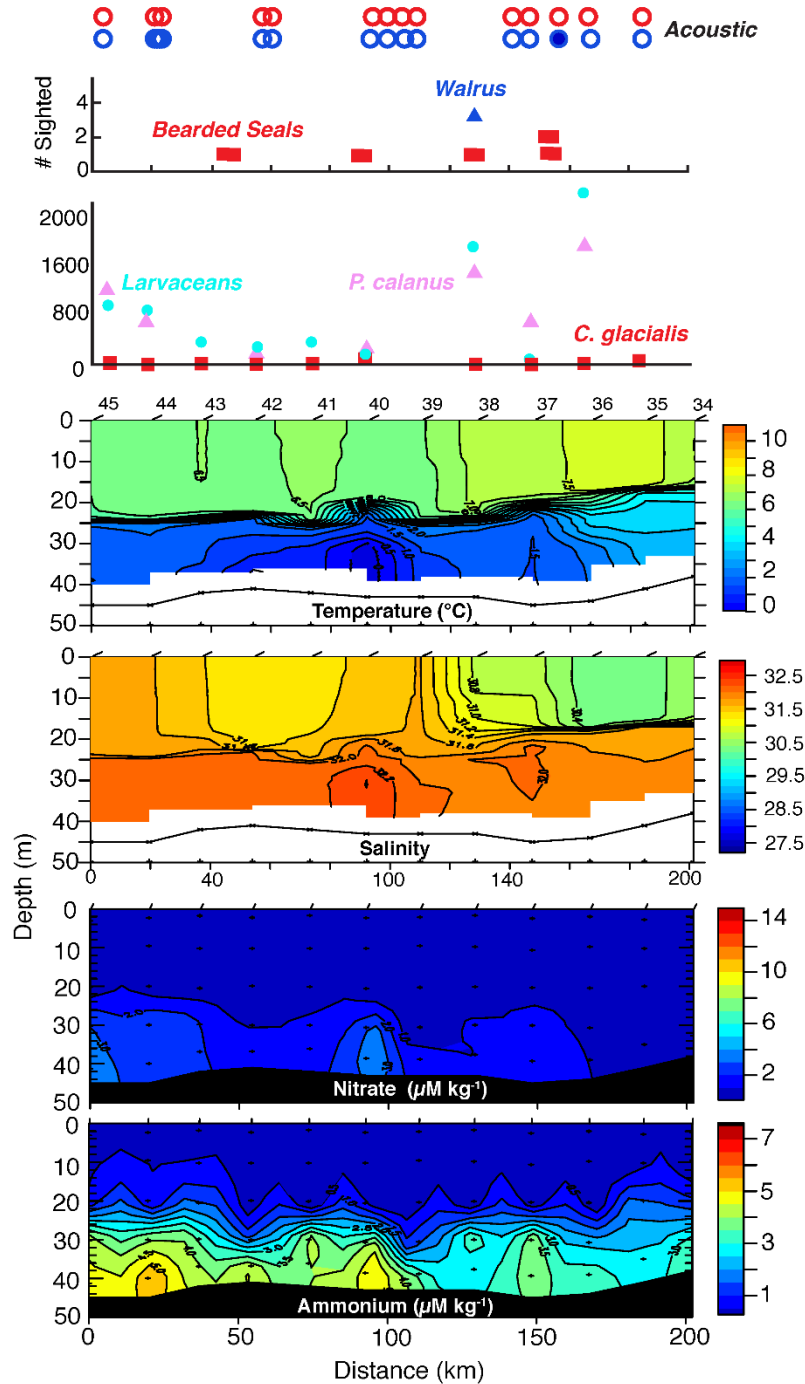


FIGURE 127. ICY CAPE TRANSECT LINE OCEANOGRAPHIC, ZOOPLANKTON, WALRUS, AND BEARDED SEAL SURVEY RESULTS, 2011. X-AXIS REFERS TO DISTANCE ALONG TRANSECT, WHERE 0 KM = STATION 1 ALONG TRANSECT. TOP ROW = SONOBUOY EFFORT AND DETECTIONS AND VISUAL SIGHTINGS (INCLUDING # OF INDIVIDUALS) OF WALRUS AND BEARDED SEALS; OPEN CIRCLE = SONOBUOY DEPLOYED BUT NO DETECTIONS, CLOSED CIRCLE = ACOUSTIC DETECTION, WALRUS = BLUE TRIANGLE, BEARDED SEALS = RED SQUARES. SECOND ROW = ZOOPLANKTON DENSITY AT EACH TRANSECT STATION; *PSEUDOCALANUS* (ABBREVIATED *P. CALANUS*) = PINK TRIANGLE, *C. GLACIALIS* = RED SQUARE, LARVACEANS = TURQUOISE CIRCLE. THIRD ROW = TEMPERATURE (°C). FOURTH ROW = SALINITY (PSU). FIFTH ROW = NITRATE (μM). BOTTOM ROW = AMMONIUM (μM).

Icy Cape, 2012

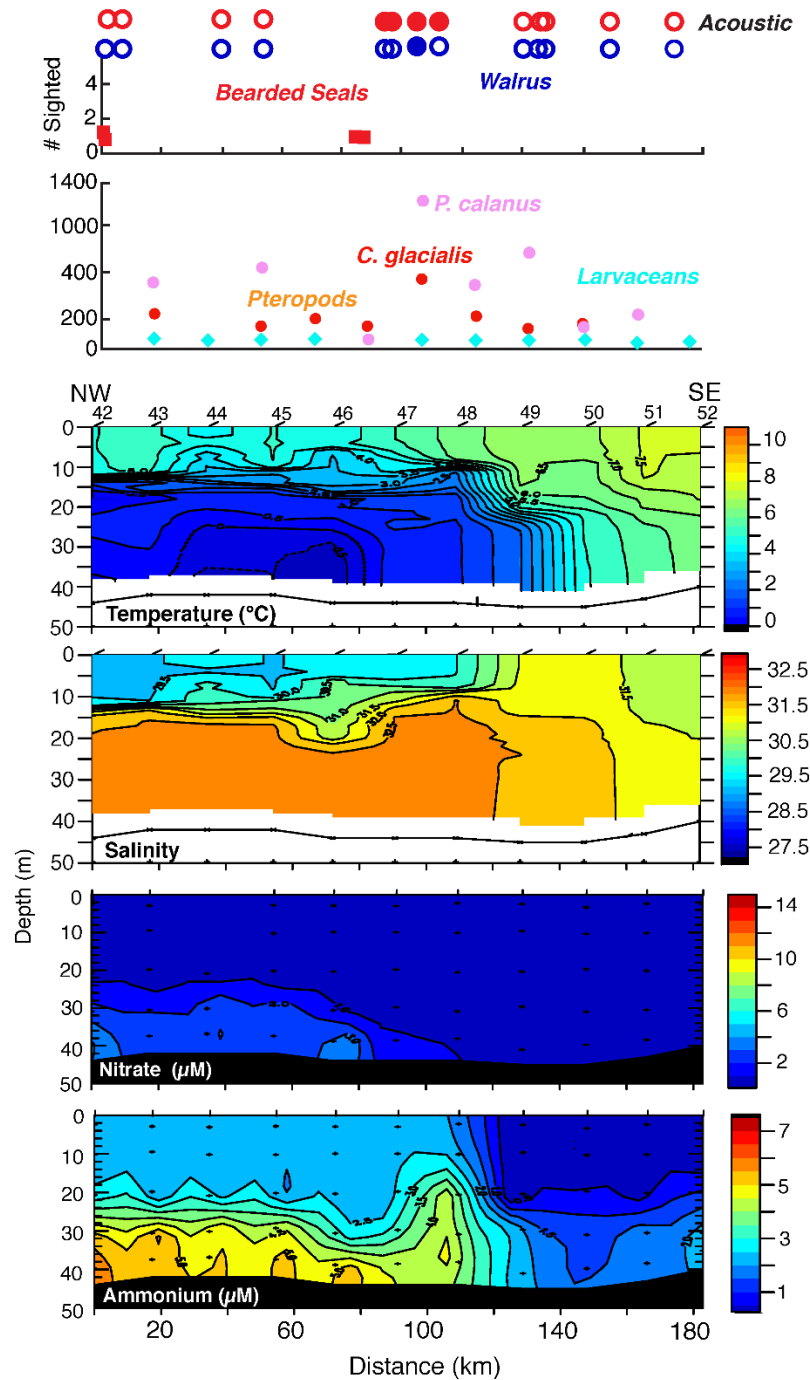


FIGURE 128. ICY CAPE TRANSECT LINE OCEANOGRAPHIC, ZOOPLANKTON, WALRUS, AND BEARDED SEAL SURVEY RESULTS, 2012. X-AXIS REFERS TO DISTANCE ALONG TRANSECT, WHERE 0 KM = STATION 1 ALONG TRANSECT. TOP ROW = SONOBUOY EFFORT AND DETECTIONS AND VISUAL SIGHTINGS (INCLUDING # OF INDIVIDUALS) OF WALRUS AND BEARDED SEALS; OPEN CIRCLE = SONOBUOY DEPLOYED BUT NO DETECTIONS, CLOSED CIRCLE = ACOUSTIC DETECTION, BEARDED SEALS = RED SQUARES. SECOND ROW = ZOOPLANKTON DENSITY AT EACH TRANSECT STATION; *PSEUDOCALANUS* (ABBREVIATED *P. CALANUS*) = PINK CIRCLE, *C. GLACIALIS* = RED CIRCLE, LARVACEANS = TURQUOISE DIAMONDS, PTEROPODS = ORANGE CIRCLE. THIRD ROW = TEMPERATURE (°C). FOURTH ROW = SALINITY (PSU). FIFTH ROW = NITRATE (µM). BOTTOM ROW = AMMONIUM (µM).

Bearded seal

The bearded seal GAM results are presented in Table 27. Of the common significant variables for the top AIC models and the top R-Squared models, only month was consistent for all locations. There were three common significant variables for the midshore location: ADCP volume backscatter (bottom), ice concentration, month, transport, and wind speed. Eleven variables were included in the top midshore model, of which seven (ADCP volume backscatter (bottom), bottom currents (V), ice concentration, month, salinity, transport, wind speed) were significant. Again, while most of the midshore data were included in the GAM (with the exception of the time period with the rapid drop in calling activity), the inshore and offshore data only included the first year, and stopped well before calling activity neared 100%.

The plots correlating bearded seal calling activity with the oceanographic variables at all locations are presented in Figure 129-131. Bearded seal calling activity was positively associated with ice. Peak calling activity occurred with ice cover, and calling activity increased simultaneously with ice thickness. Calling stopped shortly after ice concentration dropped. At the offshore location in 2011-12, there was an unusually deep, persistent ice keel, with a simultaneous drop in bearded seal calling activity (Figure 131). There is a loose association between calling activity and salinity, with both increasing simultaneously. Nitrate also increases as bearded seal calling activity increases, though with a slight delayed effect. There were no evident correlations with winds, despite wind speed being a common significant variable contributing to the top AIC and R-squared models selected by the GAM runs for both the inshore and midshore locations. There was only a slight association in 2011-12 with winds to the SSW (Figure 122, middle row).

The results of the shipboard bearded seal visual and acoustic data with the transect line sampling data are combined with the walrus data, and are presented in Figure 123-128. Generally, bearded seal results were similar to walrus. Bearded seals were associated with high densities of *Pseudocalanus* and larvaceans, and somewhat associated with nitrate and ammonium. At the Wainwright transect line, bearded seals were associated with high densities of *Pseudocalanus* (Figure 123-128). There were no bearded seals seen or acoustically detected on the transect in 2011. Interestingly, in 2012, bearded seals were generally detected at the inshore stations, unlike the walrus (Figure 125). There were high amounts of *Pseudocalanus* at these stations, though no obvious associations with the other measurements. At the Icy Cape line, there were no bearded seals seen or acoustically detected in 2010. In 2011, bearded seals were sighted all along the transect line. They were associated with high levels of *Pseudocalanus* and larvacean densities, and somewhat associated with nitrate and ammonium peaks (Figure 127). In 2012, bearded seals were associated with high ammonium levels, though interestingly there were no obvious correlations with zooplankton (Figure 128). Similar to walrus, bearded seals were visually sighted numerous times, but were rarely acoustically detected.

TABLE 27. BEARDED SEAL RESULTS OF THE GAM MODEL. RESULTS REPRESENT THE TOP AIC MODEL (LOWEST AIC VALUE), AND THE COMMON SIGNIFICANT (P<0.05) VARIABLES AMONG THE TOP AIC AND THE TOP R-SQUARED MODELS. GREEN = HIGHLY SIGNIFICANT, P<0.01. YELLOW = SIGNIFICANT, P<0.05. RED = NOT SIGNIFICANT.

	Inshore	Mid-Shore	Offshore
Top AIC model	ADCP_botSv	ADCP_botSv	ADCP_botSv
		ADCP_colSa	ADCP_colSa
	Currents_botU		
	Currents_botV	Currents_botV	
		Ice_conc	Ice_conc
	Month	Month	Month
		O2_mmol	
	Nitrate	Nitrate	
	PAR		PAR
	Salinity	Salinity	
		Transport	
		Turbidity	Turbidity
	Wind_spd	Wind_spd	
Wind_v		Wind_v	
Common sign. variables		ADCP_botV	ADCP_CoIA
	Currents_botV		
	Month	Ice_conc Month Transport	Month
	Wind_spd	Wind_spd	

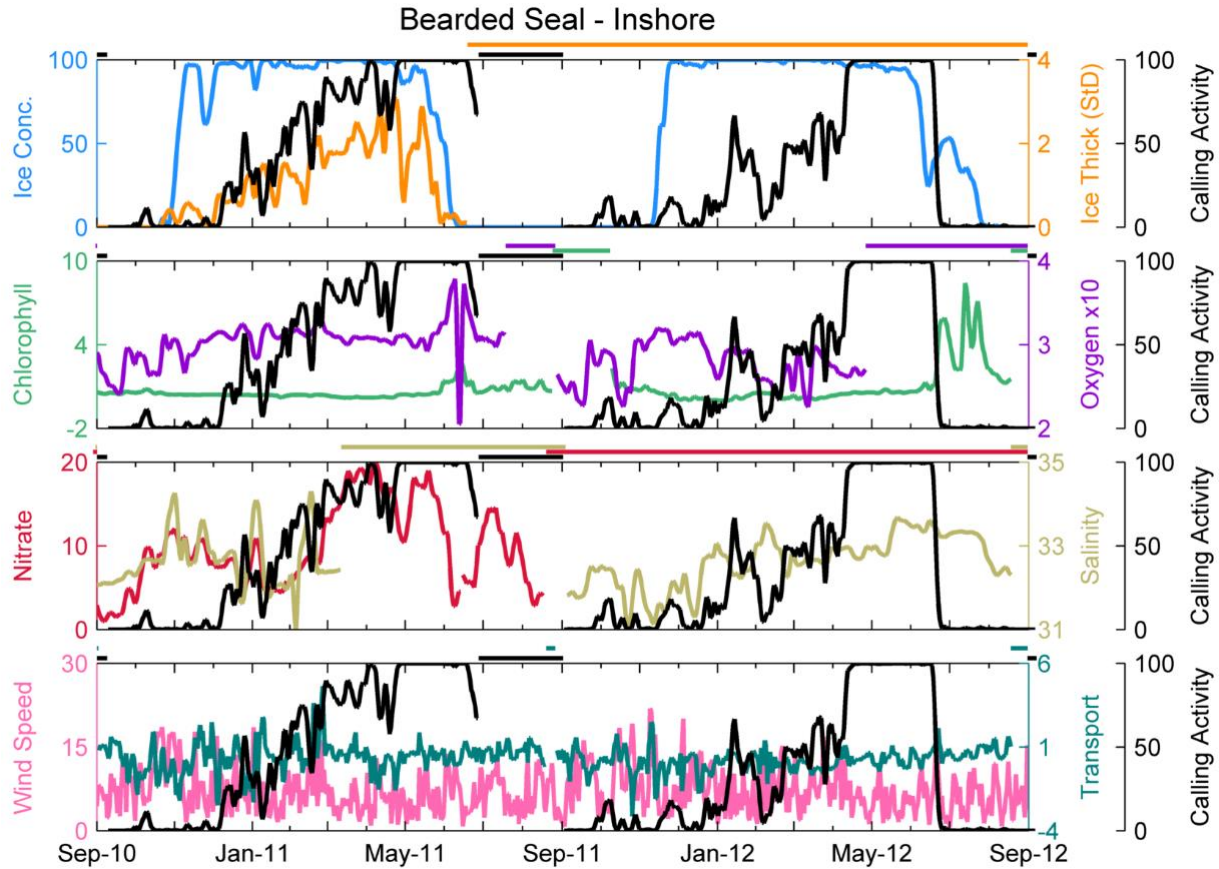


FIGURE 129. BEARDED SEAL CALLING ACTIVITY AS IT RELATES TO OCEANOGRAPHIC VARIABLES AT THE INSHORE LOCATION, 2010-2012. BLACK LINE = PERCENT OF TIME INTERVALS WITH CALLS. TOP ROW: PERCENT ICE CONCENTRATION (BLUE LINE) AND AVERAGE ICE THICKNESS (M; ORANGE LINE). SECOND ROW: CHLOROPHYLL ($\mu\text{G/L}$; GREEN LINE) AND OXYGEN (M X 10 ; PURPLE LINE). THIRD ROW: NITRATE (μM ; RED LINE) AND SALINITY (PSU; TAN LINE). BOTTOM ROW: WIND SPEED (M/S; PINK LINE) AND TRANSPORT (SV; TEAL LINE). HORIZONTAL BARS ABOVE EACH ROW INDICATE TIMES WITH NO DATA. ALL DATA EXCEPT WIND SPEED ARE PRESENTED AS A 3-DAY MOVING AVERAGE.

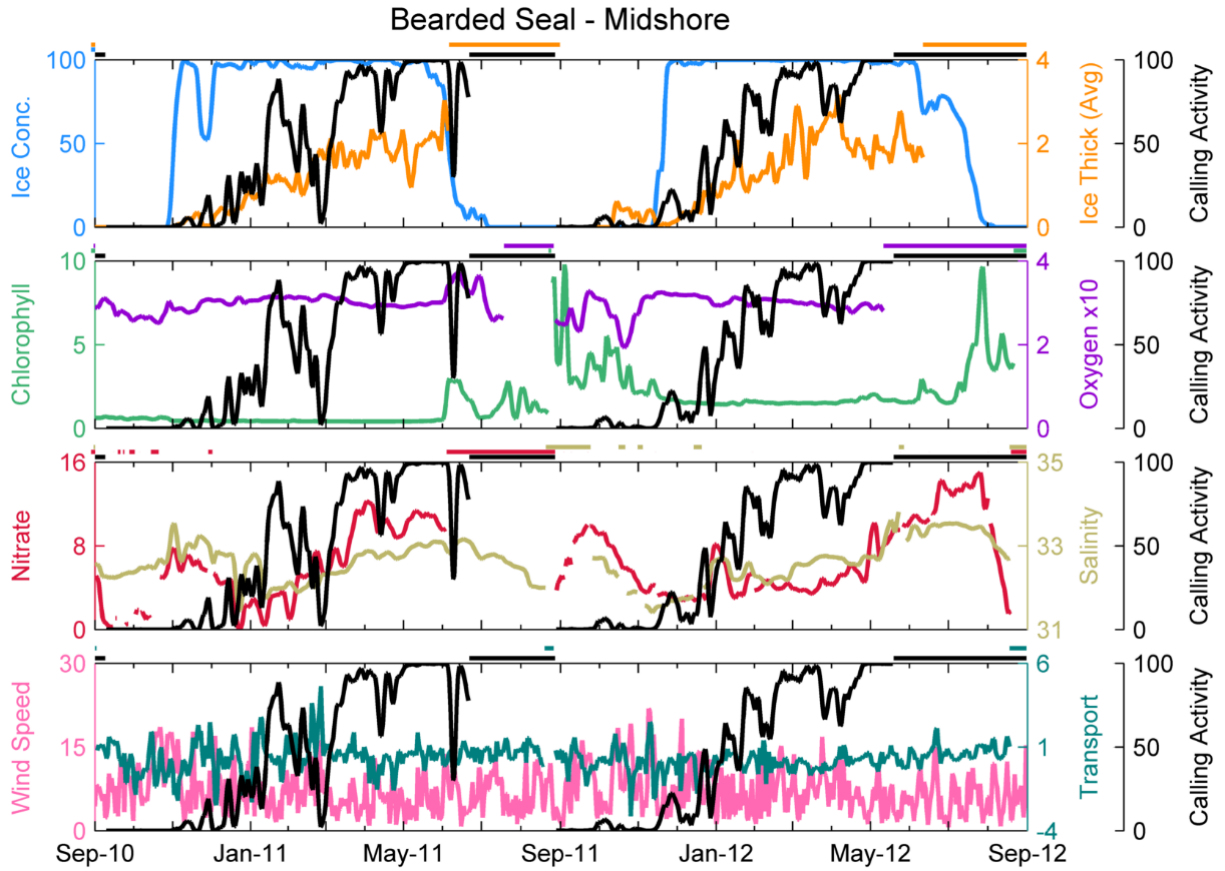


FIGURE 130. BEARDED SEAL CALLING ACTIVITY AS IT RELATES TO OCEANOGRAPHIC VARIABLES AT THE MIDSHORE LOCATION, 2010-2012. BLACK LINE = PERCENT OF TIME INTERVALS WITH CALLS. TOP ROW: PERCENT ICE CONCENTRATION (BLUE LINE) AND AVERAGE ICE THICKNESS (M; ORANGE LINE). SECOND ROW: CHLOROPHYLL ($\mu\text{G/L}$; GREEN LINE) AND OXYGEN ($\text{M} \times 10$; PURPLE LINE). THIRD ROW: NITRATE (μM ; RED LINE) AND SALINITY (PSU; TAN LINE). BOTTOM ROW: WIND SPEED (M/S; PINK LINE) AND TRANSPORT (SV; TEAL LINE). HORIZONTAL BARS ABOVE EACH ROW INDICATE TIMES WITH NO DATA. ALL DATA EXCEPT WIND SPEED ARE PRESENTED AS A 3-DAY MOVING AVERAGE.

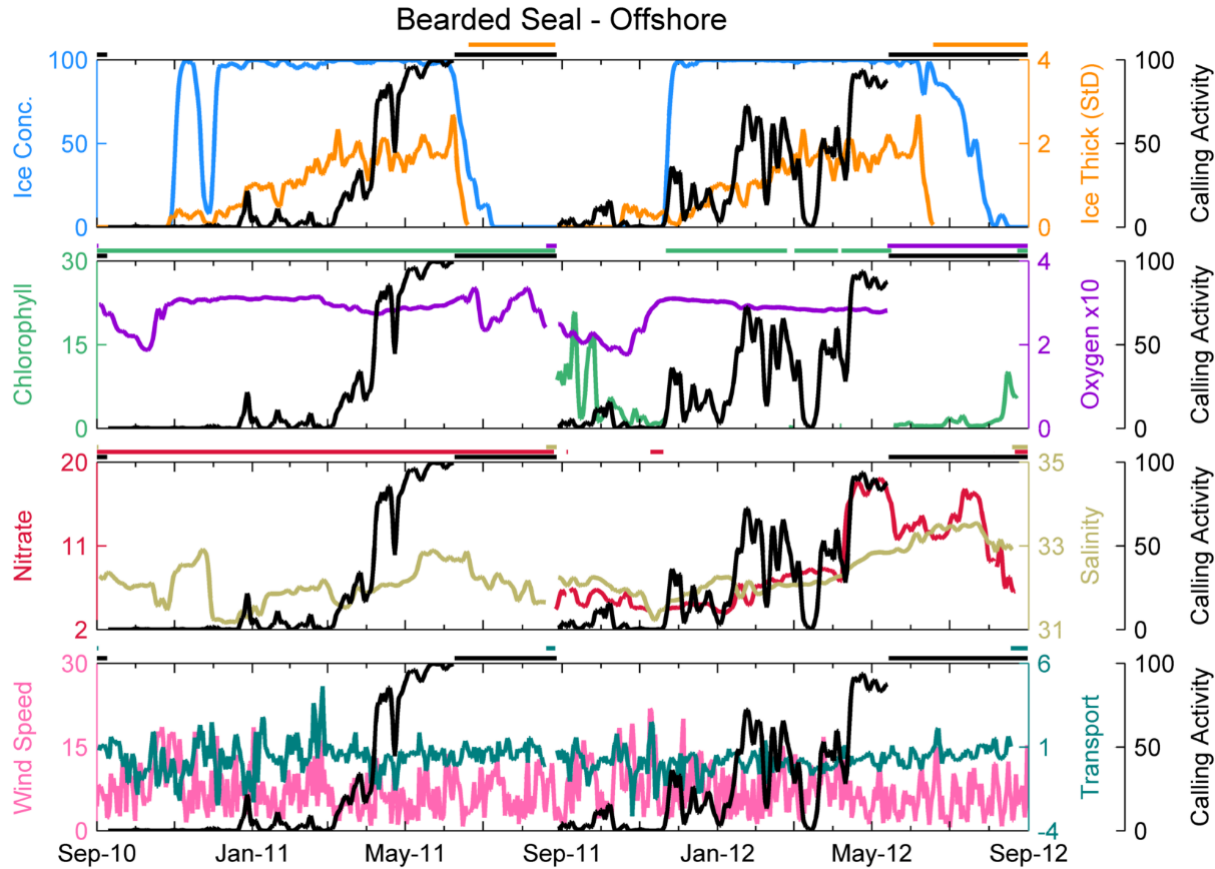


FIGURE 131. BEARDED SEAL CALLING ACTIVITY AS IT RELATES TO OCEANOGRAPHIC VARIABLES AT THE OFFSHORE LOCATION, 2010-2012. BLACK LINE = PERCENT OF TIME INTERVALS WITH CALLS. TOP ROW: PERCENT ICE CONCENTRATION (BLUE LINE) AND AVERAGE ICE THICKNESS (M; ORANGE LINE). SECOND ROW: CHLOROPHYLL ($\mu\text{G/L}$; GREEN LINE) AND OXYGEN ($\text{M} \times 10$; PURPLE LINE). THIRD ROW: NITRATE (μM ; RED LINE) AND SALINITY (PSU; TAN LINE). BOTTOM ROW: WIND SPEED (M/S; PINK LINE) AND TRANSPORT (SV; TEAL LINE). HORIZONTAL BARS ABOVE EACH ROW INDICATE TIMES WITH NO DATA. ALL DATA EXCEPT WIND SPEED ARE PRESENTED AS A 3-DAY MOVING AVERAGE.

Ice noise

The results of the GAMs for ice noise are presented in Table 28. Again, the midshore location contained the largest amount of noise activity data, only the beginning of the 2010-11 pulse of ice noise activity was included in the offshore GAM run. The inshore location did a little better with over half the 2010-11 pulse included. The midshore location had three common significant variables: chlorophyll, ice concentration, and month. The top AIC model results for all three locations had only one variable that was both consistent and significant among all locations: ice concentration. Salinity was consistent among all locations, but was not significant at the midshore location. The top AIC model selected by the GAM run at the midshore location included eleven variables, of which chlorophyll, ice concentration, month, PAR, turbidity, and winds (U, V) were significant.

The long-term correlation plots for all locations are presented in Figure 132-134. Ice noise activity required the presence of ice, but the presence of ice did not guarantee ice noise activity, indicating that other factors are involved. There was a slight delay of approximately five days between the ice beginning to form ($>0\%$ ice concentration) and the first instance of ice

noise activity. Ice noise activity is present for only the first half of the total ice presence (determined by >0% ice concentration at the midshore and offshore location, but present throughout the ice period at the inshore location. Ice noise dropped dramatically when a polynya was formed in the fall of 2010 (best seen at the offshore location, Figure 134), resuming once the polynya was gone and ice concentration reached 100% again. There was no ice noise detected in spring of 2011 at the midshore and offshore locations, when ice concentration levels were decreasing. Although the midshore passive acoustic recorder failed before ice concentration reached zero, it was still collecting data when ice concentration dropped from 100% to less than 5%. Noise activity was present at the inshore location during the rapid decrease in ice noise in spring of both years – which can be seen clearly during the 2011-12 deployment. Overall, there was more ice noise activity in 2011-2012 than in the previous year. Ice noise activity also persisted longer in the spring of 2012 than the spring of 2011. There was a strong positive correlation between ice noise and wind (Figure 122, bottom row). In 2010-11, there was a slight association with winds to the north, and in 2011-12 there was a strong correlation with high winds to the SSW. There was a negative correlation between over-winter ice noise and chlorophyll at all locations in 2011-12, this trend seems to be present in the 2010-11 data as well.

TABLE 28. ICE NOISE RESULTS OF THE GAM MODEL. RESULTS REPRESENT THE TOP AIC MODEL (LOWEST AIC VALUE), AND THE COMMON SIGNIFICANT (P<0.05) VARIABLES AMONG THE TOP AIC AND THE TOP R-SQUARED MODELS. GREEN = HIGHLY SIGNIFICANT, P<0.01. YELLOW = SIGNIFICANT, P<0.05. RED = NOT SIGNIFICANT.

	Inshore	Mid-Shore	Offshore
Top AIC models	ADCP_botSv		
		ADCP_colSa	
		Chlorophyll	
	Currents_botU		
	Ice_conc	Ice_conc	Ice_conc
			IceThick_med
		Month	
	Nitrate	Nitrate	
		PAR	PAR
	Salinity	Salinity	Salinity
	Transport		
		Turbidity	Turbidity
	Winds_spd	Winds_spd	
Winds_u	Winds_u		
	Winds_v		
Common sign. variables	Currents_botU	Chlorophyll	
		Ice_conc	
		Month	IceThick_med

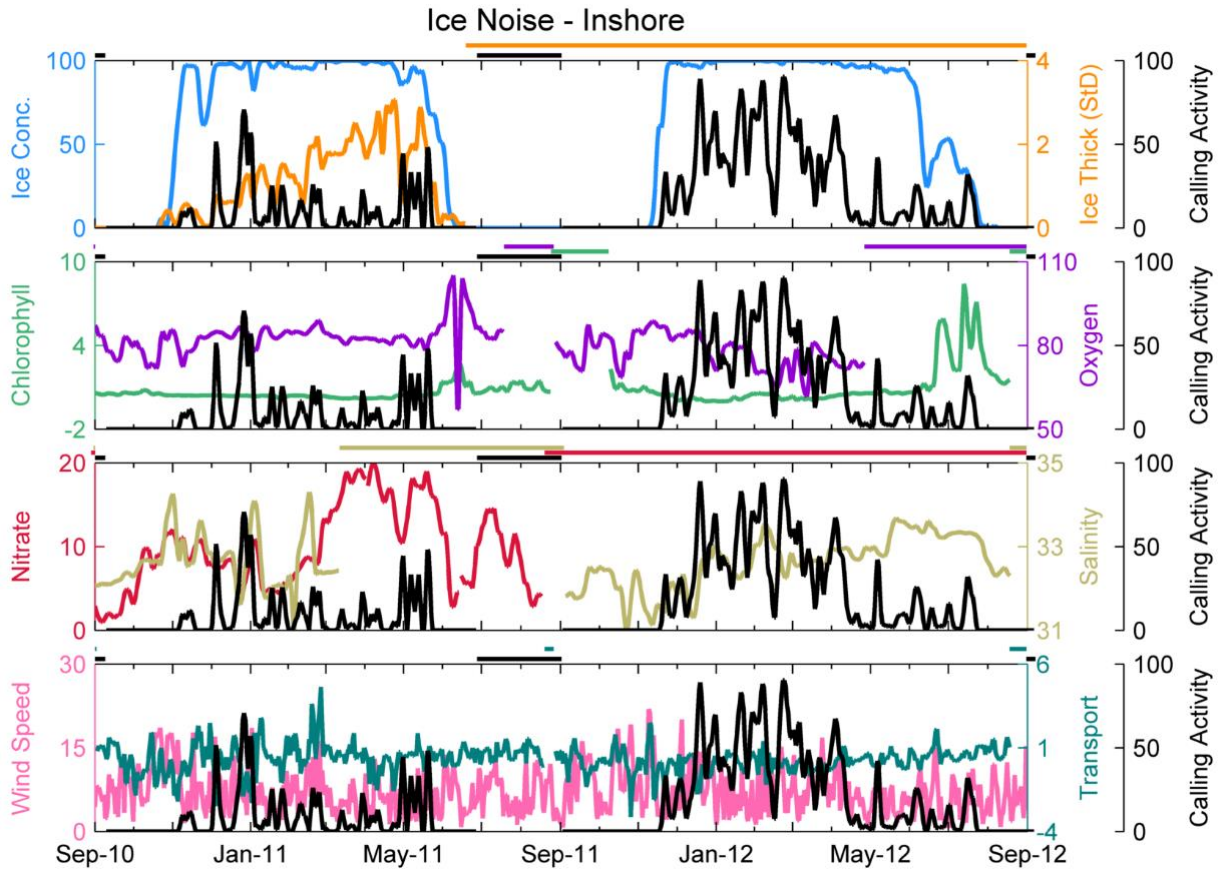


FIGURE 132. ICE NOISE PRESENCE AS IT RELATES TO OCEANOGRAPHIC VARIABLES AT THE INSHORE LOCATION, 2010-2012. BLACK LINE = PERCENT OF TIME INTERVALS WITH CALLS. TOP ROW: PERCENT ICE CONCENTRATION (BLUE LINE) AND STANDARD DEVIATION ICE THICKNESS (M; ORANGE LINE). SECOND ROW: CHLOROPHYLL ($\mu\text{G/L}$; GREEN LINE) AND OXYGEN ($\text{M} \times 10$; PURPLE LINE). THIRD ROW: NITRATE (μM ; RED LINE) AND SALINITY (PSU; TAN LINE). BOTTOM ROW: WIND SPEED (M/S; PINK LINE) AND TRANSPORT (SV; TEAL LINE). HORIZONTAL BARS ABOVE EACH ROW INDICATE TIMES WITH NO DATA. ALL DATA EXCEPT WIND SPEED ARE PRESENTED AS A 3-DAY MOVING AVERAGE.

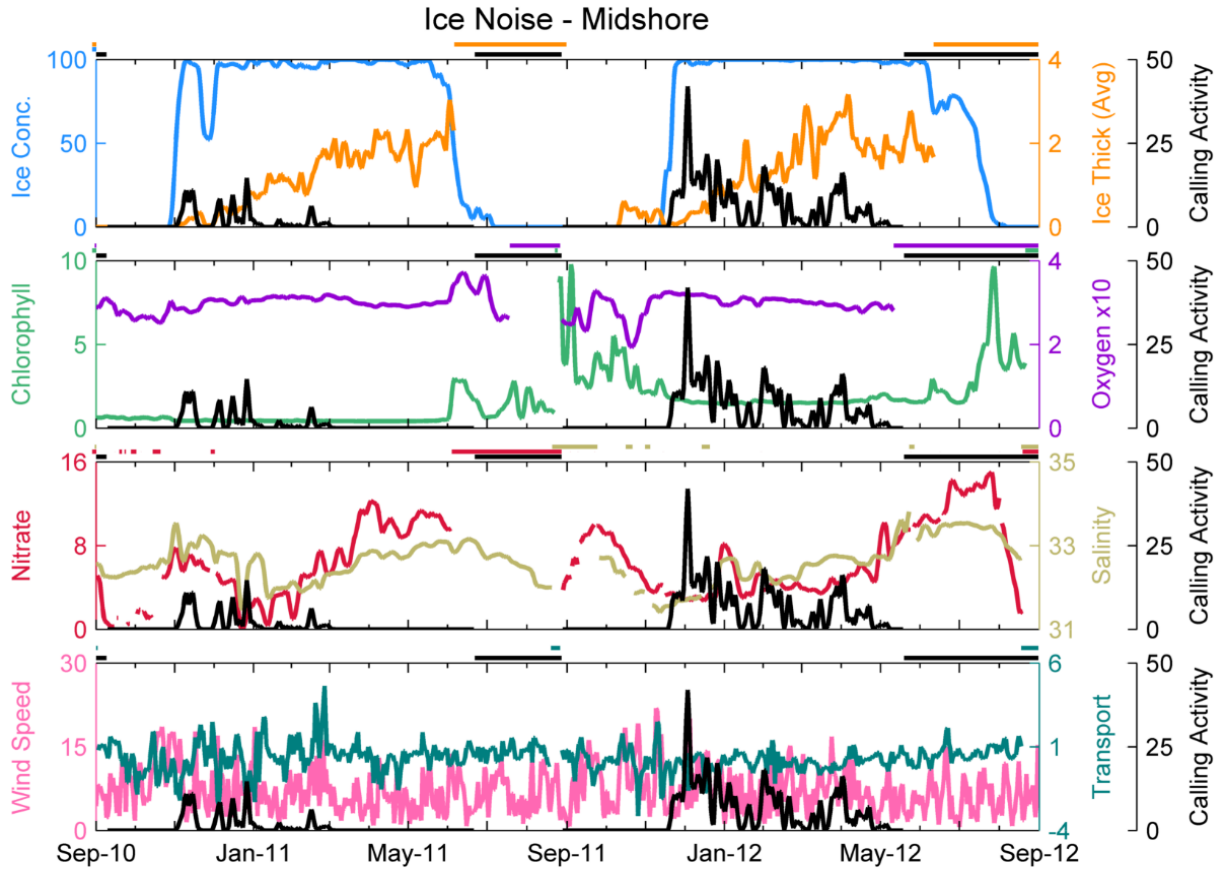


FIGURE 133. ICE NOISE PRESENCE AS IT RELATES TO OCEANOGRAPHIC VARIABLES AT THE MIDSHORE LOCATION, 2010-2012. BLACK LINE = PERCENT OF TIME INTERVALS WITH CALLS. TOP ROW: PERCENT ICE CONCENTRATION (BLUE LINE) AND STANDARD DEVIATION ICE THICKNESS (M; ORANGE LINE). SECOND ROW: CHLOROPHYLL ($\mu\text{G/L}$; GREEN LINE) AND OXYGEN ($\text{M} \times 10$; PURPLE LINE). THIRD ROW: NITRATE (μM ; RED LINE) AND SALINITY (PSU; TAN LINE). BOTTOM ROW: WIND SPEED (M/S; PINK LINE) AND TRANSPORT (SV; TEAL LINE). HORIZONTAL BARS ABOVE EACH ROW INDICATE TIMES WITH NO DATA. ALL DATA EXCEPT WIND SPEED ARE PRESENTED AS A 3-DAY MOVING AVERAGE.

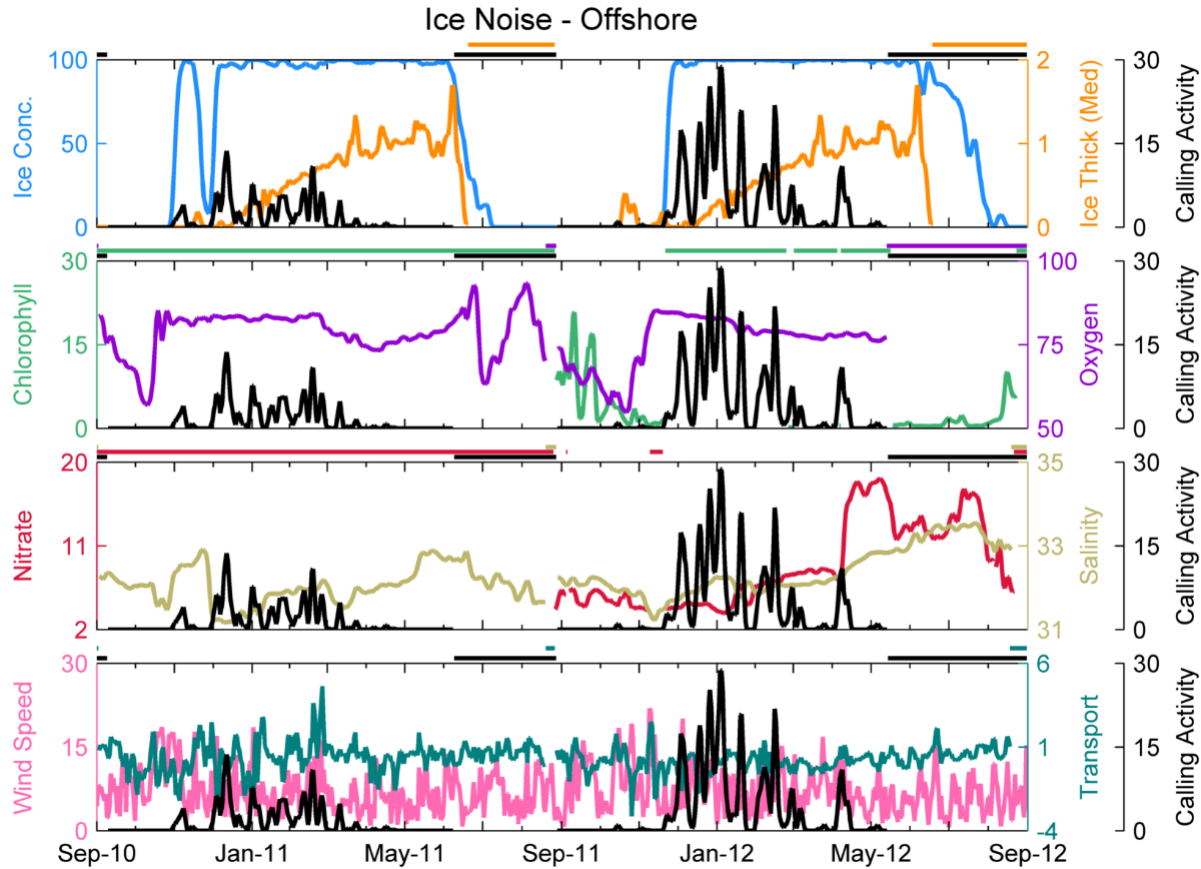


FIGURE 134. ICE NOISE PRESENCE AS IT RELATES TO OCEANOGRAPHIC VARIABLES AT THE OFFSHORE LOCATION, 2010-2012. BLACK LINE = PERCENT OF TIME INTERVALS WITH CALLS. TOP ROW: PERCENT ICE CONCENTRATION (BLUE LINE) AND STANDARD DEVIATION ICE THICKNESS (M; ORANGE LINE). SECOND ROW: CHLOROPHYLL ($\mu\text{G/L}$; GREEN LINE) AND OXYGEN ($\text{M} \times 10$; PURPLE LINE). THIRD ROW: NITRATE (μM ; RED LINE) AND SALINITY (PSU; TAN LINE). BOTTOM ROW: WIND SPEED (M/S; PINK LINE) AND TRANSPORT (SV; TEAL LINE). HORIZONTAL BARS ABOVE EACH ROW INDICATE TIMES WITH NO DATA. ALL DATA EXCEPT WIND SPEED ARE PRESENTED AS A 3-DAY MOVING AVERAGE.

Note on GAM comparison of surface vs. bottom currents

In general, there were very few differences between the models produced from the bottom and surface current iterations of the 21 separate GAM runs; the R-Squared values and sample sizes changed only slightly, especially at the midshore location where the sample sizes were high. Therefore, there is good evidence to support our initial assumptions of water current uniformity in the water column.

Note on GAM runs including TAPS6-NG variables:

The results from these runs showed that a variety of the TAPS6-NG variables provided high explanatory power for the variance in bowhead whale, bearded seal, and walrus calling activity over short time scales. In the future, every effort to collect these data simultaneous with passive acoustic recordings should be attempted to evaluate their explanatory power in understanding marine mammal distributions.

3. *Discussion*

While the results of the GAM models were run for all three locations, the midshore data had the largest sample sizes spanning the longest timeframes, and had the most consistent R-Squared values between the top AIC and top R-Squared models for each run. Furthermore, the midshore location is positioned between the Burger and Klondike study areas, and as such is best suited for representing the area of interest for this study. Thus, the discussion that follows will focus on the midshore location unless otherwise stated. Any significant differences between the three locations will be described. It is also important to note that reference to any correlations regarding the long term plots are qualitative in nature, winds were estimated from the midshore location only, and transport was averaged between the three locations.

Bowhead whale

Given that bowheads follow a regular migration pattern with fall migration occurring ahead of the advancing ice edge and the spring migration taking place in nearshore leads, the significance of both ice concentration and month in the GAMs are not surprising. Month was extremely significant (p values ranged from $1.8E^{-5}$ to $5.2E^{-29}$) for all models and all variables, indicating that the timing of the bowhead migration is driven mainly by endogenous cycles, and then secondarily by ice conditions. In the fall, bowhead calling activity is greatest just before ice forms (or in the early formation of ice), and ceases once the ice concentration reaches 100% or the ice thickness is greater than 0.5 m (see Figure 103-105). In spring, bowhead calling activity occurs in ice thicknesses greater than 0.5 m; however, it is important to note the scale of the measurements. The instrument measuring ice thickness measures a surface area of approximately $1m^2$ above the instrument, whereas ice concentrations are calculated in a $50 km^2$ area around each mooring site, and bowheads can potentially be acoustically detected up to 20 kilometers away from the recorder. Thus, in the spring, bowheads are calling in what appears to be very thick ice; rather, it is more likely that they are using a lead that is nearby, but not immediately over the ice profiling instrument. This preference for thin ice is supported by Moore (2000) who demonstrated that bowhead whales prefer shallow, coastal waters in light ice years, but preferred outer shelf/trough waters (where an open lead develops) in heavy ice years. However, other studies (Clark et al., 1986; Moore and Laidre, 2006; Quakenbush et al., 2012) do show that bowhead whales migrate through areas with heavy ice conditions and no evidence of leads.

Bowheads also showed a positive correlation with winds in the fall (Figure 109), with wind speed being one of the significant variables in the best model selected for both the inshore and midshore GAM runs. The direction and strength of the winds strongly influence ice concentration and movement throughout the Arctic (Weingartner et al., 2013). With the exception of the third peak in bowhead calling activity in fall 2010, all calling activity at the midshore location was associated with strong, consistent winds to the south-southwest. Strong persistent winds from one direction tend to push ice in that same direction (Weingartner et al., 2013). Thus, the strong winds may have been an indicator to the bowheads that ice was about to be forced southward, thus potentially cuing their migration. Winds also force surface currents, which may help the whales to conserve energy by serving as a tailwind during their fall migration to the Bering Sea.

Chlorophyll was also a highly significant variable in the best model selected from the midshore GAM run (just fall data were included) and showed a strong correlation in the long-term plots. This may be a coincidence, given that chlorophyll levels increase once the ice begins to open, allowing both ice-associated algae to fall to the bottom and light to penetrate the sea surface. It could also indicate that chlorophyll may serve as a proxy for prey availability, which is an additional factor influencing bowhead distribution. Several authors have shown that bowhead migrations may also be driven by prey aggregations and availability, rather than by ice presence, and that feeding during the spring migration is more common than previously thought (Lowry et al., 2004; Moore and Laidre, 2006; Mocklin et al., 2012). The longer tail in spring calling activity described in Section VII.A.3 may be indicative of this spring feeding. In the spring, as ice breaks up and creates leads, ice-associated algae fall to the bottom and a water column phytoplankton bloom occurs until nutrients are completely stripped from the surface waters. This is then followed by increases in zooplankton abundance, the predominant prey item for bowhead whales (Carroll et al., 1987). In fact, some authors suggest that a reduction in sea ice may enhance feeding opportunities for bowhead whales in the short-term (e.g., Moore and Laidre, 2006; Moore and Huntington, 2008). Because bowhead whales rely on the larger, older stages of zooplankton, the exact relationship between spring production of ice and water column phytoplankton and the immediate feeding of migratory bowheads is not entirely clear. If sea ice recedes much earlier and results in decreases of carbon flux to the bottom, will that result in a reduction of energy transfer to planktivorous baleen whales? The answer is not certain, as some of the phytoplankton production lost to the benthos will be transformed into primary productivity that remains in the water column. We do know that euphausiids in the Bering Sea live for up to 3-4 years and that the euphausiid *Thysanoessa raschii* may feed in the nepheloid layer (layer above the bottom that contains significant amounts of suspended sediment), particularly over winter (Hunt et al., in review). Therefore the observed relationship between chlorophyll and bowheads may also reflect a change in the distribution and availability of euphausiids during the onset of the spring bloom, rather than to the carbon contained in the phytoplankton. Although the long-term effects of reduced sea ice on bowhead whale populations remain unknown, the BCB population has increased steadily at 3.4% during two decades of sea ice loss in the Arctic (Walsh, 2008), therefore this population does not appear to be hindered by sea ice reduction at present.

Aerts et al. (2013) analyzed marine mammal (cetacean and pinniped) distribution among the Burger, Klondike, and Statoil study areas during the 2008-2010 open-water season. With the exception of one sighting of two bowheads in Statoil in September, all bowhead whales were sighted in the Burger study area in October (Aerts et al., 2013). These authors attribute this to the migration paths of bowheads across the northern Chukchi to the Chukotka coast that cross the Burger and Statoil study areas more often than the Klondike area. Although the Chukchi Sea is not listed as a Biologically Important Area for bowheads, feeding bowheads have been observed in the Chukchi Sea (see Section VII.A.3). It is also possible that the migrating bowheads are taking advantage of potential concentrations of epibenthic prey along their migratory route, and in particular in the benthic-driven Burger ecosystem. Further work (i.e., using the methods of Mocklin et al., 2012 to examine feeding behavior) is needed to determine if this is in fact the case.

Transport was a common significant variable for all top models at the inshore location. Transport in 2010-11 was very high for the Chukchi Sea, with moderate levels in 2011-12.

Positive correlations were also seen between transport and calling activity in the fall on the long term plots (Figure 106-108). Moore (2000) indicated that during fall in the northern Chukchi Sea, bowhead whales preferred coastal/shoal habitats (where our recorders are located) in high transport years, but preferred outer shelf/trough waters in years with low transport. She attributed this relationship to the advection of zooplankton through the Bering Strait into the Chukchi Sea each summer, as highly productive Bering Sea water flows into the Chukchi, driving primary productivity and high benthic biomass at the shoals. This may help explain why there is some evidence of feeding during the fall migration (see Section VII.A.3).

Nitrate and salinity both shared a similar pattern, in which they were increasing in the fall of 2010, but decreasing in the fall of 2011 at the inshore and midshore locations (Figure 35-39). It is possible that this may be related to the distinct peaks seen in the fall migration of 2010 that was not evident in fall 2011. Perhaps there was some cue in the oceanographic conditions to which different age or sex classes responded. Additional data would help confirm this hypothesis.

Gunshot calls (bowheads)

Gunshot call activity is strongly correlated to both bowhead whale calling activity and ice conditions. It was determined that peak gunshot calling occurs near the end of the peaks in bowhead whale vocal activity (Figure 110 -112). However, peak gunshot calling is also tightly associated with ice cover. Gunshot calling would often begin once ice concentration reached 100%, but while ice thickness was still less than 0.5 m. Once ice thickness increased, gunshot calling ceased, suggesting the migration of the bowheads had passed through the area. It is interesting that gunshot calls occur almost entirely in near 100% ice cover. Little is known about the function of a gunshot call, though it was first reported for this species by Würsig and Clark (1993). Perhaps this particular vocal signal is utilized by the bowheads to navigate through the ice, locate leads or openings, or possibly determine keel depths.

In fact, several authors have suggested that bowhead whales use their frequency modulated (FM) calls to estimate ice thickness (Ellison et al., 1987; George et al., 1989). Ellison et al. (1987) determined that the echoes of bowhead FM calls off thick pack ice are up to 20 dB greater than the echoes off new ice. These authors suggest that bowheads can use the echoes to determine ice thickness and thus help navigate through the ice and find areas thin enough to break through. Although the calls analyzed in those studies were FM modulated tonal calls, the impulsive nature of gunshots would make them an ideal call type for perceiving relative levels from echoes off ice keels. Given the tight correlation between gunshot calls and ice, it is likely that they are using these calls to determine ice thickness and to navigate. If so, the importance of maintaining low ambient noise in this environment during the migration period may be critical, as an increase in noise may hinder their ability to both navigate around ice, and find an ice thickness suitable for breaking. Alternatively, the positioning of the peaks of gunshot calling activity near the end of each of the regular peaks in bowhead calling activity possibly suggests it may be used as a migration cue to assemble and move.

Beluga whale

Not surprisingly, the two significant common variables among the best models obtained from the GAM runs for the inshore location were ice concentration and month for the inshore location, and month for the midshore location. Like bowheads, beluga whale migrations are likely driven primarily by endogenous rhythms and secondarily by ice. Garland et al. (2015) also found a strong positive correlation between beluga whale calling activity and both month and ice on recorders spread from the northern Bering Sea to off Barrow, AK. However, as mentioned in Section VII.A.3, not all beluga whales migrate through the inshore leads in the Chukchi Sea in the spring; this may be the reason for the lack of correlation between ice concentration and calling activity at the offshore location. Prey availability may be the driving force behind this diversion from inshore leads. As ice melts and breaks up in the spring, ice-associated algae falls to the bottom, which creates a spike in chlorophyll measurements in the water column and a subsequent increase in zooplankton, the prey of cod. Both Arctic and saffron cod, the primary fish species for the BS and ECS populations of belugas, respectively, are planktivorous; however, Arctic cod are associated with the ice edge (Gradinger and Bluhm, 2004) while saffron cod are more coastal. It could be that only the BS population travels offshore, or it could be that sampling biases exist in stomach content analyses. Since evidence is available (Section VII.A.3) to show that the ECS population does travel to the ice edge to feed, it seems likely that both populations can feed on Arctic cod. Chlorophyll was a highly significant variable in the best model selected from the midshore GAM run and showed a high qualitative correlation in the long-term plots (Figure 113-114). In the majority of cases the peak in beluga whale calling activity preceded the spike in chlorophyll levels in the spring, but lagged during the fall. This may be because ice edge was not located near our recorder locations in the spring. In fact Figure 113-114 do not appear show the ice edge over the mooring locations during the spring migrations; the calling activity ceased prior to the majority of the ice break up. It is also possible, however, that the beluga were there and feeding; our recording system is unable to detect the high frequency echolocation signals they produce while feeding (see Section VII.A.3).

Belugas are also positively associated with the presence of polynyas. As seen in Figure 113-115 (most evidently in the 2010-2011 deployment data and at the inshore and midshore locations) whenever ice concentration drops markedly (indicative of a polynya formation), beluga calling activity increases. Again, this may be due to high productivity at the ice edge, and thus high prey availability, or just availability of breathing holes. The correlation with wind speed is also likely a result of their association with the ice edge in the fall, as strong winds have a significant impact on the sea ice edge (Weingartner et al., 2013). However, no clear pattern with wind direction was seen (Figure 109).

Moore (2000) found that belugas in the fall preferred slope habitat in the northern Chukchi, rather than coastal habitat. Although we did not have any moorings located in slope waters, our results showed the opposite results of greater calling activity at the inshore recorder. This can be explained by the bifurcation in the beluga whale fall migration discussed in Section VII.A.3. She also reported that transport had little effect on habitat preference for beluga whales; they preferred slope habitats in all transport conditions. This is supported by the data presented here, in which transport was never listed as a variable in any of the top GAM models. However, Stafford et al. (2013) found higher concentrations of belugas along the Beaufort Sea slope when the Alaska Coastal Current was well-developed. These authors attribute the higher numbers to enhanced foraging opportunities, a result of the well-defined front that promotes an aggregation of prey species. Thus, movements of water masses do appear to have an effect on beluga whale

distribution. There appears to be a slight association with nitrate in the spring, however there are only nitrate data for one year at that location; more data are needed for confirmation.

Gray whale

Although gray whales were included in the GAM models, there are very few data for this species (only the inshore location had more than one day of calling activity) as they tend to remain closer to shore and have low calling rates. Therefore, the top models selected may not be the best suited to explain the variability seen in the calling activity distributions, but they are the best models for these data at this time. There was only one variable that was consistent among the top models for the midshore location ice concentration. Not surprisingly, the long-term plot at the inshore location showed a negative association with ice (Figure 116). Gray whale calling activity occurred before the ice formed in the fall, and did not resume in the spring until ice concentration dropped considerably, which is consistent with what is known about gray whale distribution (e.g., Moore et al., 2000; Clarke et al., 2012). Gray whales spend the summer in the northeastern Chukchi Sea, feeding on benthic infauna primarily in the shallow, productive shelf waters between Wainwright and Barrow, (Moore et al., 2000; Clarke et al., 2015) but also in the waters between Wainwright and Hanna Shoal – but not on the Shoal itself (Clarke and Ferguson, 2010; Hannay et al., 2013). Most gray whales begin their southern migration before the ice forms. Moore et al. (2000) found that the average percent ice cover at gray whale sightings was only 1%, indicating that gray whales prefer open water.

A weak association with chlorophyll was present in the 2011-2012 data, though this was not evident in 2010-2011. However, our acoustic recorder failed in late June of 2011, and the peak in gray whale calling in 2012 occurred in late July, so we may have missed the peak vocal activity for summer 2011. Furthermore, gray whales tend to be less vocally active while feeding and migrating than when socializing or on their breeding grounds (Rasmussen and Head, 1965; Crane and Lashkari, 1996; Section VII.B this study), so low levels of calling activity were expected.

Transport was not included as a variable in any of the models. Most likely this is due to recorder placement away from prime feeding areas. Moore (2000) found that gray whales in the northern Chukchi were strongly associated with coastal/shoal feeding areas when transport was high. Gray whales prey on benthic infauna that occur along the coast between Icy Cape and Barrow (Feder et al., 1994). In the Moore (2000) study, gray whales preferred these habitats exclusively in years of high transport when productivity was likely increased by the advection of nutrients from the Bering Strait. Although transport was not included as a significant variable in any of the models, it is interesting to note that 2010-11, a high transport year, also had considerably more gray whale calling activity than 2011-12, a year with moderate transport (Section VIII.A). Perhaps the lower amount of calling activity in 2011-12 is a result of gray whales preferring offshore waters in moderate to low transport years (Moore, 2000), positioning them further from our recording locations. This correlation with transport (and therefore high biomass) is also evident in the transect line sampling data.

Gray whales were visually sighted or acoustically detected in areas with high concentrations of zooplankton, particularly *Pseudocalanus*, *C. glacialis*, and larvaceans (Figure 117-118). High zooplankton concentrations may serve as a proxy for benthic biomass. At the Barrow Canyon transect line, gray whales were concentrated at the inshore stations, where there were high concentrations of *Pseudocalanus* and *C. glacialis*. Schonberg et al. (2014) also report

large concentrations of gray whales inshore between Wainwright and Barrow, a region with high densities of benthic amphipods. Furthermore, at the Point Hope line there was a strong correlation between gray whales and nitrate and ammonium, at the same location that there were extremely high concentrations of *Pseudocalanus*. Bluhm et al. (2009) suggest that most epifaunal biomass is between Bering Strait and Point Hope. They also correlate high relative abundances of gray whales in this area to an oceanographic front between the Bering Shelf Water and the Alaska Coastal Water (Bluhm et al., 2007). Fronts are known to support elevated biomass of hyper-benthic communities as well as marine mammal aggregations (Dewicke et al., 2002; Mendes et al., 2002). In this region, the tight benthic-pelagic coupling is driven by high sedimentation rates allowing for high benthic biomass (Grebmeier et al., 2006a; Bluhm et al., 2007).

Walrus

Month was again a highly significant variable that occurred in both the best model selected by the GAM for the midshore and offshore locations, as well as in the majority of the top five AIC and top five R-squared selected models. This again hints at endogenous cycles, which is not surprising for this species where many individuals are known to migrate between feeding grounds in the Arctic and mating grounds in the Bering Sea. Although they use the northward movement of the icepack to conserve energy on their migration, they still spend most of their time swimming (Fay, 1982), suggesting that internal timing trumps environmental factors.

Timing of the start of the summer pulse of calling activity varied slightly between mooring locations (Section VII.A.3). Although the best models obtained from the GAM run do not include ice concentration as a variable, the negative correlation between this variable (which is slightly different between locations) and the timing of the start of the summer calling pulse is clear in Figure 119-121. This lack of an ice concentration contribution is due to the patchiness in the overlap of the available datasets (see Appendix G, Section XVIII.G); no data from this summer calling pulse were used in the GAM runs. The only location to have overlapping ice thickness measurements (midshore), did show this variable to contribute significantly to the best model selected by that GAM run for the end of the summer calling pulse, indicating that the walrus move out of the area ahead of the ice front.

The presence of high levels of walrus calling throughout the winter at the offshore location, as discussed in Section VII.A.3, was an unexpected result. In addition to the sea ice images (Figure 13) that show evidence of open water near this recording location, winter calling activity appears to start immediately after a dip in ice concentration (indicating a polynya) in the 2010-11 data (Figure 121); there is a slight correlation in the 2011-12 data. These data indicate that there was, in fact, enough open water to explain the presence of this calling activity. With the presence of these open waters may come high productivity (Stirling, 1997), suggesting these individuals may prefer to remain in the Arctic instead of migrating south (see Section VII.A.3).

ADCP volume backscatter was also a highly significant variable in the best model selected from the midshore GAM run. This is indicative of a highly productive area where both plankton and walrus benthic prey are available. Several authors have shown a tight correlation between primary production and coastal benthic infauna in the northeastern Chukchi Sea (e.g.,

Dunton et al., 1989; Grebmeier et al., 2006a). High zooplankton biomass (measured by ADCP volume backscatter) may further contribute to the rain of detrital flux that fuels the benthic community, the predominant food source for walrus (Sheffield and Grebmeier, 2009). This is also supported by the inclusion of chlorophyll and oxygen as a highly significant variable in the best model obtained by the midshore GAM run. Chlorophyll, along with oxygen and salinity, were shown to peak during the summer pulse in calling activity at this location (Figure 120). This suggests productivity continued there in the fall; with oxygen present, any ice-associated algae that fell to the bottom during the spring would be able to thrive.

This correlation was also shown by Aerts et al., (2013), who compared marine mammal distributions among Burger, Klondike, and Statoil study areas. They found walrus in significantly higher densities around Burger than either Klondike or Statoil – likely a result of the more benthic-driven ecosystem and high biomass of benthos (Blanchard et al., 2013; Day et al., 2013) better suited to walrus foraging (Klondike is a more pelagic system, with currents coming from the Bering Sea bringing higher biomasses of zooplankton, and Statoil has both pelagic and benthic characteristics). This is also supported by Schonberg et al. (2014), who found that walrus aggregated in an area south of Hanna Shoal with high concentrations of bivalves and worms, although they state that this aggregation only took place when sea ice was present.

The results of the transect line sampling data with walrus visual and acoustic data also reveal a tight coupling between walrus presence and local production. At both the Wainwright and the Icy Cape transect lines, walrus were repeatedly sighted or detected at locations that had high concentrations of *Pseudocalanus*, *C. glacialis*, and larvaceans. There was also a strong correlation with high levels of nitrate and ammonium. Our results also coincide with Aerts et al. (2013) and Schonberg et al. (2014), in that there were more walrus detected on the Wainwright line near Hanna Shoal and the Burger study area than the Icy Cape line, which is situated between the two. As with the gray whales, walrus were found in high numbers at areas with tight benthic-pelagic coupling and high biomass.

Walrus were not correlated with transport, which is shown to have a direct influence on primary productivity. However, this is likely due to the summer calling activity data being left out of the GAM runs (see Appendix G, Section XVIII.G). The inclusion of the full year ARCWEST and CHAOZ-X datasets will provide opportunities to examine this relationship in the near future.

Wind speed was also a highly significant variable in the best model selected from the midshore GAM run, which is likely a result of the effect of wind on ice movements. Wind speed has been shown to strongly influence ice cover (Niebauer and Day, 1989; Weingartner et al., 2013), which would affect habitat availability for walrus. Walrus, especially females nursing pups, conserve energy by using the ice to move to potential areas of high biomass. However, walrus are not deep divers and prefer to feed in waters less than 100m deep (Fay, 1982). If this holds true, then the retreating sea ice may impact walrus populations in the future. This is explained in greater detail in Section XII.3. No consistent trends were seen between wind direction and walrus calling activity (Figure 122), although the majority of winds during the summer pulses of calling activity were heading to the southwest.

Bearded seal

It is important to note that calling activity is not a good proxy for presence of bearded seals outside of the mating season (see Section VII.B.3). Males produce elaborate vocal displays to advertise breeding condition or establish territories during the mating season (see Section VII.A.3). It is not surprising, therefore, that month was a highly significant variable that occurred in both the best model selected by the GAM as well as in the majority of the top five AIC and top five R-squared selected models for all locations. However, we did find year-round low-level bearded seal calling presence at all three locations. Little is currently known about the vocalizations of female bearded seals, therefore it is unknown what proportion of the detected calls in the non-breeding season are from each sex. Although this is in agreement with other passive acoustic studies (see Section VII.A.3), it is counter to the thought that most bearded seals winter in the Bering Sea and pass into the Arctic between April and June. Bearded seals are said to migrate south ahead of the ice edge in the fall. Figure 129-131 show that the small pulse of calling activity in October of both years and all locations precedes the increase in ice concentration by about a month.

The midshore location had the best coverage of dates included in the GAM runs (see Appendix G, XVIII.G). For this location, ice concentration was a significant variable in best model selected by the GAM and was a variable consistent among the top models (5 AIC/5 R-squared). Bearded seals spent most of their time in the drifting pack ice, preferring areas with heavier ice concentrations (70-90%) than other phocid seals, but light enough that breathing holes do not need to be maintained. Currently, however, many bearded seals spend the summer in open water. This is because, like walrus, bearded seals are benthic feeders that prefer shallow feeding areas 100-150m deep. However, unlike walrus, bearded seals rarely haul-out, and instead just distribute themselves throughout the open water (see Section VII.A.3 for more details).

Ice thickness was not included as a significant variable in the model. It is important to note, however, that the scale of resolution is important (see bowhead whale discussion above; this section). In one case (at the offshore 2011-2012 location) there was a marked decrease in bearded vocal activity that corresponds with an unusually deep and persistent ice keel (Figure 131), suggesting that the presence of thick, concentrated, multiyear ice pushed the seals out of the area temporarily, further supporting the hypothesis that bearded seals prefer areas with a specific ice thickness.

Bengtson et al. (2005) suggest that bearded seal densities may also be influenced by levels of primary productivity and benthic biomass. Volume backscatter from the ADCP (bottom), indicative of zooplankton, was a highly significant variable that occurred in both the best model selected by the GAM (for midshore and offshore locations) as well as in the majority of the top five AIC and top five R-squared selected models at the midshore location. Zooplankton are prey for many species that bearded seals rely on (e.g., larval cod, capelin, shrimp; Lowry et al., 1980; Bluhm and Gradinger, 2008). Aerts et al. (2013) also found higher densities of bearded seals at the benthic-driven Statoil and Burger study areas than at the pelagic-driven Klondike study area. Our results suggest that the benthic-driven area extends westward from the Statoil and Burger study areas. In fact, bearded seal calling activity occurred at the highest levels at our midshore recorder location, which is situated between Burger and Klondike. Transport was also highly significant variable contributing to the best model selected by the

GAM run at the midshore location. High transport levels are linked with high productivity (Grebmeier et al., 2006a). Transport has been shown to be wind forced (Roach et al., 1995), so it is not surprising that wind speed was also a significant variable contributing to the best model selected by the GAM runs at both the inshore and midshore locations. Finally, the presence of salinity, as a variable of high significance in the best model selected by the GAM run at the inshore and midshore locations suggest an influx of water up Barrow Canyon that can possibly bring zooplankton into the area.

Our shipboard survey results also coincide with the results presented by Aerts et al. (2013), indicating that bearded seals are in areas of high overall productivity (both benthic and pelagic). Along the Icy Cape and Wainwright transect lines, bearded seals were associated with high densities of *Pseudocalanus* and larvaceans, and to a lesser extent, *C. glacialis*. Bearded seals were also associated with high nitrate and ammonium levels, though not to the same degree as walrus. These differences may be a result of varying diets (see Section VII.A.3). Walrus are specialist benthic feeders, while bearded seals are more generalist feeders. This generalist diet may provide bearded seals with more habitat opportunities, as evidenced by the broader spatial distribution seen both in the long-term moorings (see Section VII.A.2) as well as the short-term shipboard surveys (Section VII.B.2). Their diet may also make the bearded seal more adaptive, and thus less vulnerable to ecosystem change (See Section XI.1). Although bearded seals were found in the same areas as walrus, bearded seals are usually not found in the immediate vicinity of large concentrations of walrus (Burns, 1970). Our study presents similar results, in which walrus and bearded seals are frequently sighted along the Icy Cape and Wainwright transects near the shoal areas, but there were few overlapping sightings between the two species.

Lastly, this correlation of bearded seals and high productivity may help to explain the variation in the ramp up of calling activity among locations and between years (Section VII.A.3). Figure 130-129 suggest that the difference in the timing of high ice concentrations among locations/years did not coincide with the increase in bearded seal calling leading up to the mating season, although it was a significant variable in the best model selected by the GAM run at the midshore location. In fact, with the exception of the ice keel mentioned above, ice thickness also did not correlate well with the differences seen among the locations/years. However, nitrate and salinity seem to show a positive correlation with the different increases of calling activity among locations/years. These variables are proxies for productivity (increases in salinity reflect possible flow up Barrow Canyon which may bring increased zooplankton into the study area). For example, the 2010-2011 inshore levels of nitrate seem to increase slightly earlier (Figure 129), than those at the midshore location (Figure 130); this follows the earlier start of calling activity at the inshore location. Furthermore, the 2010-2011 nitrate levels are delayed compared with those from 2011-2012, again mimicking the trend in calling activity between the two years. With the addition of the full-year datasets from the BOEM-funded ARCWEST and CHAOZ-X projects, we should be better able to determine if such correlations exist. For the few locations/years where recordings exist, it appears that the sharp decrease in calling activity at the end of the mating season is positively correlated with the rapid reduction in ice concentration, which is also marked by a sharp increase in chlorophyll levels (Figure 129 - 131).

Ice noise

For the midshore location, that had the greater seasonal coverage included in the GAM runs, month was a highly significant variable that occurred in both the best model selected by the GAM as well as in the majority of the top five AIC and top five R-squared selected models. This speaks to the seasonal nature of ice in the Arctic.

As expected, ice concentration was a highly significant variable contributing to the best model of ice noise activity selected by the GAM runs at all locations. Simply put, you cannot have ice noise without ice. Ice noise activity, however, cannot be used as a proxy for determining the presence of ice, since there are periods of time where ice is present but ice noise activity is absent (Figure 132-134). Nonetheless, it might be possible to determine whether certain environmental conditions exist during the periods of time while the Arctic is ice covered.

It appears that ice thickness is negatively correlated with ice noise activity at the midshore and offshore locations (Figure 132-134). This is intuitive, as thicker, more extensive ice would be less prone to fracturing and colliding than thinner, more irregular ice. Although it was a significant variable contributing to the best model selected by the offshore GAM run, the section of data with high ice thickness and low ice noise activity was not included in the GAM run; it did not contribute at all to any of the top AIC or top R-squared models selected by the midshore GAM run.

Although ice noise activity is present during ice formation in all locations/years, detection of the ice retreat was possible only at the inshore location because of recorder failure at the other two locations (Figure 132-134). The only location to have ice noise activity data included in the GAM runs for this spring retreat is the midshore location. The significant variables contributing to the best model selected by the GAM run, in addition to month and ice concentration, were chlorophyll, PAR, turbidity, and wind direction.

Niebauer and Day (1989) showed that shifts in wind regimes have strong effects on ice cover. Interannual differences in ice noise activity at the midshore location are shown in Figure 122. It appears as though ice noise activity is reduced with winds from the south, and increased with winds from the northeast. For the 2010-2011 deployment, wind direction shifted back and forth frequently and ice noise activity was at low levels. The 2011-2012 deployment saw much greater ice noise activity levels, while the winds remained fairly consistent from the northeast. Petrich et al. (2012), found that for an 11 year record of ice break up at Barrow, AK (a location they say is representative of the Chukchi coast), ice break up happened with all wind directions but those toward the north or northwest. So our results may indicate that the winds to the SSW are forcing the ice to move, while winds to the north are not. If this is the case, it is then plausible to suggest that these ice noise activity levels would be higher at the inshore location, closest to the high energy zone between the pack ice and shorefast ice.

The other variables that contributed significantly to the top model obtained from the midshore GAM run are those that are coincident with ice conditions. During the spring as the ice breaks up and melts, the ice-associated algae fall off the ice, causing bottom chlorophyll levels to spike. PAR and turbidity are measures of light levels and suspended material in the water column, and are expected to increase as the ice breaks up, melts, or is blown out of the area. Chlorophyll is the only of these variable that was plotted against ice noise activity levels in

Figure 132-134. There it is apparent that a negative correlation exists; no ice, and therefore no ice noise, is present when chlorophyll levels peak.

It is important to note, however, that the ice noise activity levels described here reflect the percentage of 90 s time intervals per day when ice noise was present. They do not indicate actual ambient noise levels. Please refer to Section XII.3 for a discussion on how ambient noise levels correlate to environmental parameters.

4. *Conclusions*

The Chukchi Sea ecosystem is complicated: landscape ecology, and regional and local forcing all combine to determine whether or not there will be favorable conditions for both the permanent and transitory residents. For example, northern Bering Sea ice dynamics and transport through the Strait via the Bering and Anadyr currents, transport nutrients and plankton to the Chukchi. The nutrient-rich currents enable local primary production on the shallow Chukchi shelf that nourishes many different trophic levels. Should the sea ice dynamics on the northern Bering Sea shelf change, this may alter nutrient concentrations in the Bering current and impact the Chukchi shelf. Similarly, terrestrial events far interior to Alaska, determine the timing and heat content of the Yukon River. The Yukon River has a strong influence on the amount of heat and salt transported to the inshore region of the Chukchi Sea as far north as Barrow. As a result, changes to the flux of Yukon River water into the Bering will impact the Chukchi. While mean transport is northeastward along the Alaskan Coast and mean winds are out the northeast, events of strong northward winds increase coastal transport and provide opportunities for residents in the form of creation of polynyas, on-shelf transport of Arctic water, and up-canyon flow at Barrow Canyon.

The Chukchi Sea is predominantly a benthic-driven ecosystem, with nutrient-rich waters being advected from the Bering Strait and episodically from the Arctic basin, augmenting primary production up to the Barrow Canyon. The current balance of benthic-pelagic production favors the benthos, but still results in high biomass of zooplankton and high biomass of benthic epifaunal and infaunal invertebrates that comprise the diets of resident Arctic benthic feeding species such as gray whales, walrus, and bearded seals. Both bowhead and beluga whales undergo consistent, predictable seasonal migrations that are strongly correlated with both month and ice concentration, but both also had several variables that can serve as proxies for prey availability show up as significant contributors to the best models selected by the GAM runs. There was a strong correlation between gunshot call activity and both ice presence and thickness, We suggest that bowhead whales use this particular call type to assess ice thickness, to cue migration, or both. Gray whale calling activity was sparse throughout the two years of long-term recordings most likely due to placement of the recorders along with low calling rates. This calling activity, however, showed a significant correlation with ice concentration and a weak one (in 2011-12) with chlorophyll. There is also a tentative correlation between increased calling activity during the high transport deployment year. Gray whales were also sighted in large clusters near the mouth of Barrow Canyon and in the middle of the transect line off Point Hope (Figure 1); areas known to have high biomass of benthic infauna and epifauna. Both of these locations also showed high concentrations of zooplankton (larvaceans and *Pseudocalanus*) as well as high amounts of nitrate and ammonium.

Month and ice thickness, along with several variables that can serve as proxies for prey availability, were significant variables contributing to the top model selected by the GAM runs for walrus calling activity, but ice concentration seems to be negatively correlated with the timing of the start of the summer pulse in calling activity. Possible presence of a polynya and prey availability make the surprising result of overwintering walrus in the northeastern Chukchi Sea plausible; we suggest these are juvenile males that did not migrate to the Bering Sea mating grounds. Month and ice concentration were significant variables contributing to the top model selected by the GAM runs for bearded seals, as well as several variables that serve as proxies for prey availability that might be the reason the ramp-up of bearded seal calling levels varies interannually and among locations. Both walrus and bearded seals were found along the Icy Cape and Wainwright transect lines near the shoals, an area known to have high biomass of benthic epifauna and infauna, but there were few overlapping sightings between the species. Ice noise activity levels were highest inshore and seemed to be influenced by wind direction. At all locations ice concentration was positively correlated and ice thickness was negatively correlated with ice noise activity levels.

5. *Recommendations*

The data collected for the CHAOZ project demonstrate the utility and benefit of concurrent zooplankton, oceanography, and marine mammal monitoring. These data, combined with those currently being collected for the ongoing BOEM-funded ARCWEST and CHAOZ-X projects represent the only long-term integrated dataset of its kind from the Chukchi Sea lease area and Alaskan Arctic in general. We therefore recommend continuation of the long-term mooring deployments. With current modifications to the moored TAPS6-NG instruments, we will be able to collect data for a full year, allowing for assessment of trophic interactions on an annual time scale. It will also be possible to establish multi-year patterns in marine mammal distributions as they relate to indices of zooplankton and oceanographic conditions. As mentioned earlier, the addition of CPODs on the passive acoustic moorings would allow for determining foraging efforts of belugas, which would aid in understanding habitat utilization as well as correlations with potential prey.

We also recommend continuation of the integrated biophysical shipboard surveys conducted during this study. These surveys provide data on the fine-scale vertical resolution of zooplankton abundance as they correlate with oceanographic indices, nutrients, and distribution of marine mammals. To maximize marine mammal detections during shipboard surveys, it is essential to have both passive acoustic monitoring and visual survey components. Since each method is well-suited to particular species, together they provide a more complete picture of marine mammal distribution. Integration of recent benthic ecology studies supported by BOEM (e.g., Grebmeier et al., 2015) will help to address prey availability for those mammals that feed on benthic epifauna and infauna.

XI. LONG-RANGE PREDICTIONS OF HABITAT USE BY ARCTIC AND SUBARCTIC MARINE MAMMAL SPECIES

1. Discussion

Current situation

The high benthic biomass and productivity in the Chukchi is driven by a combination of highly productive waters being advected through the Bering Strait and locally produced primary productivity. It is estimated that approximately 40% of the productivity in the Chukchi Sea shelf is a result of advection from the Bering Sea (Springer et al., 1989; Grebmeier et al., 2006b; Grebmeier, 2012). Dense, nutrient-rich Bering Sea water/Anadyr water flows north through Bering Strait, driven by a pressure head between the Pacific and Arctic Oceans and modified by strong north-south winds (Figure 135). This dense Bering Sea water transports high levels of nutrients to the bottom of the Chukchi Sea shelf, which then drives primary, and thus secondary, productivity. While surface nutrients are depleted, a rich supply of bottom nutrients are available to support subsurface blooms. Nutrients are recycled, providing significant concentrations of ammonium, a preferred form of nitrate for phytoplankton. Episodic wind events from the northeast also result in up-canyon flow from Barrow Canyon, introducing nutrients onto the shelf.

Locally, ice-associated algae fall to the bottom as the ice breaks up and melts. As these phytoplankton fall to the bottom, they are “trapped” in the subsurface by a strong pycnocline and the absence of strong winds. Carbon that becomes incorporated into the sediment fuels benthic secondary production. Some of the plant cells may remain suspended and be photosynthetically active depending on light concentration.

Finally, the Alaska Coastal Current consists of warm, fresh water from the Yukon and other river runoff close to shore. The predominant, but weak, winds from the southwest during summer support transport of this water mass northeast along the coast. This strengthens the front that occurs between the ACC and Bering Sea water.

In the discussion below, we use this project’s regional ocean atmosphere circulation model to forecast future conditions in the Chukchi shelf ecosystem. The models predict late arrival of the sea ice and longer open-water seasons in the Chukchi Sea (Section IX.2). Although not much changes before 2050 in the ensemble mean predictions for spring, there are episodic early sea ice retreat events predicted by the models beginning in 2020.

Although the models predict a late arrival of sea ice in the fall, this element has no bearing on future predictions. Ice is a defining characteristic of the Arctic system; it is extensive during late fall, winter, and into spring. The timing of ice retreat in the spring is important in determining ocean temperatures; an early ice retreat permits greater solar heating and results in warmer sea surface temperatures. An early ice retreat also likely results in an earlier export of chlorophyll to bottom. The arrival of ice in November is primarily a result of atmospheric conditions, with ocean temperatures playing a minor role – if the sea surface temperature is very warm, the arrival of ice may be delayed by a few days. Therefore habitat predictions that follow are based on ice extent projections of just the spring ice retreat.

Based on the strong correlation with ice that was evidenced in the GAM results (Section X), marine mammal species will likely be impacted by reductions or changes in sea ice cover. Given this, and the current state of water mass circulation in the Alaskan Arctic, we foresee two possible scenarios, both determined by wind patterns. In the first scenario, with earlier ice retreat or melting and stronger spring/ summer winds, stratification of the water column would be delayed until solar heating effected stratification and the spring phytoplankton bloom would be delayed. Weaker stratification throughout the summer and fall (due to weaker salinity gradients) would enable more summer blooms and an earlier fall bloom. In the second scenario, ice retreat is again earlier (due to melting or advection), but now the winds are weak and salinity gradients are strong. The spring phytoplankton bloom occurs earlier, but summer blooms may be less common and the fall bloom occurs later or not at all. These two scenarios, and the possible outcomes of each, are discussed below. Figure 136 is a schematic representing the current conditions in the Chukchi, as well as the two different scenarios. It is important to note that the timing of ice melt relative to the solar cycle is critical. If the ice melts early then potential ice algal production will be lost.

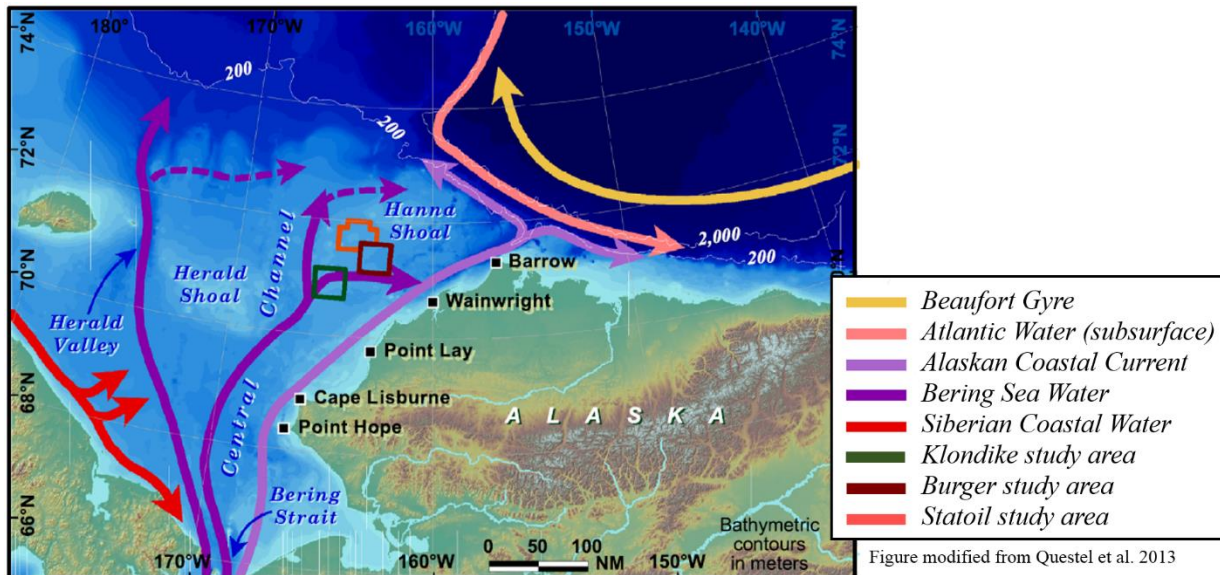


FIGURE 135. WATER MASSES AND CIRCULATION IN THE CHUKCHI SEA. FIGURE MODIFIED FROM QUESTEL ET AL. 2013.

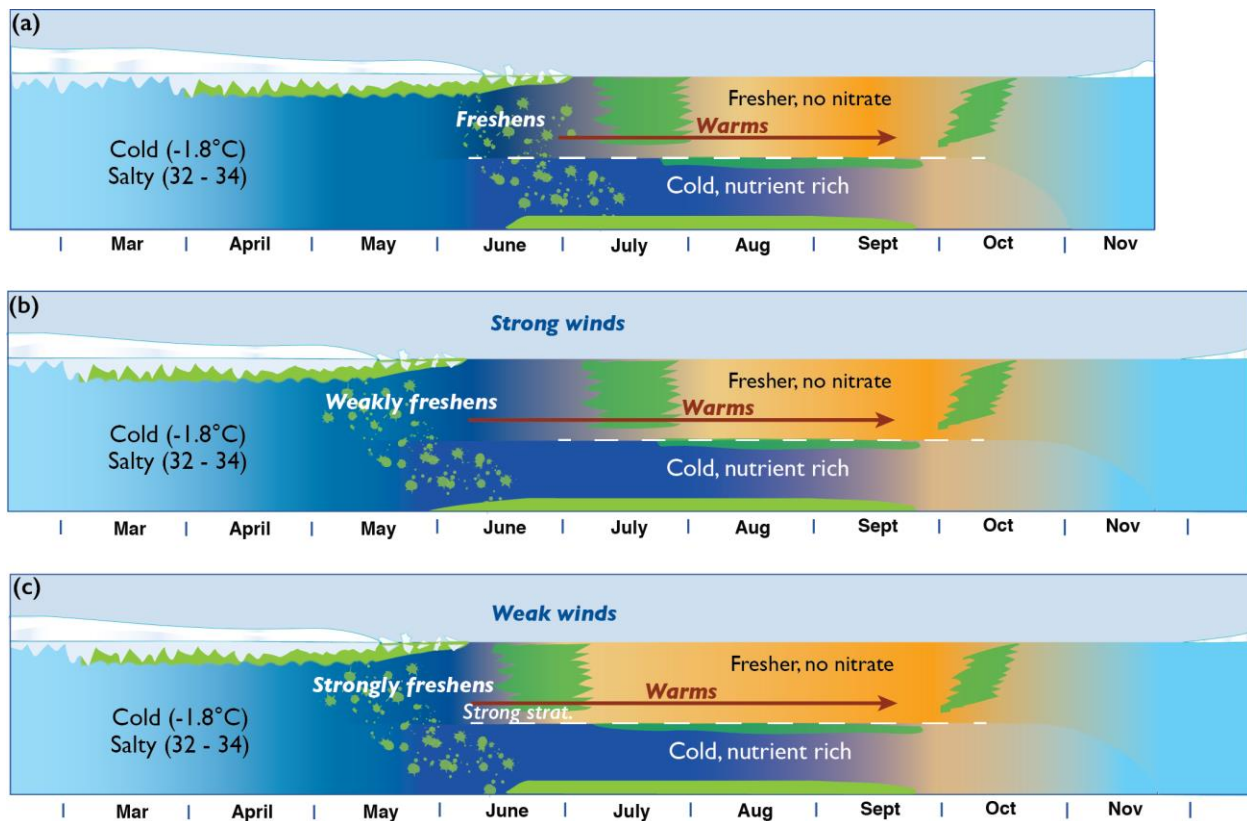


FIGURE 136. SCHEMATIC OF ECOSYSTEMS AND LOWER TROPHIC LEVELS DURING TWO POSSIBLE FUTURE SCENARIOS. A) CURRENT CONDITIONS IN THE CHUKCHI SEA. AN ICE ALGAE BLOOM OCCURS UNDER THE ICE IN LATE WINTER AND EARLY SPRING. THIS IS EXPORTED TO THE BENTHOS WITH THE MELTING ICE. IN SUMMER, A SUBSURFACE BLOOM OCCURS BELOW THE PYCNOCLINE. AFTER THE RETREAT OF ICE AND STABILIZATION OF THE WATER COLUMN, A SURFACE PHYTOPLANKTON BLOOM OCCURS. IN THE FALL, WITH THE MIXING OF NUTRIENTS INTO THE SURFACE A FALL PHYTOPLANKTON BLOOM CAN OCCUR. IN BOTH SCENARIOS ICE WILL RETREAT EARLIER B) STRONG WINDS RESULT IN A MIXING OF THE WATER COLUMN AND LOW VERTICAL SALINITY GRADIENTS AND A DELAYED SPRING PHYTOPLANKTON BLOOM. C) SCENARIO 2. LOW WINDS RESULT IN STRONG STRATIFICATION DUE TO HIGH VERTICAL SALINITY GRADIENTS AND AN EARLIER SPRING PHYTOPLANKTON BLOOM.

Scenario 1: Early ice retreat and strong winds

In the first scenario, early ice retreat is coupled with strong winds. This leads to longer open-water seasons. The strong winds mix the water column, introducing more nutrients from the bottom to the surface and erasing any vertical salinity gradient. The mixing also delays the spring bloom. Early retreat would shorten the period during which ice and associated algae cover the area and shorten the growing season for the ice algae, reducing the flux of carbon to the benthos. The spring phytoplankton bloom is then delayed until the system stratifies due to solar heating. The weaker stratification during summer would allow winds to mix into the bottom layer, introducing nutrients into the surface layer and thus supporting increased summer phytoplankton production. This would provide more food for the pelagic consumers during the short summer. Weakened stratification would also promote an earlier fall bloom. This scenario presently applies to the southern Bering Sea. The scenario predicts a shift from a benthic towards a more pelagic-dominated ecosystem. Such a regime shift may already be occurring in

the northern Bering Sea. The retreat of ice cover led to a decline in the flux of carbon to the sediments, which caused a decrease in benthic prey populations, an increase in pelagic species, and geographic displacement of marine mammal populations (Grebmeier et al., 2006b; Grebmeier, 2012).

In addition, an earlier and longer period of winds from the SW would also have the effect of forcing the ACC to remain close to shore, strengthening the northeast current and increasing advection of coastal plankton from the Bering Strait. This strengthening also tends to concentrate prey near Barrow Canyon (e.g., Stafford et al., 2013), creating enhanced foraging opportunities for higher trophic levels.

The effects of this shift to a more pelagic system on marine mammal distributions are somewhat disparate based on feeding strategies and are summarized in Table 29. Those species that are generalist feeders and prey upon both benthic and pelagic species will fare better than the specialist feeders that rely only on the benthos. Bowheads have the ability to assume a generalist diet. Although they rely heavily on energy-rich epibenthic zooplankton, they feed throughout the entire water column, and therefore are not limited to epibenthic prey (Lowry et al., 2004). While they feed predominantly in the eastern Beaufort Sea, they also engage in feeding along their migration route, taking advantage of any prey aggregations in the Chukchi Sea or near Barrow Canyon (increased in this scenario). In addition, the strengthened ACC in this scenario, combined with a slight shifting of winds from the northeast could result in localized upwelling along the coast, and potentially create “krill traps” along the Chukchi coast similar to those seen near Barrow (Okkonen et al., 2011). Although their additional resilience to changes in sea ice (as a physical structure) and ability to utilize multiple habitats increase their ability to adapt, they have still been identified as “moderately sensitive” to the effects of climate change (Laidre et al., 2008), however, because of their slow population growth and stable innate migration patterns.

Perhaps of more immediate concern, changes to the spring ice extent could have a negative impact on subsistence hunting along the Chukchi coast. Bowheads historically have relied heavily on leads that open in shallow shelf waters during their spring migration. However, as mentioned above, they have been observed in all ice conditions and a variety of habitats. Therefore, a reduction in ice in the spring may reduce the need for the bowheads to remain close to shore, allowing them to migrate further offshore. This will have a substantial effect on spring native subsistence hunting, which has already been affected due to a thinning of the ice which restricts the hunters’ access to the leads. A migration shift offshore would reduce harvest success (e.g., exceeding time limit to land whale before it spoils) while increasing risk to the hunters (e.g., rough seas, ice movements, decreased communication abilities) if they have to travel further from shore.

Beluga whale diets are even more diverse than that of bowhead whales. They prey on benthic, epibenthic, and pelagic organisms (Section VII.A.3), making them excellent feeding generalists. Currently, the ECS population feeds on benthic prey in Kasegaluk Lagoon while molting and calving, before dispersing further offshore to forage. In this scenario, they may shift their diet to take advantage of the increased pelagic prey availability and remain closer to their core summer areas, potentially increasing their presence in the lease area. They may also concentrate near Barrow Canyon, where a strong ACC causes prey aggregation, resulting in higher numbers of belugas (Stafford et al., 2013; Hauser et al., 2014). Alternatively, if the inshore pelagic prey is not ideal, they may disperse farther offshore to remain near the ice edge

and its associated productivity. On par with bowheads as far as resiliency to sea ice conditions, beluga whales can also utilize multiple habitats. In the Laidre et al. (2008) study, beluga whales were regarded as the least sensitive cetacean to climate changes; however, gray whales, which have been referred to as the most versatile and adaptable cetacean species (Moore and Huntington, 2008), were not included in the study. Finally, because the spring beluga hunt in the Chukchi Sea occurs when the whales are in Kasegaluk Lagoon for their annual molt, changes in prey distribution will likely not affect the subsistence harvest.

As mentioned above, gray whales are extremely adaptive and versatile (Moore and Huntington, 2008). Although predominantly benthic feeders, in the Chukchi, they feed on a wide variety of both benthic and pelagic invertebrates (Section VII.A.3), using several different foraging strategies (see Darling et al., 1998 for summary). As such, they are even better suited to adapting to ecosystem regime shifts than beluga whales. A shift to a more pelagic ecosystem will likely have one of two effects. Gray whales may opt to take advantage of the available pelagic prey. Their diets near Vancouver Island are predominated by pelagic invertebrates (Darling et al., 1998), so a dietary shift is not unreasonable. Another possibility is that gray whale distribution will shift farther north or east into the Beaufort Sea where there may still be a high benthic biomass. Such redistribution based on regime shift has already been reported in the northern Bering Sea (Rugh et al., 2001).

Walrus are the most specialized feeders of any Arctic marine mammal included in this study. They are benthic specialist feeders that prefer to eat bivalves, and so the decline in benthic biomass predicted by this scenario would be detrimental to the population. In fact, several authors suggest that walrus will decline if the benthic-pelagic coupling declines (e.g., Bluhm and Gradinger, 2008). In addition, Laidre et al. (2008) suggested that walrus are highly sensitive to changes in sea ice; without ice cover, exploiting such a large foraging area would be physiologically taxing. Walrus have their calves in the Bering Sea; this is therefore not affected by an early Arctic spring ice retreat as the two seas are not coupled in that way. Females nursing pups prefer to haul out on ice to rest near areas with high productivity; however, walrus are limited to shallow water depth (~100m). Unlike beluga whales that can follow the ice edge north, walrus will abandon the ice and begin hauling out on land, far from the best foraging grounds. Furthermore, a lack of sea ice haul-out locations will result in extremely large aggregations at the shore haul-outs. This has already been witnessed along the coast of Point Lay, where walrus were sighted hauled out in unprecedented numbers (ASAMM flight report 240). On September 27, 2014 an estimated 35,000 walrus were hauled out on the shore at Point Lay, whereas just four days earlier, there were only an estimated 1,500 individuals. A similar event was also reported on the far eastern Russian coast. Female walrus tend to avoid hauling out on land, perhaps due to the increased risk to calves in the presence of large herds (Laidre et al., 2008). These large haul outs not only lead to pups being separated from their mothers or perhaps crushed by large males, but also to increased local competition, exhaustion, and possible starvation. The passive acoustic data from Hannay et al. (2013) and radio tag data from Jay et al. (2012) suggest that the walrus are already moving out of the Chukchi Sea, not based on ice advance, but on the retreat of the ice edge. The tag data also found that walrus are moving to the Chukotka coast (where colder temperatures have resulted in a slower ice retreat than that seen in the Alaskan Chukchi) prior to heading down through the Bering Strait. Therefore, while the actual effect of sea ice reduction on walrus populations remains speculative, it is likely to have a negative impact (Moore and Huntington, 2008).

Bearded seal responses to ice reduction are perhaps more difficult to predict, although they have been regarded as the least sensitive marine mammal species to sea ice reduction (Laidre et al., 2008). They are generalist feeders, preying on both benthic invertebrates and pelagic fishes, and therefore, are likely to be unaffected by the pelagic shift in this scenario. They prefer moderately heavy ice cover, and so can occur further north. However, like walrus, bearded seals tend to prefer to feed in shallow water depths (< 200 m) and are limited to how far north they can go. Bearded seals rarely haul out on land, instead remaining pelagic in the open water. Although this is more energy intensive than remaining with the ice, the issues surrounding walrus young being trampled in large land haul-outs is therefore not a concern for bearded seals. Bearded seals also use the ice to whelp/mate/molt between March and late June. Weaning is complete by May, so any small changes in spring sea ice retreat will not have an immediate impact on their reproductive success.

For those Arctic species that can thrive in a pelagic-driven ecosystem, the increased open water period may allow for a longer feeding season. However, a shift to a longer feeding season may be delayed due to endogenous migratory behavior (see Section X). The lack of sea ice and longer open-water season, plus increased phytoplankton production, will also open up new habitats and provide increased foraging opportunities for subarctic species. There is already evidence of these species being reported farther north into the Chukchi (e.g., Clarke et al., 2013; Delarue et al., 2013b; Crance et al., 2015). This influx of subarctic species into the northern Chukchi may lead to increased competition with resident Arctic species. In addition to cetaceans (fin, humpback, minke, and killer whales), the longer open water season may open up new foraging habitat to ribbon seals as well. Although ribbon seals generally remain in the Bering Sea during the ice-free months, a shift to a pelagic system may provide new foraging opportunities.

As mentioned previously, longer open-water seasons and less ice cover could result in more ocean storms, and storms with higher surface wind speeds. In addition to mixing the water column, another effect of increased storms will be an increase in ambient noise. Winds and surface waves have a substantial effect on ambient noise levels. Therefore, an increase in the number and magnitude of the storms will likely result in increased ambient noise levels by an estimated 10-15 dB (see Section XII). This would negatively impact the communication efficiency of marine mammals, and increase the potential for masking of acoustic signals between conspecifics.

TABLE 29. SUMMARY OF THE EFFECTS OF SCENARIO 1 ON KEY MARINE MAMMAL SPECIES.

Species	Impacts
Bowhead whales	<ul style="list-style-type: none"> • Potential changes to timing and migration routes may impact subsistence harvest • Increased water column production and transport may increase plankton prey availability
Beluga whales	<ul style="list-style-type: none"> • Subsistence harvest will likely not be affected • Increased water column production and transport may favor pelagic fish prey, but not Arctic cod
Gray whales	<ul style="list-style-type: none"> • Decrease in ice may increase access to foraging habitat • Declining benthic prey availability; may switch to alternative foraging strategies
Walrus	<ul style="list-style-type: none"> • Decreased access to ice over shallow feeding grounds; increased haul-outs on shore and increased risk to adult females and calves • Declining benthic prey availability
Bearded Seal	<ul style="list-style-type: none"> • Decreased access to ice over shallow feeding grounds; increased energy expenditure while foraging • Declining benthic prey availability may result in a shift in foraging strategies to take advantage of increased pelagic prey availability
Ambient Noise	<ul style="list-style-type: none"> • Increases due to greater ocean storm noise as well as increased ship traffic. Estimated 10-15 dB increase in ambient noise levels • Increased ambient noise levels could result in decreased communication or foraging efficiency for all marine mammal species

Scenario 2: Early ice retreat and weak winds

The second scenario presents a very different possibility, but also includes the interaction of ice melt and winds. Ice is predicted to leave the region earlier in the year, but with weaker winds, a “cap” of low salinity water forms on the surface, which will not mix without substantial wind energy (i.e., there is strong vertical stratification). Subsequent solar heating is limited to the upper layer, which enhances the stratification. Earlier stratification will support an early surface phytoplankton bloom, which will utilize the remaining nutrients in the upper layer. This cap will then limit further surface phytoplankton blooms. Although the increased penetration of light below the pycnocline may allow subsurface phytoplankton blooms to form, the extent of the productivity of these blooms is unknown. In addition, the strong stratification can delay the mixing of the water column in the fall, thus reducing the fall phytoplankton bloom.

In addition, weak winds would allow the warm, fresh ACC water to spread out over the Chukchi shelf rather than remain along the coast. This would add to the melt water cap, further stratify the water column, and slow the transport of ACC water from the northern Bering Sea. Similar changes have already occurred near the MacKenzie River Delta (Wood et al., 2013). Studies have shown that an increase in fresh, warm water runoff into the Beaufort Sea causes the ice in that region to melt and retreat earlier than adjacent coasts with minimal runoff (Wood et al., 2013). These studies were conducted over a decade ago, and ice retreat and fresh water runoff have increased considerably since then. This increased input of fresh water will lead to larger amounts of fresh/brackish water at the coastal nearshore areas. Studies have shown that areas with brackish water at river deltas have decreased biomass, diversity, and productivity; a result of decreased light levels in the water due to suspended sediments and dissolved organic matter (Bluhm and Gradinger, 2008). Thus, with decreased ice inshore and lower light levels, less production falls to the bottom and inshore benthic prey populations may decline.

A similar situation occurring in the northern Bering Sea could have a large impact on the productivity of the Chukchi shelf. If the winds weaken on the northern Bering Sea shelf, then it will leave a stratified water column in the northern Bering Sea, which may reduce the flow of nutrient-rich Anadyr water into the Chukchi Sea. With a decreased influx of nutrients, phytoplankton production will have to rely to a greater extent on remineralization of locally-produced organic matter to produce nutrients. Furthermore, without the strong ACC moving north along the coast, there would be a lessening of the front that aggregates prey for marine mammals.

As in Scenario 1, the timing of ice melt relative to the solar cycle (light availability) is important. If the ice melts earlier, then the ice algal contribution to vertical carbon flux will be less. Similarly, the primary production in the surface waters may decline because the low salinity surface waters and weak winds prevent mixing of nutrients into the surface waters. These predicted events would reduce the amount of carbon reaching the benthos and secondary production. The effects may be most intense nearshore where the influence of the warm, fresh water is the greatest, thus the nearshore benthic biomass may decline relative to historical levels with increases in relative biomass farther offshore around the lease area or farther to the north as the ice retreats.

The effects of these changes on key marine mammal species are presented in Table 30. In this scenario, benthic production and biomass are predicted to decline, and the extent of pelagic production is unknown. As in Scenario 1, feeding generalists should fare better than feeding specialists. Bowhead whales are generalist feeders, feeding on both planktonic and benthic prey, although they rely heavily on epibenthic zooplankton. Declines in benthic biomass (under this scenario) would result in decreased foraging opportunities, especially nearshore; however, we do not know if there will be an increase in the production of their pelagic prey. If there is an increase in pelagic prey, they will likely shift to a pelagic-dominated diet. Otherwise, they will need to shift their migration offshore to take advantage of foraging opportunities. In either case, the weakened ACC will result in an increase in brackish water, decreasing overall productivity nearshore. This could negatively affect native subsistence hunting, which is currently restricted to nearshore waters, and could bring the whales much closer to the lease areas.

Beluga whales are generalist feeders, and as such may begin (or continue) relying more heavily on pelagic prey as their predominant food source. As such, their distribution and

migration patterns may shift slightly. Although they will still go to Kasegaluk lagoon to molt and calve, their distribution patterns after molting may change as a result of prey availability. If sufficient pelagic prey are available, they may shift their diet and remain closer to their summer core areas; however, insufficient pelagic biomass inshore may cause them to disperse farther offshore, following the ice edge and its associated productivity. Given the reduced nearshore biomass, gray whales may have to move farther offshore (closer to the lease area), or potentially into the Beaufort Sea to a more suitable habitat with increased foraging opportunities. Nevertheless, the versatility of the gray whale and their generalist feeding strategy make them the best suited to adapt to ecosystem shifts.

As feeding specialists, walrus are the most vulnerable under this scenario. With a lack of ice, walrus (especially females nursing calves) would have to haul out on land, then go further offshore, where benthic productivity is higher, to feed. This would be energetically unfavorable, potentially affecting survival and reproductive success. As in Scenario 1, walrus would be hauling out in extremely large numbers, which would be detrimental to calves and the overall health of the population (Udevitz et al., 2013), so they may choose instead to relocate to the Chukotka coast. Bearded seals may fare better than walrus, given both the short amount of time it takes to wean their pups, as well as their flexible foraging strategies. Although bearded seals are limited to foraging at depths less than 200 m, given the shallow depth and broad expanse of the Chukchi Sea shelf, the only limiting factor for this species would be the extent of the decreased productivity offshore.

As with Scenario 1, any decrease in sea ice will lead to an increase in subarctic species (e.g., fin, humpback, minke, and killer whales) encroaching into Arctic waters. Longer open-water seasons may increase foraging opportunities for non-resident species, and create an increase in competition with resident Arctic species. Moreover, given there is already evidence of subarctic species moving farther north into the Arctic in the current benthic-dominated system (e.g., Clarke et al., 2013; Delarue et al., 2013b; Crance et al., 2015), it is reasonable to assume that if benthic productivity is already depressed, pelagic productivity does not increase, and foraging effort outpaces primary or secondary productivity, any increase in competition will put strain on the higher trophic levels. This strain may be more than expected in Scenario 1, given that this scenario does not necessarily include an increase in pelagic biomass.

In regards to noise levels, a strong pycnocline created by the cap of fresh warm water would create a dramatic change in typical sound transmission properties such that sounds would tend to be trapped within the layer in which they were produced and be poorly transmitted between layers. This would then affect communication between vocalizing animals, reducing the communication range for individuals in different layers. As with Scenario 1, the ambient noise levels are expected to increase by an estimated 10-15 dB.

TABLE 30. SUMMARY OF EFFECTS OF SCENARIO 2 ON KEY MARINE MAMMAL SPECIES.

Species	Impacts
Bowhead whales	<ul style="list-style-type: none"> • Potential changes to timing, migration routes, and Chukchi residency to impact subsistence harvest • Decreased production and transport may decrease prey availability
Beluga whales	<ul style="list-style-type: none"> • Subsistence harvest will likely not be affected • Decreased production and transport may result in a shift in diet or further dispersal offshore
Gray whales	<ul style="list-style-type: none"> • Decreased production and transport may shift distribution farther offshore • Shift in distribution may bring them closer to lease area
Walrus	<ul style="list-style-type: none"> • Decreased access to ice over shallow feeding grounds; increased frequency of haul-outs on shore • Declining benthic prey availability, particularly nearshore
Bearded Seal	<ul style="list-style-type: none"> • Decreased access to ice over shallow feeding grounds • Declining benthic prey availability, particularly nearshore; their generalist foraging strategy may give them an advantage if pelagic prey increases
Ambient Noise	<ul style="list-style-type: none"> • Increased noise levels due to strong water column stratification and increased shipping traffic. Ambient levels may increase by 10-15 dB • Increased ambient noise levels could result in decreased communication or foraging efficiency for all marine mammal species

2. *Conclusions*

We predict two possible scenarios, both of which are dependent on the winds. If the winds remain strong and persist from the southwest, then sea ice may be forced out of the area before substantial melting and the spring ice algal bloom occurs. This will result in a loss of carbon flux to the benthos, a strengthening of the Bering Sea water and ACC into the Chukchi, and higher transport of nutrients into the system. However, an increase in ocean storms will cause mixing of the water column, resulting in a shift to a pelagic regime. Our climate model predictions estimate that the magnitude and direction of the currents will remain similar to present day levels. If this holds true, then this pelagic-shifting scenario is highly likely.

The second scenario suggests that a decrease in winds and continued warming of the atmosphere will cause the ice to melt earlier in the year, resulting in a more heavily stratified water column. Reduced winds will result in a weakening of the ACC, with reduced advection of nutrients from the Bering Sea. Benthic productivity will decrease, particularly nearshore, although effects on pelagic productivity remain unknown.

Both scenarios predict an increase in low-frequency ambient noise levels, due to both environmental as well as anthropogenic (e.g., seismic airguns, increased shipping traffic) sources, both of which are a result of predicted longer open-water seasons. The predicted increase of 10-15 dB in low-frequency ambient noise would dramatically change the acoustic environment and acoustic habitats for species that rely on the low-frequency band for basic life functions such as communication, foraging, navigating, and evading predators. This would include bowhead, beluga, and gray whales, bearded seals, and walrus, all of which could experience chronic reductions in communication space and disruptions in the adaptive benefits of lower ambient noise conditions.

Bowhead, beluga, and gray whales are the most adaptive, and are best suited to adjust to a regime or ecosystem shift. However, ecosystem changes may result in population or migration re-distribution for some species, which could have severe negative effects on native subsistence hunting. Walrus are predicted to be the most vulnerable to climate change or ecosystem shifts. They may be forced to haul out on the coast, which will impact population health; they may also move out of the Chukchi Sea, which some studies show is already happening. Bearded seals are more adaptable than walrus, and will probably adjust accordingly. Finally, longer open-water seasons will result in more subarctic species moving farther north into the Chukchi Sea and creating increased competition with resident Arctic species.

It is important to remember that no matter the scenario, most marine mammal species have innate migration patterns and reproductive cycles, as seen in the strong correlation between most of the marine mammals and month in the GAM integrative results (see Section X). As such, migration timing and patterns either may not change significantly, or those changes may be considerably delayed. This illustrates the importance of continued long-term passive acoustic monitoring, which is ideally suited to documenting migration patterns.

3. *Recommendations*

While we have some ideas of future predictions and ecosystem changes, these are based largely on only two full years of data. Thus, it is essential to continue collecting oceanographic, biophysical, and passive acoustic data to augment our current knowledge about the Alaskan Arctic ecosystem. Moorings should be deployed not only in locations where the biggest oceanographic, marine mammal, and prey distribution changes are expected to occur, but also across a range of locations and predictions. Furthermore, it is critical to know what is happening with the environmental parameters in the crucial spring and fall months. However, because the Arctic is ice-covered for 8-9 months a year, these seasons are currently inaccessible with most present technologies, the exception being passive acoustic recorders. To collect the necessary suite of crucial data, we need investments in technologies that will allow us to collect those data during time periods and in places that we are currently unable to access. This may be in the form

of new advanced moorings, subsurface gliders or AUV's, etc. In addition, it is critical that we maintain a large spatial sampling scale with the acoustic recorders to monitor changes in marine mammal distribution and ambient noise levels. Passive acoustics is currently the best means of assessing these distributions and noise levels year-round and is best suited for determining if there are changes in species composition, distribution, or migration patterns in this rapidly changing ecosystem (Hannay et al., 2013; Clark et al., 2015). Finally, to understand how whales relate to indicators from oceanographic and prey studies, it is imperative that technologies such as satellite telemetry and other animal-borne sensors fixed with dive profile instruments be included as a key component in ecosystem research. This will provide information during discrete real time sampling as well as provide long term information on habitat utilization as it relates to mooring data. This in turn will aid in strengthening future predictions.

XII. NOISE MODELING AND IMPACT MITIGATION

1. *Methods*

There were two different methods developed for each of the two primary objectives. The primary objectives were to develop and implement methods to: a) report occurrences of acoustically active marine species and ocean noise metrics in near-real-time, and b) quantify and assess the Chukchi Sea's "noise budget" (including biotic and abiotic sound sources) and assess the influences of individual source types and the aggregate of multiple sources, including different source types, on the overall acoustic environment and on the acoustic habitats of selected marine mammal species. As a result we now have a method by which to quantify the acoustic contributions from vessels and seismic airgun surveys to the aggregate noise budget (see Clark et al., 2009; Hatch et al., 2012). Throughout this report the term *impact mitigation* will be used to refer to the method of near-real-time monitoring and the term *noise modeling* will be used to refer to the method of assessing the influences of sound sources on ambient sound levels, the acoustic environment, and species-specific acoustic habitats.

Impact Mitigation

Auto-detection Buoy

Throughout this report, the term AB-2012 will be used to refer to the auto-detection buoy deployed and operated in 2012. The AB-2012 system transmitted bowhead whale detection data and ambient noise data to Cornell-BRP in near-real-time via Iridium satellite (see <http://www.listenforwhales.org>, <http://stellwagen.noaa.gov/protect/whalealert.html> for an operational example of this system). The methods implemented by this system provided the mechanism by which timely information was delivered on the presence of an endangered species in a zone leased for industrial development and on ambient noise levels in the 10-4000 Hz frequency band.

The AB-2012 was programmed to sample continuously at 8 kHz (10 - 4000 Hz effective bandwidth), detect potential bowhead sounds and compute ambient noise spectral distribution measurements. The detection process ran continuously and was maintained using an on-board data management system. The system transmitted the top 10, 2-s acoustic detections, referred to as sound clips, every hour via Iridium satellite to Cornell (Spaulding et al., 2010). A sound clip's detection rating was based on how well its acoustic features matched the features of modeled bowhead frequency-modulated calls derived from >10,000 bowhead call examples. The on-board noise analysis process computed a 1024-point discrete Fourier transform ensemble every 30 seconds and transmitted the resultant spectral data every 2 hours. The process of computing spectral distribution data was specifically motivated by the expectation that such data would provide timely information on the occurrence and received levels of abiotic acoustic events (e.g., from seismic airgun activity, vessel traffic, weather, ice) and biotic events (e.g., choruses of singing bowheads or bearded seals). It was not intended to enable observation of sparse events such as single marine mammal calls (e.g., from bowheads).

Both the detection and spectral data were available via a web-based, on-line system and visualized with a basic GUI

(<http://test.nrwbuoys.org/ab/clip/?position=Chukchi&search=pos:Chukchi>). Several of the many enhancements of the system included ruggedization of the mooring by Woods Hole Oceanographic Institution (WHOI) ocean engineers for the demanding arctic environment; modularization of the onboard data acquisition, signal conditioning, processing, management, and transmission sub-systems by Cornell-BRP engineers; and implementation of bi-directional communications by Cornell-BRP engineers. The latter improvement provided a mechanism by which, for example, Cornell-BRP could reprogram onboard code and request transmissions of selected portions of acoustic data. The buoy was outfitted with a Xeos tracker, which provided a mechanism by which WHOI and Cornell-BRP could observe the GPS position of the system in the event that it drifted from its mooring location.

Auto-detection performance evaluation

Prior to deployment of AB-2012, Cornell-BRP developed a methodology for evaluating the performance of the automated bowhead whale call detector. Since bowhead acoustic detections are relatively rare, we chose to use Precision/Recall curves to measure performance, because such curves are not subject to the issues of uneven class size that can be a problem when using Receiver Operating Characteristic (ROC) curves. The general procedure started by running the detector/classifier with a low detection threshold, yielding a large number of candidate detections, most of which would be false. We then computed *a posteriori* the Precision and Recall at various intermediate thresholds, yielding various performance curves as shown in Figure 137. We measured performance in this way for several different methods of sound classification. As a control, we scored detected events according to the maximum signal-to-noise ratio during the event.

Not surprisingly, as shown in Figure 137 (Amplitude Only, blue “x” values), precision did not change significantly as the score increased, since a higher score simply corresponds to a louder call event. Based on this performance we estimated that we could improve the threshold so as to detect about 30% of the potential calls, 80% of which would be classified as true calls.

Onboard the autobuoy deployed in 2012, we used a simple Discrete Hidden Markov Model (HMM) classifier. A short-time Fourier Transform (STFT) spectrogram was computed using a DFT size of 256 points, and an overlap of 192 point, and then a bank of four binary image filters was applied, each intended to enhance ridges in one of four “directions”, vertical, horizontal, and both diagonals. Finally, a measure of local ridge energy was computed as the max of the directional filtered energies, and a local directional estimate was assigned according to which filter produced the maximum energy output. The HMM observed symbols were represented by a pair of variables per spectrogram time slice, the modal (max) frequency index, and the estimated contour direction at the modal frequency. This gave $4 * 256$ possible symbols, but we further reduced this by integer-dividing the frequency index by 4, leaving 256 symbols. The HMMs used 16 hidden states, and were trained as “forward” models, allowing only increasing internal state index.

Using this pair of models, we were able to improve upon the trivial classifier. Some operating points offered a precision of about 80%, while keeping more than 30%. This curve is represented in Figure 137 by the red “x” marks labeled “Discrete HMM (deployed)”.

This discrete HMM was not optimal, and we later did some experiments with a vector-quantized HMM which seemed likely to improve performance. We used a standard k-means procedure to estimate the k=256 most representative frequency-direction pairs. We used the full set of true and false detected events in the training set to compute these optimal symbols, and used the full-resolution frequency values.

This evaluation is shown by the sequence of light blue “x” marks labeled as “Vector-Quantized HMM” in Figure 137. It can also be seen that when we used the vector-quantized feature set, the number of false positive events was reduced by roughly 50%, giving us more than 90% precision at 30% recall. We also ran the detector with a lower threshold to produce a greater number of candidate events for classification. The performance of the lower threshold detector/classifier is shown in Figure 137 by the two sequences of “x” marks labeled as “Amplitude Only, Lower Threshold” (green) and “Vector-Quantized HMM, Low Threshold” (purple).

The vector-quantized HMMs were trained using hold-out cross-validation, where each model was trained on 80% of the data and tested on the remaining 20%. At the lower threshold, it would be possible to have a higher recall (around 60%) at our original 70% precision. As shown in Figure 138, the performance was only slightly degraded between the training and test sets, indicating that we were most likely not over-fitting the models. For future deployments, we could use the vector-quantized models to improve detector performance. In both cases, the HMM training and test data were drawn from the same recording, so our performance estimates here are likely to be optimistic.

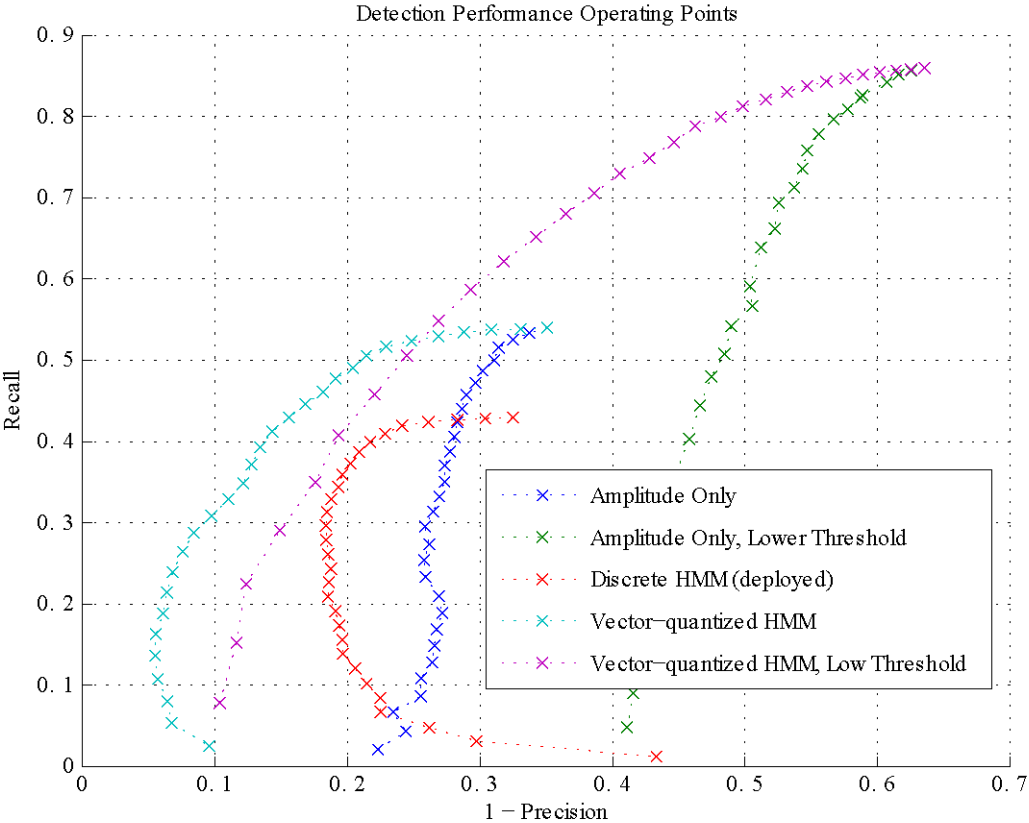


FIGURE 137. DETECTOR PERFORMANCE CURVES AS A FUNCTION OF DIFFERENT DETECTION THRESHOLD SETTINGS (SEE TEXT FOR DETAILS).

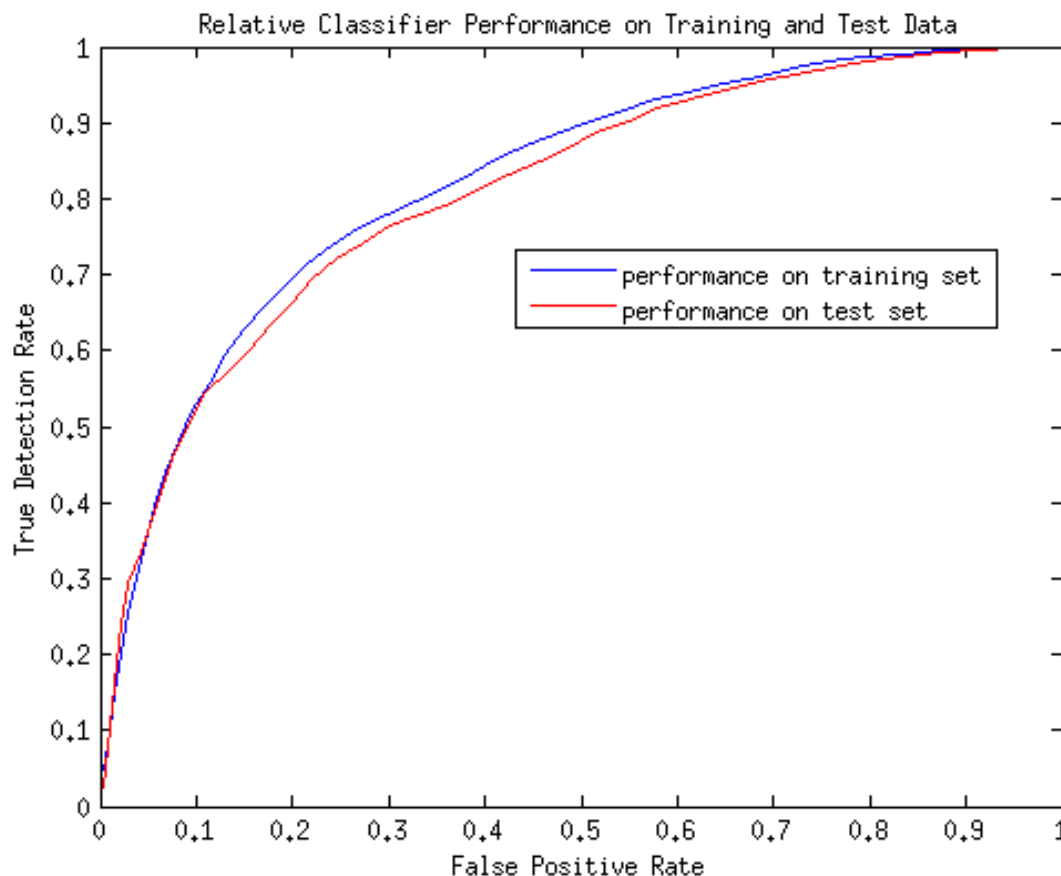


FIGURE 138. RELATIVE CLASSIFIER PERFORMANCE OF TRAINING AND TEST DATASETS.

AB-2012 Deployment and Recovery

On 9 August 2012, AB-2012 was successfully deployed and began operating in the Chukchi Sea in an area of oil and gas development: 71.17411° N by 161.558° W. The initial recovery attempt on 21-22 Oct 2012 by WHOI on board the USCGC *Healy* was unsuccessful due to high sea-state conditions. Shortly thereafter, the Xeos tracker indicated that AB-2012 was adrift. Despite this condition, the buoy continued to function properly, and even continued to report some interesting biological detections during this time. On 09 Nov 2012, with logistical help from Dr. Michael Macrander and the Shell Exploration & Production Company, the entire AB-2012 system was successfully recovered, including the mooring and anchor. Cornell-BRP's onboard data processing and recording module was eventually delivered to Ithaca, NY in January, 2013.

Upon arrival in Ithaca, the FLASH memory data from AB-2012 was downloaded into the CHAOZ-2012 acoustic data system along with the sound clips received from AB-2012 while it was operating. At this time we determined that AB-2012's on-board FLASH drive had filled to capacity on 22 October at 00:37 h local.

Noise Modeling

MARU-DB Recorders

In the summers of 2010 , 2011, and 2012 a single marine autonomous recording unit (aka MARU: Calupca et al., 2000, Clark et al., 2002, Parks et al., 2009) supplemented with a second glass sphere containing additional batteries was deployed in the Chukchi Sea (Table 31, Figure 139). Throughout this report, the term MARU-DB will be used to refer to this “double-bubble” configuration, and a suffix will be used to refer to the start and end year during which the recorder operated (e.g., MARU-DB-2010-11 refers to the recorder that started recording in 2010 and ended in 2011). This passive acoustic recording method addressed a core task of the second objective, which was to use empirical data to calculate the spatial-temporal-spectral variability of the acoustic environment in the Chukchi Sea. An expected secondary benefit of this method was that it would provide additional data on bowhead whale acoustic occurrence to compare with AB detection results. As it turned out, this secondary benefit was never realized because MARU-DB-2012-13 failed to record.

Each MARU-DB was programmed to record continuously at a 2 kHz sampling rate. In the first year’s deployment, MARU-DB-2010-11 recorded on a 50% duty cycle (30-min on, 30-min off) over a 12-month recording period. In 2011-12, the MARU-DB recorder was programmed to record continuously.

A MARU-DB recorder consisted of an HTI-94-SSQ hydrophone with a sensitivity of -168 dB re 1 V/μPa, an amplifier with a gain of 23.5 dB and an A/D converter with a sensitivity of 10³ Bit/V. The final transformation coefficient used for calculating sound level metrics was -151.2 dB re 1 μPa. The system had a flat (± 1.0 dB) frequency response between 10 – 585 Hz (Parks et al., 2009).

TABLE 31. LISTING OF THE CORNELL AUTO-DETECTION BUOY AND MARU RECORDING INFORMATION. MARU ID REFERS TO THE ACTUAL ID NUMBER OF THE MARU IN THE CORNELL-BRP FLEET. “GB DATA” REFERS TO THE TOTAL AMOUNT OF DATA RECORDED IN GIGABYTES. “SR” REFERS TO THE SAMPLING RATE.

MARU-DB Name	MARU ID	Start Date	End Date	Longitude	Latitude	No. of Days	GB data	SR (kHz)	Duty Cycle
AB-2012	--	29-Aug-2012	3-Nov-2012	-163.67602	70.99917	65	26.7	8	100%
MARU-DB-2010-11	204	11-Sep-2010	1-Sep-2011	-163.7320	71.02590	355	67	2	50%
MARU-DB-2011-12	197	1-Sep-2011	29-Aug-2012	-163.730	71.02730	364	117	2	100%

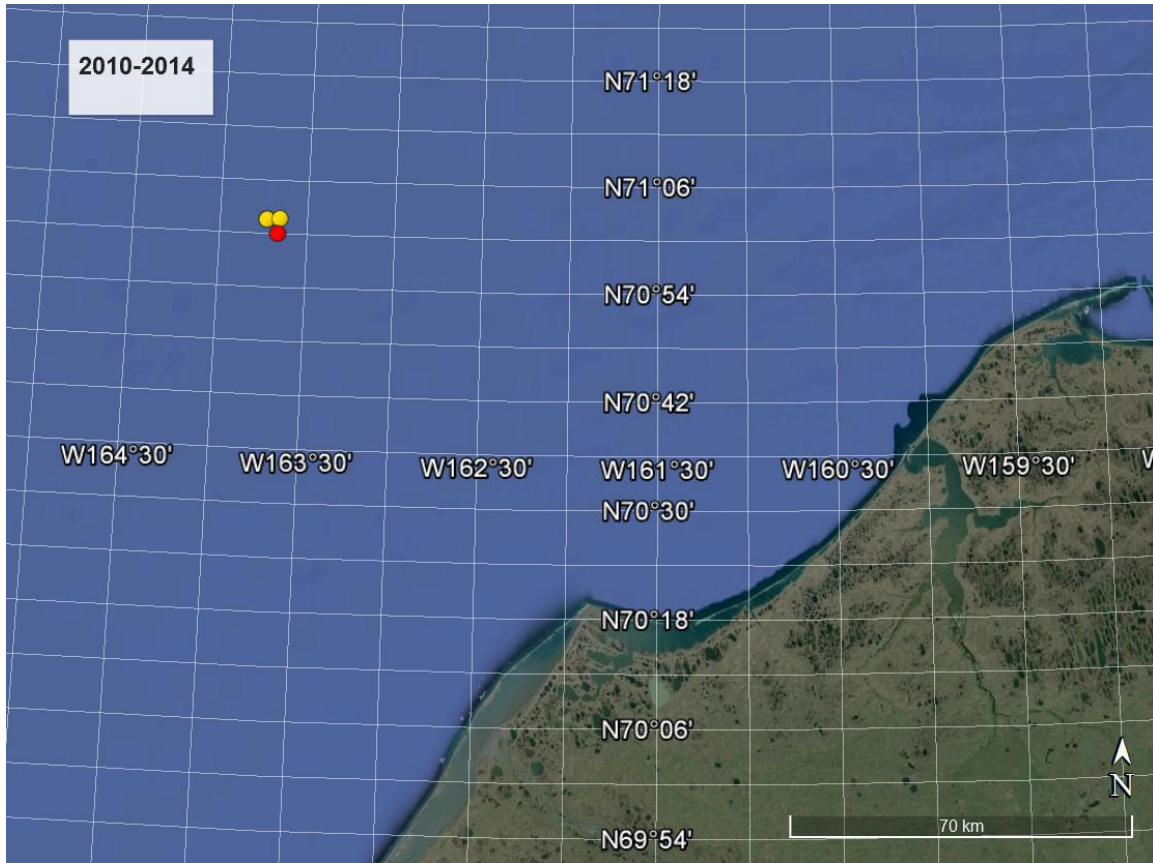


FIGURE 139. LOCATIONS OF THE AB-2012 (RED) AND MARU-DB RECORDERS (YELLOW) RELATIVE TO THE NORTH SLOPE, AK COASTLINE. NOTE THAT THE POSITIONS OF THE EQUIPMENT WERE INTENTIONALLY LOCATED IN NEARLY THE SAME SPOT YEAR AFTER YEAR.

Acoustic Detections

Data from MARU-DB -2010-11 and MARU-DB-2011-12 were analyzed for the acoustic occurrence of seismic airgun array events and bowhead sounds. Analysts with experience in both types of sound events used Raven software (Charif et al., 2004) to review and annotate the data at a 12 h resolution. By this procedure, two daily 12 h time periods (00:00 – 12:00 and 12:00 – 24:00 UTC) were scrutinized for the non-occurrence (0) or occurrence (1) of bowhead calls and bowhead songs. Given that the primary objectives for the Cornell-BRP efforts were directed at quantifying the ambient noise environment and real-time detection of bowhead sounds, the bowhead detection results from the analysis of the MARU-DB data are not included here.

Acoustic Ecology Analytical System

A combination of existing analytical acoustic technologies and newly developed analytical methods were applied to meet project objectives. Initially in the project, the analytical components were developed independently. Over the course of the project we began to convert

these components into object-oriented modules and integrate them into a more comprehensive system, which, for the sake of simplicity, we refer to as DELMA⁵.

The DELMA system provides a quantitative mechanism by which to analyze, aggregate, quantify, estimate, assess and visualize potential influences of different sound source types on the overall acoustic environment. It provides the mechanisms by which to engage the same suite of processes for either individual sound source types or aggregations of different types. When applied to a particular species of interest, it provides the mechanisms by which to assess the impact of individual or aggregated sound source types on the species' acoustic habitat. This process can be thought of as a mechanism by which to quantify the "acoustic budget" for an area of interest, where measures are calculated as functions of time, space and acoustic spectra (e.g., sound level in dB in a frequency band of interest).

DELMA was used to process all recorded data into root-mean-squared (RMS) sound level values (decibels, dB re 1 μ Pa) within the 10 – 1000 Hz frequency band at 1 sec and 1 Hz resolutions, rounded to the nearest dB. These basic sound level metrics were computed using customized sound analysis software MatLab module in DELMA. This system operated on either a high-performance computing platform, which greatly facilitated data processing speed and provided the capability to efficiently reprocess data as needed (Dugan et al., 2011), or a multi-core stand-alone computer system.

Acoustic measurement analysis was performed on all recorded data and stored as MatLab *.mat files. Additional Matlab software was developed to enable a variety of ways to visualize these *.mat files, and these visualizations were stored as Matlab *.fig files, *.png files, and *.eps files, as needed.

For comparative noise analysis, 3rd-octave sound levels were calculated for the 21 3rd-octave bands spanning the 9-891 Hz frequency band. Sound level measurements within this 9-891 Hz band, regardless of the time period over which a measurement was calculated, are referred to as broadband levels. A limited portion of the 9-891 Hz frequency band was further used to quantify noise levels for a frequency range in which bowheads produce many, if not most, of their calls and a large portion of their song notes. This band consisted of 11 3rd-octave bands spanning the 71 – 708 Hz frequency range and is referred to as the bowhead-band.

Results from the basic sound analyses were used to compute, illustrate, and compare a suite of acoustic measures for both the broadband and bowhead-band. This analytical suite included narrowband spectrograms, 1/3-octave spectrograms, and sound level percentiles for each 1 h period (5th, 25th, 50th, 75th, and 95th, where 50th percentile is the median noise level, and 25th percentile and 75th percentile levels are used to illustrate variability), and cumulative distributions of median levels. These results were also used to assess the spatial-temporal-spectral variability of the acoustic environment.

Figure 140 shows a diagrammatic schema of the components of the acoustic ecology analysis system. This system takes advantage of recently developed methodologies to calculate the noise budget contributions from different types of anthropogenic sound sources and their influences on the acoustic environment (e.g., Clark et al., 2009; Hatch et al., 2012; Williams et al., 2014). The basic input components in the system include such items as: estimates on the

⁵ In the initial years of this project we used a customized software code referred to as SEDNA, but this evolved into a more comprehensive system now referred to as DELMA.

numbers and distributions of different marine mammal species of interest (i.e., Biological Data); time-varying positions, empirical and/or estimated sound fields generated by each type of anthropogenic activity (i.e., Vessel Database and Vessel AIS/GPS); acoustic contributions from abiotic environmental sources such as wind and ice (i.e., Weather Data); sound propagation models informed by site-specific parameter values (i.e., Propagation Modeling); and empirical acoustic data (i.e., MARU-DB Data); and empirical or proxies for species specific sound source levels and auditory thresholds.

All DELMA data analysis products are archived in a Cornell “Box.” All data and data products will be fully available. Some examples of the types of results, in this case shown as figures, generated from different components of this system as diagramed in Figure 140 include:

1. Noise Report Browser: showing the analysis of MARU-DB data visualized as an annual 4-channel plot (Figure 141);
2. Spatial Analyzer: a single frame from an animated integration of a seismic survey vessel and acoustic data from the Beaufort Sea as received on an array of MARUs (Figure 142); and
3. Communication Space Visualizer: a map surface (latitude by longitude) showing communication space for a species of interest based on the integration of noise fields generated by different sound sources and a modeled sub-population of animals. In this four-panel example (Figure 143) the sound sources are noise generated by surface winds under low wind and high wind conditions and noise from a ship (R/V *Cape Flattery*).

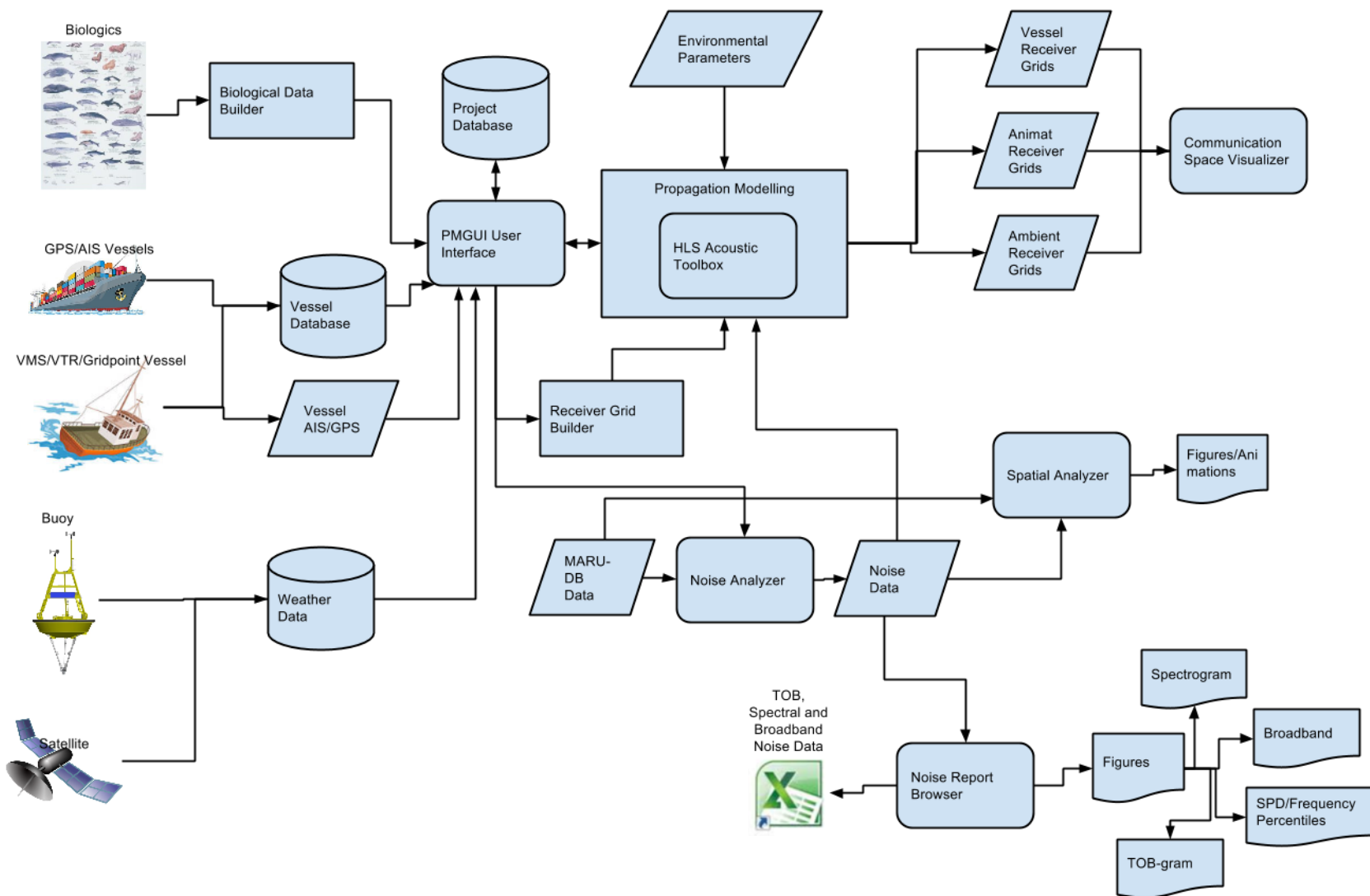


FIGURE 140. DIAGRAM SHOWING THE SCHEMA AND COMPONENTS OF THE ACOUSTIC ECOLOGY SYSTEM.

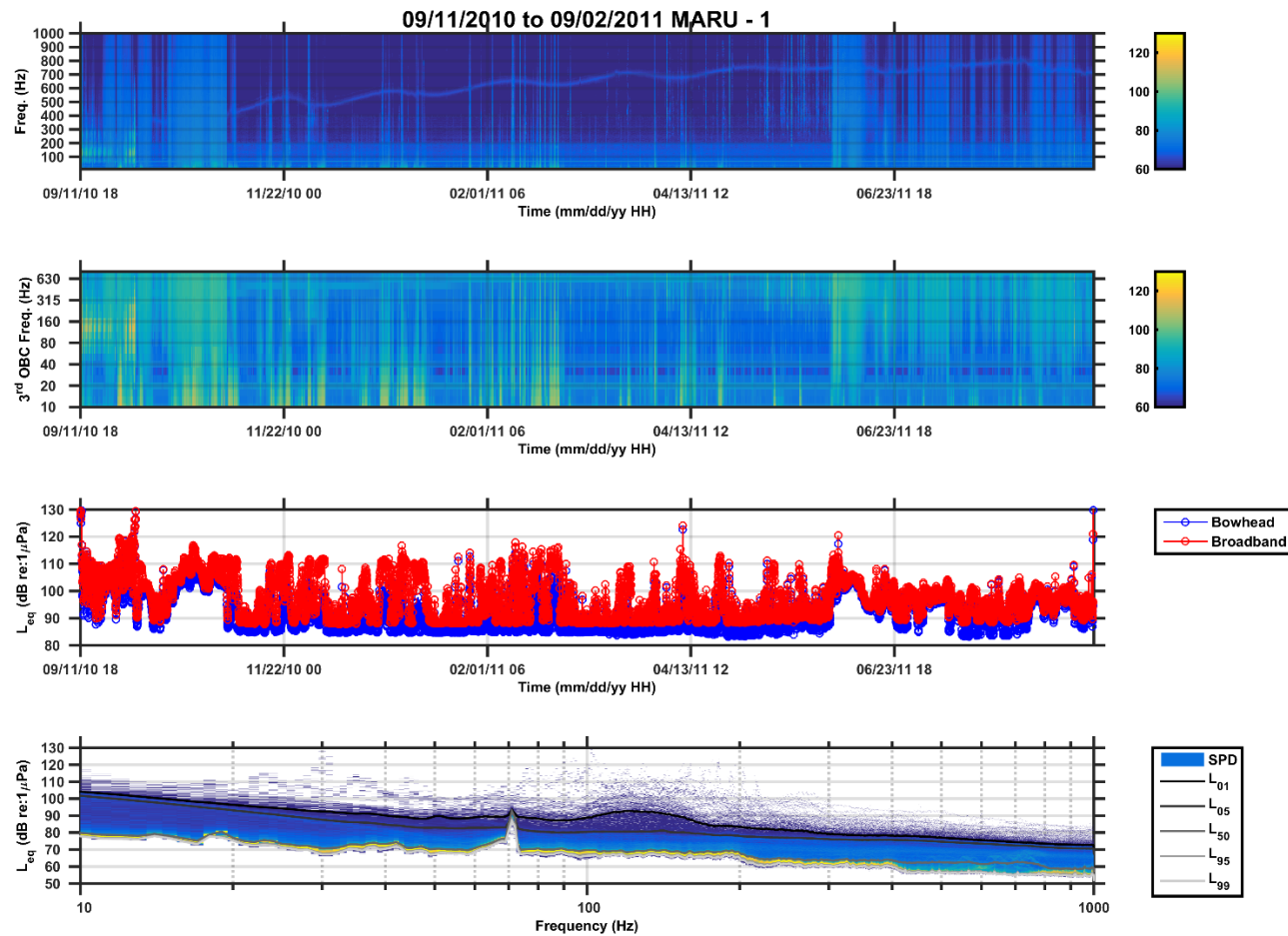


FIGURE 141. EXAMPLE OF NOISE REPORT BROWSER RESULTS, DISPLAYED AS A 4-PANEL PLOT BASED ON OUTPUT FROM THE NOISE ANALYZER (A MATLAB *.FIG FILE) (SEE FIGURE 140). THE RESULTS HERE ARE BASED ON THE ANALYSIS OF THE ENTIRE MARU-DB 2010-11 ACOUSTIC DATA RECORDED FROM 11 SEPTEMBER 2010 TO 02 SEPTEMBER 2011. THE TOP PANEL SHOWS A SPECTROGRAM AT 1-HZ RESOLUTION. THE SECOND FROM TOP PANEL SHOWS A SPECTROGRAM AT 3RD-OCTAVE BOWHEAD-BAND RESOLUTION (71-708 HZ). THE SECOND FROM BOTTOM PANEL SHOWS THE AMBIENT NOISE LEVEL FOR THE BOWHEAD-BAND RESOLUTION (71-708 HZ) AND BROADBAND (9-891 HZ) FREQUENCY BANDS. THE BOTTOM PANEL SHOWS THE SPECTRAL PROBABILITY DENSITY (SPD; MERCHANT ET AL., 2013) AND THE 5TH, 25TH, 50TH, 75TH AND 95TH PERCENTILE STATISTICAL DISTRIBUTIONS.

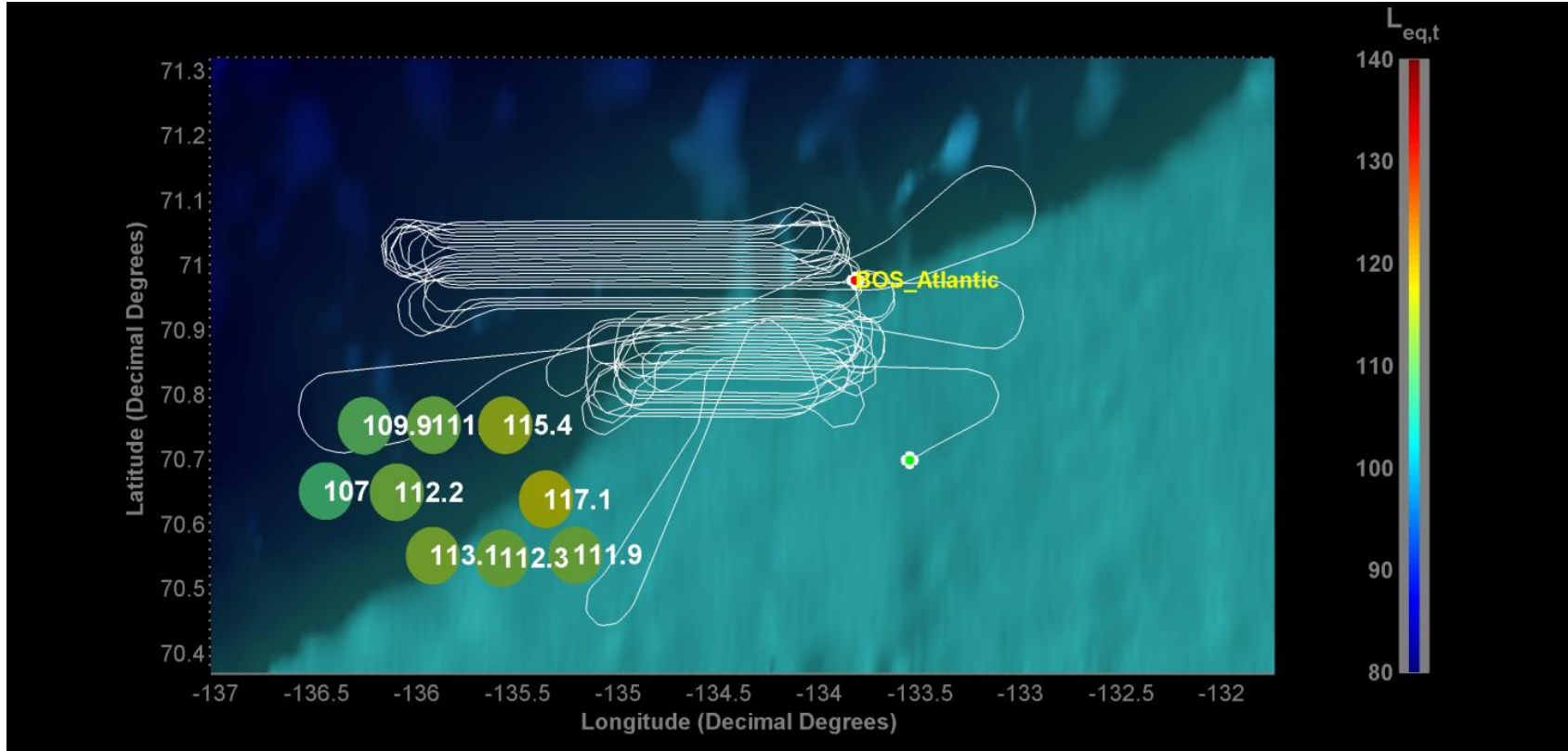


FIGURE 142. EXAMPLE FRAME FROM ONE OF THE TYPES OF OUTPUT MOVIES COMPUTED BY DELMA'S SPATIAL ANALYZER PROCESS (FIGURE 137). THIS EXAMPLE SHOWS A MAP WITH THE LOCATIONS OF NINE MARUS (COLORED CIRCLES), THE TRACK OF A SEISMIC RESEARCH VESSEL (WHITE LINE), AND THE BROADBAND NOISE LEVEL AT EACH OF THE MARUS. IN ACTUAL OPERATION, THE DELMA OUTPUT IS DYNAMIC AND ANIMATED, SUCH THAT THE USER CAN STEP FORWARDS OR BACKWARDS THROUGH THE MOVEMENT OF THE VESSEL WHILE OBSERVING THE CHANGES IN THE RECEIVED LEVELS AT EACH OF THE MARUS. THE COLOR OF A MARU CIRCLE INDICATES THE MEASURED SOUND LEVEL (DB RE 1 μ PA) AT THE RECORDER (SEE THE COLOR BAR ON THE RIGHT) ACCORDING TO THE FREQUENCY BAND AND TIME SCALE OF THE USER-SELECTED ANALYSIS PARAMETERS.

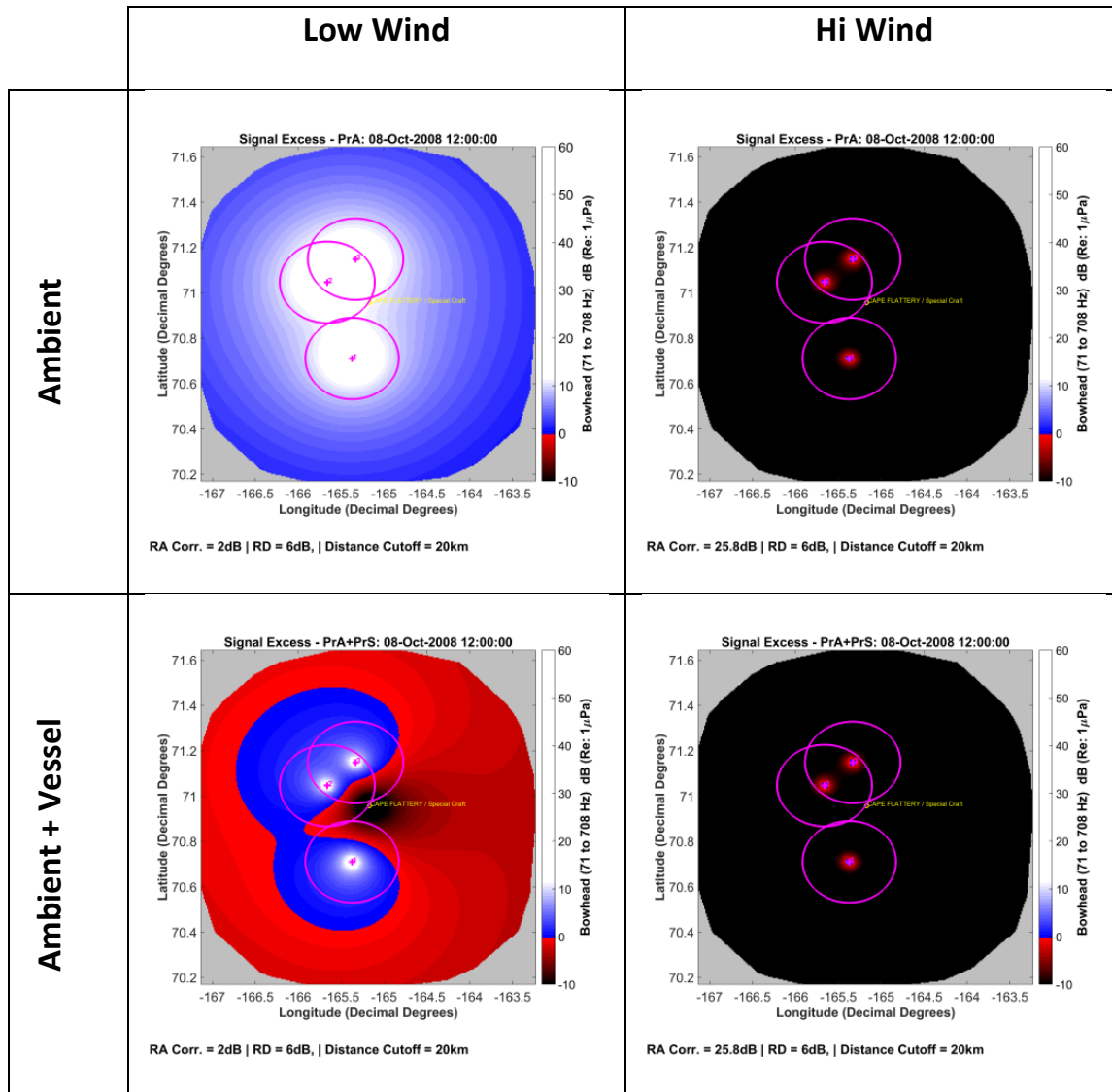


FIGURE 143. EXAMPLES OF ANOTHER TYPE OF OUTPUT FROM DELMA'S COMMUNICATION SPACE VISUALIZER PROCESS (FIGURE 140) AS APPLIED TO THE CHUKCHI SEA AB-2012 DEPLOYMENT AREA. THIS 4-PANEL EXAMPLE SHOWS THE RELATIVE DIFFERENCES IN COMMUNICATION SPACE FOR THREE BOWHEAD WHALES UNDER FOUR DIFFERENT ENVIRONMENTAL ACOUSTIC CONDITIONS AS MEASURED IN THE BOWHEAD-BAND. A: TOP LEFT- LOW SURFACE WIND (2 MPS, 85 DB). B: TOP RIGHT - HIGH SURFACE WIND (14 MPS, 102 DB). C: BOTTOM LEFT - LOW WIND (2 MPS, 85 DB) AND SINGLE SHIP (172 DB). D: BOTTOM RIGHT HIGH WIND (14 MPS, 102 DB) AND SINGLE SHIP (172 DB). (SEE CLARK ET AL., 2009 AND HATCH ET AL., 2012 FOR DETAILS OF THIS ANALYTICAL PROCESS).

Noise, Ice and Wind

DELMA data processing results (e.g., spectrogram figures, noise distribution plots, see Figure 141-138) for different time scales revealed a variety of acoustic events. These, in combination with additional analysis and careful listening were used to identify obvious biotic (e.g., bowhead whales and bearded seals) and abiotic types of sound sources (e.g., vessels, seismic airguns, wind noise and ice) that were contributors to the ambient environmental noise measurements and scenes. In particular, an effort was made to analyze the data for possible

structure in the relationships between noise metrics, wind level and percent ice coverage. This was undertaken in order to inform models to predict future ambient noise levels under reduced ice concentration conditions. Data on percent ice coverage and wind speeds were used to test for relationships between wind speed, percentage of ice cover and ambient noise metrics (see Roth et al., 2012). For this analysis we combined the satellite wind data (6 hr resolution), satellite sea ice concentration data, ambient noise metrics (6 hr resolution), while accounting for known anthropogenic source occurrence (e.g., seismic airgun survey) and bowhead whale occurrence.

We have completed an initial correlations analysis between a) daily noise level in the bowhead frequency band and daily wind speed and b) daily noise level in the bowhead frequency band and daily ice concentration. We conducted a preliminary evaluation to predict future noise levels by combining daily wind speed, sea ice concentration and both broadband and bowhead-band noise level data in a multivariate regression analysis. Results from the regression analysis can be used to estimate noise levels under future open water conditions.

2. Results

Impact Mitigation

Auto-detection Buoy, Near-real-time Bowhead Sound Detections

Of the total audio clips (N=762) detected and transmitted via satellite by AB-2012 over the duration of the deployment (between 01 September 2012 and 01 November 2012), 351 were noted as being of biological origin by Cornell-BRP research analysts with expertise in bowhead and other arctic marine mammal sound recognition (Figure 144). Figure 145 shows the daily comparison between the number of sounds detected by AB-2012 and the number of those validated as bowhead sounds (46%). While this is a significantly lower value of precision than we saw when testing the performance of the detector against the Beaufort Sea training data, it was not unexpected, since the training and test data sets were not exactly equivalent.

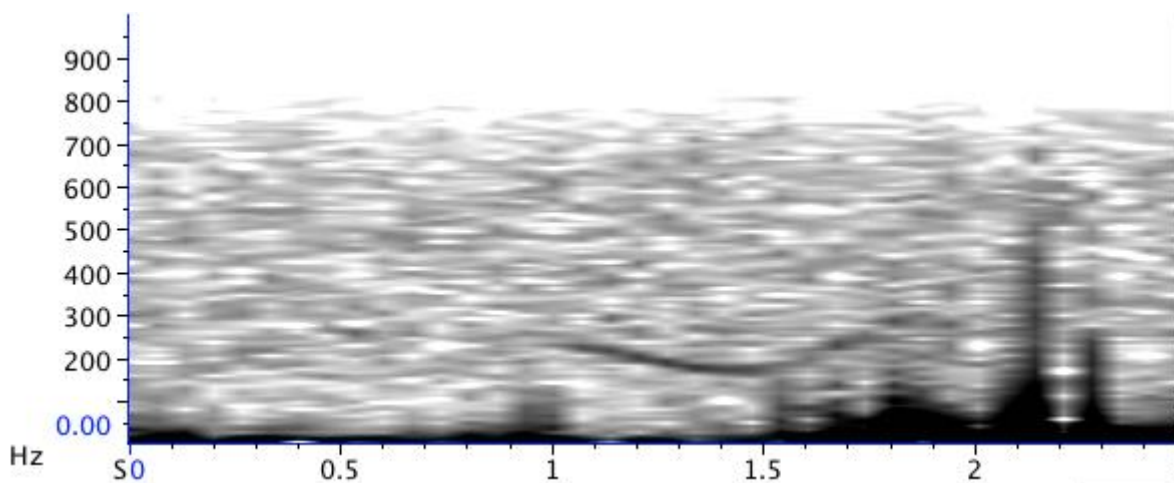


FIGURE 144. SPECTROGRAM EXAMPLE OF A FREQUENCY-MODULATED SOUND AUTOMATICALLY DETECTED BY AB-2012 OPERATING IN THE CHUKCHI SEA; 19 SEPTEMBER 2012. ANALYSTS IDENTIFIED THIS AS A BOWHEAD WHALE SOUND.

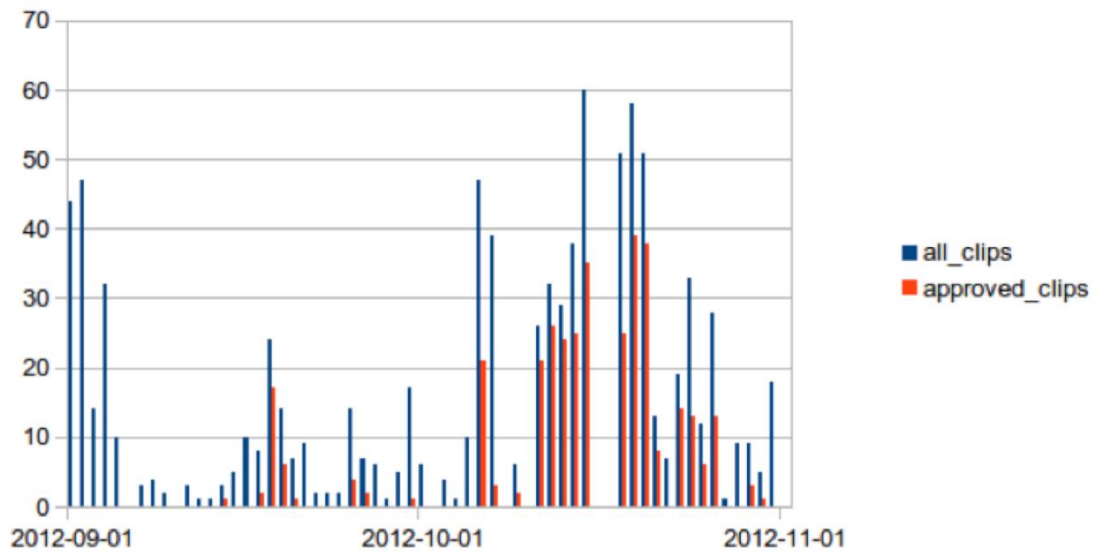


FIGURE 145. DAILY DETECTIONS OF POTENTIAL BOWHEAD WHALE SOUND CLIPS TRANSMITTED FROM AB-2012 (BLUE) OVER THE ENTIRE CHUKCHI DEPLOYMENT (N = 762) AND THOSE SOUND CLIPS IDENTIFIED AS BOWHEAD SOUNDS BY EXPERIENCED ANALYSTS UPON MANUAL REVIEW (RED, N = 351).

Auto-detection Buoy, Noise Spectral Distribution

All of the added auto-buoy features were successful and provided valuable mechanisms for observing major types of acoustic events in near-real-time. In particular, two important features included Iridium transmissions of potential bowhead sound clips of various durations (as opposed to the original fixed duration of two seconds) (Figure 146), and computing and sending spectral distribution data (Figure 147). For example, in Figure 147, a period of seismic airgun activity is evident from approximately 12 September into 18 September. The bidirectional communications feature that allowed us to request selected portions of data from the buoy was also successful. This enabled us to double check, in greater detail, any detection event (e.g., a sound that was similar to a bowhead but might have been a humpback whale) or spectral event (e.g., something that appeared to be manmade, but in fact, was noise due to weather) recorded on the AB-2012's onboard data storage system.

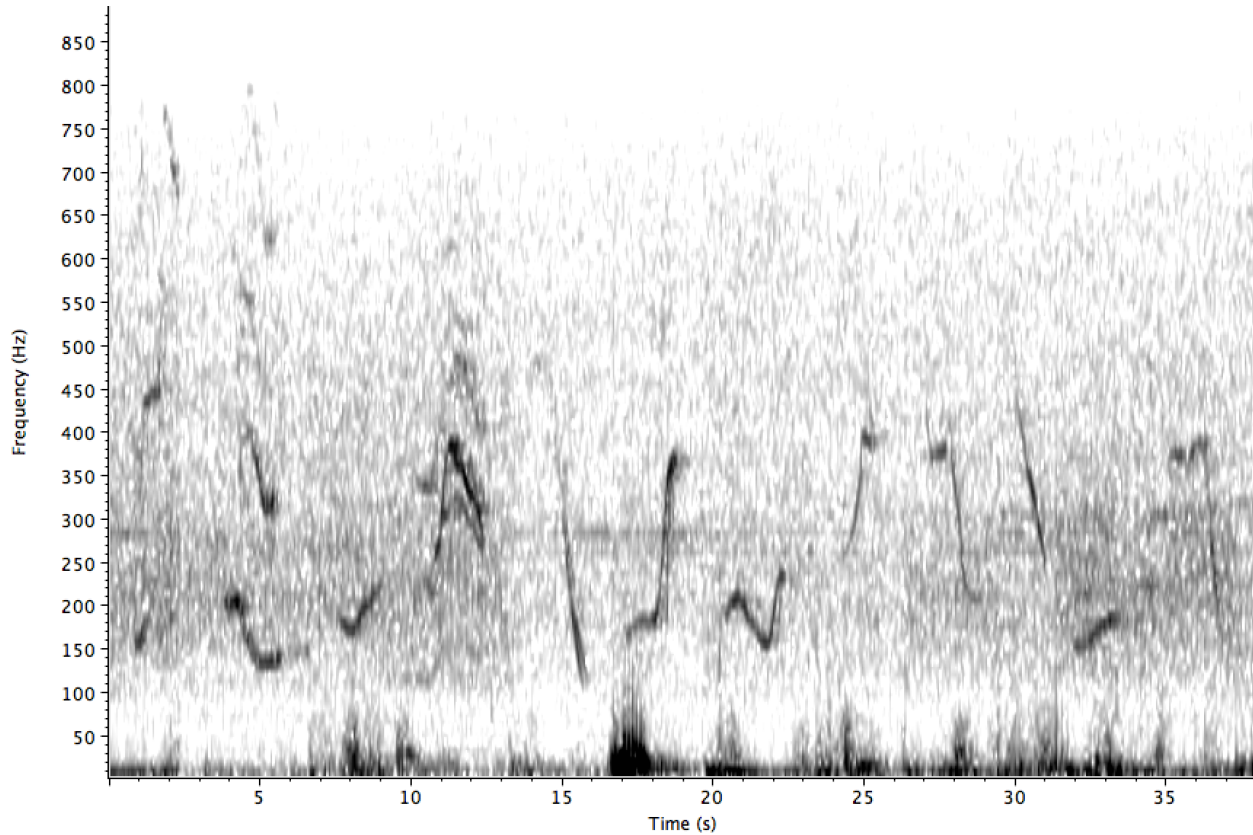


FIGURE 146. EXAMPLES OF 12 BOWHEAD SOUNDS AS FIRST DETECTED AT AND TRANSMITTED FROM THE AB-2012 AND THEN VALIDATED AT CORNELL BY EXPERIENCED ANALYSTS (DATA SAMPLES FROM 20 OCTOBER 2012, 1024 PT. FFT, 50% OVERLAP, HAMMING WINDOW).

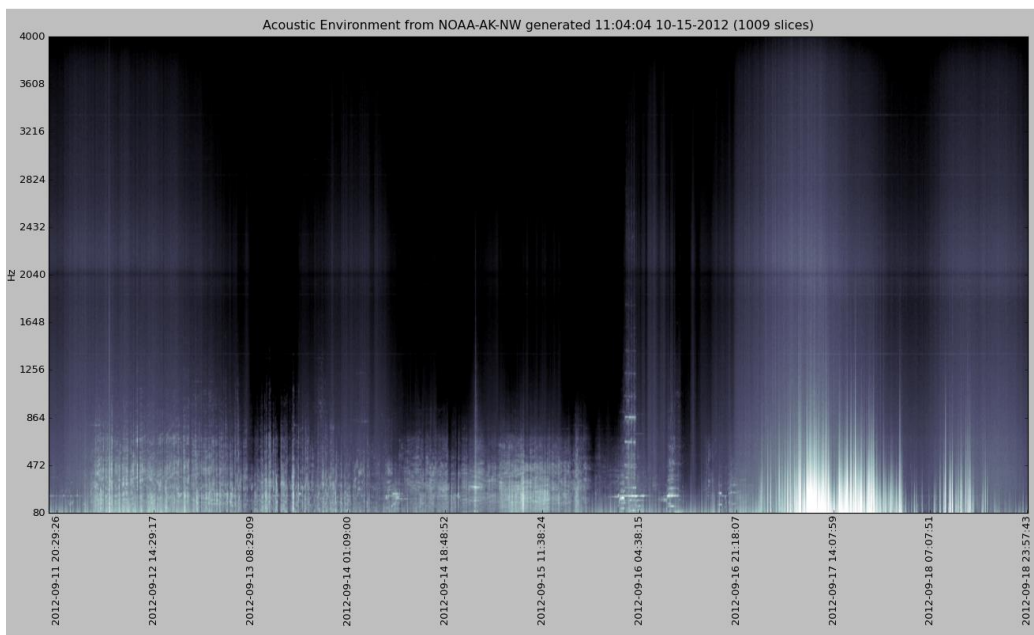


FIGURE 147. EXAMPLE OF A LONG-TERM SPECTROGRAM FOR THE PERIOD FROM 11 SEPTEMBER 2012 AT 20:29:26Z TO 18 SEPTEMBER 2012 AT 23:57:43Z. THE SPECTRAL DATA WERE COMPUTED ON THE AB AND TRANSMITTED VIA IRIDIUM SATELLITE AS PART OF THE REGULAR DATA PACKAGE.

Noise Modeling

MARU-DB Recorders

Over the two-year field season, two MARU-DBs and one AB were successfully deployed (Table 31). MARU-DB-2012-13 failed to record, so is not considered further. MARU-DB-2010-11 was programmed to only record at a 50% duty cycle, while MARU-DB-2011-12 recorded continuously at a 100% duty cycle. For the two years for which MARU-DB data collection was successful (2010-11, 2011-12), recordings were made on 718 days, resulting in a total of 184 GB of data.

Sound Analysis Measurements

Acoustic measurement analysis for all the MARU-DB recorded data were stored as Matlab *.mat files. A variety of visualizations of these *.mat files were stored as Matlab *.fig files, and some were converted into *.png files or *.mov files for illustrative purposes. Where appropriate, Matlab *.fig files were made using both bowhead-band and broadband data. These various visualization files included:

1. Annual 4-channel figures (Figure 141)
2. Daily 4-channel figures;
3. Daily summary noise statistical distributions;
4. Annual summary noise statistical distributions;
5. Time-varying noise distribution figures;
6. Time-varying noise level figures (Figure 148);
7. Customized figures (Figure 149 and Figure 150);
8. Diel plots (Figure 151);

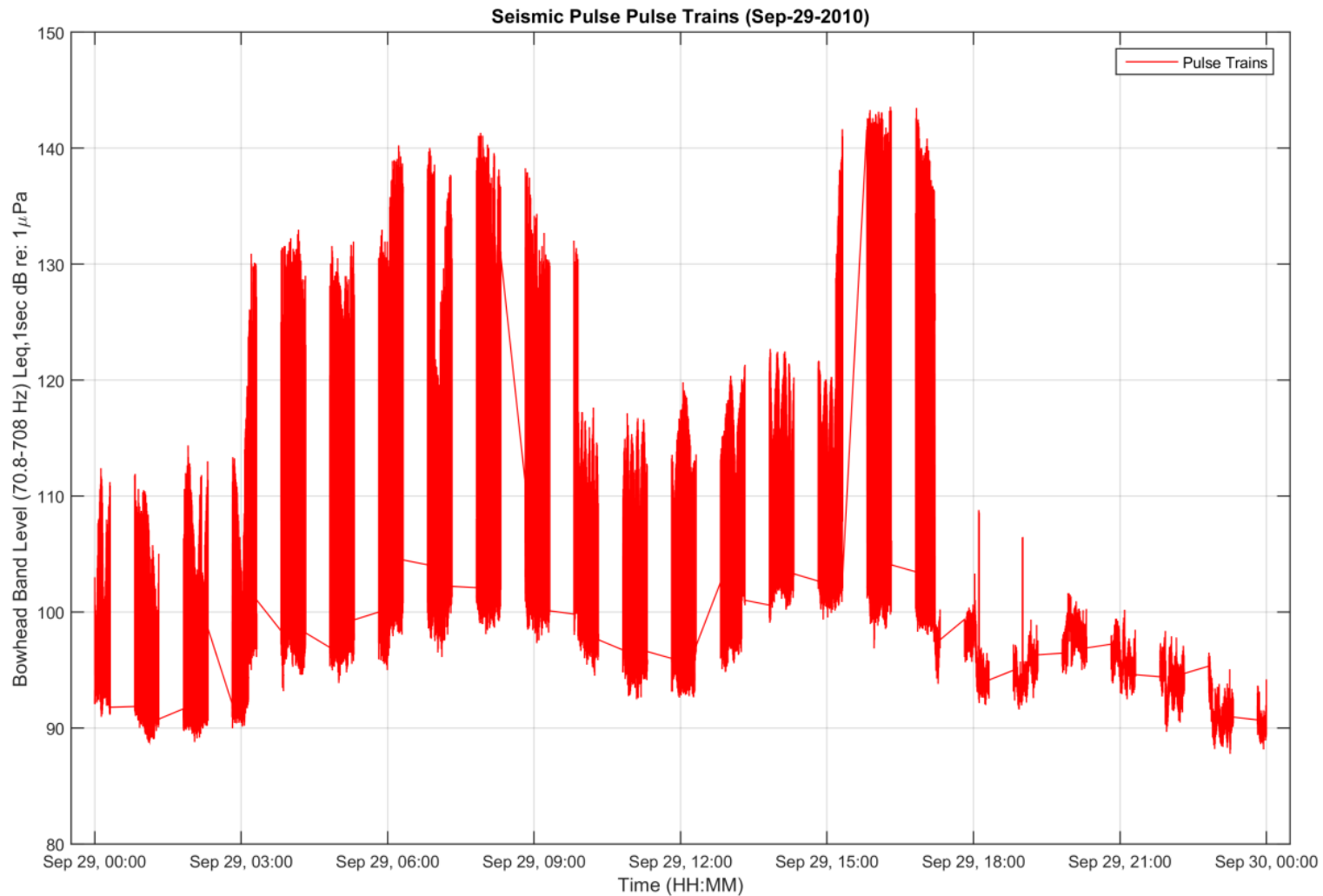


FIGURE 148. EXAMPLE OF TIME-VARYING MEDIAN NOISE LEVEL PLOT FROM MARU-DB_2010-11 FOR 29 SEPTEMBER FROM 00:00 – 24:00 (UTC) DURING A SEISMIC AIRGUN SURVEY. LEVELS ARE FOR THE BOWHEAD FREQUENCY BAND (71-708 HZ) EVERY 10 MINUTES. IN THIS EXAMPLE, THE HIGH LEVELS FROM APPROXIMATELY 00:00 – 17:00 ARE WHEN THE FULL ARRAY IS OPERATING AND THE LOWER LEVELS ARE WHEN THE MITIGATION AIRGUN IS OPERATING. NOTE THAT FOR MARU-DB-2010-11 DATA WERE RECORDED ON A 50% DUTY CYLCE, SO THE GAPS WITH FLAT LINES REPRESENT “OFF” PERIODS WHEN NO DATA WERE RECORDED.

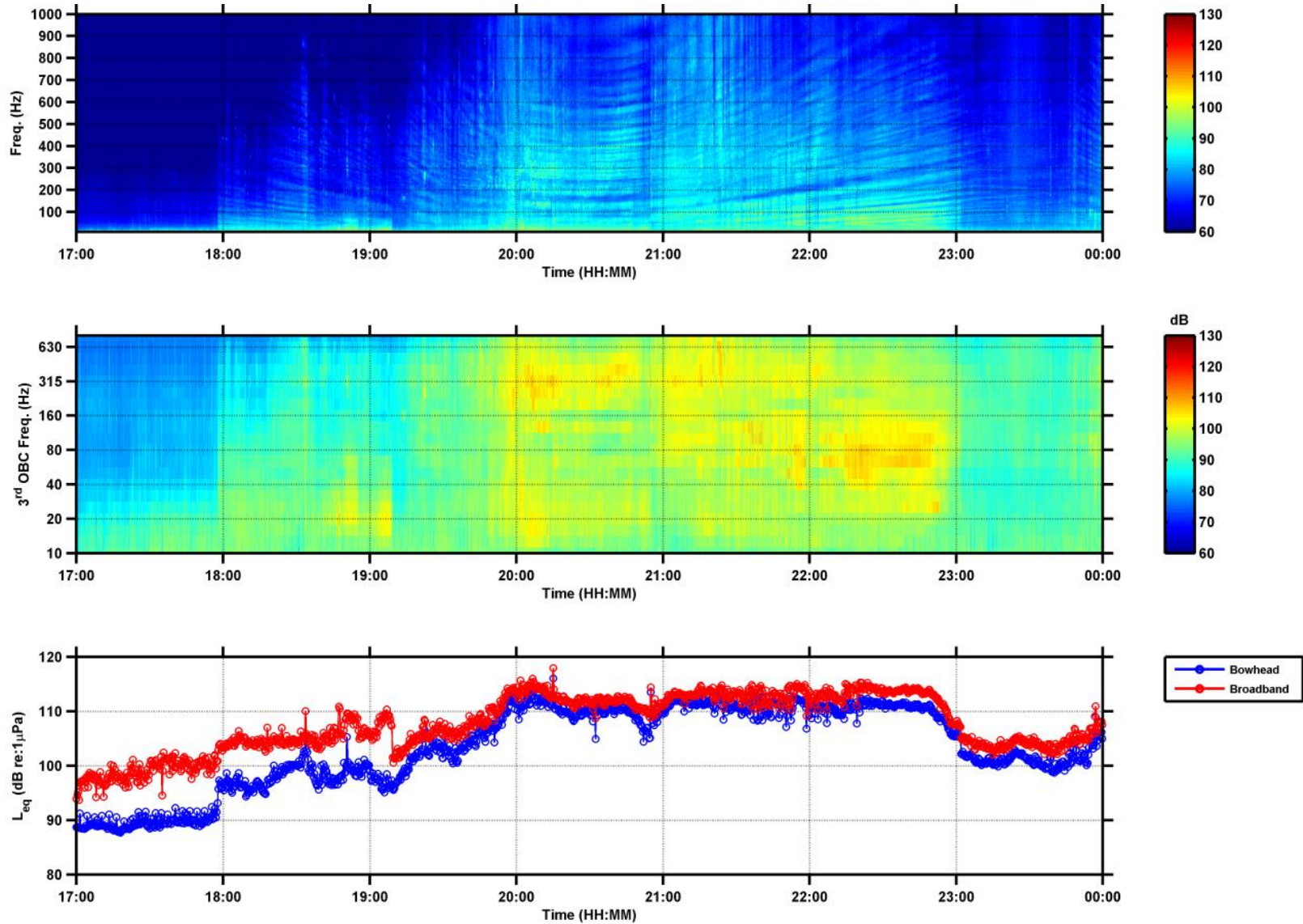


FIGURE 149. THREE-PANEL PLOT FOR MARU-DB_2011-12 SHOWING AN EXAMPLE OF NOISE FROM AN ICE MOVEMENT EVENT ON 12 DECEMBER 2012 FROM 17:00 THROUGH 23:00 (UTC).

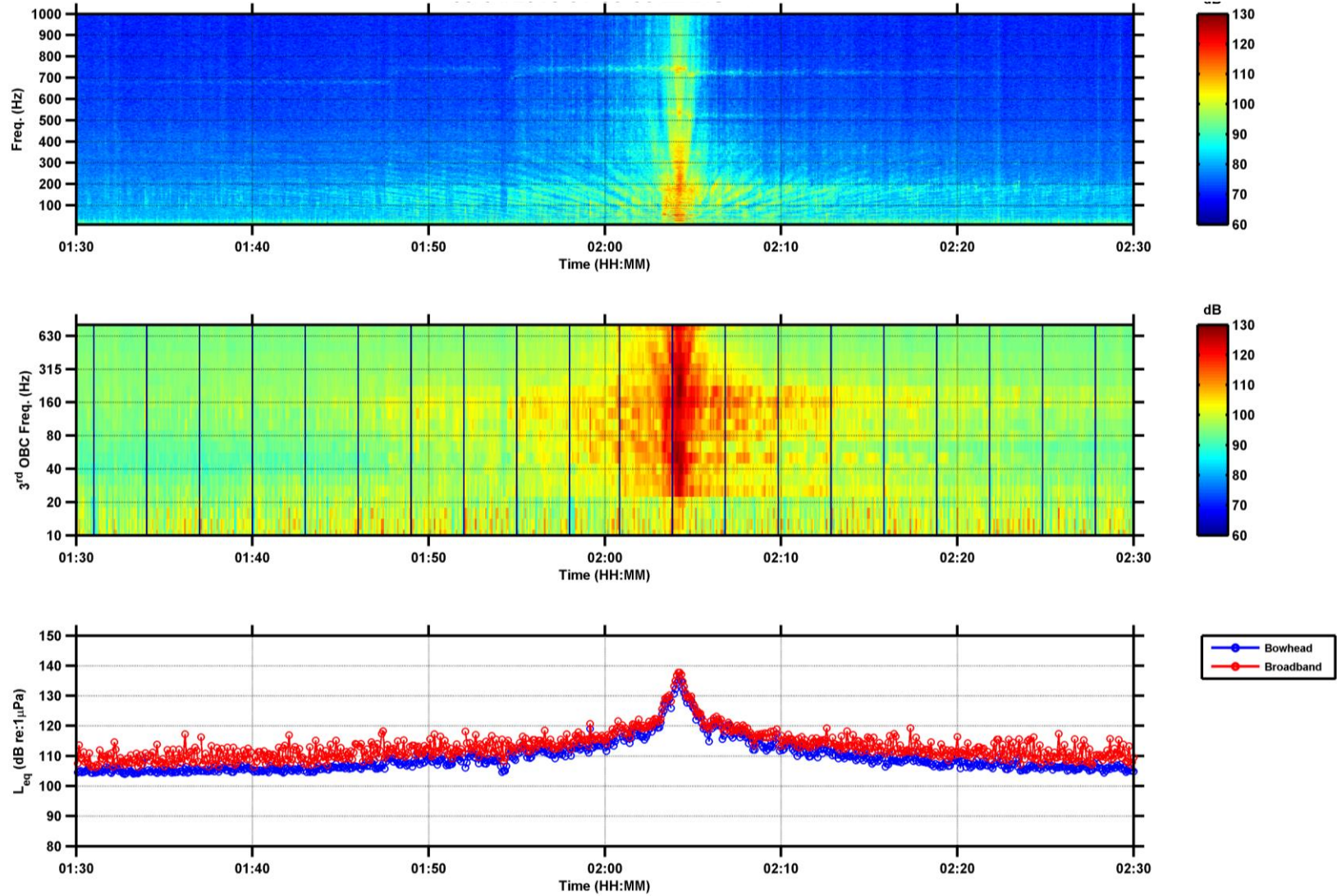


FIGURE 150. THREE-PANEL PLOT FOR MARU-DB_2013-14 WHICH SHOWS AN EXAMPLE OF NOISE FROM A SHIP PASSING CLOSE TO THE RECORDER ON 4 SEPTEMBER 2013 FROM 01:30 TO 02:30 (UTC). THIS TYPE OF EVENT WHEN AN ACOUSTIC SOURCE APPROACHES, PASSES BY, AND MOVES AWAY FROM A RECORDER IS REFERRED TO AS A CLOSEST POINT OF APPROACH (CPA).

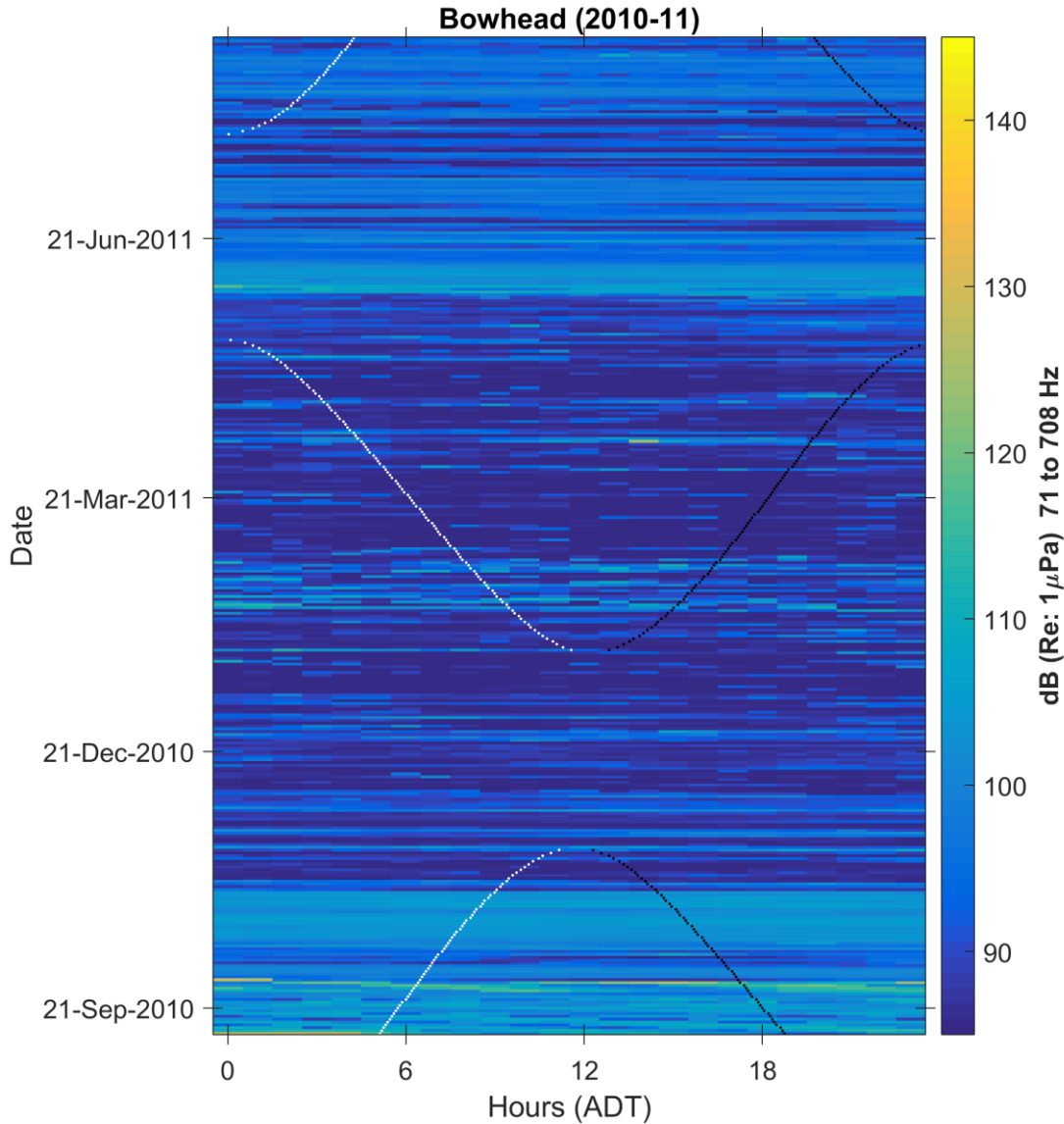


FIGURE 151. EXAMPLE OF A DIEL PLOT OF HOURLY MEDIAN NOISE LEVELS FOR THE BOWHEAD FREQUENCY BAND (71 – 708 HZ) BASED ON OUTPUT FROM THE SPATIAL ANALYZER (SEE FIGURE 140). THE RESULTS HERE ARE BASED ON THE ANALYSIS OF THE ENTIRE 2010-2011 MARU-DB_2010-11 DATA RECORDING PERIOD FROM 02 SEPTEMBER 2010 TO 11 SEPTEMBER 2011 (FIGURE 141). THE RELATIVE CHANGES IN AMBIENT NOISE LEVEL FROM FALL INTO SPRING AND FROM SPRING INTO SUMMER ARE EVIDENT AS CHANGES IN THE COLOR REPRESENTATION OF NOISE LEVEL.

Noise, Ice and Wind

Comparisons were made between ambient noise levels, wind speed and ice concentration. Satellite wind data for 2010-2012 were downloaded from NOAA’s Atlas FLK v1.1 derived surface winds (level 3.0) site

(<http://coastwatch.pfeg.noaa.gov/erddap/griddap/jplCcmpL3Wind6Hourly.html>), while sea ice

concentration data were obtained from the NOAA/NSIDC Climate Data Record of Passive Microwave Sea Ice Concentration, Version 2 site (https://nsidc.org/data/docs/noaa/g02202_ice_conc_cdr/). For each MARU-DB, the ambient noise level, surface wind and ice concentration data were plotted, compared and stored as Matlab *.mat files. A variety of visualizations of these *.mat files were stored as Matlab *.fig files, and some were converted into *.png files or *.mov files for illustrative purposes. Where appropriate, Matlab *.fig files were made using both bowhead-band and broadband data. These various visualization files include (with some illustrative examples):

1. Comparisons of daily noise levels and wind speed (Figure 152);
2. Time-series comparison of noise levels and surface wind speed (Figure 153);
3. Regression of hourly median lowest noise level and surface wind speed (Figure 154);
4. Comparisons of hourly median lowest noise level, daily satellite wind speed and sea ice concentration (Figure 155);
5. Monthly Spearman Rank correlations between daily noise level and wind speed (Figure 156).

For the correlations analysis of daily noise levels, wind speed and ice concentration (Figure 155) we used hourly broadband noise levels from the Noise Report Browser (71-708 Hz, 6 h resolution), satellite derived surface wind data (6 h resolution, level 3.0, derived from Atlas FLK v1.1), and daily satellite sea ice concentration data (NOAA/NSIDC Climate Data Record of Passive Microwave Sea Ice Concentration). Noise data were converted to daily median levels, and 6 h wind speed values were converted to average daily values. A Spearman/Pearson non-parametric test of association (right tail; assumed a positive correlation) between noise and wind speed and noise and ice concentration was run for each month (Figure 156). For noise and wind, the results revealed a strong positive relationship (Spearman's rho) between noise and wind from October 2010 through August 2011. For noise and ice concentration, the results revealed a flat relationship (Spearman's rho) between noise and ice concentration for September 2010, and for December 2010 through May 2011, but a strong negative association in November 2010 and a strong positive association in June 2011.

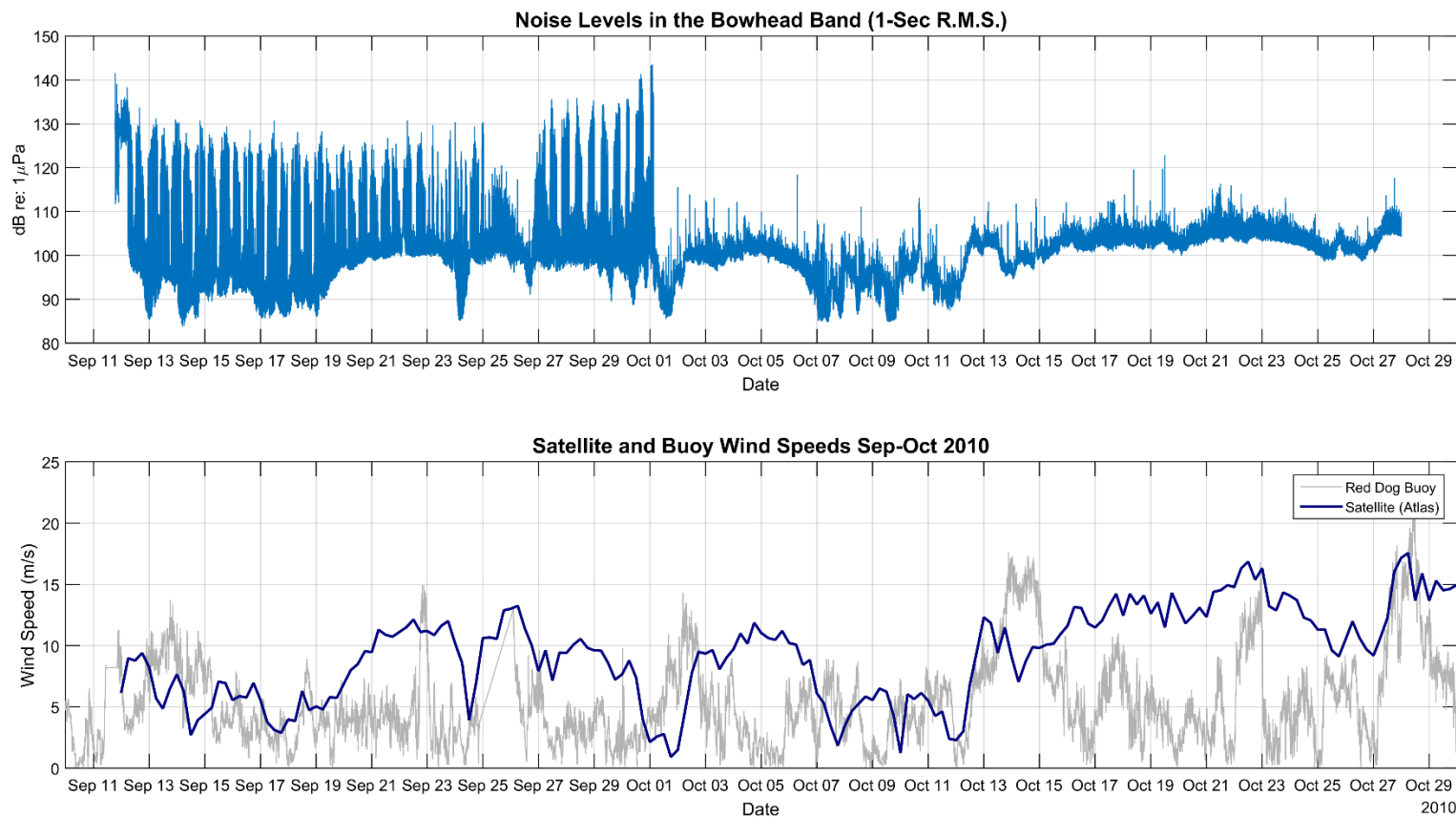


FIGURE 152. COMPARISON OF AMBIENT NOISE LEVEL IN THE BOWHEAD FREQUENCY BAND (71 – 708 HZ, MARU-DB-2010-11) AND WIND SPEED METRICS FROM THE “RED DOG” BUOY AND SATELLITE (ATLAS) DATA SOURCES.

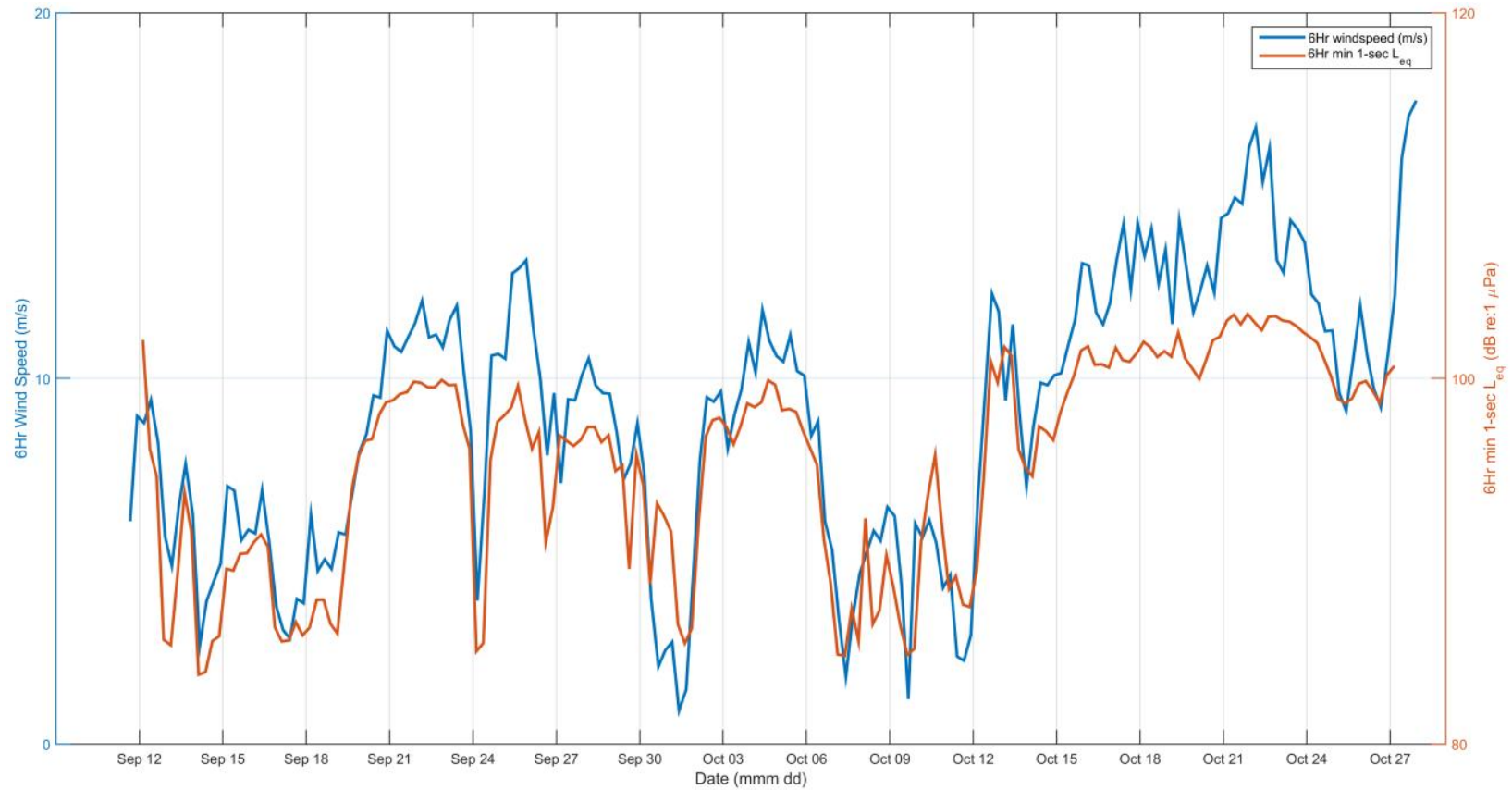


FIGURE 153. TIMES-SERIES OF NOISE LEVELS AND SURFACE WIND SPEEDS DURING THE 11 SEPTEMBER - 27 OCTOBER 2010 PERIOD. NOISE LEVELS ARE 6 HR MEDIAN LEVELS IN DB IN THE BOWHEAD FREQUENCY BAND (71-708 HZ, MARU-DB_2011-12). SURFACE WIND SPEEDS ARE DERIVED FROM SATELLITE DATA (6 H RESOLUTION, LEVEL 3.0, DERIVED FROM ATLAS FLK V1.1).

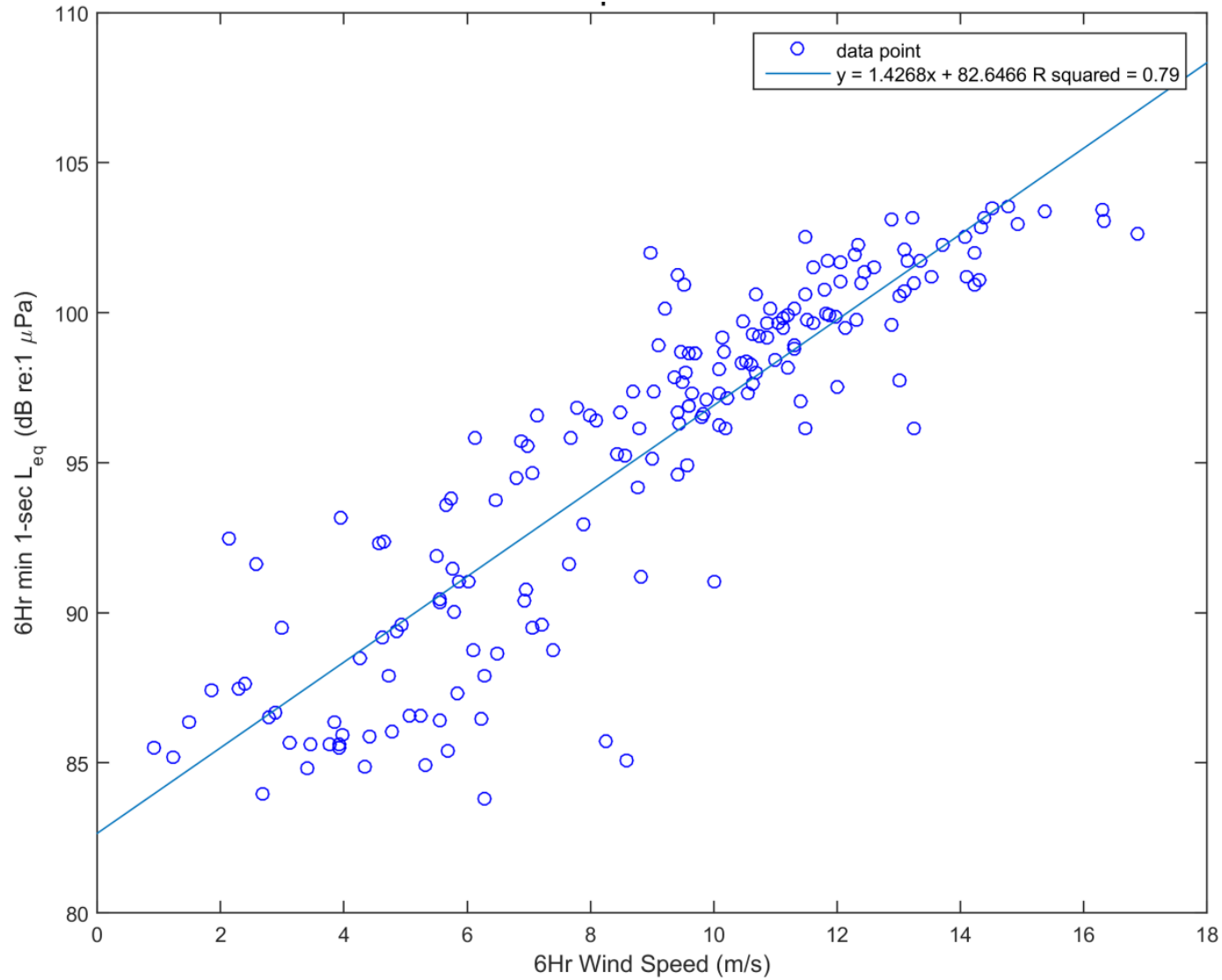


FIGURE 154. REGRESSED WIND SPEED PLOT: THE LINEAR REGRESSION OF AMBIENT NOISE LEVEL IN THE BOWHEAD FREQUENCY BAND (71 – 708 HZ, 6 HR RESOLUTION) AND WIND SPEED METRICS FROM SATELLITE (ATLAS) DATA SOURCES (6 HR RESOLUTION, LEVEL 3.0, DERIVED FROM ATLAS FLK V1.1) FOR THE 12 SEPTEMBER THROUGH 27 OCTOBER 2010 PERIOD.

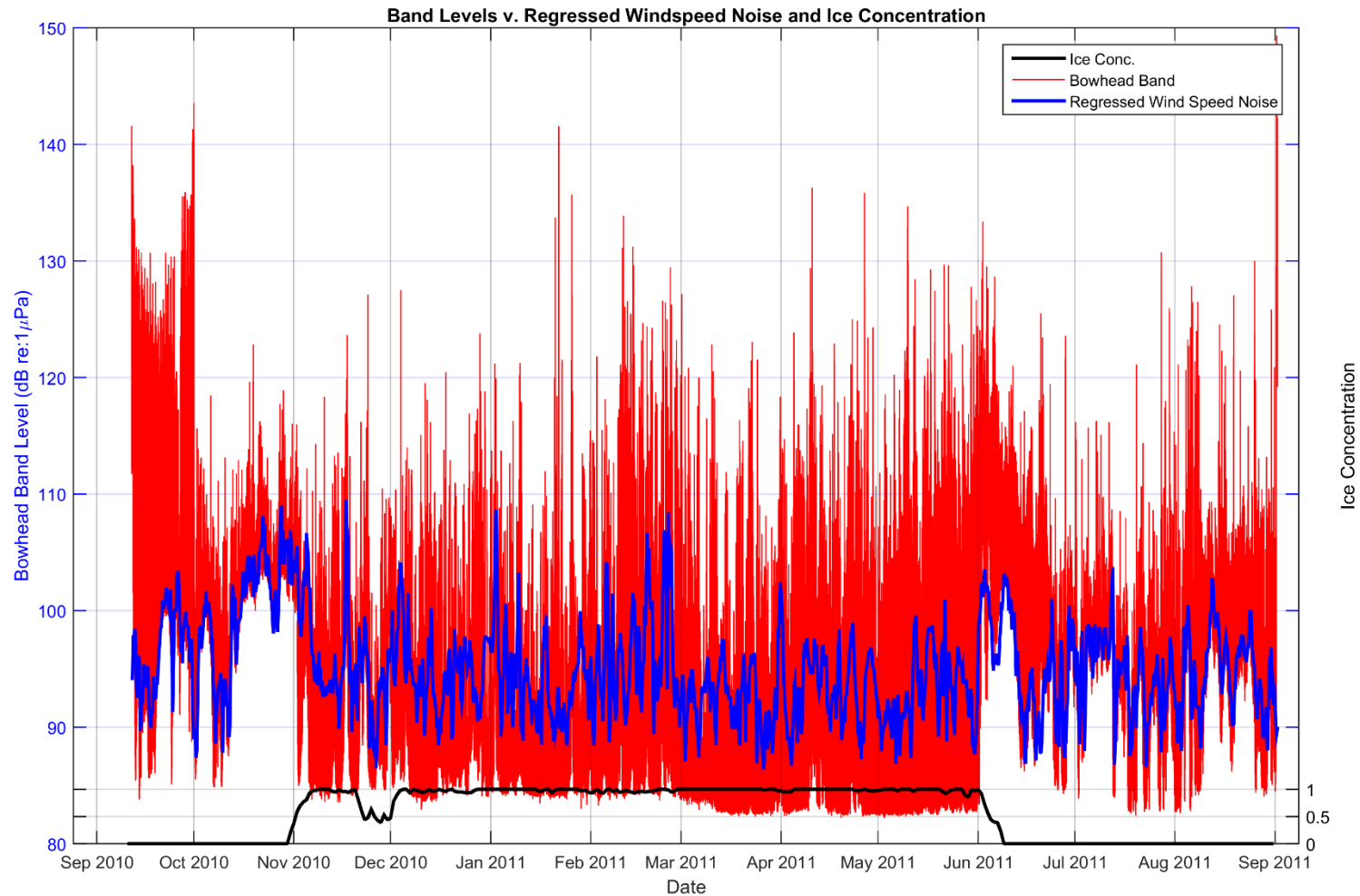


FIGURE 155. TIME SERIES COMPARISON OF BOWHEAD-BAND LEVEL NOISE (71-708 HZ, 1-SEC RESOLUTION, MARU-DB_2011-12: NOTE HIGH LEVEL OF VARIABILITY), “REGRESSED WIND SPEED” (BLUE), AND SEA ICE CONCENTRATION (BLACK). “REGRESSED WIND SPEED” WAS CALCULATED BY REGRESSING SURFACE WIND SPEED VALUES (6 HR RESOLUTION, LEVEL 3.0, DERIVED FROM ATLAS FLK V1.1 DATA) WITH NOISE LEVEL, AND APPLYING THE LINEAR REGRESSION EQUATION TO CONVERT WIND SPEED INTO ESTIMATED WIND NOISE (I.E., “REGRESSED WIND SPEED”) VALUES.

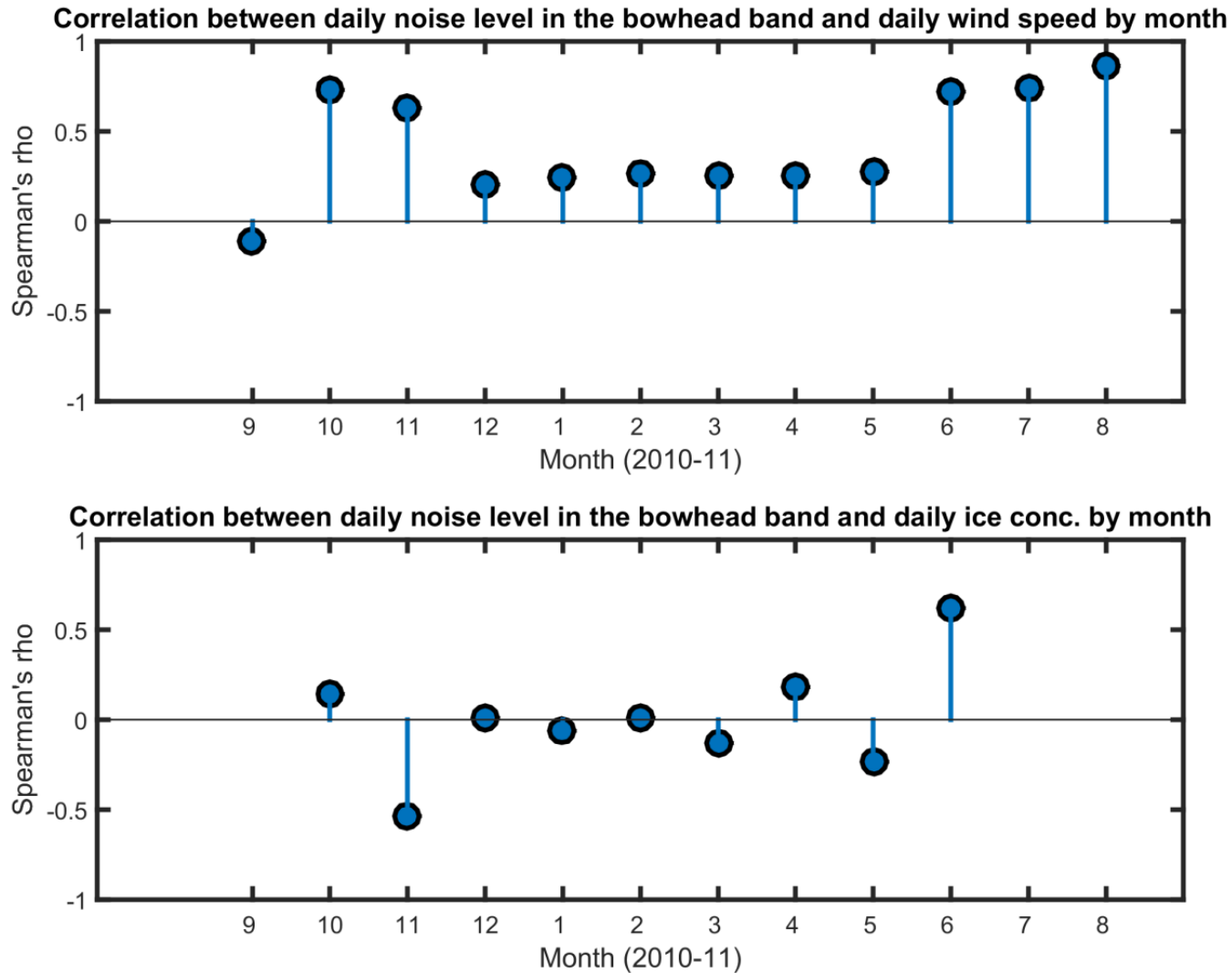


FIGURE 156. MONTHLY TIME SERIES COMPARISONS OF DAILY BOWHEAD-BAND LEVEL NOISE (71-708 HZ, 1 HR RESOLUTION, MARU-DB_2011-12) AND DAILY SURFACE WIND (6 HR RESOLUTION, DERIVED FROM ATLAS FLK V1.1); TOP PANEL. DAILY BOWHEAD-BAND LEVEL NOISE (71-708 HZ, 1 HR RESOLUTION, MARU-DB_2011-12) AND DAILY SEA ICE CONCENTRATION (NOAA/NSIDC CLIMATE DATA RECORD OF PASSIVE MICROWAVE SEA ICE CONCENTRATION); BOTTOM PANEL.

3. Discussion

This report represents an initial synthesis of the acoustic data collected from two MARU-DBs (718 days, 184 GB), and a single AB system (65 days, 26.7 GB) from 11 September 2010 through 3 November 2012 (Table 31).

Considerable effort and resources were devoted to achieving the two primary objectives, *impact mitigation* via the AB system for near-real-time monitoring, and *noise modeling* via the development of the DELMA acoustic analysis system. The overarching motivation for this research was to increase understandings of the spatial and temporal dynamics of the Chukchi Sea acoustic environment and the quantification of the various sound sources that contribute to that environment (i.e., the region's acoustic budget). Of particular concern are the short-term and long-term influences of anthropogenic activities on the marine acoustic environment and the possible impacts of those influences on the region's ecological health. An example of a short-term influence would be noise from a seismic airgun survey or drilling operation and the resultant changes in the acoustic habitats of bowhead whales, beluga whales or ice seals. An example of a long-term influence would be changes in the marine acoustic environment as a result of lower sea ice concentration and increased surface winds coupled with the expected increase in background noise due to increased commercial activities.

Impact Mitigation

Auto-detection Buoy

The task of developing an actual mechanism by which to mitigate acoustic impact focused on the application of a short-term, area-specific system, referred to as an auto-detection buoy, to monitor for sounds from bowhead whales and sounds generated by activities from the exploration and development of offshore oil and gas resources in the Chukchi Sea. Our ability to undertake this component of the project was made technically and economically possible because Cornell-BRP and WHOI had already developed the technology, and there were very few associated non-recoverable engineering costs. Furthermore, critical improvements to the technology, for example increased sampling rate and simultaneous detection algorithms, were accomplished and paid for by a totally separate industry-based whale monitoring project off Massachusetts (see <http://www.listenforwhales.org>), and were readily adapted to this Chukchi Sea context at very little cost to the project.

The mechanics for deploying, operating and recovering an auto-detection buoy in the Chukchi Sea during the open-water season were achieved in summer-fall 2012 with the successful deployment, operation and recovery of AB-2012 and with generous logistical support from Dr. Michael Macrander and the Shell Exploration & Production Company. Potential bowhead whale calls were detected, and packages of acoustic clips were transmitted back to Cornell for expert review. Acoustic data were processed in situ and resultant spectral density distribution data were transmitted back to Cornell and used to scan for natural and anthropogenic events (e.g., increased broadband noise during high wind weather events and seismic airguns). The buoy-to-Cornell bi-directional communication system was exercised and successfully used to modify buoy behavior: for example, to modify on-board detection code, request transmissions of specific sections of acoustic data, change the transmission schedule or change the data

contained in the transmission package. By exercising these technical activities, system field operational protocols were established, and on-board data processing, data management and telemetry sub-system capabilities were confirmed.

At this point, the AB's fundamental system infrastructure has been established and validated. System infrastructure has been modularized so that the firmware and software can be easily reconfigured. For example, the system's sampling rate can be increased with very little impact on power consumption and data storage. It can now simultaneously run multiple detectors for multiple species.

Some further improvements are still needed in detection capability and performance, and in the system's graphical user interface (GUI). Not surprisingly, a significant remaining challenge is the implementation of effective and efficient onboard detectors, whereby effective and efficient refers to the achievement of low false positive and false negative rates. A primary goal for the GUI is to make it more user friendly, flexible and devoid of technical idiosyncrasies such that almost anyone, not just those of us familiar with the system, can readily obtain and see information about local noise conditions, the occurrences of anthropogenic acoustic activities, and detections of marine mammals.

Noise Modeling

Sound Analysis Measurements

A significant level of effort was devoted to building the first version of the acoustic ecology analysis system (Figure 140). We applied this system to quantify and evaluate contributions of biotic and abiotic sources to the ambient noise budget. To tailor this system for this project we iterated through a series of exercises using data collected with the MARU-DB autonomous seafloor recorders. This effort took advantage of some of Cornell-BRP's existing code and ongoing development of applications of this code for other acoustic ecology projects. This effort is ongoing and has transitioned seamlessly into CHAOZ-X, the continuation of this original CHAOZ project.

A significant specification for the acoustic ecology analysis system includes having the capability to rapidly and efficiently ingest, manage and process large amounts of acoustic data. These speed and efficiency requirements have taken advantage of an existing technology development project in Cornell-BRP, called DELMA, that uses a parallelized, distributed, and multi-core high-performance-computer. A major benefit of this technology is that we can now complete the basic acoustic analysis task very rapidly: for example, we can process a year's worth of MARU-DB data in a few tens of minutes, rather than many days. As a result, during this project it became more efficient to reprocess the raw data than to store and manage all the various iterations of the analysis. At some point after we had completed a fairly large number of data analysis runs, we did save the analysis products.

The acoustic ecology analysis system includes the software infrastructure and mechanisms by which we now integrate, analyze and visualize different data types and data products. The conceptualized motivation for this system was that it would enable us to quickly explore and discover features of the analytical results to answer questions about and explain the observed structures of the ambient noise environment. In the results section above we provide some examples of the different types of data analysis products. These data analysis products

have been produced for almost all the data and will be openly available. In some cases the example was included to represent a special type of visualization product, and we have not produced figures for all the data (e.g., Figure 149-155).

Seismic Airgun Surveys and Vessel Noise

Seismic airgun survey impulses from multiple sources detected on MARU-DB-2010-11 and MARU-DB-2011-12 raised noise levels by approximately 14 dB (Guerra et al., 2013). We did not systematically annotate the acoustic data for the occurrence of vessels (Figure 150). However, analysts did notate vessel CPAs, and from these we know that vessels were only infrequently detected within the vicinity of a MARU-DB. We now have a method by which to quantify the contributions from seismic airgun surveys and vessels to the aggregate noise budget (see Clark et al., 2009; Hatch et al., 2012).

Noise, Ice and Wind

The exploration and discovery of relationships between noise level, wind speed and ice concentration are just getting underway, but some interesting results are beginning to emerge. As shown in Figure 152, there is an obvious positive relationship between low-frequency noise level and surface wind speed (but not between noise level and wind speed at the NOAA land station at Red Dog Dock, a separation distance of almost 380 km). As shown in Figure 153, when the 6-h median values of the 5th percentile noise level (i.e., representing the lowest noise levels as shown in Figure 152, top panel, and referred to as the median minimum noise level) and surface wind speed are plotted together, this association between noise and wind is even more apparent. The correlation between these 6-h median values and surface wind speed is 0.89 indicating that a 1 m/s increase in wind speed results in a 1.4 dB increase in noise level within the 71-708 Hz frequency band (Figure 154).

This resultant relationship between noise and wind is not all that surprising as the relationship between wind and noise is well known (Wenz, 1962; Urick, 1983). We recognize that the relationship presented here is for a limited subset of the data (23 days) so further analysis is warranted. Unfortunately, the satellite that provided these surface wind data stopped operating in 2011, so this source of surface wind data for the AB-2010 site was not available for further analysis. Meteorological data from buoys deployed by BOEM and CSESP programs will be incorporated in future development of noise models and statistical analyses in the BOEM-funded CHAOZ-extension study.

Our initial explorations of a relationship between wind, ice noise and ice conditions are still very preliminary. To begin, we wanted to have data for each variable over the entire year of recording, so we needed to extend the surface wind data past the expiration date of the satellite data. Therefore, we applied the correlation between noise and wind to estimate surface wind speed for the entirety of the MARU-DB-2010-12 recording period, and combined noise data with these wind estimates and ice concentration measures (Figure 155). There are several interesting features evident in this three-variable figure that are worth noting.

1. When ice concentration is above approximately 0.8, median minimum noise levels in the bowhead-band are consistently and persistently low (ca. 83-88 dB).

2. The period during the onset of ice in late October through early November 2010 was preceded by a multi-week period with high surface winds and high noise levels.
3. The period during the loss of ice in early June 2011 was coincident with a multi-week period with high surface winds and high noise levels.

We assume, but need to test the assumption, that when ice concentration is high (e.g., > 0.8) surface winds are not reliably correlated with ambient noise. Under these ice conditions we know that ice events can produce extremely loud noise events as well as a wide variety of sounds that have biological-like features (e.g., frequency-modulation, amplitude-modulation, broad-band bangs) such that ice events can sound like wolf howls, bee buzzes, whale calls and bowhead gunshot sounds.

Results from the application of the Spearman Rank correlation (Figure 156) reflect the interesting features as noted above for Figure 155 in that we find a high negative correlation between noise and ice in the fall as the ice concentration is increasing and a high positive correlation between noise and ice in the late spring as the ice concentration is decreasing.

What do these preliminary results tell us about future noise conditions in the Arctic? As stated above in Section IX: Climate Modeling, the model predicts two possible scenarios, both of which are dependent on the winds. In one model the winds are strong and persistent, in the other the winds decrease. Both scenarios predict decreases in ice concentration and an increase in the spatial and temporal extent of the open-water season. In the first scenario, there will be an increase in ocean storms, which in combination with the increase in the open-water season will lead to an increase in ambient noise conditions. In the second scenario, with the increase in the spatial and temporal extent of the open-water season and the calmer wind conditions there will be an additional increase in shipping traffic and other types of human activities, which will lead to an increase in anthropogenic background noise. Some preliminary estimates of the expected change in noise conditions can be gleaned from Figure 154 and Figure 155. In terms of the spatial and temporal change, we should expect noise level increases to follow the seasonal and geographic decrease in loss of ice. Using Figure 155 as the template, one would expect that the median minimum noise levels in the 71-708 frequency band would shift up by at least 10 dB from approximately 85 dB to approximately 95 dB. This is based on results indicating a 1.4 dB increase in noise level within the 71-708 Hz frequency band for each 1 m/s increase in wind speed (see Guerra et al. 2011). In terms of noise dynamics in any one location under the expected mid-winter, open-water condition with the expected increase in surface wind speeds one would expect to see the overall median noise level increase from approximately 95 dB to approximately 105-110 dB. These predicted median noise levels are equivalent to levels in today's shipping lanes off Boston (see Hatch et al., 2012).

4. *Conclusions*

Auto-detection Buoy

At this point, the AB's fundamental system infrastructure is established, but some further improvements are still needed in detection capability and performance, and in its graphical user

interface (GUI). The system's sampling rate can be increased with very little impact on power consumption and data storage. The detection software can now run multiple detectors. A significant remaining challenge is the implementation of effective and efficient onboard detectors, whereby effective and efficient refers to the achievement of low false positive and false negative rates. A primary goal for the GUI is to make it very user friendly, flexible and devoid of technical idiosyncrasies such that anyone, not just those of us familiar and patient with the system, can readily obtain and see information about local noise conditions and the occurrences of anthropogenic acoustic activities and various marine mammals.

Sound analysis system

In this first phase of the CHAOZ project we've made significant progress in the analytical tools. We can now process large amounts of acoustic data very rapidly. The DELMA system has specifically been designed to be scalable (i.e., the same code can run efficiently on a laptop or a high performance computer). The acoustic ecology system's flexibility has proven to be extremely valuable for visualizing analysis results at user selectable spatial, temporal and spectral scales. It is modularized and the code is nearly all converted into an object oriented format.

Biologically and scientifically, despite the rapid improvements in the technology, we are really just beginning to learn how to comprehend the very large amounts of analyses results. We are learning how to animate results to take advantage of our brains, which are so well adapted for seeing patterns through motion. We are learning how to rigorously test for the biological significance of numerical patterns, but we are still at the beginning when it comes to assimilating the complexity and scales of our collective, aggregated data sets.

5. *Recommendations*

Auto-detection Buoy

The GUI by which users obtain and interact with an operational AB can be and should be easier to use than any online weather buoy or satellite application. The system should be so comfortable for the user that it is viewed as an ocean acoustic "weather channel".

Functionally and specific to the issues surrounding near-real-time acoustic monitoring and mitigation, there is no technical reason impeding the deployment of an AB network in the Arctic. Weather and ice conditions are challenging, but buoy design can overcome many of these challenges. On-board power is a limitation, but harvesting solar and/or wind energy could help mitigate this limitation. Such a network would dramatically increase empirical evidence of biological impact and ecological risk, thereby reducing uncertainties inherent in modeled estimates of biological impact and ecological risk. This in turn would improve the use of aerial and vessel surveys, by allowing them to focus on areas and times of greatest uncertainty and when acoustic monitoring is not a viable option.

Sound analysis system

The basic system has been successfully developed but has not been fully integrated with DELMA. As expected, as we pushed to make the entire process more efficient, from data ingestion to end products, we discovered areas for improvement. These included inefficiencies in a wide range of places, from inconsistencies in data file naming conventions and file folder structures, to a lack of seamless connections between Matlab code and Java code. Some of these glitches were expected to happen as we moved to higher levels of automation, but at the time we had to accept those future difficulties in exchange for the immediate need to get something specific done. Many of these specific, late-project inefficiencies were not surprising, but the level of effort to fix any one of them has proven difficult to predict. There is also the tradeoff between a software fix that works but is a kluge and one that is robust. We are now at the point in the project where most kluge fixes are unacceptable. It cannot be understated how much mental effort and time is needed to really build a system that is scalable and capable of reliably processing large data sets.

A very significant technical issue that has enormously important implications for moving the science forward is the lack of a scalable, comprehensive data system by which to integrate all the various types of data and data formats into a data discovery environment. Without real investment in such a system, we will simply continue to spend increasing time and resources on logistical issues (e.g., moving data around, reformatting data, trying to find data, etc.). As such this is the most significant recommendation. The data scene has become far too large and complex, obscuring the very scale and detail that we seek to comprehend in our data.

XIII. ESTIMATING RELATIVE ABUNDANCE OF MARINE MAMMALS

A. Visual

1. Methods

To estimate relative abundance within Arctic waters, encounter rates (groups/km) and densities (individuals/km²) from sightings collected during “on-effort” status only (defined in Section VII) were computed. The area of analysis (198,677 km²) was defined as U.S. waters just north of the Bering Strait to the easternmost extent of effort, east of Barrow, AK (Figure 157).

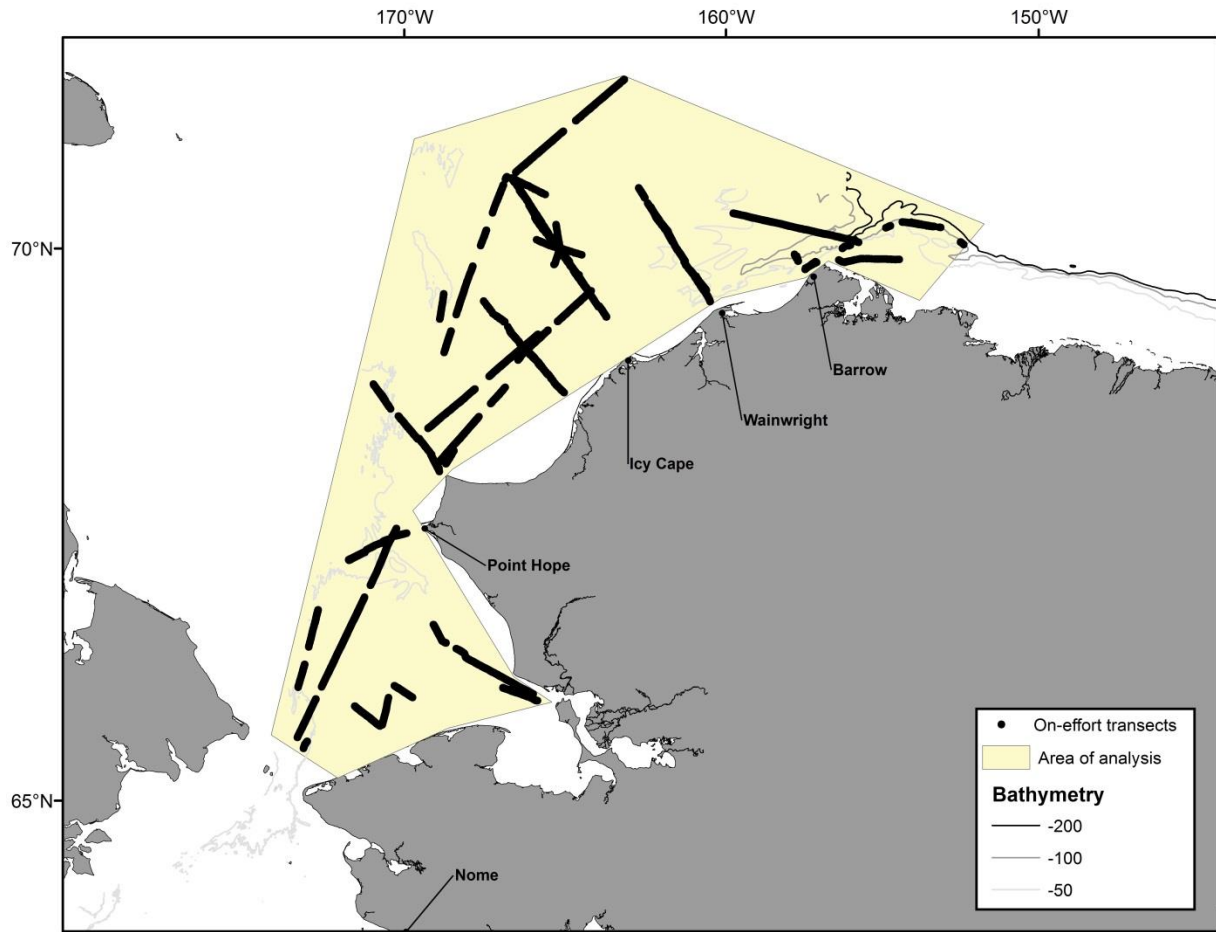


FIGURE 157. ON-EFFORT TRANSECTS AND THE AREA OF ANALYSIS WITHIN ARCTIC WATERS TO ESTIMATE RELATIVE ABUNDANCE.

Detection probability was estimated using the hazard-rate within Conventional Distance Sampling (CDS) framework (Buckland et al., 2001, 2004). For bowhead, fin, humpback, and gray whales, perpendicular distances were pooled across all “large whale” species. Pooling provided greater sample size for fitting the detection function and allowing for density to be computed for species with relatively low number of detections and for improving precision of these estimates. Pooling across species with insufficient sample sizes is a relatively common

practice (e.g., Barlow et al., 1997; Forney and Barlow, 1998) as long as pooling includes species with similar detection characteristics. In this study, perpendicular distance data were combined across species detected at similar average distances (e.g., Barlow et al., 2001). Modeling of perpendicular distance was conducted with ungrouped data truncated at 3 km for all whale species. Truncation was set at these distances after exploratory analyses were conducted to assess best truncation points (i.e., balance between sample size and appropriate fit model). The procedures and values selected for truncation are consistent with the literature (e.g., Buckland et al., 2001; Zerbini et al., 2006; Friday et al., 2013).

Model selection was conducted following the Akaike Information Criterion (AIC; Akaike, 1973). A model with species as a covariate was run and was not well supported by AIC; therefore, no covariates were included in this analysis. The detection function was used to estimate species-specific density for all years combined (that is, an average across years). Encounter rate and its variance were estimated empirically from the data (Innes et al., 2002). For the purpose of this analysis, detection probability on the trackline was assumed to be $(g[0] = 1)$. Detection probability and density estimates were computed using the R package *mrds* version 2.1.0 (Laake et al., 2012).

2. Results

On-effort trackline used to estimate densities totaled 1,230 nm (2,278 km) (Figure 157). Estimated parameters for the hazard rate model (most supported by AIC) across all species were: average detection probability (P) – 0.32, CV(P) – 0.23, and effective strip width (ESW) – 0.96 km. The number of sightings used in the estimation of density (after truncation) are shown in Table 32. Estimates of encounter rate (Table 33) and density (

Table 34) were calculated for cetaceans with adequate sample sizes only. Estimates were not corrected for the proportion of animals missed on the trackline. The effort included for these estimates was as follows: August 24, 2010-September 15, 2010, August 19, 2011 – September 3, 2011, and August 15-31, 2012.

TABLE 32. THE NUMBER OF SIGHTINGS (GROUPS) USED IN THE ESTIMATION OF DENSITY (AFTER TRUNCATION) OF CETACEANS WITHIN ARCTIC WATERS, 2010-2012. THE EFFORT INCLUDED FOR THESE ESTIMATES WAS: AUGUST 24, 2010-SEPTEMBER 15, 2010, AUGUST 19, 2011 – SEPTEMBER 3, 2011, AND AUGUST 15-31, 2012.

Species	Sightings (groups)
Bowhead whale	16
Fin whale	5
Humpback whale	2
Gray whale	15

TABLE 33. ESTIMATES OF ENCOUNTER RATE (GROUPS/KM) AND CV (IN PARENTHESIS) ACROSS ALL YEARS FOR CETACEANS WITHIN ARCTIC WATERS, 2010-2012. THE EFFORT INCLUDED FOR THESE ESTIMATES WAS: AUGUST 24, 2010-SEPTEMBER 15, 2010, AUGUST 19, 2011 – SEPTEMBER 3, 2011, AND AUGUST 15-31, 2012.

Species	Encounter Rate
Bowhead whale	0.0059 (0.59)
Fin whale	0.0022 (0.79)
Humpback whale	0.0007 (0.94)
Gray whale	0.0051 (0.86)

TABLE 34. ESTIMATES OF DENSITY (INDIVIDUALS/KM²) AND CV (IN PARENTHESIS) ACROSS ALL YEARS FOR CETACEANS WITHIN ARCTIC WATERS, 2010-2012. THE EFFORT INCLUDED FOR THESE ESTIMATES WAS: AUGUST 24, 2010-SEPTEMBER 15, 2010, AUGUST 19, 2011 – SEPTEMBER 3, 2011, AND AUGUST 15-31, 2012.

Species	Density
Bowhead whale	0.0043 (0.65)
Fin whale	0.0019 (0.88)
Humpback whale	0.0004 (0.97)
Gray whale	0.0030 (0.86)

3. Discussion

Visual estimates of relative abundance presented in this study assumed that no cetaceans were missed on the trackline ($g[0]=1$). Failure to meet this assumption (referred to as ‘visibility bias’) is common in marine mammal surveys and causes negative biases in density estimates (Laake, 1999; Buckland et al., 2001). Marsh and Sinclair (1989) coined the terms ‘perception’ and ‘availability’ bias to differentiate two forms of visibility bias. Perception bias occurs when marine mammal groups are available to be seen but are missed by the observers while availability bias corresponds to animals that are missed because they are submerged. Except for long-diving species such as sperm whales and beaked whales and for species that are only seen at close ranges such as harbor porpoise, the latter is typically not as important an issue as perception bias in ship surveys (see discussion in Barlow, 1995); animals are often at the surface and within the visual range of observers due to the relatively slow speed of the vessel. The magnitude of visibility bias is possibly small in the estimates of large whales with visible bodies and conspicuous blows such as humpback, bowhead, fin and gray whales. Studies to assess the proportion of whales missed on the trackline have shown that nearly 90-100 percent of humpback whales are detected during ship surveys, depending on visibility conditions and group size (Barlow and Gerrodette, 1996; Calambokidis and Barlow, 2004). On the other hand,

visibility bias is more substantial for species that are more difficult to detect (e.g., porpoise) or for deep-diving species (e.g., sperm whales) leading to more severe negative bias in their estimates; neither were analyzed here. The magnitude of the bias is unknown in this study. Surveys with two independent observer teams would allow for experiments to estimate $g(0)$ and should therefore be considered in future surveys for which abundance and density estimates are a priority.

Summer and fall density estimates for bowhead and gray whales in the Chukchi Sea have been calculated using the 2008-2010 COMIDA aerial survey data (Clarke et al., in review). However, estimates are not comparable to estimates presented here given differences in platforms and geographic coverage. Small sample sizes typically result in large uncertainty around the estimates. Estimates were calculated for bowhead, gray, humpback and fin whales despite their small numbers of visual detections (Table 32) in order to provide predictions on presence within the Chukchi Sea during August/September. The effects of the small sample sizes are reflected in the high CVs for these species.

4. *Conclusions*

Despite the small sample sizes, results from this survey did provide a measure of densities of four species within the Chukchi Sea during August and September. Furthermore, identifying species within the area provided invaluable information for the other key components of this study. Visuals provided species identification for calls detected by acoustics as well as providing information on species and numbers within areas of oceanographic moorings and sampling stations. Additionally, visuals provided information on interannual differences in the spatial distribution of these key Arctic species.

5. *Recommendations*

Visual survey methods for this project differed from standard line-transect or abundance surveys due to constraints of the overall project. To improve estimates, surveys should be designed with density and abundance estimates as a main objective. This would require additional ship time, observers, and ideally, be designed with predetermined tracklines. Depending on the objective, shipboard surveys may or may not be appropriate to fulfill requirements. If the question is density within the Chukchi Sea, an aerial survey (i.e., Aerial Surveys of Arctic Marine Mammals, ASAMM) may be a more appropriate platform to meet objectives given the ability to cover greater distances within a large survey area. However, calculating densities within smaller regions (e.g., the lease area) could be achieved in a reasonable amount of time with a shipboard survey.

B. *Acoustic*

No relative abundance estimates were calculated from the passive acoustic data collected during the CHAOZ project. As detailed below, the field is still in its infancy, but we now have a plan as to how to begin to collect the field data necessary to mine our long-term passive acoustic datasets and eventually estimate relative abundance for all marine mammal species included in this study.

In recent years, considerable effort has been spent developing methods for incorporating towed passive acoustic arrays into survey designs to improve estimates of animal density and/or abundance. These methods have proved successful at obtaining density estimates on par with those from visual methods (e.g., Barlow and Taylor, 2005) for species such as sperm whales that vocalize at high calling rates and source levels. However, for the shallow Chukchi Sea shelf (~40 m), towed arrays are not feasible as they require at least 100m depth so that masking from the tow ship, and the risk that they would become tangled on something on the bottom, would be minimized. Towed arrays are even less practical than visual surveys for cruises that stop at numerous stations for biophysical sampling and mooring deployments. Furthermore, they are better suited to species with higher frequency call repertoires, since lower frequencies on the recordings are masked by flow noise. Finally, as with visual line transect surveys, they are limited to the short time window of the open water season.

As shown in Section VII.A above, passive acoustic moorings are an excellent platform for obtaining long-term datasets on the year-round seasonal distribution of multiple species of cetaceans and pinnipeds. There are even certain subarctic species where passive acoustic monitoring methods surpassed visual survey techniques for detecting individuals (see Section VII.B.3). Is it possible to use these data to obtain relative abundance estimates for Arctic and subarctic marine mammal species? Marques et al. (2009) answer concisely: “... *estimating absolute density or abundance from such data is considerably more difficult, although considerably more useful too.*” Their paper describes the steps needed to accomplish this task: cue counting, estimating average detection probability, and determining the false positive proportion.

The first two methods (cue counting and average detection probability) provide information on the ‘availability bias’ defined in Section XIII.A.3 above. The main problem with passive acoustic methods is that they are only capable of detecting animals that are making sounds. Like animals that are below the surface when the visual survey passes by, silent animals cannot be counted. Cue counting is a method that estimates the probability that an animal is calling. For the upcoming field season, we plan to begin building a dataset of these probability estimates with the following method⁶. The visual team will conduct their line transect survey as usual (Section VII.B.1). Sightings will then be randomly selected for a focused cue count session. The visual team will take detailed notes on all animals within their field of view, while the passive acoustics team deploys and monitors a sonobuoy and notes the presence of any calls for that species. At the end of the ten-minute session, the cue count will be entered into the database as ‘calling’ or ‘not calling’. The bigger the sample size, the more accurate the resulting estimate of calling probability will be.

It is important that the selected sightings be obtained from the visual sightings as opposed to the sonobuoy detections so as to not bias the cue counts by leaving out silent animals. It is equally important to conduct these cue counts under a variety of situations; e.g., at various times of the day, at different locations, with different group sizes, and during a variety of behaviors, so that corrections for these factors can be applied. It would also be beneficial to collect these data throughout the year. Although impractical on a shipboard survey, training of local native hunters

⁶ Another way to obtain cue counts is to use acoustic recorder tags (e.g., DTAGs). These instruments are able to collect call counts from individual whales quite accurately, but the amount of extra ship time needed to conduct this type of effort will be cost-prohibitive (and also limited to the open water season).

and participation on platforms of opportunity (see www.aoots.org for more information) could provide the means of obtaining these data beyond the open water season. Since the visual survey method (i.e., Big Eyes) and passive acoustic method (sonobuoys) can be used at five mile distances – the influence of the survey vessel on the calling behavior of the animal can be reduced.

If two or more sonobuoys are deployed during these cue counts, cross-fixes to the calling animals, and therefore detection distance, can be calculated. This can then be used to estimate the average detection probability for that species. As mentioned above (Section VII.A.1), and by other studies (Stafford et al., 2007a), the detection range is influenced by a variety of oceanographic factors as well as the presence of ambient noise (of biological, environmental, and anthropogenic sources) that can mask the calls of interest. Again, this is a source of availability bias that has to be determined before relative density and abundance estimates can be obtained. However, on our multi-disciplinary cruises, oceanographic sampling equipment is on board and available for measuring many of the environmental variables that contribute to sound propagation.

Call localization techniques from moored recorder arrays are another way of obtaining these average detection probabilities (although not cue counts). For the CHAOZ study we deployed five-element arrays positioned with the elements spaced 2-4 m apart. The critical component of any array localization study is time synchronization of all recorders in the array. Typically, high precision crystals are used to maintain the time synchronization, but temperature differences can cause fluctuations among times. A linear time drift is generally assumed, with the difference in start and end times smoothed linearly over the entire length of the deployment. Less than perfect drifts (e.g., 5 minutes over 3-4 months) have been seen with recorders that were expected to perform better (C. Berchok, pers. observation). For this reason we equipped each mooring with an acoustic pinger that sent a small (<7 s) series of chirps every half hour. Localization of these chirps with all elements of the array would provide an estimate of the localization error correction for that location that would account for all oceanographic conditions at that time of day/year. However, in an attempt to limit the amount of sounds produced, the source level of the pings was not sufficient in the 2010-11 deployment for the signal to be detected on any of the other recorders in the array. For the 2011-12 deployment, the signal was boosted slightly and the duty cycle reduced to hourly transmissions. These data exist and can be used to determine detection distances of the calling animals within the arrays (localizations always have smaller error bounds within the array (Berchok et al., 2006)). The current limiting factor is the lack of accurate auto-detection algorithms that can quickly compile the detections on the other four recorders of each array and provide the core data needed to perform these localizations.

The last piece of the puzzle is obtaining an estimate of the false positive rate of the acoustic analysis methods (i.e., the percentage of times a signal was falsely identified as belonging to a certain species). This provides information on the perception bias. Work has been done (Caillat et al., 2013) on other data sets that suggests these techniques are appropriate. However, in speaking with the author about the current level of performance for Arctic auto-detectors it was clear that the variance in any resulting abundance estimates would be impractically high. Therefore, more work is needed to develop auto-detectors that can perform well in the Arctic environment where very few species have stereotyped calls, and many species (and environment sources such as ice noise) make similar, often overlapping sounds. In the

meantime, we will continue with our manual analysis while concurrently working on improving our auto-detectors (Section VII.A.5). With our manual analysis method, a random blind cross-check by a couple of experienced analysts can provide the metrics needed to obtain this false detection rate; however, manual analysts tend to be conservative with their detections (e.g., Hannay et al., 2013), and a low false detection rate is expected. After these components are in place, estimates of relative density and abundance can then be calculated following the methods described in Marques et al. (2009).

Finally, it is very important to emphasize at this point that although it will most likely take some time to establish an Arctic database of cue counts and detection probabilities, the long-term passive acoustic data sets collected during the CHAOZ project will be available and ready for the suitable abundance techniques (Marques et al., 2009) to be applied. The field methods needed to build this database can be readily integrated into multidisciplinary cruises, and therefore will not require the substantial ship time nor personnel of a traditional visual survey. Furthermore, the sample size in this Arctic database will only increase over time, leading to more accurate recalculations of relative density and abundance, which will then be available for comparisons between years, and eventually decades.

XIV. SUMMARY

A. *Overall summary*

This integrative five year study was able to correlate marine mammal distributions with oceanographic parameters, and indices of potential prey availability. The technologies utilized in this study allowed us to assess complex trophic interactions, and illustrated the benefit of these complex analyses being conducted on an annual scale. Furthermore, by including climate and ocean atmosphere modeling, we were able to not only predict ecosystem-wide changes as a result of a reduction in sea ice, but also to assess potential impacts to marine mammal populations and distribution. Although the current marine mammal dataset was too brief to determine if there was a northward shift of subarctic species into the Arctic, anecdotal evidence (i.e., walrus and ribbon seals detected in the Chukchi during off-season months, the acoustic detection of a fin whale off Barrow Canyon) possibly suggests that such a northward shift of subarctic species may be underway.

This project included two years of continuous year-round data at a location that is well suited to document changes to the ecosystem. However, with this limited spatio-temporal scale, it is difficult to determine if our results are representative of true annual patterns, or merely reflect the high interannual variability in this region. By including additional data that are currently being collected in the ongoing BOEM-funded ARCWEST and CHAOZ-X (CHAOZ extension) projects, we will not only increase the temporal time scale of our dataset, but greatly expand our spatial coverage to include other areas that are critical to marine mammal migrations as well. This will allow us to more fully assess year-round distributions as well as quantify interannual variation, better predict future oceanographic conditions and ecosystem shifts, and evaluate potential impacts of climate change on both lower and upper trophic levels.

B. *Recommendations for future work*

The data collected for the CHAOZ project demonstrate the utility and benefit of concurrent zooplankton, oceanography, and marine mammal monitoring. These data, combined with those currently being collected for the ongoing BOEM-funded ARCWEST and CHAOZ-X projects represent the only long-term integrated dataset of its kind from the Chukchi Sea lease area and Alaskan Arctic in general. We therefore recommend continuation of the long-term mooring deployments. With current modifications to the moored TAPS6-NG instruments, we will be able to collect data for a full year, allowing for assessment of trophic interactions on an annual time scale. It will also be possible to establish multi-year patterns in marine mammal distributions as they relate to indices of zooplankton and oceanographic conditions.

We also recommend continuation of the integrated biophysical shipboard surveys conducted during this study. These surveys provide data on the fine-scale vertical resolution of zooplankton abundance as they correlate with oceanographic indices, nutrients, and distribution of marine mammals. To maximize marine mammal detections during shipboard surveys, it is essential to have both passive acoustic monitoring and visual survey components. Since each method is well-suited to particular species, together they provide a more complete picture of

marine mammal distribution. In addition, joint passive acoustic/visual survey focal follows enable future calculations of relative abundance. Addition of a benthic ecology component would help to address prey availability for those mammals that feed on benthic epifauna and infauna.

XV. LITERATURE CITED

- Aerts, L.A.M., A. Kirk, C. Schudel, B. Watts, P. Seiser, A. McFarland, and K. Lomac-Macnair. 2012. Marine Mammal Distribution and Abundance in the Northeastern Chukchi Sea, July-October 2008-2011. Report prepared by LAMA Ecological for ConocoPhillips Alaska, Inc., Shell Exploration and Production Company and Statoil USA E&P, Inc. 69 pp.
- Aerts, L.A.M., A.E. McFarland, B.H. Watts, K.S. Lomac-MacNair, P.E. Seiser, S.S. Wisdom, A.V. Kirk, and C.A. Schudel. 2013. Marine mammal distribution and abundance in an offshore sub-region of the northeastern Chukchi Sea during the open-water season. *Continental Shelf Research* 67: 116-126.
- Akaike, H. 1973. Information theory and an extension of the maximum likelihood principle. In B. N. Petran and F. Csáki (eds.), *International symposium on information theory*, 2nd edition, pp. 267-281. Budapest, Hungary: Acadèmiai Kiadi.
- Allen, B.M. and R.P. Angliss. 2013. Alaska marine mammal stock assessments: Bearded Seal (*Erignathus barbatus nauticus*). NOAA-TM-AFSC-277: 55-61.
- Angliss, R.P., D.J. Rugh, D.E. Withrow and R.C. Hobbs. 1995. Evaluations of aerial photogrammetric length measurements of the Bering-Chukchi-Beaufort Seas stock of bowhead whales (*Balaena mysticetus*). *Reports of the International Whaling Commission* 45: 313-324.
- Argos. 1990. User's manual. Service Argos, Inc. Landover, MD, USA.
- ASAMM (Aerial Surveys of Arctic Marine Mammals) daily flight report. Chukchi Sea Flight 240, 27 September 2014.
http://www.afsc.noaa.gov/nmml/cetacean/bwasp/2014/ASAMM-Chukchi_Flight240_27September2014.pdf
- Ashjian, C.J., R.G. Campbell, J.C. George, J. Kruse, W. Maslowski, S.E. Moore, C.R. Nicolson, S.R. Okkonen, B.F. Sherr, E.B. Sherr, and Y.H. Spitz. 2010. Climate variability, oceanography, bowhead whale distribution, and Inupiat subsistence whaling near Barrow, Alaska. *Arctic* 63: 179-194.
- Au, W.W.L., D.A. Carder, R.H. Penner, and B.L. Scronce. 1985. Demonstration of adaptation in beluga whale echolocation signals. *Journal of the Acoustical Society of America* 77(2): 726-730.
- Barlow, J. 1995. The abundance of cetaceans in California waters. Part I: Ship surveys in the summer and fall of 1991. *Fishery Bulletin* 93: 1-14.
- Barlow, J. and T. Gerrodette. 1996. Abundance of cetaceans in California waters based on 1991 and 1993 ship surveys. NOAA Technical Memorandum NMFS-SWFSC-233. La Jolla, CA: National Marine Fisheries Service. 15 pp.
- Barlow, J., T. Gerrodette, and G. Silber. 1997. First estimates of vaquita abundance. *Marine Mammal Science* 13: 44-58.
- Barlow, J., T. Gerrodette, and T. Forcada. 2001. Factors affecting perpendicular sighting distances on shipboard line-transect surveys for cetaceans. *Journal of Cetacean Research and Management* 3: 201-212.

- Barlow, J. and B.L. Taylor. 2005. Estimates of sperm whale abundance in the northeastern temperate Pacific from a combined acoustic and visual survey. *Marine Mammal Science* 21(3): 429-445.
- Bengtson, J.L., L.M. Hiruki-Raring, M.A. Simpkins, and P.L. Boveng. 2005. Ringed and bearded seal densities in the eastern Chukchi Sea, 1999-2000. *Polar Biology* 28: 833-845.
- Berchok, C.L., G.L. D'Spain, and J.A. Hildebrand. 2006. Reducing source localization errors: a visualization method to help guide the design, calibration, and use of widely-separated acoustic sensor arrays. *Journal of the Acoustical Society of America*. 120: 2999.
- Berge, J., F. Cottier, K.S. Last, Ø.Varpe, E. Leu, J. Søreide, K. Eiane, S. Falk-Petersen, K. Willis, H. Nygård, D. Vogedes, C. Griffiths, G. Johnsen, D. Lorentzen, and A.S. Brierley. 2009. Diel vertical migration of Arctic zooplankton during the polar night. *Biology Letters* 5: 69–72.
- Berline, L., Y.H. Spitz, C.J. Ashjian, R.G. Campbell, W. Maslowski, S.E. Moore. 2008. Euphausiid transport in the western Arctic Ocean. *Marine Ecology Progress Series* 360: 163-178.
- Blackwell, S.B., W.J. Richardson, C.R. Greene, Jr., and B. Streever. 2007. Bowhead whale (*Balaena mysticetus*) migration and calling behavior in the Alaskan Beaufort Sea, Autumn 2001-04: an acoustic localization study. *Arctic* 60: 255-270.
- Blackwell, S.B., C.S. Nations, T.L. McDonald, C.R. Greene, Jr., A.M. Thode, M. Guerra, and A. M. Macrander. 2013. Effects of airgun sounds on bowhead whale calling rates in the Alaskan Beaufort Sea. *Marine Mammal Science* 29: E342-E365. DOI: 10.1111/mms.12001
- Blanchard, A.L., C.L. Parris, A.L. Knowlton, and N.R. Wade. 2013. Benthic ecology of the northeastern Chukchi Sea. Part I. Environmental characteristics and macro faunal community structure 2008-2010. *Continental Shelf Research* 67: 52-66.
- Blees, M.K., K.G. Hartin, D.S. Ireland, and D. Hannay. (eds.) 2010. Marine mammal monitoring and mitigation during open water seismic exploration by Statoil USA E&P Inc. in the Chukchi Sea, August–October 2010: 90-day report. LGL Rep. P1119. Rep. from LGL Alaska Research Associates Inc., LGL Ltd., and JASCO Research Ltd. for by Statoil USA E&P Inc., Nat. Mar. Fish. Serv., and U.S. Fish and Wild. Serv. 102 pp, plus appendices.
- Bluhm, B.A., K.O. Coyle, B. Konar, and R. Highsmith. 2007. High gray whale relative abundances associated with an oceanographic front in the south-central Chukchi Sea. *Deep-Sea Research II* 54: 2919-2933.
- Bluhm, B.A. and R. Gradinger. 2008. Regional variability in food availability for Arctic marine mammals. *Ecological Applications* 18: S77-S96.
- Bluhm, B.A., K. Iken, S. Mincks Hardy, B.I. Sirenko, and B.A. Holladay. 2009. Community structure of epibenthic megafauna in the Chukchi Sea. *Aquatic Biology* 7: 269-293.

- Boveng, P.L., J.L. Bengtson, M.F. Cameron, S.P. Dahle, E.A. Logerwell, J.M. London, J.E. Overland, J.T. Sterling, D.E. Stevenson, B.L. Taylor, and H.L. Ziel. 2013. Status review of the ribbon seal (*Histiophoca fasciata*). U.S. Department of Commerce, NOAA Technical Memorandum NMFS-AFSC-225. 175 pp.
- Braham, H.W., C. Fiscus, and D. J. Rugh. 1977. Marine mammals of the Bering and southern Chukchi seas. Environmental Assessment of Alaska Outer Continental Shelf 1: 1-99.
- Braham, H.W., M.A. Fraker, and B.D. Krogman. 1980. Spring Migration of the Western Arctic Population of Bowhead Whales. Marine Fisheries Review 42: 36-46.
- Braham, H.W., B.D. Krogman, and G.M. Carroll. 1984. Bowhead and white whale migration, distribution, and abundance in the Bering, Chukchi, and Beaufort Seas, 1975-78. NOAA Technical Report NMFS SSRF-778.
- Buckland, S.T., D.R. Anderson, K.P. Burnham, J.L. Laake, D.L. Borchers, and L. Thomas. 2001. Introduction to distance sampling estimating abundance of biological populations. Oxford, UK: Oxford University Press. 432 pp.
- Buckland, S.T., D.R. Anderson, K.P. Burnham, J.L. Laake, D.L. Borchers, and L. Thomas. 2004. Advanced distance sampling. Oxford, UK: Oxford University Press. 411 pp.
- Burns, J.J. 1967. The Pacific bearded seal. Alaska Department of Fish and Game, Pittman-Robertson Project Report W-6-r and W-14-R.
- Burns, J.J. 1970. Remarks on the distribution and natural history of pagophilic pinnipeds in the Bering and Chukchi Seas. Journal of Mammalogy 51: 445-454.
- Burns, J.J. 1981. Bearded seal, *Erignathus barbatus*. In S.H. Ridgeway and R.J. Harrison, F.R.S. (eds.), Handbook of Marine Mammals, pp.145-170. London: Academic Press.
- Burns, J.J. and T.J. Eley. 1978. The Natural History and Ecology of the Bearded Seal (*Erignathus Barbatus*) and the Ringed Seal (*Phoca Hispida*). Environmental Assessment of the Alaskan Continental Shelf Annual Reports of Principal Investigators for the Year Ending March 1, 1978.
- Burns, J.J. and K.J. Frost. 1979. The natural history and ecology of the bearded seal, *Erignathus barbatus*. Alaska Department of Fish and Game. 77pp.
- Caillat, M., L. Thomas, and D. Gillespie. 2013. The effects of acoustic misclassification on cetacean species abundance estimation. Journal of the Acoustical Society of America 134: 2469-2476.
- Caillat, M., L. Thomas, and D. Gillespie. 2013. The effects of acoustic miscalculation on cetacean species abundance estimation. Journal of the Acoustical Society of America. 134: 2469-2476.
- Calambokidis, J. and J. Barlow. 2004. Abundance of blue and humpback whales in the eastern North Pacific estimated by capture-recapture and line-transect methods. Marine Mammal Science 20: 63-85.
- Calupca T.A., K.M. Fristrup, and C.W. Clark. 2000. A compact digital recording system for autonomous bioacoustic monitoring. Journal of the Acoustical Society of America. 108: 2582-2582.

- Cameron, D., E. Ellis, A. Harrison, H. Ingram, and M. Piercy. 2012. Plate boundaries around the Chukchi borderland: An integrated geophysics cruise to test models for the formation of the Canada Basin. Protected Species Mitigation and Monitoring Report of the Coakley Marine Geophysical Survey in the Arctic Ocean. Prepared for Lamont-Doherty Earth Observatory of Columbia University, Palisades, NY, and Nat. Mar. Fish. Serv., Silver Spring, MD. 54 pp, plus appendices.
- Carroll, G.M., J.C. George, L.F. Lowry, and K.O. Coyle. 1987. Bowhead whale (*Balaena mysticetus*) feeding near Point Barrow, Alaska, during the 1985 spring migration. *Arctic* 40: 105-110.
- Castellote, M., R.J. Small, M.O. Lammers, J. Jenniges, J. Mondragon, and S. Atkinson. In review. Dual instrument passive acoustic monitoring of belugas in Cook Inlet, Alaska. Submitted to *Journal of the Acoustical Society of America*.
- Castellote, M., T. McGuire, C. McKee, and M. Lammers. 2011. Can we hear Cook Inlet beluga whales feeding? Poster presentation at the Alaska Marine Science Symposium, 17-21 January, 2011. Anchorage, AK.
- Castellote, M., R.H. Leeney, G. O’Corry-Crowe, R. Lauhakangas, K.M. Kovacs, W. Lucey, V. Krasnova, C. Lydersen, K.M. Stafford, and R. Belikov. 2013. Monitoring white whales (*Delphinapterus leucas*) with echolocation loggers. *Polar Biology* 36: 493-509.
- Castellote, M., T.A. Mooney, L. Quakenbush, R. Hobbs, C. Goertz, and E. Gaglione. 2014. Baseline hearing abilities and variability in wild beluga whales (*Delphinapterus leucas*). *Journal of Experimental Biology* 217(10): 1682-1691.
- Cerchio, S., S. Strindberg, T. Collins, C. Bennett, and H. Rosenbaum. 2014. Seismic surveys negatively affect humpback whale singing activity off Northern Angola. *PLoS ONE* 9: e86464. doi: 10.1371/journal.pone.0086464
- Charif, R.A., C.W. Clark, and K.M. Fristrup. 2004. Raven 1.2 User’s Manual. Cornell Laboratory of Ornithology, Ithaca, NY.
- Citta, J.J., R.S. Suydam, L.T. Quakenbush, K.J. Frost, and G.M. O’Corry-Crowe. 2013. Dive behavior of Eastern Chukchi beluga whales (*Delphinapterus leucas*), 1998-2008. *Arctic* 66: 389-406.
- Clapham, P.J., A.S. Kennedy, B.K. Rone, A.N. Zerbini, J.L. Crance, and C.L. Berchok. 2012. North Pacific right whales (*Eubalaena japonica*) in the southeastern Bering Sea. Final Report. OCS Study BOEM 2012-074. National Marine Mammal Laboratory, Alaska Fisheries Science Center, NOAA. 175pp.
- Clark, C.W. 1983. Acoustic communication and behavior of the southern right whale. In R.S. Payne (ed.), *Communication and Behavior of Whales*, pp. 163-198. American Association for the Advancement of Science Selected Symposium 76. Boulder, Colorado: Westview Press.
- Clark, C.W., W.T. Ellison, and K. Beeman. 1986. A preliminary account of the acoustic study conducted during the 1985 spring bowhead whale, *Balaena mysticetus*, migration off Point Barrow, Alaska. Report of the International Whaling Commission 36: 311-316.

- Clark, C.W. and W.T. Ellison. 2000. Calibration and comparison of the acoustic location methods used during the spring migration of the bowhead whale, *Balaena mysticetus*, off Pt. Barrow, Alaska, 1984-1993. *Journal of the Acoustical Society of America*. 106: 3509-3517.
- Clark, C. W., J.F. Borsani, and G. Notarbartolo-di-Sciara. 2002. Vocal activity of fin whales, *Balaenoptera physalus*, in the Ligurian Sea. *Marine Mammal Science* 18: 286–295.
- Clark, C.W., W.T. Ellison, B.L. Southall, L. Hatch, S. Van Parijs, A. Frankel, and D. Ponirakis. 2009. Acoustic Masking in Marine Ecosystems: Intuitions, Analysis, and Implications. *Marine Ecology Progress Series* 395: 201-222.
- Clark, C.W., C.L. Berchok, S.B. Blackwell, D.E. Hannay, J. Jones, D. Ponirakis and K.M. Stafford. 2015. A year in the acoustic world of Western Arctic bowhead whales in the Bering, Chukchi and Beaufort seas. *Progress in Oceanography* 136: 223-240
<http://dx.doi.org/10.1016/j.pocean.2015.05.007>.
- Clarke, J.T., S.E. Moore, and M.M. Johnson. 1993. Observations on beluga fall migration in the Alaskan Beaufort Sea, 1982-87, and northeastern Chukchi Sea, 1982-91. *Report of the International Whaling Commission* 43: 387-396.
- Clarke, J.T. and M.C. Ferguson. 2010. Aerial surveys of large whales in the northeastern Chukchi Sea, 2008-2009, with review of 1982-1991 data. IWC Scientific Committee, pp. 1-18.
- Clarke, J.T., M.C. Ferguson, C.L. Christman, S.L. Grassia, A.A. Brower, and L.J. Morse. 2011. Chukchi Offshore Monitoring in Drilling Area (COMIDA) Distribution and Relative Abundance of Marine Mammals: Aerial Surveys. Final Report, OCS Study BOEMRE 2011-06. National Marine Mammal Laboratory, Alaska Fisheries Science Center, NMFS, NOAA, 7600 Sand Point Way NE, F/AKC3, Seattle, WA 98115-6349.
- Clarke, J., C.L. Christman, A.A. Brower, and M.C. Ferguson. 2012. Distribution and relative abundance of marine mammals in the Alaskan Chukchi and Beaufort Seas, 2011. Annual Report, OCS Study BOEM 2012-009. National Marine Mammal Laboratory, Alaska Fisheries Science Center, NMFS, NOAA, 7600 Sand Point Way NE, F/AKC3, Seattle, WA 98115-6349.
- Clarke, J.T., C.L. Christman, A.A. Brower, and M.C. Ferguson. 2013. Distribution and Relative Abundance of Marine Mammals in the Northeastern Chukchi and Western Beaufort Seas, 2012. Annual Report, OCS Study BOEM 2013-00117. National Marine Mammal Laboratory, Alaska Fisheries Science Center, NMFS, NOAA, 7600 Sand Point Way NE, F/AKC3, Seattle, WA 98115-6349.
- Clarke, J., K. Stafford, S.E. Moore, B.K. Rone, L. Aerts, and J.L. Crance. 2013. Subarctic cetaceans in the southern Chukchi Sea: Evidence of recovery or response to a changing ecosystem. *Oceanography* 26: 136-149. doi: 10.5670/oceanog.2013.81
- Clarke, J., M.C. Ferguson, C. Curtice, and J. Harrison. 2015. Biologically Important Areas for cetaceans within U.S. waters – Arctic region. *Aquatic Mammals* 41: 94-103. doi: 10.1578/AM.41.1.2015.94

- Clarke, J.T., A.S. Kennedy, and M.C. Ferguson. Bowhead (*Balaena mysticetus*) and gray whale (*Eschrichtius robustus*) distribution, relative abundance and habitat selection in summer and fall in the northeastern Chukch Sea, 2009-2012. Arctic, in review.
- Cleator, H.J., I. Stirling, and T.G. Smith. 1989. Underwater vocalizations of the bearded seal (*Erignathus barbatus*). Canadian Journal of Zoology 67: 1900-1910.
- Clutter, R.I. and M. Anraku. 1968. Avoidance of samplers. In Zooplankton Sampling, UNESCO Monograph on Oceanographic Methodology, vol. 2, pp. 57-643. Paris, France: UNESCO Press.
- Cottier, F.R., G.A. Tarling, A. Wold, and S. Falk-Petersen. 2006. Unsynchronised and synchronised vertical migration of zooplankton in a high Arctic fjord. Limnology and Oceanography 51: 2586–2599.
- Crance, J.L., C.L. Berchok, J. Bonnel, and A.M. Thode. 2015. Northeasternmost record of a north Pacific fin whale (*Balaenoptera physalus*) in the Alaskan Chukchi Sea. Polar Biology doi: 10.1007/s00300-015-1719-7
- Crane, N.L. and K. Lashkari. 1996. Sound production of gray whales, *Eschrichtius robustus*, along their migration route: a new approach to signal analysis. Journal of the Acoustical Society of America 100: 1878-1886.
- Cummings, W.C., P.O. Thompson, and R. Cook. 1968. Underwater Sounds of Migrating Gray Whales, *Eschrichtius glaucus*. Journal of the Acoustical Society of America 44 (5): 1278-1281.
- Dahlheim, M.E. 1987. Bio-acoustics of the gray whale (*Eschrichtius robustus*). Ph.D. Dissertation, University of British Columbia.
- Dahlheim, M., T. Bray, and H. Braham. 1980. Vessel survey for bowhead whales in the Bering and Chukchi Seas, June-July 1978. Marine Fisheries Review 42: 51-57.
- Danielson, S.L., L. Eisner, C. Ladd, C. Mordy, L. Sousa and T.J. Weingartner. Submitted (July 2015). A comparison between late summer 2012 and 2013 water masses, macronutrients, and phytoplankton standing crops in the northern Bering and Chukchi Seas. Deep-Sea Res. II.
- Darling, J.D, K.E. Keogh, and T.E. Steeves. 1998. Gray whale (*Eschrichtius robustus*) habitat utilization and prey species off Vancouver Island, B.C. Marine Mammal Science 14: 692-720.
- Day, R.H., T.J. Weingartner, R.R. Hopcroft, L.A.M. Aerts, A.L. Blanchard, A.E. Gall, B.J. Gallaway, D.E. Hannay, B.A. Holladay, J.T. Mathis, B.L. Norcross, J.M. Questel, and S.S. Wisdom. 2013. The offshore northeastern Chukchi Sea, Alaska: A complex high-latitude system. Continental Shelf Research 67: 147–165.
- Deecke, V.B., J.K.B. Ford, and P.J.B. Slater. 2005. The vocal behaviour of mammal-eating killer whales (*Orcinus orca*): Communicating with costly calls. Animal Behaviour 69: 395-405.
- Deines, K.L. 1999. Backscatter estimation using Broadband acoustic Doppler current profilers. Proceedings of the IEEE Sixth Working Conference on Current Measurement, pp. 249 – 253. San Diego, California.

- De Jesus, M., G. Heckel, J.M. Breiwick, and S.B. Reilly. 2014. Migration timing and distance from shore of southbound eastern Pacific gray whales (*Eschrichtius robustus*) off Ensenada, Baja California, Mexico. *Marine Mammal Science* 30: 674-690.
- Delarue, J., M. Laurinolli, and B. Martin. 2009. Bowhead whale (*Balaena mysticetus*) songs in the Chukchi Sea between October 2007 and May 2008. *Journal of the Acoustical Society of America* 126: 3319-3328.
- Delarue, J., M. Laurinoll, and B. Martin. 2011. Acoustic detections of beluga whales in the Northeastern Chukchi Sea, July 2007 to July 2008. *Arctic* 64: 15-24.
- Delarue, J., B. Martin, D. Hannay, and C.L. Berchok. 2013a. Acoustic occurrence and affiliation of fin whales detected in the northeastern Chukchi Sea, July to October 2007-10. *Arctic* 66: 159-172.
- Delarue, J., B. Martin, and D. Hannay. 2013b. Minke whale boing sound detections in the northeastern Chukchi Sea. *Marine Mammal Science* 29(3): E333-E341.
- DeRobertis, A., D. McKelvey, and P.H. Ressler. 2010. Development and application of empirical multi-frequency methods for backscatter classification. *Canadian Journal of Fisheries and Aquatic Sciences* 67: 1459-1474.
- Dewicke, A., V. Rottiers, J. Mees, and M. Vincx. 2002. Evidence for an enriched hyperbenthic fauna in the Frisian front (North Sea). *Journal of Sea Research* 47: 121-139.
- Dougherty, A., C. Harpold, and J. Clark. 2010. Ecosystems and Fisheries-Oceanography Coordinated Investigations (EcoFOCI) field manual. AFSC Processed Report 2010-02, 213 pp. Alaska Fisheries Science Center, NMFS, NOAA, 7600 Sand Point Way NE, Seattle WA 98115. <http://www.afsc.noaa.gov/Publications/ProcRpt/PR2010-02.pdf>
- Dugan, P.J., D.W. Ponirakis, J.A. Zollweg, M.S. Pitzrick, J.L. Morano, A.M. Warde, A.N. Rice, and C.W. Clark. 2011. SEDNA - Bioacoustic Analysis Toolbox Matlab Platform to Support High Performance Computing, Noise Analysis, Event Detection and Event Modeling. IEEE Xplore, vol. OCEANS-11, Kona, Hawaii.
- Dunton, K.H., S.M. Saupe, A.N. Golikov, D.M. Schell, and S.V. Schonberg. 1989. Trophic relationships and isotopic gradients among arctic and subarctic marine fauna. *Marine Ecology Progress Series, Oldendorf* 56: 89-97.
- Ellison, W.T., C.W. Clark, and G.C. Bishop. 1987. Potential use of surface reverberation by bowhead whales, *Balaena mysticetus*, in under-ice navigation: Preliminary considerations. *Report of the International Whaling Commission* 37: 329-332.
- Fadely, B.S., B.W. Robson, J.T. Sterling, A. Greig, and K.A. Kall. 2005. Immature Steller sea lion (*Eumetopias jubatus*) dive activity in relation to habitat features of the eastern Aleutian Islands. *Fisheries Oceanography* 14: 243-258.
- Fay, F.H. 1982. Ecology and biology of the Pacific walrus, *Odobenus rosmarus divergens* Illiger. *North American Fauna* 74: 1-279.
- Fay, F.H., Y.A. Bukhtiyarov, S.W. Stoker, and L.M. Shults. 1984a. Foods of the Pacific walrus in winter and spring in the Bering Sea. *NOAA Technical Report NMFS*, 12: 81-88.

- Fay, F.H., G.C. Ray, and A.A. Kibal'chich. 1984b. Time and location of mating and associated behavior of the Pacific walrus, *Odobenus rosmarus divergens* Illiger. Soviet-American cooperative research on marine mammals 1: 89-99.
- Feder, H.M., A.S. Naidu, S.C. Jewett, J.M. Hameedi, W.R. Johnson, and T.E. Whitledge. 1994. The northeastern Chukchi Sea: benthos-environmental interactions. Marine Ecology Press Series 111: 171-190.
- Flinn, R.D., A.W. Trites, E.J. Gregr, and R.I. Perry. 2002. Diets of fin, sei, and sperm whales in British Columbia: An analysis of commercial whaling records, 1963-1967. Marine Mammal Science 18: 663-679.
- Freitas, C., C. Lydersen, M.A. Fedak, and K.M. Kovacs. 2008. A simple new algorithm to filter marine mammal Argos locations. Marine Mammal Science 24: 315-325.
- Forney, K.A. and J. Barlow. 1998. Seasonal patterns in the abundance and distribution of California cetaceans, 1991-1992. Marine Mammal Science 14: 460-489.
- Friday, N.A., A.N. Zerbini, J.M. Waite, S.E. Moore, and P.J. Clapham. 2013. Cetacean distribution and abundance in relation to oceanographic domains on the eastern Bering Sea shelf in June and July of 2002, 2008, and 2010. Deep Sea Research II 94: 244-256. doi: 10.1016/j.dsr2.2013.03.011
- Frost, K.J., L.F. Lowry, and G. Carroll. 1993. Beluga whale and spotted seal use of a coastal lagoon system in the northeastern Chukchi Sea. Arctic 46: 8-16.
- Garland, E.C., M. Castellote, and C.L. Berchok. 2015. Beluga whale (*Delphinapterus leucas*) vocalizations and call classifications from the eastern Beaufort Sea population. Journal of the Acoustical Society of America 137:3054-3067 doi: 10.1121/1.4919338.
- Garland, E.C., C.L. Berchok, and M. Castellote. 2015. Temporal peaks in beluga whale (*Delphinapterus leucas*) acoustic detections in the northern Bering, northeastern Chukchi, and western Beaufort Seas: 2010-2011. Polar Biology. doi: 10.1007/s00300-014-1636-1
- George, J.C., C.W. Clark, G.M. Carroll, and W.T. Ellison. 1989. Observations on the ice-breaking and ice navigation behavior of migrating bowhead whales (*Balaena mysticetus*) near Point Barrow, Alaska, Spring 1985. Arctic 42: 24-30.
- Gostiaux, L. and H. Van Haren. 2010. Extracting meaningful information from uncalibrated backscattered echo intensity data. Journal of Atmospheric and Oceanic Technology 27: 943-949.
- Gradinger, R.R. and B.A. Bluhm. 2004. In-situ observations on the distribution and behavior of amphipods and Arctic cod (*Boreogadus saida*) under the sea ice of the High Arctic Canada Basin. Polar Biology 27: 595-603.
- Grebmeier, J.M., L.W. Cooper, H.M. Feder, and B.I. Sirenko. 2006a. Ecosystem dynamics of the Pacific-influenced Northern Bering and Chukchi Seas in the Amerasian Arctic. Progress in Oceanography 71: 331-361.
- Grebmeier, J.M., J.E. Overland, S.E. Moore, E.V. Farley, E.C. Carmack, L.W. Cooper, K.E. Frey, J.H. Helle, F.A. McLaughlin, and S.L. McNutt. 2006b. A major ecosystem shift in the northern Bering Sea. Science 311: 1461-1464.

- Grebmeier, J.M. 2012. Shifting patterns of life in the Pacific Arctic and sub-Arctic Seas. *Annual Review of Marine Science* 4. doi: 10.1146/annurev-marine-120710-100926.
- Grebmeier, J.M., B.A. Bluhm, L.W. Cooper, S.L. Danielson, K.R. Arrigo, A.L. Blanchard, J.T. Clarke, R.H. Day, K.E. Frey, R.R. Gradinger, M. Kedra, B. Konar, K.J. Kuletz, S.H. Lee, J.R. Lovvorn, B.L. Norcross, and S.R. Okkonen. 2015. Ecosystem characteristics and processes facilitating persistent macrobenthic biomass hotspots and associated benthivory in the Pacific Arctic. *Progress in Oceanography* 136: 92-114. doi: 10.1016/j.pocean.2015.05.006
- Greene, C.R., M.W. McLennan, R.G. Norman, T.L. McDonald, R. Jakubczak, and W.J. Richardson. 2004. Directional frequency and recording (DIFAR) sensors in seafloor recorders to locate calling bowhead whales during their fall migration. *Journal of the Acoustical Society of America*. 116: 799-813.
- Greenlaw, C.F. 1979. Acoustical estimation of zooplankton populations. *Limnology and Oceanography* 24: 226–242.
- Greenlaw, C.F. and R.K. Johnson. 1983. Multiple-frequency acoustical estimation. *Biological Oceanography* 2: 227–252.
- Guerra, M., A.M. Thode, S.B. Blackwell, and A.M. Macrander. 2011. Quantifying seismic survey reverberation off the Alaskan North Slope. *Journal of the Acoustical Society of America* 130: 3046-3058.
- Guerra, M., A.N. Rice, D.W. Ponirakis, and C.W. Clark. 2013. Characterization of the interannual ambient noise baseline off Icy Cape, AK and its primary noise sources (2010-2012). Alaska Marine Science Symposium, Anchorage, AK, January 2013.
- Hannay, D.E., J. Delarue, X. Mouy, B.S. Martin, D. Leary, J.N. Oswald, and J. Vallarta. 2013. Marine mammal acoustic detections in the northeastern Chukchi Sea, September 2007-July 2011. *Continental Shelf Research* 67: 127-146.
- Hartin K.G., L.N. Bisson, S.A. Case, D.S. Ireland, and D. Hannay (eds.). 2011. Marine mammal monitoring and mitigation during site clearance and geotechnical surveys by Statoil USA E&P Inc. in the Chukchi Sea, August–October 2011: 90-day report. LGL Rep. P1193. Rep. from LGL Alaska Research Associates Inc., LGL Ltd., and JASCO Research Ltd. for Statoil USA E&P Inc., Nat. Mar. Fish. Serv., and U.S. Fish and Wild. Serv. 202 pp, plus appendices.
- Hatch, L.T., C.W. Clark, S. Van Parijs, A.S. Frankel, and D.W. Ponirakis. 2012. Quantifying loss of acoustic communication space for right whales in and around a U.S. National Marine Sanctuary. *Conservation Biology* 26: 983-994.
- Hauser, D.D.W., K.L. Laidre, R.S. Suydam, and P.R. Richard. 2014. Population-specific home ranges and migration timing for Pacific Arctic beluga whales (*Delphinapterus leucas*). *Polar Biology* 37: 1171-1183. doi: 10.1007/s00300-014-1510-1
- Heide-Jørgensen, M.P., L. Kleivane, N. Øien, K.L. Laidre, and M.V. Jensen. 2001. A new technique for deploying satellite transmitters on baleen whales: tracking a blue whale (*Balaenoptera musculus*) in the North Atlantic. *Marine Mammal Science* 17: 949-953.

- Holliday, D.V. 1977. Extracting bio-physical information from the acoustic signatures of marine organisms. In N.R. Anderson and B.J. Zahuranec (eds.), *Oceanic Sound Scattering Prediction*, pp. 619-624. New York: Plenum Press.
- Holliday, D.V. 1992. Zooplankton Acoustics. In B.N. Desai (ed.), *Oceanography of the Indian Ocean*, pp. 733–740. New Delhi: Oxford-IBH.
- Holliday D.V., P.L. Donaghay, C.F. Greenlaw, D.E. McGehee, M.M. McManus, J.M. Sullivan, and J.L. Miksis. 2003. Advances in defining fine- and micro-scale patterns in marine plankton. *Aquatic Living Resources* 16: 131–136.
- Holliday, D.V., P.L., Donaghay, C.F. Greenlaw, J.M. Napp, and J.M. Sullivan. 2009. High-frequency acoustics and bio-optics in ecosystems research. *ICES Journal of Marine Science* 66: 974-980.
- Hopcroft, R.R. and R.H. Day (eds.). 2013. Seasonal and interannual dynamic s of the northeastern Chukchi Sea ecosystem. *Continental Shelf Research, Special Issue 67*: 1-166.
- Hunt, G.L., Jr., P. Ressler, G. Gibson, A. De Robertis, K. Aydin, M.F. Sigler, I. Ortiz, E. Lessard, B.C. Williams, A. Pinchuk, and T. Buckley. Euphausiids of the eastern Bering Sea: A synthesis of recent studies of euphausiid production, consumption, and population control. *Deep Sea Res., II*, submitted.
- Huntington, H.P. and L.T. Quakenbush. 2009. Traditional knowledge of bowhead whale migratory patterns near Kaktovik and Barrow, Alaska. Report to the Alaska Eskimo Whaling Commission.
- Innes, S., M.P. Heide-Jørgensen, J. Laake, K.L. Laidre, H. Cleator, P. Richard, and R.E.A. Stewart. 2002. Surveys of belugas and narwhals in the Canadian High Arctic in 1996. *Scientific Publications of the North Atlantic Marine Mammal Commission* 4: 169-190.
- Jay, C.V., A.S. Fischbach, and A.A. Kochnev. 2012. Walrus areas of use in the Chukchi Sea during sparse sea ice cover. *Marine Ecology Progress Series* 468: 1-13.
- Jay, C.V., J.M. Grebmeier, A.S. Fischbach, T.L. McDonald, L.W. Cooper, and F. Hornsby. 2014. Pacific Walrus (*Odobenus rosmarus divergens*) resource selection in the northern Bering Sea. *PLoS ONE* 9: e93035. doi:10.1371/journal.pone.0093035
- Jones, J.M., B.J. Thyre, E.H. Roth, M. Mahoney, I. Sia, K. Mercurief, C. Jackson, C. Zeller, M. Clare, A. Bacon, S. Weaver, Z. Gentes, R.J. Small, I. Stirling, S.M. Wiggins and J.A. Hildebrand. 2014. Ringed, bearded, and ribbon seal vocalizations north of Barrow, Alaska: Seasonal presence and relationship with sea ice. *Arctic* 67: 203-222.
- Jonsen, I.D., J.M. Flemming, and R.A. Myers. 2005. Robust state-space modeling of animal movement data. *Ecology* 86: 2874-2880.
- Kareiva P. and G. Odell. 1987. Swarms of predators exhibit ‘prey-taxis’ if individual predators use area-restricted search. *American Naturalist* 130: 233-270.

- Kastelein, R.A., P. Mosterd, B. Van Santen, M. Hagedoorn, and D. de Haan. 2002. Underwater audiogram of a Pacific walrus (*Odobenus rosmarus divergens*) measured with narrow-band frequency-modulated signals. *The Journal of the Acoustical Society of America* 112: 2173-2182.
- Kennedy, A.S., D.R. Salden, and P.J. Clapham. 2011. First high-to low-latitude match of an Eastern North Pacific right whale (*Eubalaena japonica*). *Marine Mammal Science*. doi: 10.1111/j.1748-7692.2011.00539.x.
- Kennedy, A.S., A.N. Zerbini, B.K. Rone, and P.J. Clapham. 2014. Individual variation in movements of satellite-tracked humpback whales in the eastern Aleutian Islands and Bering Sea. *Endangered Species Research* 23: 187-195.
- Koski, W.R. and G.W. Miller. 2009. Habitat use by different size classes of bowhead whales in the central Beaufort Sea during late summer and autumn. *Arctic* 62: 137-150.
- Kwok R., G.F. Cunningham, M. Wensnahan, I. Rigor, H.J. Zwally, and D. Yi. 2009. Thinning and volume loss of Arctic sea ice: 2003-2008. *Journal of Geophysical Research: Oceans* 114: C07005. doi: 10.1029/2009JC005312
- Kwok, R. and N. Untersteiner. 2011. The thinning of Arctic sea ice. *Physics Today* 64: 36-41.
- Laake, J. 1999. Distance sampling with independent observers: Reducing bias from heterogeneity by weakening the conditional independence assumption. In G.W. Garner, S.C. Amstrup, J.L. Laake, B.J.F. Manly, L.L. McDonald, and D.G. Robertson (eds.), *Marine mammal survey and assessment methods*, pp. 137-148. Rotterdam, Netherlands: A. A. Balkema.
- Laake, J.L., D.L. Borchers, L. Thomas, D. Miller, and J. Bishop. 2012. Mark-recapture distance sampling (MRDS). Version 2.1.0.
- Laidre, K.L., I. Stirling, L.F. Lowry, Ø. Wiig, M.P. Heide-Jørgensen, and S.H. Ferguson. 2008. Quantifying the sensitivity of Arctic marine mammals to climate-induced habitat change. *Ecological Applications* 18: S97-S125.
- Ljungblad, D.K. and S.E. Moore. 1983. Killer whales (*Orcinus orca*) chasing gray whales (*Eschrichtius robustus*) in the northern Bering Sea. *Arctic*: 361-364.
- Ljungblad, D.K., S.E. Moore, and D.R. Van Schoik. 1983. Aerial Surveys of Endangered Whales in the Beaufort, Eastern Chukchi, and Northern Bearing Seas, 1982. No. NOSC/TD-605. Naval Ocean Systems Center, San Diego, CA.
- Ljungblad, D.K., S.E. Moore, J.T. Clarke, and J.C. Bennett. 1986. Aerial surveys of endangered whales in the northern Bering, eastern Chukchi, and Alaskan Beaufort Seas, 1985: with a seven year review, 1979-85. Naval Ocean Systems Center, San Diego, Technical Report 1111, pp. 440. (NTIS PB87-115929/AS.)
- Ljungblad, D.K., S.E. Moore, J.T. Clarke, and J.C. Bennett. 1987. Distribution, Abundance, Behavior, and Bioacoustics of Endangered Whales in the Alaskan Beaufort and Eastern Chukchi Seas, 1979-86. No. NOSC/TR-1177. Naval Ocean Systems Center, San Diego, CA.

- Lowry, L. F. 1985. The ribbon seal (*Phoca fasciata*). in J. J. Burns, K. J. Frost, and L. F. Lowry (eds.), Marine Mammals Species Accounts, pp. 71-78. Alaska Department Fish and Game, Juneau, AK.
- Lowry, L.F. 1993. Foods and feeding ecology. In J.J. Burns, J.J. Montague, and C.J. Cowles, (eds.), The Bowhead Whale, pp. 201-238. Lawrence, Kansas: Allen Press.
- Lowry, L.F., K.J. Frost, and J.J. Burns. 1980. Feeding of bearded seals in the Bering and Chukchi Seas and trophic interaction with Pacific walruses. Arctic 33: 330-342.
- Lowry, L.F., and K.J. Frost. 1984. Foods and feeding of bowhead whales (*Balaena mysticetus*) in western and northern Alaska. Scientific Reports of the Whales Research Institute 35: 1-16.
- Lowry, L.F., G.A. Seaman, and K.J. Frost. 1985. Investigations of belukha whales in coastal waters of western and northern Alaska – I: Distribution, abundance, and movements. U.S. Department of Commerce, NOAA OCS Final report NA-81-RAC-00049, pp. 60.
- Lowry, L.F., G. Sheffield, and J.C. George. 2004. Bowhead whale feeding in the Alaskan Beaufort Sea, based on stomach contents analyses. Journal of Cetacean Research and Management 6: 215-223.
- MacIntyre, K.Q., K.M. Stafford, C.L. Berchok, and P.L. Boveng. 2013. Year-round acoustic detection of bearded seals (*Erignathus barbatus*) in the Beaufort Sea relative to changing environmental conditions, 2008–2010. Polar Biology 36: 1161-1173.
- Marques, T.A., L. Thomas, J. Ward, N. DiMarzio, and P.L. Tyack. 2009. Estimating cetacean population density using fixed passive acoustic sensors: an example with Blainville’s beaked whales. Journal of the Acoustical Society of America 125(4): 1982-1994.
- Marsh, H. and D.F. Sinclair. 1989. Correcting for visibility bias in strip transect aerial surveys of aquatic fauna. Journal of Wildlife Management 53: 1017-1024.
- Mayo, C.A. and M.K. Marx. 1990. Surface foraging behavior of the north Atlantic right whale, *Eubalaena glacialis*, and associated zooplankton characteristics. Canadian Journal of Zoology 68: 2214-2220.
- Mellinger, D.K. 2001. Ishmael 1.0 User’s Guide. NOAA Technical Memorandum OAR PMEL-120, available from NOAA/PMEL, 7600 Sand Point Way NE, Seattle, WA 98115, USA.
- Mendes, S., W. Turrell, T. Lu’tkebohle, and P. Thompson. 2002. Influence of the tidal cycle and a tidal intrusion front on the spatio-temporal distribution of coastal bottlenose dolphins. Marine Ecology Progress Series 239: 221–229.
- Merchant, N.D., T.R. Barton, P.M. Thompson, E. Pirotta, D.T. Dakin, and J. Dorocicz. 2013. Spectral probability density as a tool for ambient noise analysis. Journal of the Acoustical Society of America. 133: 262-267, DOI:10.1121/1.4794934
- Miller, E.H. 1975. Walrus ethology. I. The social role of tusks and applications of multidimensional scaling. Canadian Journal of Zoology 53: 590-613.
- Miller, E.H. 1976. Walrus ethology. II. Herd structure and activity budgets of summering males. Canadian Journal of Zoology 54: 704-715.

- Miksis-Olds, J.L. and S.E. Parks. 2011. Seasonal trends in acoustic detection of ribbon seal (*Histriophoca fasciata*) vocalizations in the Bering Sea. *Aquatic Mammals* 37(4): 464-471.
- Mizroch, S.A., D.W. Rice, and J.M. Breiwick. 1984. The fin whale, *Balaenoptera physalus*. *Marine Fisheries Review* 46: 20-24.
- Mizroch, S.A., D.W. Rice, D. Zwiefelhofer, J. Waite, and W.L. Perryman. 2009. Distribution and movements of fin whales in the North Pacific Ocean. *Mammal Review* 39: 193-227.
- Mocklin, J.A., D. J. Rugh, S.E. Moore, and R.P. Angliss. 2012. Using aerial photography to investigate evidence of feeding by bowhead whales. *Marine Mammal Science* 28: 602-619.
- Moore, S.E. and J.T. Clarke. 1992. Distribution, abundance and behavior of endangered whales in the Alaskan Chukchi and western Beaufort seas, 1991: with a review of 1982-91. Report of Science Applications International Corporation (SAIC), Maritime Services Division, for Minerals Management Service, Anchorage, Alaska.
- Moore, S.E. and R.R. Reeves. 1993. Distribution and movement. In J.J. Burns, J.J. Montague, and C.J. Cowles (eds.), *The Bowhead Whale*, pp. 313-386. Lawrence, Kansas: Allen Press.
- Moore, S.E., J.T. Clarke and M.M. Johnson. 1993. Beluga Distribution and movements offshore northern Alaska in spring and summer, 1980-1984. Report of the International Whaling Commission 43: 375-386.
- Moore, S.E. 2000. Variability of cetacean distribution and habitat selection in the Alaskan Arctic, Autumn 1982-91. *Arctic* 53: 448-460.
- Moore, S.E., D.P. DeMaster, and P.K. Dayton. 2000. Cetacean habitat selection in the Alaskan Arctic during summer and autumn. *Arctic* 53(4): 432-447.
- Moore, S.E. and J.T. Clarke. 2002. Potential impact of offshore human activities on gray whales (*Eschrichtius robustus*). *Journal of Cetacean Research and Management* 4: 19-25.
- Moore, S.E., J.M. Waite, N.A. Friday, and T. Honkalehto. 2002. Cetacean distribution and relative abundance on the central-eastern and southeastern Bering Sea shelf with reference to oceanographic domains. *Progress in Oceanography* 55: 249-261, [http://dx.doi.org/10.1016/S0079-6611\(02\)00082-4](http://dx.doi.org/10.1016/S0079-6611(02)00082-4).
- Moore, S.E. and K.L. Laidre. 2006. Trends in sea ice cover within habitats used by bowhead whales in the western Arctic. *Ecological Applications* 16: 932-944.
- Moore, S.E., K.M. Stafford, D.K. Mellinger, and J.A. Hildebrand. 2006. Listening for large whales in the offshore waters of Alaska. *Bioscience* 56: 49-55.
- Moore, S.E. and H.P. Huntington. 2008. Arctic marine mammals and climate change: impacts and resilience. *Ecological Applications* 18: S157-165.
- Moore, S.E., K.M. Stafford, H. Melling, C. Berchok, O. Wiig, K.M. Kovacs, C. Lydersen, and J. Richter-Menge. 2012. Comparing marine mammal acoustic habitats in Atlantic and Pacific sectors of the High Arctic: year-long records from Fram Strait and the Chukchi Plateau. *Polar Biology* 35: 475-480.

- Napp, J. M., L.S. Incze, P.B. Ortner, D.L.W. Siefert, and L. Britt. 1996. The plankton of Shelikof Strait, Alaska: Standing stock, production, mesoscale variability and their relevance to larval fish survival. *Fisheries Oceanography* 5: 19-38.
- Nerini, M. 1984. A review of gray whale feeding ecology. In M.L. Jones, S.L. Swartz, and S. Leatherwood (eds.), *The Gray Whale, Eschrichtius robustus*, pp. 423-450. Orlando, Florida: Academic Press Inc.
- Niebauer, H.J. and R.H. Day. 1989. Causes of interannual variability in the sea ice cover of the eastern Bering Sea. *GeoJournal* 18: 45-59.
- Okkonen, S.R., C.J. Ashjian, R.G. Campbell, J.T. Clarke, S.E. Moore, and K.D. Taylor. 2011. Satellite observations of circulation features associated with a bowhead whale feeding 'hotspot' near Barrow, Alaska. *Remote Sensing of Environment* 115: 2168-2174. doi: 10.1016/j.rse.2011.04.024
- Panova, E.M., R.A. Belikov, A.V. Agafonov, and V.M. Bel'Kovich. 2012. The relationship between the behavioral activity and the underwater vocalization of the beluga whale (*Delphinapterus leucas*). *Oceanology* 52(1): 79-87.
- Parkinson, C.L. and J.C. Comiso. 2013. On the 2012 record low Arctic sea ice cover: Combined impact of preconditioning and an August storm. *Geophysical Research Letters* 40(7): 1356-1361.
- Parks, S.E., P.K. Hamilton, S.D. Kraus, and P.L. Tyack. 2005. The gunshot sound produced by male North Atlantic right whales (*Eubalaena glacialis*) and its potential function in reproductive advertisement. *Marine Mammal Science* 21: 458-475.
- Parks, S., I. Urazghildiiev, and C.W. Clark. 2009. Variability in ambient noise levels and call parameters of North Atlantic right whales in three habitat areas. *Journal of the Acoustical Society of America* 125: 1230-1239.
- Perry, S.L., D.P. DeMaster, and G.K. Silber. 1999. The great whales: History and status of six species listed as endangered under the US Endangered Species Act of 1973. *Marine Fisheries Review* 61: 1-74.
- Petrich, C., H. Eicken, J. Zhang, J. Krieger, Y. Fukamachi, and K. I. Ohshima. 2012. Coastal landfast sea ice decay and breakup in northern Alaska: Key processes and seasonal prediction, *J. Geophys. Res.* 117 C02003 doi:10.1029/2011JC007339.
- Quakenbush, L.T., J.J. Citta, J.C. George, R.J. Small, and M.P. Heide- Jørgensen. 2010. Fall and winter movements of bowhead whales (*Balaena mysticetus*) in the Chukchi Sea and within a potential petroleum development area. *Arctic* 63: 289-307.
- Quakenbush, L.T., J.J. Citta, J.C. George et al. 2012. Seasonal movements of the Bering-Chukchi-Beaufort stock of bowhead whales: 2006-2011 satellite telemetry results. *International Whaling Commission Science Committee Report SC/64/BRG1*.
- Quakenbush, L.T., R.J. Small, and J.J. Citta. 2013. Satellite tracking of bowhead whales: Movements and analysis from 2006 to 2012. US Department of the Interior, Bureau of Ocean Energy Management, Alaska Outer Continental Shelf Region, Anchorage, Alaska. OCS Study BOEM 2013-01110, pp. 56.

- Quakenbush, L.T., R.S. Suydam, A.L. Bryan, L.F. Lowry, K.J. Frost, and B.A. Mahoney. 2015. Diet of Beluga Whales, *Delphinapterus leucas*, in Alaska from stomach contents, March–November. *Marine Fisheries Review* doi: dx.doi.org/10.7755/MFR.77.1.7.
- Questel, J.M., C. Clarke, and R.R. Hopcroft. 2013. Seasonal and interannual variation in the planktonic communities of the northeastern Chukchi Sea during the summer and early fall. *Continental Shelf Research* 67: 23-41.
- Rankin, S. and J. Barlow. 2005. Source of the North Pacific “boing” sound attributed to minke whales. *Journal of the Acoustical Society of America* 118: 3346-3351.
- Rasmussen, R.A. and N.E. Head. 1965. The quiet gray whale *Eschrichtius glaucus*. *Deep-Sea Research* 12: 869–877.
- Ray, C., W.A. Watkins, and J. Burns. 1969. The underwater song of *Erignathus* (Bearded seal). *Zoologica* 54: 79-83.
- R Development Core Team (2012) R: A language and environment for statistical computing. 2.11.0. R Foundation for Statistical Computing, Vienna.
- Reiser, C.M, D.W. Funk, R. Rodrigues, and D. Hannay (eds.). 2011. Marine mammal monitoring and mitigation during marine geophysical surveys by Shell Offshore, Inc. in the Alaskan Chukchi and Beaufort seas, July–October 2010: 90-day report. LGL Rep. P1171E–1. Rep. from LGL Alaska Research Associates Inc., Anchorage, AK, and JASCO Applied Sciences, Victoria, BC for Shell Offshore Inc, Houston, TX, Nat. Mar. Fish. Serv., Silver Spring, MD, and U.S. Fish and Wild. Serv., Anchorage, AK. 240 pp, plus appendices.
- Ressler, P.H., A. De Robertis, J.D. Warren, J.N. Smith, and S. Kotwicki. 2012. Developing an acoustic index of euphausiid abundance to understand trophic interactions in the Bering Sea ecosystem. *Deep-Sea Research II* 65-70: 184-195.
- Richard, P.R., M.P. Heide-Jorgensen, J.R. Orr, R. Dietz, and T.G. Smith. 2001. Summer and autumn movements and habitat use by belugas in the Canadian High Arctic and adjacent areas. *Arctic* 54: 207–222.
- Risch, D. R., C.W. Clark, P.J. Corkeron, A. Elepfandt, K.M Kovacs, C. Lydersen, I. Stirling, S.M Van Parijs. 2007. Vocalizations of male bearded seals, *Erignathus barbatus*: classification and geographical variation. *Animal Behaviour*. 73: 747-762.
- Roach, A.T., K. Aagaard, C.H. Pease, S.A. Salo, T. Weingartner, V. Pavlov, and M. Kulakov. 1995. Direct measurements of transport and water properties through the Bering Strait. *Journal of Geophysical Research* 100: 18443–18457. doi:10.1029/95JC01673
- Roth, E.H., J.A. Hildebrand, and S.M. Wiggins. 2012. Underwater ambient noise on the Chukchi Sea continental slope from 2006-2009. *Journal of the Acoustical Society of America* 131: 104-110. doi: 10.1121/1.3664096
- Rugh, D.J. and M.A. Fraker. 1981. Gray whale (*Eschrichtius robustus*) sightings in the eastern Beaufort Sea. *Arctic* 34: 186-187.
- Rugh, D.J., K.E.W. Shelden, and A. Schulman-Janiger. 2001. Timing of the gray whale southbound migration. *Journal of Cetacean Research and Management* 3: 31-39.

- Rugh, D.J., R.C. Hobbes, J.A. Lerczak, and J.M. Breiwick. 2005. Estimates of abundance of the eastern North Pacific stock of gray whales (*Eschrichtius robustus*) 1997-2002. *Journal of Cetacean Research and Management* 7: 1-12.
- Sameoto, D., N. Cochrane, and A. Herman. 1993. Convergence of acoustic, optical, and net-catch estimates of euphausiid abundance – use of artificial light to reduce net avoidance. *Canadian Journal of Fisheries and Aquatic Sciences* 50: 334-346.
- Schonberg, S.V., J.T. Clarke, and K.H. Dunton. 2014. Distribution, abundance, biomass and diversity of benthic infauna in the Northeast Chukchi Sea, Alaska: Relation to environmental variables and marine mammals. *Deep Sea Research II* 102: 144-163.
- Schusterman, R.J. and C. Reichmuth. 2008. Novel sound production through contingency learning in the Pacific walrus (*Odobenus rosmarus divergens*). *Animal cognition* 11: 319-327.
- Seaman, G.A., L.F. Lowry, and K.L. Frost. 1982. Foods of belukha whales (*Delphinapterus leucas*) in western Alaska. *Cetology* 44: 1-19.
- Seymour, J., Horstmann-Dehn, L., & Wooller, M. J. (2014). Interannual variability in the proportional contribution of higher trophic levels to the diet of Pacific walruses. *Polar biology*, 37(5), 597-609.
- Sheffield, G. and J.M. Grebmeier. 2009. Pacific walrus (*Odobenus rosmarus divergens*): Differential prey digestion and diet. *Marine Mammal Science* 25: 761-777.
- Shelden, K.E.W. and J.A. Mocklin, Editors. 2013. Bowhead Whale Feeding Ecology Study (BOWFEST) in the western Beaufort Sea. Final Report, OCS Study BOEM 2013-0114. National Marine Mammal Laboratory, Alaska Fisheries Science Center, NMFS, NOAA, 7600 Sand Point Way NE, Seattle, WA 98115-6349.
- Simpkins, M.A., L.M. Hiruki-Raring, G. Sheffield, J.M. Grebmeier, and J.L. Bengtson. 2003. Habitat selection by ice-associated pinnipeds near St. Lawrence Island, Alaska in March 2001. *Polar Biology* 26: 577-586.
- Sjare, B.L. and T.G. Smith. 1986. The vocal repertoire of white whales, *Delphinapterus leucas*, summering in Cunningham Inlet, Northwest Territories. *Can. J. Zool.* 64, 407-415
- Spaulding, E., M. Robbins, T. Calupca, C.W. Clark, C. Tremblay, A. Waack, A. Warde, J. Kemp, and K. Newhall. 2010. An autonomous, near-real-time buoy system for automatic detection of North Atlantic right whale calls. *Proceedings of Meetings on Acoustics* 6: 010001-01000122.
- Springer, A.M., C.P. McRoy, and K.R. Turco. 1989. The paradox of pelagic food webs in the northern Bering Sea – II. Zooplankton communities. *Continental Shelf Research* 9: 359–386.
- Stabeno, P.J., N. Kachel, C. Ladd, K. Martini, and C. Mordy. In prep. Currents and transport on the Chukchi Shelf: 2010 – 2014. To be submitted to *Continental Shelf Research*.
- Stafford, K.M., D.K. Mellinger, S.E. Moore, and C.G. Fox. 2007a. Seasonal variability and detection range modeling of baleen whale calls in the Gulf of Alaska, 1999–2002. *Journal of the Acoustical Society of America* 122: 3378–3390.

- Stafford, K.M., S.E. Moore, M. Spillane, and S. Wiggins. 2007b. Gray whale calls recorded near Barrow, Alaska, throughout the winter of 2003-04. *Arctic* 60: 167-172.
- Stafford, K.M., S.R. Okkonen, and J.T. Clarke. 2013. Correlation of a strong Alaska Coastal Current with the presence of beluga whales *Delphinapterus leucas* near Barrow, Alaska. *Marine Ecology Progress Series* 474: 287-297. doi: 10.3354/meps10076
- Stanton, T.K., P.H. Wiebe, D. Chu, M.C. Benfield, L. Scanlon, L. Martin, and R.L. Eastwood. 1994. On acoustic estimates of zooplankton biomass. *ICES Journal of Marine Science*: 51: 505-512.
- Stirling, I., W. Calvert, and C. Spencer. 1987. Evidence of stereotyped underwater vocalizations of male Atlantic walruses (*Obodenus rosmarus rosmarus*). *Canadian Journal of Zoology* 65: 2311-2321.
- Stirling, I. 1997. The importance of polynyas, ice edges, and leads to marine mammals and birds. *Journal of Marine Systems* 10: 9-21.
- Suydam, R.S., L.F. Lowry, K.J. Frost, G.M. O’Corry-Crowe, and D. Pikkok, Jr. 2001. Satellite tracking of eastern Chukchi Sea beluga whales into the Arctic Ocean. *Arctic* 54: 237-243.
- Suydam, R.S. 2009. Age, growth, reproduction, and movements of beluga whales (*Delphinapterus leucas*) from the eastern Chukchi Sea. Dissertation, University of Washington.
- Swartz, S.L., B.L. Taylor, and D.J. Rugh. 2006. Gray whale *Eschrichtius robustus* population and stock identity. *Mammal Review* 36: 66-84.
- Tikhomirov, E.A. 1961. Distribution and migration of seals in waters of the far east. Pages 199-210 in Conference on Pelagic Mammals, 1959. Ichthyological Commission of the Academy of Sciences of the USSR, Moscow, Russia. (Translated from Russian by L.V. Sagen, U.S. Fish and Wildlife Service, Marine Mammal Biological Laboratory, Seattle, WA, 26 p.)
- Torrence, C. and G.P. Compo. 1998. A practical guide to wavelet analysis. *Bulletin of the American Meteorological Society* 79: 61-78.
- Udevitz, M.S., R.L. Taylor, J.L. Garlich-Miller, L.T. Quakenbush, and J.A. Snyder. 2013. Potential population-level effects of increased haul-out-related mortality of Pacific walrus calves. *Polar biology* 36: 291-298.
- Urick, R.J. 1983. *Principles of Underwater Sound*, 3rd edition. New York, NY: McGraw Hill.
- Van Opzeeland, I., L. Kindermann, O. Boebel, and S. Van Parijs. 2008. Insights into the acoustic behaviour of polar pinnipeds—current knowledge and emerging techniques of study. In E.A. Weber and L.H. Krause (eds.), *Animal Behavior: New Research*, pp. 133-161. Hauppauge, New York: Nova Science Publishers, Inc.
- Van Parijs, S.M., K.M. Kovacs, and C. Lydersen. 2001. Spatial and temporal distribution of vocalizing male bearded seals: Implications for male mating strategies. *Behaviour* 138: 905-922.

- Wallace, M.I., F.R. Cottier, J. Berge, G.A. Tarling, C. Griffiths, and A.S. Brierley. 2010. Comparison of zooplankton vertical migration in an ice-free and a seasonally ice-covered Arctic fjord: An insight into the influence of sea ice cover on zooplankton behaviour. *Limnology and Oceanography* 55: 831-845.
- Walsh, J.E. 2008. Climate of the Arctic marine environment. *Ecological Applications* 18: S3-S22.
- Wang, M. and J.E. Overland. 2009. An ice free summer Arctic within 30 years? *Geophysical Research Letters* 36: L07502. doi: 10.1029/2009GL037820
- Wang, M. and J.E. Overland. 2012. A sea ice free summer Arctic within 30 years—an update from CMIP5 models. *Geophysical Research Letters* 39: L18501. doi: 10.1029/2012GL052868
- Wang, M. and J.E. Overland. 2015. Projected future duration of the sea-ice-free season in the Alaskan Arctic. *Progress in Oceanography* 136: 50-59. doi:10.1016/j.pocean.2015.01.001.
- Watkins, W.A. and G.C. Ray. 1977. Underwater sounds from ribbon seal, *Phoca (Histriophoca) fasciata*. *Fishery Bulletin* 75: 450-453.
- Watkins, W.A., M.A. Daher, G.M. Reppucci, J.E. George, D.L. Martin, N.A. DiMarzio, and D.P. Gannon. 2000. Seasonality and distribution of whale calls in the North Pacific. *Oceanography* 13: 62–67.
- Weingartner, T., E. Dobbins, S. Danielson, W. Winsor, R. Potter, and H. Statscewich. 2013. Hydrographic variability over the northeastern Chukchi Sea shelf in summer-fall 2008-2010. *Continental Shelf Research* 67: 5-22.
- Wenz, G.M. 1962. Acoustic ambient noise in the ocean: spectra and sources. *Journal of the Acoustical Society of America* 334: 1936-1956.
- Williams, R., C.W. Clark, D. Ponirakis, and E. Ashe. 2014. Acoustic quality of critical habitats for three threatened whale populations. *Animal Conservation* 17: 174-185. doi: 10.1111/acv.12076
- Winn, H.E. and P.J. Perkins. 1976. Distribution and sounds of the minke whale, with a review of mysticete sounds. *Cetology* 19: 1-12.
- Wood, S.N. 2006. *Generalized additive models: An introduction with R*. Chapman and Hall, Boca Raton, Florida.
- Wood, K.R., J.E. Overland, S.A. Salo, N.A. Bond, W.J. Williams, and X. Dong. 2013. Is there a “new normal” climate in the Beaufort Sea? *Polar Research* 32: 19552, doi: <http://dx.doi.org/10.3402/polar.v32i0.19552>.
- Wood, K.R., N.A. Bond, S.L. Danielson, J.E. Overland, S.A. Salo, P.J. Stabeno and J. Whitefield. 2015. A decade of environmental change in the Pacific Arctic region. *Progress in Oceanography* 36: 12-31.
- Woodgate, R.A., K. Aagaard, and T.J. Weingartner. 2005. Monthly temperature, salinity, and transport variability of the Bering Strait through flow. *Geophysical Research Letters* 32: L04601. doi: 10.1029/2004GL021880

- Würsig, B. E. M. Dorsey, W. J. Richardson, and R. S. Wells. 1989. Feeding, aerial and play behavior of bowhead whales, *Balaena mysticetus*, summering in the Beaufort Sea. *Aquatic Mammals* 15:27-27.
- Würsig, B. and C.W. Clark. 1993. Behavior. In J.J. Burns, J.J. Montague, and C.J. Cowles (eds.), *The Bowhead Whale*, pp. 157-200. Lawrence, Kansas: Allen Press.
- Xie, Y. and D.M. Farmer. 1992. The sound of ice break-up and floe interaction. *Journal of the Acoustical Society of America* 91: 1423-1428.
- Zerbini, A.N., J.M. Waite, J.L. Laake, and P.R. Wade. 2006. Abundance, trends and distribution of baleen whales off western Alaska and the central Aleutian Islands. *Deep Sea Research* I 53: 1772-1790.

XVI. ACKNOWLEDGEMENTS

This project would not have been possible without the help of a great number of people. First and foremost, we thank Heather Crowley (BOEM) for her endless support. Chuck Monnett was instrumental in starting the CHAOZ project. The authors would also like to acknowledge the following people:

North Slope residents

Craig George, Robert Suydam, and Lesley Pierce (North Slope Borough) for helping us develop and distribute our cruise information flyers; Sheyna Wisdom (Fairweather Science, LLC) for providing information on contacting the village communication centers during the field surveys; the villages of Barrow, Point Hope, Point Lay, Wainwright, Kivalina, Kotzebue; Gay Sheffield (UAF); and the whaling captains.

Vessel captains and crew

Captain Atle Remme, F/V *Alaskan Enterprise*; Captain Fred Roman, F/V *Mystery Bay*; and Captain Kale Garcia, R/V *Aquila*, as well as all crew members.

Sonobuoys

Theresa Yost (Naval Operational Logistics Support Center); Jeffrey Leonhard, Todd Mequet, and Edward Rainey (Naval Surface Warfare Center, Crane Division); and Robin Fitch (I&E Director Marine Science, Office of the Assistant Secretary of the Navy) for providing the sonobuoys used during the field surveys, and Don Ljungblad for teaching us about sonobuoy modifications.

At sea science crew

William Floering, Sigrid Salo, Adam Spear, Sam Denes, Dan Naber, Stephanie Grassia, Amy S. Kennedy, Dana Wright, Laura Morse, Andy Bankert, Jason Michalec, Jessica Thompson, Misty E. Niemeyer, Lisa DeForest, Heather Riley, Elizabeth Küsel, Colleen Harpold, Chris Tessaglia-Hymes, Robert Ambrose, Steve Porter, John Kemp

Analysts/technicians

Ellen Garland for her assistance with the GAMs, Eliza Ives for incorporating the LFDCS on our dataset and for assistance with this report, Charles Greenlaw for his guidance and expertise, Benjamin Bloss and David Strausz for helping construct, tune, and calibrate the TAPS6-NG, Stephanie Grassia, Alexandra Ulmke, and Dawn Grebner for their acoustic analysis, Sigrid Salo, Nancy Kachel, Alexandre N. Zerbini, Amy S. Kennedy, Janice M. Waite

XVII. LIST OF PUBLICATIONS AND PRESENTATIONS

Publications

- Cheng, W., E. Curchitser, C. Ladd, P. Stabeno, and M. Wang. 2014. Ice-Ocean Interactions in the Eastern Bering Sea: NCAR CESM Simulations and Comparison with Observations. Deep Sea Research II. doi: 10.1016/j.dsr2.2014.03.002.
- Clark, C.W., C.L. Berchok, S. Blackwell, J. Citta, D. Hannay, J. Jones, L. Quakenbush, and K.M. Stafford. 2015-accepted. A year in the acoustic world of Western Arctic bowhead whales. Progress in Oceanography.
- Crance, J.L., C.L. Berchok, J. Bonnel, and A.M. Thode. 2015. Northeastern-most record of a north Pacific fin whale (*Balaenoptera physalus*) in the Alaskan Chukchi Sea. Polar Biology, doi: 10.1007/s00300-015-1719-7.
- Garland, E.G., C.L. Berchok, and M. Castellote. 2015. Temporal peaks in beluga whale (*Delphinapterus leucas*) acoustic detections in the northern Bering, northeastern Chukchi, and western Beaufort Seas: 2010-2011. Polar Biology, doi: 10.1007/s00300-014-1636-1.
- Garland, E.C., M. Castellote, and C.L. Berchok. 2015. Beluga whale (*Delphinapterus leucas*) vocalizations and call classification from the eastern Beaufort Sea population. Journal of the Acoustical Society of America, 137: 3054-3067, doi: 10.1121/1.4919338. .
- Overland, J.E. and M. Wang. 2013. When will the summer Arctic be nearly sea ice free? Geophysical Research Letters 40, DOI: 10.1002/grl.50316.
- Overland, J.E., M. Wang, J. Walsh, and J.C. Stroeve. 2014. Future Arctic climate changes: Adaptation and mitigation timescales. Published online, Earth's Future. doi: 10.1002/2013EF000162.
- Wang, M. and J.E. Overland. 2012. A sea ice free summer Arctic within 30 years-an update from CMIP5 models. Geophysical Research Letters 39, DOI: 10.1029/2012GL052868.
- Wang, M., J.E. Overland, and P.J. Stabeno. 2012. Future climate of the Bering and Chukchi Seas projected by global climate models. Deep-Sea Research II, 65-70: 46-57.
- Wang, M. and J.E. Overland. 2015. Projected future duration of the sea-ice-free season in the Alaskan Arctic. Progress in Oceanography. doi:10.1016/j.pocean.2015.01.001

Oral Presentations

- Berchok, C.L., J. Crance, B. Rone. 2010. North Pacific Right Whale Survey Acoustics. 26 May 2010. Sonobuoy conference at the Naval Air Station, Whidbey Island, Oak Harbor, WA.
- Berchok, C.L. and J. Crance. 2015. Chukchi Sea whale ecology. 28 May 2015. Sonobuoy conference at the Naval Air Station, Whidbey Island, Oak Harbor, WA.
- Clark, C.W., Berchok, C.L., Blackwell, S.B., Hannay, D.E., Jones, J., Ponirakis, D., and Stafford, K.M. 2015. A year in the acoustic world of Western Arctic bowhead whales. Oral presentation at the Alaska Marine Science Symposium, 21-25 January 2013. Anchorage, AK.
- Delarue, J., D.K. Mellinger, K.M. Stafford, and C.L. Berchok. 2010. Where do the Chukchi Sea fin whales come from? Looking for answers in the structure of songs recorded in the Bering Sea and Western N. Pacific. Oral presentation at the 159th meeting of the Acoustical Society of America, 19-23 April 2010. Baltimore, MD.

- Garland, E.C., C.L. Berchok, and M. Castellote. 2012. Acoustic monitoring of belugas (*Delphinapterus leucas*) in the eastern Chukchi Sea. Oral presentation at the 164th Meeting of the Acoustical Society of America, 22-26 October 2012. Kansas City, MO.
- Guerra, M., A.N. Rice, and C.W. Clark. 2013. Acoustic environment as context to understand patterns in Arctic marine biodiversity. Invited talk at the Zoological Society of London. 17 May 2013.
- MacIntyre, K. 2013. Acoustic detection of bearded seals (*Erignathus barbatus*) in the Bering, Chukchi, and Beaufort Seas 2008-2011. Oral presentation at the Alaska Marine Science Symposium, 21-25 January 2013. Anchorage, AK.
- Moore, S., K. Kuletz, and J. Murphy. 2011. Fish, seabird, and marine mammal observations during the 2010-2011 Pilot DBO. Distributed Biological Observatory (DBO) workshop and Pacific Arctic Group (PAG) meeting, 15-16 November 2011. Sidney, BC.
- Moore, S.E. 2012. Science Lecture aboard the USCGC HEALY entitled "Marine Mammals in the 'New Normal' Pacific Arctic", where sampling protocols and mammal distributions from the CHAOZ cruises were highlighted. August 15, 2012.
- Napp, J.M., C.L. Berchok, P.J. Stabeno, and S.E. Moore. 2013. An integrated ocean observing approach to understanding the effects of climate variability in the NE Chukchi Sea. Oral presentation at the Alaska Marine Science Symposium, 21-25 January 2013. Anchorage, AK.
- Napp, J.M. and P.J. Stabeno. 2012. CHAOZ in the Arctic: Go North Young Scientist! EcoFOCI Seminar, 10 April 2012. Seattle, WA.
- Napp, J.M., C.L. Berchok, P.J. Stabeno, and S.E. Moore. 2013. Steps toward an integrated ocean observing approach to understanding the effects of climate variability in the NE Chukchi Sea. Oral presentation by Moore at the 28th Lowell Wakefield Symposium, 26-29 March 2013. Anchorage, AK.
- Overland, J.E. 2010. Hot Arctic-Cold Continents: Climate Impacts of the Newly Open Polar Sea. Rapid changes in Arctic sea ice: Assessing drivers and future trajectories workshop, 6-8 October 2010. Fairbanks, AK.
- Stabeno, P.J., N.B. Kachel, C. Ladd, and J.M. Napp. 2014. The CHAOZ project: Influence of climate variability on the northeastern Chukchi ecosystem. Oral presentation at the American Geophysical Union Ocean Sciences Meeting, February 26, 2014. Honolulu, HI.
- Stabeno, P.J., C.L. Berchok, S.E. Moore, C. Mordy, J.M. Napp, and S. Salo. 2012. Chukchi Acoustics, Oceanography, and Zooplankton (CHAOZ): Observations on the Chukchi Sea. Oral presentation at the Alaska Marine Science Symposium, 16-20 January 2012. Anchorage, AK.
- Stabeno, P.J. and J.E. Overland. 2012. The New Normal in U. S. Arctic. Presented to the NOAA Senior Res. Council. July 19, 2012. Seattle, WA.
- Stabeno, P.J. and J.M. Napp. 2012. Observations in the Chukchi Sea. Oral presentation for Pacific Marine Environmental Laboratory (PMEL) seminar series, April 10, 2012.
- Wang, M. 2010. Melting pond in the Arctic Sea ice: How much can we learn from the NPEO? Rapid changes in Arctic sea ice: Assessing drivers and future trajectories workshop, 6-8 October 2010. Fairbanks, AK.
- Wang, M. 2013. A sea ice free summer Arctic within 30 years: An update from CMIP5 models. Oral presentation at the Alaska Marine Science Symposium, 21-25 January 2013. Anchorage, AK.

Poster Presentations

- Berchok, C.L., S. Moore, J. Napp, J. Overland, and P. Stabeno. 2011. Bringing CHAOZ to the Arctic. Poster presentation at the Alaska Marine Science Symposium, 17-21 January 2011. Anchorage, AK.
- Crance, J.L., C.L. Berchok, A. Kennedy, B. Rone, E. Küsel, J. Thompson, and P.J. Clapham. 2011. Visual and acoustic survey results during the 2010 CHAOZ cruise. Poster presentation at the Alaska Marine Science Symposium, 17-21 January 2011. Anchorage, AK.
- Crance, J.L., C.L. Berchok, B. Rone, A. Kennedy, E. Küsel, L. Morse, J. Thompson, and P.J. Clapham. 2011. Short-term trends in the summer distribution of cetaceans in the Chukchi Sea. Poster presentation at the 19th Biennial Conference on the Biology of Marine Mammals, Nov 28 – Dec 2, 2011. Tampa, FL.
- Crance, J.L., C.L. Berchok, B. Rone, A. Kennedy, E. Küsel, L. Morse, J. Thompson, and P.J. Clapham. 2012. Short-term trends in the summer distribution of Cetaceans in the Chukchi Sea. Poster presentation at the Alaska Marine Science Symposium, 16-20 January 2012. Anchorage, AK.
- Garland, E.C., C.L. Berchok, and M. Castellote. 2013. Spatio-temporal distribution of Alaskan beluga (*Delphinapterus leucas*) populations based on acoustic monitoring. Poster presentation at the Alaska Marine Science Symposium, 21-25 January 2013. Anchorage, AK.
- Garland, E.G., C.L. Berchok, and M. Castellote. 2014. Spatio-temporal movement patterns of Alaskan beluga whale (*Delphinapterus leucas*) populations based on vocal peaks from passive acoustic monitoring. Poster presentation at the Alaska Marine Science Symposium, January 20-24, 2014. Anchorage, AK.
- Grassia, S.L., C.L. Berchok, Crance, J.L., B.K. Rone, A. Kennedy, and P.J. Clapham. 2013. Short- and long-term distribution of marine mammals in the Chukchi Sea. Poster presentation at the Alaska Marine Science Symposium, 21-25 January 2013. Anchorage, AK.
- Guerra, M. A.N. Rice, D.W. Ponirakis, and C.W. Clark. 2013. Characterization of the interannual ambient noise baseline off Icy Cape, Alaska, and its primary sources (2010-2012). Poster presentation at the Alaska Marine Science Symposium, 21-25 January 2013. Anchorage, AK.
- Napp, J. and P. Stabeno. 2011. Summer 2010 hydrography and zooplankton on the Chukchi Sea shelf (the CHAOZ project). Poster presentation at the Alaska Marine Science Symposium, 17-21 January 2011. Anchorage, AK.
- Napp, J.M., A.H. Spear, and P.J. Stabeno. 2012. Acoustic detection of zooplankton in the Chukchi Sea. Poster presentation at the Alaska Marine Science Symposium, 16-20 January 2012. Anchorage, AK.
- Wang, M., J.E. Overland, and P. Stabeno. 2011. Future status of the Chukchi Sea seen from global climate models. Poster presentation at the Alaska Marine Science Symposium, 17-21 January 2011. Anchorage, AK.
- Wang, M., W. Cheng, J.E. Overland, and P.J. Stabeno. 2012. Chukchi Sea climate variability seen from CESM. Poster presentation for Community Earth System Model (CESM) annual workshop. Breckenridge, CO, June 18-21, 2012.

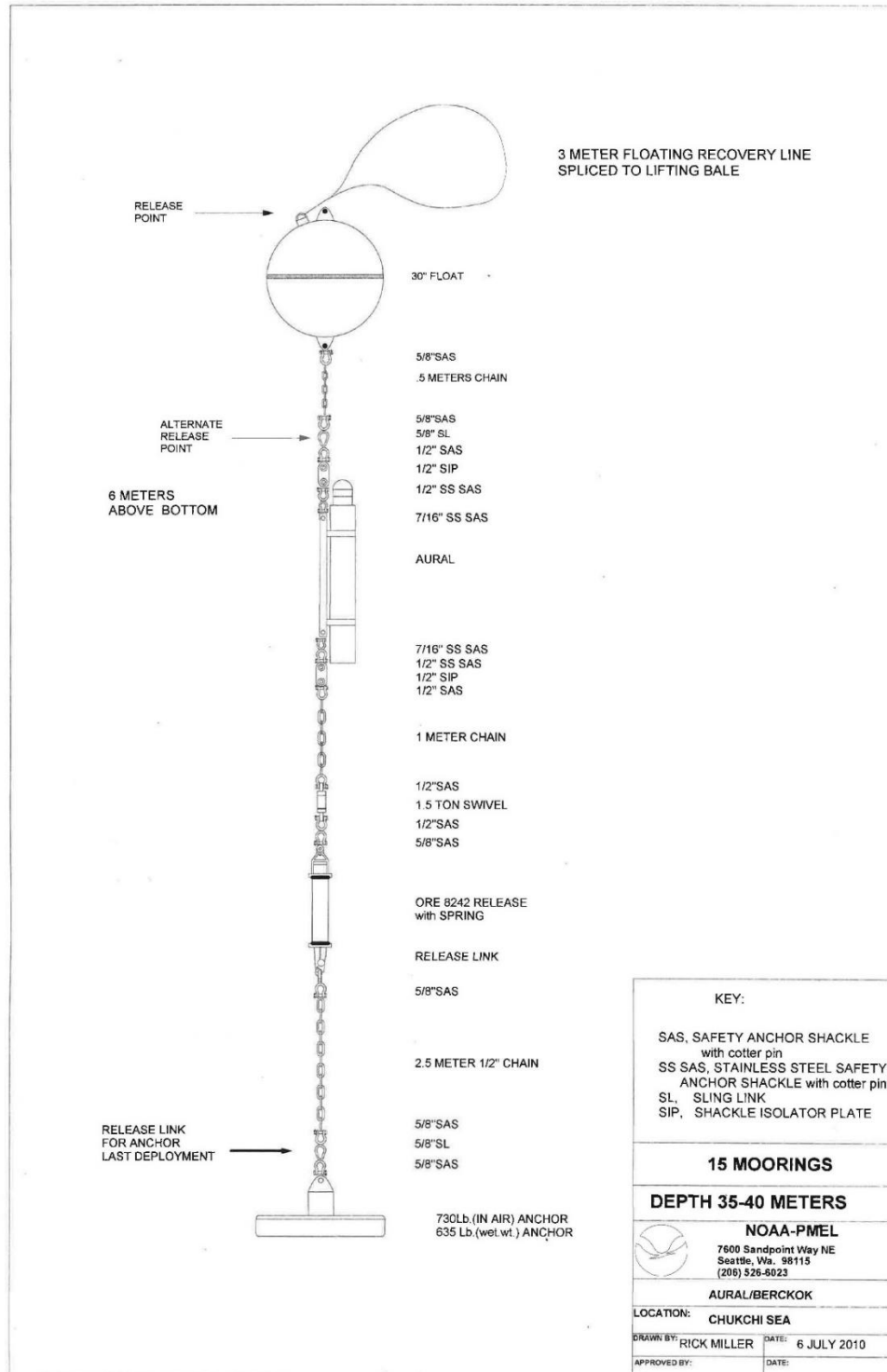
Wang, M. and J.E. Overland. 2014. Projected future duration of the sea-ice-free season in the Alaskan Arctic. Poster presentation at the Alaska Marine Science Symposium, January 20-24, 2014. Anchorage, AK.

XVIII. APPENDICES

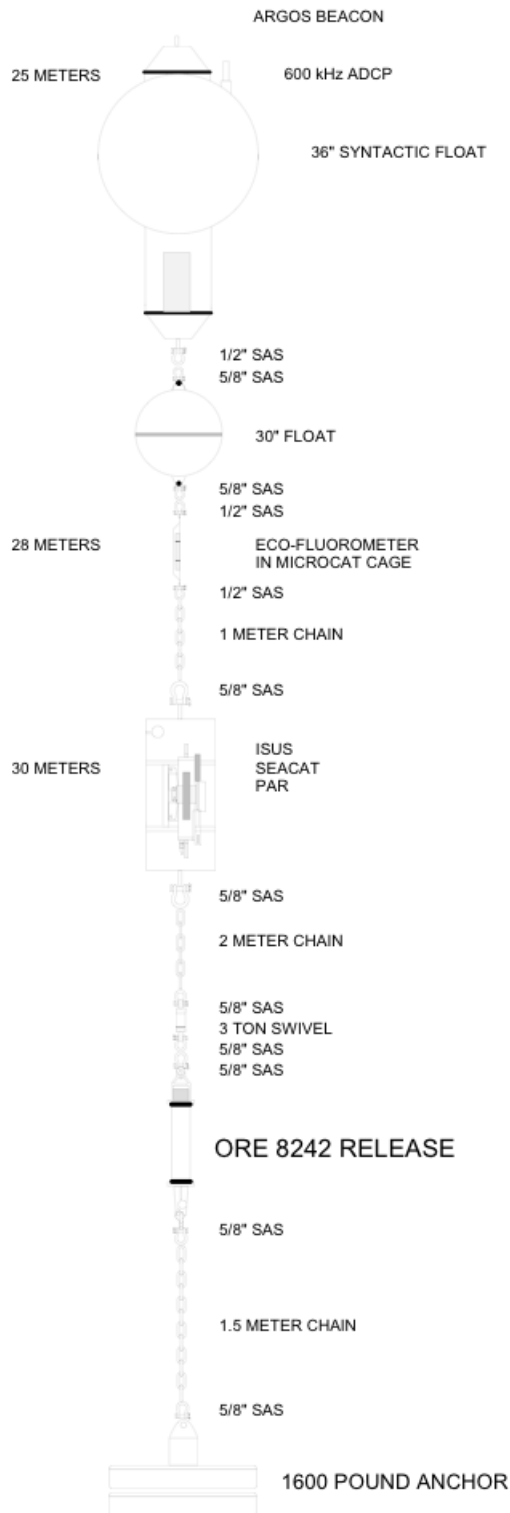
A. *Field survey summary table*

Year	Start date	End date	Start port location	End port location	Vessel	Captain	Chief Scientist
2010	8/24/2010	9/20/2010	Nome, AK	Dutch Harbor, AK	<i>F/V Alaskan Enterprise</i>	Atle Remme	Dr. Catherine Berchok
2011	8/12/2011	9/11/2011	Dutch Harbor, AK	Dutch Harbor, AK	<i>F/V Mystery Bay</i>	Fred Roman	Dr. Catherine Berchok
2012	8/8/2012	9/7/2012	Dutch Harbor, AK	Dutch Harbor, AK	<i>R/V Aquila</i>	Kale Garcia	Dr. Catherine Berchok

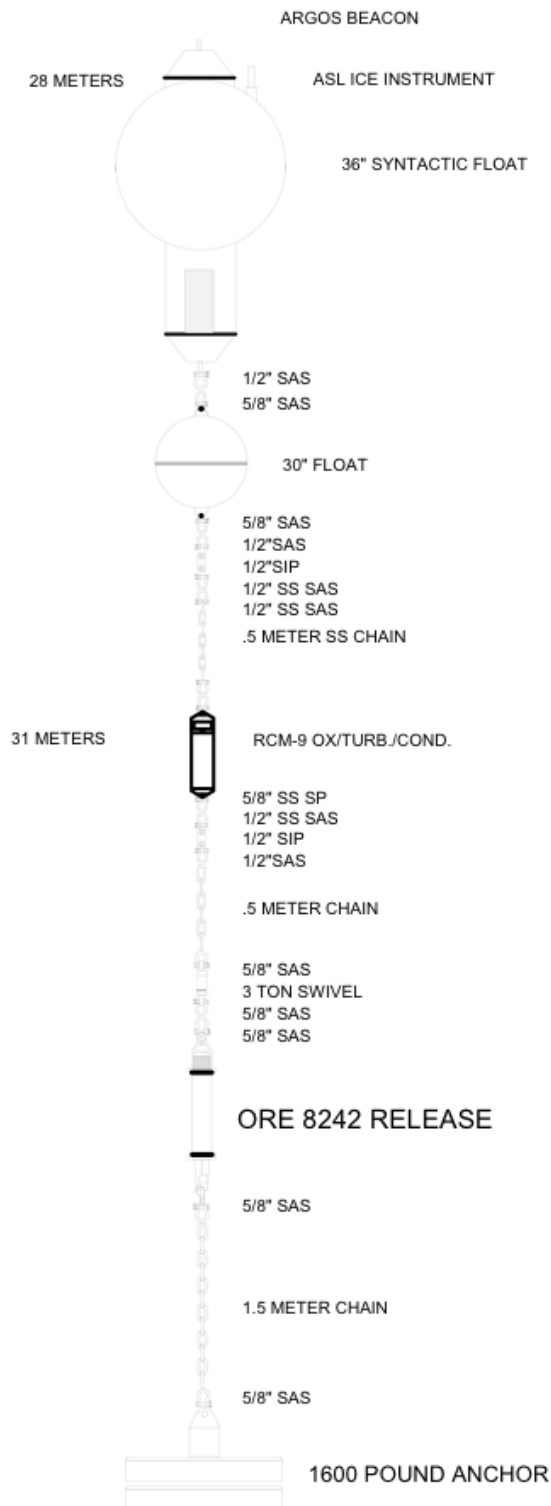
B. Mooring diagrams.



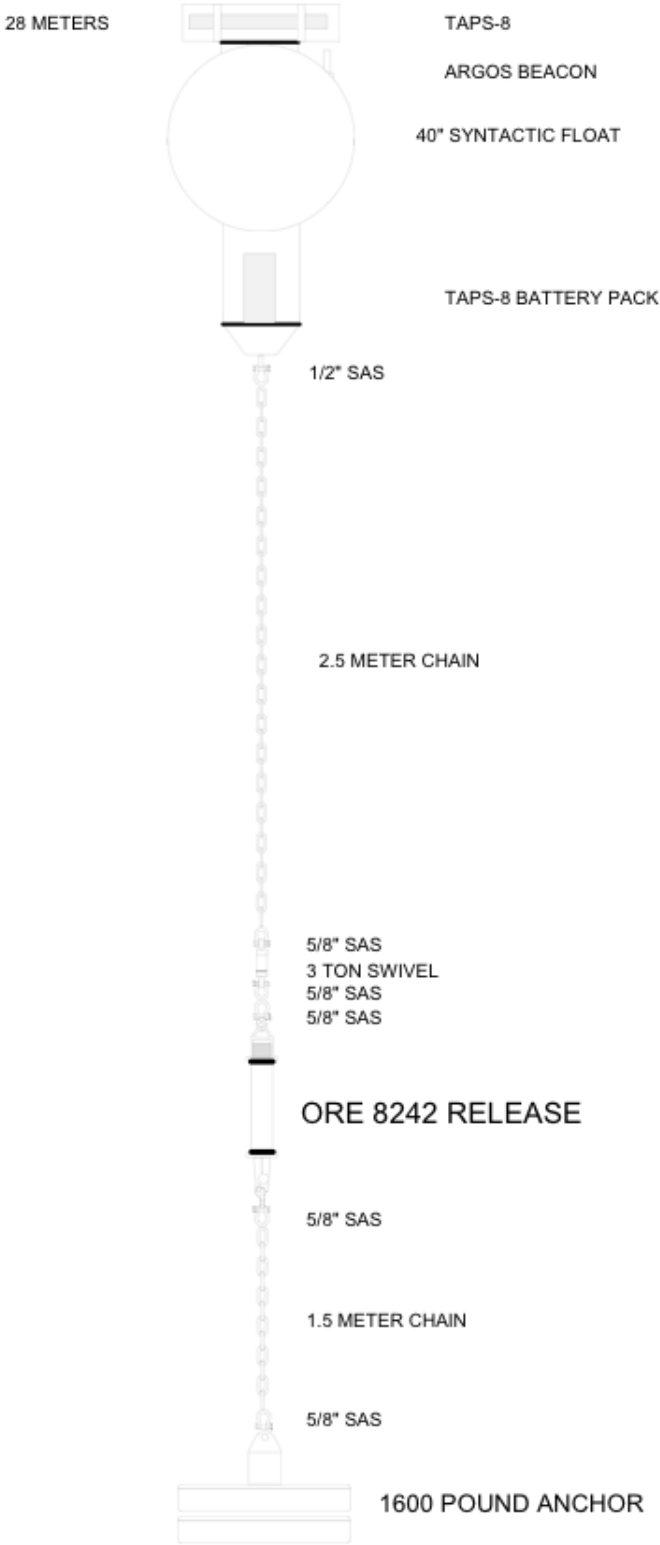
APPENDIX B. 1. MOORING DIAGRAM FOR PASSIVE ACOUSTIC RECORDERS.



APPENDIX B. 2. MOORING DESIGN FOR CKP1A, CKP2A, AND CKP3A. IN ADDITION TO THE 600 KHZ ADCP (CURRENTS), THIS MOORING CONTAINS INSTRUMENTS TO MEASURE NITRATE (ISUS), TEMPERATURE AND SALINITY (SEACAT), FLUORESCENCE (ECOFLUOROMETER) AND PHOTOSYNTHETICALLY ACTIVE RADIATION (PAR).



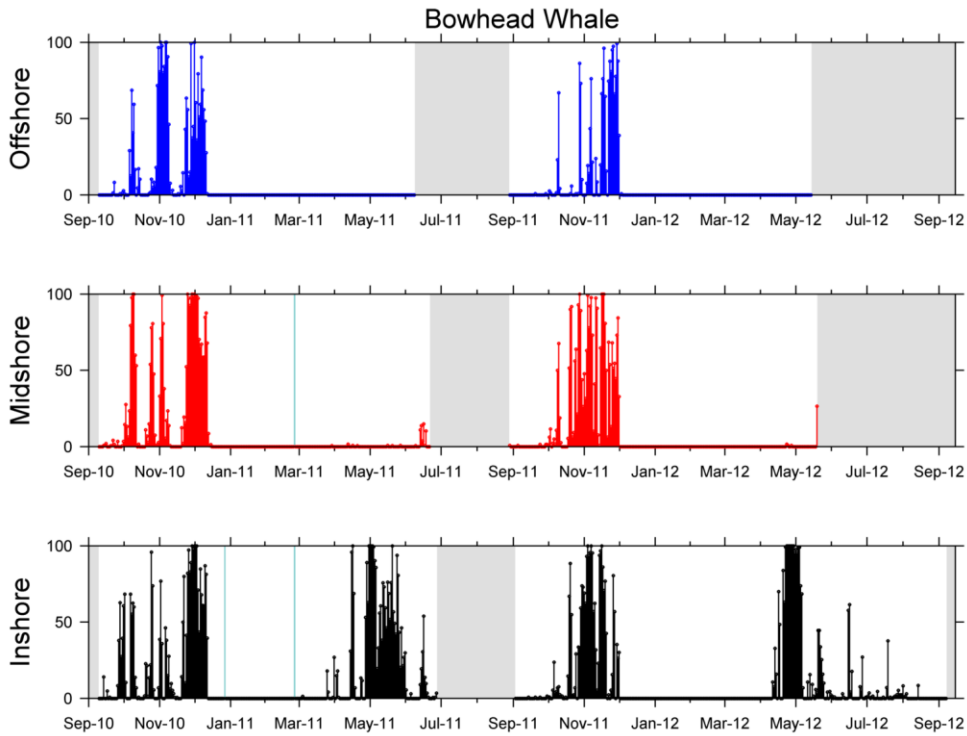
APPENDIX B. 3. MOORING DESIGN FOR CKIP1A, CKIP2A AND CKIP3A. IN ADDITION TO THE ASL ICE INSTRUMENT (MEASURES ICE THICKNESS), THIS MOORING CONTAINS RCM9 THAT MEASURES CURRENTS AT ONE DEPTH, TEMPERATURE, OXYGEN, AND TURBIDITY.



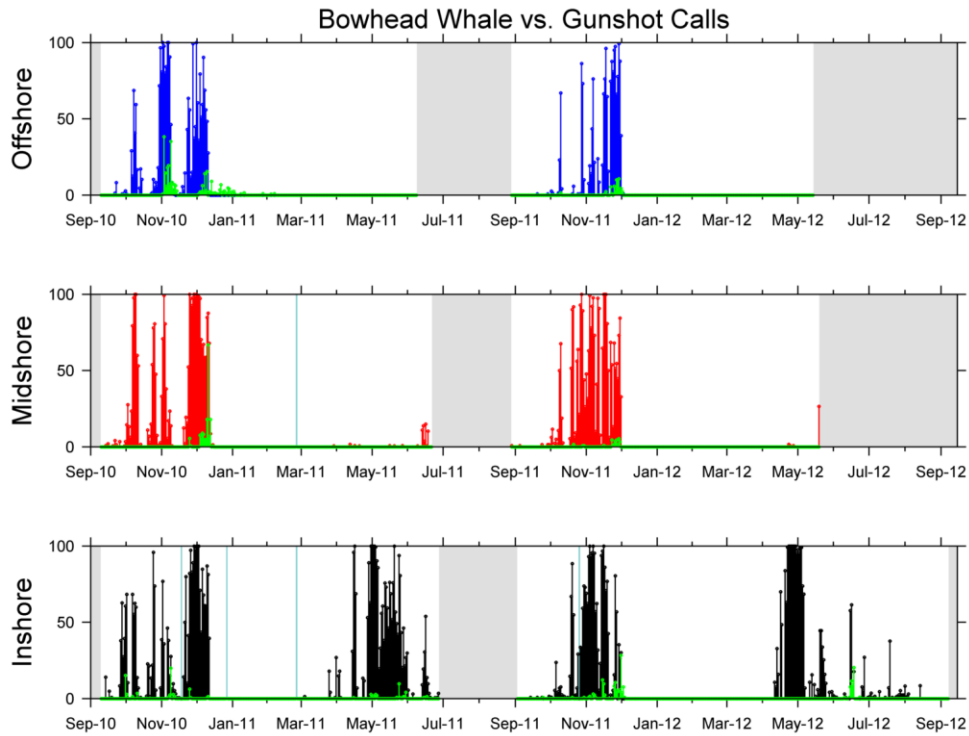
APPENDIX B. 4. MOORING DESIGN FOR CKT. THE TAPS-8 IS AN INSTRUMENT THAT ACOUSTICALLY MEASURES ZOOPLANKTON BIO-VOLUME.

C. Long-term passive acoustic data by species

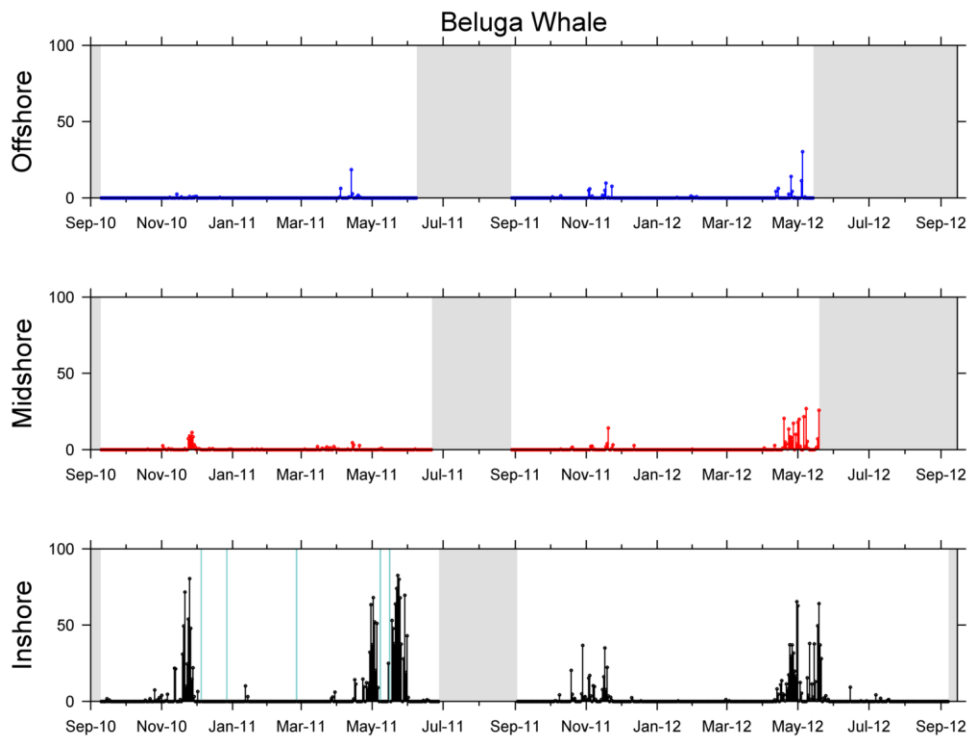
Data are presented as the percentage of time intervals with calls) for inshore (lower panel), midshore (middle panel), and offshore (upper panel) locations 2010-2012. Dark gray shading indicates no data and teal shading indicates days where detections were masked by noise.



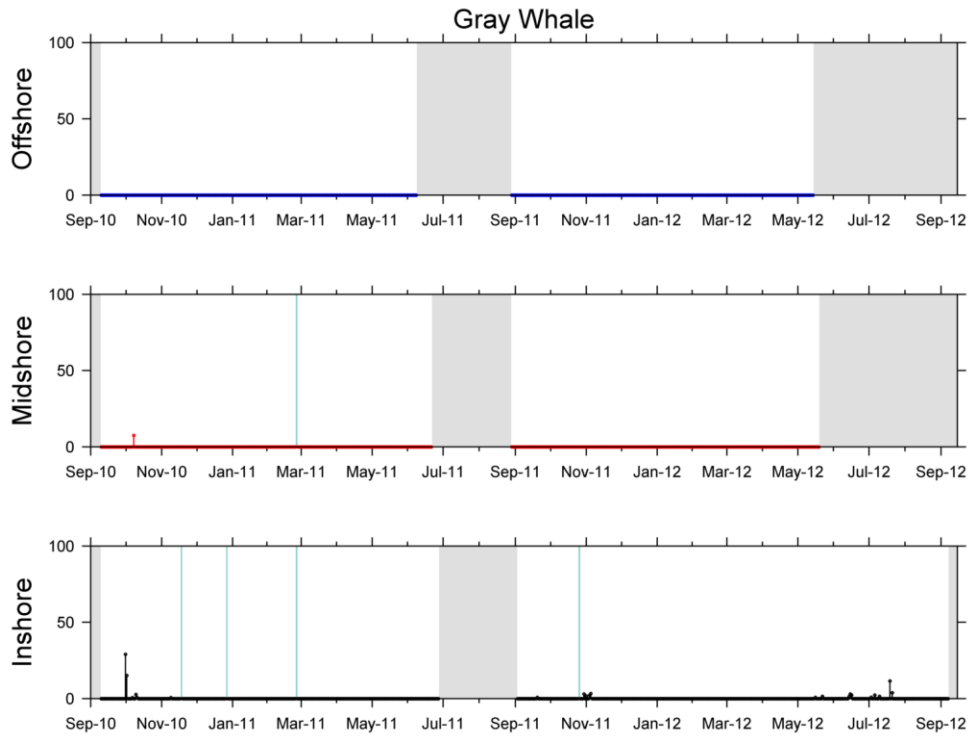
APPENDIX C. 1. BOWHEAD WHALE ACOUSTIC DETECTIONS.



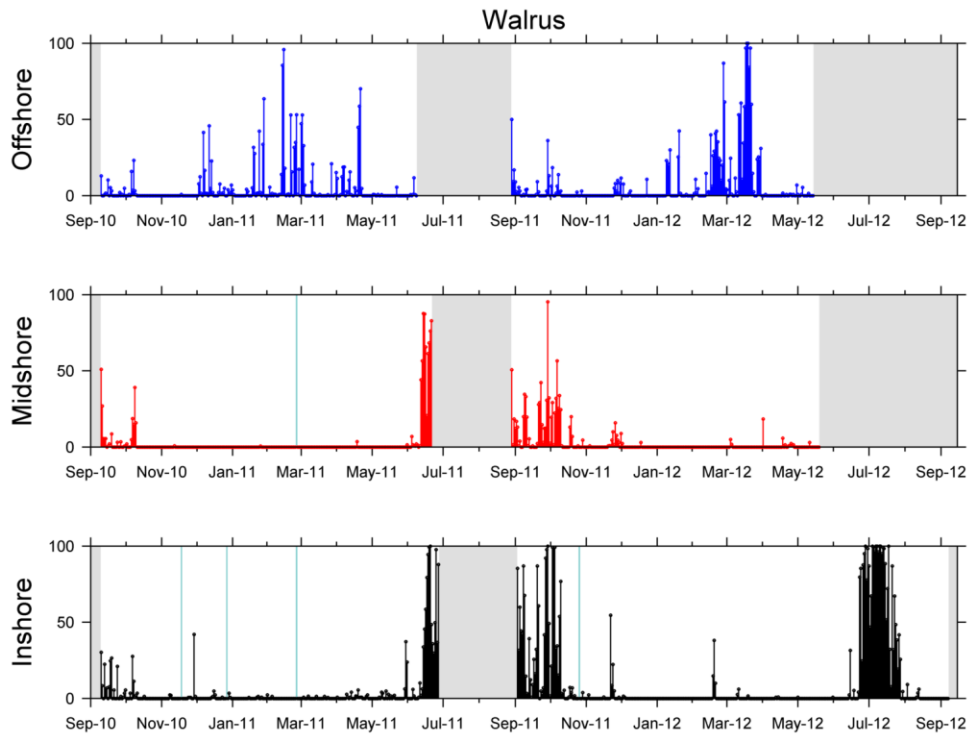
APPENDIX C. 2. GUNSHOT CALL ACOUSTIC DETECTIONS.



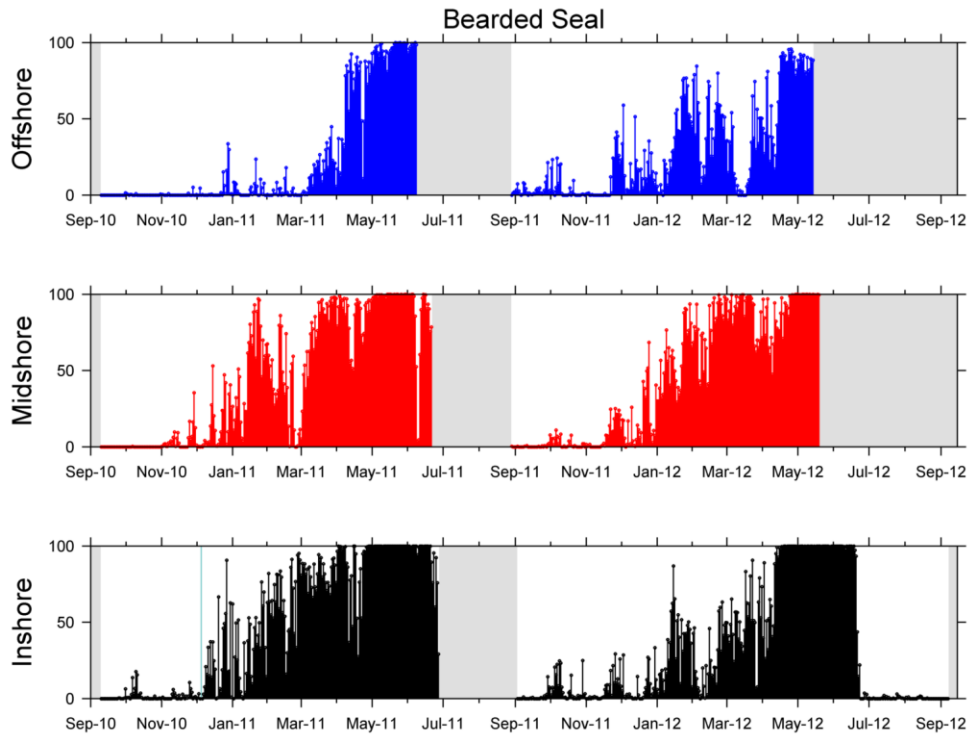
APPENDIX C. 3. BELUGA ACOUSTIC DETECTIONS.



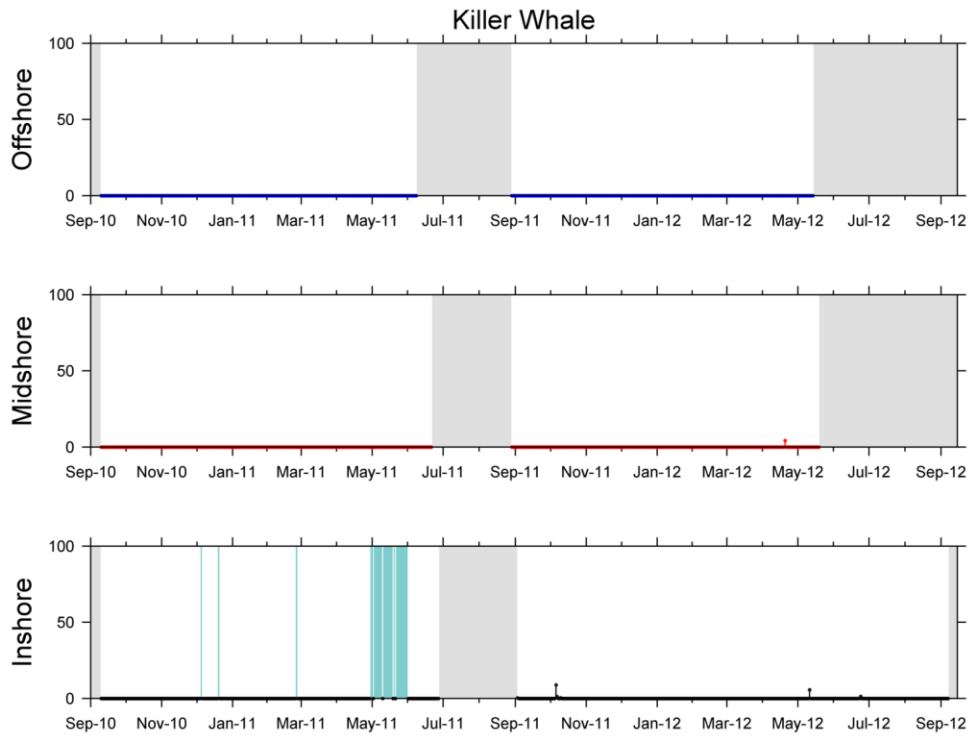
APPENDIX C. 4. GRAY WHALE ACOUSTIC DETECTIONS.



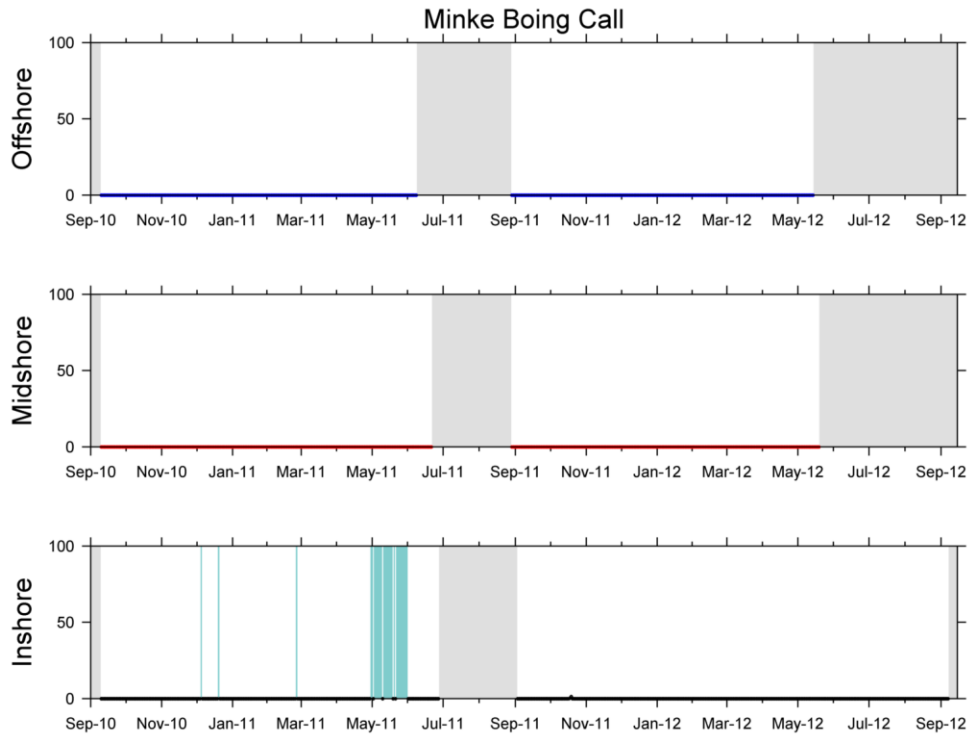
APPENDIX C. 5. WALRUS ACOUSTIC DETECTIONS.



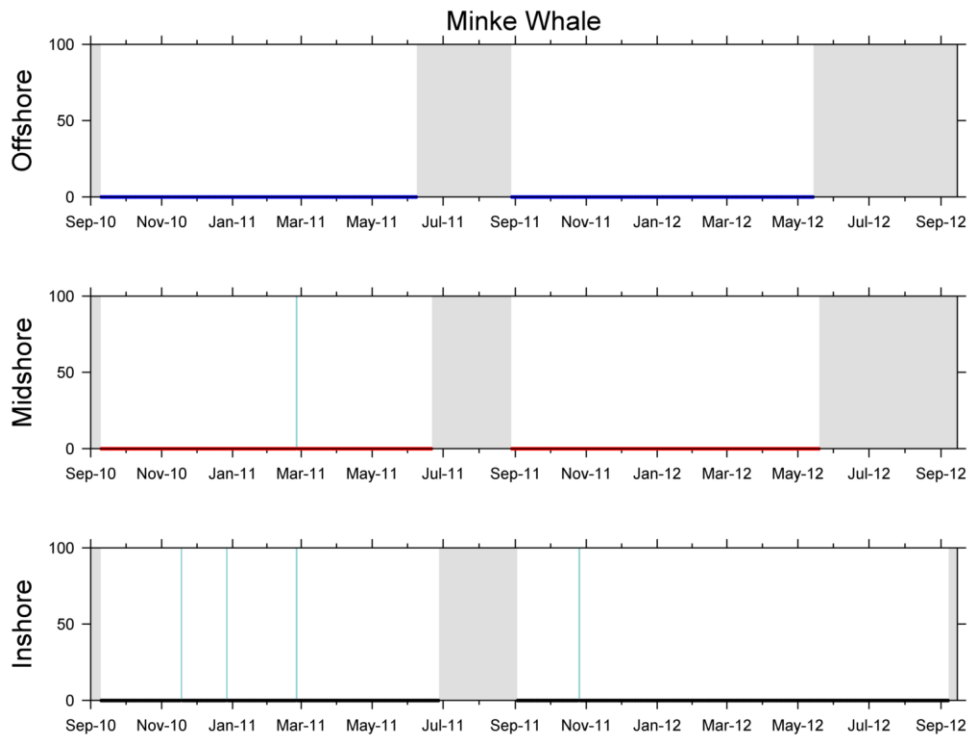
APPENDIX C. 6. BEARDED SEAL ACOUSTIC DETECTIONS.



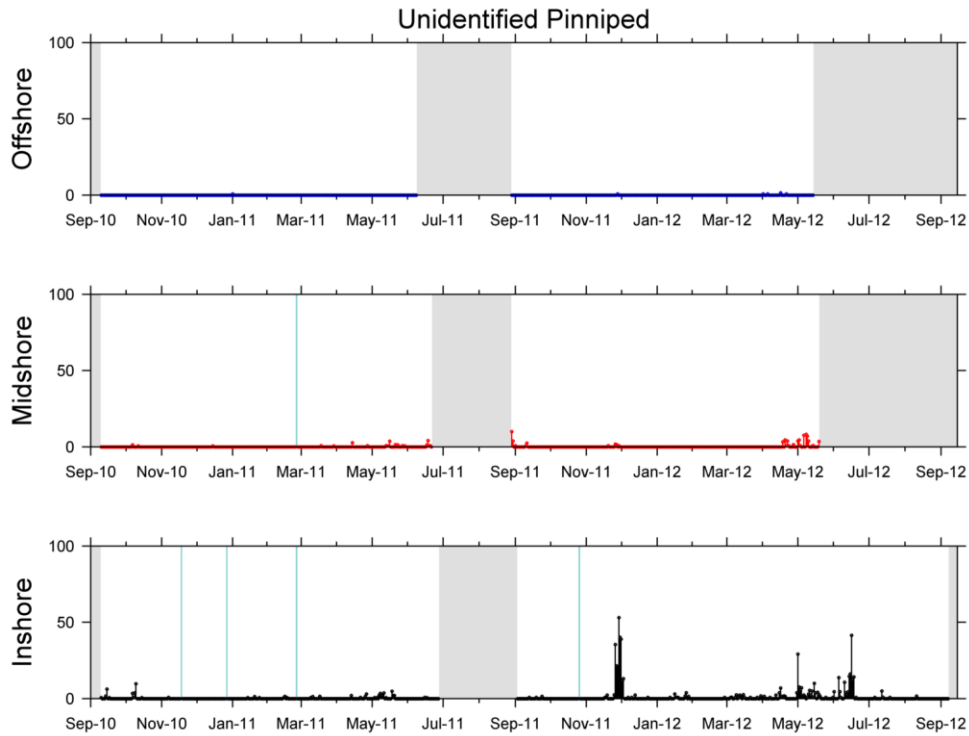
APPENDIX C. 7. KILLER WHALE ACOUSTIC DETECTIONS.



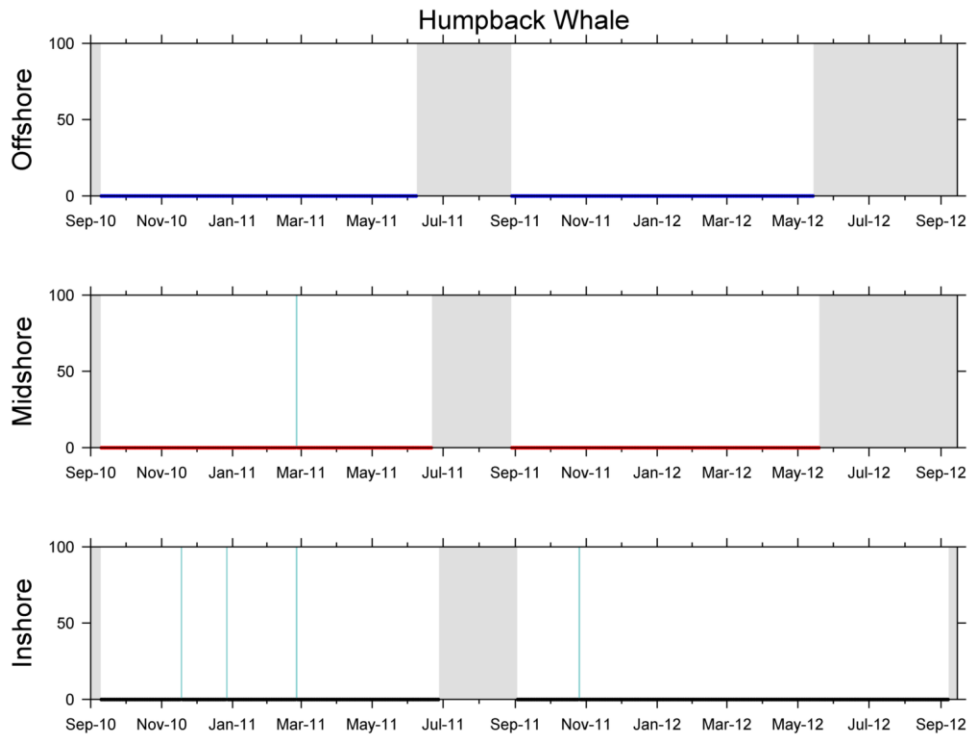
APPENDIX C. 8. MINKE “BOING” ACOUSTIC DETECTIONS.



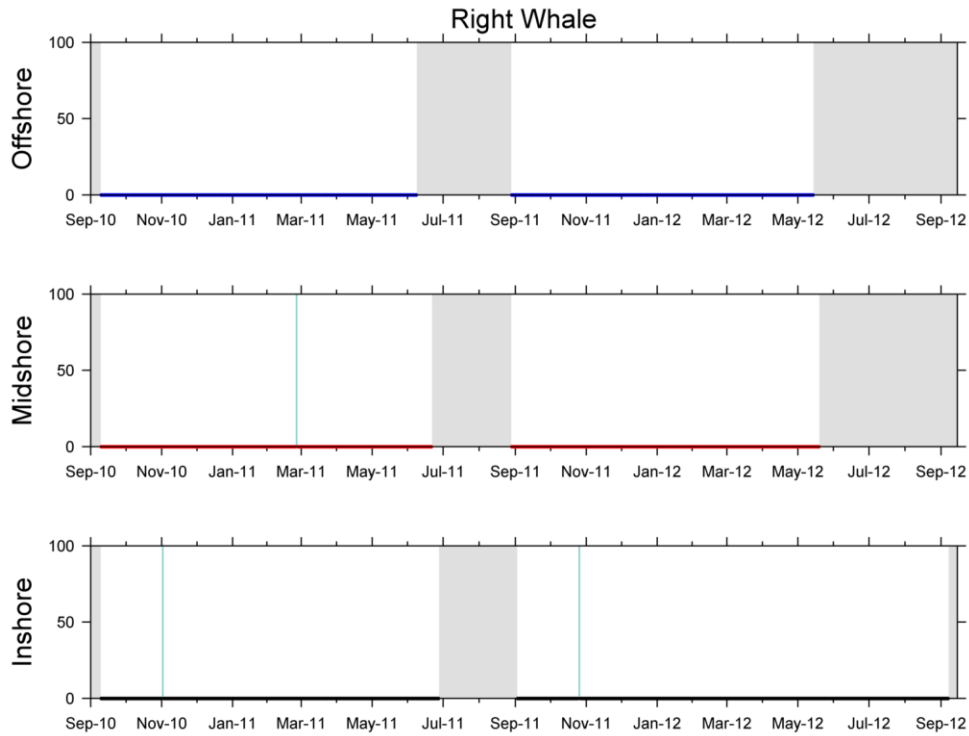
APPENDIX C. 9. MINKE WHALE ACOUSTIC DETECTIONS (NONE).



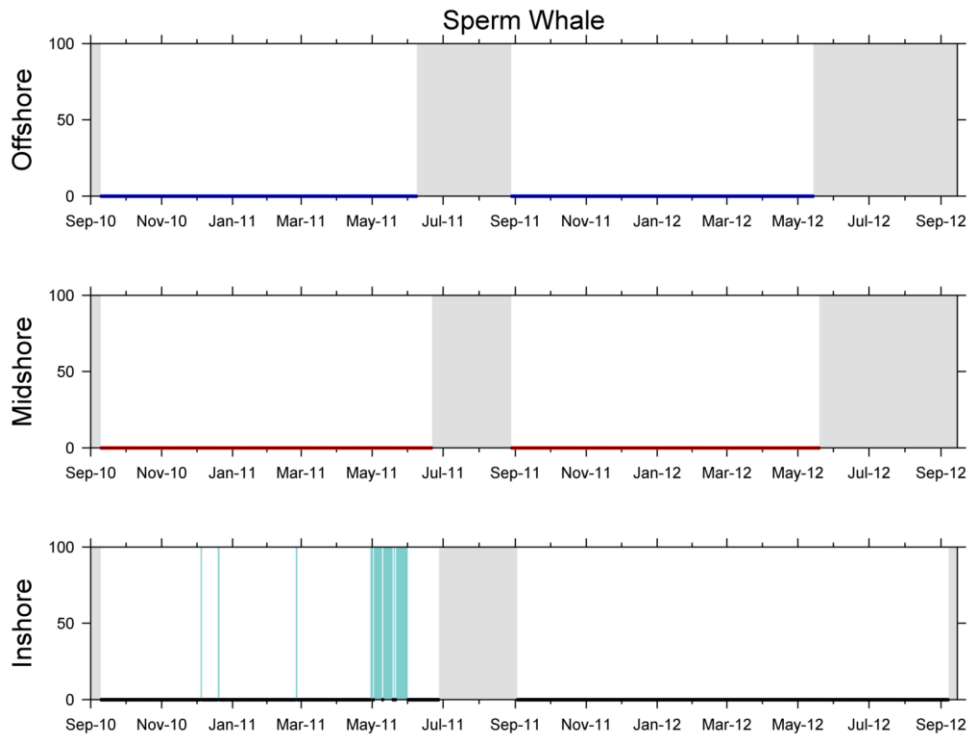
APPENDIX C. 10. UNIDENTIFIED PINNIPED ACOUSTIC DETECTIONS.



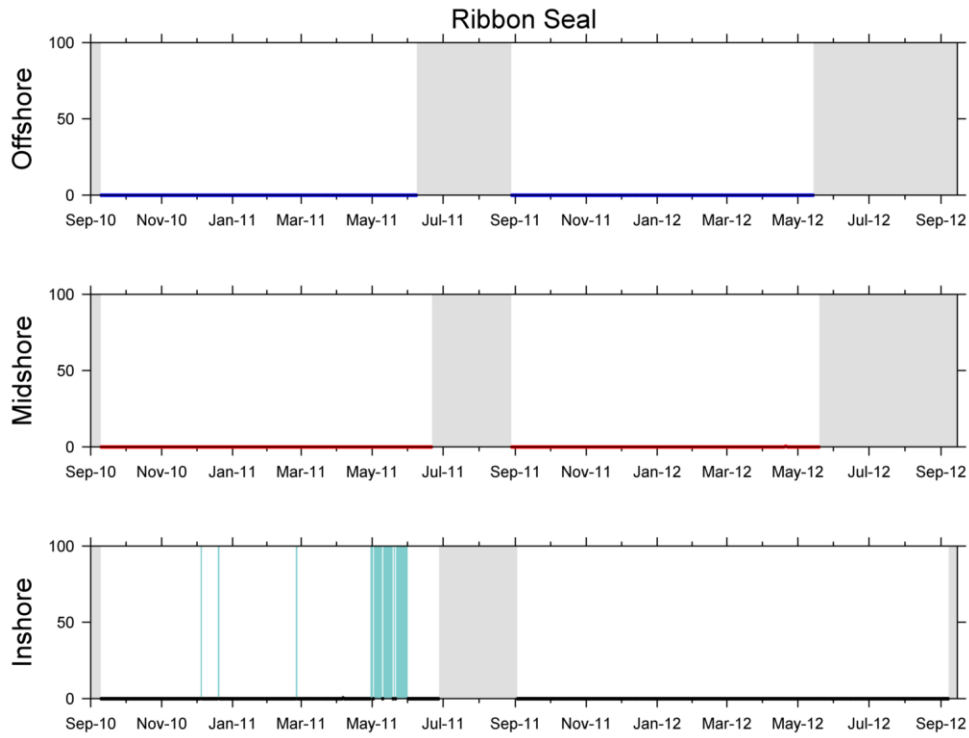
APPENDIX C. 11. HUMPBACK WHALE ACOUSTIC DETECTIONS (NONE).



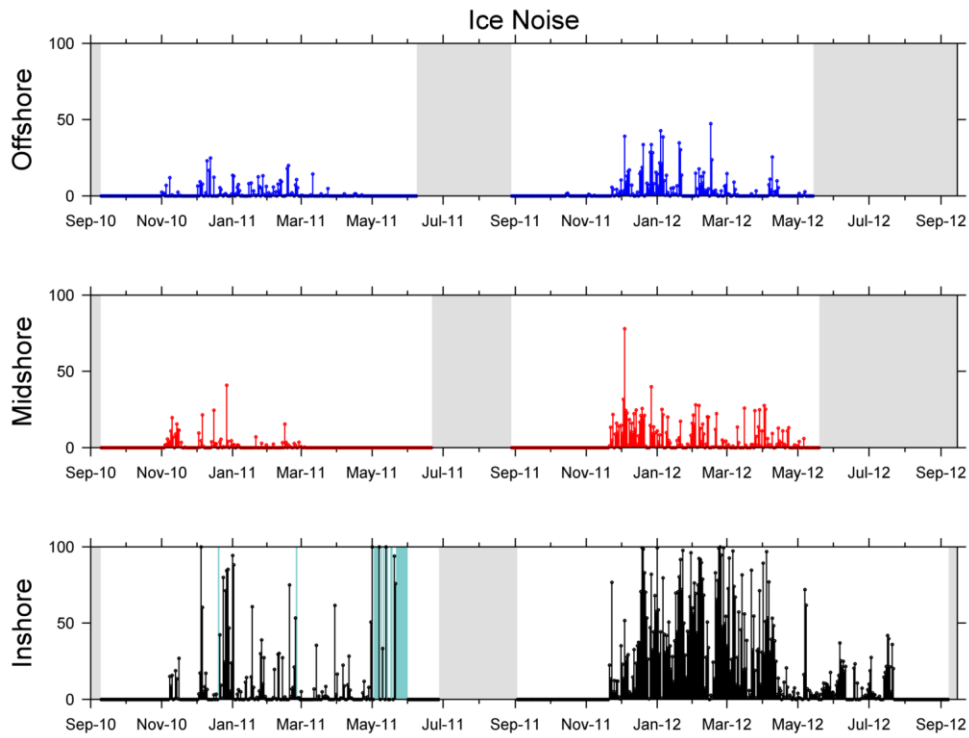
APPENDIX C. 12. RIGHT WHALE ACOUSTIC DETECTIONS (NONE).



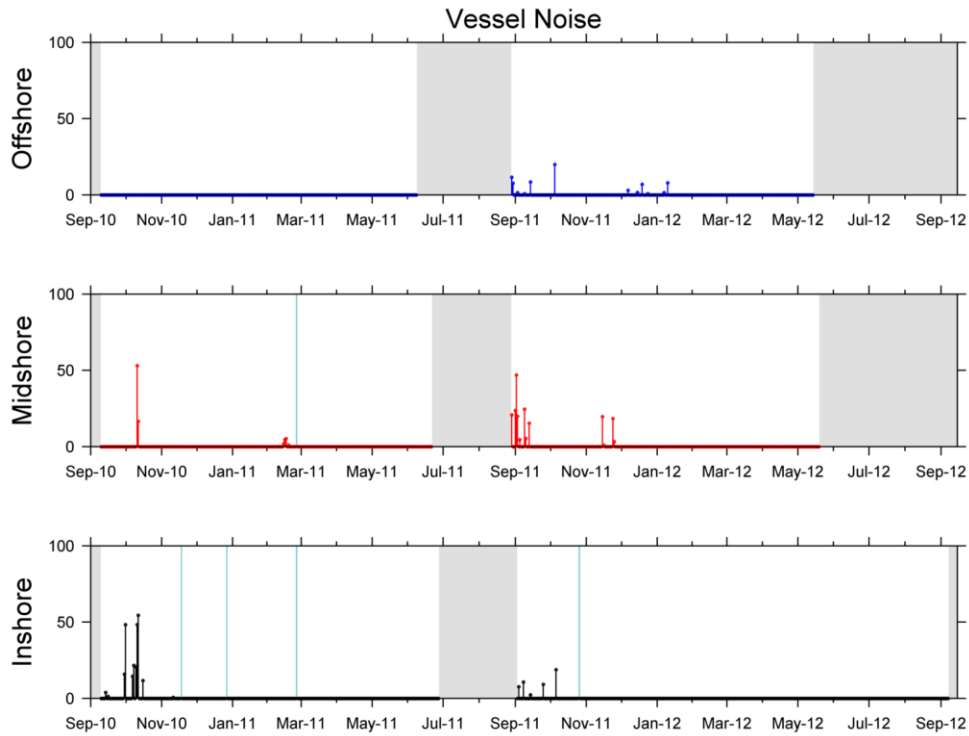
APPENDIX C. 13. SPERM WHALE ACOUSTIC DETECTIONS (NONE).



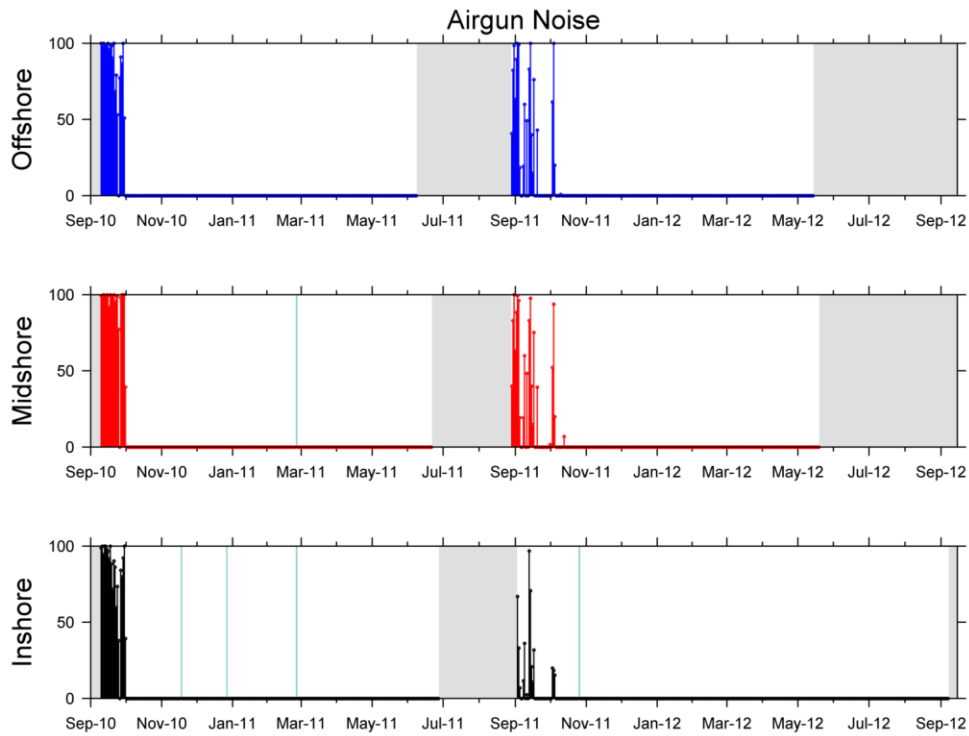
APPENDIX C. 14. RIBBON SEAL ACOUSTIC DETECTIONS (NONE).



APPENDIX C. 15. ICE NOISE ACOUSTIC DETECTIONS.



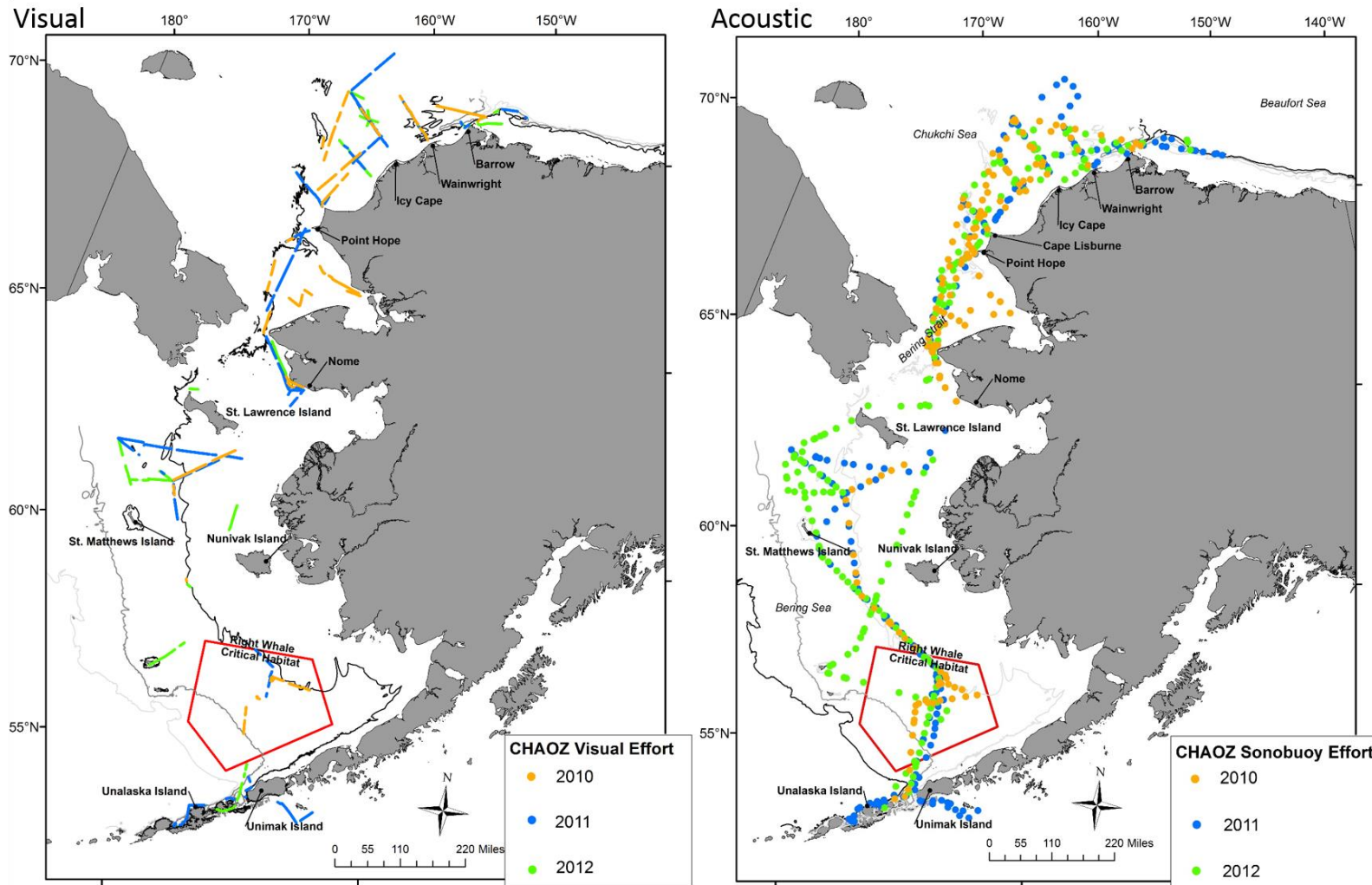
APPENDIX C. 16. VESSEL NOISE ACOUSTIC DETECTIONS.



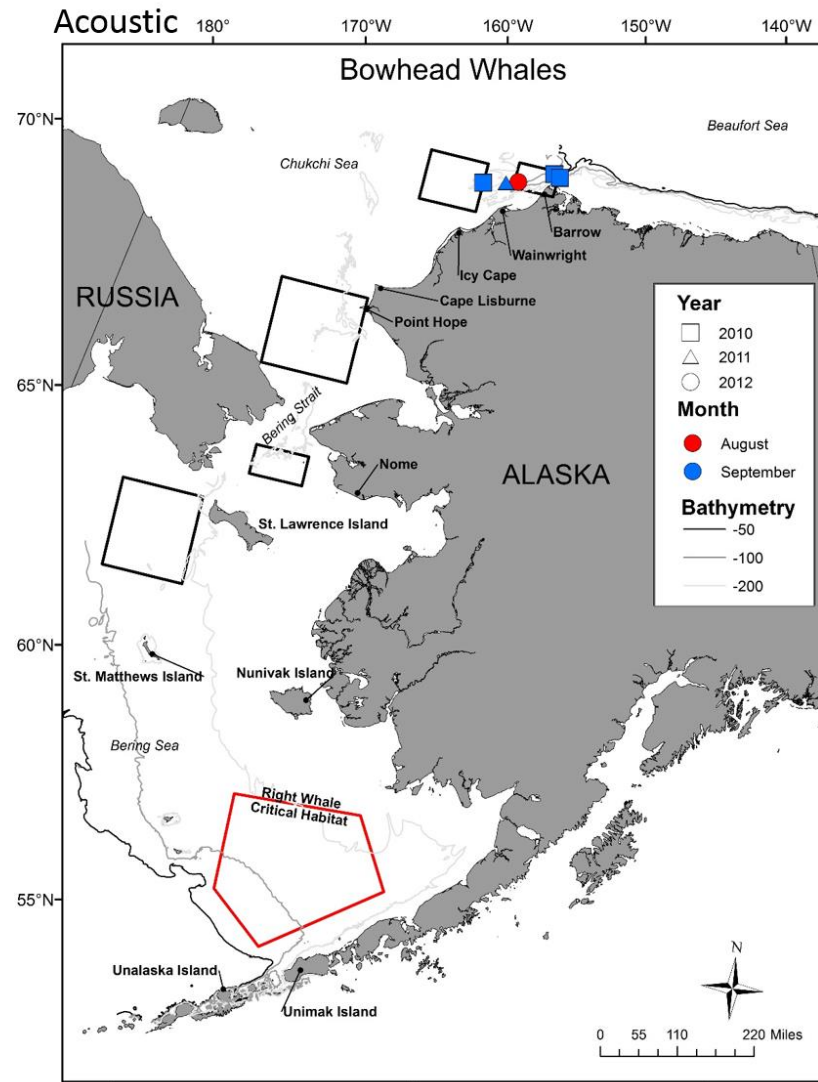
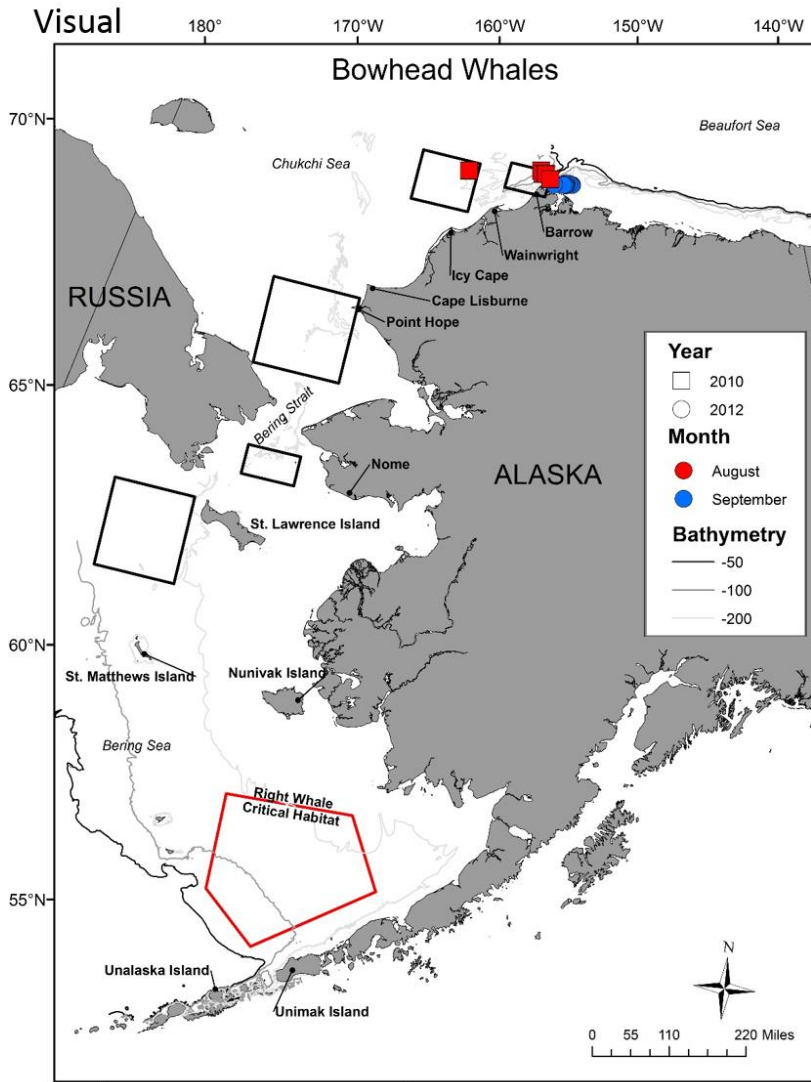
APPENDIX C. 17. SEISMIC AIRGUN ACOUSTIC DETECTIONS.

D. Sonobuoy and visual survey data

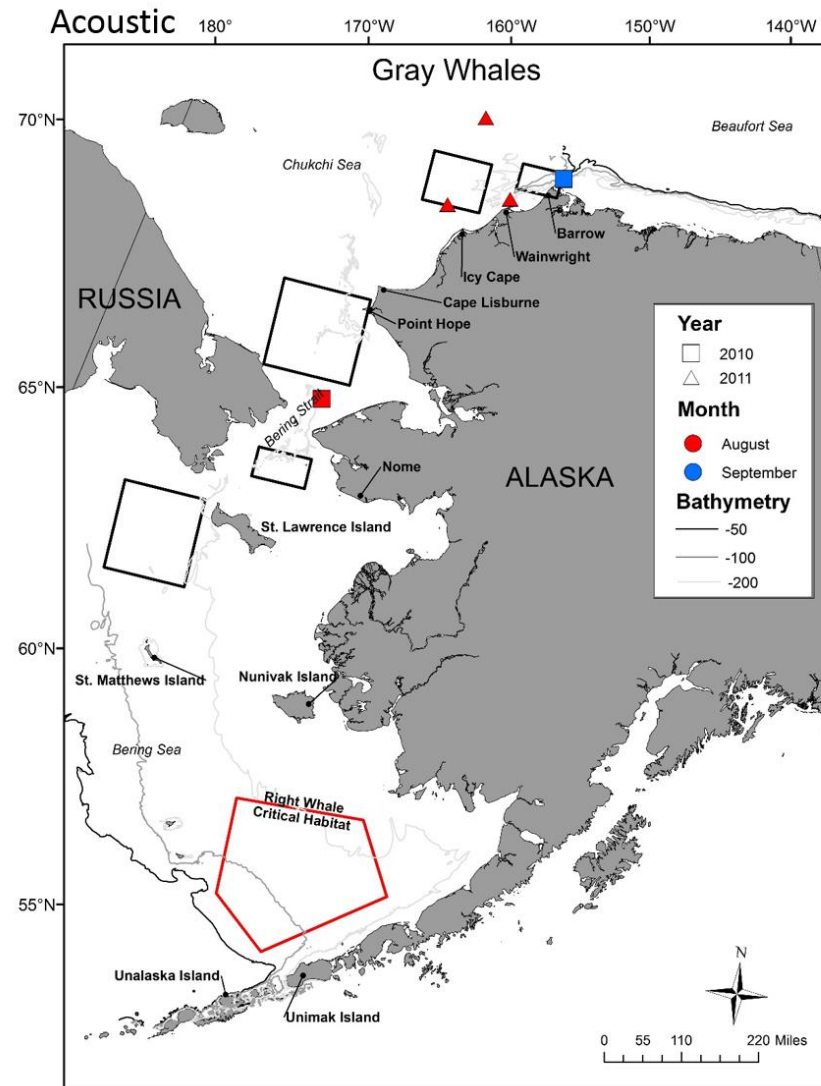
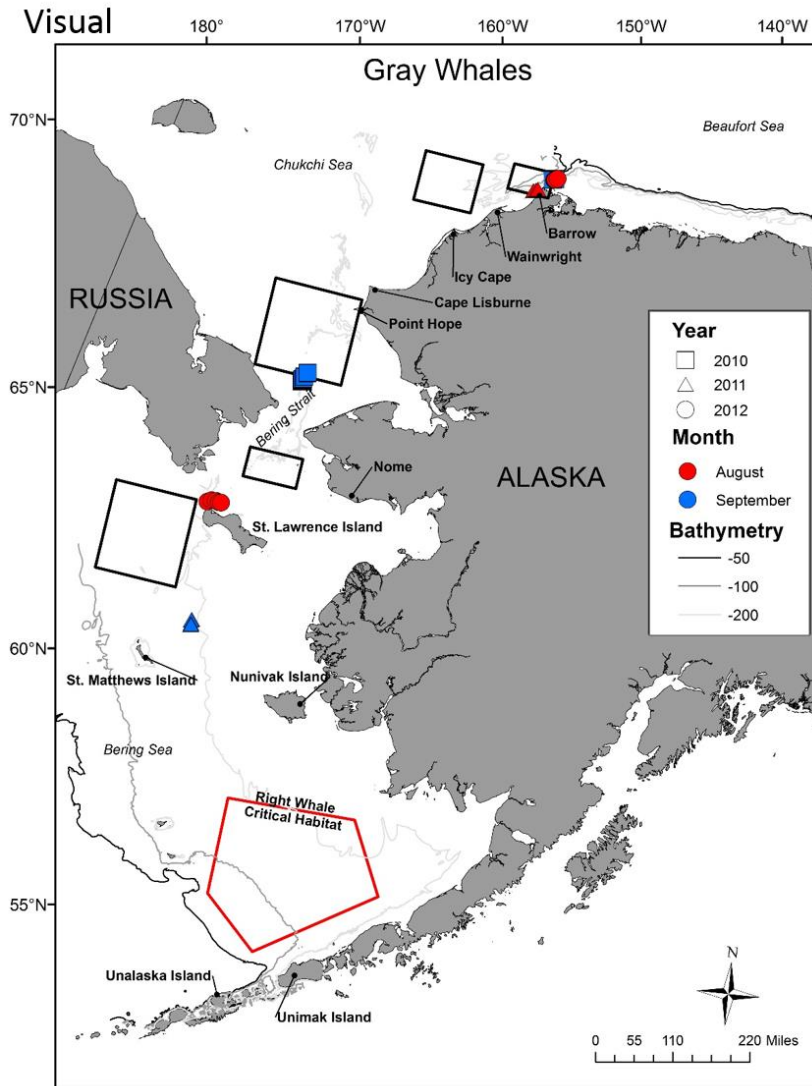
Visual sightings (left) and acoustic detections (right) of each species in the Bering, Chukchi, and Beaufort Seas by month for 2010-2012. DBO regions outlined in black.



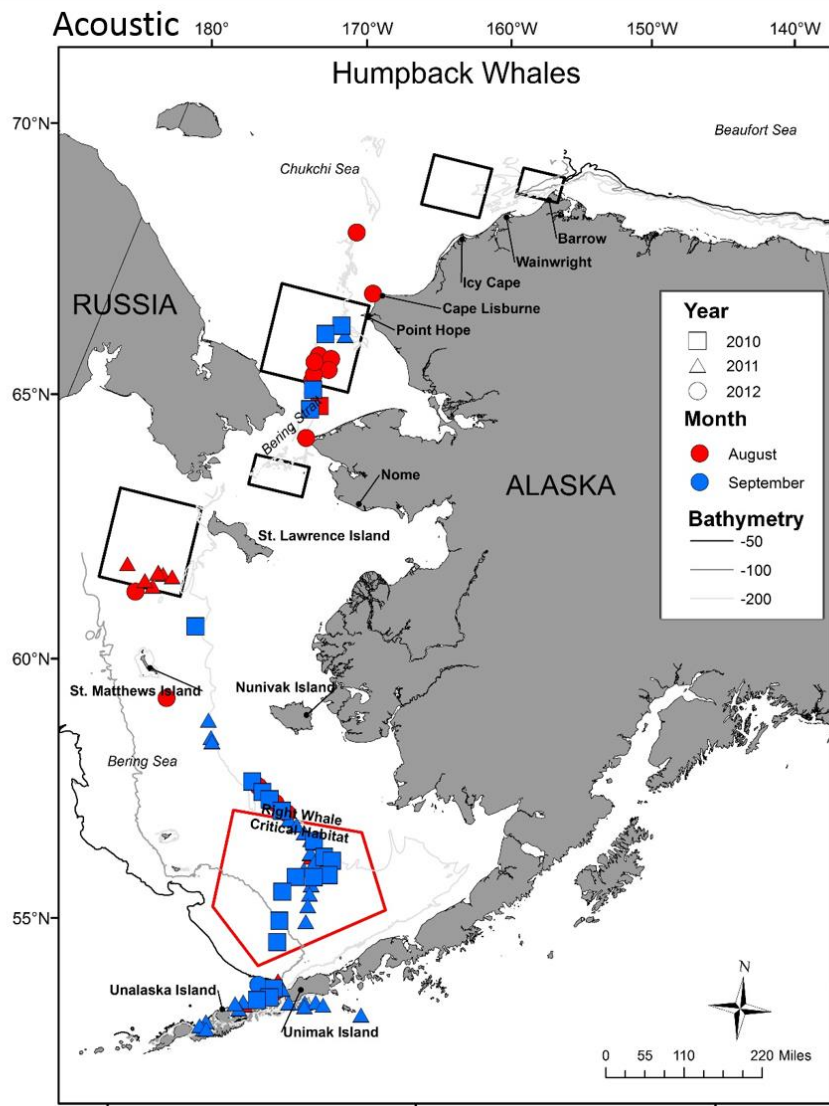
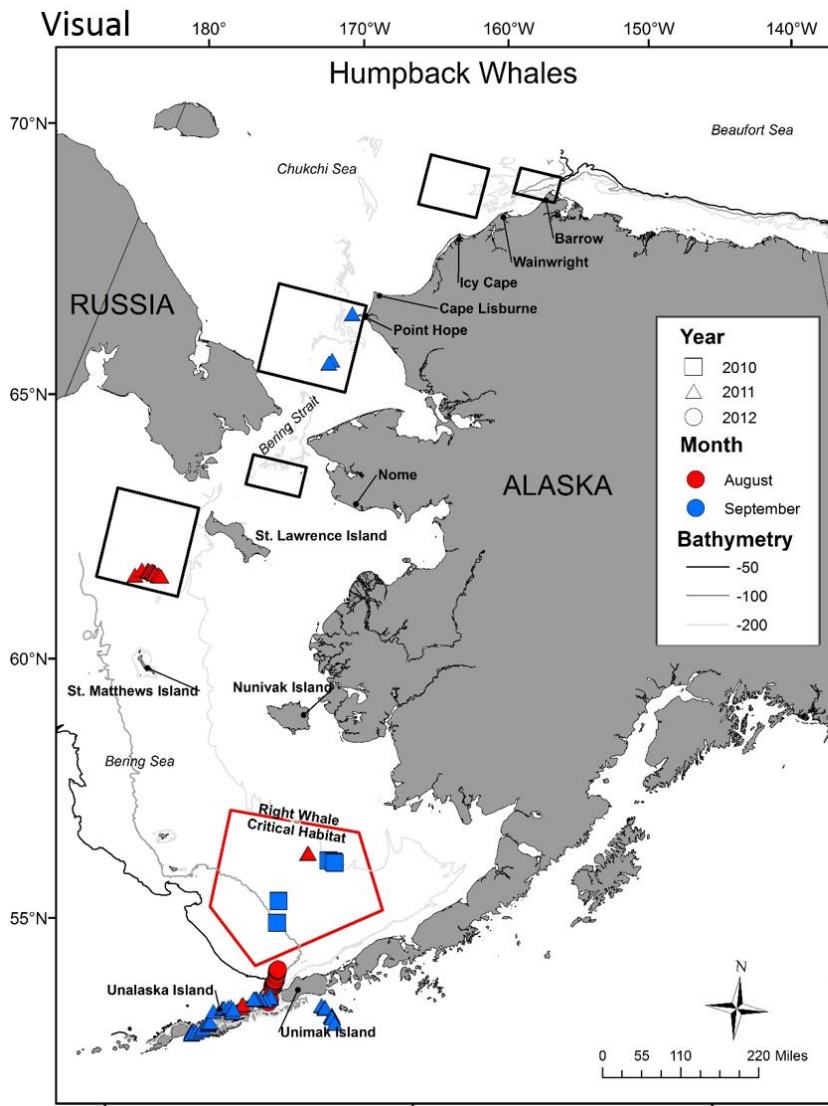
APPENDIX D. 1.SUMMARY OF TOTAL VISUAL AND SONOBUOY EFFORT, 2010-2012.



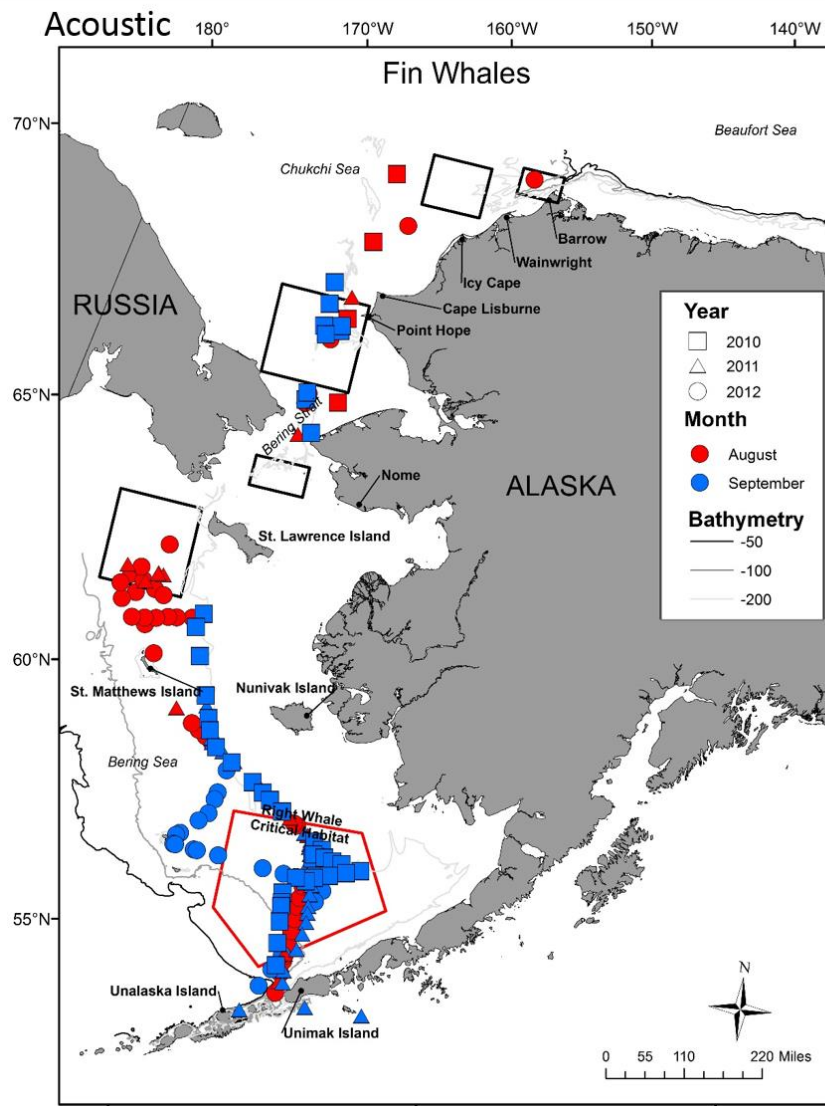
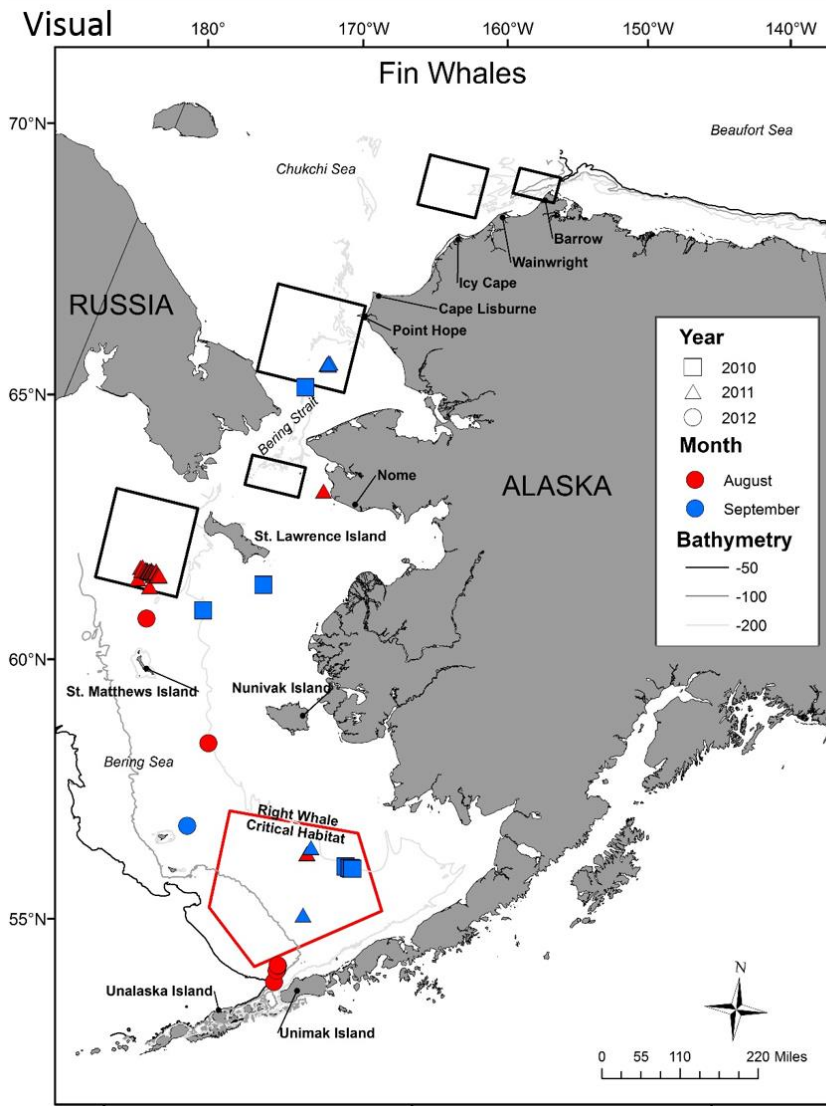
APPENDIX D. 2. BOWHEAD WHALE SIGHTINGS AND ACOUSTIC DETECTIONS, 2010-2012.



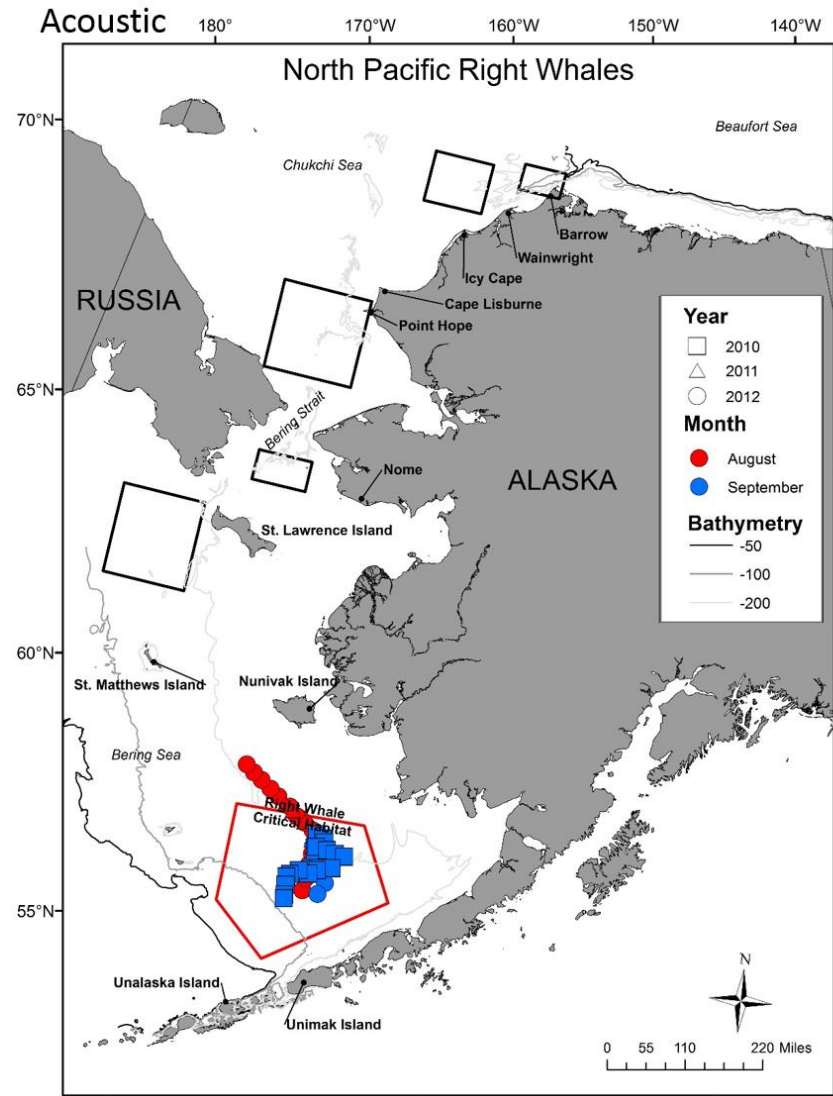
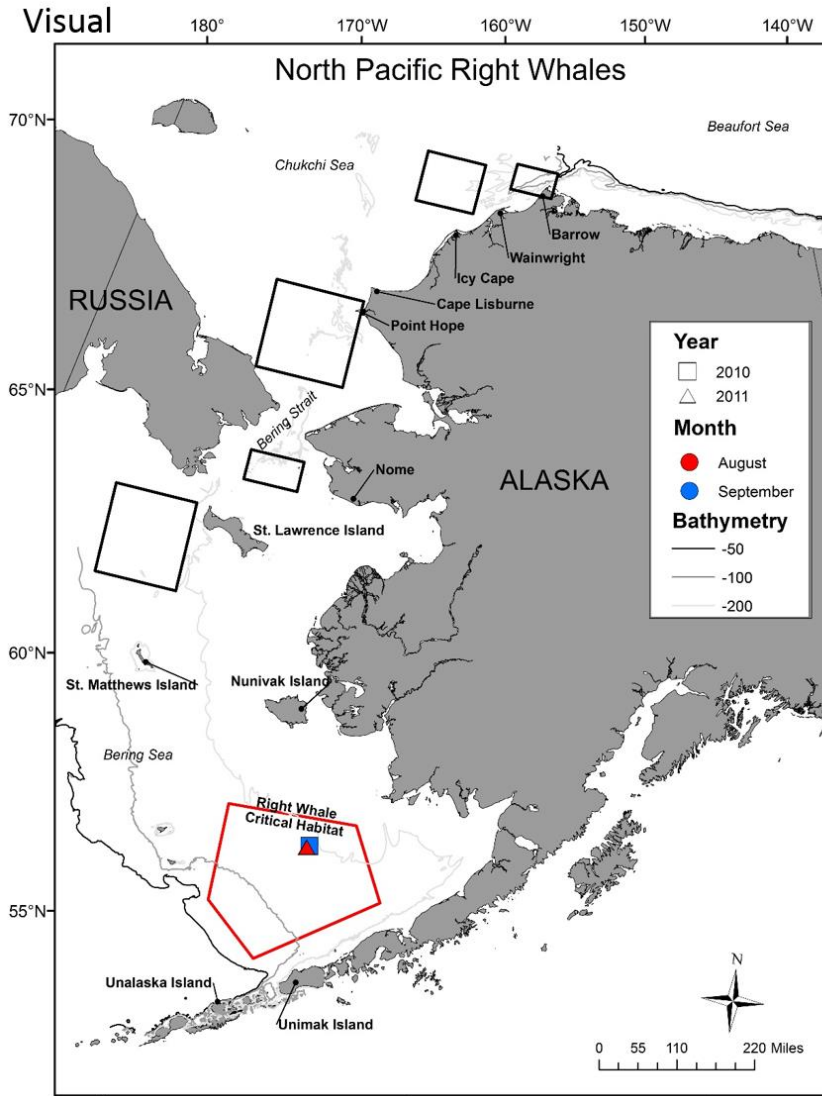
APPENDIX D. 3. GRAY WHALE SIGHTINGS AND ACOUSTIC DETECTIONS, 2010-2012.



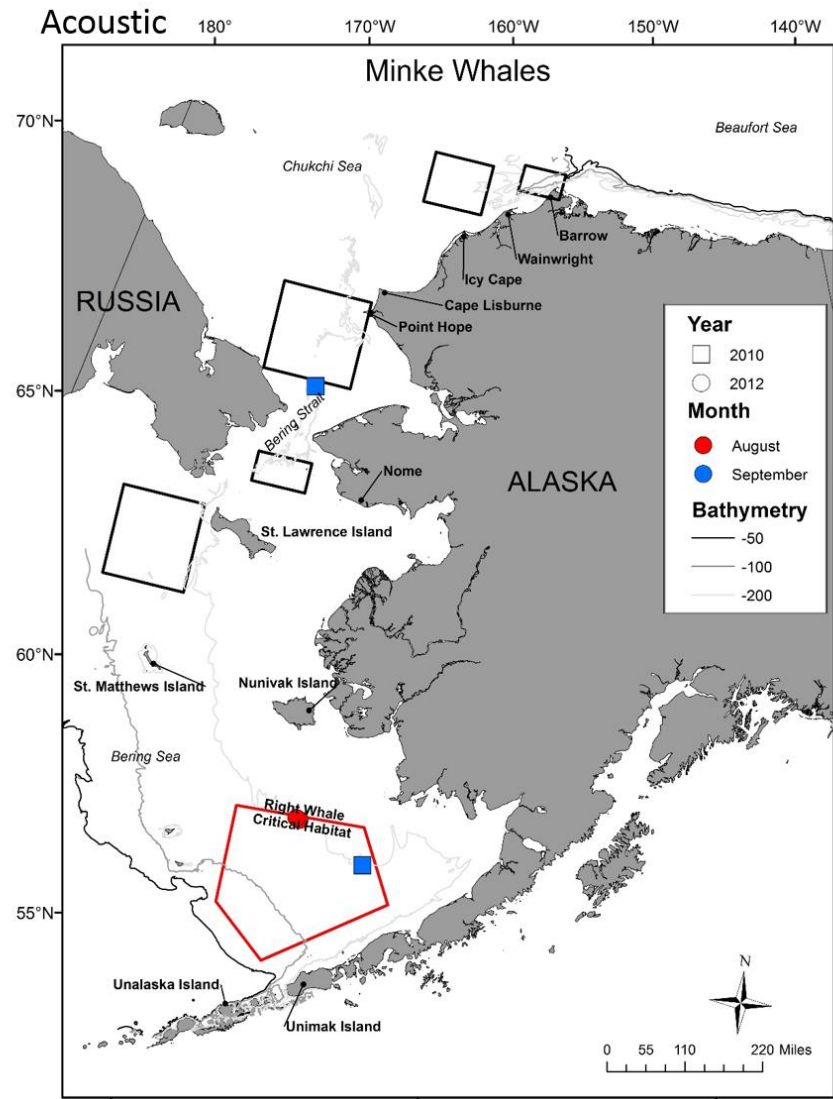
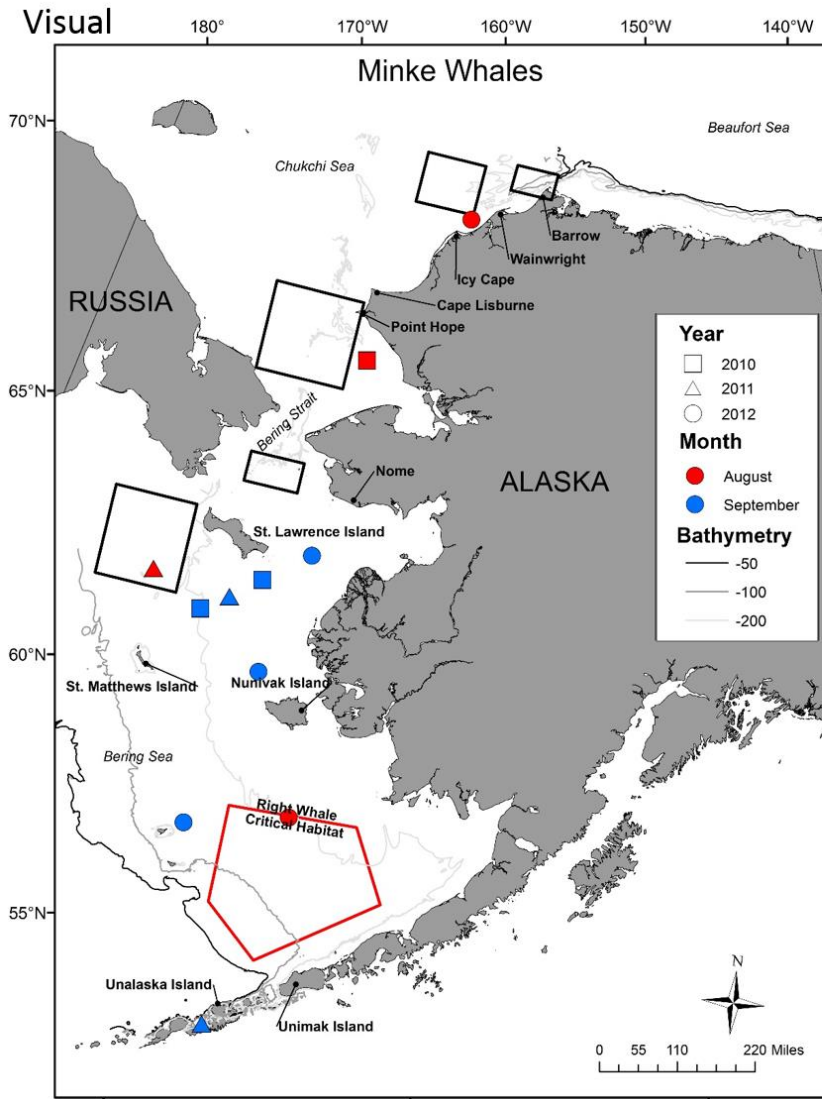
APPENDIX D. 4. HUMPBACK WHALE SIGHTINGS AND ACOUSTIC DETECTIONS, 2010-2012.



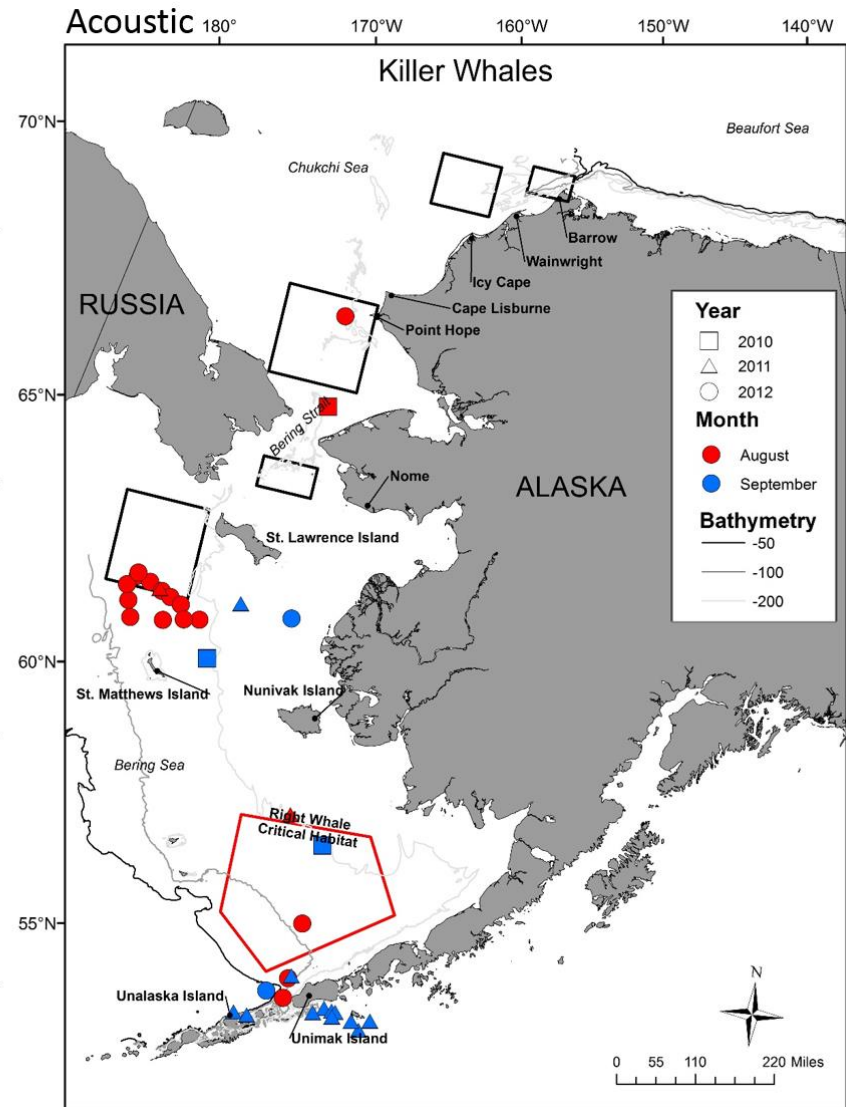
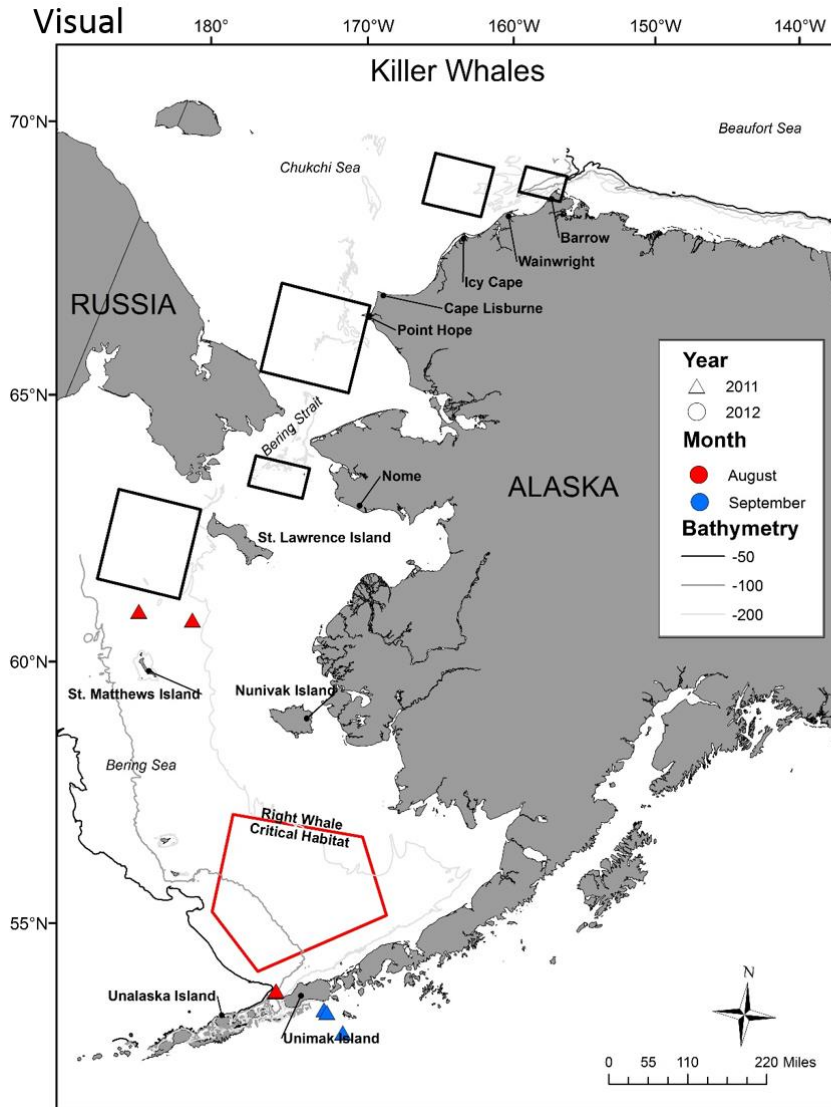
APPENDIX D. 5. FIN WHALE SIGHTINGS AND ACOUSTIC DETECTIONS, 2010-2012.



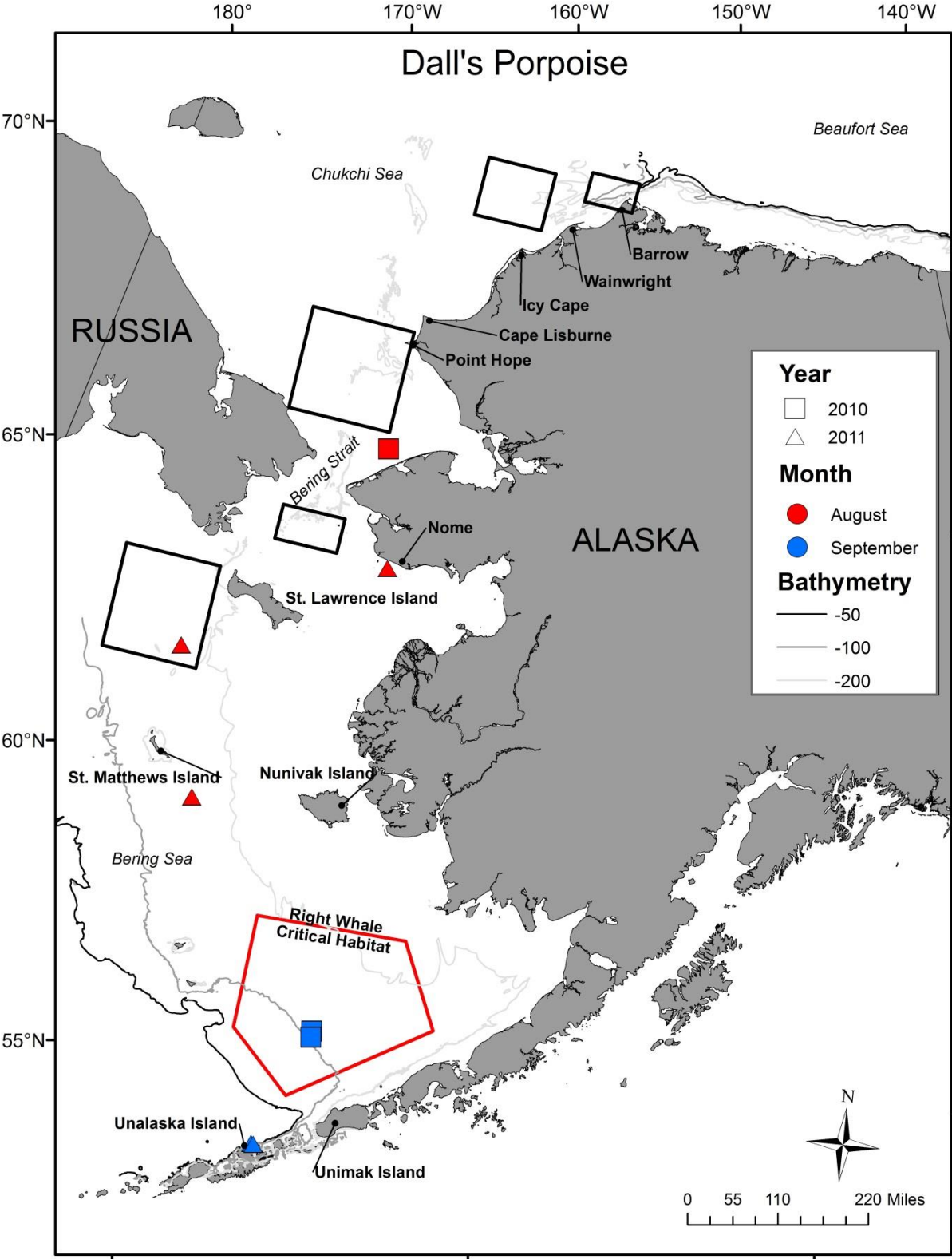
APPENDIX D. 6. NORTH PACIFIC RIGHT WHALE SIGHTINGS AND ACOUSTIC DETECTIONS, 2010-2012.



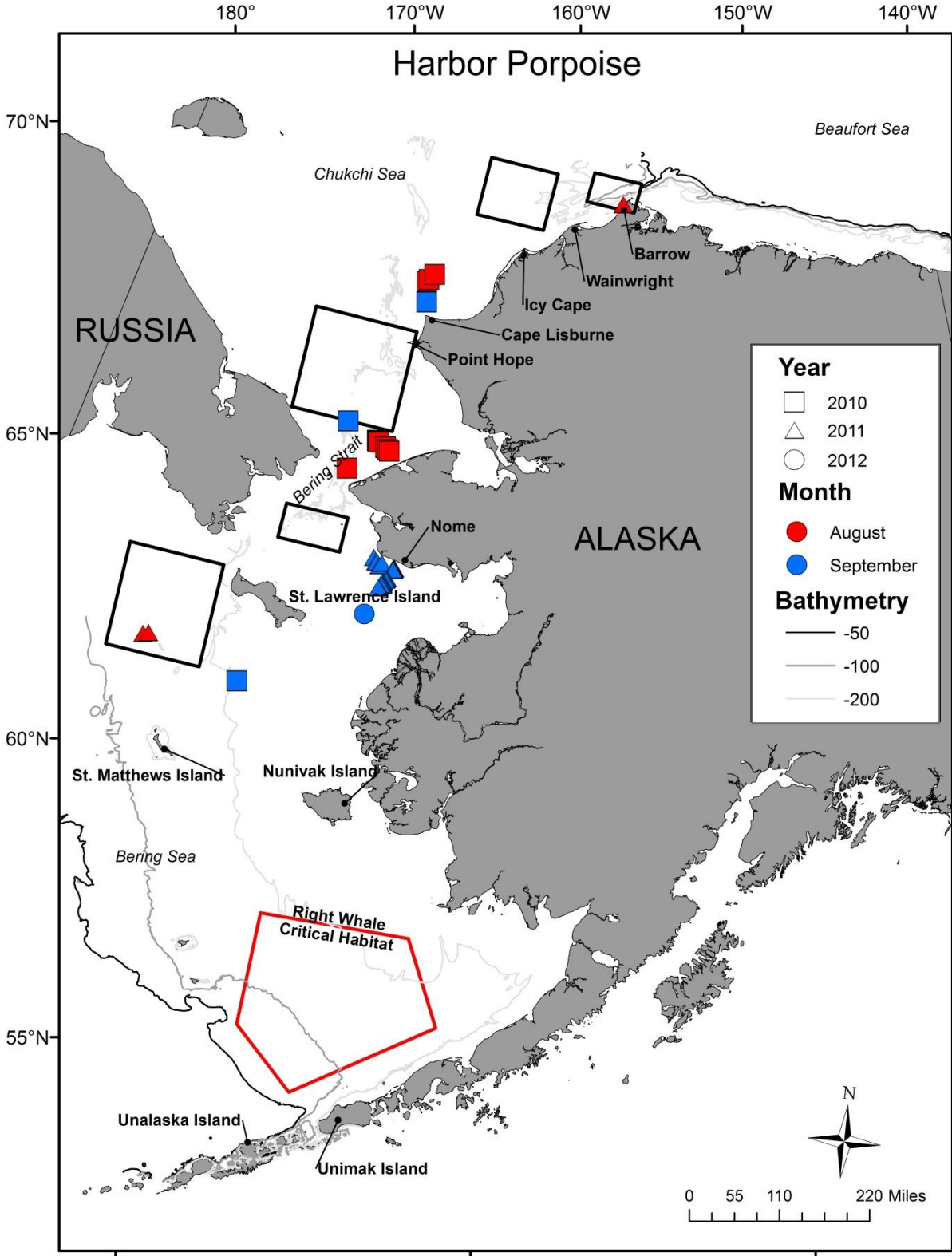
APPENDIX D. 7. MINKE WHALE SIGHTINGS AND ACOUSTIC DETECTIONS, 2010-2012.



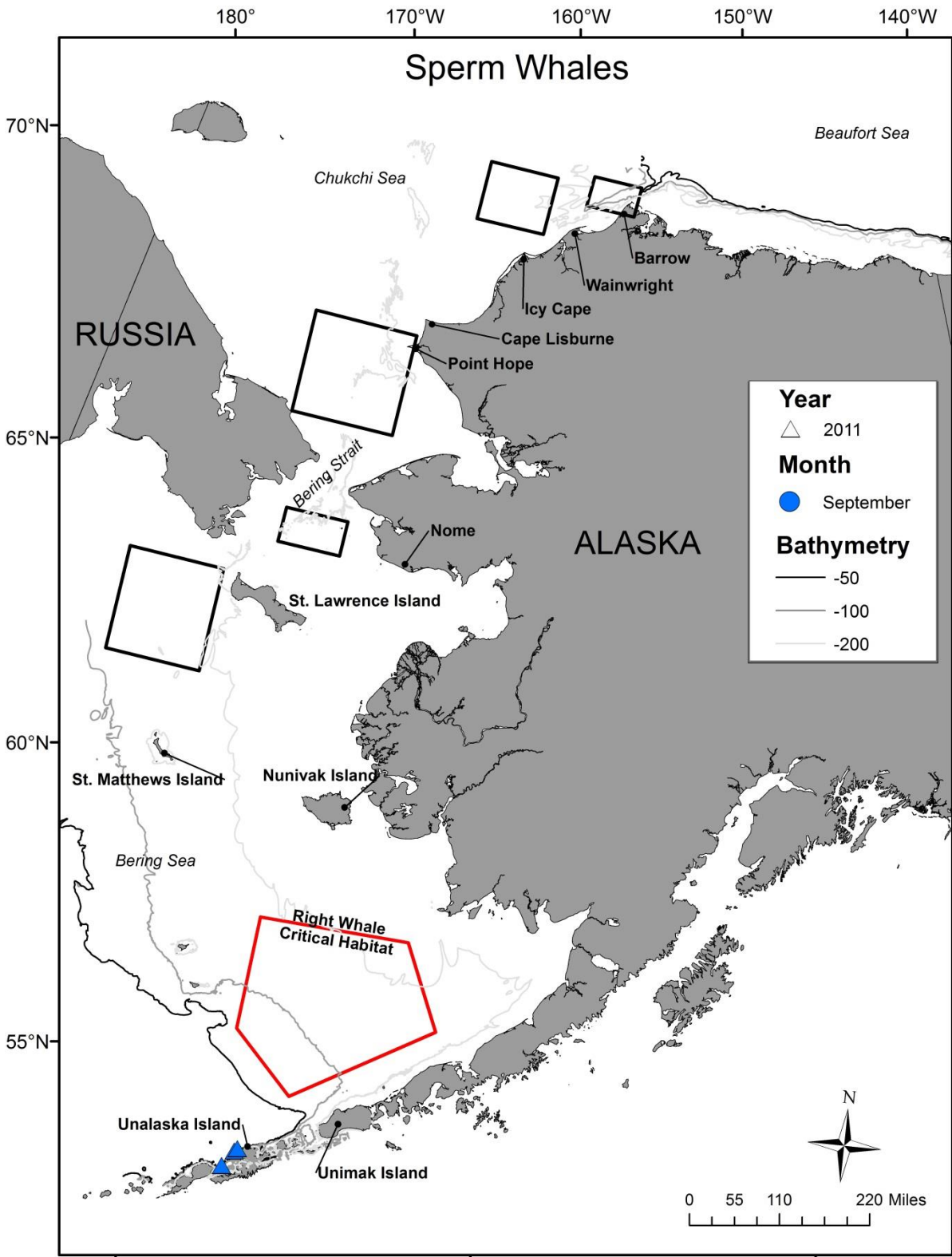
APPENDIX D. 8. KILLER WHALE SIGHTINGS AND ACOUSTIC DETECTIONS, 2010-2012.



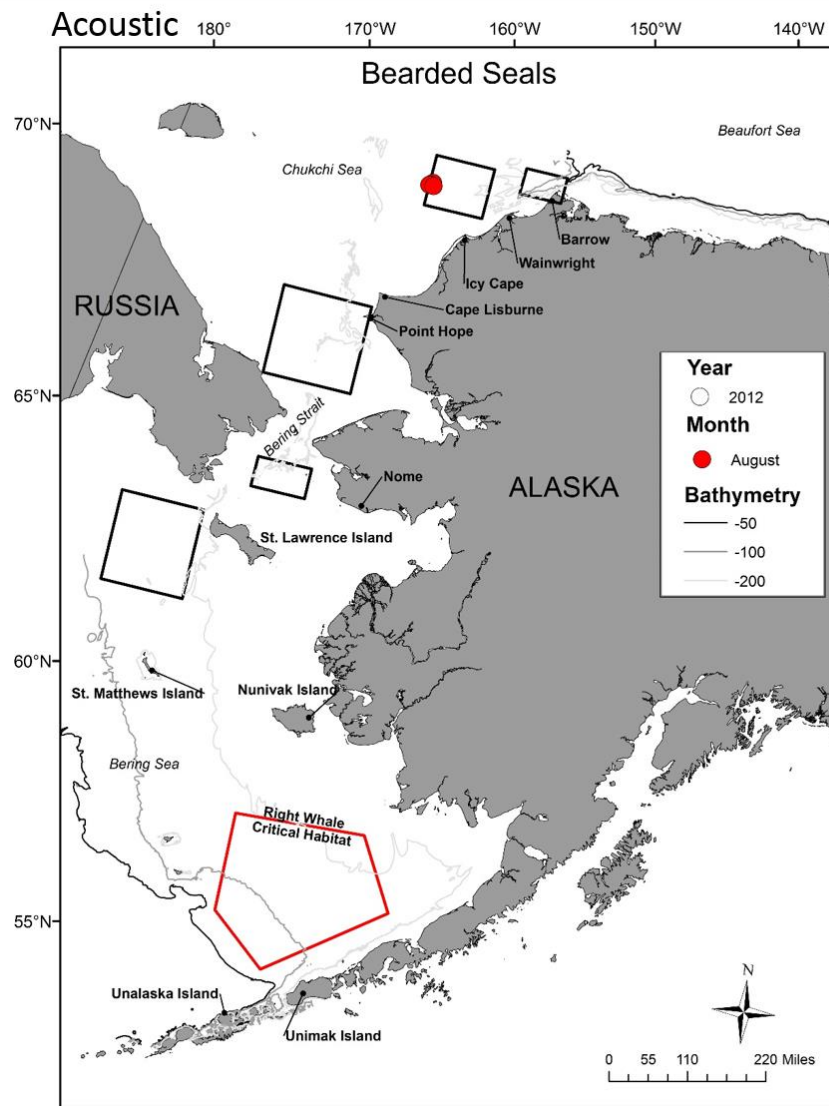
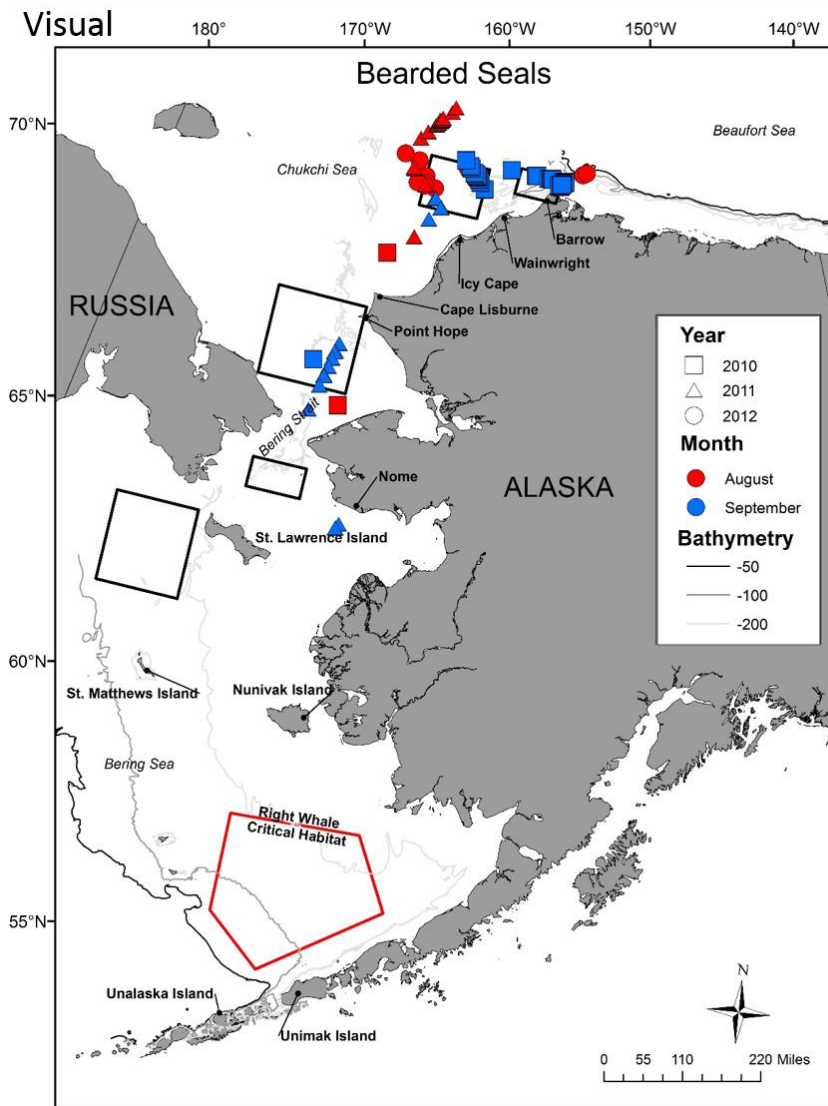
APPENDIX D. 9. DALL'S PORPOISE SIGHTINGS, 2010-2012.



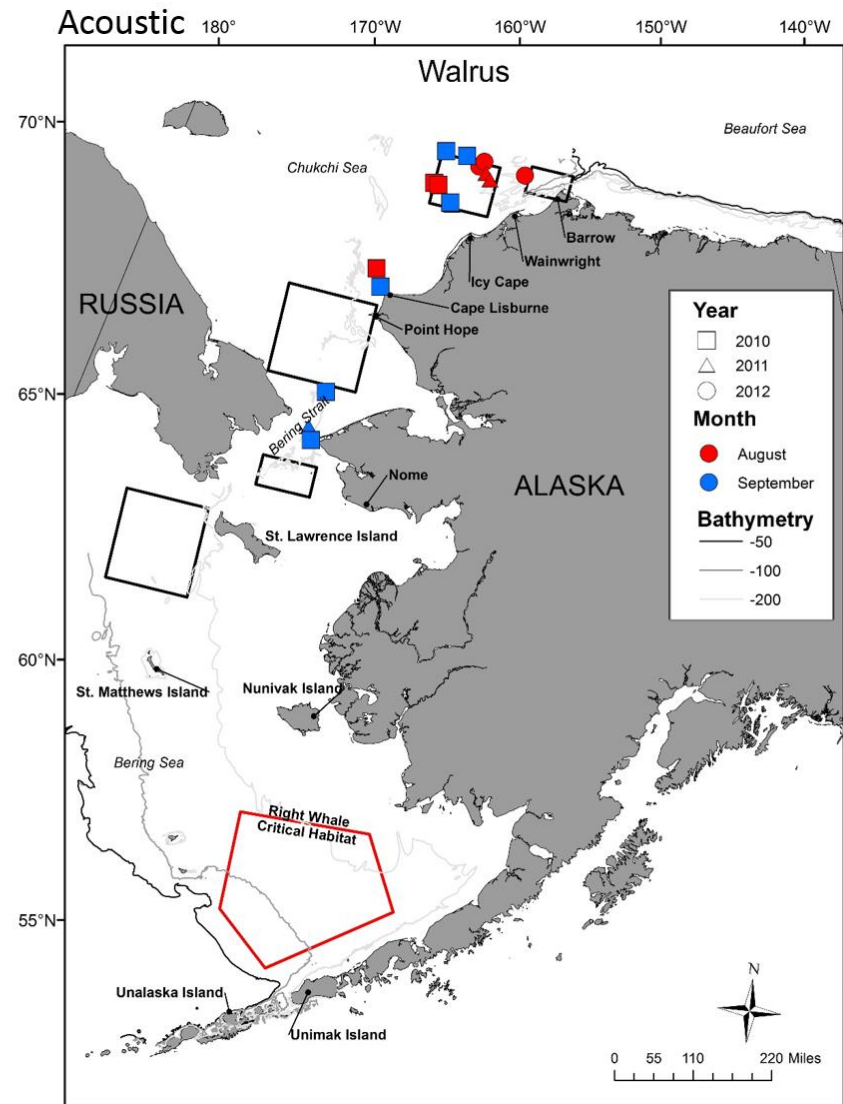
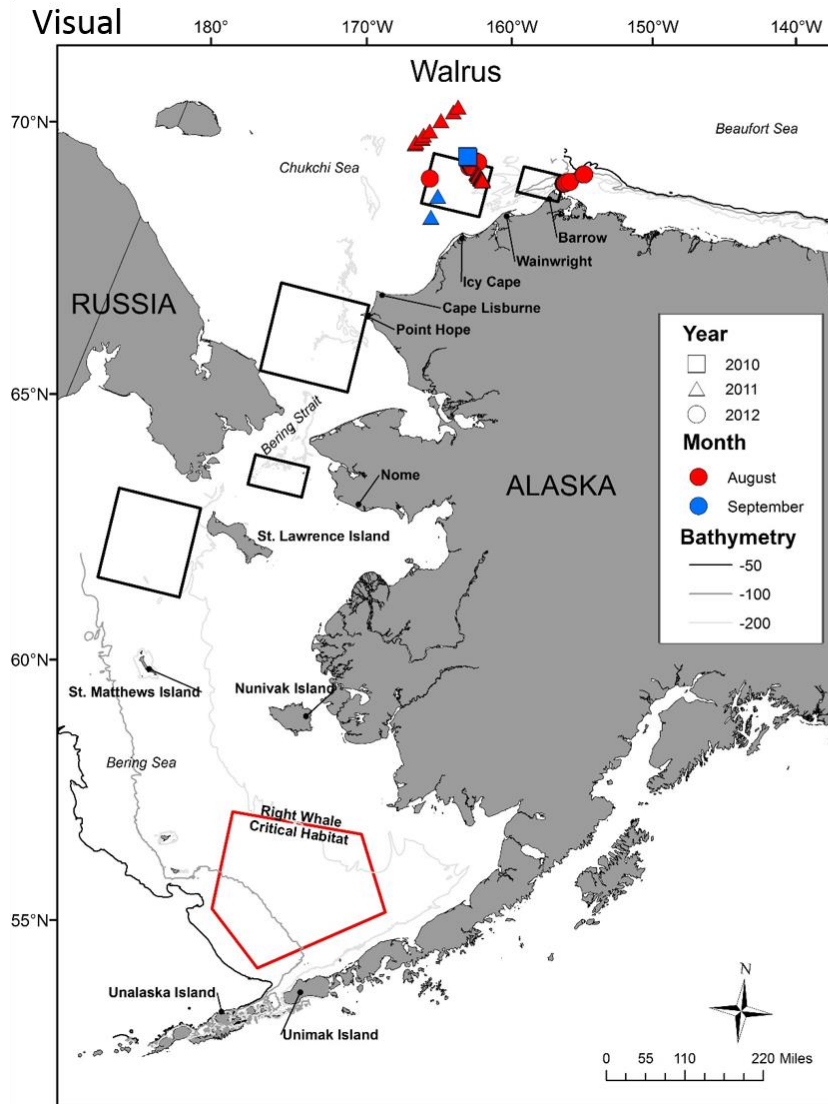
APPENDIX D. 10. HARBOR PORPOISE SIGHTINGS, 2010-2012.



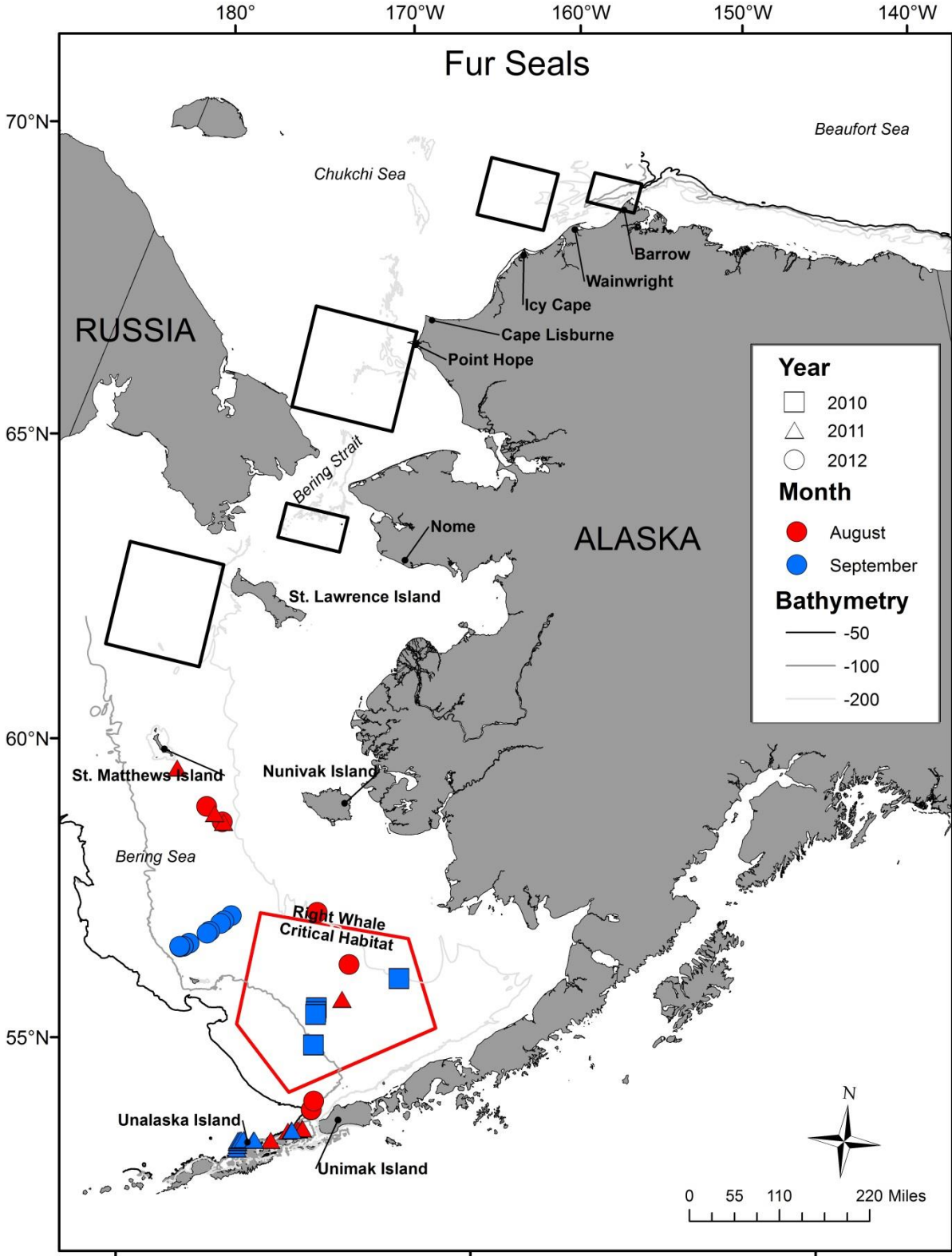
APPENDIX D. 11. SPERM WHALE ACOUSTIC DETECTIONS, 2010-2012.



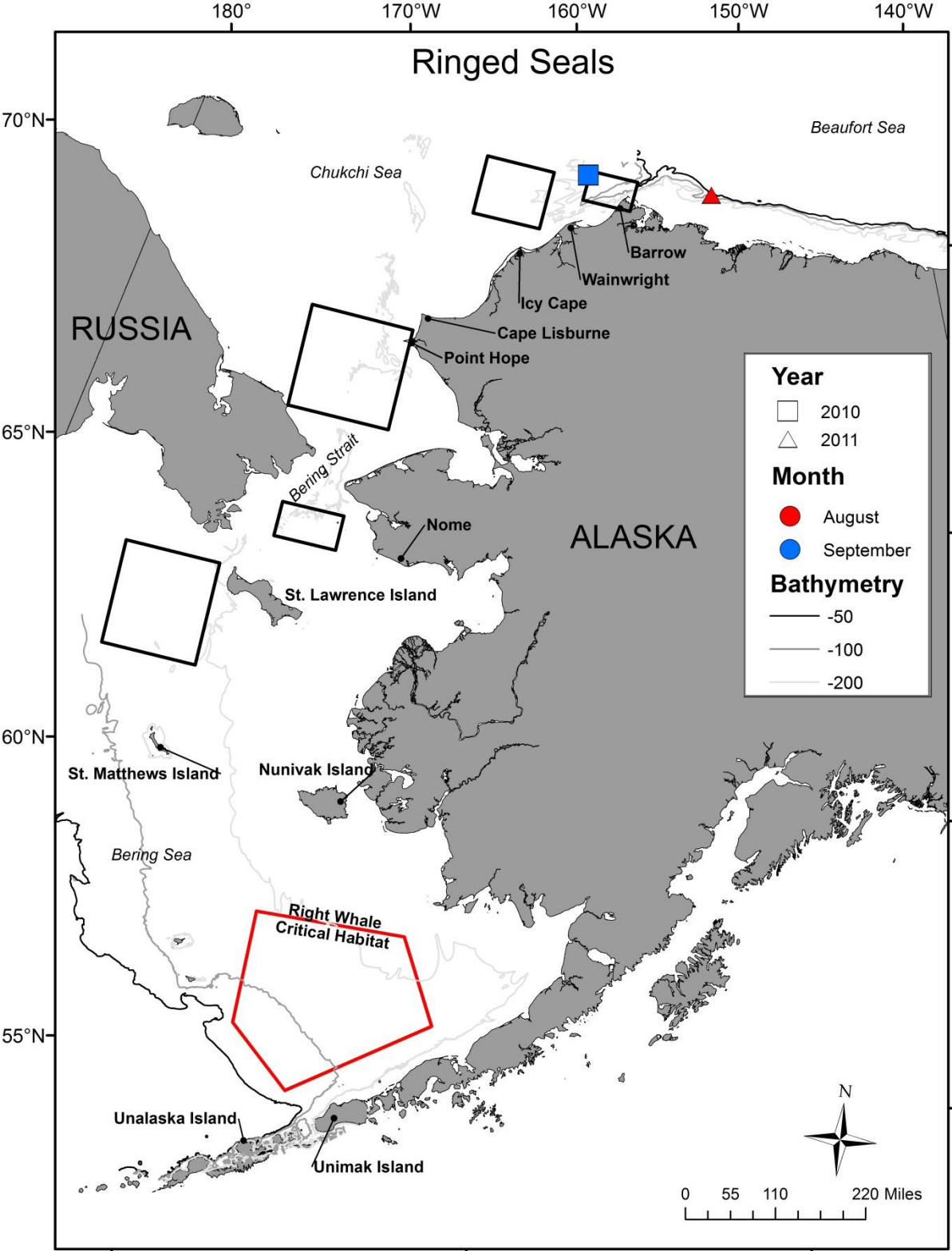
APPENDIX D. 12. BEARDED SEAL SIGHTINGS AND ACOUSTIC DETECTIONS, 2010-2012.



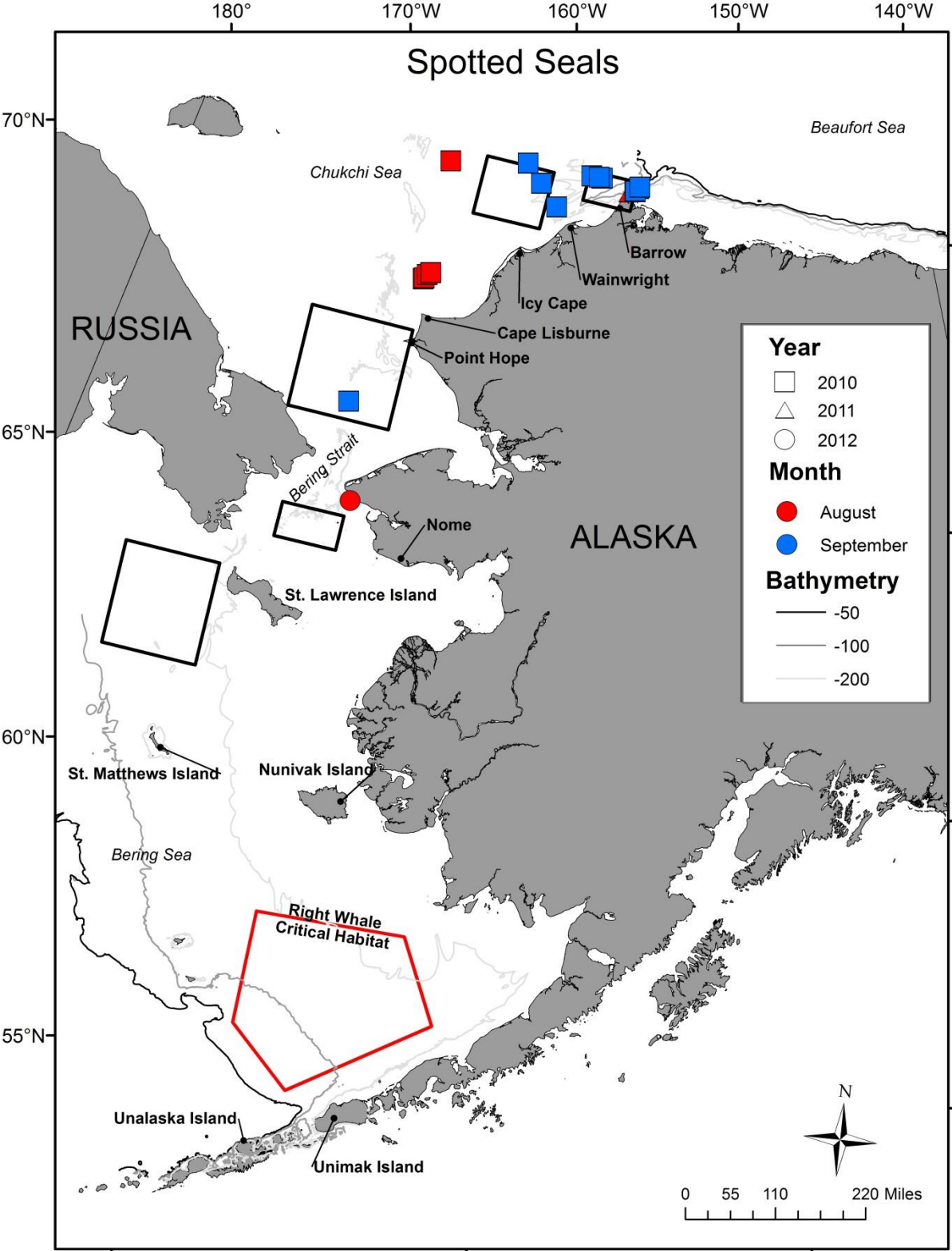
APPENDIX D. 13. WALRUS SIGHTINGS AND ACOUSTIC DETECTIONS, 2010-2012.



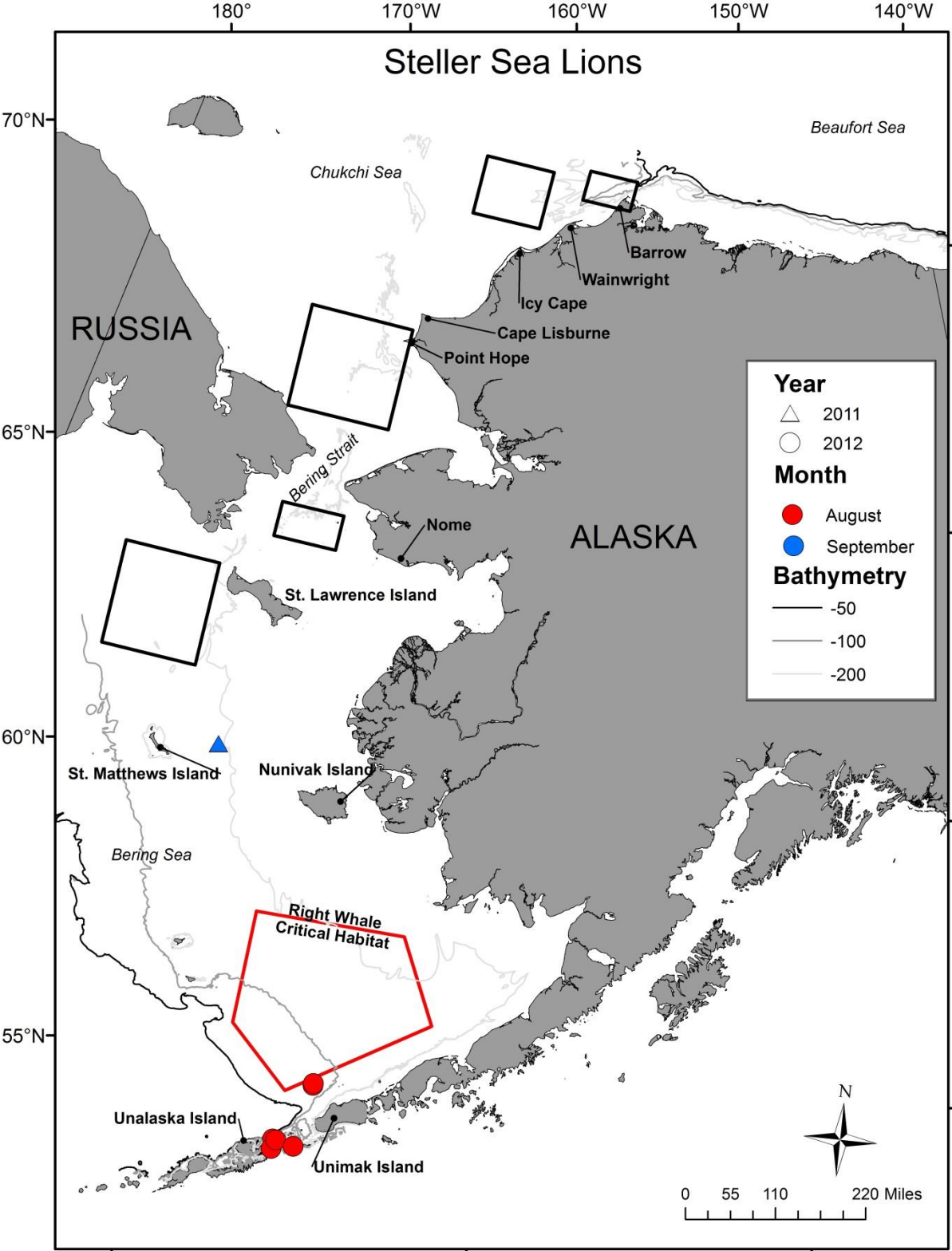
APPENDIX D. 14. NORTHERN FUR SEAL SIGHTINGS, 2010-2012.



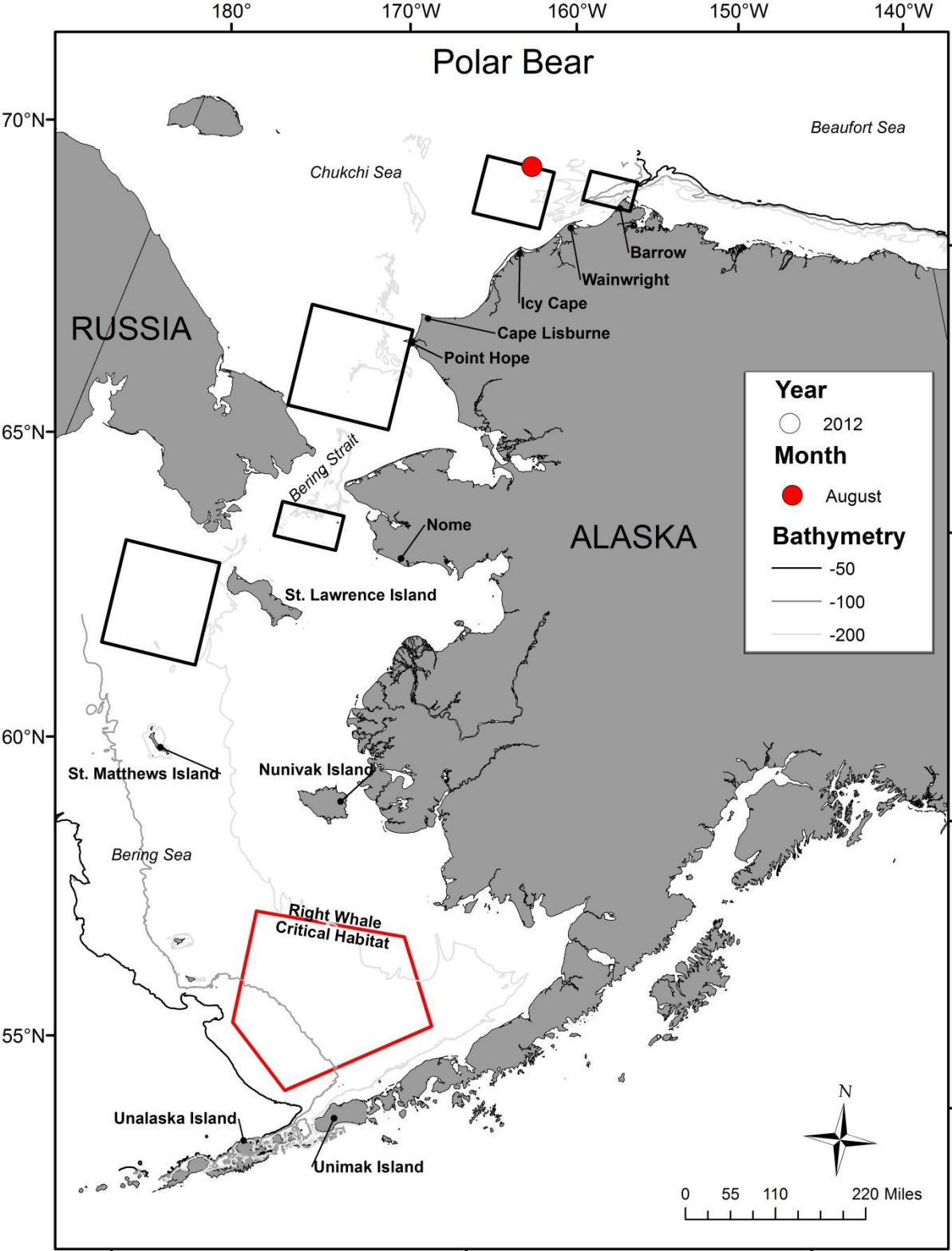
APPENDIX D. 15. RINGED SEAL SIGHTINGS, 2010-2012.



APPENDIX D. 16. SPOTTED SEAL SIGHTINGS, 2010-2012.



APPENDIX D. 17. STELLER SEA LION SIGHTINGS, 2010-2012.



APPENDIX D. 18. POLAR BEAR SIGHTINGS, 2010-2012.

E. Passive acoustics table showing percentage of days with calls for each species by month.

Species	Mooring	September	October	November	December	January	February	March	April	May	June	July	August
Bowhead whale	Inshore	21.4	72.6	85.0	21.0	0	0	8.1	51.7	85.5	43.9	58.1	16.1
	Midshore	25.5	80.6	85.0	25.8	0	0	1.6	10.0	8.0	33.3	n/a	33.3
	Offshore	11.8	53.2	78.3	22.6	1.6	0	0	1.7	0	0	n/a	0
Gunshot call	Inshore	1.8	9.7	33.3	9.7	0	0	0	3.3	14.5	17.5	0	0
	Midshore	0	4.8	18.3	17.7	0	0	0	0	0	0	n/a	0
	Offshore	0	1.6	38.3	43.5	8.1	3.5	0	0	0	0	n/a	0
Beluga whale	Inshore	3.6	25.8	58.3	6.5	4.8	1.8	6.5	46.7	67.7	14.0	12.9	0
	Midshore	0	6.5	36.7	14.5	6.5	0	14.5	31.7	28.0	4.8	n/a	0
	Offshore	0	3.2	23.3	3.2	4.8	3.5	0	26.7	4.4	0	n/a	0
Walrus	Inshore	71.4	43.5	23.3	14.5	8.1	7.0	12.9	25.0	21.0	56.1	93.5	12.9
	Midshore	68.6	37.1	20.0	4.8	1.6	0	3.2	15.0	4.0	81.0	n/a	100.0
	Offshore	47.1	24.2	11.7	41.9	33.9	71.9	58.1	38.3	20.0	50.0	n/a	100.0
Bearded seal	Inshore	21.4	67.7	66.7	82.3	96.8	96.5	100.0	100.0	100.0	93.0	41.9	22.6
	Midshore	19.6	33.9	73.3	91.9	100.0	96.5	100.0	100.0	100.0	100.0	n/a	33.3
	Offshore	54.9	40.3	31.7	71.0	77.4	75.4	90.3	100.0	100.0	100.0	n/a	66.7
Gray whale	Inshore	1.8	9.7	6.7	0	0	0	0	0	3.2	5.3	16.1	0
	Midshore	0	1.6	0	0	0	0	0	0	0	0	n/a	0
	Offshore	0	0	0	0	0	0	0	0	0	0	n/a	0
Killer whale	Inshore	1.8	4.8	0	0	0	0	0	0	1.6	1.8	0	0
	Midshore	0	0	0	0	0	0	0	1.7	0	0	n/a	0
	Offshore	0	0	0	0	0	0	0	0	0	0	n/a	0
Humpback whale	Inshore	0	0	0	0	0	0	0	0	0	0	0	0
	Midshore	0	0	0	0	0	0	0	0	0	0	n/a	0
	Offshore	0	0	0	0	0	0	0	0	0	0	n/a	0
Fin whale	Inshore	0	0	0	0	0	0	0	0	0	0	0	0
	Midshore	0	0	0	0	0	0	0	0	0	0	n/a	0
	Offshore	0	0	0	0	0	0	0	0	0	0	n/a	0
Minke whale	Inshore	0	0	0	0	0	0	0	0	0	0	0	0
	Midshore	0	0	0	0	0	0	0	0	0	0	n/a	0
	Offshore	0	0	0	0	0	0	0	0	0	0	n/a	0
Minke boing	Inshore	0	1.6	0	0	0	0	0	0	0	0	0	0
	Midshore	0	0	0	0	0	0	0	0	0	0	n/a	0
	Offshore	0	0	0	0	0	0	0	0	0	0	n/a	0
Right whale	Inshore	0	0	0	0	0	0	0	0	0	0	0	0
	Midshore	0	0	0	0	0	0	0	0	0	0	n/a	0
	Offshore	0	0	0	0	0	0	0	0	0	0	n/a	0
Unidentified pinniped	Inshore	12.5	8.1	16.7	11.3	17.7	7.0	24.2	23.3	50.0	28.1	12.9	3.2
	Midshore	5.9	3.2	6.7	1.6	0	0	3.2	13.3	34.0	19.0	n/a	66.7
	Offshore	0	0	1.7	0	1.6	0	0	6.7	0	0	n/a	0
Ribbon seal	Inshore	0	0	0	0	0	0	0	1.7	0	0	0	0
	Midshore	0	0	0	0	0	0	0	3.3	0	0	n/a	0
	Offshore	0	0	0	0	0	0	0	0	0	0	n/a	0
Sperm whale	Inshore	0	0	0	0	0	0	0	0	0	0	0	0
	Midshore	0	0	0	0	0	0	0	0	0	0	n/a	0
	Offshore	0	0	0	0	0	0	0	0	0	0	n/a	0
Ice noise	Inshore	0	0	30.0	83.9	80.6	75.4	69.4	66.7	53.2	36.8	61.3	0
	Midshore	0	0	38.3	75.8	45.2	59.6	29.0	35.0	4.0	0	n/a	0
	Offshore	0	4.8	28.3	71.0	64.5	70.2	25.8	21.7	6.7	0	n/a	0
Vessel	Inshore	12.5	12.9	1.7	0	0	0	0	0	0	0	0	0
	Midshore	13.7	3.2	6.7	0	0	7.0	0	0	0	0	n/a	33.3
	Offshore	5.9	1.6	0	6.5	3.2	0	0	0	0	0	n/a	66.7
Airguns	Inshore	55.4	6.5	0	0	0	0	0	0	0	0	0	0
	Midshore	66.7	9.7	0	0	0	0	0	0	0	0	n/a	100.0
	Offshore	66.7	6.5	0	0	0	0	0	0	0	0	n/a	100.0

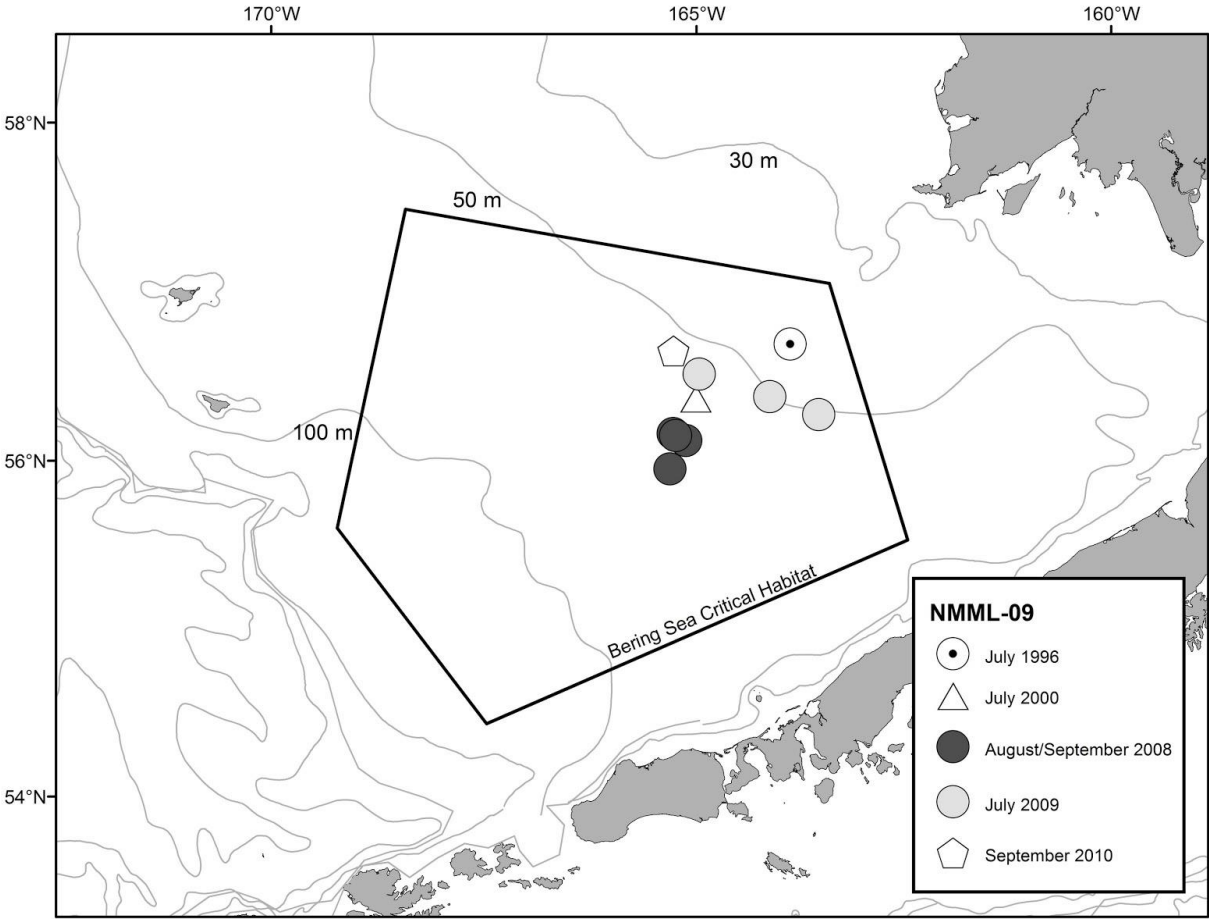
F. Photo-identification results within the Bering Sea and Gulf of Alaska.

Individuals (Appendix F. 1) were matched to NMML catalogs (humpback and right whale), and to the Western Alaska Transient and Resident Catalogs (killer whale, WATC/WARC). Of the three North Pacific right whales photographed, two were previously sighted and one was a new addition. NMML-09 has been sighted in five years (1996, 2000, 2008, 2009, 2010). NMML-85 has been sighted in three years (2009, 2010, 2011). In 2010, NMML-85 was sighted with a new individual designated as NMML-94. There were no matches found for humpback whales or the one adult male killer whale.

APPENDIX F. 1. SUMMARY OF PHOTOS COLLECTED AND ANALYSIS RESULTS, 2010-2012.

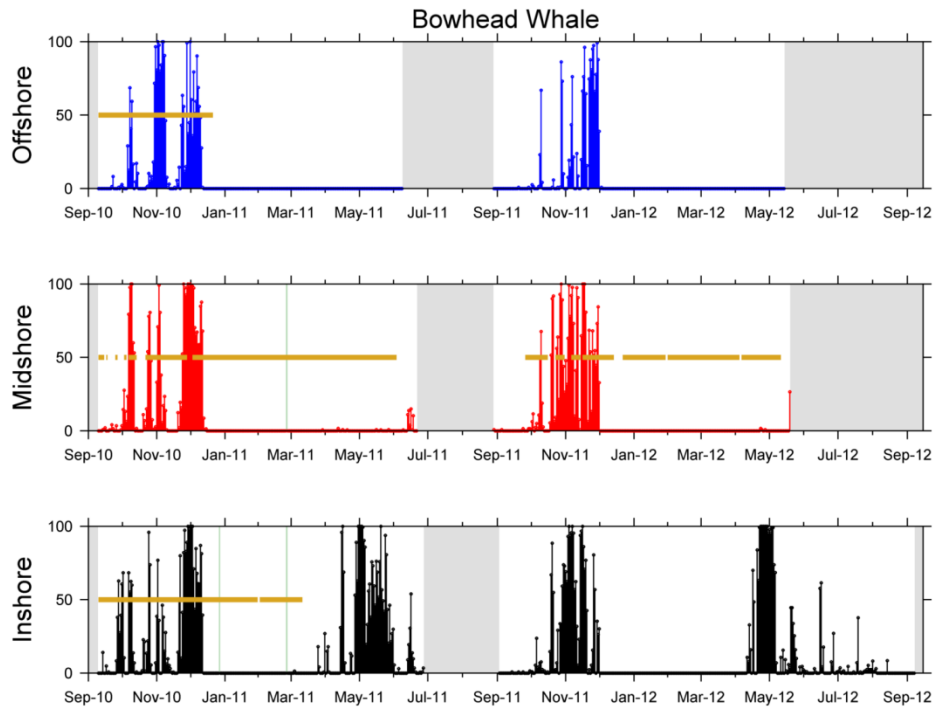
Year	Species	No. Individuals	Catalogs	Matches
2010	North Pacific right whale	1	NMML	NMML-09
2011	North Pacific right whale	2	NMML	NMML-85, NMML-94*
All	Humpback whale	27	NMML	No matches
2012	Killer whale	1	WATC/WARC	No match

Photo-identification of North Pacific right whales, although opportunistically collected, provided an invaluable contribution to insights into this critically endangered species. Most notably, the sightings of NMML-09 reinforce the importance of the Bering Sea Critical Habitat. Over five years, NMML-09 was sighted within the same general location with multiple sightings occurring within 2008 (Clapham et al., 2012) (Appendix F. 2). This animal has provided a significant contribution to understanding summertime foraging habitat use as well as providing the first high- to low-latitude match of a North Pacific right whale (Kennedy et al., 2011). Photo contributions spanning all of the North Pacific date back to 1979. In over 30 years, only 23 individuals have been added to the NMML North Pacific right whale catalog. The documentation of a new individual in 2011 provided a significant contribution to this catalog.

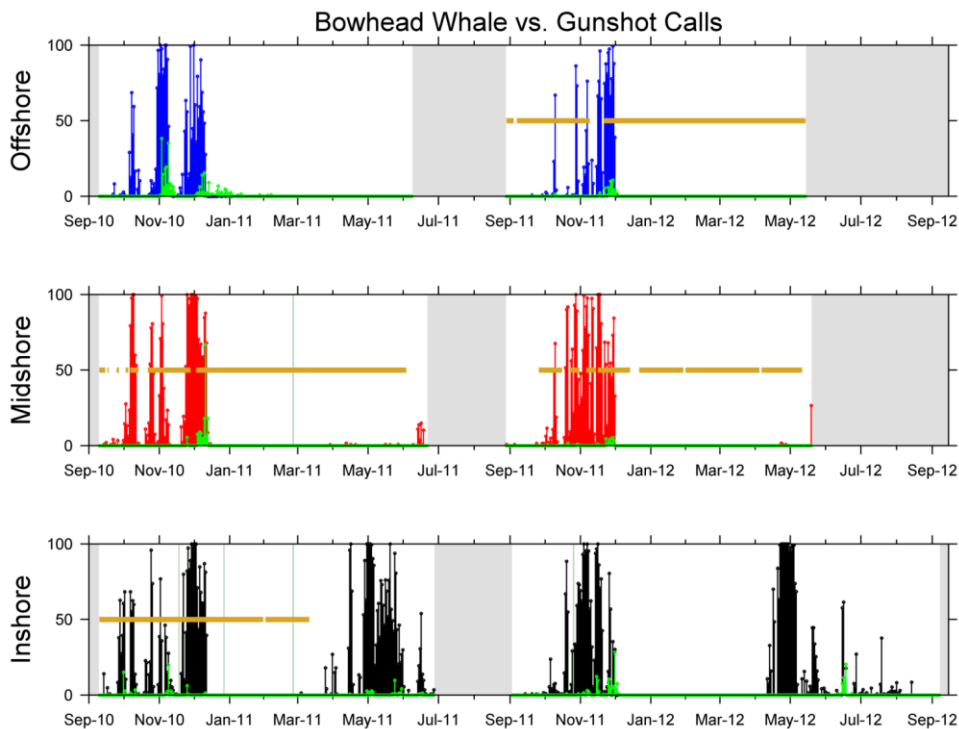


APPENDIX F. 2. SIGHTING HISTORY OF A NORTH PACIFIC RIGHT WHALE (NMML-09) OVER FIVE YEARS WITHIN THE BERING SEA CRITICAL HABITAT.

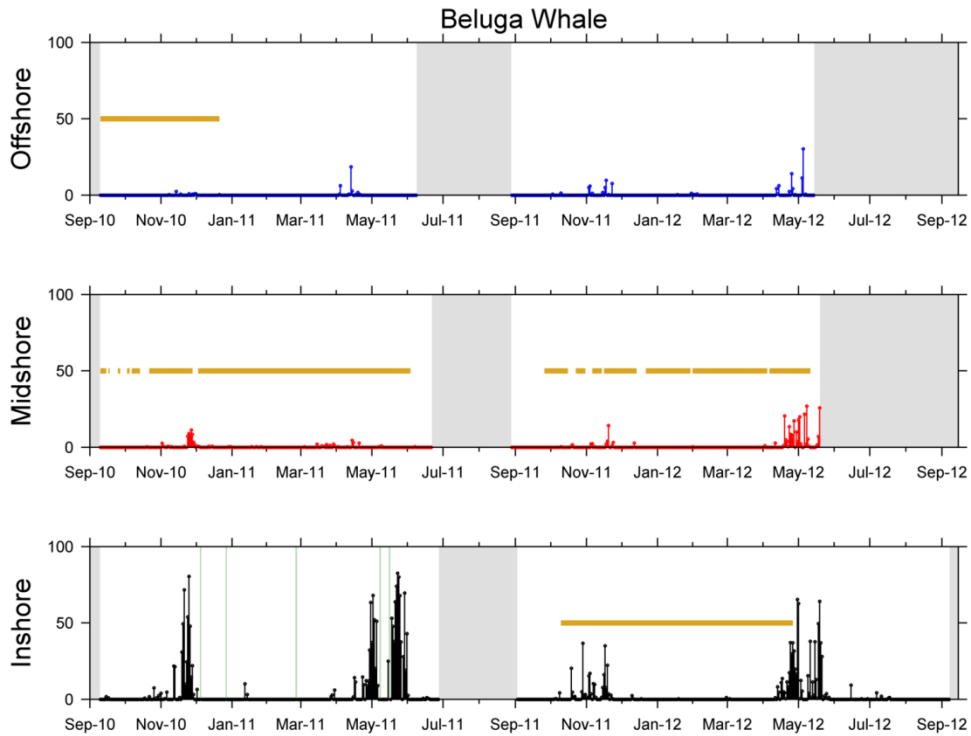
G. Long-term passive acoustic data showing timespans (orange) included in the GAMs for each species or signal.



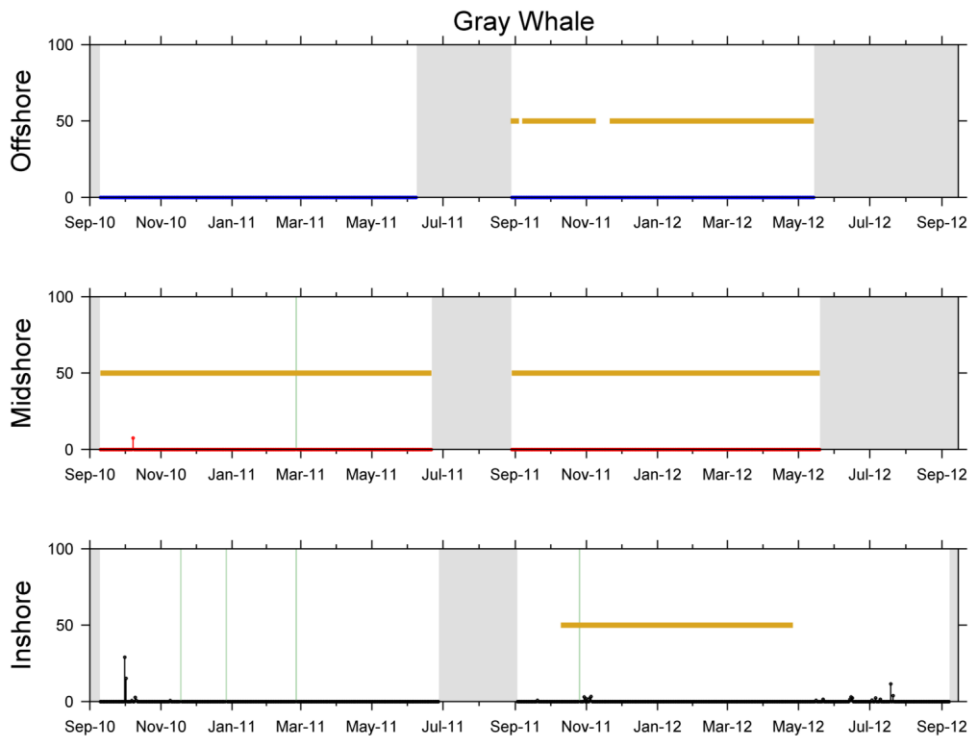
APPENDIX G. 1. LONG-TERM PASSIVE ACOUSTIC RESULTS SHOWING TIMESPANS INCLUDED IN GAM FOR BOWHEAD WHALES.



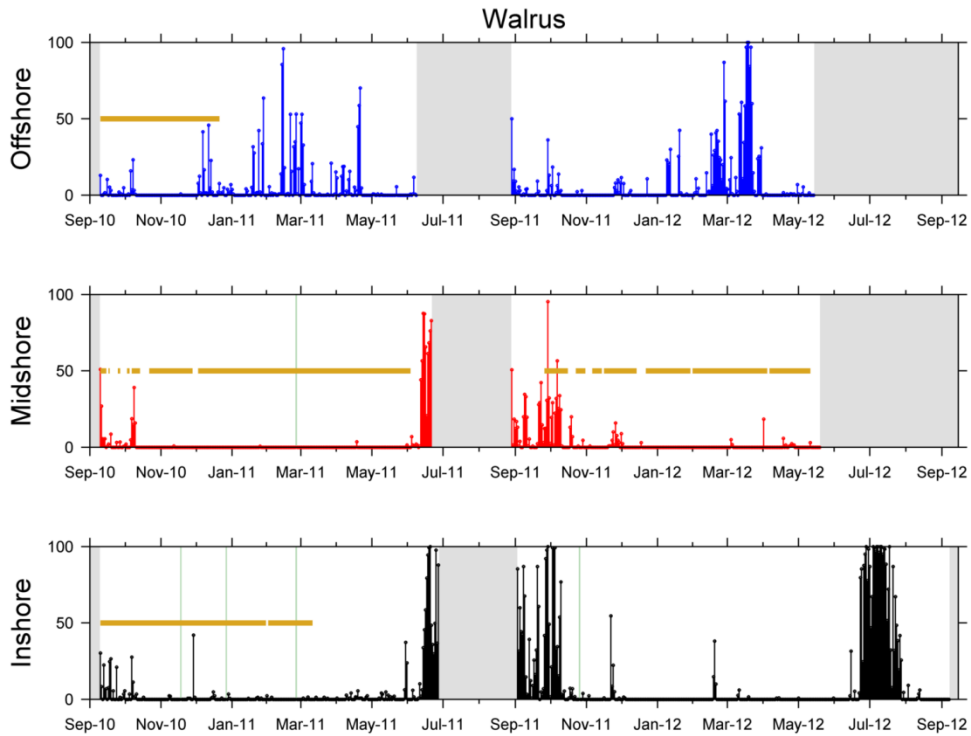
APPENDIX G. 2. LONG-TERM PASSIVE ACOUSTIC RESULTS SHOWING TIMESPANS INCLUDED IN GAM FOR BOWHEAD WHALES AND GUNSHOT CALLS.



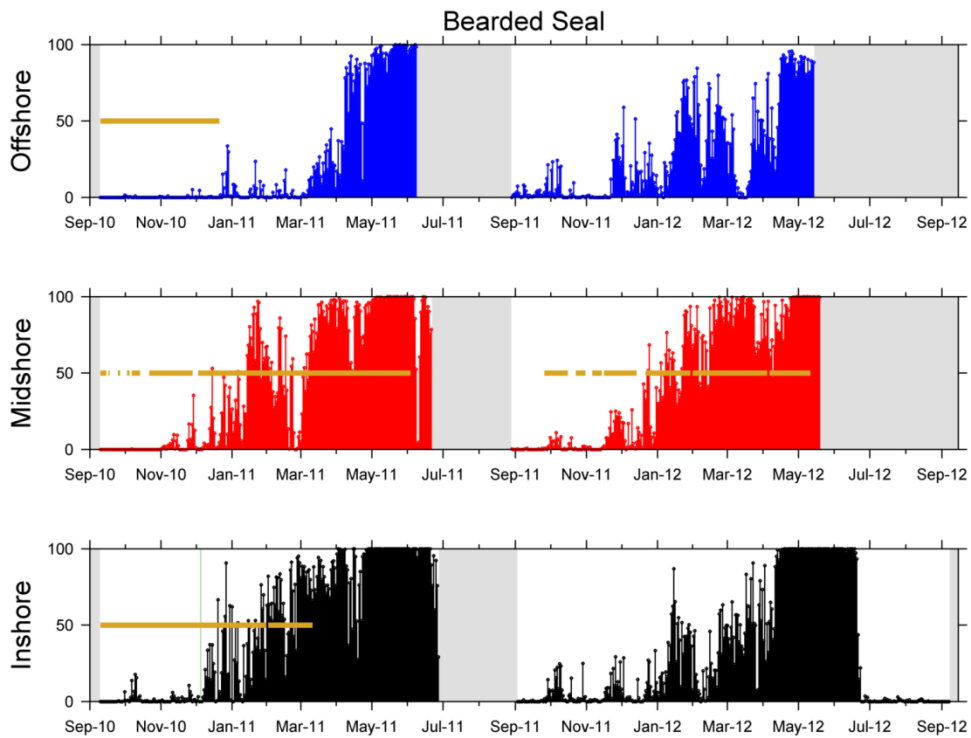
APPENDIX G. 3. LONG-TERM PASSIVE ACOUSTIC RESULTS SHOWING TIME SPANS INCLUDED IN GAM FOR BELUGA WHALES.



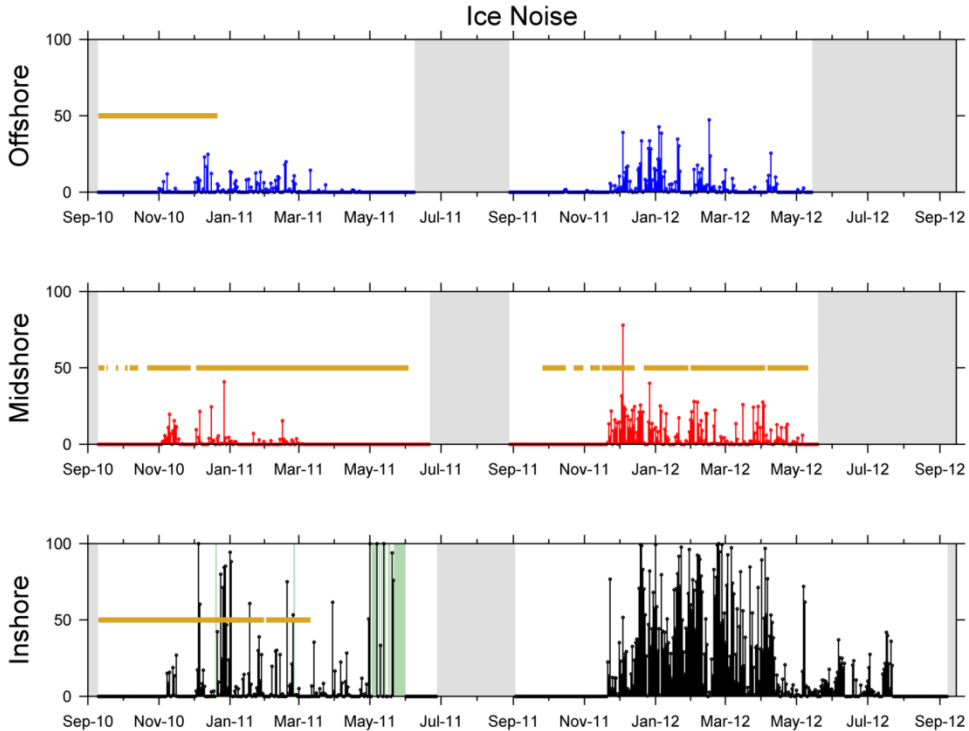
APPENDIX G. 4. LONG-TERM PASSIVE ACOUSTIC RESULTS SHOWING TIME SPANS INCLUDED IN GAM FOR GRAY WHALES.



APPENDIX G. 5. LONG-TERM PASSIVE ACOUSTIC RESULTS SHOWING TIMESPANS INCLUDED IN GAM FOR WALRUS.



APPENDIX G. 6. LONG-TERM PASSIVE ACOUSTIC RESULTS SHOWING TIMESPANS INCLUDED IN GAM FOR BEARDED SEALS.



APPENDIX G. 7. LONG-TERM PASSIVE ACOUSTIC RESULTS SHOWING TIMESPANS INCLUDED IN GAM FOR ICE NOISE.

H. GAM results including TAPS6-NG variables

Additional Methods

The TAPS6-NG GAM runs were limited to the calling activity of three species: bearded seal, bowhead whales, and walrus. The remainder of the species/sound sources that were included in the main GAM models had no calling/noise activity for any of the days with TAPS6-NG measurements and were not included in the TAPS6-NG analysis. In addition, not all of the oceanographic variables from the main GAM models were included in the TAPS6-NG GAM runs. Salinity was excluded as no data were available. Month and year variables were excluded as the data came from a single month and year. Ice concentration and ice thickness were excluded, as there was no ice present during TAPS6-NG data collection.

Two separate sets of runs were conducted for the TAPS6-NG analysis; one included the four full water column variables (Type I), and the second one included the four bottom layer (Type II) variables. This was necessary, as the computing power limit would have been reached if all eight variables had been included (i.e., 22 variables would have produced 4.1 million models; all attempts at running a 20-variable GAM crashed after 24 hours of running). For all runs, the entire two-year midshore dataset was used. This allowed examination of how strongly correlated the TAPS6-NG variables were to the calling data. If a TAPS6-NG variable rose to the top of the GAM runs, this would indicate the variable provided a high level of explanatory power to explain the variance in calling activity during the short period of time that the TAPS6-NG was collecting data, higher than other models containing more data.

Results

Because there were only 36 days of data available from the TAPS6-NG instrument (25 Aug - 29 Sep 2011), and four of these days occurred before the passive acoustic recordings began, there is a very limited dataset (32 days) available. Typically models having this sample size would be automatically excluded from being ranked high in the GAM analysis. In this case, however, the motivation was to see if any of the TAPS6-NG variables contributed significantly to the variability seen in the seasonal distributions of calling activity. Therefore, no models were excluded due to a low ($n < 100$) sample size. A summary table of the results of the two runs is presented in Appendix H. Table 1.

Discussion

The results from this set of GAM runs indicate a variety of the TAPS6-NG variables provided high explanatory power for the variance in bowhead whale, bearded seal, and walrus calling activity. In the future, every effort to collect these data simultaneous with passive acoustic recordings should be attempted to evaluate their explanatory power in understanding marine mammal distributions.

APPENDIX H. TABLE 1. TAP6-NG GAM RESULTS SUMMARY OF THE TOP VARIABLES, THE % R-SQUARED VALUE, AND THE SAMPLE SIZE, FOR BOTH THE TOP AIC MODEL AND THE TOP R-SQUARED MODEL, AND THE COMMON SIGNIFICANT VARIABLES AMONG THE TOP FIVE AIC AND R-SQUARED MODELS FOR EACH SPECIES OR SIGNAL.

		Type I Midshore		Type II Midshore	
Bearded Seal	Top 1 Models	Top AIC	Q + t + a	Q + R + t + f	
		AIC, % AIC, n	9, 48.5%, 32	14, 41.0%, 32	
		Top Rsqr	A + Q + P + T + V + R + N + C + t + n + G	A + Q + P + T + V + R + N + C + t + n + G	
		AIC, % R ² , n	4625, 59.6%, 495	4625, 59.6%, 495	
	Top 5 Models: Common Vars*	Sig < 0.01	Q	Q	
		Sig < 0.05	Q t	Q R t	
Bowhead Whale	Top 1 Models	Top AIC	F + p	P + T + N + d + h	
		AIC, % AIC, n	28, 28.0%, 32	32, 25.3%, 29	
		Top Rsqr	F + p	A + Q + P + T + U + R + N + C + t + n	
		AIC, % R ² , n	28, 28.0%, 32	4489, 26.8%, 495	
	Top 5 Models: Common Vars*	Sig < 0.01	p	-	
		Sig < 0.05	F p	-	
Walrus	Top 1 Models	Top AIC	N + u + a + r	Q + V + R + N + d + f + h + O	
		AIC, % AIC, n	244, 48.2%, 29	241, 58.1%, 29	
		Top Rsqr	Q + P + T + U + V + R + N + a + O	Q + V + R + N + d + f + h + O	
		AIC, % R ² , n	245, 52.5%, 29	241, 58.1%, 29	
	Top 5 Models: Common Vars*	Sig < 0.01	-	Q h O	
		Sig < 0.05	a	Q d h O	

* To be included, variable had to be in at least 3 of each set of models; U = U bottom currents (cm s-1); R = transport (Sv, averaged across all locations); N = nitrate (bottom); t = V winds at midshore location; n = wind speed at midshore location; G = bottom O2 (mMol kg-1); A = ADCP (600) column Sa (area backscattering dB re 1 m-1); F = chlorophyll (fluorescence); P = PAR (mE in cm-2 s-1); V = V bottom currents (cm s-1); C = Turbidity (FNU); O = % oxygen saturation; Q = ADCP (600 kHz) bottom Sv (volume backscattering dB re 1 m-1); T = temperature (°C); u = U winds at midshore location; f = TAPS 420 kHz Volume backscatter (Sv) bottom (dB re 1 m-1); p = TAPS Euphausiid abundance (/m3) full column; d = TAPS Euphausiid abundance (/m3) bottom; h = TAPS 50 kHz Volume backscatter (Sv) bottom (dB re 1 m-1); a = TAPS Total BioVolume (mm3/m3) full column; r = TAPS 50 kHz Volume backscatter (Sv) full column (dB re 1(m2))

I. List of attached electronic files:

1. Sonobuoy deployment tables. These are tables showing every sonobuoy deployed during the CHAOZ cruises, as well as species detected, for 2010-2012. File name: “CHAOZ 2010-12 sonobuoy deployments.pdf”
2. Table of GAM daily averaged variables across disciplines. This table contains daily average values for each variable that was included in the GAMs. This spreadsheet also contains one tab per mooring location (inshore, midshore, and offshore). File name: “CHAOZ_GAM_AllComponents_FINAL.xls”
3. CTD and plankton reports, detailing samples and measurements collected at each transect sampling station for the 2010-2012 field surveys.
 - a. 2010: “CHAOZ_2010_CTD&planktonReport.pdf”
 - b. 2011: “CHAOZ_2011_CTD&planktonReport.pdf”
 - c. 2012: “CHAOZ_2012_CTD&planktonReport.pdf”
4. Archived Samples list. This document contains a list of all data samples, their approximate file size, and their location, for all data collected during the CHAOZ study. File name: “CHAOZ Archived Samples List.pdf”
5. Technical Summary. This is a brief (3-4 page) summary report of the CHAOZ project. File name: “CHAOZ M09PG00016 Technical Summary.pdf”



The Department of the Interior Mission

Protecting America's Great Outdoors and Powering Our Future

The U.S. Department of the Interior protects America's natural resources and heritage, honors our cultures and tribal communities